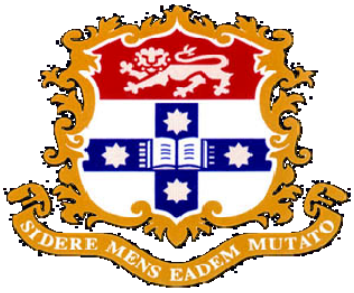

CHARACTERISING SOIL STRUCTURAL STABILITY AND FORM OF SODIC SOIL USED FOR COTTON PRODUCTION

SIMON DOUGLAS SPEIRS
BScAgr (Hons)

Faculty of Agriculture, Food and Natural Resources
The University of Sydney
New South Wales
Australia

A thesis submitted in fulfilment of the requirements for the Degree of Doctor of Philosophy

2006

CERTIFICATE OF ORIGINALITY

The text of this thesis contains no material which has been accepted as part of the requirements for any other degree or diploma in any university or any material previously published or written, unless due reference to the material has been made

Simon D Speirs

ABSTRACT

In eastern Australia, Vertosols are widely utilised for the production of irrigated cotton (*Gossypium hirsutum*) due to their inherent fertility and large water–holding capacity. However, irrigated agriculture in eastern Australia is faced with a decline in the availability of good quality irrigation water sources *i.e.* waters with low electrolyte concentrations and small Na^+ contributions. Consequently, alternative water resources that contain larger contributions of Na^+ are becoming increasingly relevant as potential irrigation sources. It is known that the application of Na^+ rich waters as irrigation has the potential to increase the Na^+ content of the soil, and that this will affect the structural condition of Vertosols. However, the extent to which these poor quality water resources will influence the structural characteristics of different Vertosols is unknown. In addition to this knowledge gap, there is currently no suitable predictor of dispersive behaviour for this soil type, particularly where Vertosols are irrigated with different water quality solutions.

The research conducted in this study aimed to characterise the impact of different increments of water quality on the structural stability of different Vertosols. Once this was concluded, the study looked to assess the impact of irrigation water quality on the structural stability, structural form and soil water retention properties of intact soil columns. Knowledge of the structural stability of the soils investigated was then used to derive a model describing the impact of water quality on the structural stability of different cotton producing soils.

To achieve the aims nine different soil profiles were sampled from the Bourke, lower Gwydir, Hillston and lower Namoi cotton–producing regions. Eight of these soils are Grey and Black Vertosols with clay phyllosilicate suites dominated to different extents by 2:1 expanding clays, and the ninth soil is an illitic Red Vertosol containing small contributions of 2:1 expanding clays. The soils investigated have ESPs that range between 1 and 10, ECs of 0.1 to 1.2 dS m^{-1} and CEC_{eff} values that are largest for those soils that contain more 2:1 expanding clays.

This study shows that the clay phyllosilicate suite of different Vertosols is the primary determinant of structural stability, structural form and soil water retention properties. For example, the Gwydir and Namoi soils contain more 2:1 expanding lattice phyllosilicate clays, have the largest CEC_{eff} values of all nine soils and are the most dispersive after all applied immersion treatments. The Bourke and Hillston soils contain less 2:1 expanding lattice clay, have smaller CEC_{eff} values and are generally more stable.

Irrigation of structurally–intact soils with solutions of larger SAR_w resulted in larger exchangeable Na^+ contents for each soil (and larger ESPs) and smaller contributions of exchangeable Ca^{2+} and

Mg^{2+}. For each soil, larger ESPs are reflected by decreased stability, but generally the soils dominated by 2:1 expansive clays are much less stable than the soils containing smaller contributions of these clay mineral types.

Irrigating the structurally–intact Vertosols dominated by 2:1 expansive clays generally resulted in structural form attributes that do not indicate any impact of the applied water treatments, but the Vertosols with less of these mineral types tend to have less desirable structural form attributes after irrigation with solutions of larger Na^+ content. Similarly, where the water retention properties of two soils were assessed, the illitic Red Vertosol has less structural pore space after treatment using the large SAR_w solutions, while the other soil (a Black Vertosol dominated by 2:1 expansive clays) does not show any differences between water retention properties that can be linked to irrigation water quality. These results were clarified for the water retention properties by the assessment of pore–solid space relations, which show both these soils to contain less solid space after irrigation with clean water or solutions of large SAR_w. This is attributed to increased swelling of clays in the presence of larger Na^+ contributions, but both soils have different structural arrangements as shown by the water retention properties and structural form assessment. The red illitic Vertosol shows signs of structural collapse, while the black Vertosol maintains its structural arrangement.

Finally, a model describing the structural stability of different Vertosols was developed from the stability assessment of soils, both in different water quality treatments and after the irrigation of structurally–intact columns. The model presented uses a surface response function to describe the impact of increased EC_w and SAR_w of irrigation solutions on soil stability after immersion according to specific soil physico–chemical attributes. In this model increased exchangeable Na^+, SAR and a larger CEC_{eff} (and consequently, an increased proportion of 2:1 swelling clays) are associated with increases in clay dispersion, while a smaller Ca^{2+}:Mg^{2+} ratio, EC and less total clay are associated with decreases in clay dispersion.

ACKNOWLEDGEMENTS

I would like to sincerely thank Dr Stephen Cattle, who after initially providing me with the opportunity to undertake this project, has tirelessly guided me as I pursued this research. As I prepared this thesis he spent many hours critiquing written material, and his insights and assistance have been most warmly appreciated.

To my associate supervisors within the University, Dr Damien Field and Dr Balwant Singh, thankyou for your patience and assistance. The assistance Damien provided with a number of analytical techniques, with concepts of soil structural stability and soil water retention has been invaluable. In addition, I complete this postgraduate experience richer for the experience of having had Damien as a colleague, to challenge and to debate what exists beyond soil science.

I thank Balwant for his time. It has been a pleasure to have his assistance in this research project and he has been strongly supportive of my candidature. Furthermore, I wish to thank him for the time he has given to the postgraduate group as a whole.

To Dr Nilantha Hulugalle I give my thanks for his role as an associate Supervisor. We have had the opportunity on many occasions to sit and discuss my research and he has provided some helpful insights and much encouragement.

Many thanks must go to Dr Willem Vervoort whose constant assistance has provided me with considerable encouragement for both this research and for involvement with other Faculty initiatives.

To the Soil Science group at the University of Sydney; Professor Alex McBratney, Dr Inakwu Odeh, Dr Raphael Viscarra Rossel, Dr Budiman Minasny and all those not mentioned, thankyou for your assistance, encouragement and for friendship.

Thankyou to Mr Colin Bailey, Ms Iona Gregory, Mr Kevin McLauchlan and all other staff of the Faculty. The assistance, support and friendship you have all provided have been a wonderful blessing to my time as a postgraduate student.

Fellow comrades in arms, the postgraduate students, thankyou for assistance and friendship. I thankyou for your support, friendship and encouragement.

I would like to thank the Cotton Research and Development Corporation for their generous financial support of this research. Further, thanks go to the Australian Cotton Cooperative Research Centre for the assistance they have provided. I would also like to thank the cotton–growers and industry extension staff that have been involved in this project. In addition, I must thank both the CRDC and the Cotton CRC organisations for the lengths to which they have extended themselves in order to educate postgraduate students in industry practices as a whole.

Finally, most heart felt thanks must go to those not part, yet so much a part. Mum and Dad, Kate and James, Mike and Greta; they have given me so much care and support during the last four years. No words can show my gratitude, but from this point I finish with so much more than with what I began. The journey is far from complete, yet I am prepared and only time shall tell what lies in front.

~

"When I was a child, I talked like a child, I thought like a child, I reasoned like a child.
When I became a man, I put childish ways behind me."

1 CORINTHIANS 13 VS 11

~

PUBLICATIONS

The following paper has been published based on work presented for this thesis:

Speirs SD, Cattle SR (2004) Soil structural form: the effect of irrigation water with varying SAR on several Vertosols. In 'SuperSoil 2004, 3rd Australian New Zealand Soils Conference' (ED. B Singh). The University of Sydney, Australia.

TABLE OF CONTENTS

ABSTRACT ..... *iii*
ACKNOWLEDGMENTS ..... *v*
PUBLICATIONS ..... *vii*
TABLE OF CONTENTS ..... *viii*
LIST OF TABLES ..... *xiii*
LIST OF FIGURES ..... *xvi*
GLOSSARY, SYMBOLS AND ABBREVIATIONS ..... *xxii*

GENERAL INTRODUCTION AND AIMS

0.1 Introduction ..... *xxv*
0.2 Aims ..... *xxvii*

CHAPTER 1 FACTORS INFLUENCING THE STRUCTURAL CONDITION OF VERTOSOLS

1.1 Vertosols in Australia 1
1.1.1 Definition 1
1.1.2 Distribution of Vertosols 2
1.1.3 Genesis 2
1.1.4 General soil properties 3
1.1.5 Current landuse practices and their potential impact on Vertosol structure 4
1.2 The integrity of soil structure: definitions applicable to Vertosols 6
1.2.1 Soil structural form 6
1.2.2 Soil structural stability 7
1.2.3 Soil structural resilience 8
1.2.4 Soil structural vulnerability 9
1.3 Soil physical processes that influence the structural form of Vertosols 9
1.3.1 Swelling and shrinkage: the wet–dry process 10
1.3.2 Self–mulching 10
1.3.3 Slaking of aggregates 11
1.3.4 Churning 12
1.4 The physico–chemical properties that influence the structure of Vertosols 12
1.4.1 The importance of clay content and the mineral suite 13
1.4.1.1 Clay content and size 13
1.4.1.2 Clay mineral suite 14
1.4.1.3 The swelling of clay minerals 15
1.4.2 The cation exchange complex 18
1.4.1.4 The principles of double layer theory and the influence of ionic state 19
1.4.2.2 The role of exchangeable Na^+ in determining structural characteristics 22
1.4.2.3 The role of exchangeable Ca^{2+} and Mg^{2+} in determining structural characteristics 25
1.4.2.4 The role of exchangeable K^+ in determining structural characteristics 26
1.4.3 The soil solution 27
1.4.3.1 The concentration of the soil solution 27
1.4.3.2 The speciation of cations in the soil solution 29
1.4.4 Soil pH 30
1.4.5 Soil organic material 30
1.4.6 Sulfates, carbonates and oxides 31

1.5 The structural degradation of Vertosols 32
1.5.1 The physical disintegration of Vertosols 33
1.5.2 The chemical disintegration of Vertosols 34
1.6 Methods of determining the relative importance of structure–affecting soil attributes 34
1.6.1 Determining the structural stability of Vertosols 35
1.6.2 Determining the structural form of Vertosols 37
1.7 Predicting structural changes in Vertosols 39
1.7.1 Critical levels of Na^+ and the relationship between exchangeable Na^+ and electrical conductivity 39
1.7.2 Multifactorial relationships 40
1.8 Current knowledge deficiencies regarding the structural condition of Vertosols 42

CHAPTER 2 A DESCRIPTION OF NINE VERTOSOLS USED FOR COTTON PRODUCTION

2.1 Introduction 45
2.2 Sampling regions 45
2.3 Soil profiles 46
2.3.1 The Bourke cotton–producing region 47
2.3.2 The lower Gwydir cotton–producing region 49
2.3.3 The Hillston cotton–producing region 50
2.3.4 The lower Namoi cotton–producing region 52
2.4 The physico–chemical properties of the nine Vertosols 53
2.4.1 Physico–chemical methods 54
2.4.2 Physico–chemical properties of cotton–producing Vertosols 56
2.4.2.1 Three profiles from the Bourke region 57
2.4.2.2 Two profiles from the lower Gwydir valley 59
2.4.2.3 Two profiles from the Hillston region 61
2.4.2.4 Two profiles from the lower Namoi valley 62
2.5 The soil mineral suite 64
2.5.1 The primary mineral suite of each Vertosol 65
2.5.2 The phyllosilicate suite of each Vertosol 67
2.6 Classification of the nine soils 72
2.7 Comparing these Vertosols with other cotton–producing Vertosols 74
2.8 Summary 75

CHAPTER 3 DETERMINING THE STRUCTURAL STABILITY OF NINE SURFACE SOILS

3.1 Introduction 77
3.2 Methods 78
3.2.1 Fundamental soil physico–chemical properties 78
3.2.2 Spontaneous clay dispersion 79
3.2.3 EOE–disruption 79
3.2.4 Ultrasonic agitation 80
3.2.5 Water quality and end–over–end disruption 80
3.2.6 Estimation of structural stability 82
3.3 Results 83
3.3.1 Fundamental soil properties 83
3.3.2 Structural stability of Vertosols measured using de–ionised water and three disruptive forces 85
3.3.3 Comparing the structural stability of the nine topsoils after treatment with solutions T102 and FW00i using EOE–disruption 87
3.3.4 Comparing the structural stability of the nine topsoils after treatment with solutions of EC_{iw} 0.0, 0.2, 0.5 and 2.7 dS m^{-1}, where SAR_{iw} is equal to zero, using EOE–disruption 88

3.3.5 Structural stability of nine surface soils after EOE–disruption using different increments of water quality (3 increments of EC_w each with 4 levels of SAR_w) 91
3.3.5.1 Water quality and the stability of the Bourke soils 92
3.3.5.2 Water quality and the stability of the lower Gwydir soils 93
3.3.5.3 Water quality and the stability of the Hillston soils 95
3.3.5.4 Water quality and the stability of the lower Namoi soils 96
3.3.6 Correlation of the soil physico–chemical attributes with $SI_{<100}$ and $SI_{<2}$ values for each applied treatment 97
3.4 Discussion 99
3.4.1 Comparing the nine different furrow surface soils with the properties of each profile 99
3.4.2 Critical thresholds of dispersion 101
3.4.3 Comparing the effect of dispersive energy on the stability of the nine furrow topsoils 103
3.4.4 The effect of water quality on the liberation of soil material during end–over–end shaking 105
3.4.5 Comparisons of soil physico–chemical attributes with the $SI_{<100}$ and $SI_{<2}$ values 107
3.5 Conclusions 108

CHAPTER 4 ASSESSING THE IMPACT OF IRRIGATION ON SELECTED PHYSICO–CHEMICAL ATTRIBUTES

4.1 Introduction 111
4.2 Materials and Methods 112
4.2.1 Laboratory irrigation of soil columns 113
4.2.2 The six solutions used to irrigate soil columns 114
4.2.3 Monitoring the irrigation of soil columns 115
4.2.4 Selected chemical properties and the structural stability of laboratory irrigated Vertosols 115
4.2.5 Data analysis 116
4.3 Results 116
4.3.1 The bulk density and the field wetness of columns at the time of sampling 116
4.3.2 The impact of irrigating columns on selected soil properties 117
4.3.2.1 The effect of irrigation treatment on the exchangeable cations 117
4.3.2.2 The effect of treatment solution on the soil solution and the quantity of dispersed clay 125
4.3.3 The effect of selected soil properties on the $SI_{<2}$ values determined for the six Vertosols 133
4.4 Discussion 135
4.4.1 Irrigating in the laboratory 135
4.4.2 Comparing the chemical properties of soil columns with the chemical attributes of the irrigation furrow 136
4.4.3 Comparison of the assessed soil attributes for these irrigated Vertosols 138
4.4.4 Comparing $SI_{<2}$ values with soil properties 140
4.5 Conclusions 141

CHAPTER 5 ASSESSING THE IMPACT OF IRRIGATION ON SOIL STRUCTURAL FORM

5.1 Introduction 143
5.2 Soil structural form characteristics determined using Solicon© 144
5.3 Methods 145
5.3.1 Sample preparation and the laboratory irrigation of soil columns 145
5.3.2 Image acquisition and analysis 146
5.3.3 Analysis of soil structural form attributes 147
5.4 Results 148
5.4.1 The effect of irrigation water quality on selected structural parameters for the nine soils investigated 150
5.4.1.1 Comparative effects of the T40i solutions on structural form attributes 151
5.4.1.2 Comparative effects of the T401 and T102 solutions on structural form attributes 156

5.4.1.3 Comparative effects of the FW00i and T102 solutions on structural form attributes 156
5.4.2 Comparing the effect of water quality on selected structural parameters of each soil using three depth increments 156
5.4.3 Comparing the structural form attributes of the nine Vertosols 164
5.4.4 Determining the effect of water quality on pore sieve distributions 165
5.4.5 Determining the effect of water quality on pore star–shape distributions 167
5.5 Discussion 170
5.5.1 The impact of irrigation water quality on the different Vertosols 170
5.5.2 The pore sieve and pore star–shape distributions 172
5.5.3 Structural form and the impact of soil physico–chemical properties 174
5.6 Conclusions 175

CHAPTER 6 WATER QUALITY AND THE WATER RETENTION CURVES OF TWO VERTOSOLS

6.1 Introduction 177
6.2 Materials and Methods 178
6.2.1 Determining the water potential and moisture content using the ku/pF–Apparatus 178
6.2.2 The soil–water retention curves 179
6.2.3 The water capacity function 181
6.2.4 Total porosity of the treated columns 182
6.3 Results 182
6.3.1 The simulated water retention curves of G001 and H001 182
6.3.2 The water capacity of irrigation treatments for G001 and H001 187
6.3.3 The effect of irrigation water quality on the total soil porosity 190
6.4 Discussion 191
6.4.1 Determination of unknown parameters using the van Genuchten equation 191
6.4.2 The moisture retention of soils G001 and H001 191
6.4.3 Water capacity as a function of effective pore drainage radii for the two Vertosols investigated 193
6.4.4 The soil solid, liquid and gaseous phases 194
6.4.5 Comparing the pore distributions obtained from the soil moisture retention curve and from the image analysis procedure 195
6.5 Conclusions 196

CHAPTER 7 DEVELOPING A DESCRIPTIVE MODEL OF THE STRUCTURAL STABILITY OF IRRIGATED VERTOSOLS

7.1 Introduction 197
7.2 Estimating the structural stability of the nine Vertosols using current methods 198
7.2.1 The soil samples and data used for comparisons 198
7.2.2 Factors affecting the structural stability of cotton–producing Vertosols in water 198
7.2.3 Comparing ESP, ESI and $EC_{1:5}/Na^{+}_{exch}$ with the stability index of clay dispersion 201
7.2.3.1 Comparing all chapter 3 soils and all chapter 4 soils 201
7.2.3.2 Differentiating the irrigated Vertosols (chapter 4 soils) according to the suite of clay phyllosilicates 202
7.2.4 The Rengasamy classification scheme 203
7.2.4.1 The furrow topsoils (chapter 3 soils) 204
7.2.4.2 The laboratory irrigated soils (chapter 4 soils) 205
7.2.5 The problems with these current predictive models 206
7.3 Developing predictions of structural stability according to soil physico–chemical properties and water quality 207
7.3.1 The association between soil physico–chemical properties and $SI_{<2}$ 208
7.3.2 The impact of water quality on $SI_{<2}$ 210
7.3.2.1 Development of a prediction of $SI_{<2}$ according to water quality characteristics 210

7.3.2.2 Predicting $SI_{<2}$ for individual Vertosols according to water quality characteristics 212
7.3.3 Summary of the dispersion classes 215
7.4 A model of the structural stability of the nine Vertosols 215
7.4.1 The structural stability of irrigated Vertosols 215
7.4.2 Modelling the stability of each of the nine Vertosols 216
7.5 Conclusions 221

CHAPTER 8 DISCUSSION, FUTURE RESEARCH OPPORTUNITIES AND CONCLUSIONS

8.1 The structural integrity of cotton–producing Vertosols 223
8.1.1 The irrigated Vertosols: their physico–chemical properties 223
8.1.2 The irrigated Vertosols: structural stability 224
8.1.3 The impact of irrigation water quality on selected soil properties, structural form and water retention 226
8.1.4 A model describing the stability of Vertosols in solutions of different EC_{iw} and SAR_{iw} characteristics 228
8.1.5 Cotton soils that are most likely to exhibit structural degradation where poor quality solutions are applied as irrigation supplies 229
8.2 Conclusions 231
8.3 Future research opportunities 233
8.3.1 Current methods of determining structural stability and the clay mineral suite 233
8.3.2 The impact of organic carbon contributions 233
8.3.3 The structural form of Vertosols: the impact of moisture content 234
8.3.4 Developing a model of structural stability 235
8.3.5 Remediation of sodic conditions in Vertosols 235

BIBLIOGRAPHY 237

APPENDICES 251

LIST OF TABLES

CHAPTER 1

Table 1.1 Mineral suite composition of Vertosol topsoils from eastern Australia (Vervoort *et al.* 2003) 14

Table 1.2 The ionic and hydrated radii of the four common exchangeable cations in Vertosols 21

Table 1.3 Classification units based on the map of Northcote and Skene (1972) (from McKenzie *et al.* 1995) 23

Table 1.4 Classes applied by Rengasamy *et al.* (1984) in their structural stability classification scheme for red–brown earths 42

CHAPTER 2

Table 2.1 The average annual rainfall and temperature for each sampling region 46

Table 2.2 Field description of three soil profiles from the Bourke cotton–growing region 49

Table 2.3 Field description of two soil profiles from the lower Gwydir cotton–growing region 50

Table 2.4 Field description of two soil profiles from the Hillston cotton–growing region 52

Table 2.5 Field description of two soil profiles from the lower Namoi cotton–growing region 53

Table 2.6 Physical properties of profiles B001, B002 and B003 58

Table 2.7 Chemical properties of profiles B001, B002 and B003 59

Table 2.8 Physical properties of profiles G001 and G002 60

Table 2.9 Chemical properties of profiles G001 and G002 60

Table 2.10 Physical properties of profiles H001 and H002 61

Table 2.11 Chemical properties of profiles H001 and H002 62

Table 2.12 Physical properties of profiles N001 and N002 63

Table 2.13 Chemical properties of profiles N001 and N002 64

Table 2.14 Measurement criteria applied during the use of XRD–techniques for the identification of the soil mineral suite and for the identification and quantification of the clay phyllosilicates 65

Table 2.15 The primary mineral suite for each of the nine Vertosols investigated 66

Table 2.16 The contribution of various secondary phyllosilicates to the coarse clay fraction (2–0.2 μm) 68

Table 2.17 The contribution of various secondary phyllosilicates to the fine clay fraction (<0.2 μm 69

Table 2.18 Classification of the nine Vertosols using the Australian Soil Classification (Isbell 1996), Soil Taxonomy (ASSS 2003) and World Reference Base for soil resources (FAO 1998) 73

Table 2.19 Mean physico–chemical soil properties of surface samples (0.0–0.2 m) from five cotton–growing Vertosols of eastern Australia (adapted from Vervoort *et al.* 2003) 74

CHAPTER 3

Table 3.1 Field water (FW00*i*) sampled from irrigation sources for each cotton–field investigated 81

Table 3.2 Target attributes of each synthetic water solution, including those of de–ionised water (T102), and the actual attributes of each solution 82

Table 3.3 Physico–chemical properties of the irrigation furrow for each Vertosol investigated 85

Table 3.4 The <100 μm and the <2 μm fractions for all soils, disrupted using EOE–shaking in either FW00*i* or T102 87

Table 3.5 The <100 μm (dag kg^{-1}) fraction of all soils treated with four solutions of increasing salt concentration using EOE–disruption 89

Table 3.6 The <2 μm (dag kg^{-1}) fraction of all soils treated with four solutions of increasing salt concentration using EOE–disruption 90

Table 3.7 Correlation of $SI_{<100}$ and $SI_{<2}$ with selected physico–chemical properties of the nine Vertosols, determined for the three disruptive forces 98

Table 3.8 Correlation of $SI_{<100}$ and $SI_{<2}$ and selected physico–chemical properties of the nine Vertosols, determined for each treatment solution 99

Table 3.9 Comparing the values of $SI_{<20}$ for the nine furrow soils after spontaneous dispersion with the $SI_{<2}$ values obtained after spontaneous dispersion and after EOE–shaking 102

Table 3.10 Dispersion classes applied for the description of $SI_{<2}$ (EOE–disruption) for the nine irrigated Vertosols 102

CHAPTER 4

Table 4.1 Mean values of exchangeable Ca^{2+}, Mg^{2+}, Na^{+} and K^{+} and of ESP following each irrigation treatment (FW00*i*, T102 and T401–4) of the G001 soil columns 119

Table 4.2 Mean values of exchangeable Ca^{2+}, Mg^{2+}, Na^{+} and K^{+} and of ESP following each irrigation treatment (FW00*i*, T102 and T401–4) of the G002 soil columns 120

Table 4.3 Mean values of exchangeable Ca^{2+}, Mg^{2+}, Na^{+} and K^{+} and of ESP following each irrigation treatment (FW00*i*, T102 and T401–4) of the H001 soil columns 121

Table 4.4 Mean values of exchangeable Ca^{2+}, Mg^{2+}, Na^{+} and K^{+} and of ESP following each irrigation treatment (FW00*i*, T102 and T401–4) of the H002 soil columns 122

Table 4.5 Mean values of exchangeable Ca^{2+}, Mg^{2+}, Na^{+} and K^{+} and of ESP following each irrigation treatment (FW00*i*, T102 and T401–4) of the N001 soil columns 123

Table 4.6 Mean values of exchangeable Ca^{2+}, Mg^{2+}, Na^{+} and K^{+} and of ESP following each irrigation treatment (FW00*i*, T102 and T401–4) of the N002 soil columns 124

Table 4.7 Mean values of EC, SAR and Dispersed clay following the completion of each irrigation treatment (FW00*i*, T102 and T401–4) of the G001 soil columns 127

Table 4.8 Mean values of EC, SAR and Dispersed clay following the completion of each irrigation treatment (FW00*i*, T102 and T401–4) of the G002 soil columns 128

Table 4.9 Mean values of EC, SAR and Dispersed clay following the completion of each irrigation treatment (FW00*i*, T102 and T401–4) of the H001 soil columns 129

Table 4.10 Mean values of EC, SAR and Dispersed clay following the completion of each irrigation treatment (FW00*i*, T102 and T401–4) of the H002 soil columns 130

Table 4.11 Mean values of EC, SAR and Dispersed clay following the completion of each irrigation treatment (FW00*i*, T102 and T401–4) of the N001 soil columns 131

Table 4.12 Mean values of EC, SAR and Dispersed clay following the completion of each irrigation treatment (FW00*i*, T102 and T401–4) of the N002 soil columns 132

Table 4.13 Correlation values comparing the $SI_{<2}$ (%) of dispersed clay with the measured soil properties determined from air–dry soil layers for all treatments of all soils and for each soil 133

CHAPTER 5

Table 5.1 Mean structural parameters derived using image analysis for soils B001 and B003 (50–90 mm) after laboratory irrigation 159

Table 5.2 Mean structural parameters derived using image analysis for soils G001 and G002 (50–90 mm) after laboratory irrigation 160

Table 5.3 Mean structural parameters derived using image analysis for soils H001 and H002 (50–90 mm) after laboratory irrigation 161

Table 5.4 Mean structural parameters derived using image analysis for soils N001 and N002 (50–90 mm) after laboratory irrigation 162

Table 5.5 Mean structural parameters comparing the effects of treatment solution (T102 and T402) on the soils B001, B003, G00*i*, H00*i* and N00*i* 163

Table 5.6 Comparing the different structural parameters for the three B00*i* soils after irrigation using the field water treatment (FW001) 164

CHAPTER 6

Table 6.1 Parameter values for the van Genuchten Model of the treated soils and the associated RMSE values. The θ_s, θ_r, α and n values were used to derive the water capacity function for each treatment of each soil (G001 and H001) 183

CHAPTER 7

Table 7.1 Thresholds associated with the structural stability or structural instability of cotton–growing Vertosols (McKenzie 1998) 199

Table 7.2 Selected physico–chemical chemical attributes of the nine furrow soils described in chapter 3 200

CHAPTER 8

Table 8.1 A generalised summary of selected physico–chemical properties for the nine Vertosols 224

Table 8.2 A summary of the dispersion of the nine Vertosols 225

LIST OF FIGURES

CHAPTER 1

Figure 1.1 The distribution of Australian Vertosols (Isbell et al. 1997) 2

Figure 1.2 The 'ideal' structural condition of a Vertosol used in cotton production (McKenzie 1998) 5

Figure 1.3 The morphological changes associated with the development of the structural form of Vertosols (Dudal and Eswaran 1988) 9

Figure 1.4 The churning or pedoturbation model describing the development of uniform structures in Vertosols (Wilding and Tessier 1988) 12

Figure 1.5 The schematic representation of the microstructure of Na^{+}–smectites (A) and Ca^{2+}–smectites (B) at near saturation (-0.032×10^{5} Pa) and prepared in low electrolyte concentrations (10^{-3} M) (Wilding and Tessier 1988) 16

Figure 1.6 Schematic representation of relative swelling and consolidation volumes of different clay minerals as a function of matric potential (e = void ratio – volume of pore space to solid particle volume) (Wilding and Tessier 1988) 18

Figure 1.7 Schematic distribution of charges in the diffuse electrical double layer surrounding clay particles according to the Gouy-Chapman model (adapted from van Olphen 1963) 20

Figure 1.8 The distribution of Vertosols (Isbell 1996), *(a)*, and the distribution of sodic and saline soils in NSW including various intergrades of sodic–saline soils according to Northcote and Skene 1972 (from McKenzie *et al.* 1995), *(b)* 23

Figure 1.9 The relationship between exchangeable Na^{+} and dispersible clay for two Australian Vertosols; Waco (●), Langlands (▽) (from Sumner 1993) 24

Figure 1.10 Comparison of particle arrangements in a homeoionic Na–smectite (right) with that in a Ca–Na system (left) illustrating the formation of 'tactoids or Quasi-crystals' with 'de–mixing' of Na^{+} and Ca^{2+} (Sumner 1993) 25

Figure 1.11 The general relationship of dispersion and coagulation for kaolin, illite and smectite as affected by SAR and TCC (from Field 2000) 29

Figure 1.12 A model describing the stability of clay in red–brown earths (Rengasamy *et al.* 1984) 41

CHAPTER 2

Figure 2.1 Cotton–producing regions of eastern Australia, including the nine soil sampling locations; three cotton–fields from Bourke (●) and two cotton–fields each from Hillston (●), Moree (●) and Narrabri (●) 46

Figure 2.2 Cotton fields B001 *(a)* and B003 *(b)*. These were sampled from the Bourke cotton–growing area 48

Figure 2.3 Cotton fields G001 *(a)* and G002 *(b)*. These were sampled from the lower Gwydir cotton–growing area 50

Figure 2.4 Cotton field H001 sampled from the Hillston cotton–growing area 51

Figure 2.5 Cotton field N001 sampled from the lower Namoi cotton–growing area 53

Figure 2.6 The suite of primary soil minerals from site G001 at depths of 0.2–0.4 and 1.0–1.2m 66

Figure 2.7 The suite of primary soil minerals from site H001 at depths of 0.2–0.4 and 1.0–1.2m 67

Figure 2.8 The secondary suite of soil minerals of the fine clay (▬) and the coarse clay (▬) fractions of site G001 at depths of 0.2–0.4 and 1.0–1.2m and using 2 M KCl to treat samples 70

Figure 2.9 The secondary suite of soil minerals of the fine clay (▬) and the coarse clay (▬) fractions of site G001 at depths of 0.2–0.4 and 1.0–1.2m and using 2 M $MgCl_2$ to treat samples 70

Figure 2.10 The secondary suite of soil minerals of the fine clay (▬) and the coarse clay (▬) fractions of site H001 at depths of 0.2–0.4 and 1.0–1.2m and using 2 M KCl to treat samples 71

Figure 2.11 The secondary suite of soil minerals of the fine clay (▬) and the coarse clay (▬) fractions of site H001 at depths of 0.2–0.4 and 1.0–1.2m and using 2 M $MgCl_2$ to treat samples 71

CHAPTER 3

Figure 3.1 $SI_{<100}$ and $SI_{<2}$ values for each soil after being treated in de–ionised water with each of the three disruptive forces; spontaneous dispersion (□), EOE–disruption (■) and ultrasonic agitation (■) 86

Figure 3.2 $SI_{<100}$ and $SI_{<2}$ values for all soils treated with solutions of de–ionised water (T102) (■) and field water (FW00*i*) (■) during EOE–disruption 88

Figure 3.3 $SI_{<100}$ values for all soils treated with four solutions of increasing salt concentration [T102 (■), T301 (■), T401 (■) and T501 (□)] using EOE–disruption 90

Figure 3.4 $SI_{<2}$ values for all soils treated with four solutions of increasing salt concentration [T102 (■), T301 (■), T401 (■) and T501 (□)] using EOE–disruption 91

Figure 3.5 The $SI_{<100}$ (%) and the $SI_{<2}$ (%) values of soil B001 (*a*), B002 (*b*) and B003 (*c*) using the treatment solutions T301–4 (◇), T401–4 (□) or T501–4 (○) and EOE–disruption 93

Figure 3.6 The $SI_{<100}$ (%) and the $SI_{<2}$ (%) values of soil G001 (*a*) and G002 (*b*) using treatment solutions T301–4 (◇), T401–4 (□) or T501–4 (○) and EOE–disruption 94

Figure 3.7 The $SI_{<100}$ (%) and the $SI_{<2}$ (%) values of soil H001 (*a*) and H002 (*b*) using treatment solutions T301–4 (◇), T401–4 (□) or T501–4 (○) and EOE–disruption 95

Figure 3.8 The $SI_{<100}$ (%) and the $SI_{<2}$ (%) values of soil N001 (*a*) and N002 (*b*) using treatment solutions T301–4 (◇), T401–4 (□) or T501–4 (○) and EOE–disruption 96

Figure 3.9 Comparing the change in the 2–100 μm fraction after end–over–end treatment of the nine Vertosols using solutions T102 (■) and FW00*i* (□) 105

Figure 3.10 Comparing the change in the 2–100 μm fraction after end–over–end treatment of the nine Vertosols using solutions T102 (■), T301 (■), T401 (■) and T501 (□) 106

Figure 3.11 Comparing the change in the 2–100 μm fraction determined after end–over–end treatment of the nine Vertosols using the solutions, *(a)*, T30*i*, *(b)*, T40*i*, and *(c)*, T50*i* each at increments of SAR 0 (■), SAR 7.5 (■), SAR 15 (■) and SAR 30 (□) 107

CHAPTER 4

Figure 4.1 Excavation of soil columns from an irrigation furrow of the N001 sampling site 112

Figure 4.2 The apparatus employed to irrigate soil cores in the laboratory 114

Figure 4.3 Comparison of the $SI_{<2}$ (%) values for all soils with the corresponding values of EC ($y=47.9x+11.8$, $R^2=0.13$) and SAR ($y=3.6x+9.9$, $R^2=0.34$) following each of the treatment solutions and for each soil layer analysed 134

Figure 4.4 Comparison of the $SI_{<2}$ (%) values for all soils with the corresponding values of exchangeable Na^+ ($y=4.7x+9.0$, $R^2=0.48$) and Ca^{2+}:Mg^{2+} ($y=5x+5.9$, $R^2=0.07$) following each of the treatment solutions and for each soil layer analysed 134

Figure 4.5 Comparison of the $SI_{<2}$ (%) values for all soils with the corresponding, *(a)*, values of ESP ($y=1.5x+10.1$, $R^2=0.27$), *(b)*, ESI ($y=19.5e^{-7.8x}$, $R^2=0.06$) and, *(c)*, $EC_{1:5}/Na^+_{exch.}$ ($y=0.6e^{44.3x}$, $R^2=0.14$) following each of the treatment solutions and for each soil layer analysed 135

CHAPTER 5

Figure 5.1 Horizontal image samples were collected at 10 mm increments in the 0–100 mm depth of soil columns and then at 20 mm increments in the 100–160 mm zone. In this Figure the horizontal images are given for one of the irrigated soil columns at sampling points of, *(a)*, 10 mm depth, *(b)*, 30 mm depth, *(c)*, 50 mm depth, *(d)*, 70 mm depth and, *(e)*, 90 mm depth 147

Figure 5.2 The treatment of G001 with each of the irrigation treatment solutions [FW00*i*, *(a)*, T102, *(b)*, T401, *(c)*, T402, *(d)*, T403, *(e)*, and T404, *(f)*]. These selected images were taken from the 50 mm depth increment of soil columns 149

Figure 5.3 The treatment of H001 with each of the irrigation treatment solutions [FW00*i*, *(a)*, T102, *(b)*, T401, *(c)*, T402, *(d)*, T403, *(e)*, and T404, *(f)*]. These selected images were taken from the 50 mm depth increment of soil columns 150

Figure 5.4 Response of selected structural parameters (P, S_v *and* l_p^*) of soil G001 to four treatments; T401 (▬), T402 (▬), T403 (▬) and T404 (▬) 152

Figure 5.5 Response of selected structural parameters (l_s^*, g_p *and* g_s) of soil G001 to four treatments; T401 (▬), T402 (▬), T403 (▬) and T404 (▬) 153

Figure 5.6 Response of selected structural parameters (P, S_v *and* l_p^*) of soil H001 to four treatments; T401 (▬), T402 (▬), T403 (▬) and T404 (▬) 154

Figure 5.7 Response of selected structural parameters (l_s^*, g_p *and* g_s) of soil H001 to four treatments; T401 (▬), T402 (▬), T403 (▬) and T404 (▬) 155

Figure 5.8 The distribution of the pore sieve diameter (s_p) for the 50–90 mm depth of the G001 soil. Comparisons are made between the irrigation treatments; *(a)*, for solutions of increasing SAR_w [T401 (▬), T402 (▬), T403 (▬) and T404 (▬)], *(b)*, for salinity treatments [T102 (▬) and T401] and, *(c)*, for field water and clean water [FW00*i* (▬) and T102 (▬)] 166

Figure 5.9 The distribution of the pore sieve diameter (s_p) for the 50–90 mm depth of the H001 soil. Comparisons are made between the irrigation treatments; *(a)*, for solutions of increasing SAR_w [T401 (—), T402 (—), T403 (—) and T404 (—)], *(b)*, for salinity treatments [T102 (—) and T401] and, *(c)*, for field water and clean water [FW00*i* (—) and T102 (—)]. 167

Figure 5.10 The distribution of the pore star shape (Ra_p^*) for the 50–90 mm depth of the G001 soil. Comparisons are made between the irrigation treatments; *(a)*, for solutions of increasing SAR_w [T401 (—), T402 (—), T403 (—) and T404 (—)], *(b)*, for salinity treatments [T102 (—) and T401] and, *(c)*, for field water and clean water [FW00*i* (—) and T102 (—)] 168

Figure 5.11 The distribution of the pore star shape (Ra_p^*) for the 50–90 mm depth of the H001 soil. Comparisons are made between the irrigation treatments; *(a)*, for solutions of increasing SAR_w [T401 (—), T402 (—), T403 (—) and T404 (—)], *(b)*, for salinity treatments [T102 (—) and T401] and, *(c)*, for field water and clean water [FW00*i* (—) and T102 (—)] 169

CHAPTER 6

Figure 6.1 The ku/pF apparatus. Individual soil cores were hung in each of the ten baskets. This apparatus determines changes in matric potential and soil weight as moisture evaporates from the surface of individual soil cores 179

Figure 6.2 The soil moisture characteristics of two differently structured soils (adapted from Hillel 1982) 181

Figure 6.3 Predicted water retention curves for the soils G001 and H001 for each of the laboratory irrigation treatments [*FW00i** (—), *T102** (—), *T401** (—), *T402** (—), *T403** (—) and *T404** (—)] 185

Figure 6.4 Predicted water retention curves, using a natural log scale, for the soils G001 and H001 for each of the laboratory irrigation treatments [*FW00i** (—), *T102** (—), *T401** (—), *T402** (—), *T403** (—) and *T404** (—)] 186

Figure 6.5 Water capacity as a function of matric potential and of effective pore radii for each of the laboratory irrigation treatments of G001 [*FW00i** (—), *T102** (—), *T401** (—), *T402** (—), *T403** (—) and *T404** (—)] 188

Figure 6.6 Water capacity as a function of matric potential and of effective pore radii for each of the laboratory irrigation treatments of H001 [*FW00i** (—), *T102** (—), *T401** (—), *T402** (—), *T403** (—) and *T404** (—)] 189

Figure 6.7 The contribution of each phase (solid, liquid and air) to soil volume for soils G001 *(a)* and H001 *(b)* 190

CHAPTER 7

Figure 7.1 The ASWAT dispersion classes (Field 2000). ASWAT scores (0–4) are determined at intervals of 10 minutes and 2 hrs by immersing air–dry soil aggregates, and then re–moulded soil, in de–ionised water. The result is an ASWAT score out of 16, where 0–1 represents negligible dispersion, 2–6 represents moderate dispersion and 7–16 represents serious dispersion 199

Figure 7.2 The $SI_{<2}$ values for the furrow soils related to, *(a)*, ESP (*y=0.9x+16.3* R^2*=0.12*), *(b)*, ESI ($y=23.3x^{0.1}$ $R^2=0.03$) and, *(c)*, $EC_{1:5}/Na^+_{exch}$ (*y=18.1x*$^{-0.1}$ R^2*=0.00*) and the $SI_{<2}$ values for the laboratory–irrigated soils according to, *(d)*, ESP (*y=1.5x+10.1*

R^2=0.27), (e), ESI ($y=11.1x^{-0.1}$ R^2=0.01) and, (f), $EC_{1:5}/Na^+_{exch}$ ($y=2.3x^{-0.4}$ R^2=0.11) 202

Figure 7.3 The $SI_{<2}$ values determined for the laboratory–irrigated soils as a function of ESI and of $EC_{1:5}/Na^+_{exch}$ 203

Figure 7.4 The Rengasamy classification scheme (Rengasamy *et al.* 1984); the nine Vertosols from chapter 3 have been added to estimate stability according to this classification scheme 204

Figure 7.5 The Rengasamy classification scheme (Rengasamy *et al.* 1984) is presented for the furrow soils according to, *(a)*, $SI_{<2}$ values [0–5 (○), 5–10 (□), 10–15 (△), 15–20 (●), 20–25 (■), 25–30 (●) and >30 (■) %] and, *(b)*, as a function of sampling region [B00*i* (▲),G00*i* (●), H00*i* (○), and N00*i* (●)] 205

Figure 7.6 The Rengasamy classification scheme (Rengasamy *et al.* 1984) showing all soil layers from the laboratory–irrigated Vertosols (chapter 4) 206

Figure 7.7 The Rengasamy classification scheme (Rengasamy *et al.* 1984) is presented for the soils irrigated in the laboratory according to, *(a)*, $SI_{<2}$ values for each soil [0–5 (○), 5–10 (□), 10–15 (△), 15–20 (●), 20–25 (■), 25–30 (●) and >30 (■) %] and, *(b)*, as a function of sampling region [B00*i* (▲),G00*i* (●), H00*i* (○), and N00*i* (●)] 206

Figure 7.8 The measured $SI_{<2}$ values for all soil samples as a function of the *Dispersion in water* (D_w) prediction ($y=x+0.03$, $R^2=0.65$ *and correlation*=0.81) 209

Figure 7.9 Values of $SI_{<2}$, at each of three different EC_w intervals of 0.2 *(a)*, 0.5 *(b)* and 2.7 *(c)* (dS m^{-1}), with increasing SAR_w [B001 (○), B002 (□), B003 (△), G001 (○), G002 (□), H001 (○), H002 (□), N001 (○) and N002 (□)] 210

Figure 7.10 The predicted *Dispersion under irrigation* (D_i) response surface fitted to all EC_w values between 0.0 and 3.0 (dS m^{-1}) and all SAR_w values between 0 and 30 ($mmol_{(+)}$ $L^{-1})^{1/2}$. The predicted average $SI_{<2}$ value for these Vertosols where EC_w and SAR_w are both equal to 0 is indicated by ○ 212

Figure 7.11 The actual values of $SI_{<2}$ obtained after the EOE–disruption of the G001 (○) soil in solutions of, *(a)*, EC 0.19, *(b)*, EC 0.47 and, *(c)*, EC 2.35 (dS m^{-1}) and of the H001 (○) soil in solutions of, *(d)*, EC 0.19, *(e)*, EC 0.47 and, *(f)*, EC 2.35 (dS m^{-1}). For each of the soils the D_iV [G001 (▬) and H001 (▬)] and D_i (▬) are given 214

Figure 7.12 The predictive model, describing the structural stability of the nine different Vertosols in solutions of different EC_w and SAR_w. In this model the dispersion class limits occur at D_iV values of 10 (■), 15 (■), 20 (■) and 30 (■) %. The impact of water quality on the stability of different Vertosols is described by D_iV, where the D_w function gives the predicted value of $SI_{<2\ (T102)}$. The regions of 'No water use restrictions' and 'Some water use restriction for agriculture' represent the degree of restrictions applied by the FAO on irrigation supplies according to crop water availability (Ayers and Westcot 1985) 216

Figure 7.13 A predictive model for describing the structural stability of the nine different Vertosols in solutions of different EC_w and SAR_w. In this model the dispersion class limits occur at D_iV values of 10 (■), 15 (■), 20 (■) and 30 (■) %. The impact of water quality on the stability of different Vertosols is described by D_iV, where the D_w function gives the predicted value of $SI_{<2\ (T102)}$. The cross section slices (*(i)*, *(ii)* and *(iii)*) represent the irrigation water EC_w intervals used during the treatment of each of the nine Vertosols using the different T30*i*, T40*i* and T50*i* solutions 217

Figure 7.14 Predicted D_iV for the soils, *(a)*, B001, *(b)*, B002, and *(c)*, B003. For each soil, the three slices *(i)*, *(ii)* and *(iii)* represent predicted mechanically dispersed clay after

EOE–disruption using solutions of EC_w 0.19 (—), 0.47 (—) and 2.35 (—) dSm^{-1}, between the SAR_w values of 0 and 30. The dispersion class thresholds are given where D_iV equals 10 (—), 15 (—), 20 (—) and 30 (—) %. The actual values of $SI_{<2}$ are given according to the EC_w of the treatment solutions applied; EC 0.19 (◇), 0.47 (□) and 2.35 (○) dS m^{-1} 218

Figure 7.15 Predicted D_iV for the soils, *(a)*, G001, and *(b)*, G002. For each soil, the three slices *(i)*, *(ii)* and *(iii)* represent predicted mechanically dispersed clay after EOE–disruption using solutions of EC_w 0.19 (—), 0.47 (—) and 2.35 (—) dSm^{-1}, between the SAR_w values of 0 and 30. The dispersion class thresholds are given where D_iV equals 10 (—), 15 (—), 20 (—) and 30 (—) %. The actual values of $SI_{<2}$ are given according to the EC_w of the treatment solutions applied; EC 0.19 (◇), 0.47 (□) and 2.35 (○) dS m^{-1} 219

Figure 7.16 Predicted D_iV for the soils, *(a)*, H001, and *(b)*, H002. For each soil, the three slices *(i)*, *(ii)* and *(iii)* represent predicted mechanically dispersed clay after EOE–disruption using solutions of EC_w 0.19 (—), 0.47 (—) and 2.35 (—) dSm^{-1}, between the SAR_w values of 0 and 30. The dispersion class thresholds are given where D_iV equals 10 (—), 15 (—), 20 (—) and 30 (—) %. The actual values of $SI_{<2}$ are given according to the EC_w of the treatment solutions applied; EC 0.19 (◇), 0.47 (□) and 2.35 (○) dS m^{-1} 219

Figure 7.17 Predicted D_iV for the soils, *(a)*, N001, and *(b)*, N002. For each soil, the three slices *(i)*, *(ii)* and *(iii)* represent the predicted increments of mechanically dispersed clay after EOE–disruption using solutions of EC_w 0.19 (—), 0.47 (—) and 2.35 (—) dSm^{-1}, between the SAR_w values of 0 and 30. The dispersion class thresholds are given where D_iV equals 10 (—), 15 (—), 20 (—) and 30 (—) %. The actual values of $SI_{<2}$ are given according to the EC_w of the treatment solutions applied; EC 0.19 (◇), 0.47 (□) and 2.35 (○) dS m^{-1} 220

GLOSSARY, SYMBOLS AND ABBREVIATIONS

GLOSSARY

Aggregate – natural unit of soil that encompasses groupings of clusters, microaggregates and macroaggregates

Clusters – cohesion of clay particles, quasi–crystals, domains and assemblages responsible for the formation of the next higher level of aggregation

De–mixing – segregation of cations (*i.e.* Ca^{2+} and Na^{+}) between the interlayer spaces and external surfaces of clay minerals

Dispersion – the liberation of discrete soil particles after the immersion of soil aggregates in water, which forms a stable suspension of clay particles in suspension

Flocculation – the dominance of net attractive forces over repulsive forces enabling clay particles to remain close together in solution

Irrigation furrow – non–wheeled furrow between two adjacent cotton beds down which water flows during irrigation events.

Macroaggregate – unit of soil greater than 250 μm in size which consists of enmeshed microaggregates

Microaggregate – unit of soil less than 250 μm in size which consists of sand, silt and clusters of clay

Rengasamy classification scheme – Classification scheme for dispersive behaviour in red–brown earths (Rengasamy *et al.* 1984)

Structural Form – the heterogeneous arrangement of solid and void space existing in a soil at a given time (t_i); it refers to the total porosity, pore size distribution and the continuity of the pore system

Structural Stability – the resistance of soil structural form to change, where stress is applied; it is characterised for different types of stress and at different scales of structural form

Structural resilience – describes the ability of a soil to recover its structural form through natural processes when external disruptive forces are reduced or removed

Slaking – the explosive breakdown of aggregates after immersion in water; this does not include the liberation of discrete clay particles to solution (*see* Dispersion)

Sodicity – Soil containing excessive exchangeable Na^{+}; in Vertosols used for cotton production an ESP_{crit} of 5 delineates the sodic from the non–sodic soils

Structural porosity – All pore space with a radius greater then 15 μm (Quirk 1994)

SYMBOLS

Treatment solutions:–

FW00*i*	Field water solutions, collected for each of the soils investigated
T102	EC_w 0 (dS m^{-1}) and SAR_w 0 $(mmol_{(+)}\ L^{-1})^{1/2}$
T30*i*	EC_w 0.2 (dS m^{-1}) and SAR_w 0, 7.5, 15 or 30 $(mmol_{(+)}\ L^{-1})^{1/2}$ (T301–4)
T40*i*	EC_w 0.5 (dS m^{-1}) and SAR_w 0, 7.5, 15 or 30 $(mmol_{(+)}\ L^{-1})^{1/2}$ (T401–4)
T50*i*	EC_w 2.7 (dS m^{-1}) and SAR_w 0, 7.5, 15 or 30 $(mmol_{(+)}\ L^{-1})^{1/2}$ (T501–4)

Image analysis:–

P	Porosity ($mm^3\ mm^{-3}$)
S_v	Surface area ($mm^2\ mm^{-3}$)
l_p^* and l_s^*	Pore and Solid star lengths (mm)
g_p	Pore connectivity ($\times 10^{-2}\ mm^2$)
g_s	Solid connectivity ($\times 10^{-2}\ mm^2$)

ABBREVIATIONS

ASC	Australian Soil Classification
ASWAT	Aggregate Stability in WATer test
Ca^{2+}_{exch}	Exchangeable Calcium ($cmol_{(+)}\ kg^{-1}$)
CEC_{eff}	effective Cation Exchange Capacity (the sum of Ca^{2+}_{exch}, Mg^{2+}_{exch}, K^{+}_{exch} and Na^{+}_{exch}) ($cmol_{(+)}\ kg^{-1}$)
$C_w(h)$	Soil water capacity
D_i	*Dispersion under irrigation* function (%)
D_iV	*Dispersion of irrigated Vertosols* function (%)
D_w	*Dispersion in water* function (%)
EC or $EC_{1:5}$	Electrical Conductivity of the soil solution, determined using a 1:5 soil:water ratio (dS m^{-1})
EC_w	Electrical Conductivity of a water solution (dS m^{-1})
EOE	End–Over–End method of mechanical disruption
ESI	Electrochemical Stability Index ($EC_{1:5}$ dS m^{-1}/ESP)
ESP	Exchangeable Sodium Percentage ($Na^+/CEC_{eff}\times 100$)

K^+_{exch}	Exchangeable Potassium ($cmol_{(+)}\ kg^{-1}$)
Mg^{2+}_{exch}	Exchangeable Magnesium ($cmol_{(+)}\ kg^{-1}$)
Na^+_{exch}	Exchangeable Sodium ($cmol_{(+)}\ kg^{-1}$)
OC	Organic Carbon content (%)
PSD	Particle Size Distribution ($dag\ kg^{-1}$)
SAR	Sodium Adsorption Ratio of a soil solution $(Na^+/[(Ca^{2+}+Mg^{2+})/2]^{1/2})$ $(mmol_{(+)}\ L^{-1})^{1/2}$
SAR_w	Sodium Adsorption Ratio of a water solution $(Na^+/[(Ca^{2+}+Mg^{2+})/2]^{1/2})$ $(mmol_{(+)}\ L^{-1})^{1/2}$
$SI_{<100}$	Stability index describing the percentage of particles of <100 μm liberated after the imposition of disruptive force
$SI_{<2\ (T102)}$	Stability index describing the percentage of particles of <2 μm liberated after the imposition of EOE–disruption using clean water (solution T102)
$SI_{<2}$	Stability index describing the percentage of particles of <2 μm liberated after the imposition of disruptive force
$SI_{<20}$	Stability index describing the percentage of particles of <20 μm liberated after the imposition of disruptive force
TCC	Total Cation Concentration (Sum[Ca^{2+}, Mg^{2+}, Na^+ and K^+]) ($mmol_{(+)}\ L^{-1}$)
WRB	World Reference Base for soil resources
XRD	X–ray diffraction

GENERAL INTRODUCTION AND AIMS

0.1 Introduction

Irrigation water supplies of good quality (*i.e.* low electrolyte concentration and small contributions of Na^+) are becoming increasingly sought after for agricultural production in Australia. In addition, there exists a strong requirement that a portion of current water resources should be retained for environmental purposes (*e.g.* riverine ecosystems). However, recent dry periods have highlighted the pressures placed on Australia's current water resources and have led to reduced water allocations for irrigated agriculture. This is likely to be an ongoing issue for irrigated cotton–producers and will potentially lead to the use of moderate or poor quality irrigation supplies, containing elevated electrolyte concentrations and/or large Na^+ contributions, to supplement good quality water allocations. In addition to increasing the risk of salt cycling through the topsoil, such a practice is likely to impact immediately on the structural behaviour of soil. This in turn, will impact on soil hydraulic properties and alter the water use efficiency of crops.

In Australia, irrigated cotton (*Gossypium hirsutum*) is produced using highly fertile heavy clay soils, or Vertosols (Isbell 1996). However, soils of this type are widely regarded as having large exchangeable Na^+ contributions, either in subsoil layers or throughout the soil profile. Vertosols that contain large levels of exchangeable Na^+ are described as sodic. Sodic soils are defined in the cotton industry as soils that contain greater than 5 % exchangeable sodium (McKenzie 1998); these soils swell excessively and are often dispersive. Consequently, sodic Vertosols are potentially unstable and this instability can lead to a loss of aggregation and porosity, and reduced hydraulic conductivity. In addition, fine–textured Vertosols are known to be extremely unstable even at ESPs less than 5 (*e.g.* Cook *et al.* 1992). This occurs because the extent of clay dispersion is influenced by a myriad of soil physico–chemical properties in addition to the ESP (*e.g.* the electrolyte concentration and the clay phyllosilicate suite). Therefore, the use of a critical ESP of 5 in Vertosols to describe sodicity, and to infer structural instability, is not always correct. Furthermore, crop yields may be maintained in sodic soils if these sodic layers are deep within the profile, or if dispersion is avoided by managing the application of irrigation waters to reduce the risk of dispersion *i.e.* applying irrigation solutions with large electrolyte concentrations (*e.g.* 1 dS m^{-1}). Consequently, the behaviour of sodic soils when subjected to poor quality water may not be much different to that displayed when good quality water is applied during irrigation. This behaviour results from many interactions between soil physico–chemical attributes and irrigation water properties. For example, clean water has a small ionic

strength and in sodic soils, promotes the swelling of clay minerals. This occurs because the ionic strength of solution is insufficient to suppress the expansion of clay minerals where excessive amounts of exchangeable Na^+ are present and these soils will be unstable. In contrast, solutions of larger ionic strength will suppress clay swelling and limit dispersion. Therefore, the challenge is to assess the impact of differing water quality solutions on the structural condition of these soils. During the last 20 years, much research into the impact of sodicity on soil structural stability in Australia has referred to the data presented by Rengasamy *et al.* (1984), which describes the dispersive behaviour of red–brown earth profiles with varying soil solution concentrations and varying soil solution Na^+ contents (SAR). In their research, Rengasamy *et al.* (1984) included only red–brown earths and did not include any heavy clay soils (Vertosols). They excluded Vertosols because they recognised differences in the structural behaviour of these soils, and they associated these differences with different clay mineral suites. However, since their work a similar prediction has not been formulated to describe the dispersive behaviour of Vertosols and current predictors of structural stability are incomplete. Consequently, the need for a suitable predictor of stability in Vertosols is widely recognised (*e.g.* Surapaneni *et al.* 2002).

0.2 Aims

In order to characterise the structural stability and form of sodic Vertosols used for irrigated cotton production in New South Wales, there were four principal aims. These aims are defined as:

Aim 1 ~ To characterise the structural stability of different cotton–growing Vertosols – to comprehensively investigate the structural stability of a range of different cotton–producing soils. This will provide an understanding of the impact of different soil physico–chemical properties on aggregate breakdown and clay dispersion where different disruptive forces and different water quality solutions are introduced.

Aim 2 ~ To characterise the impact of irrigation water quality on soil chemical attributes and structural stability – to determine the impact of irrigation water quality on selected properties of different structurally–intact Vertosols. This will demonstrate the impact of irrigation water quality on exchangeable cation contributions, the soil solution and the structural stability of different Vertosols.

Aim 3 ~ To characterise the impact of irrigation water quality on soil structural form and water retention properties – to determine the impact of irrigation water quality on the structural form and water retention properties of selected structurally–intact field soils. In so doing, changes in the volume fractions of solid, pore and solution phases will be identified. This assessment will assist in determining the extent of change in the soil structural arrangement of different Vertosols, where solutions of different electrolyte concentration and different Na^+ contributions were used to irrigate intact soils.

Aim 4 ~ To develop a descriptive model of structural stability – using the soil structural stability assessments a descriptive model of stability will be developed. This model will consider the physico–chemical properties that influence the stability of different Vertosols and will provide a prediction of stability based on the impact of different irrigation solution parameters. A model of this kind will characterise the potential dispersion of Vertosols where these soils are subjected to alternative irrigation waters containing different electrolyte concentrations and/or Na^+ contributions.

Chapter 1

FACTORS INFLUENCING THE STRUCTURAL CONDITION OF VERTOSOLS

FACTORS INFLUENCING THE STRUCTURAL CONDITION OF VERTOSOLS

~

Vertic: *vertere (L): to turn or invert; to turn into, change.*

~

1.1 Vertosols in Australia

The term Vertosol is applied to Australian soils that exhibit vertic properties, including shrinkage during drying and swelling during wetting. These soils are strongly structured and frequently develop a surface mulch of aggregates. Vertosols sustain a high level of production due to their inherent chemical fertility and have a recognised ability for retaining large quantities of moisture. As a result, these soils are utilized widely for irrigated (*e.g.* cotton, sugar cane and rice) and dryland agriculture (*e.g.* wheat and grazing). However, their fine texture and their ability to swell during wetting make Vertosols highly susceptible to aggregate disintegration and clay dispersion. This leads to reduced porosity and reductions in hydraulic conductivity. The degradation observed is influenced by the presence of excessive exchangeable Na^+, and Vertosols that have a small electrical conductivity and a low calcium–magnesium ratio can exhibit dispersive behaviour at exchangeable sodium percentages as low as 2 (McKenzie 1998).

1.1.1 Definition

The properties of vertic soils have been recognised for many years (*e.g.* Kossovitch 1912; Del Villar 1944; FAO 1998) and their unique characteristics have been classified using a number of descriptive terms; as *Dark Clay Soils* (Oakes and Thorp 1950; Dudal 1963, 1965), as *Black Earths* and *Grey, Brown and Red Clays* (Stace *et al.* 1968) and as *Vertisols* (Soil Survey Staff 1998; FAO 1998). The Australian Soil Classification (ASC) defines *Vertosols* as uniform soils with a clay contribution in excess of 35 %; as they dry these soils shrink and are characterised by extensive cracking. Vertosols frequently develop a 'self–mulching' or 'crusty' surface horizon and as soil depth increases they become strongly pedal, including an arrangement of lenticular peds and/or slickensides at some depth in the solum (Isbell 1996).

1.1.2 Distribution of Vertosols

The global distribution of Vertosols has been estimated by several authors. Most recently, Coulombe *et al.* (1996b) estimated that Vertosols cover a global land area of 308 M ha, or 2.2 % of surface soils. However, this estimate does not account for current differences between the soil classification schemes and utilizes the incomplete inventories of national soil survey resources.

In Australia, Vertosols account for 88 M ha (Isbell *et al.* 1997) or 11.5 % of all surface soils (Figure 1.1). They occur primarily throughout New South Wales, Queensland and the Northern Territory. These Vertosols occupy regions of tropical, subtropical and warm–temperate climates (Probert *et al.* 1987; Isbell 1989) and are generally found on the wide floodplains of inland water ways where altitude is less than 500 m (Isbell *et al.* 1997).

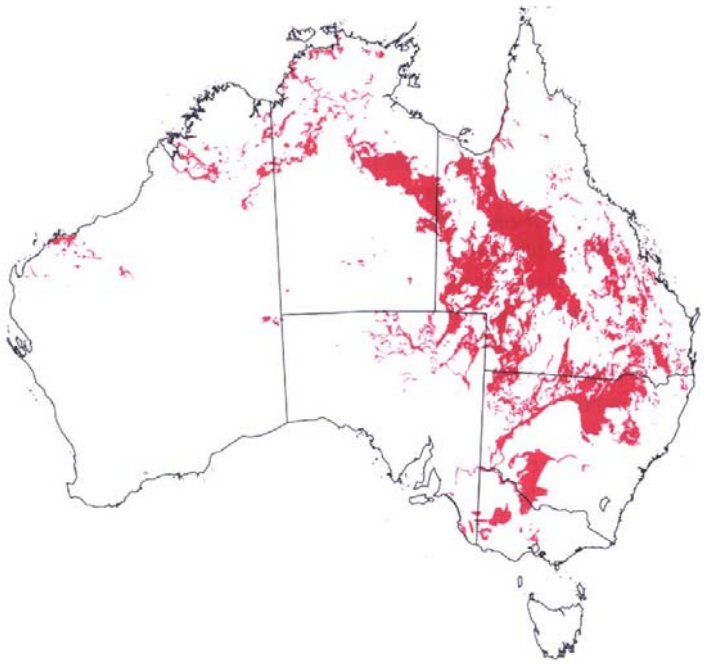

Figure 1.1 The distribution of Australian Vertosols (Isbell *et al.* 1997)

1.1.3 Genesis

Australian Vertosols are derived from a variety of parent materials deposited as alluvium and less frequently as aeolian sediments. Parent rocks include sedimentary materials such as shale, mudstone and impure limestone, and basic igneous materials, particularly basalt (Isbell *et al.* 1997). Irrespective of the depositional environment, these soils form as a direct consequence of the weathering of materials abundant in ferromagnesian minerals and which contain large concentrations of basic ions (Coulombe *et al.* 1996a). This provides Vertosols with their large clay content, which is often

dominated by 2:1 expanding lattice minerals of extensive surface area and considerable base saturation, particularly the smectite clays, *e.g.* montmorillonite.

In regions where Vertosols are found, the climatic regime will invariably control the rate of clay mineral decomposition and the rate of profile development (Jewitt *et al.* 1979). The Vertosols of Australia occur across a wide array of soil temperature regimes, ranging from thermic in the south to hyperthermic throughout the greater part of tropical Australia (Isbell *et al.* 1997). These soils are subject to seasonal wetting, but as a consequence of their prominence in arid and semi–arid environments the formation and longevity of 2:1 expanding phyllosilicate clays is favoured. This provides the opportunity for the development of lenticular peds and/or slickensides (Mermut *et al.* 1996).

In terms of colour class, the Black Vertosols are generally derived from basalt and are usually dominated by the smectites. Some of the Grey, Brown and Red Vertosols are also dominated by smectites, but in contrast many contain large proportions of illite and kaolinite minerals, with some containing only a subdominant contribution of smectitic clays (Isbell 1989). This reduces the degree of swelling and shrinkage during wet–dry cycles, thereby reducing the extent of expression of the characteristic structural features (Norrish and Pickering 1977) that are prerequisites for this soil class.

1.1.4 General soil properties

The general properties of Australian Vertosols have been described in depth by Isbell (1989). These soils exhibit uniform texture profiles with clay contents ranging from 40–80 % (*e.g.* Stace *et al.* 1968), and clear colour changes in the upper metre are uncommon. The colour classification ranges from red in the more arid and semi–arid regions, to brown, grey and black. However, colour class does not necessarily relate to rainfall or to organic matter content and reflects other soil characteristics such as the mineral suite. Vertosols are characterised by their structural form; they have medium to coarse blocky or polyhedral peds which occur below various surface structural arrangements *e.g.* a surface–mulch of soil aggregates. At depth, typically beyond 0.3–0.5 m, the structural form is characterised by moderate, medium or coarse lenticular peds containing prominent shear planes and/or slickensides. These features extend to the full depth of the solum. The surface behaviour (water infiltration and aggregate development) of Vertosols commonly results in the formation of a layer of 'mulched' aggregates or, less frequently, in the development of a 'massive' layer (Hubble 1984). Such characteristics are dependent on the clay content, the mineral suite and the interaction of other physico–chemical properties; specifically, the association of exchangeable and solution cations with the mineral suite (Blokhuis 1982). These soils have a relatively large water–holding

capacity at all potentials; for example, 35–75 % moisture at -0.33 MPa and 15–35 % moisture at -1.5 MPa (Coulombe *et al.* 1996b). This is attributed to the fine texture of these soils and the predominance of montmorillonite in the mineral suite (Ahmad 1983). Due to the climatic regimes in which Vertosols develop, they frequently contain inclusions of calcium carbonate ($CaCO_3$) in the form of discrete nodules or diffuse soft masses. In addition, variable amounts of gypsum are almost ubiquitous in the more arid Vertosols (Isbell 1989; Ahmad 1996). The contributions of organic carbon and nitrogen vary considerably, *e.g.* Isbell (1989) quotes organic carbon contents of 2.2 % for Black Vertosols and 0.8 % for Grey, Brown and Red Vertosols. There are three pH trends in these soils; the alkaline soils (pH >6.5 at the surface), the alkaline/acid soils (pH >6.5 at the surface but strongly acid at depth) and the acid soils (pH <6.5 at the surface) (Isbell 1989).

In Vertosols that do not contain large amounts of gypsum or carbonates, sodium chloride frequently dominates soluble salts (40–80 %) (Isbell 1989; Ahmad 1996). The cation exchange capacity (CEC) and exchangeable cation concentrations vary considerably. This depends on the clay mineral suite, the quantity of clay and the base status of parent materials. Generally, the CEC ranges from 10–80 $cmol_{(+)}\ kg^{-1}$ (Murthy *et al.* 1984; Isbell 1989; Coulombe *et al.* 1996a; Singh and Heffernan 2002) and is usually dominated by calcium (Ca^{2+}) in the upper horizons. In most Vertosols the exchangeable Ca^{2+}:Mg^{2+} ratio may range between 3:1 and 1:1 (Blokhuis 1982) and occasionally exchangeable Mg^{2+} dominates, particularly at depth (Hubble 1984). A large proportion of Vertosols are classed as sodic with an Exchangeable Sodium Percentages (ESP) ($[Na^{+}_{exch}/CEC]\times100$) of >6 and large ESPs (>30) are not infrequent in the subsoil horizons of these soils (Jewitt *et al.* 1979; Ahmad 1996).

1.1.5 Current landuse practices and their potential impact on Vertosol structure

The availability of rainfall and/or irrigation water dictates current landuse practices. In many arid and semi–arid environments, Vertosols are widely utilized for native pastures in livestock production (Isbell 1989). In regions where rainfall is suitable (300–800 mm), dryland agriculture increases in prominence (Isbell 1989). Here winter crops (*e.g.* wheat or legumes) and summer crops (*e.g.* sorghum or soybeans) are grown, taking advantage of stored moisture and inherent soil fertility. In situations where water of good quality is available, *e.g.* low salinity (EC <1 dS m^{-1}) and a small Na^{+} content, extensive irrigation is practised, particularly for the production of cotton (Singh and Heffernan 2002).

The cotton industry depends on the availability of good quality water supplies, but like other cultivated and/or irrigated activities, cotton production places a high demand on the soil environment. Irrigated cotton production often requires potentially damaging soil operations,

including field levelling and cut–and–fill activities (NSW Agriculture 1995). In addition, the crop requires large quantities of water but is sensitive to waterlogging and large soil strength (NSW Agriculture 1995). These soils need to have good porosity to promote adequate water infiltration and internal drainage (McKenzie 1998). These attributes are demonstrated in Figure 1.2, which gives the 'ideal' structural condition of a cotton–producing Vertosol.

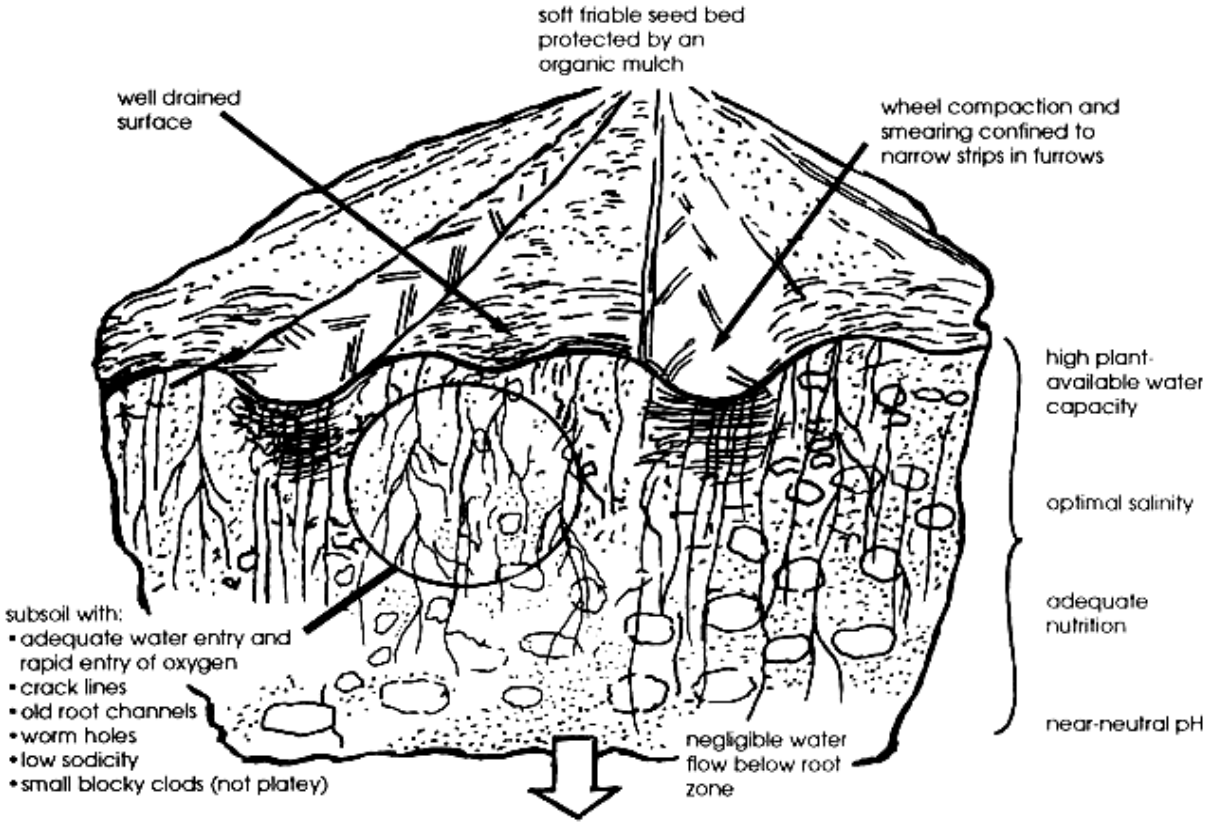

Figure 1.2 The 'ideal' structural condition of a Vertosol used in cotton production (McKenzie 1998).

The introduction of certain cropping practices, *e.g.* tillage of or traffic across wet soil, have been shown to cause substantial damage to soil structural condition (*i.e.* compaction), with associated losses in crop production (Daniells 1989). This occurs primarily as a result of reduced porosity and increased bulk density, which restricts water movement and internal drainage (Dalal 1989; Daniells 1989). Damage to soil structural condition can also lead to a substantial decrease in organic matter contributions and an increase in the pH and ESP of these soils (Dalal and Mayer 1986a, 1986b; McKenzie *et al.* 1991). In addition, McKenzie *et al.* (1991) identified reductions in soil solution electrical conductivity (EC) where Vertosols were irrigated, suggesting that the leaching of salts from the profile was occurring. This becomes an issue primarily because of the suppressive effect of soluble salts on the dispersive influence of exchangeable Na^+. Complicating this problem is the prospect of increased use of irrigation water containing elevated levels of Na^+ (Halliwell *et al.* 2001; Oster and Shainberg 2001). This has been brought about by the reduced availability of suitable

irrigation waters. The increasing and continued use of Na^+–rich irrigation water is likely to result in the ESP of some Vertosols being increased. This will have repercussions on the structural stability of these soils and affect the shrink–swell process, aggregate liberation and clay dispersion.

1.2 The integrity of soil structure: definitions applicable to Vertosols

Maintaining soil structural integrity is paramount for achieving sustainable agricultural production (McGarry 1993; Horn *et al.* 1994; Amézketa 1999), particularly as degradation of the structure results in reductions in moisture availability, root penetration and gas transport. Soil structure is defined in terms of *structural form*, *structural stability* and *structural resilience* (Kay 1990).

1.2.1 Soil structural form

The group of characteristics explaining the arrangement of soil solid and pore space is described by *soil structural form* (*e.g.* Nikiforoff 1941; Thomasson 1978; Black 1986; Brewer and Sleeman 1988; Kay 1990; Kay *et al.* 1994; Miller and Donahue 1995; McGarry 1996; SSSA 1997). Frequently, however, definitions have not adequately accounted for the properties of vertic soils, and most current descriptions reflect individual areas of research. In this work the definition applied by Field (2000) is used. The *structural form* of Vertosols is described by the heterogeneous arrangement of solid and void space existing in a soil at a given time (t_i); it refers to the total porosity, pore size distribution and the continuity of the pore system. It considers the arrangement of primary particles into hierarchical structural states that are identified on the basis of failure zones and which are bound by regions of differing strength.

The structural form of Vertosols is dependent on soil physico–chemical properties, landuse and climatic conditions. Consequently, a number of descriptions have been applied and a generalised view of the structural form of Vertosols is widely understood (*e.g.* Blokhuis 1982; Hubble 1984; Dudal and Eswaran 1988; McGarry 1996). This was summarised by Dudal and Eswaran (1988). They divided a typical Vertosol profile into five distinct zones of pedogenic development. These are:

Zone 1. 0–0.25 m, or to the depth of tillage: This zone is subject to cracking and the formation of large aggregates with prism lengths <0.3 m in size. Aggregates are hard to very hard when dry. These prismatic units can break giving secondary aggregates that are coarse and angular blocky. In *zone 1*, soil structural form is most complex and the development processes are more rapid than at greater depth (Warkentin 1982). This is the result of

more complete drying and more rapid wetting. Subsequently, a 'surface mulch' frequently develops. In soils where less desirable physico–chemical conditions occur, a pale laminated seal of dispersed clay or a massive layer (Hubble 1984) is often evident.

Zone 2. Beneath *zone 1* a layer of 0.1–0.3 m thickness occurs. The aggregates of this zone are hard to very hard, coarse and angular blocky. They develop as the profile dries and in some cases discernable prisms are evident.

Zone 3. Beneath *zone 2*, lies a zone with a thickness of <0.1 to >1.0 m. In this zone structural units form wedge–shaped peds ('lenticular' or 'parallela' peds) of 50–100 mm length. These ped structures have long axes tilted 10–60 ° from the horizontal and have ped faces that are smooth or striated. In soils where these striated faces are observed, strias generally occur in lines sub–parallel to the long axis.

Zone 4. This is the zone of slickensides (0.25–1.0 m thick): the term 'slickensides' refers to a surface having a polished and shiny appearance, and which may be striated or grooved. Slickensides form the faces of lenticular peds, described in *zone 3*. This zone is differentiated by an increased size of peds (600–2000 cm^2).

Zone 5. Generally, *zone 5* is found underlying *zone 4*, but it is common for this to occur directly below *zone 3*. There are only small variations of moisture content and structural form is most often massive. In this zone accumulations of carbonates and gypsum are observed, particularly in arid and semi–arid regions where the leaching of soluble salts occurs infrequently.

1.2.2 Soil structural stability

The terms *soil structural stability* and *aggregate stability* are largely synonymous. They differ only on point of scale and both have been discussed widely throughout the literature (*e.g.* Cass and Sumner 1982, 1982; Matkin and Smart 1987; Barlow and Nash 2002). In this review the definition of Field (2000) will be used. *Soil structural stability* describes the resistance of soil structural form to change, where stress is applied; it is characterised for different types of stress and at different scales of structural form.

Soil structural stability does not infer resistance to change (Lal 1998), but implies that a level of energy is required to alter the stability of a given system. As a result, characteristics of structural stability are often specific for particular soil types. These depend on soil physico–chemical properties and the applied stress (Kay *et al.* 1994). For example, the stability of a soil's structural

form to an applied compressive stress will be different to the stability of that same soil if an osmotic stress were to be introduced (Kay, 1990). In this research, the imposition of osmotic stresses, rather than compressive stresses, is addressed.

The dominant factors affecting the structural stability of Vertosols to osmotic stresses are soil physico–chemical properties such as texture, the clay mineral suite, exchangeable cation concentrations, the soil solution and organic carbon contributions. In particular, these soils are susceptible to changes in electrolyte concentration and in the increased presence of exchangeable Na^+ and soil solution Na^+. This was demonstrated by Mukhtar *et al.* (1974), who compared the effects of $CaCl_2$ and NaCl treatments. They demonstrated that the stability of Vertosols was enhanced by increased electrolyte concentration, but that increasing the contribution of solution Na^+ led to increased clay dispersion. Shainberg *et al.* (1997) support this finding by observing the formation of a surface seal as a result of two complementary mechanisms; *(i)*, a rapid disintegration of surface aggregates brought about by rapid wetting and raindrop impact and, *(ii)*, the dispersion of clay resulting from soil physico–chemical properties such as the EC of the soil solution and the exchangeable Na^+ content. In addition, Reichert and Norton (1994) implicate the importance of expanding lattice clay minerals (*e.g.* smectite) in aggregate stability. They showed that stability was controlled by soil swelling and found that soils with larger CEC values were less stable than those soils with smaller CEC values.

1.2.3 Soil structural resilience

Associated with soil structural stability is the capacity of a system to recover structural form after disturbance, or the *structural resilience* (*e.g.* Kay 1990; Lal 1993; Kay *et al.* 1994; Hewitt and Shepherd 1997; Herrick and Wander 1998; Lal 1998; Seybold *et al.* 1999). *Soil structural resilience* describes the ability of a soil to recover its structural form through natural processes when external disruptive forces are reduced or removed (Field 2000). Vertosols have a widely documented ability to resile structural form through swelling and shrinkage during intermittent periods of wetting and drying (Pillai and McGarry 1999). These processes combine with other soil properties (*e.g.* OC, EC and ESP) to influence the re–development of soil structural form (Figure 1.3).

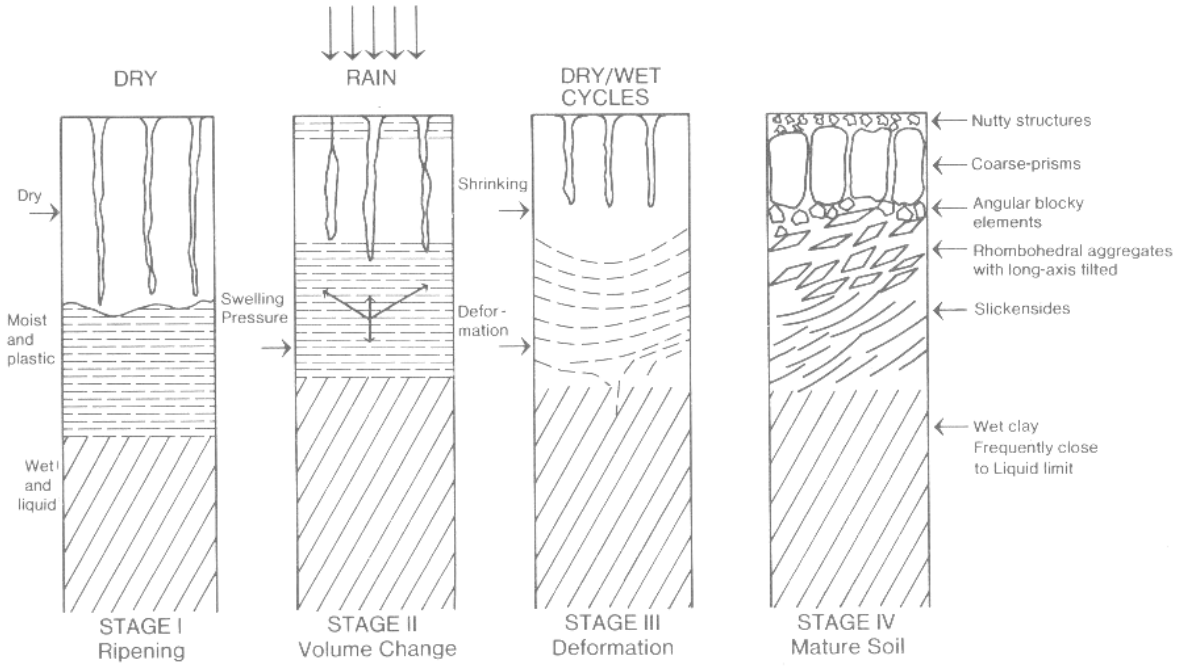

Figure 1.3 The morphological changes associated with the development of the structural form of Vertosols (Dudal and Eswaran 1988).

1.2.4 Soil structural vulnerability

Soils which are least stable under a given stress and which do not recover when the stress is reduced or removed (or which recover very slowly) are said to be vulnerable. This occurs regardless of whether the stress applied is natural or anthropogenic (Kay 1998). The term *structural vulnerability* reflects the combined characteristics of *structural stability* and *structural resilience* (Hewitt and Shepherd 1997). It relates to the distribution of bonding mechanisms and of failure zones (Kay 1990). Kay (1998) described this relationship and indicated that a soil with a large capacity for resilience and which is highly stable has low vulnerability. The characteristic properties of Vertosols make this soil class very resilient. However, their physico–chemical attributes do not instil stability. Consequently, these soils generally have intermediate vulnerability.

1.3 Soil physical processes that influence the structural form of Vertosols

The structural form of Vertosols is distinguished from that of other soil classes by the formation of distinctive characteristics such as deep, wide cracks and the ability to self–mulch (*e.g.* Dudal 1963, 1965; Blokhuis 1982; Probert *et al.* 1987). The processes that contribute to this characteristic development are addressed throughout the literature (*e.g.* Jewitt *et al.* 1979; Probert *et al.* 1987; Wilding and Puentes 1988; Ahmad and Mermut 1996; McGarry 1996). In this review, processes that

influence structural development over limited time scales (*i.e.* 1–5 years) are considered. Those pedogenic processes that generally require greater time periods to be significant (*i.e.* weathering and leaching) are not discussed.

1.3.1 Swelling and shrinkage: the wet–dry process

The development of structural form and the structural resilience of Vertosols relies on the swelling and shrinkage of phyllosilicate clays during alternate wet–dry cycles (Jewitt *et al.* 1979; Coughlan 1984; Mermut *et al.* 1996; Favre *et al.* 1997; Hussein and Adey 1998; Pillai and McGarry 1999). The extent of swelling is determined by the clay mineral suite, particularly the type and proportion of 2:1 expanding lattice clays. These minerals swell when water is adsorbed between clay structural layers and between individual clay particles through the process of osmosis, whereby water moves toward the greater salt concentration and results in expansion of the diffuse double layer (Blokhuis 1982). Consequently, this process depends not only on the proportions of phyllosilicate clay species but on the distribution of cations in the soil solution and at the exchange surface. In those Vertosols where 2:1 expanding lattice clays are subordinate (*e.g.* Shiel *et al.* 1988), the wide–deep cracks that characterise the structural form of vertic soils also develop, but the frequency of cracking in these soils is much reduced and structural characteristics are expressed to a lesser degree. Regardless of the suite of phyllosilicate clays, all Vertosols have a structural form that appears massive when wet, but as the soil dries, stresses develop causing aggregates to fracture along zones of least resistance. This results in the development of the features characteristic of this soil class, *e.g.* lenticular peds, numerous deep–wide cracks and in many, an aggregate layer of surface–mulch. The development of a surface–mulch over repeated cycles of wetting and drying results in some Vertosols being described as *self–mulching*.

1.3.2 Self–mulching

Many Vertosols have the ability to self–mulch as a consequence of repeated wetting and drying phases (De Vos and Virgo 1969; Blokhuis 1982; Mermut *et al.* 1996) and this characteristic is of crucial importance to the structural form of these soils. It influences moisture infiltration and water–holding properties (*e.g.* evaporation) (Probert *et al.* 1987) by reducing the frequency of large cracks at the soil surface and by decreasing the size of packing voids between aggregates. The process occurs during drying, when these Vertosols fragment to form a thin surface layer (<50 mm) of water stable aggregates less than 5 mm *d.* (McDonald and Isbell 1998). The formation of this layer is dependent on three factors: the mode of wetting (Hussein and Adey 1998), the number and extent of intermittent periods of wetting and drying (McGarry 1996) and the physico–chemical conditions of

the soil. These self–mulching soils generally have a very small ESP (<1), a very large Ca^{2+}:Mg^{2+} ratio, small indices of dispersion and mineral suites dominated by clays with large exchange capacities (Pillai–McGarry and Collis–George 1990).

1.3.3 Slaking of aggregates

The process of *slaking* occurs where soil aggregates lack the strength to withstand introduced stresses brought about by wetting (Warkentin 1982; Chan and Mullins 1994). As soil aggregates are wetted, entrapped air and the differential swelling of clay minerals (Emerson and Greenland 1990) may cause soil aggregates to fragment explosively, giving a distribution of microaggregates. This reduces infiltration by impeding pore space (Chan and Mullins 1994) where liberated aggregates block the pore network. In most Vertosols, which possess a strong inherent ability to resile structural form through intermittent wetting and drying, this is a desirable process (McKenzie 1998). This is because after slaking, drying allows the development of a fine granular surface structure at the soil surface, comprising the self–mulched layer (Grant and Blackmore 1991).

The slaking process is dependent on four principal soil factors; *(i)*, the degree of desiccation prior to wetting, *(ii)*, the rate of wetting, *(iii)*, the proportion of clay present and, *(iv)*, the size and suite of clay minerals (Warkentin 1982; Emerson and Greenland 1990; Chan and Mullins 1994; Curtin *et al.* 1994c; Hussein and Adey 1998). The degree of desiccation and the rate of wetting determine the extent to which air pressure is increased within the pore structure of aggregates. The greater the degree of desiccation, the larger the proportion of pore space that is occupied by soil air. During wetting clay minerals swell as water moves to particle surfaces. This increases intra–aggregate air pressures and results in explosive aggregate breakdown. In the same way, increasing the rate of wetting increases the degree of slaking, as larger quantities of air are entrapped and microaggregates are forced apart once tensile strength is exceeded. The greater the contribution of clay–sized particles, the more susceptible are aggregates to the slaking process, while soils with increasingly fine clay mineral contributions have an even greater capacity to swell and thus, to slake during rapid wetting. The mineral suite is of primary importance, where clay contributes large proportions of the total particle size distribution. The rate of water entry into soil aggregates decreases as clay particles pack together more closely, and where intra–aggregate pressures increase during wetting, stresses can be relieved by the bending of clay particles. The ability of some clay species to deform in response to increased pressure was shown by Emerson and Greenland (1990) for aggregates of a fine Ca^{2+}–illite and a fine Ca^{2+}–smectite. However, kaolinite clay, which contained much larger packing voids than the previous systems, slaked readily as a result of entrapped air and its less flexible structure (Tessier *et al.* 1990).

1.3.4 Churning

The theory of churning, or pedoturbation, is one model applied to describe the homogenisation of Vertosols (Figure 1.4). This process occurs where surface–connected cracks are filled to varying extents by aggregates, primarily from a surface–mulch, during dry seasons. This prevents cracks from closing completely as the soil adsorbs moisture and swells (Wilding and Tessier 1988; Mermut *et al.* 1996). Subsequently, pressure develops and swelling occurs along the path of least resistance and the subsoil pushes toward the soil surface. This leads to a cyclic inversion of the profile (Blokhuis 1982; Mermut *et al.* 1996).

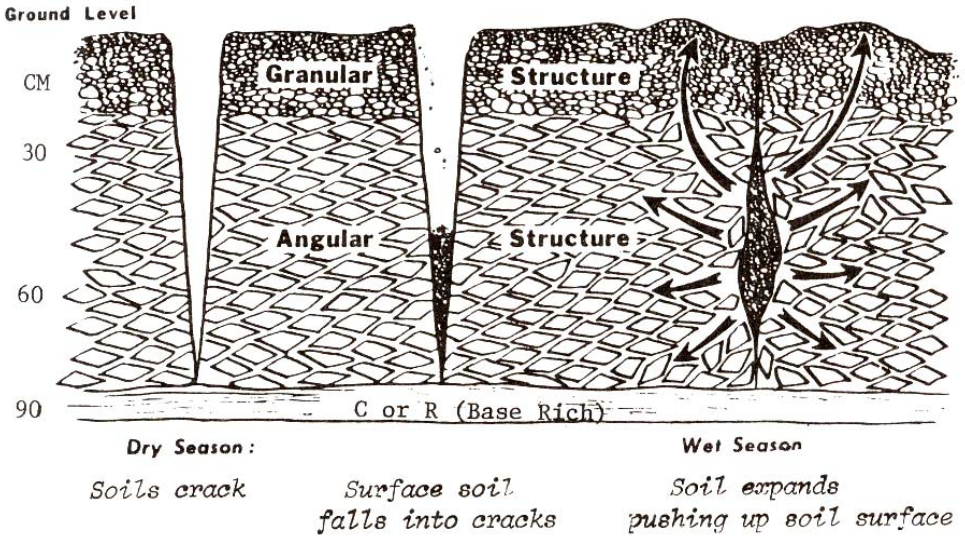

Figure 1.4 The churning or pedoturbation model describing the development of uniform structures in Vertosols (Wilding and Tessier 1988).

This process of homogenisation has been used to account for the lack of clear or abrupt boundaries between the horizons of Vertosols (Mermut *et al.* 1996). However, it does not completely explain the development of these soils (Wilding and Tessier 1988). This is because churning contributes to the mixing of the profile and the development of *zone 1* and *zone 2*, (*part* 1.2.1), but does not explain the formation of the lenticular structure or the occurrence of carbonate inclusions at specific depths.

1.4 The physico–chemical soil properties that influence the structure of Vertosols

The physico–chemical properties of Vertosols influence the development and vulnerability of soil structural form. These properties have been studied extensively and the physico–chemical properties

that provide the basis for the structural condition of Vertosols are texture, clay mineral suite and the capacity for cation exchange. Different expression of form and stability then depends on the contributions of specific cations to the exchange complex and to the soil solution. Furthermore, the soil pH, organic contributions and inclusions, *e.g.* carbonates and oxides, can all impact on the structural form and stability to varying extents.

1.4.1 The importance of clay content and the mineral suite

The content and suite of clay minerals are the most significant contributors to the structural characteristics observed in Vertosols, *e.g.* swelling is attributed primarily to the rate of wetting and to the clay mineral suite. Consequently, extensive research has characterised the clay fraction and the activity of the phyllosilicate suite of minerals.

1.4.1.1 Clay content and size

The clay content of Vertosols is important to their structural characteristics; increased total clay is associated with greater cohesive strength and larger ped structures (Warkentin 1982; McGarry 1996), it imparts an increased water–holding capacity and contains the phyllosilicate minerals that determine shrink–swell capacity. The clay fraction is composed of an array of different sized particles congregated during sedimentation and/or weathering. Of this fraction, fine clay (<0.2 μm) can constitute more than 80 % of total clay (<2 μm) (Ahmad 1983). This contribution differs according to the mineral suite and the depositional environment, *e.g.* Vervoort *et al.* (2003) found a Black Vertosol from the Darling Downs, Queensland, to contain 60 % fine clay in the <2 μm fraction, but this compares with 44 % fine clay in a Grey Vertosol from the lower Gwydir region of NSW.

The capacity of Vertosols to shrink and swell has been linked to the proportions of fine clay by Anderson *et al.* (1973). They found that smaller clay particles have a greater surface area relative to volume, allowing particles to fit more closely after desiccation and giving a greater potential for the adsorption of water. Furthermore, increasingly fine phyllosilicate particles have greater flexibility which allows them to distort during intermittent periods of applied pressure; this increases aggregate stability (Quirk 1994) and influences slaking and swelling activity. As a consequence, soils which contain large proportions of fine clay have a greater capacity to swell than those soils with increased proportions of coarse phyllosilicates. This is critical in determining the stability and the extent of structural development in Vertosols (Anderson *et al.* 1973).

1.4.1.2 Clay mineral suite

The phyllosilicate suite in Vertosols is frequently dominated by the smectites, and in general, illites and kaolinites are of lesser abundance (*e.g.* Hubble 1984; Shainberg and Letey 1984; Wilding and Tessier 1988; Hussein and Adey 1995). This is not absolute, and in Australia all three of these clay mineral species (smectites, illites and kaolinites) have been shown to dominate different Vertosols (*e.g.* Norrish and Pickering 1977; Stannard and Kelly 1977; Sarmah *et al.* 1996; Singh and Heffernan 2002). This relates principally to differences in parent materials and to alternate rates of mineral weathering (Ahmad 1983; Hubble 1984). Vervoort *et al.* (2003) determined the clay mineral suites of several Vertosols from eastern Australia and demonstrated the large variation in clay mineral contributions (Table 1.1).

Table 1.1
Clay mineral suite composition of Vertosol topsoils from eastern Australia (Vervoort *et al.* 2003)
Abundance of the individual clay minerals is indicated by the number of (+) signs

	Darling Downs, QLD	Lower Gwydir valley, NSW	Lower Namoi valley, NSW	Macquarie valley, NSW	Lachlan valley, NSW
			Total clay fraction (<2 µm)		
Illite	+	Trace	++	++	++ ½
Kaolinite	+	+	++	++	+ ½
Smectite		+++		Trace	
Other 2:1 minerals[a]	++	+	+++	++	+
			Fine clay fraction (<0.2 µm)		
Illite	Trace	Trace	Trace	+ ½	+
Kaolinite	+	+	+/ Trace	++	+ ½
Smectite	+	+++	+++	++	
Other 2:1 minerals[a]	++	+	++	++	++ ½

[a] Mineral thought to be interstratified mica smectite or another smectite intergrade

The differences in mineral suite and the size of clay particles impacts on the exchange capacity and the ability of Vertosols to swell during wetting events. However, there exists conjecture regarding the relationship between mineral species and the way in which the clay size distribution affects physical behaviour, *e.g.* Yerima *et al.* (1985, 1987) and Wilding and Tessier (1988). These authors report similarities between the physical activity of smectite–based systems and of smectite–kaolinite systems. Two examples of Vertosols from Queensland (Stace *et al.* 1968) show how soils with different phyllosilicate clays have similar structural form. These soils have different contributions of smectite and of kaolinite, but according to profile descriptions have a similar soil surface structure, with structural similarities decreasing with depth.

Example 1:

A Brown Vertosol from the Chinchilla district, clay content of 55–65 % in the top metre of the profile, where the clay mineral suite consists of 40–50 % kaolinite and 30–40 % montmorillonite. At the surface this profile had a thin surface crust overlying strong granular to polyhedral aggregates. At depths >0.4 m structure is strongly blocky and grading to polyhedral aggregates (size: 0.05 m) (*from* Stace *et al.* 1968).

Example 2:

A Black Vertosol from the Darling Downs, clay content of 35–55 % in the top metre of the profile, where the clay mineral suite consists of 20–30 % kaolinite and 50–65 % montmorillonite. This soil had a very minimal surface crust and at depths less than 0.45 m structure was very similar to that of example 1. However, characteristic lenticular peds became apparent (size: 0.15 m) at depths >0.45 m (*from* Stace *et al.* 1968).

1.4.1.3 The swelling of clay minerals

Clay systems swell in two ways: *(i)*, crystalline swelling (*e.g.* intra–crystal), or *(ii)*, osmotic or extensive swelling (Churchman *et al.* 1993). In general, the hydration and swelling of smectite results in water molecules penetrating into both interparticle pores and interlayer space (McGarry 1996). This causes the separation of mineral sheets and the expansion of lattice structures. The extent of this expansion depends on the proportions of exchangeable cation species and on the electrolyte concentration of the soil solution (Shainberg and Letey 1984).

It is generally accepted that clays with greatest negative charge have the highest degree of hydration, the most complete interlayer exchange, the most flexible clay particles and the greatest shrink–swell potential (Wilding and Tessier 1988). Wilding and Tessier (1988) described two modes of activity; the first addresses the activity of Na^+–smectites, and the second, the activity of Ca^{2+}– and Mg^{2+}–smectites (Figure 1.5).

Na^+–smectites:

The microstructure of Na^+–smectites consists of interparticle pores (<1 μm *d.*) that are filled with water. The walls of interparticle pores consist of laterally extensive and overlapping quasicrystals. The individual quasicrystals are composed of 5–10 layers of clay particles stacked face–to–face to form a structure of approximately 500 nm in size. The individual clay particles have a d–spacing of 3.5–10 nm (35–100 Å), and have a hydrated interlayer space

where the diffuse double–layer structure is formed. The layer charge is balanced by exchangeable cations and as negative charge approaches zero, the water content decreases and the number of clay layers comprising each of the quasicrystals increases. This results in a less flexible and less extensive structure. These structures combine to form more rigid microstructures that are less conducive to shrink–swell activity. In addition, these require greater energy input to open and close microstructures (Wilding and Tessier 1988).

Ca^{2+} and Mg^{2+}–smectites:

There are three important differences between the Ca^{2+}– and Mg^{2+}–smectites and the Na^{+}–smectite system at electrolyte concentrations <0.3 M. The interparticle pores of the divalent system are much larger (1–2 μm *d.*). In this model, the diffuse double layer of Ca^{2+}– and Mg^{2+}–smectites is absent, and therefore less interlayer water adsorption occurs and leads to a reduced interlayer space of 1.86 nm (18.6 Å). Thirdly, the number of layers comprising individual quasicrystals is much larger, generally >50, resulting in less flexible systems than for Na^{+}–smectite (Wilding and Tessier 1988).

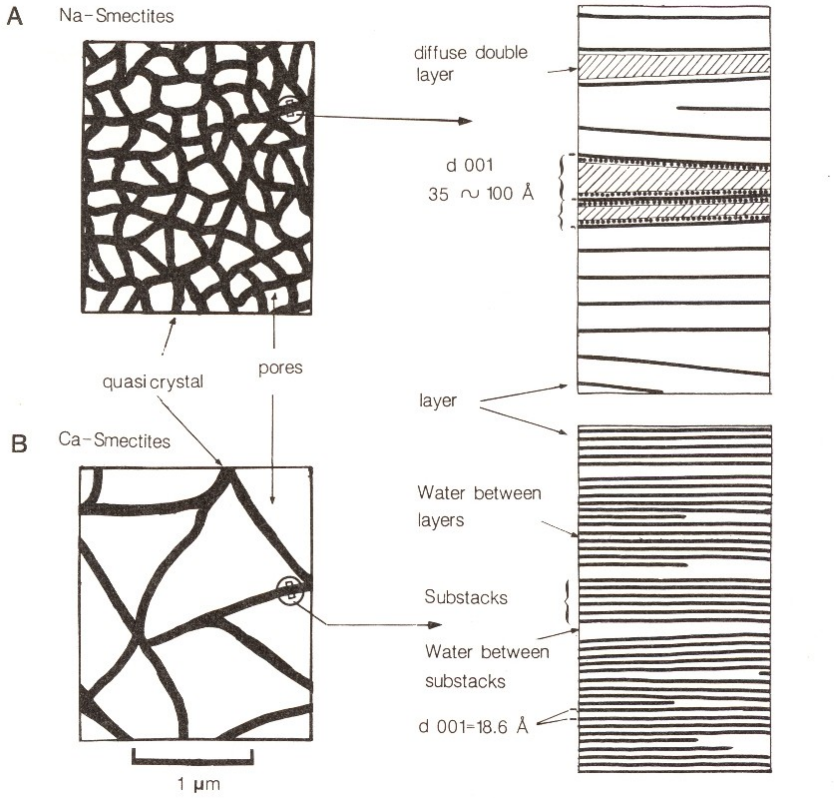

Figure 1.5 The schematic representation of the microstructure of Na^{+}–smectites (A) and Ca^{2+}–smectites (B) at near saturation (-0.032×10^{5} Pa) and prepared in low electrolyte concentrations of chloride solutions (10^{-3} M) (Wilding and Tessier 1988).

The example in Figure 1.5 compares clay microstructures in small electrolyte concentrations, *i.e.* less than 0.3 M. The ability of electrolyte concentrations above 0.3 M to limit swelling in smectites was later presented by Tessier (1990). In these systems microstructures of Na^+–smectite acted in a similar way to microstructures of Ca^{2+}– and Mg^{2+}–smectites. Alternatively, microstructures of illite and kaolinite clay minerals act differently to the smectite systems (Alperovitch *et al.* 1985; Wilding and Tessier 1988). These clays have been described as being brittle, forming rigid domains of illite and large crystallites of kaolinite. The formation of these structures is not favourable for the development of the flexible, extensive and overlapping quasicrystals described by Wilding and Tessier (1988) in Figure 1.5, and they concluded by showing that the resulting volume change during shrink–swell activity for illite and kaolinite clays is about $\frac{1}{2}$–$\frac{1}{5}$ that of the smectite systems (Figure 1.6).

The expanded microstructure of smectite clays can collapse completely as matric potential is increased (Wilding and Tessier 1988). This allows smectite systems to occupy less volume per given mass than illite or kaolinite clays, which maintain a minimum level of porosity (Figure 1.6). The shrink–swell properties of these different systems can therefore be ranked: smectites have the greatest ability to shrink–swell and kaolinite has the least (Na^+–smectites > Ca^{2+} and Mg^{2+}–smectites > illites > kaolinites). These conditions describe the activity of pure clay systems. In soil environments, heterogeneous mineral arrangements will reduce the expression of specific species activity. This is because clay particles exist in an arrangement of macromolecules consisting of different mineral species. In addition to these mineral associations, bonding occurs between clay particles and organic molecules and/or polymers, which will further influence the expression of mineral activity.

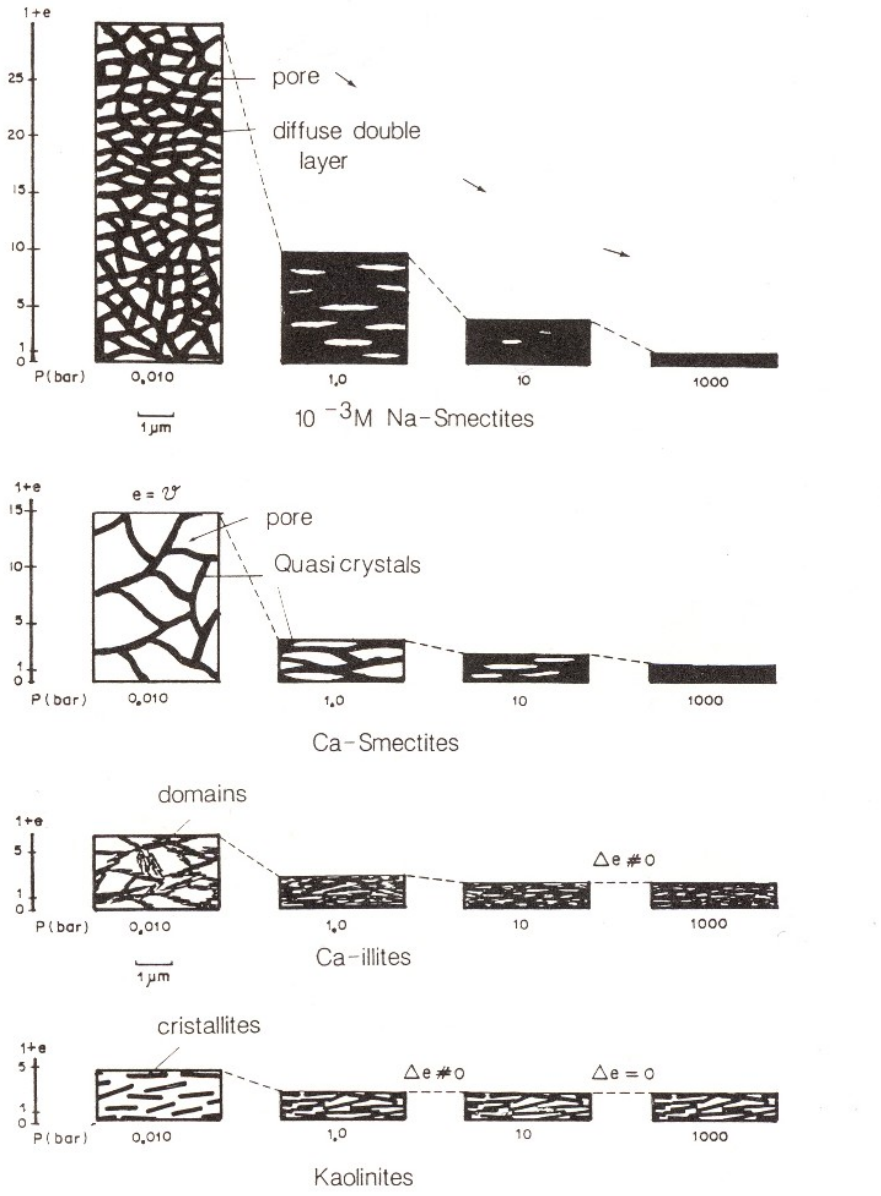

Figure 1.6 Schematic representation of relative swelling and consolidation volumes of different clay minerals as a function of matric potential (e = void ratio – volume of pore space to solid particle volume) (Wilding and Tessier 1988).

1.4.2 The cation exchange complex

The term 'charge' is applied throughout this discussion to represent excess negative charge on the lateral face of clay particles brought about by isomorphous substitution (*e.g.* substitution of Si^{4+} by Al^{3+} and of Al^{3+} by Fe^{2+} and Mg^{2+}). The excess negative charge is compensated by the adsorption of cations onto layer surfaces, because cations are too large to be accommodated in the interior lattice structure (van Olphen 1963). In the presence of water, the compensating cations on this layer surface are easily exchanged by other cations from solution; thus these are *exchangeable cations* (van Olphen 1963). Vertosols frequently have a much larger *cation exchange capacity* (CEC) than other soils.

This ranges from approximately 10 to greater than 80 $cmol_{(+)}\ kg^{-1}$ (Murthy *et al.* 1984; Isbell 1989; Coulombe *et al.* 1996a; Singh and Heffernan 2002) and depends on the mineral suite and on organic contributions.

Irrespective of CEC, the cations Ca^{2+}, Mg^{2+}, K^{+} and Na^{+} generally dominate the exchange complex of Vertosols (SSSA 1997). The strongly structured Vertosols usually exhibit an exchange complex dominated by Ca^{2+}. This contrasts with soils containing elevated concentrations of exchangeable Mg^{2+} and exchangeable Na^{+}; these soils tend to have poor structural stability and undesirable structural form (Hubble 1984). This acknowledgement implicates the importance of exchangeable cation contributions in the development of soil structure (Coughlan 1984). The basic cations exert an influence in two ways: *(i)*, through the affect of cation valence, *i.e.* whether monovalent *or* divalent species dominate and, *(ii)*, through the different impacts of monovalent cations (*i.e.* Na^{+} or K^{+}) and of divalent cations (*i.e.* Ca^{2+} or Mg^{2+}) (Kanwar and Kanwar 1968; Chen *et al.* 1983; Levy and van der Watt 1990).

1.4.2.1 The principles of double layer theory and the influence of ionic state

Electronic double layer theory is discussed by van Olphen (1963, 1987) and by Quirk (1994, 2001). This theory describes the activity of charged matter (*e.g.* clay surfaces, cations or anions) at the lateral face of clay minerals and is summarised by Sumner (1993) and by Halliwell *et al.* (2001). The electrical double layer is composed of two individual layers. The surface charge of clays (–ve charge) provides the first layer. A layer of compensating charge (counter–ions) then accumulates in the solution near this surface layer (Shainberg and Letey 1984). The counter–ions are electrostatically attracted by the oppositely–charged surface. These form a distribution of ions at equilibrium in solution, and the concentration of ions decreases with increasing distance from the charged surface (Figure 1.7). This theory proposes that divalent ions are attracted to the surface with a force twice that of monovalent ions. As a result, the diffuse double layer in a divalent system has much greater compression towards the layer surface (Shainberg and Letey 1984). This was shown by Wilding and Tessier (1988), who suggested that a diffuse double layer is absent from Ca^{2+}– and Mg^{2+}–smectites (Figure 1.5). In addition, the extent or thickness of the counter ion layer is determined by the charge neutral difference of this layer with the outside solution (Quirk 2001). The result is that the greater the ionic concentration, the more compressed the diffuse double layer becomes.

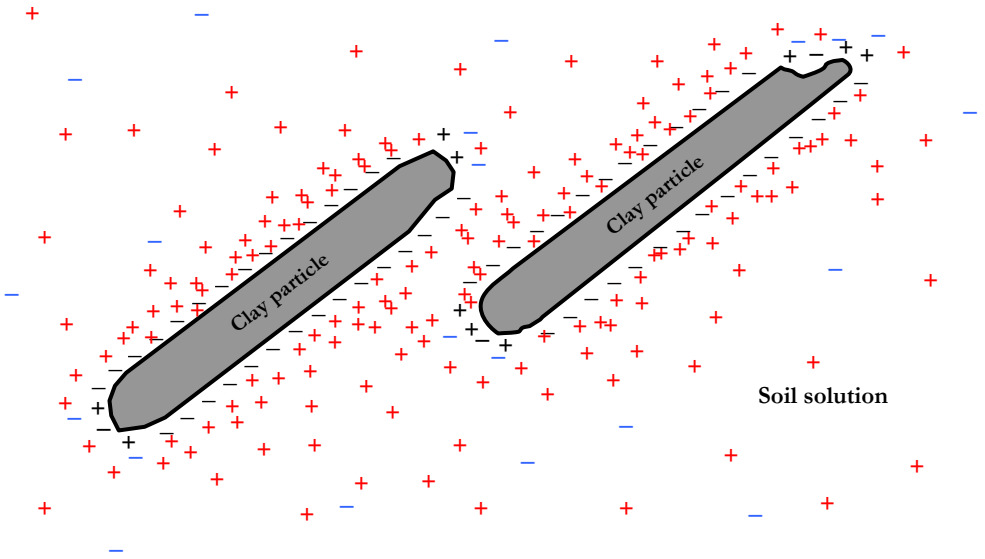

Figure 1.7 Schematic distribution of charges in the diffuse electrical double layer surrounding clay particles according to the Gouy-Chapman model (adapted from van Olphen 1963). The charge of clay particles is represented by (–) and (+) and the charge of ions in solution by (–) and (+). This model demonstrates the attraction of ions in solution toward opposite charge at the surface of clay particles.

In Vertosols, the counter–layer is formed by an abundance of cations and a deficit of anions. The difference between the cations and anions is therefore representative of the surface charge of a particular mineral. Thus, when two clay particles approach each other in solution, a consequence of Brownian motion, diffuse double layers overlap and repulsion occurs. This repulsion of particles is suppressed by the addition of electrolytes to the soil solution. An increased electrolyte concentration reduces the tendency of ions to move outward from the charged surface by compressing the double layer. This reduces the range at which clay particles can repel each other and as a result, influences the colloidal stability of suspensions, the potential for osmotic swelling and the ion exchange process.

The speciation of ions is significant for the formation of the diffuse double layer. The valence and the hydrated radius of each cation influences the extent of double layer compression; the greater the proportion of ions of larger valence (*e.g.* Ca^{2+} or Mg^{2+}, rather than Na^{+} or K^{+}) the greater the compression of the double layer. In the same way, the smaller the hydrated radii (Table 1.2) of cations present, the greater the compression of the diffuse double layer. The *hydrated radius* represents the effective size of an ion or molecule in solution, so includes associated water molecules attracted by the imbalance in ionic charge. Therefore, unlike ionic radius, which is dependent only upon the attractive force of an atom's nuclei, hydraulic radius is dependent also upon the valence of the ion considered (Rengasamy 1982). Thus, increasing the size of a cation's radius will lead to more diffuse electrical charge and subsequently the attraction of fewer water molecules. This led some

early researchers to discount the difference between ions of the same valence (*i.e.* Ca^{2+} and Mg^{2+}, or Na^{+} and K^{+}) (*e.g.* Quirk and Schofield 1955; van Olphen 1963). Currently, estimators of potential instability, such as ESP ($[Na^{+}_{exch}/CEC]\times100$) and ESI ($EC_{1:5}/ESP$) do not discriminate ionic size or hydrated radii, with both Ca^{2+} and Mg^{2+} having often been considered together despite recognition of their different activity in soils. Similarly, K^{+} was rarely given any consideration as a contributor to stability. Later research supported the theory that different cations exhibit different effects on the exchange complex (*e.g.* Emerson and Chi 1977). For example, Ca^{2+} is widely recognised as being more beneficial for structural development than Mg^{2+}, and K^{+} less detrimental to structural stability than Na^{+}. This was supported by Emerson and Bakker (1973), who found that for illitic red–brown earths in Victoria, the ESP required for dispersion was approximately halved when Mg^{2+} replaced Ca^{2+} as the complementary ion. The effects of K^{+} were summarised by Levy and van der Watt (1990), who found that K^{+}–saturated soils have larger aggregates with greater aggregate stability than Na^{+}–saturated soils. Although K^{+} has an additional shell of electrons (e^{-}) and a larger ionic radius than Na^{+}, the more diffuse electrical charge observed in K^{+} results in a hydraulic radius approximately $^{2}/_{3}$ that of Na^{+} (Table 1.2). Therefore, hydrated K^{+} ions pack together more closely against the negative layer charge than hydrated Na^{+} ions.

Table 1.2
The ionic and hydrated radii of the four common exchangeable cations in Vertosols

Cation [a]	Ionic Radius (nm)	Hydrated Radius [b] (nm)
Na^{+} (22.99)	0.190	0.40–0.45
K^{+} (39.10)	0.266	0.30
Mg^{2+} (24.31)	0.130	0.8
Ca^{2+} (40.08)	0.198	0.6

[a] In brackets is the atomic mass of each cation
[b] Hydrated radii obtained from Narawimha and Mathew (1995).

In contrast to the ionic activity at the lateral face of minerals, activity along edges is quite different. At these edge surfaces, charge occurs as a result of broken bonds and can be either +ve or –ve. This *variable charge* is determined by the activity of H^{+} and OH^{-} in solution. In these soils, pH determines the expression of charge; in acid and neutral solutions the edges of variably charged clays carry a positive double layer, but this becomes negative with an increasingly alkaline soil solution. Subsequently, the stability of some clay systems will be influenced by the presence of variable charge, particularly those soils containing large proportions of highly weathered clay minerals, *e.g.* kaolinite.

1.4.2.2 The role of exchangeable Na^+ in determining structural characteristics

More than 28 % of the total land area of Australia is classed as sodic and more than 50 % of arable land is potentially influenced by sodicity–related problems (Keren and Ben–Hur 2003). Contributing to this, many Australian Vertosols fall into this sodic soil class with ESP values greater than 6 (Northcote and Skene 1972). Consequently, the distribution of Vertosols across NSW (Figure 1.8*a*) (Isbell 1996) tends to be reflected by the distribution of uniformly–textured, sodic, alkaline soils (Map unit AS1) (Figure 1.8*b*) (Northcote and Skene 1972). The classification units used in Figure 1.8*b* are described in Table 1.3.

Generally, Vertosols that have large proportions of exchangeable Na^+, *e.g.* ESP >6, swell more extensively when wetted and are susceptible to spontaneous dispersion (Sumner 1993). These soils are described as *sodic*. A *sodic soil* is a non-saline soil containing exchangeable Na^+ at levels that adversely affect crop production and soil structure in most soil conditions and for most plant species (Sumner 1993; SSSA 1997). The US Salinity Laboratory Staff (1954) give the critical ESP value of 15 to delineate non–sodic soils from the sodic soils. In Australia, Northcote and Skene (1972) and later Isbell (1996), define sodic soils as those that have an ESP >6. Northcote and Skene (1972) qualified this definition by assigning three classes of sodicity; *(i)* the non–sodic (ESP< 6), *(ii)*, the sodic (ESP 6–14) and, *(iii)*, the strongly sodic (ESP >15). In cotton–producing Vertosols, McKenzie (1998) encourages the use of an ESP_{crit} of 5 to delineate the non–sodic soils from the sodic systems. This was qualified with the understanding that ESPs as low as 2 can have detrimental effects on the structural condition of some Vertosols (*e.g.* Cook *et al.* 1992). The extent of instability expression is therefore determined by the ESP and other physico–chemical properties, in particular the electrolyte concentration of the soil solution. As a consequence numerous authors have accounted for clay dispersion using exchangeable Na^+ or ESP in conjunction with the electrical conductivity of the soil solution (*e.g.* Blackwell *et al.* 1991; Hulugalle and Finlay 2003).

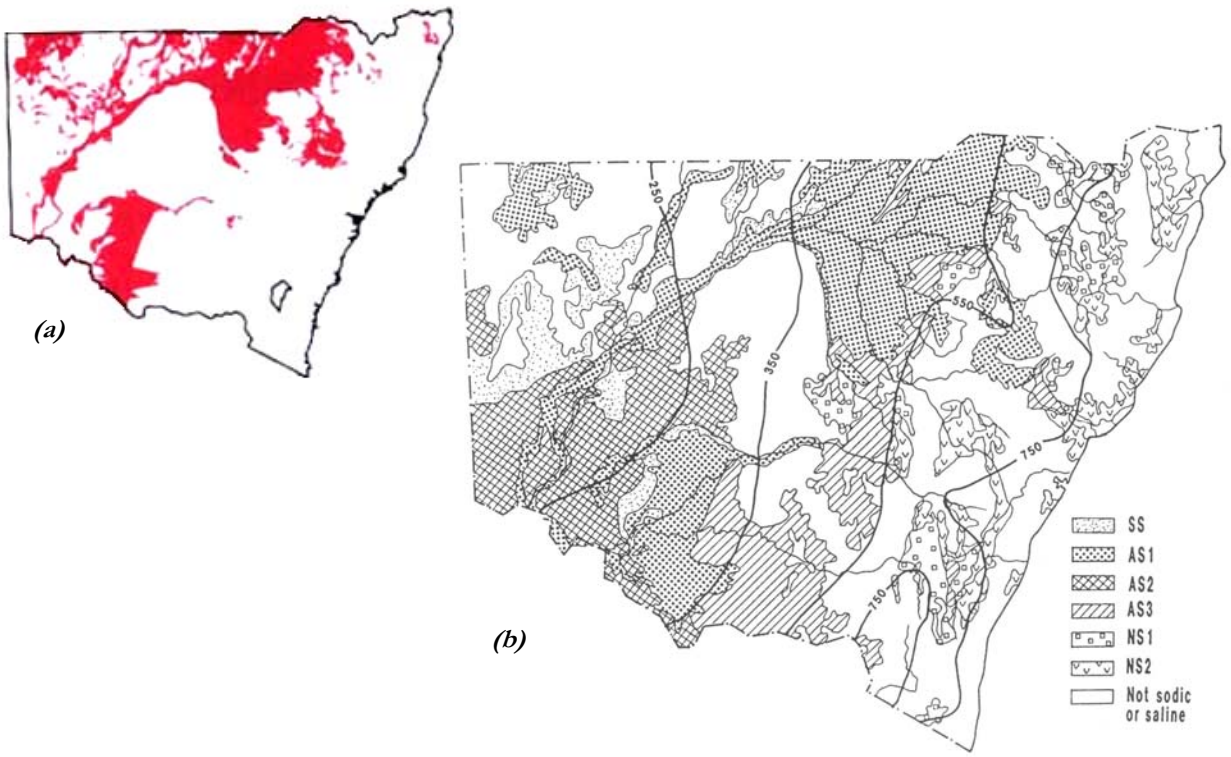

Figure 1.8 The distribution of Vertosols (Isbell 1996), *(a)*, and the distribution of sodic and saline soils in NSW including various intergrades of sodic–saline soils according to Northcote and Skene 1972 (from McKenzie *et al.* 1995), *(b)*.

Table 1.3
Classification units based on the map of Northcote and Skene (1972) (from McKenzie *et al.* 1995)

Map unit	Soil category[a]
SS	Saline soils (dominated by chlorides either in at the soil surface, in the subsoil or throughout)
AS1	Alkaline soils with ESP >6, clay textures and uniform texture profiles
AS2	Alkaline soils with ESP >6, sandy/loamy textures and uniform/gradational texture profiles
AS3	Alkaline soils with ESP >6 and duplex texture profiles
NS1	Sodic and strongly sodic, pH 6.5–7.9 and duplex profile form
NS2	Sodic and strongly sodic, pH <6.5 and duplex profile form

[a] Saline soil defined as NaCl >0.1 % (soil texture class of loam or more coarse) or >0.2 % (clay loam and clay soils) at the surface (0–0.2 m) and/or >0.3 % below 0.2 m depth. Sodic soil defined as having an ESP 6–14 within depth of 1 m; strongly sodic defined as having an ESP >15 within depth of 1 m. Alkaline $pH_{1:5}$ (soil:water) 8.0–9.5 within depth of 1 m; strongly alkaline $pH_{1:5}$ (soil:water) >9.5 within depth of 1 m.

Regardless of definitions applied to describe sodicity, the exchangeable Na^+ content is conceivably the most important of all physico–chemical properties influencing the stability of Vertosols. It is arguably the most intensively studied and frequently discussed exchangeable cation from the soil environment (*e.g.* Fireman and Bodman 1939; Shainberg and Letey 1984; Chiang *et al.* 1987; Levy *et al.* 1993; Rengasamy and Naidu 1993; Naidu *et al.* 1995; Sumner *et al.* 1998). Its detrimental influence on soil systems is widely recognised (*e.g.* Chang and Dregne 1955; Chen and Banin 1975; Curtin *et al.* 1994a, 1994c) and it affects soil moisture retention, soil swelling and the dispersion of clay (Oster *et al.* 1980). Increasing the contribution of Na^+, relative to Ca^{2+} and Mg^{2+}, is a dominant factor contributing to increased dispersion. This was demonstrated by So and Cook (1993) who showed a significant relationship between dispersed clay and exchangeable Na^+ using two Vertosols (Figure 1.9). The impact of Na^+ is particularly evident in soils that have low electrolyte concentrations in the soil solution (Wilding and Tessier 1988), as a large electrolyte concentration reduces the thickness of the diffuse double layer. As the proportion of Na^+ is increased the thickness of the counter layer increases and the clay particles begin to separate (Figure 1.10) resulting in accentuated swelling during hydration. Furthermore, hydration dilutes the soil solution (*e.g.* rainfall or irrigation) and where the electrical conductivity is sufficiently low, soils with large ESPs undergo spontaneous dispersion (Rengasamy and Naidu 1993; Sumner 1993).

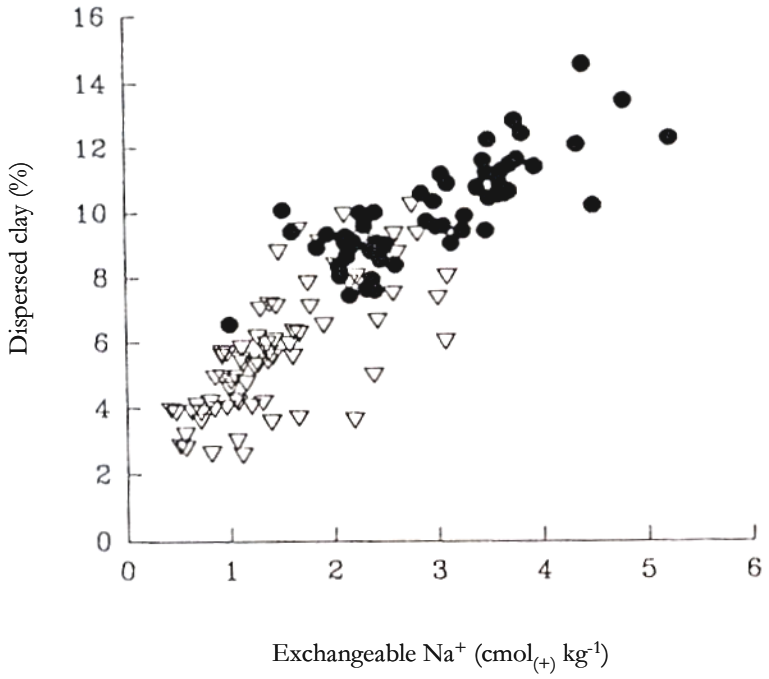

Figure 1.9 The relationship between exchangeable Na^+ and dispersible clay for two Australian Vertosols; Waco (●), Langlands (▽) (from So and Cook 1993).

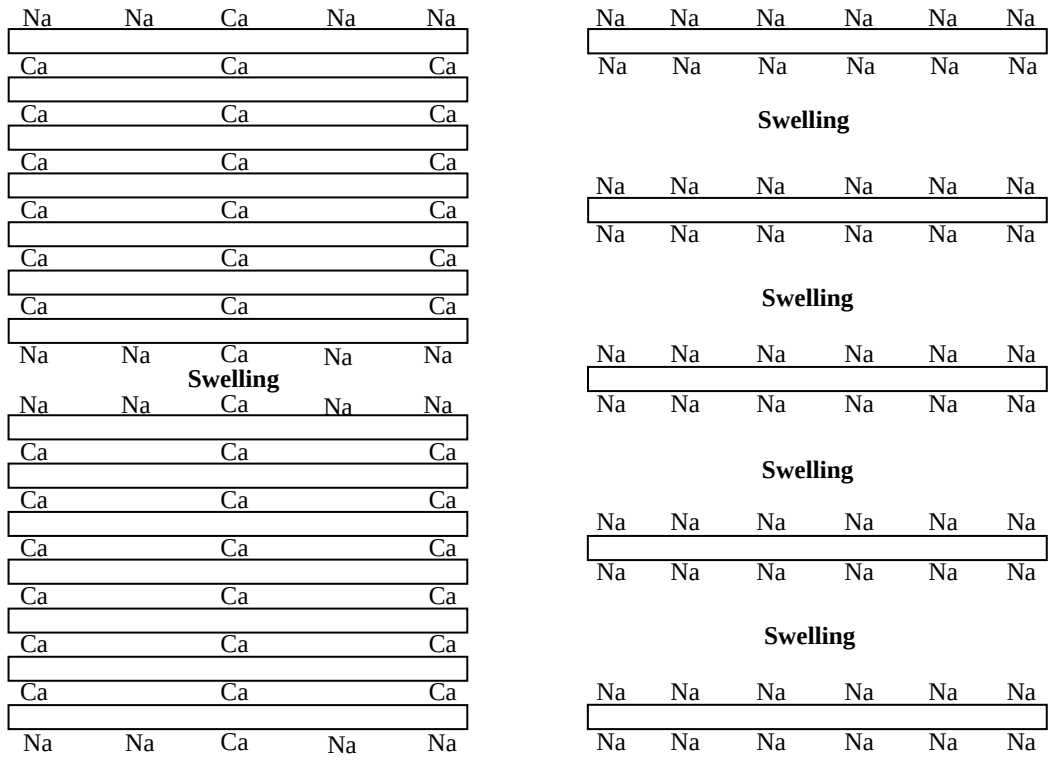

Figure 1.10 Comparison of particle arrangements in a homeoionic Na–smectite (right) with that in a Ca–Na system (left) illustrating the formation of 'tactoids or Quasi-crystals' with 'de–mixing' of Na^+ and Ca^{2+} (Sumner 1993).

1.4.2.3 The role of exchangeable Ca^{2+} and Mg^{2+} in determining structural characteristics

Vertosols that have good structure and which are strongly self–mulching have an overwhelming dominance of exchangeable Ca^{2+} throughout. They contain only small to moderate quantities of exchangeable Mg^{2+} and have a very small amount of exchangeable Na^+ (Hubble 1984). In contrast, soils that swell excessively, disperse spontaneously and which develop undesirable structure contain Mg^{2+} as a co–dominant cation with Ca^{2+}. These soils can contain significant exchangeable Na^+ at or close to the soil surface (Hubble 1984).

An alternate view is that exchangeable Ca^{2+} and Mg^{2+} affect soil structural condition in similar ways (*e.g.* Ahmed *et al.* 1969). For example, Rengasamy (1982) studied homeoionic systems free of solution electrolytes. Here there was no difference in the dispersion of three Mg^{2+}– and Ca^{2+}–saturated clays; *(i)*, Wyoming bentonite, *(ii)*, Grundy illite, and *(iii)*, Shepparton fine sand loam (30 % kaolinite, 55 % illite and 15 % smectite). However, most research has tended to show that exchangeable Mg^{2+} is less beneficial than Ca^{2+} in maintaining soil structural condition. This was first shown by the early permeability studies of Quirk and Schofield (1955) where they separated the effect of valence and related permeability to the hydrated radius of ionic species (Table 1.2). Many of these studies were carried out using homeoionic clays and clays equilibrated using either Ca^{2+} or

Mg^{2+} in combination with Na^{+} (*e.g.* Emerson and Smith 1970). Later, Emerson and Chi (1977) investigated illite clays and found that for a given exchangeable Na^{+} content the Ca^{2+}–Na^{+} clay had greater aggregate stability and dispersed less than Mg^{2+}–Na^{+} clay. They related this to the lower repulsive force present in the Ca^{2+}–Na^{+} system. Then they compared these clays to homeoionic systems. They found that approximately 10 times as much exchangeable Mg^{2+} was required to disperse a Ca^{2+}–illite than exchangeable Na^{+}. These findings are supported by Curtin *et al.* (1994b) who investigated a clay fraction dominated by smectitic clay. Here they found that the ability of the soil to resist swelling and dispersive pressures in the presence of Na^{+} was greater in Ca^{2+}–systems than in Mg^{2+}–systems. In addition, they showed that the exchangeable Ca^{2+}:Mg^{2+} ratio affected dispersion even in the absence of Na^{+}, and that Mg^{2+}–systems had greater susceptibility to surface sealing caused by aggregate disintegration and clay dispersion. More recently, Dontsova and Norton (2002) began by questioning whether any significant difference between Mg^{2+} and Ca^{2+} occurred in relation to swelling. However, they concluded that Mg^{2+} had less flocculating effect on clays than Ca^{2+} and observed minor decreases in the hydraulic conductivity of some soils saturated with Mg^{2+} rather than Ca^{2+}. They attributed this to the smaller ionic radius of Mg^{2+} and its larger hydrated radius.

1.4.2.4 The role of exchangeable K^{+} in determining structural characteristics

In contrast to the enormous store of literature describing the effect of exchangeable Na^{+} and Ca^{2+}, and to a lesser extent Mg^{2+}, very little research has focused on the activity of exchangeable K^{+}. In addition, the results of many K^{+} studies are conflicting. Consequently, the influence of exchangeable K^{+} on soil structure is much less understood. For example, Levy and Torrento (1995) studied the extent of dispersion in two soils dominated by smectite clays. They found that 10–15 % exchangeable K^{+} had no effect on the dispersion of clay. This is broadly reflected in the work of Chen *et al.* (1983), who investigated the effect of K^{+} on the permeability of three soils dominated by smectite clays. They showed for two of these soils that increasing exchangeable K^{+} from 0 toward 20 % increased relative hydraulic conductivity. However, increasing K^{+} beyond 20 % led to a decrease in the hydraulic conductivity of these soils. In contrast, their third soil, which had 10 % less smectite, showed decreasing relative hydraulic conductivity as exchangeable K^{+} was increased from 0 %. The reasons for these differences did not correlate to the other soil properties in their study. A third study by Levy and van Der Watt (1990) looked at three soils dominated by illite and kaolinite clay mineral suites. They found that exchangeable K^{+}, while not as efficient as exchangeable Ca^{2+} in maintaining high permeability, did not reduce permeability to the extent observed in Na^{+} systems.

Current work is inconclusive, but results generally relate to the method of study and to the soil mineral suite. Further, while elevated exchangeable K^+ does not always positively influence soil structural condition, it is clear that its effect does not cause soil to swell and disperse to the same extent as soils containing similar contributions of Na^+.

1.4.3 The soil solution

The soil liquid phase, the *soil solution*, contains all liquid phase electrolytes in equilibrium with exchangeable ions and precipitate compounds. The electrolyte concentration increases as moisture loss occurs (*e.g.* evaporation) and is diluted by moisture additions (*e.g.* rainfall or irrigation) (Oster and Shainberg 2001). This, and the effects of ion valence and size (Le Bissonnais 1996), influences the extent of flocculation or dispersion, particularly where the soil Na^+ content is large (exchangeable and solution Na^+) (Shainberg *et al.* 1981; Rengasamy *et al.* 1984; Mullins *et al.* 1991). Furthermore, increasing or decreasing the concentration and composition of ions in solution can increase precipitation or cause preferential exchange for the dominant cations. This was shown by Loveday (1984), where increasing the Na^+ content of applied water led to an increased ESP of the soils used.

1.4.3.1 The concentration of the soil solution

The concentration of ions present in the soil solution is described by the electrical conductivity (EC, dS m^{-1}). In soils containing excessive soluble salts, the term *saline* is applied. Saline soils tend to contain large concentrations of Cl^- and SO_4^{2-} salts of Ca^{2+}, Mg^{2+}, Na^+ and K^+ (Sumner *et al.* 1998). In cotton–growing Vertosols, a 'very highly saline' medium clay soil has an $EC_{1:5}$ >1.33 dS m^{-1} (1:5, soil:de–ionised water extraction) and a 'very highly saline' heavy clay soil has an $EC_{1:5}$ >1.72 dS m^{-1} (McKenzie 1998). This is the salt content above which crop plants are adversely affected (SSSA 1997), resulting in reduced plant production.

The concentration of the soil solution, specifically the Total Cation Concentration (TCC) and the Sodium Adsorption Ratio (SAR), are of greater relevance to soil structural condition than descriptions of salinity. These attributes are described by equation 1 (TCC is approximately 10 times the value of $EC_{1:5}$) and equation 2:

$$TCC\ mmol_{(+)}\ L^{-1} = \Sigma(Ca^{2+}, Mg^{2+}, Na^{+}\ and\ K^{+}) \qquad [1]$$

$$SAR\,(mmol_{(+)}\,L^{-1})^{1/2} = \frac{Na^{+}}{\sqrt{\left(\frac{Ca^{2+} + Mg^{2+}}{2}\right)^{2}}} \qquad [2]$$

In soils containing large ESPs the concentration of the soil solution is particularly important. The importance of the TCC was demonstrated by Rengasamy *et al.* (1984), who derived a model describing the stability of red–brown earths (Chromosols and Sodosols). In their model, increasing the TCC was shown to benefit structural stability and increasing SAR was shown to increase instability. This model reveals a number of characteristics of the soils they investigated, including a propensity for clay dispersion at very low values of SAR (Wilding and Tessier 1988) when TCC is small. Shainberg *et al.* (1989) summarized a number of works that had applied 'tap water' to soil for the study of hydraulic conductivity. Different sources of 'tap water' contained different solute concentrations; when water with a TCC of 3.13 $mmol_{(+)}\ L^{-1}$ was applied, there was no reduction in the hydraulic conductivity of prepared soils for all but the very sodic systems. In contrast, the use of 'tap water' containing 0.7 $mmol_{(+)}\ L^{-1}$ of soluble salts resulted in large reductions in hydraulic conductivity, even at small ESPs. Finally, Hulugalle and Finlay (2003) recently compared ESP, Electrochemical Stability Index (ESI) ($EC_{1:5}$/ESP) and $EC_{1:5}/Na^{+}_{exch}$ as predictors of soil dispersion. The ESI and $EC_{1:5}/Na^{+}_{exch}$ values obtained show a significantly better relationship with dispersion than ESP alone.

The extent to which the electrolyte concentration influences the stability of soils is dependent on the mineral suite (Figure 1.11); for example, as the SAR of kaolinite clay solutions is increased, small increases in TCC are required to maintain flocculation. In contrast, small increases in the SAR of smectite clay solutions require large increases in TCC to maintain flocculation. In addition to the impact of phyllosilicate species, the influence of electrolyte concentration also depends on the dominant exchangeable cations in a soil. Rengasamy *et al.* (1986) showed that preserving an adequate electrolyte concentration maintained clays in a flocculated state, but that Mg^{2+}–Na^{+} systems require more electrolyte than the Ca^{2+}–Na^{+} systems. Oster *et al.* (1980) looked at the flocculation of smectite systems and observed that; *(i)*, the flocculation rate increased with increasing electrolyte concentration, except for systems of very large ESP (40 %), *(ii)*, the rate of flocculation decreased with increasing ESP, *(iii)*, the rate of flocculation depended on the concentration of clay in suspension, but this did not influence the flocculation value (TCC required to initiate flocculation) and, *(iv)*, the rate of flocculation decreased exponentially with time.

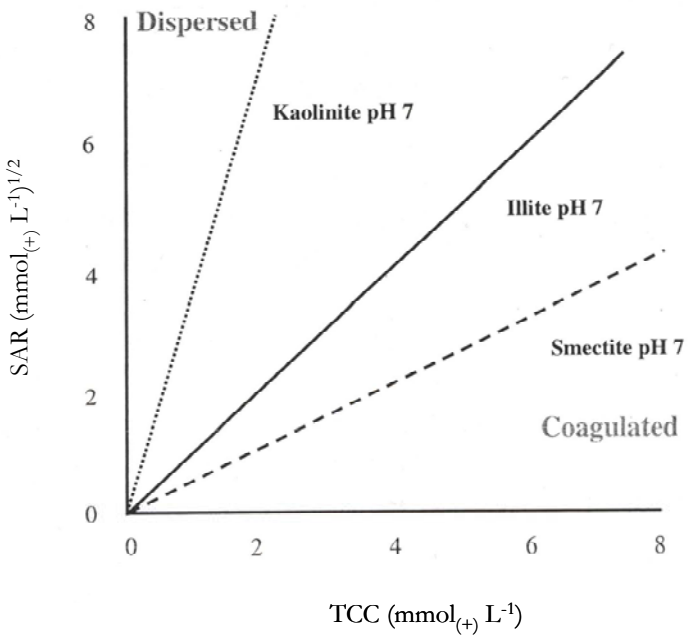

Figure 1.11 The general relationship of dispersion and coagulation for kaolinite, illite and smectite as affected by SAR and TCC (from Field 2000).

1.4.3.2 The speciation of cations in the soil solution

The TCC influences soil structural form through the impact of cations held in, and associated with, the double layer. Subsequently, increasing the contribution of a particular cation to the TCC, *e.g.* through the application of gypsum ($CaSO_4.H_2O$), will cause a new equilibrium to develop between the solution and the exchange complex. For example, raising the concentration of a particular index cation (*e.g.* Na^+) in solution causes a decrease in the solution concentrations of Ca^{2+} and Mg^{2+}. This leads to an increase in the index cation (Na^+) on exchange sites (Fireman and Bodman 1939; Kanwar and Kanwar 1968; Lieffering and McLay 1996) and the contributions of exchangeable Ca^{2+} and Mg^{2+} become less. In the case of infiltrating solutions where the concentration of salts approaches zero, the soil solution becomes more dilute. This will lead to an increase in the size of the diffuse double layer and the result is decreasing stability as charged particles move apart and the soil swells. In situations where the repulsion force is large enough to overcome attraction, soil dispersion occurs and clay particles move into suspension. For example, Felhendler *et al.* (1974) used hydraulic conductivity (HC) as a measure of the structural condition of two swelling soils; a sandy loam and a silty loam. They found that reductions in HC were minimal provided the electrolyte concentration of the percolating solution exceeded 10 $mmol_{(+)}\ L^{-1}$. Similar results were obtained by Shainberg *et al.* (1981) using solutions with low SAR. Here, they demonstrated that raising the SAR resulted in a requirement for increasing the TCC of solution so as to maintain structural condition.

1.4.4 Soil pH

The pH of any soil system develops predominantly from the parent material (Coulombe *et al.* 1996a; Coulombe *et al.* 1996b). It influences the solubility of ionic species (*e.g.* Al^{3+}) and the charge balance of variably–charged sites. In general, acidic Vertosols develop from acidic parent material, while neutral and alkaline Vertosols develop from calcareous or base–rich parent materials (Coulombe *et al.* 1996a).

The physico–chemical properties of Vertosols are most stable at pH values approaching neutral. In Vertosols that become either increasingly acid or increasingly alkaline, degradation of the physico–chemical properties may occur. In soils where acidic conditions prevail the stability of clay phyllosilicates is compromised. This results in the gradual formation of highly weathered products, and kaolinites form as smectite clays are degraded (Coulombe *et al.* 1996a).

In alkaline Vertosols, the large pH is the result of the increasing presence of Na^+ and carbonates in solution (Kanwar and Kanwar 1968; Coulombe *et al.* 1996b; Barzegar *et al.* 1997). This results in the decreased solubility of $CaCO_3$ (Ahmad 1996) and thus the precipitation of Ca^{2+} occurs. Furthermore, increased pH (7–9) leads to an increase in the net negative charge of variably–charged minerals (iron and aluminium oxides and kaolinite clay) and organic material binds increasing amounts of OH^-. Structural stability is compromised (Emerson 1983; Coulombe *et al.* 1996b) through swelling and the dispersion of both clay and organic material (Coulombe *et al.* 1996a). This was demonstrated by Suarez *et al.* (1984) using three soils (20–30 % clay). They studied the effect of increasing pH (6–9) and found reductions in the saturated hydraulic conductivity to be primarily the result of changes in dispersive forces. The conclusion they reached was that the sensitivity of soils to changes in pH is dependent on the quantity of variable charge present. Therefore, in soils with large quantities of variable charge the structural conditions are more susceptible to increasing pH than soils that contain smaller quantities of variably–charged materials.

1.4.5 Soil organic material

Organic matter is highly regarded for its beneficial effect on soils both as a source of plant nutrition and for its influence on soil physical properties. However, many Australian Vertosols have quite small organic contributions, generally containing <2 % organic matter (Hulugalle and Entwistle 1997; Hulugalle *et al.* 2001; Vervoort *et al.* 2003). Consequently, several authors have questioned the importance of organic material to the structural stability and form of Vertosols (*e.g.* Jewitt *et al.* 1979; Coughlan 1984; Lu *et al.* 1998). The general view opposes this observation (*e.g.* Mukhtar *et al.* 1974;

Hubble 1984; Lal 1993; Coulombe *et al.* 1996a). The effects of organic matter on Vertosols was investigated by Warkentin (1982), who proposed that organic matter is important at a finer scale in swelling soils than in the non–swelling soil types. He suggested that organic matter was important at two scales; primarily to soil clusters (1–50 μm), and to a lesser extent, to soil micropeds (50–500 μm). This is contrary to the scale of influence in other soil types, where organic matter impacts on aggregates in the 500–5000 μm range. The absence of significant contributions of organic material to the >500 μm scale in Vertosols is associated with self–mulching behaviour. In the same way that tillage increases the loss of organic constituents, so to the self–mulching behaviour of Vertosols increases the rate of organic mineralisation.

Organic matter in Vertosols is frequently found on both external and internal clay surfaces. It forms clay–organic complexes strongly bound to small aggregates (Blokhuis 1982). However, the different organic fractions influence the formation of stable aggregates differently. Roots and fungal hyphae have an important role in stabilizing microaggregates and preventing dispersion. The importance of these in stabilizing aggregates, irrespective of the exchange cations present, was suggested by Barzegar *et al.* (1997). Furthermore, they found that the presence of organic matter in general, had a positive influence on the water stability of aggregates irrespective of clay type or sodicity. Chenu (1989) showed that the polysaccharide *scleroglucan* decreased the size of clay quasi-crystals of a smectite. This led to improved stability but increased the extent of soil swelling, thereby increasing the soil's void ratio and raising the moisture holding capacity. Kaolinite clays were affected differently; in these soils, the size of quasi-crystals was not affected, but stability was improved. Piccolo and Mbagwu (1989) found humic acids to generally be successful in improving stability of soil micro–aggregates and macro–aggregates, but they noted that excessive humic acid (>1 %) decreased the stability of micro–aggregates. This they attributed to the displacement of weakly bound clay particles by strongly chelating divalent and trivalent cations in complexes.

1.4.6 Sulfates, carbonates and oxides

In many Vertosols, carbonates (particularly lime), gypsum, and oxides act as binding agents and assist in buffering the soil system (Hubble 1984). In addition, these soils contain an array of silicates (*e.g.* Ca^{2+}, Na^{+} and K^{+} feldspars) other than the phyllosilicates, which are particularly sensitive to soil moisture and environmental conditions. Coulombe *et al.* (1996b) indicated that mineral dissolution, translocation, and precipitation due to wet–dry cycles, and the subsequent redistribution of various mineral phases in a soil profile, can impact on soil structure.

The Ca^{2+} and Na^{+} carbonates ($CaCO_3$ and Na_2CO_3) and gypsum ($CaSO_4.H_2O$) strongly influence the structural condition of soil. The solubility of these salts depends on pH and solution composition, with lime ($CaCO_3$) commonly present as concretions (Jewitt *et al.* 1979) in alkaline Vertosols (Ahmad 1996). Consequently, the rate of release of these soluble salts influences the ability of a soil to buffer changes in the soil solution from water applications (Shainberg *et al.* 1981). In solution $CaCO_3$ donates Ca^{2+}, which assists in reducing soil pH and in maintaining the TCC; this then, suppresses chemical dispersion forces (*e.g.* excessive ESP). Lime also acts as a binding agent (Keren and Ben–Hur 2003), cementing soil mineral material in soils with an alkaline pH. Gypsum is a common feature of the more arid Vertosols reflecting its relatively high solubility. Consequently, the depth of gypsum in a soil profile provides a guide to the depth of leaching under applied moisture (Jewitt *et al.* 1979; Ahmad 1996). The Na^{+} carbonates are also highly soluble and are readily leached. In soils, the presence of these carbonates is an indicator of very alkaline conditions (pH >9.5) (Coulombe *et al.* 1996b); such soils will have very large contributions of exchangeable Na^{+} and as a result, very poor structural stability.

The sesquioxides of Fe^{3+} and Al^{3+} act as binding or cementing agents of soil fabric (Wilding and Tessier 1988), but soils rich in iron oxides are generally acidic (*e.g.*, Oxisols and Krasnozems) (Mullins *et al.* 1991). The clay mineral suite of Vertic soils is degraded where abundant H^{+} is present; subsequently, oxides play a less significant role in alkaline Vertosols, particularly those dominated by smectitic phyllosilicates. The more reddish, better drained and more weathered Vertosols containing moderate amounts of kaolinite have relatively high contents of free iron oxide; these have greater structural stability and smaller aggregates. Free iron oxides reduce the ability of Vertosols to swell and consequently the characteristic properties of these soils are less pronounced (Blokhuis 1982).

1.5 The structural degradation of Vertosols

Soil structural failure occurs as soils undergo cycles of swelling and shrinkage. This is dependent on the texture and mineral suite and on the contributions of particular cations to the exchange complex and the soil solution. However, failure does not necessarily imply degradation. *Soil degradation* is defined as a loss or a reduction of actual or potential productivity, and is equal to a loss or reduction of soil structural function (Blum 1998; Lal 1998). There are two main forces involved in the degradation of Vertosols; the natural, due to soil forming factors and the anthropogenic, due to agricultural activities. These contribute to two principal forms of structural degradation: physical degradation and chemical degradation. The processes of physical disintegration (Ben-Hur *et al.* 1992)

and chemical dispersion result in clay dispersion, its migration (Felhendler *et al.* 1974; Levy and van der Watt 1988) and the plugging of soil pores (McIntyre 1956; Agassi *et al.* 1981). This is a major cause of decreased hydraulic conductivity in montmorillonitic, vermiculitic, and kaolinitic soils at ESP values less than 20 (Frenkel *et al.* 1978). In addition, Abu–Sharar *et al.* (1987) showed that in some cases dispersion has to be associated with slaking to reduce hydraulic conductivity because dispersed clay particles are mobile, easily illuviated and not able to clog large conducting pores.

1.5.1 The physical disintegration of Vertosols

It is well established that soil structural form will remain completely stable if an applied stress is less than the strength of the soil failure zones (Kay 1990). However, when attractive forces are overcome, aggregates fail (Kemper and Rosenau 1984). The deformation of structural form takes place where stress is applied, and where the weakest zones of the structural matrix fail. Thus, the application of increasing disruptive energy will result in the failure of aggregates of increasing strength (Kay 1990). This pattern implies a hierarchy of aggregates (Oades and Waters 1991); smaller aggregates are most resistant to disruption, and subsequently the ability of aggregates to resist failure reflects the arrangement of strength within this hierarchy. This hierarchical organisation exists in soils where the stability of aggregates is controlled by organic materials, but is of less relevance where cementing agents bind aggregates to one another (Oades and Waters 1991).

Physical degradation can be caused by the slaking of aggregates, the infilling of shrinkage cracks during wetting or by excessive overburden pressures (during tillage) that cause soil compaction (Yule and Willcocks 1996). This degradation results in a compacted soil structural form with an increased density and less porosity. The resulting structural arrangement is increasingly difficult to resile, and the work of Pillai and McGarry (1999) shows the importance of shrink–swell cycles in the structural repair of a physically degraded Vertosol. In addition to shrink–swell activity, soil moisture assists in maintaining aggregate strength. However, once water pressure becomes equal to or greater than the air pressure (Kemper and Rosenau 1984) aggregate coherence is no longer supported. The consequence of this is that freshly cultivated and weakly structured soils can slump or settle (Levy and van der Watt 1990). This reduces the distribution of soil porosity and impacts on water movement and the exploration and function of plant roots. Aggregate breakdown by water results from a variety of physico–chemical interactions (*e.g.* mineral suite and cation composition) and physical mechanisms (*e.g.* rainfall or tillage). It involves different scales of soil structure, from the interaction of clay particles to the macroscopic behaviour of aggregates (Tisdall and Oades 1982; Elliott 1986; Oades and Waters 1991). Coughlan (1979) studied 12 cracking clay soils and found that aggregate breakdown increased rapidly with wetting rate and reached a maximum at a rate equivalent

to rainfall of 50 mm hr^{-1}. Later, Loch (1982) found surface sealing to occur in a cracking clay soil at a rainfall intensity of 75 mm hr^{-1}. Raindrop impact releases a disruptive force and, where applied force exceeds cohesive force, aggregates break apart forming an array of microaggregates and individual particles (Quirk and Schofield 1955). In solution, these microaggregates and soil particles block near surface porosity (Le Bissonnais 1996). This results in increased bulk density of surface soils and reduced water infiltration (Rengasamy *et al.* 1984).

1.5.2 The chemical degradation of Vertosols

In Vertosols, chemical degradation occurs through two primary processes; either the pH becomes too acidic or to alkaline, or the contribution of exchangeable Na^+ increases sufficiently to cause excessive mineral swelling and clay dispersion. Halliwell *et al.* (2001) discussed increased soil sodicity that occurred through the application of irrigation waste waters containing elevated concentrations of Na^+. The mechanisms by which Na^+ contributes to degradation have already been discussed at length; increased swelling and clay dispersion lead to reductions in hydraulic conductivity and increases the soil bulk density. However, these processes rarely occur in the absence of mechanical stress. For example, Le Bissonnais (1996) described clay dispersion as a function of the physical force imparted by raindrop impact and the rate of wetting, and of the soil chemical attributes; exchangeable Na^+ content and EC.

1.6 Methods for determining the relative importance of structure–affecting soil attributes

Since the work of Fireman and Bodman (1939) and of Quirk and Schofield (1955), there has been a strong research emphasis aimed at studying the effect of water quality on soil structural characteristics. This has generally focused on the effects of water quality on the hydraulic conductivity of soils, providing an initial understanding of the way in which Na^+ influences swelling and dispersion. Consequently, hydraulic conductivity has sometimes been used as a surrogate measure of stability and desirable structural condition (*e.g.* Rengasamy *et al.* 1986; Keren and Ben–Hur 2003). More direct measures of structural stability and structural form are now widely applied. The determination of the stability of aggregates is generally based on three principles: *(i)*, the availability of simple procedures, *(ii)*, the ability to correlate results of stability measurements with aggregate–size distributions and field phenomena and, *(iii)*, the limitations of the method applied (Kemper and Rosenau 1986; Nimmo and Perkins 2002). The quantification of structural form for assessing the effects of management practices initially proved more elusive. Procedures commonly

involved surrogate measures to describe total porosity (*e.g.* bulk density) and effective pore size distributions (*e.g.* the moisture characteristic). However, in the last 20 years advances in computing power and stereological techniques have improved capabilities in this area. This has provided the ability to quantify structural form based on the differentiation of pore and solid phase components.

1.6.1 Determining the structural stability of Vertosols

Methods for determining the stability of soil aggregates were discussed by Kemper and Rosenau (1986). Two primary forces hold aggregates together in moist soils; the surface tension of the air–water interface and the cohesive tension in the liquid phase. These two forces pull adjacent particles of an aggregate together with increasing force as a soil dries and as drying continues, solute molecules and ions precipitate as inorganic semicrystalline compounds or amorphous organic compounds around particle–particle contacts, cementing particles to one another. Once the cohesive forces of the liquid phase no longer assist in maintaining aggregate stability (humidity <30 %) cementation maintains the structural arrangement. However, this cementation is crystalline and generally brittle, and once acted upon by mechanical force, will not re–form without the wetting and drying process.

Measuring the stability of soil aggregates is important for the development of diagnostic and management principles for different Vertosols. Consequently, a diversity of methods have been undertaken to characterise aggregate liberation (*e.g.* Rowell *et al.* 1969; Emerson and Chi 1977; Rengasamy 1982; Kemper and Rosenau 1984; Rengasamy *et al.* 1984; Raine and So 1993; Levy and Torrento 1995; Dontsova and Norton 2002). These methods were summarised by Field (2000) into six categories; *(i)*, immersion wetting techniques, *(ii)*, wet–sieving procedures, *(iii)*, end–over–end (EOE) shaking, *(iv)*, ultrasonic agitation, *(v)*, raindrop impact simulations and, *(vi)*, the assessment of surrogate soil properties. These all involve the wetting process, which itself is highly disruptive, where ion hydration and osmotic swelling forces pull water into inter–clay spaces. This forces layers apart and causes aggregates to swell (Kemper and Rosenau 1986). If the rate of wetting causes uneven swelling of individual aggregates, then shear planes develop and aggregates disintegrate.

The methods used to determine the stability of wet aggregates are classified into two types: *(i)*, those studying the macro–aggregate distribution (*e.g.* Emerson 1954, 1967; Matkin and Smart 1987) and, *(ii)*, those studying the micro–aggregate distribution (*e.g.* Quirk 1950). The micro–aggregate distribution is classed as particles <250 μm (Tisdall and Oades 1982; Oades and Waters 1991; Field and Minasny 1999), which consist chiefly of clay complexes, polyvalent cations and organic materials (Field and Minasny 1999). North (1976) describes the study of the micro–aggregate distribution as

being potentially more realistic in the study of surface soils where mechanical forces are prevalent. Three methods have been broadly adapted to study this size fraction: spontaneous dispersion (Rengasamy *et al.* 1984; Rengasamy *et al.* 1987), end–over–end disruption (Middleton 1930; Quirk 1950; So and Cook 1987; Field *et al.* 1997; Raine and So 1997; So *et al.* 1997; Field 2000) and ultrasonic agitation (North 1976; Raine and So 1994, 1997; Field and Minasny 1999; Field 2000). The use of spontaneous dispersion determines the quantity of clay–sized particles in suspension after minimal disruptive force (*e.g.* Rengasamy *et al.* 1984). This reflects the behaviour of surface soils during rainfall events where the soil is effectively protected by organic material, but where rapid wetting takes place. The EOE–disruption technique (*e.g.* So *et al.* 1997) and the ultrasonic agitation procedure are similar in that both apply disruptive energy to soil aggregates in water solutions in order to determine the proportion of liberated material or the particle size distribution of soils (*e.g.* Edwards and Bremner 1967). The level of aggregate disruption occurring after either EOE–disruption or ultrasonic agitation depends on the total energy applied and the uniform mixing of the soil suspension. Thus, Raine and So (1993) asserted that differences in dispersive energy consumed would represent differences in the quantity and type of bonding mechanisms in a soil. However, the application of these methods contain a number of inherent difficulties (North 1976). Currently, there is no standard method of assessment (*e.g.* Quirk 1950; So *et al.* 1997; Field 2000). This means that stability tests from different studies are not easily compared to each other, and that comparing structural stability assessments to field conditions is difficult.

To rank the stability of a number of soils for a given activity, in this case cotton production, soils must be considered on the same basis. In some cases this will involve ranking the various size fractions assessed in order of their importance *e.g.* in agricultural soils it is generally considered that a specific weight of large aggregates is more indicative of good structure than an equal weight of small aggregates (Kemper and Rosenau 1986). This is characterised by the *mean weight diameter*, which was summarized by Kemper and Rosenau (1986). The mean weight diameter is equal to the sum of products of the mean diameter of each size fraction and the proportion of the total sample weight occurring in the corresponding size fraction. This method of estimating stability is not suitable where a single or very few particle size fractions are sampled. Consequently, the comparison of soils is frequently conducted by determining a stability index. The stability index represents the quantity of a particular size fraction (*e.g.* dispersed <20 μm g g^{-1}), after aggregate liberation, as a percentage of the total original mass of that fraction (*e.g.* total soil mass <20 μm g g^{-1}). Hulugalle and Finlay (2003) determined a dispersion index for soil material less than 20 μm:

$$DI\,(\%) = \frac{weight\ of\ dispersed\ soil\ particles < 20\,\mu m}{total\ weight\ of\ soil\ particles < 20\,\mu m} \times 100 \qquad [3]$$

Despite the extent of work in this area there remain three primary concerns: *(i)*, the lack of a standard method of assessment has meant that much information cannot be compared between different studies and particularly between the work of different laboratories, *(ii)*, the evaluation of surrogate soil properties have not been strongly associated with observed differences in structural stability for different soil types, *i.e.* linking predictors with observed properties (*e.g.* Field *et al.* 1997; Surapaneni *et al.* 2002) and, *(iii)*, there has been limited comparison of laboratory measures of aggregate stability with the structural activity of Vertosols in the field; this has sparked much debate of the management applications of stability assessments.

1.6.2 Determining the structural form of Vertosols

The physical condition of soils can be determined from their structural form; for example, where the soil surface has been exposed to rain, any disintegration of aggregates can be used as an indicator of structural instability (Batey 2001). The structural form of soil profiles has historically been described in the field using visual assessment to give structure grade, ped shape and size, the soil fabric and soil macroporosity characteristics. For example, Ringrose–Voase and Sanidad (1996) used the intercept method 'in field' to measure the development of cracks in two puddled Vertosols of the Philippines as drying occurred. This was done by moving along a 7 m transect using a semi–cycle (1 m *r.*) to sample crack size either side of the transect and to gain an understanding of the development of cracks during drying. Descriptions of structural form are qualitative or semi–quantitative and can be used to detect hardsetting surfaces, plough layers, cracking patterns or soil compaction (*e.g.* Batey 2001).

Other methods provide a quantitative measure of the total porosity and the pore size distribution. Total porosity has often been obtained from bulk density determinations. However, such measurements provide no knowledge of the pore size distribution; this can be obtained from hydraulic conductivity studies (*e.g.* Cass and Sumner 1982) or the soil moisture characteristic. As an example, Barlow and Nash (2002) compared the moisture characteristics of an intact Ferrosol and an intact Dermosol. After repeated wet–dry cycles using different water quality treatments they were able to characterise small changes in structural condition. This technique has the obvious advantages of being rapid and descriptive, but the disadvantage of not allowing pore shape characteristics to be determined.

The quantitative assessment of soil structural form can be accomplished using image analysis. The application of various algorithms assist in determining the characteristics of binary images of soil sections (*see* Serra 1982). Currently this is conducted using image analysis software (*e.g.* Cattle *et al.*

2001), where structural attributes are defined using pixel counting procedures that characterise the pore space, solid space and the pore–solid interface. The problem, however, has remained the collection of images representative of soil structural form at a desired scale.

There are three broad methods of image analysis: *(i)*, the use of thin sections, *(ii)*, the increasingly popular application of X–ray computed tomography (CT–scanning) and, *(iii)*, the impregnation of soil columns with fluorescent resin. Thin sections have been used for many years to identify structural attributes and soil morphological characteristics. The advent of quantitative analysis has led to the reinvention of micromorphology as a procedure for identifying structural characteristics at a fine resolution. For example, Lebron *et al.* (2002) used thin sections and scanning electron microscopy to identify changes in the characteristics of porosity and aggregation of two soils, a silty loam and a fine sandy loam. Later, Fox *et al.* (2004) used thin sections to quantify changes in soil porosity with depth in a soil crust, and Nordt *et al.* (2004) used thin sections in their study of the genesis of Vertisols in humid climates. The process of image acquisition using micromorphology provides well–defined structural components. However, sample preparation and image acquisition can be laborious. In comparison, CT–scanning is a rapid and non–destructive method of identifying structural characteristics. This procedure has been applied predominantly in studies of soil–plant interactions (*e.g.* Heeraman *et al.* 1997; Hamza *et al.* 2001; Pierret *et al.* 2003; McNeill and Kolesik 2004). For example, Mooney (2002) and Pierret *et al.* (2002) used CT–scanning to describe root growth in soils by preparing 3D visualisations of pore structure. This technique has many advantages, *e.g.* it is neither labour intensive nor time consuming. However, equipment expenses, resolution limits (greater than ≈200 μm) and sample size limitations currently restrict its application. These problems are being rapidly overcome, *e.g.* Gregory *et al.* (2003) report on a prototype instrument being developed to assess samples up to ≈120 mm *d.* at resolutions greater than ≈50 μm. Consequently, CT–scanning is likely to provide a significant method of determining structural form in the near future. This will depend on equipment costs or availability of suitable medical scanners. The alternative to CT–scanning is the use of resins to impregnate soil columns or blocks. Using an epoxy–based fluorescent resin Moran *et al.* (1989), McBratney and Moran (1990) and McBratney *et al.* (1992) developed a relatively rapid and inexpensive method of obtaining images of soil sections. They applied stereological techniques to describe and estimate soil structural attributes from large soil samples. Similar techniques have been applied throughout the research community for the determination of structural characteristics (*e.g.* Ringrose–Voase 1996) and are described by Roesner (2003). These methods have used an array of different resin compounds to prepare soils for image acquisition and subsequent image analysis. In general, these procedures involve irrigating soil either in the laboratory or in the field with a resin mixture. Soil samples are sectioned in the horizontal or

vertical orientation and images obtained using film or digital media. Then each image is prepared and analysed for an array of pore and solid space descriptors.

The structural form obtained using image analysis procedures depends on the arrangement of soil aggregates and the distribution of void space. Currently there are two inherent problems in applying this procedure to Vertosols: *(i)*, in Vertosols, which shrink and swell, the development of cracking patterns is determined by differences in cohesion and cohesion is influenced by soil water content (Warkentin 1982) and, *(ii)*, the moisture content at sampling which most suitably represents the structural form is unknown. These concerns are well documented, *e.g.* Ringrose–Voase and Sanidad (1996). Recently, Pierret *et al.* (2003) studied the water content around developing roots using CT–scanning. This method is likely to provide a means by which crack development and changing soil moisture content can be monitored in Vertosols.

1.7 Predicting structural changes in Vertosols

Many authors have attempted to describe the roles of different soil physico–chemical properties in determining soil hydraulic properties, aggregate breakdown and clay dispersion. This has led to the use of several descriptive comparisons of observed soil behaviour. Descriptors have been developed in two ways; *(i)*, by addressing the critical levels of exchangeable Na^+, ESP or SAR in combination with electrical conductivity and, *(ii)*, by considering multifactorial relationships observed for different soil classes.

1.7.1 Critical levels of Na^+ and the relationship between exchangeable Na^+ and electrical conductivity

In comparing observations of structural stability, the majority of research has historically focused on the relationship between aggregate breakdown/dispersion and exchangeable Na^+, ESP or SAR. Subsequently, ESP has been widely used as a descriptor of potential instability and several critical levels have been proposed. However, the impact of electrical conductivity in reducing the affect of exchangeable Na^+ has been well established *e.g.* Quirk and Schofield (1955). This has led to the use of ESP or exchangeable Na^+ in combination with electrical conductivity as descriptors of potential stability. These are not the only important properties pertaining to aggregate stability and clay dispersion. Much work has investigated relationships between structural stability and the soil mineral suite, organic carbon content and exchange/solution chemistry. The relationships between organic matter and aggregate stability in different soil types were summarised by Tisdall and Oades (1982).

However, the physical behaviour of Vertosols has meant that the importance of organic material to structural stability is not well understood. In addition, descriptors of potential instability have avoided the inclusion of Vertosols, or have compared Vertosols alone as a soil class.

Vertosols with an ESP above a specific level, *i.e.* 5 (McIntyre 1979; McKenzie 1998) are described as sodic and are often considered to be potentially unstable. However, the principle of ESP was developed on the basis of the exchangeable Na^+ loading and not as a function of clay dispersion. Consequently, the use of a specific ESP as a single descriptor of dispersive behaviour is a flawed practice. This was demonstrated by Cook *et al.* (1992), who showed that Vertosols with ESP values as low as 2 can be dispersive if other soil properties are inadequate *e.g.* soils with small values of electrical conductivity are dispersed more readily, even at small exchangeable Na^+ contents, than soils with larger electrolyte concentrations. Consequently, in a review of knowledge gaps in current sodicity research, Surapaneni *et al.* (2002) cited the need for determination of the 'best' predictors of clay dispersion in Vertosols. Attempts have been made to overcome the use of ESP alone by considering ESP or exchangeable Na^+ relative to the $EC_{1:5}$ *e.g.* the ESI value (Blackwell *et al.* 1991; McKenzie 1998; Hulugalle and Finlay 2003). This was a response to the observation that increasing the electrical conductivity of solution assisted in suppressing expansion of the diffuse double layer of phyllosilicate clays. ESI was introduced by Blackwell *et al.* (1991) to facilitate comparisons between the macropore space and the electrochemical status of treated red–brown earths. These comparisons were based on the observed association between SAR–TCC and soil saturated hydraulic conductivity. They suggested that an increase in SAR (or ESP) or a decrease in TCC (or electrical conductivity), or changes in both, would cause changes in the extent of macroscopic swelling of clay phyllosilicate minerals, thereby influencing permeability, macroporosity and spontaneous dispersion. More recently, Hulugalle *et al.* (2003) compared ESP, ESI and $EC_{1:5}/Na^+_{exch}$ to describe observations of dispersed <20 μm soil particles. Using $EC_{1:5}/Na^+_{exch}$, they discounted the influence of CEC in an attempt to improve the ESI descriptor for predictions of dispersive behaviour in several Grey Vertosols. They found that the $EC_{1:5}/Na^+_{exch}$ and the ESI had greater correlation with dispersion than the ESP. However, they made no account for other soil physico–chemical properties such as the clay mineral suite or the contributions of exchangeable Ca^{2+} or Mg^{2+}.

1.7.2 Multifactorial relationships

Relationships between soil physico–chemical attributes (*e.g.* exchangeable cations, soil solution, organic carbon and mineral suites) have often been considered in defining the stability of soils. Yet currently there exists a dearth of information relating these characteristics, in combination, to the observed patterns of soil structural stability in Vertosols. In an early attempt at predicting the

stability of soils, Rengasamy *et al.* (1984) developed a scheme for the classification of dispersive potential in red–brown earths (Chromosols and Sodosols). Initially, they had included seven Vertosols (black earths) and the dispersion of all the soil samples did not show a significant correlation with the SAR or TCC. However, they found a significant correlation between the dispersion of only the red–brown earth samples and values of TCC and SAR. As a result, they restricted their model to soils with similar clay mineral suites. This model compares the dispersion of red–brown earths at different intervals of SAR and TCC (Figure 1.12). A description of classification terms used in Figure 1.12 is given in Table 1.4.

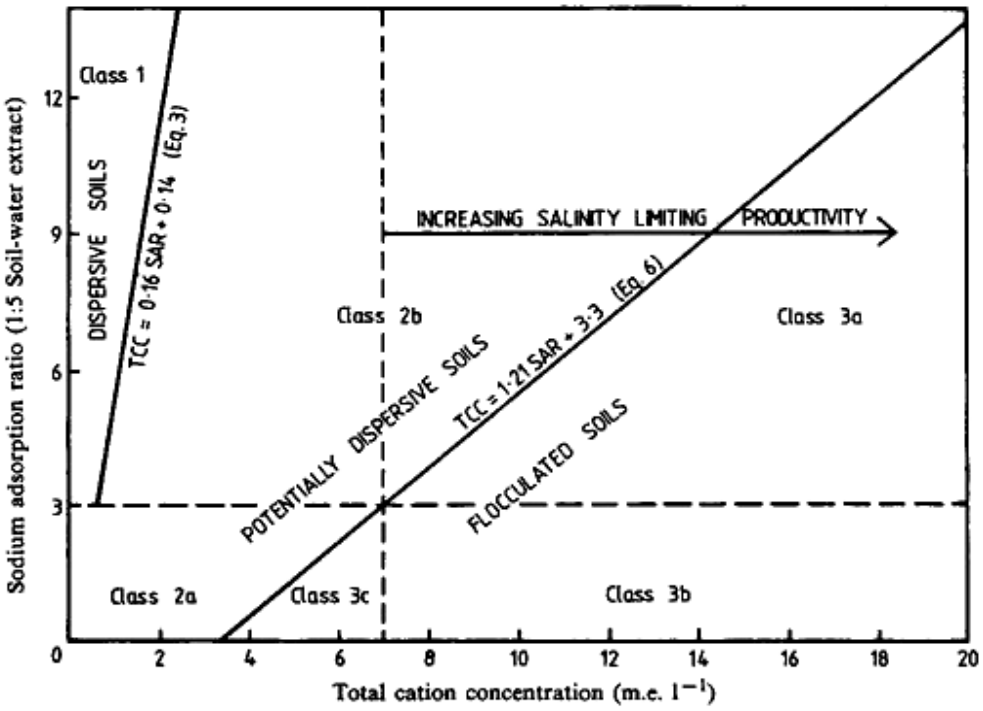

Figure 1.12 A model describing the stability of clay in red–brown earths (Rengasamy *et al.* 1984).

This work provided the basis for the future development of predictive indices of structural stability. However, there are deficiencies in this classification scheme that prevent its application across all soil types; the most significant of these being that clay mineral suites are not considered in the scheme. Unlike the red–brown earths used by Rengasamy *et al.* (1984), there is significant variation in the clay phyllosilicate suites of Vertosols (*e.g.* Shiel *et al.* 1988; Hussein and Adey 1995; Vervoort *et al.* 2003), which will affect the propensity for dispersion. A predictive tool for determination of the structural stability of Vertosols must include this parameter or a surrogate estimate of the phyllosilicate suite, *e.g.* CEC. In addition to these considerations, the role of organic matter in Vertosols is poorly understood, and subsequently the total organic contribution is often used to describe wet–aggregate stability (*e.g.* Tisdall and Oades 1982). However, more consideration must be given to the contribution of organic materials in determining the stability of Vertosols.

Table 1.4
Classes applied by Rengasamy *et al.* (1984) in their structural stability classification scheme for red–brown earths

Class			Description
1.	Dispersive soils		Soils that undergo spontaneous dispersion where TCC <0.16 SAR + 0.14. The stability of such soils is generally controlled by Na^+ and these soils have severe problems associated with crusting and reduced porosity.
2.	Potentially dispersive soils *(soils which disperse after shaking)*	*(a)*	Soils from the A–horizon with a SAR <3, requiring a TCC >1.21 SAR + 3.3 to maintain structural stability. Therefore these soils will have problems when in contact with water of low TCC and can form surface crusts
		(b)	Soils from the A–horizon with a SAR >3, requiring a TCC >1.21 SAR + 3.3 to maintain flocculation. Unlike 2*a*, these soils have the potential to disperse spontaneously when leached without the addition of Ca^{2+} compounds.
3.	Flocculated soils *(EC large enough to maintain flocculation)*	*(a)*	Soils in which the SAR >3 and where TCC exceeds flocculation value are deemed saline–sodic.
		(b)	Soils in which the SAR <3 and where TCC exceeds flocculation value are deemed saline and are dominated by non–Na^+ salts. These soils have no physical problems, and leaching requirements depend on the salt tolerance of prospective crops.
		(c)	Soils in which the SAR <3 and where TCC is ideally similar to the flocculation value. These soils are neither saline nor sodic.

During the early 1990s, Quirk and Murray (1991) reviewed the structural stability literature with a focus on swelling pressures and interparticle forces present at the surfaces of clay mineral species, in relation to double layer theory and both exchangeable Ca^{2+} and Na^+. They discussed the micro–aggregate environment and gave brief consideration to organic material and its various components. However, they remained focussed on the concept of threshold concentration for describing solution constraints that limit clay dispersion, as defined by Quirk and Schofield (1955). The threshold concentration represents the concentration of an electrolyte solution which results in a 10–15 % reduction in soil permeability, or the concentration at which there is a drastic increase in aggregate breakdown, swelling and dispersion. This will vary according to other soil physico–chemical characteristics. Subsequently, current predictors of structural stability in Vertosols are incomplete and this was highlighted by Surapaneni *et al.* (2002). They cited the need for the modelling of sodification processes in relation to irrigation water composition and identified a requirement for the development of a more suitable understanding of salinity–sodicity interactions, specifically in relation to clay mineralogy, organic carbon and ionic chemistry.

1.8 Current knowledge deficiencies regarding the structural condition of Vertosols

Maintaining or improving soil structural condition is important to agricultural producers using Australian soils. Currently, there is a vast body of work focusing on the structural condition of many of these soil types, particularly red–brown earths (Chromosols, Sodosols and Kurosols). However,

there is significant conjecture as to the relevance of the various indicators currently applied to predict structural instability. It is also apparent that much of the existing information is not applicable to Vertosols and there appears to be a lack of work characterising the structural condition of this soil type. Specifically, there is a dearth of descriptive information relating the combined effects of sodicity, salinity and soil physico–chemical properties to the structural form and structural stability of Vertosols. In cases where this information is available, from moisture characteristics or surrogate measures of porosity, this has not been directly compared with other measures of structural form such as pore/solid descriptors obtained from image analysis. McGarry (1996) indicated that the present challenge with research into the structural condition of Vertosols is not to discuss the range of soil structures possible, but to investigate the interaction between physico–chemical properties, external influences and soil forming processes in order to explain the difference between 'good structure', desirable physical properties, inherent agricultural potential and sustainability.

Furthermore, the availability of good quality water is potentially a serious constraint for future irrigated agricultural production in Australia (Ashton and Hanna 2002). This is particularly applicable in regions where river waters are already showing a trend of increasing EC, *e.g.* the Darling River (Bourke) or the Lachlan River (Hillston) (Jolly *et al.* 2001). Subsequently, it is anticipated that water supplies of decreasing quality will become more important for the irrigation of Vertosols. This will influence the structural condition of this soil type and the potential effects should be estimated to assist in sustainable soil management. A predictive tool of the sort required was proposed by Rengasamy *et al.* (1984), but it is not directly transferable to the characterisation of dispersion in Vertosols. Consequently, a similar prediction describing the stability of irrigated Vertosols is required. To develop such a model a database must be prepared containing a description of the structural stability of different Vertosols used in irrigated agriculture. The stability of these soils must be assessed using different disruptive forces and using different increments of water quality. Then, the effect of irrigating Vertosols with different levels of water quality can be compared to determine the effect of increased solution Na^+ on the soil chemical properties (*e.g.* exchangeable cations), structural stability, structural form and water retention attributes.

Chapter 2

A DESCRIPTION OF NINE VERTOSOLS USED FOR COTTON PRODUCTION

A DESCRIPTION OF NINE VERTOSOLS USED FOR COTTON PRODUCTION

~

Profile: *ōis līmeāmenta (L): a formal summary or analysis of data representing descriptive features or characteristics*

~

2.1 Introduction

Vertosols are widely distributed across central and western regions of eastern Australia and typically occur in close proximity to various river systems. The parent materials of these soils are usually alluvial deposits transported from higher positions in each catchment. The depositional environments of the various valleys each have significant climatic variation, influencing soil formation and rates of mineral weathering. Consequently, Vertosols in NSW tend to have different physico–chemical properties and cotton production practices must account for a variety of soil attributes. This chapter describes the basic physico–chemical attributes and the mineral composition of a number of Vertosols sampled for this work from various cotton–producing regions distributed throughout NSW.

2.2 Sampling regions

Soil was collected from nine cotton–producing Vertosol profiles across four regions of NSW; from the Bourke and Hillston cotton–growing regions and from the lower Gwydir (Moree) and lower Namoi (Narrabri) catchments. Figure 2.1 shows the distribution of sampling regions across the irrigated cotton–producing regions of eastern Australia, the topographic and geological maps are given for each site in appendix 1. Table 2.1 details the average temperatures and rainfall of each region. The Köppen system classifies these climatic regimes as semi–arid grasslands (Bourke), as temperate (Hillston) and as subtropical (Gwydir and Namoi) (Australian Department of Trade and Resources 1982).

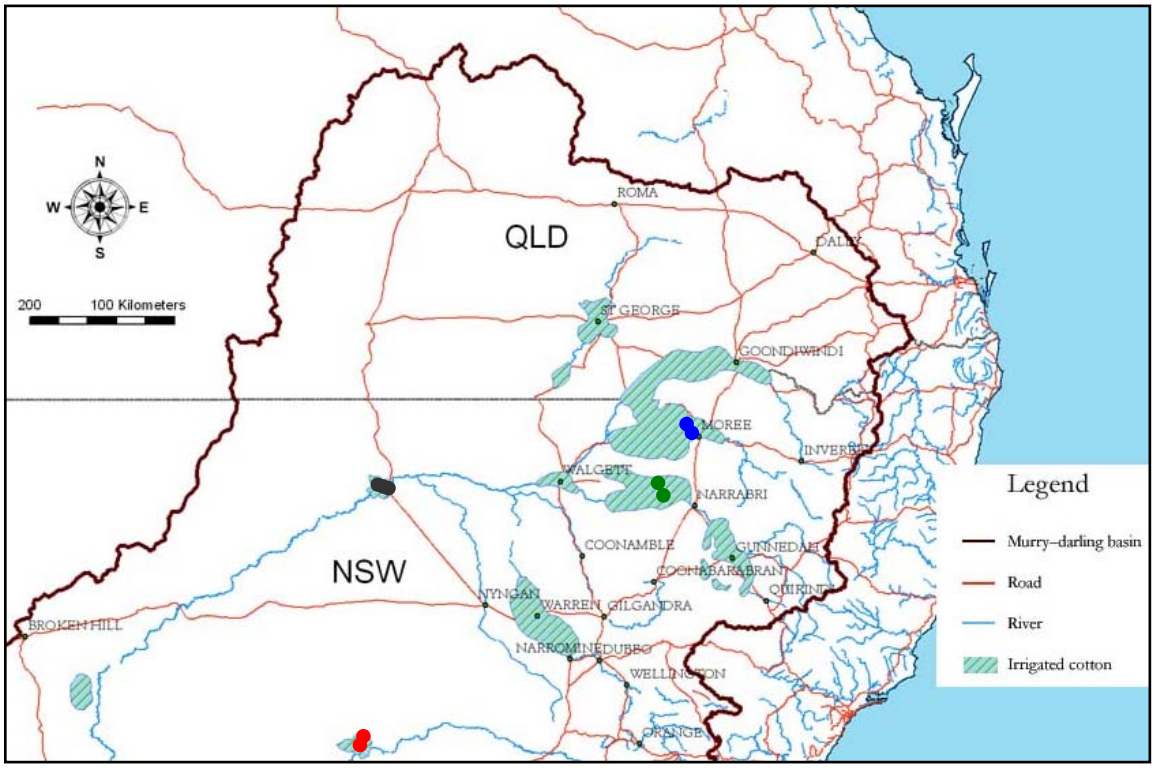

Figure 2.1 Cotton–producing regions of eastern Australia, including the nine soil sampling locations; three cotton–fields from Bourke (●) and two cotton–fields each from Hillston (●), Moree (●) and Narrabri (●) (Odeh *et al.* 2004).

Table 2.1
The average annual rainfall and temperature for each sampling region

Valley	Annual Rainfall[a]	Annual Temperature[a] (°C)	
	(mm)	Minimum	Maximum
Darling River Bourke	355	13	28
Lachlan River Hillston	366	11	24
Lower Gwydir Valley Moree	579	12	28
Lower Namoi Valley Narrabri	643	12	27

[a] Obtained from the Australian Government, Bureau of Meteorology (www.bom.gov.au/climate/averages).

2.3 Soil profiles

In each region, soil profiles were sampled to reflect different degrees of sodicity; this generally involved the sampling of one field with desirable structural condition and one field with undesirable structural condition, where undesirable conditions were thought to be the result of soil sodicity. Each soil profile was sampled by vertically inserting a hydraulically driven corer into a planting ridge at the tail drain end of an irrigated cotton field and away from any wheeled furrows. Soil cores were obtained according to the techniques described by McIntyre (1974).

The soil cores (50 mm *d.*) were collected to a depth of 1.0–1.2 m, and each core was segmented to give a series of soil samples at increments of 0.2 m from the soil surface. The soil was characterised in this way as smearing was evident at the outer surface of each core and this made it difficult to distinguish each horizon.

In the field, an array of soil attributes were described for each depth increment (Tables 2.2–2.5); the Munsell® soil colour, soil texture, Raupach pH, the presence of carbonates (using HCl) and/or inclusions and soil dispersion by immersion of aggregates in water. At sampling each soil profile was strongly structured and several had a surface mulch of aggregates. These soils were classified as Vertosols according to the Australian Soil Classification scheme (Isbell 1996), and range in colour class from red to grey and black. In Australia, the suborder classes of Red, Grey and Black are thought to represent 10 %, 27 % and 41 % of all assessed Vertosols respectively (Isbell *et al.* 1997). The texture grade of these Vertosols varied between light and medium clays at the soil surface, to between light–medium and heavy clays in the subsoil. They had surface pH values of 7–9 and exhibited increasing alkalinity with depth. In general, the surface samples did not disperse when immersed in water, but dispersion tended to increase with depth.

2.3.1 The Bourke cotton–producing region

In the Bourke cotton–growing region three irrigated cotton fields were sampled; B001 (0391759 m E, 6675838 m N) (Figure 2.2*a*), B002 (0387008 m E, 6672194 m N) and B003 (0382867 m E, 6674031 m N) (Figure 2.2*b*). The surface of each of these profiles is self–mulching, and they are classified as Grey Vertosols. These profiles, on inspection, are similar and there was little evidence from field observation of differences in soil characteristics (Table 2.2). A uniform increase in clay content occurs with depth, increasing from light and medium clay textures at the soil surface to medium and heavy clay texture groups in the subsoil. Using hand texturing, profiles B002 and B003 both show fluctuations in texture class, generally becoming 3–4 texture grades heavier between the surface soil and subsoil. This characteristic may be attributed to variations in the alluvial deposits that formed the soil parent material. An alkaline reaction is evident at the soil surface of each profile using Raupach reagent (pH 8.0–8.5), and only slight increases in pH are observed as depth increases. Dispersion tests indicate moderate to serious dispersion for all depths when aggregates from B001 and B003 are placed in de–ionised water. The only exception for these soils is the 0.0–0.2 m depth of profile B002, where negligible dispersion was observed. This site is situated approximately 100 m from an irrigation storage facility and at distances less than 50 m from this facility, a thin surface crust of salt is evident, suggesting surface salination. This appears to have affected the growth of cotton plants at B002, which at sampling were visibly smaller than plants at greater distances from

the storage facility. This salt crust is not observed at sites B001 or B003. At these sites inclusions are evident; B001 contained visible gypsum crystals at depths greater than 0.6 m, and B003 contained visible inclusions of $CaCO_3$ at depths greater than 0.4 m.

Figure 2.2 Cotton fields B001 *(a)* and B003 *(b)*. These were sampled from the Bourke cotton–growing area.

Table 2.2
Field description of three soil profiles from the Bourke cotton–growing region

	B001	B002	B003
0.0 m	Dark greyish brown light clay (10 YR $4/2_{moist}$, 7.5 YR $4/2_{dry}$) with a pH of 8.0 and moderate dispersion	Dark greyish brown medium clay (10 YR $4/2_{moist}$, 10 YR $5/2_{dry}$) with a pH of 8.5 and negligible dispersion	Greyish brown light medium clay (2.5 Y $5/2_{moist}$, 2.5 Y $5/2_{dry}$) with a pH of 8.5 and moderate dispersion
0.2 m	Dark greyish brown medium clay (10 YR $4/2_{moist}$, 10 YR $5/2_{dry}$) with a pH of 8.5 and serious dispersion	Brown light medium clay (7.5 YR $5/3_{moist}$, 10 YR $5/2_{dry}$) with a pH of 8.5 and negligible to moderate dispersion	Greyish brown medium clay (2.5 Y $5/2_{moist}$, 2.5 Y $5/2_{dry}$) with a pH of 8.0 and serious dispersion
0.4 m	Greyish brown light clay (10 YR $5/2_{moist}$, 10 YR $6/2_{dry}$) with a pH of 8.0 and serious dispersion	Brown light medium clay (10 YR $5/3_{moist}$, 10 YR $6/2_{dry}$) with a pH of 8.5, serious dispersion but with small infrequent carbonate inclusions	Greyish brown medium clay (10 YR $5/2_{moist}$, 10 YR $5/2_{dry}$) with a pH of 9.0, serious dispersion and gave a minor reaction for carbonates
0.6 m	Light brownish grey heavy clay (10 YR $6/2_{moist}$, 10 YR $6/2_{dry}$) with a pH of 8.0, serious dispersion but with gypsum crystals present	Brown medium clay (10 YR $5/3_{moist}$, 10 YR $6/3_{dry}$) with a pH of 8.5 and serious dispersion	Greyish brown medium clay (10 YR $5/2_{moist}$, 10 YR $6/2_{dry}$) with a pH of 9.0, serious dispersion and visible carbonates
0.8 m	Brown heavy clay (10 YR $5/3_{moist}$, 10 YR $6/3_{dry}$) with a pH of 8.0, serious dispersion but with gypsum crystals present	Brown light medium clay (10 YR $5/3_{moist}$, 10 YR $6/3_{dry}$) with a pH of 8.5 and serious dispersion	Greyish brown heavy clay (10 YR $5/2_{moist}$, 10 YR $6/3_{dry}$) with a pH of 8.5, serious dispersion and visible carbonates
1.0 m	Brown heavy clay (10 YR $5/3_{moist}$, 10 YR $6/3_{dry}$) with a pH of 8.0, serious dispersion but with gypsum crystals present	Brown heavy clay (10 YR $5/3_{moist}$, 10 YR $6/3_{dry}$) with a pH of 8.5 and serious dispersion	Brown medium clay (10 YR $5/3_{moist}$, 10 YR $6/3_{dry}$) with a pH of 8.5, serious dispersion and visible carbonates
1.2 m			

2.3.2 The lower Gwydir cotton–producing region

Two cotton fields were sampled from the lower Gwydir valley; G001 (0770426 m E, 6740299 m N) (Figure 2.3*a*) and G002 (0756000 m E, 6767307 m N) (Figure 2.3*b*). These soils have a self–mulching surface and are classified as Black Vertosols (Table 2.4). These profiles are uniformly clayey throughout; with depth, G001 becomes slightly lighter in texture, while G002 becomes slightly heavier. These soils exhibit a neutral topsoil pH, and are increasingly alkaline with depth. The topsoils are not dispersive in de–ionised water, but at increasing depth serious dispersion occurs. All layers of soil profile G001 at depths greater than 0.4 m show serious dispersion. This contrasts with the intermediate surface layers (<0.8 m) of G002; in these layers only negligible to slight dispersion occurs. Carbonate inclusions are not observed in any layer of profile G001. These are evident near the soil surface of G002, but are not observed at depths greater than 0.4 m.

Figure 2.3 Cotton fields G001 *(a)* and G002 *(b)*. These were sampled from the lower Gwydir cotton–growing area.

Table 2.3
Field description of two soil profiles from the lower Gwydir cotton–growing region

	G001	G002
0.0 m	Very dark brown light medium clay (10 YR $2/2_{moist}$, 10 YR $3/2_{dry}$) with a pH of 7.5 and negligible dispersion	Black light medium clay (7.5 YR $2.5/1_{moist}$, 10 YR $3/1_{dry}$) with a pH of 8.0, negligible dispersion and carbonates to 3 mm *d.*
0.2 m	Black light medium clay (7.5 YR $2.5/1_{moist}$, 10 YR $3/1_{dry}$) with a pH of 8.0 and negligible dispersion	Very dark grey medium clay (2.5 Y $3/1_{moist}$, 2.5 Y $4/1_{dry}$) with a pH of 8.5, negligible dispersion and carbonates to 2 mm *d.*
0.4 m	Very dark greyish brown light medium clay (2.5 Y $3/2_{moist}$, 2.5 Y $4/2_{dry}$) with a pH of 8.5, some carbonates and serious dispersion	Very dark grey medium clay (10 YR $3/1_{moist}$, 2.5 Y $3/1_{dry}$) with a pH of 8.5 and negligible dispersion
0.6 m	Very dark greyish brown light medium clay (2.5 Y $3/2_{moist}$, 2.5 Y $4/2_{dry}$) with a pH of 8.0 and serious dispersion	Dark grey light medium clay (10 YR $4/1_{moist}$, 2.5 Y $4/1_{dry}$) with a pH of 8.0 and negligible to moderate dispersion
0.8 m	Dark yellowish brown light clay (10 YR $3/4_{moist}$, 10 YR $5/4_{dry}$) with a pH of 8.0, some carbonates and serious dispersion	Dark grey light medium clay (10 YR $4/1_{moist}$, 2.5 Y $4/1_{dry}$) with a pH of 8.5 and serious dispersion
1.0 m	Very dark greyish brown light clay (10 YR $3/2_{moist}$, 10 YR $4/2_{dry}$) with a pH of 8.5 and serious dispersion	Dark grey medium clay (10 YR $4/1_{moist}$, 2.5 Y $4/1_{dry}$) with a pH of 9.0 and serious dispersion
1.2 m		

2.3.3 The Hillston cotton–producing region

Two irrigated cotton fields, H001 (0355195 m E, 6304641 m N) (Figure 2.4) and H002 (0360751 m E, 6319373 m N) were sampled in the Hillston cotton–growing region. Profile H001 has a strongly structured epipedal surface horizon. This contrasts with the H002 profile, which appeared massive

at the time of sampling due to a recent irrigation application. These profiles are classified as Red and Grey Vertosols respectively (Table 2.4).

The H001 soil profile contains a rapid colour change, from red in the upper soil layers, to a yellowish brown (0.6–0.8 m) and then to a light olive brown (>0.8 m). This is associated with a decrease in clay content at these depths. The upper layers (<0.6 m) show serious dispersion when aggregates are placed in de–ionised water. In contrast, the soil layers >0.6 m do not disperse and carbonate inclusions are present in these layers.

The H002 profile has a grey colour class in the upper soil layers, but like H001 this profile becomes yellowish brown at depths >0.8 m. Similarly, this soil has less clay in soil layers greater than 0.6 m depth, than nearer the surface. Like H001, where pH increases with depth, H002 shows increasing alkalinity with depth, but is more alkaline than H001. Carbonate inclusions are present at all depths in this profile. Surface aggregates of the H002 profile are not dispersive when immersed in de–ionised water. However, as depth increases from the topsoil layer, aggregates are increasingly dispersive.

Figure 2.4 Cotton field H001 sampled from the Hillston cotton–growing area.

Table 2.4
Field description of two soil profiles from the Hillston cotton–growing region

	H001	H002
0.0 m	Dark reddish brown light medium clay (5 YR $3/4_{moist}$, 5 YR $4/4_{dry}$) with a pH of 7.5, visible quartz grains to 2 mm *d.* and moderate to serious dispersion	Dark greyish brown light clay (10 YR $4/2_{moist}$, 10 YR $5/2_{dry}$) with a pH of 9.0, carbonate inclusions and negligible dispersion
0.2 m	Dark reddish brown light medium clay (5 YR $3/4_{moist}$, 7.5 YR $4/4_{dry}$) with a pH of 8.5 and serious dispersion	Dark greyish brown light medium clay (10 YR $4/2_{moist}$, 10 YR $5/2_{dry}$) with a pH of 9.5, carbonate inclusions and negligible to moderate dispersion
0.4 m	Reddish brown light medium clay (5 YR $4/4_{moist}$, 7.5 YR $4/6_{dry}$) with a pH of 9.0, carbonates to 2 mm *d.* and serious dispersion	Brown heavy clay (10 YR $4/3_{moist}$, 10 YR $5/3_{dry}$) with a pH of 9.5, carbonate inclusions and serious dispersion
0.6 m	Yellowish brown medium clay (10 YR $5/4_{moist}$, 2.5 Y $6/4_{dry}$) with a pH of 9.0, carbonates to 2 mm *d.*, slight mottling and negligible dispersion	Dark yellowish brown light medium clay (10 YR $4/4_{moist}$, 10 YR $5/4_{dry}$) with a pH of 9.5, carbonate inclusions and serious dispersion
0.8 m	Light olive brown light clay (2.5 Y $5/4_{moist}$, 2.5 Y $6/4_{dry}$) with a pH of 9.0, carbonates, slight mottling and negligible dispersion	Yellowish brown light medium clay (10 YR $5/4_{moist}$, 10 YR $6/4_{dry}$) with a pH of 9.5, carbonate inclusions and serious dispersion
1.0 m	Light olive brown light clay (2.5 Y $5/4_{moist}$, 5 Y $7/4_{dry}$) with a pH of 8.5, slight mottling and negligible dispersion	Yellowish brown light clay (10 YR $5/4_{moist}$, 10 YR $6/4_{dry}$) with a pH of 9.5, carbonate inclusions and negligible dispersion
1.2 m		

2.3.4 The lower Namoi cotton–producing region

Two irrigated cotton fields were sampled from the lower Namoi valley; N001 (0731394 m E, 6684351 m N) (Figure 2.5) and N002 (0750001 m E, 6655992 m N). Profiles N001 and N002 are Black Vertosols, and have largely uniform Munsell® colour throughout (Table 2.5). Profile N001 had, at the time of sampling, a self–mulched surface layer. The second profile (N002) had a strongly structured topsoil, but was not self–mulching. Both of these Vertosols have a consistent texture grade; N001 has a light medium clay texture, while N002 has a medium clay texture throughout. The pH values of both profiles are strongly alkaline. The layers of N002 are not dispersive at depth, where aggregates are immersed in de–ionised water. In comparison, N001 is moderately to seriously dispersive in all the soil layers sampled.

Figure 2.5 Cotton field N001 sampled from the lower Namoi cotton–growing area.

Table 2.5
Field description of two soil profiles from the lower Namoi cotton–growing region

	N001	N002
0.0 m		
	Very dark grey light medium clay (10 YR $3/1_{moist}$, 10 YR $4/1_{dry}$) with a pH of 9.5, carbonate inclusions and moderate dispersion	Very dark grey medium clay (5 YR $3/1_{moist}$, 7.5 YR $3/2_{dry}$) with a pH of 9.5, few carbonates and negligible dispersion
0.2 m		
	Dark brown medium clay (7.5 YR $3/2_{moist}$, 10 YR $3/2_{dry}$) with a pH of 9.0, carbonate inclusions and moderate dispersion	Very dark brown medium clay (7.5 YR $2.5/2_{moist}$, 10 YR $3/2_{dry}$) with a pH of 9.0, carbonates and negligible dispersion
0.4 m		
	Very dark greyish brown light medium clay (10 YR $3/2_{moist}$, 10 YR $4/2_{dry}$) with a pH of 9.0, carbonate inclusions and serious dispersion	Very dark brown light medium clay (7.5 YR $2.5/2_{moist}$, 10 YR $3/3_{dry}$) with a pH of 8.5, carbonates and negligible dispersion
0.6 m		
	Very dark greyish brown medium clay (10 YR $3/2_{moist}$, 10 YR $3/3_{dry}$) with a pH of 9.5, carbonate inclusions and serious dispersion	Very dark brown light medium clay (7.5 YR $2.5/2_{moist}$, 10 YR $3/2_{dry}$) with a pH of 8.5, carbonates and negligible dispersion
0.8 m		
	Dark brown light medium clay (7.5 YR $3/3_{moist}$, 7.5 YR $3/4_{dry}$) with a pH of 9.5, carbonates and moderate dispersion	Very dark greyish brown medium clay (10 YR $3/2_{moist}$, 10 YR $4/2_{dry}$) with a pH of 9.0, carbonates and negligible dispersion
1.0 m		

2.4 The physico–chemical properties of the nine Vertosols

Sampled soil profiles were transported to the laboratory and prepared for analysis by grinding air–dry aggregates to pass through a 2 mm sieve. Prior to grinding small quantities of air–dry soil aggregates were retained for specific tests. Soil samples from each field were assessed for an array of soil physico–chemical characteristics; soil organic carbon content, the particle size distribution, Aggregate Stability in WATer (Field *et al.* 1997), soil pH and a number of attributes describing the soil solution and the exchangeable cations. Following are the methods used to determine these

characteristics and the average values of these properties for each soil depth increment of the nine soil profiles.

2.4.1 Physico–chemical methods

The *organic carbon* content was determined for each soil sample according to an adjusted method of Walkley and Black (McLeod 1975). Two grams of air–dry soil were ground to pass through a 200 µm sieve and digested in $K_2Cr_2O_7$. The resultant soil solution was titrated against $FeSO_4$ and the organic carbon content was determined according to the quantity of $K_2Cr_2O_7$ consumed in reaction with $FeSO_4$. Soil organic carbon content is presented as an oven–dry percentage of total soil mass.

The *particle size distribution* (PSD) was determined by adapting the pipette method of Gee and Bauder (1986). Thirty grams of air–dry soil were placed on an end–over–end shaker for 48 hrs after 50 ml sodium hexa–metaphosphate solution (HMP) and 300 ml of de–ionised water were added. The resultant soil solution was transferred to a 50 µm sieve and after wet sieving, the coarse sand fraction (>50 µm) was retained. The remaining soil solution was transferred to a measuring cylinder, filled to 1 L using de–ionised water, homogenised and after appropriate sedimentation periods, the silt (20–2 µm) and the total clay (<2 µm) fractions were sampled using a 25 ml pipette. All fractions were oven dried (105 °C) and the fine sand fraction was determined by difference. The contribution of each of the four size fractions was determined as a percentage of the total soil oven–dry mass: >50, 50–20, 20–2, <2 µm (%). In general, no pre–treatments were applied, but where flocculation occurred during sedimentation, soils were treated to remove soluble salts. This was done by placing the required quantity of air–dry soil into 40 mm dialysis tubing after soil was dispersed in 50 ml sodium hexa–metaphosphate solution (HMP) and 300 ml of de–ionised water on an end–over–end shaker for 48 hrs. The soil solution filled dialysis tubing was placed in a bucket of de–ionised water. The de–ionised water was changed at intervals of three days over a period of three weeks, giving successive dilution of soluble soil salts. An estimate of each size fraction (>50, 50–20, 20–2, <2 µm) was obtained, after each soil solution was transferred to a 1 L measuring cylinder, using the pipette method described.

After the particle size distribution was determined for each soil sample, 0.1 L of each clay suspension was obtained from each measuring cylinder after the appropriate settling period. The clay fraction was separated using centrifugal force (Jackson 1956) to give the *coarse clay fraction* (2–0.2 µm) and the *fine clay fraction* (<0.2 µm). The sedimentation time (T) for a particle of radius r (0.2×10^{-3} cm) to fall a specified depth was determined as:

$$T = \frac{\eta \log_{10}\left(R/S\right)}{3.81N^2 r^2 \Delta S} \qquad [4]$$

where, η is the viscosity of solution at 20 °C, R is the radius (cm) of rotation at the desired sampling depth, S is the radius (cm) of rotation at the surface of the solution, ΔS is the difference in specific gravity (*i.e.* that between clay and water), and N is the number of revolutions per second.

The *Aggregate Stability in WATer* (ASWAT) test was carried out according to Field *et al.* (1997). Three air–dry soil aggregates (2–5 mm) were gently placed in a Petri dish filled with de–ionised water. The degree of dispersion was assessed after 10 mins and after 2 hrs and a qualitative score between 0 and 4 assigned at each time step; a score of 0 represents no dispersion and that of 4 corresponds to maximum dispersion. If aggregates had not dispersed after 2 hrs, soil was worked at its plastic limit to remove soil structure; 3 re–moulded soil units (2–5 mm) were then placed in de–ionised water and the dispersion assessment was repeated as for soil aggregates. A final ASWAT score was derived according to the observed dispersion. If aggregates dispersed after 10 mins, 12 was added to the score, and where aggregates dispersed after 2 hrs, 8 was added to the score. This gave a range of values of 9–16 for air–dry aggregates. If re–moulded soil dispersed after 10 mins, 4 was added to the score and where re–moulded samples dispersed after 2 hrs this score was recorded, giving values between 0 and 8 for re–moulded soils. This gives a final ASWAT score of between 0 and 16: scores 0–1 are representative of soils with negligible dispersion, scores 2–6 are representative of soils with moderate dispersion on re–moulding and scores 7–16 are representative of soils with the potential for serious dispersion (McKenzie 1998).

The *soil pH* was determined for each soil sample using a 1:5 (soil:$CaCl_2$) ratio. To five grams of air–dry soil, 25 ml of 1 M $CaCl_2$ solution was added. Soil solutions were shaken for 1 hr and pH was determined at 20 °C using a combined glass electrode.

The *soil solution* was extracted for each soil using a ratio of 1:5 (soil:de–ionised water) (Rhoades 1982). Soil solutions were shaken end–over–end for 1 hr and then a clear supernatant was obtained by centrifugation at 10,000 rpm (15 mins). The supernatant solution was used for measurement of EC (dS m^{-1}) using a conductivity cell. Then each supernatant was diluted to the appropriate level and an ionising suppressant added, containing 2222 µg ml^{-1} CsCl and 1650 µg ml^{-1} $SrCl_2$. The prepared dilutions were used to determine the contributions of Ca^{2+}, Mg^{2+} and Na^{+} ($mmol_{(+)}$ L^{-1}) to the soil solution using the air–acetylene flame of an Atomic Absorption Spectrometer. The concentrations of each cation were used to determine the SAR (($mmol_{(+)}$ L^{-1})$^{1/2}$) (equation 2) of each soil solution.

The suite of *exchangeable cations* was determined for each soil using a 1 M NH_4Cl displacing solution prepared in 60 % ethanol at pH 8.5 according to Rayment and Higginson (1992). For the Vertosols studied here, 2.5 g air–dry soil were mixed with 5 g acid–washed sand and placed in a syringe barrel lined with 32–17 grade filter pulp. Using a mechanical leaching device (Holmgren *et al.* 1977) soluble salts were removed by washing each soil sample in 3×1 hr time steps using 50 ml of 60 % ethanol solution. In the same way, exchangeable cations were displaced by leaching the prepared samples for 10 hrs with 60 ml of the 1 M NH_4Cl displacing solution. To each extract, 40 ml of 0.5 M HCl was added and solutions made to 100 ml using the NH_4Cl solution. Extract preparations were diluted to the appropriate level and an ionising suppressant added, containing 2222 μg ml^{-1} CsCl and 1650 μg ml^{-1} $SrCl_2$. These dilutions were passed through the air–acetylene flame of an Atomic Absorption Spectrometer to quantify the contributions of Ca^{2+}, Mg^{2+}, Na^{+} and K^{+} ($cmol_{(+)}$ kg^{-1}). The effective Cation Exchange Capacity (CEC_{eff} $cmol_{(+)}$ kg^{-1}) was calculated as the sum of Ca^{2+}, Mg^{2+}, Na^{+} and K^{+} ($cmol_{(+)}$ kg^{-1}) and the ESP determined.

2.4.2 Physico–chemical properties of cotton–producing Vertosols

The soils sampled for this investigation contain small quantities of organic carbon and none of the topsoils have more than 1 % organic carbon. The sand, silt and clay contributions to the soil mineral fraction vary according to region. In general, the sand contribution to the surface soils increases in the order G00*i*<N00*i*<B00*i*<H00*i*, while silt decreases in the same order. The total clay content of the soils increases according to region in the order H00*i*<G00*i*<N00*i*<B00*i* and the contribution of fine clay (to the total clay content) is between 60 and 70 % for all soils. The ASWAT dispersion technique broadly shows the surface soils to have negligible dispersion, but with increasing soil depth, aggregates tend to be seriously dispersive.

The nine soils have neutral pH values at the soil surface and become increasingly alkaline with depth. These profiles generally have small values of electrical conductivity in the topsoil, but EC increases at depth. This appears to be strongly influenced by the presence of carbonate inclusions observed in some of the field descriptions. In soils that do not contain carbonates, the SAR increases with soil depth. The CEC_{eff} values are generally between 40 and 60 $cmol_{(+)}$ kg^{-1}. The exception is the H00*i* sites; these have the smallest values of total clay and smaller CEC_{eff} values than the other Vertosols. Commonly, Ca^{2+} dominates the exchange complex of these nine, and the surface layers are generally not sodic. These profiles all have sodic subsoils (ESP >5).

2.4.2.1 Three profiles from the Bourke region

The fundamental physico–chemical attributes of profiles B001, B002 and B003 are given in Tables 2.6 and 2.7. The small organic carbon contents decrease with depth from an average of 0.37 % in the topsoil of planting ridges to 0.08 % in the 1.0–1.2 m soil layer. These three soil profiles generally have similar particle size fractions. They contain an average of 38 % sand (>20 μm), 10 % silt (20–2 μm) and 52 % clay (<2 μm) at the soil surface. Of the clay fraction in these topsoils, approximately 69 % is fine clay. For each of these soil profiles, the silt content is generally consistent throughout the sampling depth. The contribution of total clay increases with depth, but the proportion of fine clay is less in the subsoils of B001 and B002 than in their topsoils. In the subsoil (1.0–1.2 m), the sand content is largest for B003 and least for B001. This negatively correlates to the clay content, which is greatest at this depth for B001 and least for B003. The ASWAT dispersion procedure describes all three subsoils (0.4–1.2 m) as having the potential for serious dispersion. In addition, B001 and B003 have the potential for moderate–serious dispersion in the topsoil layers (0.0–0.4 m), while profile B002 is unlikely to have dispersion problems in these layers. This reflects field–observed characteristics and the influence of a large electrical conductivity value (Table 2.7) in the top soil layer of this profile.

The electrical conductivity values of soil profiles B001 and B003 are small for the surface layers but increase with depth. In B003 the carbonates described during field analysis do not appear to influence soluble salt contents, but in the subsoil layers of B001 substantial soluble salt concentrations are indicated by the very large values of electrical conductivity. Soil B002 contrasts with the other soils, as it is saline in the top soil layer (EC 2.8 dS m^{-1}) (*see* McKenzie 1998). All other B002 soil layers have electrical conductivity values in the range 1.1–1.8 dS m^{-1} and are non–saline. The general trend for larger values of electrical conductivity at depth is frequently accompanied by larger SARs for these B00*i* soils. However, the effect of soluble salts, including $CaCO_3$ observed during field description, on the subsoil SAR of profile B001 led to similar SARs in the topsoil and subsoil layers except between 0.6 and 0.8 m depth. In this region of the profile the EC is much less than that observed between depths of 0.8 and 1.2 m and as a result it is expected that soluble salts are not contributing to the EC value obtained for the 0.6–0.8 m depth.

Table 2.6
Physical properties of profiles B001, B002 and B003

Depth (m)	Organic carbon (%)	Coarse sand (>50 μm) (%)	Fine sand (50–20 μm) (%)	Silt (20–2 μm) (%)	Coarse clay (2–0.2 μm) (%)	Fine clay (<0.2 μm) (%)	ASWAT score
				Site B001			
0.0–0.2	0.39	22.0	15.5	11.4	14.6	36.5	3
0.2–0.4	0.31	23.0	14.3	11.5	14.5	36.7	9
0.4–0.6	0.20	18.5	15.7	11.1	17.0	37.7	12
0.6–0.8	0.11	11.9	16.7	12.5	20.2	38.7	12
0.8–1.0[a]	0.08	11.7	7.8	13.7	26.0	40.8	12
1.0–1.2[a]	0.08	9.9	9.0	13.9	27.7	39.5	12
				Site B002			
0.0–0.2 [a]	0.34	19.8	17.3	11.2	16.2	35.5	0
0.2–0.4	0.18	18.3	18.2	8.4	19.2	35.9	2
0.4–0.6	0.11	16.8	14.6	13.1	19.1	36.4	12
0.6–0.8	0.11	18.8	14.5	11.4	20.0	35.3	12
0.8–1.0	0.10	16.1	17.7	11.4	19.6	35.2	12
1.0–1.2	0.08	13.5	13.2	12.9	23.2	37.2	12
				Site B003			
0.0–0.2	0.38	23.2	15.6	8.0	17.3	35.9	5
0.2–0.4	0.22	20.7	17.2	9.2	15.1	37.8	9
0.4–0.6	0.12	20.6	17.7	8.9	19.2	33.6	12
0.6–0.8	0.11	18.3	17.7	11.9	18.5	33.6	12
0.8–1.0	0.10	18.4	19.7	8.2	18.0	35.7	12
1.0–1.2	0.08	17.0	18.1	10.5	17.3	37.1	12

[a] Soil samples requiring pre–treatment for soluble salts

The CEC_{eff} of each sampled layer is relatively constant throughout each of these profiles. The B001 and B003 profiles have similar exchange capacities of between 35 and 40 $cmol_{(+)}$ kg^{-1} throughout, whereas B002 has a larger CEC_{eff} (44–47 $cmol_{(+)}$ kg^{-1}). The subsoil layers of B001 (0.8–1.2 m) have CEC_{eff} values approximately 5 $cmol_{(+)}$ kg^{-1} larger than the overlying layers. This is potentially a consequence of some soluble Ca^{2+} contributing to exchangeable Ca^{2+} content, thereby increasing the summation of CEC_{eff}. The ESP of these soils is commonly larger than the prescribed delineator of sodicity in Vertosols (ESP 5, McIntyre 1979). In all sampled layers the ESP is above 2; this is described as a potential lower threshold of dispersion in Vertosols with certain physico–chemical properties (McKenzie 1998). Soil B002 has a particularly high ESP in the topsoil layer (ESP 10.8), but this soil does not have the large ESP values (>20) observed in the subsoils (0.4–1.2 m) of profiles B001 and B003. ASWAT dispersion is strongly associated with the ESP values described. In all three soil profiles, where moderate to serious dispersion is evident, ESP values are above the critical level for 'sodic' soils. An exception is the topsoil layer of profile B002. In this layer, the ESP is more than 10 but the potential for dispersion is negligible according to the ASWAT test. In this soil layer it is likely that the saline conditions are limiting excessive expansion of the diffuse double layer and restricting the capacity of this soil to disperse.

Table 2.7
Chemical properties of profiles B001, B002 and B003

Depth	$pH_{1:5}$ $CaCl_2$	$EC_{1:5}$ dS m^{-1}	$SAR_{1:5}$ $(mmol_{(+)}\ L^{-1})^{1/2}$	CEC_{eff} $cmol_{(+)}\ kg^{-1}$	Exchangeable cations $cmol_{(+)}\ kg^{-1}$				ESP
					Ca^{2+}	Mg^{2+}	K^{+}	Na^{+}	
				Site B001					
0.0–0.2	6.9	0.41	4.24	35.86	21.46	11.01	1.85	1.55	4.3
0.2–0.4	7.3	0.28	5.16	35.12	20.45	10.28	1.42	2.98	8.5
0.4–0.6	7.3	0.41	4.63	32.43	14.31	9.70	0.91	7.50	23.1
0.6–0.8	7.2	0.84	22.20	35.04	14.93	10.59	1.13	8.38	23.9
0.8–1.0	7.0	3.54	5.23	40.27	20.63	10.84	1.05	7.77	19.3
1.0–1.2	7.0	3.72	5.84	40.47	20.16	11.62	1.02	7.67	19.0
				Site B002					
0.0–0.2	7.5	2.76	13.55	45.00	28.34	9.30	2.43	4.84	10.8
0.2–0.4	7.7	1.19	11.42	44.02	28.83	9.66	1.43	4.10	9.3
0.4–0.6	7.7	1.11	21.23	43.56	24.51	9.86	1.65	7.54	17.3
0.6–0.8	7.9	1.31	25.47	44.80	24.61	10.35	1.79	8.06	18.0
0.8–1.0	7.7	1.29	22.85	46.77	27.75	9.82	1.84	7.35	15.7
1.0–1.2	7.8	1.78	19.30	44.50	25.80	9.78	1.64	7.27	16.3
				Site B003					
0.0–0.2	7.2	0.10	1.71	37.15	24.94	9.59	1.85	0.76	2.1
0.2–0.4	7.3	0.10	1.70	37.03	24.21	9.43	1.36	2.03	5.5
0.4–0.6	7.8	0.36	4.26	36.64	17.43	9.62	1.12	8.46	23.1
0.6–0.8	8.1	0.51	8.04	38.75	18.05	9.73	1.27	9.70	25.0
0.8–1.0	7.9	0.61	14.97	37.39	17.55	9.37	1.24	9.23	24.7
1.0–1.2	8.0	0.81	19.78	38.76	18.44	9.69	1.22	9.41	24.3

2.4.2.2 Two profiles from the lower Gwydir valley

The fundamental physico–chemical properties of profiles G001 and G002 are given in Tables 2.8 and 2.9. The organic carbon content of both profiles decreases with depth. In the topsoil, the organic carbon content of G001 is approximately double that of G002, and in all subsequent soil layers the G001 soil has much larger organic carbon values. The coarse mineral fraction (>20 μm) is the same for these two soils. However, profile G001 has 10 % more silt throughout, while G002 has a 10 % larger clay fraction. The fine clay fraction of both these soils is approximately 64 % of total clay. The silt–clay difference between these soils reflects different positions in the current landscape (appendix 1). Site G002 is situated at a greater distance from the Gwydir River, indicating sedimentation of a finer size fraction during deposition of alluvial material.

Table 2.8
Physical properties of profiles G001 and G002

Depth (m)	Organic carbon (%)	Coarse sand (>50 μm) (%)	Fine sand (50–20 μm) (%)	Silt (20–2 μm) (%)	Coarse clay (2–0.2 μm) (%)	Fine clay (<0.2 μm) (%)	ASWAT score
				Site G001			
0.0–0.2	0.99	7.2	15.8	28.7	18.1	30.2	0
0.2–0.4	0.72	5.2	12.9	30.6	17.0	34.3	0
0.4–0.6	0.62	4.3	15.2	32.1	15.7	32.7	9
0.6–0.8	0.43	5.7	22.0	32.0	13.5	26.8	8
0.8–1.0	0.40	6.2	20.2	34.8	13.5	25.3	8
1.0–1.2	0.55	4.8	14.4	37.8	17.2	25.8	9
				Site G002			
0.0–0.2	0.48	9.7	11.9	19.6	21.0	37.8	0
0.2–0.4	0.39	9.4	11.9	20.4	18.9	39.4	1
0.4–0.6	0.36	10.7	12.2	20.7	19.6	36.8	0
0.6–0.8	0.32	10.3	12.6	21.8	18.6	36.7	3
0.8–1.0	0.29	10.5	13.8	21.1	17.1	37.5	10
1.0–1.2	0.27	9.1	12.4	22.4	18.1	38.0	7

Table 2.9
Chemical properties of profiles G001 and G002

Depth	$pH_{1:5}$ $CaCl_2$	$EC_{1:5}$ dS m^{-1}	$SAR_{1:5}$ $(mmol_{(+)}\ L^{-1})^{1/2}$	CEC_{eff} $cmol_{(+)}\ kg^{-1}$	Exchangeable cations $cmol_{(+)}\ kg^{-1}$				ESP
					Ca^{2+}	Mg^{2+}	K^{+}	Na^{+}	
				Site G001					
0.0–0.2	7.0	0.11	2.56	48.31	36.63	9.76	1.28	0.65	1.3
0.2–0.4	6.9	0.10	4.50	50.13	37.20	10.81	0.68	1.44	2.9
0.4–0.6	6.9	0.09	5.46	48.51	35.22	10.33	0.57	2.39	4.9
0.6–0.8	7.2	0.09	7.67	48.09	34.76	9.70	0.48	3.15	6.6
0.8–1.0	7.5	0.10	7.40	43.32	30.21	9.07	0.49	3.55	8.2
1.0–1.2	7.3	0.12	8.47	48.94	33.99	9.80	0.63	4.52	9.2
				Site G002					
0.0–0.2	7.3	0.23	2.17	54.56	40.10	12.11	1.69	0.66	1.2
0.2–0.4	7.4	0.15	4.47	52.84	38.02	12.04	1.33	1.45	2.7
0.4–0.6	7.4	0.14	7.32	50.62	35.04	12.13	1.13	2.33	4.6
0.6–0.8	7.5	0.17	9.87	48.35	30.40	12.75	1.22	3.98	8.2
0.8–1.0	7.9	0.23	10.93	47.23	28.94	12.17	1.09	5.03	10.6
1.0–1.2	7.6	0.24	10.17	45.09	26.73	11.87	1.14	5.35	11.9

The ASWAT dispersion test categorises G001 as being seriously dispersive at depths 0.4–1.2 m. In contrast, soil profile G002 is seriously dispersive only in the 0.8–1.2 m layers. The electrical conductivity values are very small throughout these soil profiles. However, the SAR increases with depth; SARs of 2.6 and 2.2 occur in G001 and G002 topsoils and increase to values of 8.5 and 10.2 in subsoil layers (1.0–1.2 m). The CEC_{eff} of profile G001 is generally constant (48–50 $cmol_{(+)}\ kg^{-1}$) throughout. In contrast, the CEC_{eff} of G002 decreases with sampling depth; 55 in the topsoil to 45

$cmol_{(+)}\ kg^{-1}$ in the subsoil. For both profiles, the ESP of soil layers above 0.6 m are less than 5, but with the exception of each topsoil layer, all soil layers have ESPs greater than 2. The lower layers (0.6–1.2 m) of these soils are sodic.

2.4.2.3 Two profiles from the Hillston region

The fundamental physico–chemical properties of profiles H001 and H002 are given in Tables 2.10 and 2.11. The organic carbon content is approximately 0.5 % for these two topsoils and is less at depth; approximately 0.05 % in subsoils (1.0–1.2 m). These profiles, particularly H002, have large sand contents throughout, but have small silt contents. The clay contents for the surface soil layers of H001 and H002 are 50 and 44 % respectively.

In H001, the contribution of clay decreases with depth, but the clay content of H002 tends to be constant throughout. Contributions of fine clay are approximately 70 % of total clay throughout each of these soils. The ASWAT procedure describes soil H001 as moderate–seriously dispersive in the topsoil layers (0.0–0.6 m). Below 0.6 m the ASWAT test indicates that this soil is not dispersive. Conversely, the H002 profile has ASWAT values for surface layers suggesting little or no dispersion, but at depths of 0.4–1.0 m, H002 has the potential for serious dispersion. Like H001, this soil is not dispersive in the 1.0–1.2 m layer. This layer, according to field description, appears to have similar characteristics to the 0.6–0.8 m depth of H001.

Table 2.10
Physical properties of profiles H001 and H002

Depth (m)	Organic carbon (%)	Coarse sand (>50 μm) (%)	Fine sand (50–20 μm) (%)	Silt (20–2 μm) (%)	Coarse clay (2–0.2 μm) (%)	Fine clay (<0.2 μm) (%)	ASWAT score
				Site H001			
0.0–0.2	0.48	22.3	18.0	10.3	14.1	35.3	6
0.2–0.4	0.30	21.5	17.1	10.4	14.2	36.8	9
0.4–0.6	0.18	18.7	22.2	11.8	22.6	24.7	9
0.6–0.8	0.10	20.6	18.3	17.7	15.6	27.8	0
0.8–1.0	0.07	24.3	19.8	17.0	18.1	20.8	0
1.0–1.2	0.04	33.0	25.1	8.5	14.1	19.3	0
				Site H002			
0.0–0.2	0.54	30.5	20.5	4.8	13.4	30.8	0
0.2–0.4	0.38	32.4	18.1	4.7	13.6	31.2	3
0.4–0.6	0.21	30.6	18.3	6.6	13.9	30.6	9
0.6–0.8	0.10	28.8	16.5	6.9	14.5	33.3	9
0.8–1.0	0.08	25.6	19.9	7.9	15.3	31.3	9
1.0–1.2	0.06	26.5	17.7	8.3	16.8	30.7	1

The electrical conductivity values are very small in the surface layers of these soils, but increase substantially with depth. In the subsoil layers of H001 (0.6–1.2 m) and in the 1.0–1.2 m layer of

H002 electrical conductivity values are greater than 1 dS m^{-1}. The SAR tends to increase between the surface and the 0.6 to 0.8 m depth for the H001 and H002 profiles, but then decreases in the lower soil layers where the EC values are ≥0.9 dS m^{-1}. These electrical conductivity and SAR values reflect the possible presence of soluble salts, *e.g.* $CaCO_3$ (lime) or $CaSO_4.2H_2O$ (gypsum), which were evidenced during the field examination of these soils. The CEC_{eff} of H001 is generally constant for all soil layers in the 0.0–0.8 m depth, but is less for the subsoil layers (0.8–1.2m). This reflects the smaller contribution of fine clay in this zone of the H001 profile. In contrast, the CEC_{eff} of profile H002 increases with sampling depth; 25 $cmol_{(+)}$ kg^{-1} at the soil surface increasing to 34 $cmol_{(+)}$ kg^{-1} at 1.0–1.2 m, reflecting a small increase in the total clay content. These profiles are sodic throughout with ESPs ranging from 6 in the topsoil layer to greater than 10 at depth. The ESPs and the electrical conductivity values of each soil layer are reflected in the determined ASWAT estimates, where soil layers tend to be dispersive at EC <1 dS m^{-1}, and non–dispersive at larger values of electrical conductivity, irrespective of the extent of soil sodicity.

Table 2.11
Chemical properties of profiles H001 and H002

Depth	$pH_{1:5}$ $CaCl_2$	$EC_{1:5}$ dS m^{-1}	$SAR_{1:5}$ $(mmol_{(+)}\ L^{-1})^{1/2}$	CEC_{eff} $cmol_{(+)}\ kg^{-1}$	Exchangeable cations $cmol_{(+)}\ kg^{-1}$				ESP
					Ca^{2+}	Mg^{2+}	K^+	Na^+	
				Site H001					
0.0–0.2	6.7	0.24	4.20	29.87	19.20	7.76	1.11	1.79	6.0
0.2–0.4	7.7	0.26	5.10	32.88	19.64	9.12	0.77	3.35	10.2
0.4–0.6	7.8	0.18	5.82	30.50	16.97	8.87	0.69	3.96	13.0
0.6–0.8	7.8	1.41	3.82	31.03	18.87	8.10	0.60	3.46	11.1
0.8–1.0	7.6	1.99	2.31	25.29	15.93	6.30	0.40	2.65	10.5
1.0–1.2	7.4	2.37	1.95	22.36	14.03	5.77	0.46	2.10	9.4
				Site H002					
0.0–0.2	7.7	0.17	3.07	24.51	13.02	8.82	1.24	1.43	5.8
0.2–0.4	7.8	0.24	5.12	32.68	18.91	10.34	0.87	2.55	7.8
0.4–0.6	8.1	0.40	8.26	30.06	13.00	10.50	0.69	5.86	19.5
0.6–0.8	8.2	0.50	14.21	33.14	15.15	10.62	0.78	6.60	19.9
0.8–1.0	8.2	0.90	8.98	35.65	17.24	11.49	0.89	6.03	16.9
1.0–1.2	8.2	1.39	5.93	33.68	15.74	11.35	0.81	5.78	17.1

2.4.2.4 Two profiles from the lower Namoi valley

The fundamental physico–chemical properties of the N001 and N002 profiles are given in Tables 2.12 and 2.13. The contribution of organic carbon at the soil surface is small in these soils. These two Namoi soils contain approximately 29 % sand at the soil surface, 20 % silt and 52 % clay. The fine clay fraction is approximately 65 % of the clay fraction. These profiles are texturally uniform and the subsoils (0.8–1.0 m) have sand, silt and clay contents that are similar to the topsoil. The

ASWAT test categorises soil N001 as moderately to seriously dispersive throughout. In contrast, the N002 soil layers <0.6 m tended to be non–dispersive, while at increased depth (0.6–1.0 m) soil layers have the potential for serious dispersion.

The electrical conductivity values are generally very small in both surface soils, but increase with depth. This attribute increases sufficiently in N001 (0.8–1.0 m) that the EC (2.26 dS m^{-1}) is much larger than the limit for a 'very highly saline' medium clay (McKenzie 1998). The SAR of the soil solution increases with sampling depth for both sites N001 and N002, and the N001 soil also has the largest values of SAR of all nine Vertosols studied. The CEC_{eff} of profile N001 is generally constant throughout the profile. This is different to the N002 profile, which has decreasing values of CEC_{eff} with depth; CEC_{eff} of 50 $cmol_{(+)}$ kg^{-1} in the topsoil and 42 $cmol_{(+)}$ kg^{-1} in the subsoil (0.8–1.0 m). This decrease is indicative of the smaller clay content in the subsoil of this profile. The large SAR of N001 is reflected in the ESP of this soil. N001 is sodic in the surface layer (McIntyre 1979) and strongly sodic in all other soil layers. In comparison, the topsoil layers (0.0–0.6 m) of N002 are non–sodic. The subsoil layers of N002 (0.6–1.0 m) are sodic (ESP of 7.8 at depth interval 0.8–1.0 m), and this is broadly reflected by ASWAT dispersion, where scores of 5 or greater occur for the sodic layers of these soils.

Table 2.12
Physical properties of profiles N001 and N002

Depth (m)	Organic carbon (%)	Coarse sand (>50 μm) (%)	Fine sand (50–20 μm) (%)	Silt (20–2 μm) (%)	Coarse clay (2–0.2 μm) (%)	Fine clay (<0.2 μm) (%)	ASWAT score
				Site N001			
0.0–0.2	0.59	17.9	11.1	18.5	17.2	35.3	5
0.2–0.4	0.44	19.8	11.6	16.8	16.7	35.1	5
0.4–0.6	0.49	17.4	10.8	16.6	18.8	36.4	9
0.6–0.8	0.38	16.0	13.0	14.9	17.7	38.4	7
0.8–1.0	0.26	13.5	12.3	17.2	17.3	39.7	3
				Site N002			
0.0–0.2	0.80	17.2	11.1	21.1	18.4	32.2	0
0.2–0.4	0.51	14.4	10.9	23.5	17.5	33.7	0
0.4–0.6	0.47	14.0	11.8	22.4	17.2	34.6	2
0.6–0.8	0.34	14.2	11.4	23.9	16.2	34.3	6
0.8–1.0	0.32	13.6	17.1	22.1	16.8	30.4	7

Table 2.13
Chemical properties of profiles N001 and N002

Depth	$pH_{1:5}$ $CaCl_2$	$EC_{1:5}$ dS m^{-1}	$SAR_{1:5}$ $(mmol_{(+)}\ L^{-1})^{1/2}$	CEC_{eff} $cmol_{(+)}\ kg^{-1}$	Exchangeable cations $cmol_{(+)}\ kg^{-1}$				ESP
					Ca^{2+}	Mg^{2+}	K^+	Na^+	
				Site N001					
0.0–0.2	7.9	0.32	9.74	54.46	37.13	10.78	1.97	4.58	8.4
0.2–0.4	8.1	0.42	14.52	53.85	31.74	13.04	1.24	7.84	14.6
0.4–0.6	8.3	0.62	18.49	54.52	27.81	14.33	1.10	11.29	20.7
0.6–0.8	8.2	0.87	23.69	53.18	25.52	14.46	1.32	11.89	22.4
0.8–1.0	7.8	2.26	14.40	51.77	24.59	14.60	1.51	11.08	21.4
				Site N002					
0.0–0.2	7.6	0.17	2.17	50.46	38.33	9.90	1.58	0.66	1.3
0.2–0.4	7.8	0.19	2.67	44.62	31.85	10.91	0.98	0.87	2.0
0.4–0.6	7.9	0.22	4.35	43.32	28.41	12.25	0.99	1.68	3.9
0.6–0.8	7.8	0.22	6.85	40.95	25.52	11.97	0.98	2.48	6.0
0.8–1.0	8.0	0.23	8.71	41.53	25.41	11.88	1.01	3.25	7.8

2.5 The soil mineral suite

The mineral composition of each soil provides information describing parent materials and the potential for structural development in Vertosols. To identify the mineral components of each soil profile, X–ray diffraction (XRD) techniques were used to characterize soil minerals from two sampling intervals; the second topsoil layer (0.2–0.4 m) and the subsoil, either the 0.8–1.0 m or the 1.0–1.2 m increment. These procedures are described by Brindley and Brown (1984) and by Whittig and Allardice (1986).

The primary minerals of each soil were determined from a random–powder arrangement of soil material. To prepare these samples, air–dry soil was ground to <50 μm and placed into a *well* at the centre of an aluminium holder backed with a glass slide. Each sample was placed in a Siemens Diffraktometer D5000 coupled with a Siemens Kristalloflex 710D X–ray generator, and the diffraction pattern obtained. The measurement criteria for this analysis are presented in Table 2.14.

Table 2.14
Measurement criteria applied during the use of XRD techniques for the identification of the soil mineral suite and for the identification and quantification of the clay phyllosilicates

Treatment	Particle size fraction (μm)	Step size (°2θ)	Step time (sec)	mA	kV	°2θ range
Mg^{2+} salt	2–0.2	0.02	2	40	40	2–30
	<0.2	0.02	2	40	40	2–30
K^+ salt	2–0.2	0.02	2	40	40	2–15
	<0.2	0.02	2	40	40	2–15
Random–powder	<50	0.02	2	40	40	15–70

Once the primary minerals were identified, the clay phyllosilicate suite was determined using the Siemens Diffraktometer from preparations of orientated clay. The measurement criteria for this series of analyses are given in Table 2.14. The coarse (2–0.2 μm) and fine (<0.2 μm) clay fractions were prepared for XRD analysis by placing a 10 mm band of clay solution onto a ceramic tile. Duplicate clay tiles were prepared for each clay solution; one was saturated with 2 M KCl solution, and the other was saturated using 2 M $MgCl_2$ solution. Diffraction patterns were obtained from the K^+ treated clay tiles in air–dry condition and then after successive heat treatments (100, 300 and 550 °C), while diffraction patterns were obtained for the Mg^{2+} treated clay tiles in air–dry condition and after saturation with glycerol. The proportions of smectite, vermiculite, illite and kaolinite contributing to the fine and coarse clay phyllosilicate fractions were estimated according to Bullock and Loveland (1974). Using this method the proportion of illite is determined as the peak area of the 1.0 nm peak determined from the XRD–diffractogram of the glycerated Mg^{2+} treatment. The same trace is used to determine the proportion of kaolinite; this is determined as the peak area of the 0.7 nm peak divided by three. The proportion of expansive clay (smectite and vermiculite) is determined by subtracting the peak area of the 1.0 nm peak (glycerated Mg^{2+}) from the peak area of the 1.0 nm peak determined from the XRD–trace of the 550 °C K^+ treatment and then dividing this value by two. The presence of smectite and vermiculite was then assigned proportionally depending on the presence or absence of these minerals in diffractograms for each clay tile.

2.5.1 The primary mineral suite of each Vertosol

The primary mineral suites of each of the nine Vertosols are given in Table 2.15. Figures 2.6 and 2.7 give the diffraction patterns of all soil minerals from soil profiles G001 and H001 at each of the two depth intervals (0.2–0.4 m and 1.0–1.2 m). The diffraction patterns of all soil minerals for the seven remaining Vertosols are presented in appendix 2 (Figures A2.1–A2.7).

Table 2.15
The primary mineral suite for each of the nine Vertosols investigated[a]

	Profile								
	B001	**B003**	**B002**	**G001**	**G002**	**H001**	**H002**	**N001**	**N002**
Quartz	✓	✓	✓	✓	✓	✓	✓	✓	✓
Plagioclase				✓	✓	½		✓	✓
Alkali–feldspars							✓	✓	✓

[a] Dominant soil minerals were similar at both depths investigated for each of the nine Vertosols

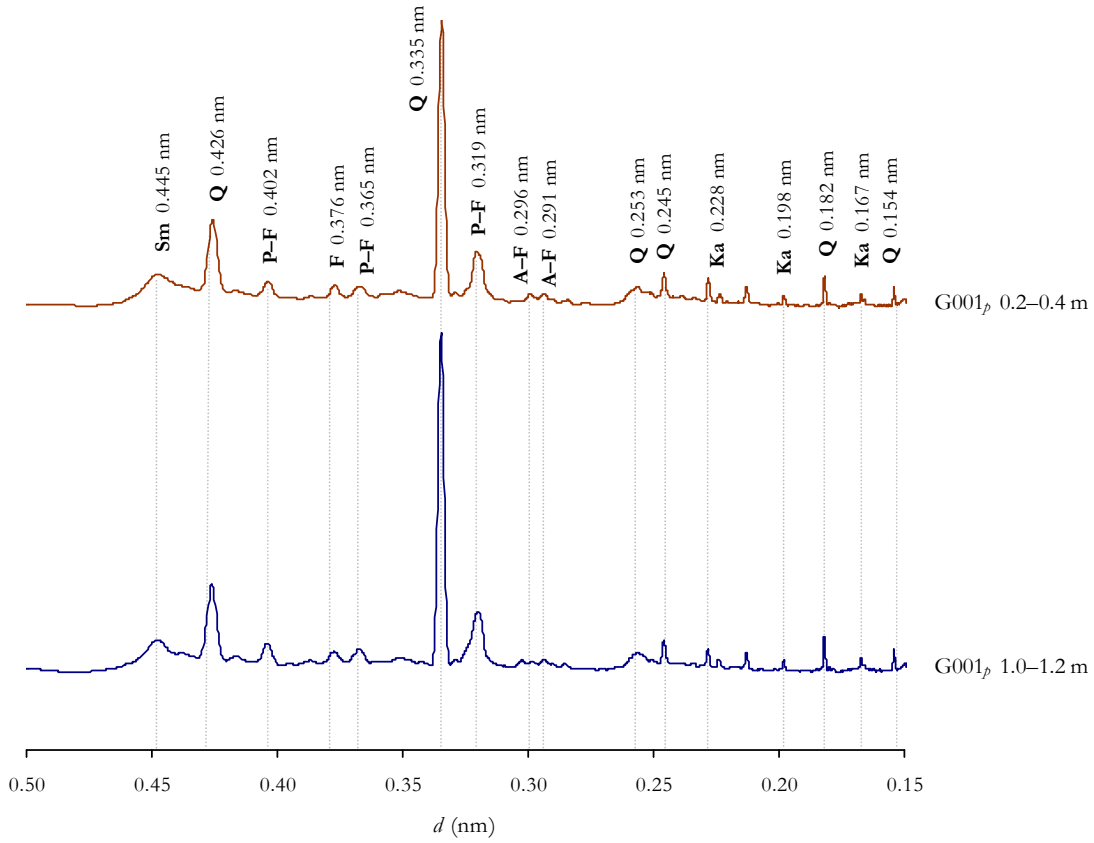

Figure 2.6 The suite of primary soil minerals from site G001 at depths of 0.2–0.4 and 1.0–1.2m. The labels identify the basal spacings (nm) corresponding to the minerals quartz (Q), feldspars (F), plagioclase feldspars (P–F), alkali–feldspars (A–F), smectite clay (Sm) and kaolinite clay (Ka).

The primary mineral suites of the nine Vertosols are generally the same for soil profiles from the same cotton–producing region *e.g.* all B00*i* soils generally have the same primary mineral suite. This presumably reflects differences in differing depositional conditions and in weathering and/or in parent material. The predominant primary mineral in each soil is quartz, a mineral almost ubiquitous in soils and which is the most common component of the sand and silt fractions (Allen and Hajek 1989). The soil profiles B001, B002 and B003 do not show other primary silicates in quantities detected using this XRD technique. The other six soils contain varying contributions of plagioclase and/or alkali–feldspars. The feldspars are the most common mineral in the earth's crust, but are less stable than quartz (Allen and Hajek 1989), and therefore suggest a measure of the degree of mineral

weathering. Consequently, the B00*i* soils appear to contain more highly weathered primary minerals than the G00*i* or N00*i* soils. The H00*i* soils appear to contain primary minerals that are less weathered than those of the B00*i* soils, but are more highly weathered than those minerals of the G00*i* and N00*i* soils. The N00*i* soils appear to contain primary minerals which show least weathering.

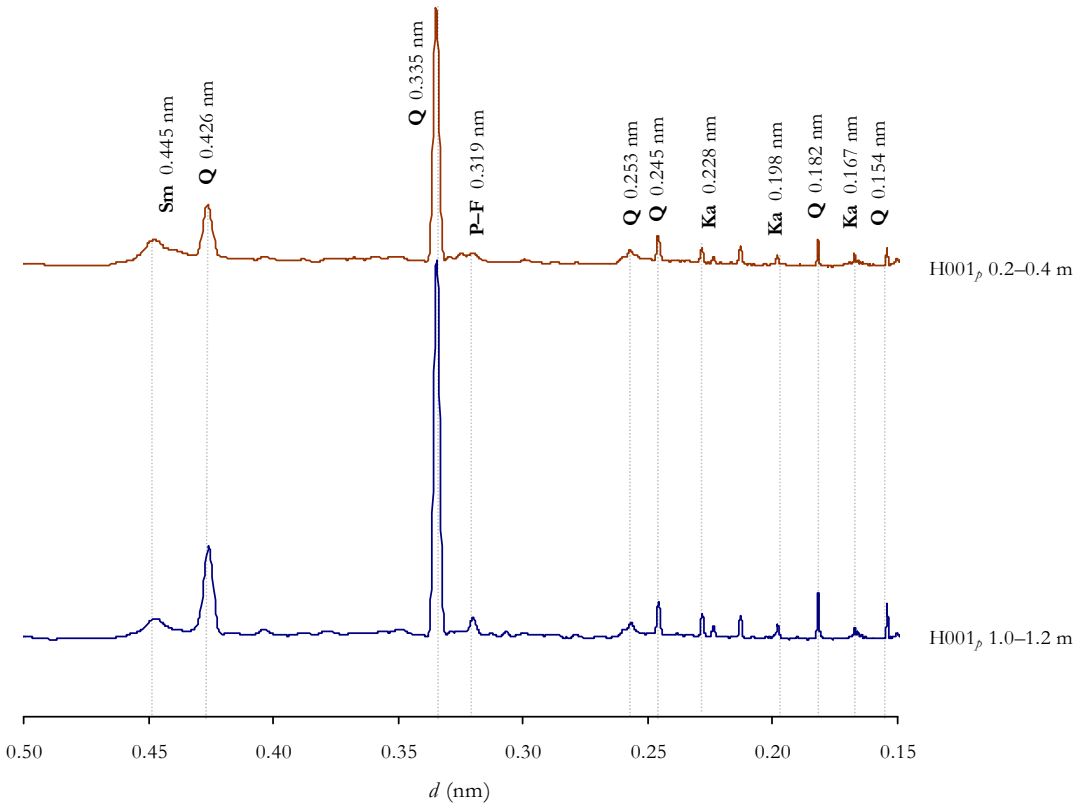

Figure 2.7 The suite of primary soil minerals from site H001 at depths of 0.2–0.4 and 1.0–1.2m. The labels identify the basal spacings (nm) corresponding to the minerals quartz (Q), plagioclase feldspars (P–F), smectite clay (Sm) and kaolinite clay (Ka).

2.5.2 The phyllosilicate suite of each Vertosol

The contribution of secondary phyllosilicates to the coarse clay (2–0.2 µm) and the fine clay (<0.2 µm) fractions of the Vertosols investigated are given in Tables 2.16 and 2.17. The Figures 2.8, 2.9, 2.10 and 2.11 give the diffractograms of clay tiles after treatment with K^+ (air–dry, 100, 300 and 550 °C) and Mg^{2+} (air–dry and glycerol) for profiles G001 and H001. The diffraction patterns for the seven remaining Vertosols are presented in appendix 2 (Figures A2.8–A2.14).

Table 2.16
The contribution of various secondary phyllosilicates to the coarse clay fraction (2–0.2 μm)[a]

		Profile								
		B001	**B002**	**B003**	**G001**	**G002**	**H001**	**H002**	**N001**	**N002**
Surface soil[b]	**Smectite**	Trace	+	½	+½	+++		+	++½	++½
	Vermiculite				+					
	Kaolinite	+½	+½	+½	+	½	½	+++½	+	½
	Illite	+++½	++½	+++	+½	+½	++++½	½	+½	++
Subsoil[c]	**Smectite**	++½	++½	+½	+++	++½	++	++	+	+++
	Vermiculite				+		Trace			Trace
	Kaolinite	½	+	+½	½	½	Trace	+	+½	½
	Illite	++	+½	++	½	++	++½	++	++½	+½

[a] Number of (+) symbols represent approximate proportions of particular minerals present in the 2–0.2 μm clay fraction
[b] Surface soil represents the depth interval 0.2–0.4 m
[c] Subsoil represents the greatest depth interval sampled; either 0.8–1.0 m or 1.0–1.2 m

Generally, the phyllosilicate suite of the coarse clay fraction of each of these nine Vertosols is dominated by either smectite or illite. The B00*i* and H00*i* soils have larger contributions of illite, while G00*i* and N002 soils tend to have coarse fractions dominated by expanding lattice phyllosilicates (smectite and vermiculite). These soils all contain various contributions of kaolinite, but with the exception of the H002 profile, this is less common than either smectite or illite in each coarse fraction. In addition, the G001 soil is the only soil to contain vermiculite in the topsoil layer. The topsoil layers of the B00*i* and H001 profiles are dominated by illite and they contain small proportions of kaolinite. The H002 surface layer is dominated by kaolinite and contains only small proportions of smectite and illite minerals. The G001 soil contains similar amounts of smectite, vermiculite, kaolinite and illite in the upper part of the profile. In contrast, the G002 and N00*i* soils are all either dominated by smectite or have co–dominant quantities of smectite and illite in the topsoil. The subsoil layer of most of these soils tends to be dominated by larger amounts of smectite clay rather than that at the surface, which is indicative of different rates of mineral weathering between the topsoil and subsoil. The N001 soil has much less smectite in the subsoil and is dominated by illite in the coarse fraction. The B003 soil has similar contributions of smectite, kaolinite and illite in the coarse clay fraction.

The fine clay fraction (<0.2 μm) generally contributes 30–40 % of the total particle size distribution in all these Vertosols; this is approximately 60–70 % of all clay. All nine of these Vertosols generally have a fine clay fraction dominated by smectites, but contain small amounts of kaolinite and illite at both depths. Two of the soils investigated have clay mineral suites that are different to the other soils. The Red Vertosol, H001, is dominated by illite in the topsoil. The field characteristics of this soil and its physico–chemical attributes indicate that the topsoil layers (0.0–0.6 m) are different to the subsoil layers (0.6–1.2 m) (*e.g.* Munsell® colour). In the subsoil layer, the secondary mineral suite

of this soil is dominated by smectite clays. The Black Vertosol, N002, is dominated in the topsoil layer by smectite clays, however in the subsoil; illitic clay is the dominant phyllosilicate.

The nine Vertosols can be distinguished on the basis of 2:1 expanding phyllosilicate contributions (smectite and vermiculite) to the surface soil and subsoil layers of either the coarse or fine clay fractions. In the coarse fraction, the 2:1 expanding phyllosilicate content increases in the order: B00*i* ≈ H00*i* < N00*i* ≈ G001 < G002 (topsoil) and N001 < H00*i* ≈ B003 < B001 ≈ B002 ≈ G002 < N002 < G001 (subsoil). In the fine fraction, the 2:1 expanding phyllosilicate content increases in the order: H001 < N002 < H002 < B00*i* ≈ G002 ≈ N001 < G001 (topsoil) and N002 < B001 ≈ N001 < B003 ≈ G001 < H001 < B002 ≈ G002 ≈ H002 (subsoil).

Table 2.17
The contribution of various secondary phyllosilicates to the fine clay fraction (<0.2 μm)[a]

		Profile								
		B001	**B002**	**B003**	**G001**	**G002**	**H001**	**H002**	**N001**	**N002**
Surface soil[b]	**Smectite**	++++	++++½	++++	+++++	++++½	+½	+++½	++++½	+++
	Vermiculite	Trace								
	Kaolinite	½	Trace	Trace	Trace	½	+	½	Trace	½
	Illite	½	Trace	+			++½	+	½	+½
Subsoil[c]	**Smectite**	+++	++++½	++++	++++	++++½	++++	++++½	+++	+
	Vermiculite									
	Kaolinite	½	Trace	½	½	Trace	½	Trace	½	+
	Illite	+½	Trace	½	½	Trace	½	Trace	+½	+++

[a] Number of (+) symbols represent approximate proportions of particular minerals present in the <0.2 μm clay fraction
[b] Surface soil represents the depth interval 0.2–0.4 m
[c] Subsoil represents the greatest depth interval sampled; either 0.8–1.0 m or 1.0–1.2 m

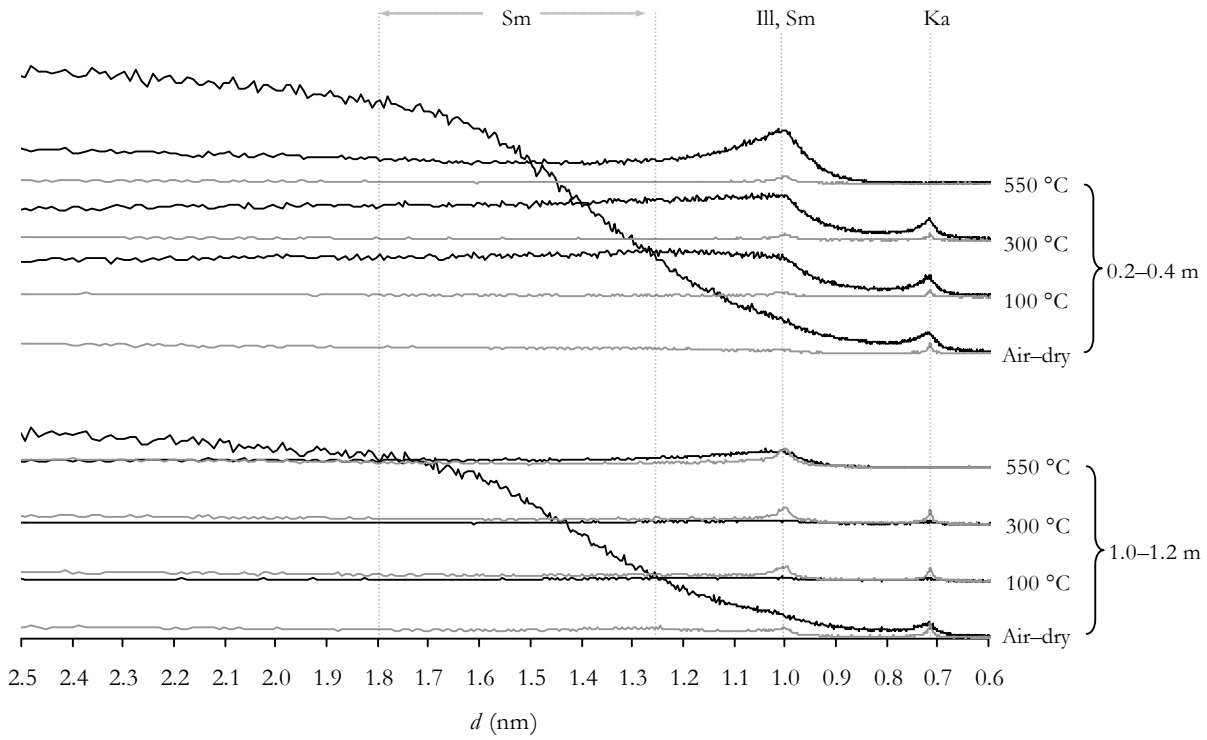

Figure 2.8 The secondary suite of soil minerals of the fine clay (━) and the coarse clay (━) fractions of site G001 at depths of 0.2–0.4 and 1.0–1.2m and using 2 M KCl to treat samples. The labels identify the basal spacings (nm) corresponding to smectite clay (Sm) ($d_{(air–dry)}$=1.25–1.80 nm, $d_{(100–550\ °C)}$=1.00 nm), illite clay (Ill) (d=1.00 nm) and kaolinite clay (Ka) (d=0.71 nm).

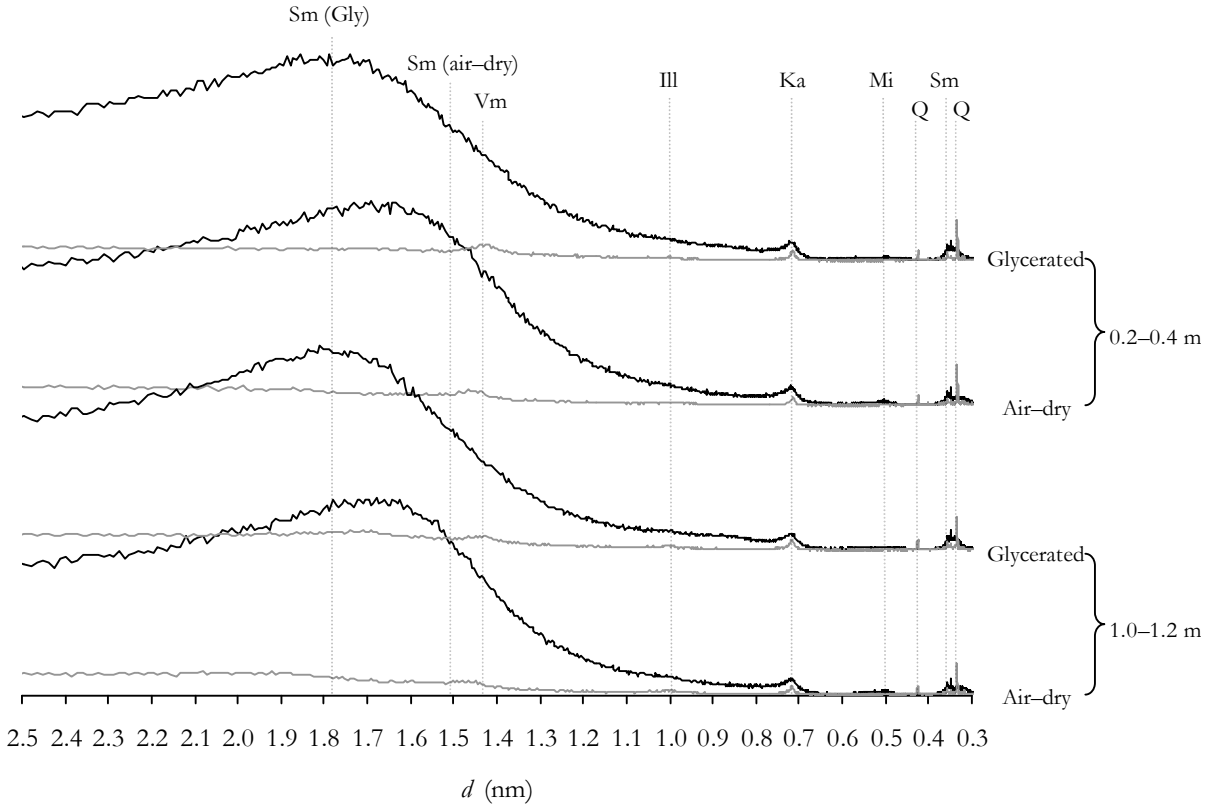

Figure 2.9 The secondary suite of soil minerals of the fine clay (━) and the coarse clay (━) fractions of site G001 at depths of 0.2–0.4 and 1.0–1.2m and using 2 M $MgCl_2$ to treat samples. The labels identify the basal spacings (nm) corresponding to smectite clay (Sm) ($d_{(air–dry)}$=1.51 nm, $d_{(Gly.)}$=1.78 nm and d=0.35), vermiculite (Vm) (d=1.45 nm), illite clay (Ill) (d=1.00 nm) and kaolinite clay (Ka) (d=0.71 nm), quartz (Q) (d=0.42 nm, d=0.33) and mica (Mi) (d=0.48 nm).

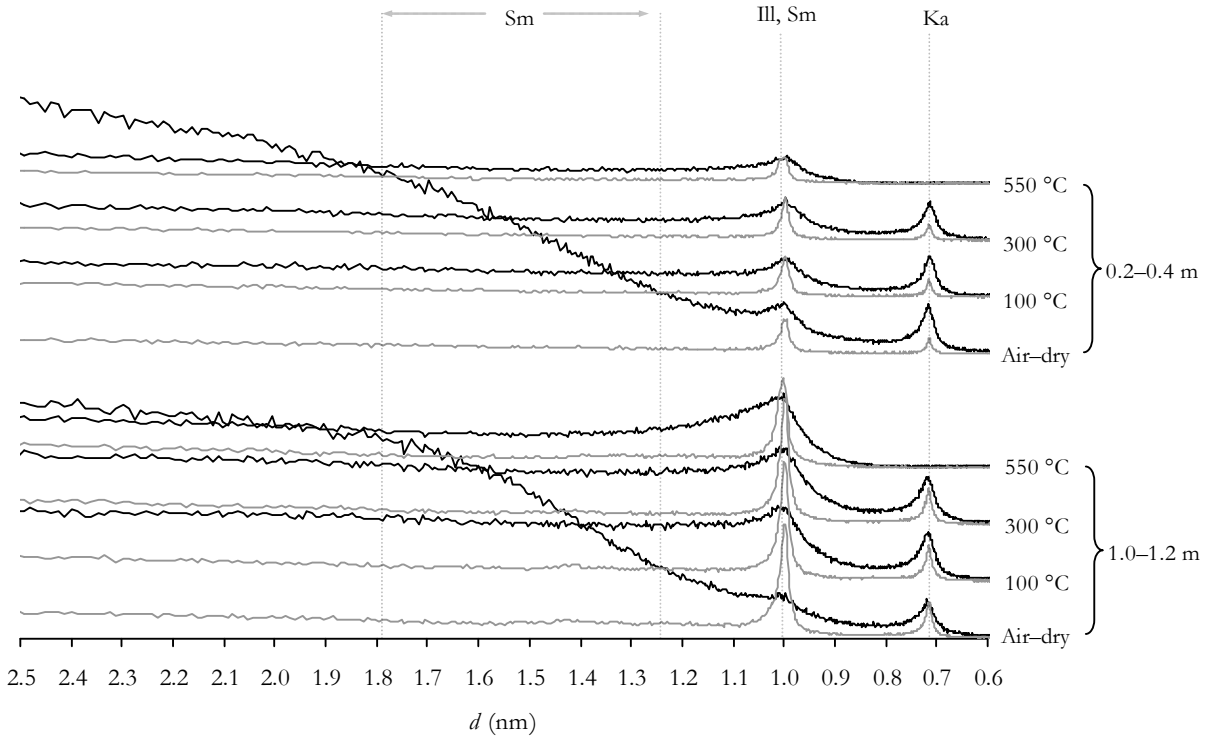

Figure 2.10 The secondary suite of soil minerals of the fine clay (▬) and the coarse clay (▬) fractions of site H001 at depths of 0.2–0.4 and 1.0–1.2m and using 2 M KCl to treat samples. The labels identify the basal spacings (nm) corresponding to smectite clay (Sm) ($d_{(air–dry)}$= 1.25–1.80 nm, $d_{(100–550\ °C)}$=1.00 nm), illite clay (Ill) (d=1.00 nm) and kaolinite clay (Ka) (d=0.71 nm).

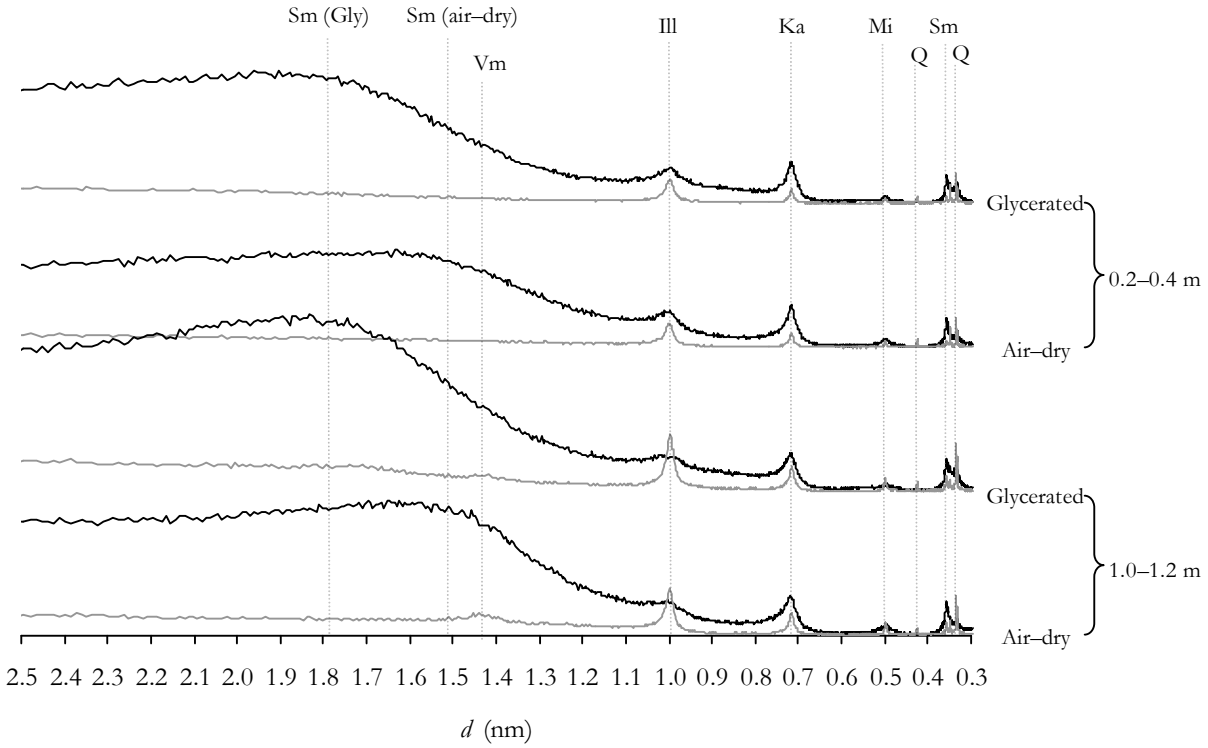

Figure 2.11 The secondary suite of soil minerals of the fine clay (▬) and the coarse clay (▬) fractions of site H001 at depths of 0.2–0.4 and 1.0–1.2m and using 2 M $MgCl_2$ to treat samples. The labels identify the basal spacings (nm) corresponding to smectite clay (Sm) ($d_{(air–dry)}$=1.51 nm, $d_{(Gly.)}$=1.78 nm and d=0.35), vermiculite (Vm) (d=1.45 nm), illite clay (Ill) (d=1.00 nm) and kaolinite clay (Ka) (d=0.71 nm), quartz (Q) (d=0.42 nm, d=0.33) and mica (Mi) (d=0.48 nm).

2.6 Classification of the nine soils

The field descriptions were used to classify each of the nine soils, using the Australian Soil Classification scheme (ASC), as either Red, Grey or Black Vertosols (Isbell 1996). To classify these nine Vertosols, it was assumed that slickensides and/or lenticular peds were present within 1 m of the soil surface. These attributes are used to give evidence of shrink–swell behaviour. The sampling regime imposed made it impossible to identify these characteristics, but for these soils shrink–swell activity was demonstrated by the extensive large cracks that were evident at the soil surface, and in the case of the H002 soil, in nearby soil not recently irrigated. Then, the soil surface condition at the time of sampling was used to describe the great groups to which each of these Vertosols belonged. The physico–chemical attributes, determined in the laboratory, were used to assign each of these nine soils to appropriate subgroups (Isbell 1996). The nine Vertosols were then classified to subgroups of Soil Taxonomy (Soil Survey Staff 2003) and to soil reference groups of the World Reference Base for soil resources (FAO 1998). The classes assigned to each of these Vertosols using the three classification schemes are given in Table 2.18.

The G00*i* soils could not be distinguished at the subgroup level using the ASC scheme. However, using the ASC the profiles of each of the other cotton–growing regions could be distinguished at the subgroup level. The B001 and B003 soils are both described as soils with large ESPs at depths greater than 0.5 m (*Endohypersodic*), whereas the B002 soil is an *Episodic* soil, with an ESP greater than 6 occurring in the uppermost soil layer. This soil also exhibits *Salic* characteristics, where a seasonal saline watertable (EC >2 dS m^{-1}) is present in the upper 0.5 m of the profile. The very large electrical conductivity of the uppermost soil layer appeared to result from leakage occurring from an irrigation storage facility in close proximity to this site and salic properties were not observed beyond the upper most soil layer; it was consequently concluded that this did not represent a saline watertable. Overall, three of the nine Vertosols are described as *Endohypersodic* soils (B001, B003 and H002), three are described as *Episodic* (B002, H001 and N001), while three are *Haplic* Vertosols (G00*i* and N002). These soils commonly have *self–mulching* topsoils (B00*i*, G00*i* and N001), but both H001 and N002 have an epipedal surface structure, and H002 has a surface structure that appeared massive at the time of sampling. In the case of H002, the surface structure described is a reflection of the soil moisture content at the time of sampling.

Soil Taxonomy and the World Reference Base for soil resources (WRB) did not tend to delineate differences between these soils as clearly as the ASC scheme. Soil Taxonomy delineated between the different types of Vertisols using the climatic regimes and the average temperature and rainfall

attributes of each region (Table 2.1). Consequently, the B00*i* soils were considered Torrerts, the H00*i* soils as Xererts, and the G00*i* and N00*i* soils Usterts. There is no further delineation between the B00*i* soils or the G00*i* soils, but the H00*i* and N00*i* soils are described differently. These H00*i* and N00*i* soils are classed based on their different levels of sodicity. For example, using Soil Taxonomy H002 is classed as a Sodic Vertisol, while H001 is a Typic Vertisol. Likewise, N001 is sodic throughout, with ESP values for most soil layers (0.0–1.0 m) much larger than 15, while the N002 soil has no distinguishing descriptive features and is described as a Typic Vertisol. Using the WRB, all nine of these soils are characterised according only to different levels of sodicity.

Table 2.18
Classification of the nine Vertosols using the Australian Soil Classification (Isbell 1996), Soil Taxonomy (ASSS 2003) and World Reference Base for soil resources (FAO 1998)

Profile	Australian Soil Classification (subgroups)[a]	Soil Taxonomy[b]	WRB reference groups[c]
B001	Endohypersodic Self–mulching Grey Vertosol	Sodic Haplotorrert	Hypersodic Vertisol
B002	Episodic Self–mulching Grey Vertosol	Sodic Haplotorrert	Hypersodic Vertisol
B003	Endohypersodic Self–mulching Grey Vertosol	Sodic Haplotorrert	Hypersodic Vertisol
G001	Haplic Self–mulching Black Vertosol	Typic Haplustert	Haplic Vertisol
G002	Haplic Self–mulching Black Vertosol	Typic Haplustert	Haplic Vertisol
H001	Episodic Epipedal Red Vertosol	Typic Haploxerert	Hypersodic Vertisol
H002	Endohypersodic Massive Grey Vertosol	Sodic Haploxerert	Hypersodic Vertisol
N001	Episodic Self–mulching Black Vertosol	Sodic Haplustert	Sodic Vertisol
N002	Haplic Epipedal Black Vertosol	Typic Haplustert	Haplic Vertisol

[a] In the ASC, *Endohypersodic* refers to soils with an ESP of at least 15 in some subsoil horizon below 0.5 m depth. *Episodic* refers to soils with an ESP of at least 6 in upper 0.1 m of a soil profile. *Haplic* soils are those soils in which the major part of the upper 0.5 m of a profile is whole coloured.

[b] In Soil Taxonomy, *Sodic* refers to soils with an ESP of at least 15 % in the upper 1 m of a soil profile, *Typic* refers to other soils not characterised by specific attributes. The denotation *Haplo* refers to soils not characterised by given criteria. The terms *torrert (i)*, *xerert (ii)* and *ustert (iii)* refer to Vertisols that have either, *(i)*, cracks closed for 60 days or less consecutive days during a period where the soil temperature at 0.5 m depth is at least 8 °C, *(ii)*, a thermic (annual soil temperature 15–20 °C at 0.5 m with a minimum of 6 °C change) or mesic (annual soil temperature 8–15 °C at 0.5 m with a minimum of 6 °C change) temperature regime, and cracks that open at least 5 mm wide and to at least 0.25 m depth for 60 or more days of a 90 day period following the summer solstice but which are closed for 60 days or more of a 90 day period following the winter solstice, and *(iii)*, other Vertisols not described by the diagnostic criteria.

[c] In the WRB reference groups, *Sodic* refers to soils with an ESP of at least 15 % within 0.5 m of the soil surface, *Hypersodic* refers to soils with an ESP of at least 6 % within 1 m of the soil surface, and *Haplic* refers to Vertisols with no special characteristics.

2.7 Comparing these Vertosols with other cotton–producing Vertosols

According to the ASC classes applied to these nine Vertosols, they are delineated based primarily on the levels of sodicity they exhibited, on surface structure and according to dominant colours. Soil Taxonomy and the WRB for soil resources highlighted the differences between the variations in climate between the sampling regions and the sodicities of these soils. To further demonstrate the differences between these nine Vertosols, the physico–chemical properties and phyllosilicate suites were compared with those Vertosols described by Vervoort *et al.* (2003). In Table 2.19 the physico–chemical properties of the Vertosols they studied are given, while in Table 1.1 the phyllosilicate minerals of these soils are shown.

Table 2.19
Mean physico–chemical soil properties of surface samples (0.0–0.2 m) from five cotton–growing Vertosols of eastern Australia (adapted from Vervoort *et al.* 2003)
To determine these mean values 12 soils were assessed; 2 soils from the Lachlan valley, 4 soils from the Gwydir valley and 6 soils from the Namoi valley. The average subsoil values (depth >0.4 m) were determined from 5 soils; 2 soils from the Gwydir valley and 3 soils from the Namoi valley. Average values were taken directly from Vervoort *et al.* (2003).

	By cotton–growing valley			By soil depth	
	Gwydir	**Namoi**	**Lachlan**	**Average surface**	**Average subsoil**
Organic carbon (%)	0.8	0.8	0.6	0.8	0.5
Coarse sand (>50 μm) (%)	10.2	18.0	22.5	15.7	7.4
Fine sand (50–20 μm) (%)	4.6	5.8	9.6	5.5	4.9
Silt (20–2 μm) (%)	23.9	18.5	13.7	20.0	19.6
Coarse clay (2–0.2 μm) (%)	34.1	27.1	18.7	29.1	33.2
Fine clay (<0.2 μm) (%)	27.2	30.6	35.5	29.6	34.9
$EC_{1:5}$ (dS m^{-1})	0.07	0.16	0.15	0.13	0.50
CEC_{eff} ($cmol_{(+)}$ kg^{-1})	38.4	38.2	26.9	33.3	38.3
$Ca^{2+}_{exch.}$ ($cmol_{(+)}$ kg^{-1})	23.9	23.9	16.4	21.1	23.9
$Mg^{2+}_{exch.}$ ($cmol_{(+)}$ kg^{-1})	12.5	11.6	8.3	9.8	11.8
$Na^{+}_{exch.}$ ($cmol_{(+)}$ kg^{-1})	0.9	1.1	0.9	0.9	1.1
$K^{+}_{exch.}$ ($cmol_{(+)}$ kg^{-1})	1.1	1.5	1.4	1.5	1.4
ESP (%)	2.6	3.2	3.6	2.6	2.9

The surface soil properties of the nine Vertosols used in this work are similar to those determined for twelve Vertosols by Vervoort *et al.* (2003). However, there are differences between the laboratory measured attributes given by Vervoort *et al.* (2003) and those of the nine Vertosols studied. For example, the fine clay content, CEC_{eff} and the Ca^{2+}:Mg^{2+} ratios of the nine topsoils are different. The fine clay fractions of the soils investigated by Vervoort *et al.* (2003) are smaller than those determined for the nine Vertosols. Specifically, their Gwydir and Namoi soils only had 40–50 % fine clay, which is much less than that determined for the G00*i* and N00*i* soils in study. The total clay contents of the nine surface soils are similar (for each region) to clay contents presented by Vervoort

et al. (2003). The CEC_{eff} values and Ca^{2+}:Mg^{2+} ratios they present for the Gwydir and Namoi soils are also smaller than those of the G00*i* and N00*i* soils. The sodicities of the Gwydir and Namoi soils are similar to those of the G00*i* and the N002 soils, but are much lower than those of the H00*i* and N001 soils. However, the soils in this work were selected to show different ESPs and this is highlighted by the classes applied to each soil using the three classification schemes.

The average subsoil characteristics of the soils Vervoort *et al.* (2003) studies tend to be similar to those of the G00*i* and N00*i* soils investigated in this study, with the exception being the quantities of fine clay and the ESPs. The fine clay contributions to the Vervoort *et al.* (2003) subsoils are approximately 50 % of total clay; this is between 10 and 20 % less than those of the G00*i* and N00*i* soils investigated in this study. Furthermore, the average subsoil ESPs of the profiles used by Vervoort *et al.* (2003) do not suggest subsoil sodicity. This may be a function of sampling depth, but here the G00*i* and N00*i* soils both tend to show some level of subsoil sodicity. In addition to these soils, the B00*i* and H00*i* soils all have subsoil ESPs indicative of sodicity.

The phyllosilicate minerals determined for the clay fraction by Vervoort *et al.* (2003) tend to be similar for each region to those identified for the nine Vertosols. In their study, the Gwydir and Namoi soils tend to be dominated by 2:1 expanding lattice phyllosilicates, while the Lachlan soils contain much larger contributions of illite and kaolinite clays.

2.8 Summary

The nine soils represent a spectrum of Vertosol textures; the G002 soil has greatest clay content, the B00*i* and N00*i* soils have clay contents of approximately 50 %, while the G001 and H00*i* soils tend to have lightest texture, with clay contents of approximately 45 %. All of these soils have very small amounts of organic carbon. However, there is a clear distinction in organic carbon contributions for the climatic regions from which soils were sampled. For example, the B00*i* soils have organic carbon contributions of 0.35–0.40 % in the topsoil, the G002, H00*i* and N001 soils, of approximately 0.50 %, while the G001 and N002 soils have the largest contribution of organic carbon (0.99 % and 0.80 % respectively). These small contributions of organic carbon are expected for the Red and Grey Vertosols, but are less than anticipated for the Black Vertosols (Isbell 1989). Only one of the soils has a saline topsoil layer (B002), but the B00*i*, H00*i* and N001 soils all have very large values of electrical conductivity in the subsoil. The differences in clay content tend to be reflected by differences in CEC_{eff}. For these soils, the G00*i* and N00*i* soils tend to have exchange capacities of

approximately 50 $cmol_{(+)}$ kg^{-1}, whereas the B00*i* and H00*i* soils generally have exchange capacities of 30–40 $cmol_{(+)}$ kg^{-1}. All profiles exhibit subsoil sodicity, and according to the criteria of McIntyre (1979), the B002, H00*i* and N001 Vertosols are sodic throughout. The soils from B00*i* and H00*i* appear to be more highly weathered than the soils from G00*i* and N00*i*. This conclusion is based on the presence of felsic minerals and the larger contributions of smectite to the G00*i* and N00*i* soils. All of these profiles tend to be dominated by 2:1 expanding lattice clays (smectite and vermiculite), but the B00*i*, H00*i* and N002 soils (particularly H001) appear to have greater contributions of kaolinite and illite than the G00*i* and N001 soils. In these nine Vertosols, the contributions of smectite, or other expanding phyllosilicates, tend to increase in the order H00*i*≈B00*i*≈N002<N001 ≈ G00*i* (surface soil) and H00*i* ≈ N00*i* < B00*i* < G00*i* (subsoil). Consequently, these nine profiles, according to their physico–chemical properties and mineral suites, appear to represent a wide range of Vertosols found across eastern Australia.

Chapter 3

DETERMINING THE STRUCTURAL STABILITY OF NINE SURFACE SOILS

DETERMINING THE STRUCTURAL STABILITY OF NINE SURFACE SOILS

~

Disperse: *dispergere (L.): to distribute (particles) evenly throughout a medium.*

~

3.1 Introduction

The propensity of soil aggregates to breakdown with the addition of disruptive force has been recognised since early last century. For example, Ellison (1947) documented the effect of raindrop impact on increasing 'muddiness' at the soil surface. Since this time a large body of research, focusing on the identification and alleviation of structural instability across all soil types, has accumulated. The structural stability of soils is determined according to the force required to break aggregates or peds into smaller units or individual particles. This occurs when sufficient mechanical stress is applied to overcome the attractive forces between two or more particles. The stability of an aggregate in the presence of an applied force then depends on the strength of bonding mechanisms operating within that aggregate (Raine and So 1997). If these mechanisms are not sufficient to maintain stability, aggregates begin to break apart.

The structural stability of soil is influenced by physico–chemical characteristics and extensive research has explored the complex relationships between structural stability, exchangeable Na^+, electrical conductivity, clay content, clay phyllosilicate suite and soil hydraulic conductivity (e.g. Quirk and Schofield 1955; Cass and Sumner 1982). Australian Vertosols are particularly prone to structural instability; this is because these soils have large volumes of expansive phyllosilicate clays and often contain large quantities of exchangeable Na^+. However, the current understanding of soil physico–chemical properties has not been linked unequivocally with measures of structural stability in Vertosols. Consequently, the inability to determine associations between physico–chemical properties and structural instability remains a key difficulty in the management of Vertosols. As a result, a soil's ESP has historically been applied as a guide to potential instability (*e.g.* USSL Staff 1954; McIntyre 1979; Isbell 1996).

The critical ESP proposed for use in Australian cotton–producing Vertosols is 5; this delineates *non–sodic* from *sodic* Vertosols (McKenzie 1998). However, soil ESP does not wholly describe the dispersive potential of this soil class, and Cook *et al.* (1992) showed that some Vertosols disperse with ESP values as low as 2 where the electrical conductivity is sufficiently small. This discrepancy

has led to the introduction of other critical predictors of stability, *e.g.* ESI (EC/ESP) and $EC_{1:5}/Na^{+}_{exch.}$ (Blackwell *et al.* 1991; Hulugalle and Finlay 2003), to accommodate the effects of soil solution electrical conductivity in combination with the soil exchangeable Na^{+} content.

In this chapter, the structural stability of topsoil from each of the nine sampling sites, described in chapter 2, is compared and critical dispersion classes are discussed. To do this, soil was sampled from an *irrigation furrow* of each of the B00*i*, G00*i*, H00*i* and N00*i* soils, where an irrigation furrow is the region between two adjacent cotton rows down which irrigation water flows. The stability of these soils is compared in two ways: *(i)*, using three methods of aggregate liberation (spontaneous dispersion, EOE–disruption and ultrasonic agitation) when soil is immersed in clean water (de–ionised water) and, *(ii)*, using EOE–disruption to compare structural stability when soil is immersed in solutions of varying total salt content and increasing sodium content.

3.2 Methods

Bulk soil was excavated from an irrigation furrow (0.0–0.2 m), which did not appear to have undergone trafficking, adjacent to each of the nine Vertosol profiles characterised in chapter 2. This topsoil layer represents the interface between the soil environment and applied irrigation water.

All topsoil samples from the nine sites (B00*i* G00*i*, H00*i* and N00*i*) were air–dried and ground to pass through a 2 mm sieve. The ground fraction was placed into a 0.1 mm sieve and later the <0.1 mm soil fraction was discarded. The 2.0–0.1 mm fraction was retained for the analysis of a series of fundamental soil properties and for the assessment of soil structural stability attributes using immersion techniques. For all physico–chemical and structural stability attributes determined, the analyses were performed in triplicate and the mean values are presented.

3.2.1 Fundamental soil physico–chemical properties

The fundamental soil properties were determined for the 0.0–0.2 m layer of each irrigation furrow in the same way as the physico–chemical properties of soil layers assessed in chapter 2; these methods are outlined in chapter 2.3.1. The particle size distribution (PSD) analysis (Gee and Bauder 1986) was used to determine the >100 μm, the <20 μm and the <2 μm size fractions (dag kg^{-1}) once soils had been shaken EOE in 50 ml Sodium Hexa Metaphosphate solution and 300 ml de–ionised water. Soil pH was determined using a 1:5 (soil:0.01 M $CaCl_2$) soil suspension. The amount of soil organic carbon was estimated using an adjusted method of Walkley and Black (McLeod 1975). The soil solution was extracted using a 1:5 (soil:de–ionised water) ratio and the electrical conductivity ($EC_{1:5}$)

determined. Exchangeable cations were extracted using a 60 % ethanol, 1 M NH_4Cl solution at pH 8.5 (Rayment and Higginson 1992). Cations from the extracted *soil solution* and the exchangeable phase cations (Ca^{2+}, Mg^{2+}, Na^+ and K^+) were quantified using Atomic Absorption Spectroscopy (AAS). The effective cation exchange capacity (CEC_{eff}), ESP, ESI, $EC_{1:5}/Na^+_{exch}$ and SAR were calculated. The ASWAT test (Field *et al.* 1997) was used to provide a preliminary description of soil stability.

3.2.2 Spontaneous clay dispersion

Spontaneous dispersion was used to simulate the breakdown of soil aggregates during a light rainfall event where the soil is effectively protected by plant material (Rengasamy *et al.* 1984). To determine spontaneous breakdown, the air–dry equivalent of six grams soil was weighed into a 500 ml measuring cylinder and 100 ml of de–ionised water was carefully added (Rengasamy *et al.* 1984). The soil solution was left to equilibrate for 24 hrs at 20 °C. The volume was made to 500 ml using de–ionised water and dispersed clay was homogenised in solution by carefully upending each cylinder twice. After the appropriate sedimentation period, the <20 μm and the dispersed clay (<2 μm) fractions were sampled using a 25 ml pipette (Gee and Bauder 1986). The remaining soil solution was transferred to a 100 μm sieve, immersed in de–ionised water, and after gentle wet–sieving, the >100 μm soil fraction was retained. The >100 μm, the <20 μm and the <2 μm size fractions of each soil were oven dried (105 °C) and quantified gravimetrically (dag kg^{-1}), and then the <100 μm fraction was determined by difference. The <100 μm and the <2 μm fractions were used to determine differences in the stability of these soils. The <20 μm fraction was used to develop critical classes of dispersion for the classification of each Vertosol.

3.2.3 EOE–disruption

EOE–disruption was used to simulate the breakdown of soil aggregates during a moderate rainfall or irrigation event where the soil surface is not protected (Rengasamy *et al.* 1984). To do this, the method of Field (2000) was used to determine the extent of clay dispersion after end–over–end shaking. Accordingly, the air–dry equivalent of six grams of soil was weighed into a centrifuge bottle (58 mm *i.d.* × 134 mm *h.*). To each centrifuge bottle, 100 ml of de–ionised water was added at 20 °C. Samples were placed on a shaking wheel (205 mm *o.d.*) in the vertical position and shaken end–over–end at 30 rpm for 30 minutes. Each soil solution was transferred to a sieve immersed in de–ionised water and after gentle wet–sieving, the >100 μm fraction was obtained (Gee and Bauder 1986). The remaining soil solution was transferred to a 500 ml measuring cylinder and made to volume using de–ionised water. After the appropriate sedimentation period, the dispersed clay (<2 μm) fraction

was sampled using a 25 ml pipette (Gee and Bauder 1986). The >100 μm and the <2 μm size fractions of each soil were oven dried (105 °C) and quantified gravimetrically (dag kg^{-1}), and then the <100 μm fraction was determined by difference.

3.2.4 Ultrasonic agitation

Ultrasonic agitation was used to simulate the breakdown of soil aggregates during an intense rainfall event where the soil surface is not protected. This was done using the procedure of Field (2000); soil samples were prepared in glass specimen tubes (21 mm *i.d.* × 76 mm *h.*) by immersing the equivalent of four grams of air–dry soil in 20 ml of de–ionised water at 20 °C. The ultrasonic instrument used was a Misonix (Microson, ultrasonic cell disrupter) type instrument, which dissipated approximately 9.6 W. This disruptive force was delivered using ultrasound applied via a conical probe 112 mm in length, with a tip surface area of 28.2 mm^2. The probe was immersed to a depth of 22 mm in the soil solution, and disruptive energy applied for a period of 120 seconds. The soil suspension was transferred to a sieve immersed in de–ionised water and after gentle wet–sieving, the >100 μm fraction was obtained (Gee and Bauder 1986). The remaining soil solution was transferred to a 500 ml measuring cylinder and made to volume using de–ionised water. After the appropriate sedimentation period, the dispersed clay (<2 μm) fraction was sampled using a 25 ml pipette (Gee and Bauder 1986). The >100 μm and the <2 μm size fractions were oven dried (105 °C) and quantified gravimetrically (dag kg^{-1}), and then the <100 μm fraction was determined by difference.

3.2.5 Water quality and end–over–end disruption

To test the impact of water quality treatments on structural stability, the EOE–disruption procedure was repeated for each soil using an array of different solutions. Sub–samples of each soil were treated using one of thirteen different water solutions in addition to the de–ionised water treatment (solution T102) applied in chapter 3.2.3. In this experiment, six gram sub–samples of each of the nine Vertosols were shaken end–over–end using the respective *field water* solutions (FW00*i*) (Table 3.1) and with each of twelve *electrolyte solutions* (T301–4, T401–4 and T501–4) (Table 3.2). For the FW00*i* treatment, each soil was shaken using the field water sample collected from corresponding irrigation sources only, *e.g.* the B00*i* soils were treated with FW001, G001 was treated with FW002 and G002 was treated with FW003. The seven FW00*i* solutions were collected from the Darling River (FW001), and from water sources closest to each sampling site in the lower Gwydir (FW002–3), Hillston (FW004–5) and the lower Namoi (FW006–7) cotton–growing areas. For each FW00*i* solution, the EC_w (dS m^{-1}), the cations in solution and the SAR_w ($(mmol_{(+)}\ L^{-1})^{1/2}$) were determined using a conductivity electrode and an Atomic Absorption Spectrometer, which gave the content of

Ca^{2+}, Mg^{2+} and Na^{+} in solution (Table 3.l). The SAR_w of each solution was then determined using equation 2.

Table 3.1
Field water (FW00*i*) sampled from irrigation sources for each cotton–field investigated

	Origin	EC_w	SAR_w	Cations ($mmol_{(+)}\ L^{-1}$)			
		($dS\ m^{-1}$)	($(mmol_{(+)}\ L^{-1})^{1/2}$)	Ca^{2+}	Mg^{2+}	K^{+}	Na^{+}
FW001	B00*i* River[a]	0.98	4.69	1.14	1.14	0.11	5.02
FW002	G001 Storage[b]	0.22	1.00	1.52	1.06	0.14	1.13
FW003	G002 Storage[b]	0.31	1.56	1.31	1.07	0.12	1.71
FW004	H001 Bore[c]	0.45	3.38	0.45	0.58	0.05	2.43
FW005	H002 Bore[c]	0.31	3.44	0.27	0.37	0.04	1.94
FW006	N001 Storage[b]	0.41	5.84	0.69	0.55	0.03	4.07
FW007	N002 River[d]	0.26	2.48	0.93	0.81	0.04	2.02

[a] Sampled from the Darling River, Bourke, and used to treat B001, B002 and B003.
[b] Sampled from water storage facilities on each property.
[c] Sampled from individual bores at each property.
[d] Sampled from an irrigation channel adjacent to site N002.

The T30*i*, T40*i* and T50*i* solutions (Table 3.2) were prepared to give twelve different electrolyte solutions. The target EC_w of each solution was set as either 0.2, 0.5 or 2.7 dS m^{-1} and, for each increment of electrical conductivity, four different SAR_w levels were proposed (0, 7.5, 15 or 30 $(mmol_{(+)}\ L^{-1})^{1/2}$). These solutions were each prepared by combining $CaCl_2.2H_2O$, $MgCl_2.6H_2O$ and NaCl so that the Ca^{2+}:Mg^{2+} ratio was always equal to one. Quantities of Ca^{2+}, Mg^{2+} and Na^{+} were then combined to obtain desired values of EC_w and SAR_w (equations 5 and 6). The actual and the targeted values of EC_w and SAR_w are given in Table 3.2. The actual EC_w and SAR_w values are in all cases smaller than the target values. This is particularly evident in the solutions with a target EC_w of 0.2 dS m^{-1}. The very small values of actual SAR_w are a direct consequence of the difficulties of mixing the small quantities of $CaCl_2.2H_2O$, $MgCl_2.6H_2O$ and NaCl required in solution and the hydrophilic nature of each of the salts used. For example, to prepare the target EC_w 0.2, SAR_w 7.5 solution the salt contributions per litre of de–ionised water were: 4.6×10^{-3} g L^{-1} of $CaCl_2.2H_2O$, 6.4×10^{-3} g L^{-1} of $MgCl_2.6H_2O$ and 1.1×10^{-1} g L^{-1} of NaCl. These salt contributions are similar to the salt requirements of the EC_w 0.2, SAR_w 15 solution (1.3×10^{-3} g L^{-1} of $CaCl_2.2H_2O$, 1.7×10^{-3} g L^{-1} of $MgCl_2.6H_2O$ and 1.1×10^{-1} g L^{-1} of NaCl).

Table 3.2
Target attributes of each synthetic water solution, including those of de–ionised water (T102), and the actual attributes of each solution

Solution	Target EC_w[a] (dS m^{-1})	Target SAR_w[a] ($(mmol_{(+)} L^{-1})^{1/2}$)	Actual EC_w (dS m^{-1})	Actual SAR_w ($(mmol_{(+)} L^{-1})^{1/2}$)
T102	0.0	0.0	0.00	0.00
T301	0.2	0.0	0.19	0.02
T302		7.5		3.81
T303		15.0		4.39
T304		30.0		4.40
T401	0.5	0.0	0.47	0.00
T402		7.5		6.90
T403		15.0		10.40
T404		30.0		28.60
T501	2.7	0.0	2.35	0.00
T502		7.5		7.10
T503		15.0		14.30
T504		30.0		28.20

[a] Target thresholds of water quality as described by Muhammed (1996) and by Ayers and Westcot (1985)

$$Na^{+}\ mmol_{(+)}\ L^{-1} = SAR_{w} \times \sqrt{\frac{\left(Ca^{2+} + Mg^{2+}\right)}{2}} \qquad [5]$$

$$EC_{w}\ dS\ m^{-1} \approx \frac{\Sigma(Ca^{2+}, Mg^{2+}, Na^{+}\ mmol_{(+)}\ L^{-1})}{10} \qquad [6]$$

3.2.6 Estimation of structural stability

In order to compare the stability of all nine Vertosols, a stability index (SI) was developed according to Hulugalle and Finlay (2003). In this study the mass of particles <100 μm and <2 μm obtained after applying each different disruptive force were compared to the total mass of the <100 μm and the <2 μm fractions. The mean values of $SI_{<100}$ and $SI_{<2}$ were used to compare the nine soils, and different treatments of these nine Vertosols. The total mass of each size fraction was obtained from the particle size distribution (chapter 3.2.1). In this work:

$$SI_{<100}\ (\%) = \frac{<100\ \mu m_{stability}\ (dag\ kg^{-1})}{<100\ \mu m_{PSD}\ (dag\ kg^{-1})} \times 100 \qquad [7]$$

$$SI_{<2}\ (\%) = \frac{<2\ \mu m_{stability}\ (dag\ kg^{-1})}{<2\ \mu m_{PSD}\ (dag\ kg^{-1})} \times 100 \qquad [8]$$

After the determination of $SI_{<100}$ and $SI_{<2}$ values, the responses of each soil to the applied stresses and water quality treatments were compared in two ways; *(i)*, the effect of the three disruptive forces on the SI values of these soils were compared (spontaneous dispersion, EOE–disruption and ultrasonic agitation) and, *(ii)*, comparisons were made between the effects of solution treatments on either the <2 μm or <100 μm fractions (dag kg^{-1}) of each soil. For the latter comparisons, the Tukey Kramer test (P=0.05) was used to indicate significant differences between the mean values of the <2 μm fraction following the T102 and FW00*i* treatments and following the T102, T301, T401 and T501 treatments. This was repeated for the <100 μm fraction for the T102 and FW00*i* treatment comparisons and for the T102, T301, T401 and T501 treatment comparisons. Then, using the $SI_{<100}$ and $SI_{<2}$ values for each soil, the effects of water quality treatments were compared as follows; *(a)*, the responses of each soil to solutions T102 and FW00*i* were compared, *(b)*, the responses of each soil to solutions T102, T301, T401 and T501 were compared and, *(c)*, the effects of SAR_w were compared for each soil, where solutions T30*i*, T40*i* and T50*i* had been applied during EOE–disruption.

To further investigate the stability of the nine Vertosols, correlation values (equation 9) were determined between all calculated mean values of $SI_{<100}$ and $SI_{<2}$ and the selected physico–chemical properties for each of the disruptive forces and for each of the treatment solutions. The selected physico–chemical properties used were the organic carbon content, electrical conductivity, SAR, exchangeable Na^+, CEC_{eff}, Ca^{2+}:Mg^{2+} ratio, ESP, ESI and $EC_{1:5}/Na^+_{exch}$.

$$r = \frac{\sum (x - \bar{x})(y - \bar{y})}{\sqrt{\left[\sum (x - \bar{x})^2 (y - \bar{y})^2\right]}} \qquad [9]$$

In equation 9, *r* is the correlation coefficient for variables *x* and *y*. $\bar{x}$ and $\bar{y}$ are mean values for the *x* and *y* values used in the estimation.

3.3 Results

3.3.1 Fundamental soil properties

The nine furrow soils generally have physico–chemical properties (Table 3.3) that are similar to those of the 0.2–0.4 m layer of their respective soil profiles (chapter 2.4.2). In the irrigation furrow, each of the nine soils have clay textures, but soils B001 and H002 have a much larger coarse fraction (>100 μm) than the other soils. The organic carbon contents of the B00*i* and H00*i* sampling sites are

much less than those of sites G001 and N00*i*, but G002 has an organic carbon content equivalent to that of the two H00*i* soils. This range of organic carbon contents tends to show large regional variation, but all soils are still very low in organic material (McKenzie 1998).

The electrical conductivity of the soil solutions shows all the soils to be non–saline. The electrical conductivity values are all <0.5 dS m^{-1} with the exception of the B002 and N001 topsoils. These two soils are non–saline, but their large electrical conductivities mean that they are potentially problematic for agricultural production (*see* McKenzie 1998). The contribution of Na^+ to the soil solution is much more variable than the electrical conductivity values, and these soils have SARs of 0.2–7.5 $(mmol_{(+)}\ L^{-1})^{1/2}$. The B003, G00*i* and N002 soils all have SARs less than 2, but of the remaining furrow soils, only the B002 topsoil has a SAR larger than 5. The B00*i*, H00*i* and N002 sites have the smallest values of CEC_{eff}; this reflects the differences between the clay phyllosilicate suites of these soils and the G00*i* and N001 soils. The G00*i* and N001 soils have topsoil clay phyllosilicate suites dominated by expanding minerals (smectite and vermiculite).

The B00*i* and H00*i* soils have the smallest contributions of exchangeable Ca^{2+}. The Mg^{2+} contribution to the CEC_{eff} values is similar for all nine of these surface soils. However, the Ca^{2+}:Mg^{2+} ratio of the B00*i* and H00*i* soils is distinctly less than that of the other soils. The ESP values of each of these topsoils broadly reflect the respective SAR values. In particular, soils B001, B002 and N001 all have ESPs in excess of 5, and are regraded as sodic (McIntyre 1979). The surface soils B003 and H001 both have ESP values above 2 and it is anticipated that all five of these surface soils (B00*i*, H001 and N001) are potentially unstable (Cook *et al.* 1992; McKenzie 1998). The ASWAT test confirmed this potential instability. In particular, B001, B003 and N001 all contain aggregates that disperse when immersed in de–ionised water, while the B002 and H001 topsoils show dispersion only after aggregates are remoulded. Given their ESPs, soils B002 and B003 do not disperse as anticipated and this reflects different electrical conductivities between these soils. B002 is a sodic soil, but in this soil the large electrical conductivity is expected to influence the extent of clay swelling, and consequently, the extent of clay dispersion. In contrast, B003 is non–sodic but has a very small electrolyte concentration, which appears insufficient to restrict the dispersion of clay particles during the ASWAT assessment. However, this observed association between ESP and electrical conductivity is not described by comparisons between ASWAT dispersion scores and the determined ESI or $EC_{1:5}/Na^+_{exch}$ values.

Table 3.3
Physico–chemical properties of the irrigation furrow for each Vertosol investigated

	Sampled field								
	B001	**B002**	**B003**	**G001**	**G002**	**H001**	**H002**	**N001**	**N002**
Size fraction (%)									
<100 μm	80.3	87.3	88.0	97.5	93.4	90.1	77.3	86.2	85.3
<2 μm	60.5	60.0	63.0	54.9	63.7	59.9	54.1	57.3	55.3
pH (1:5 $CaCl_2$)	7.2	7.6	7.2	7.0	7.6	7.2	7.9	7.9	7.7
Organic Carbon (%)	0.22	0.27	0.32	0.96	0.39	0.45	0.40	0.62	0.88
EC (1:5 water) (dS m^{-1})	0.37	1.19	0.14	0.09	0.15	0.21	0.20	0.96	0.17
SAR ($(mmol_{(+)}\ L^{-1})^{1/2}$)	4.9	7.5	1.9	1.3	1.9	3.0	2.4	3.2	0.2
Ca^{2+}_{exch} ($cmol_{(+)}\ kg^{-1}$)	20.4	25.7	26.9	37.1	33.6	18.6	24.7	32.9	31.4
Mg^{2+}_{exch} ($cmol_{(+)}\ kg^{-1}$)	10.7	11.1	10.4	12.7	13.0	9.9	11.7	11.4	10.3
Na^{+}_{exch} ($cmol_{(+)}\ kg^{-1}$)	2.86	2.16	1.46	0.64	0.77	0.94	0.70	3.13	0.29
K^{+}_{exch} ($cmol_{(+)}\ kg^{-1}$)	1.53	1.51	1.85	0.88	1.35	1.43	1.11	1.58	1.72
CEC_{eff} ($cmol_{(+)}\ kg^{-1}$)	35.5	40.5	40.5	51.3	48.8	30.8	38.2	49.0	43.7
Ca^{2+}:Mg^{2+}	1.9	2.3	2.6	2.9	2.6	1.9	2.1	2.9	3.0
ESP	8.1	5.3	3.6	1.3	1.6	3.1	1.8	6.4	0.7
ESI	0.05	0.22	0.04	0.07	0.09	0.07	0.11	0.15	0.24
$EC_{1:5}/Na^{+}_{exch}$	0.13	0.55	0.10	0.14	0.19	0.22	0.29	0.31	0.59
ASWAT dispersion[a]	9	3	9	0	0	4	0	9	0

[a] 0=no dispersion of aggregates, 1–8=dispersion after re–moulding of aggregates, 9–16=dispersion of aggregates.

3.3.2 Structural stability of Vertosols measured using de–ionised water and three different disruptive forces

The imposition of the three disruptive forces (spontaneous dispersion, EOE–disruption and ultrasonic agitation) results in more complete aggregate breakdown where larger forces are imposed (Figure 3.1). This is expected and is demonstrated, for all these soils, by the larger values of $SI_{<100}$ and $SI_{<2}$ following EOE–disruption than following spontaneous dispersion, and by the larger values of $SI_{<100}$ and $SI_{<2}$ following ultrasonic agitation rather than following EOE–disruption.

The extent of liberation is different after each of the disruptive forces, for each of the furrow topsoils. The $SI_{<100}$ value after spontaneous dispersion is largest for soil B001 where 55 % of particles less than <100 μm are liberated. The furrow soils B002, B003 and G001 have intermediate values for $SI_{<100}$ (34–38 %), while G002, H00*i* and N00*i* have the most stable >100 μm fraction.

The treatment of these soils with EOE–disruption results in the liberation of 39–62 % of soil material <100 μm for the nine Vertosols. Using this treatment soils H001 and N001 are least stable for this size fraction, while soil B002 is the most stable. Comparing $SI_{<100}$ values of spontaneous dispersion and EOE–disruption shows two distinct soil categories: *(i)*, B00*i* soils have similar $SI_{<100}$ values after the application of each of these disruptive forces and, *(ii)*, the G00*i*, H00*i* and N00*i* soils

show a large increase in aggregate liberation after EOE–disruption. These six topsoils (G00*i*, H00*i* and N00*i*) have $SI_{<100}$ values that are 18–36 % larger after EOE–disruption than after spontaneous dispersion.

Treating the B00*i*, G00*i*, H00*i* or N00*i* topsoils using ultrasonic agitation results in the liberation of ≥90 % of soil particles of the <100 μm size fraction for all these Vertosols. In particular, almost all of the <100 μm size fraction of B001 is liberated after ultrasonic agitation, while the $SI_{<100}$ values for soils B003 and H001 are greater than 95 %. The remaining soils (B002, G00*i*, H002 and N00*i*) all tend to have $SI_{<100}$ values of 90–95 % after this disruptive force is applied.

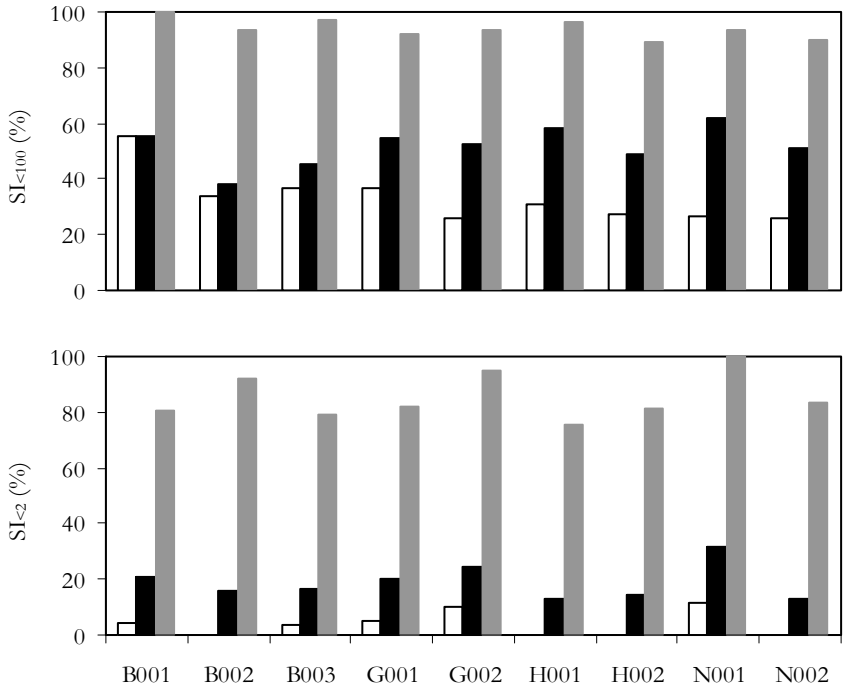

Figure 3.1 $SI_{<100}$ and $SI_{<2}$ values for each soil after being treated in de–ionised water with each of the three disruptive forces; spontaneous dispersion (□), EOE–disruption (■) and ultrasonic agitation (■).

The $SI_{<2}$ values show similar trends to the $SI_{<100}$ values for each topsoil (Figure 3.1). After treating the nine topsoils using spontaneous dispersion, the G002 and N001 topsoils are the least stable. These soils have $SI_{<2}$ values of approximately 10 %, which are distinctly larger than those of the other soils ($SI_{<2}$ <5 %), and four soils do not have any observed dispersion (B002, H00*i* and N002).

Treating the nine topsoils using EOE–disruption results in all soils having $SI_{<2}$ values that are 10–15 % larger than the $SI_{<2}$ values determined after spontaneous dispersion. The EOE–disruption technique results in the dispersion of 13–30 % of the clay fractions of these soils. N001 and G002 are the least stable in this case, while H00*i* and N002 have the smallest $SI_{<2}$ values for this treatment.

A comparison of these $SI_{<2}$ values with those values obtained using ultrasonic agitation shows that soils N001 and G002 are again the least stable of the nine topsoils. These two soils and soil B002 all have greater than 90 % of clay dispersed where ultrasonic agitation is applied. All the other topsoils have $SI_{<2}$ values of 77–83 % and of these, the H001 soil has the smallest $SI_{<2}$ values.

3.3.3 Comparing the structural stability of the nine topsoils after treatment with solutions T102 and FW00i using EOE–disruption

The <100 μm and <2 μm size fractions, obtained after treating each of the nine soils with the T102 and FW00*i* solutions, are presented in Table 3.4 and the associated $SI_{<100}$ and $SI_{<2}$ values are presented in Figure 3.2. The stabilities of these soil are generally similar when the <100 μm size fractions are compared following the T102 and FW00*i* treatments. Four furrow topsoils (B001, G001, H001 and N001) all have $SI_{<100}$ values that are greater than 50 % after treatment with T102 and these soils are the least stable. In contrast, the B002 topsoil has the smallest $SI_{<100}$ value after treatment using T102.

Four of the topsoils investigated (B002, G002, H001 and N001) show significantly different <100 μm fractions following the two treatments; of these four surface soils, the H001 and N001 soils have the largest difference in aggregate liberation between these treatments. These two soils have approximately 10 dag kg^{-1} more <100 μm soil material liberated after shaking in T102 than after shaking in FW00*i*. Similarly, G002 has significantly larger <100 μm values after shaking in T102. However, the B002 topsoil shows a different response to treatment. This soil has significantly larger <100 μm values where FW00*i*, rather than T102, is applied.

Table 3.4
The <100 μm and the <2 μm fractions for all soils, disrupted using EOE–shaking in either FW00*i* or T102

	De–ionised water (T102)				Field water (FW00*i*)			
	<2 μm (dag kg^{-1})		<100 μm (dag kg^{-1})		<2 μm (dag kg^{-1})		<100 μm (dag kg^{-1})	
B001	12.77*a*	± 0.18	44.90	± 0.95	4.69*b*	± 0.58	43.53	± 1.16
B002	9.61	± 0.78	33.01*d*	± 0.14	7.39	± 0.68	37.99*c*	± 1.36
B003	10.29*a*	± 0.32	39.58	± 0.53	4.42*b*	± 0.51	38.46	± 0.90
G001	11.01*b*	± 0.37	53.32	± 1.44	21.45*a*	± 1.09	59.35	± 1.94
G002	15.40*b*	± 1.12	48.86*c*	± 0.78	27.69*a*	± 0.25	44.76*d*	± 0.53
H001	7.71	± 0.36	52.38*c*	± 1.11	8.45	± 1.04	43.72*d*	± 0.79
H002	7.72	± 0.33	37.91	± 0.28	9.01	± 0.85	36.74	± 0.75
N001	18.12*b*	± 0.97	53.46*c*	± 0.49	28.79*a*	± 0.42	44.43*d*	± 0.30
N002	7.30*b*	± 0.73	43.50	± 0.47	25.99*a*	± 0.57	41.48	± 1.04

Within rows the letters *a* and *b* represent significant difference between treatments for the <2 μm particle class and the letters *c* and *d* represent significant difference between treatments for the <100 μm particle class. Comparison of means was carried out using the Tukey–Kramer test (P=0.05).

The clay fractions of these soils are affected very differently by the two solutions. In the <2 μm fraction, soils B001 and B003 have significantly more dispersed clay in solution after treatment with solution T102 rather than after treatment with solution FW00*i* (Table 3.4). In contrast, the G00*i* and N00*i* soils each have significantly less dispersed clay after shaking in the T102 treatment than after shaking in the FW00*i* solution. The B002 and H00*i* soils show no significant difference in quantities of dispersed clay following the two solution treatments.

Comparing all soils using these treatments for the $SI_{<2}$ values, there are two clear trends (Figure 3.2). The B00*i* soils have larger $SI_{<2}$ values after treatment with solution T102 than after treatment with solution FW001, and overall the B00*i* and H00*i* topsoils have the least dispersive clay fractions. In comparison, the G00*i* and N00*i* topsoils have larger $SI_{<2}$ values after treatment with the FW00*i* solution. These soils have the most dispersive clay fractions after each of the treatments. The N001 topsoil is least stable in T102, while the N00*i* soils are least stable of all the soils when their respective FW00*i* solutions are used as treatments during EOE–disruption.

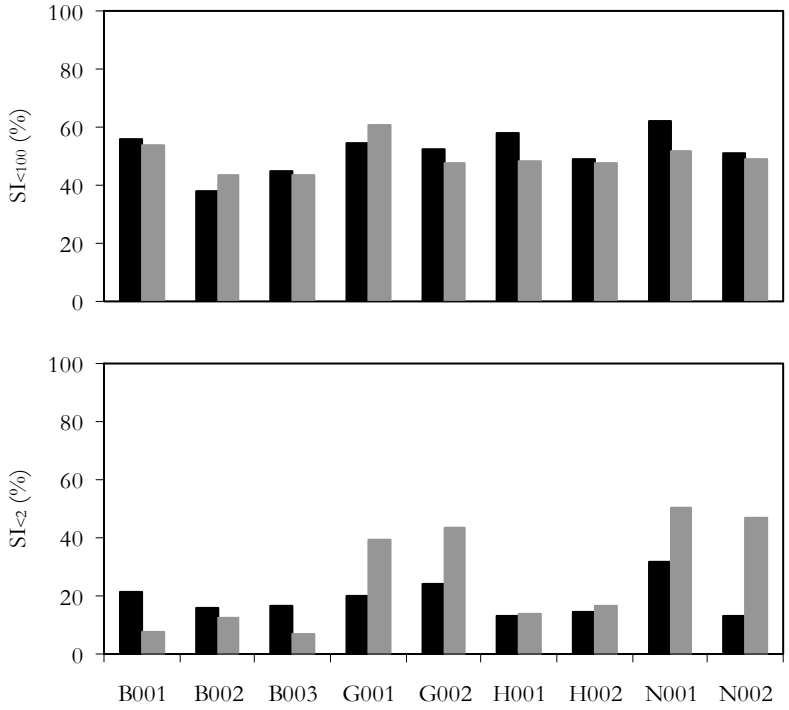

Figure 3.2 $SI_{<100}$ and $SI_{<2}$ values for all soils treated with solutions of de–ionised water (T102) (■) and field water (FW00*i*) (■) during EOE–disruption.

3.3.4 Comparing the structural stability of the nine topsoils after treatment with solutions of EC_w 0.0, 0.2, 0.5 or 2.7 dS m^{-1}, where SAR_w is equal to zero, using EOE–disruption

The <100 μm and <2 μm size fractions, obtained after treating each of the nine topsoils with solutions T102, T301, T401 and T501, are presented in Tables 3.5 and 3.6 and the associated $SI_{<100}$

and $SI_{<2}$ values are presented in Figures 3.3 and 3.4. The stability of all these soils shows a significant influence of the EC_w of the applied treatment solution. The common trend for the <100 μm fraction shows that these topsoils are more stable in solutions of larger EC_w. However, two topsoils (B002 and G001) are less stable in solutions T301 and T401 than in solution T102. Seven of the topsoils (B001, B002, G002, H00*i* and N00*i*) have <100 μm fractions that are significantly smaller after mechanical disruption in the T501 treatment. In this case, the exceptions are the B002 and G001 topsoils, both of which have similar <100 μm fractions after treatment with T102 or T501.

Shaking these soils in solutions T301, T401 and T501 shows the G001 topsoil to have the largest values of $SI_{<100}$ (Figure 3.3), while B002, B003 and H00*i* consistently have the smallest $SI_{<100}$ values. Five of the nine Vertosols have $SI_{<100}$ values that appear to be strongly influenced by the electrolyte concentration of treatment solutions. These topsoils (B001, B003, H00*i* and N001) all have $SI_{<100}$ values that are at least 10 % smaller after treatment with solution T301 rather than after treatment with solution T102. Applying solutions of larger EC_w does not have the same effect on the $SI_{<100}$ values of these five topsoils *e.g.* treating the B003 and H00*i* soils with each of these three solutions gives $SI_{<100}$ values that differed by less than 5 %.

Table 3.5
The <100 μm (dag kg^{-1}) fraction of all soils treated with four solutions of increasing salt concentration using EOE–disruption

	Solution T102 *EC_w 0.0 (dS m^{-1})*			**Solution T301** *EC_w 0.2 (dS m^{-1})*			**Solution T401** *EC_w 0.5 (dS m^{-1})*			**Solution T501** *EC_w 2.7 (dS m^{-1})*		
B001	44.90*a*	±	0.95	37.23*b*	±	1.00	31.84*c*	±	0.32	27.16*d*	±	0.65
B002	33.01*b*	±	0.14	35.57*b*	±	0.66	40.54*a*	±	0.50	32.87*b*	±	1.09
B003	39.58*a*	±	0.53	32.01*b*	±	0.56	30.87*b*	±	0.18	26.85*c*	±	1.17
G001	53.32*b*	±	1.44	56.73a*b*	±	0.58	58.73*a*	±	0.64	53.74*b*	±	0.30
G002	48.86*a*	±	0.78	47.13*a*	±	0.43	46.43*a*	±	0.86	38.29*b*	±	0.18
H001	52.38*a*	±	1.11	36.30*b*	±	0.37	35.98*b*	±	0.20	32.02*c*	±	0.46
H002	37.91*a*	±	0.28	29.83*bc*	±	0.75	31.40*b*	±	0.59	27.63*c*	±	0.56
N001	53.46*a*	±	0.49	43.31*b*	±	0.95	39.13*c*	±	0.89	32.86*d*	±	0.04
N002	43.50*a*	±	0.47	42.27*a*	±	0.83	43.65*a*	±	0.45	38.12*b*	±	1.14

Within rows the letters represent significant difference between treatments using the multiple comparison Tukey–Kramer test (P=0.05).

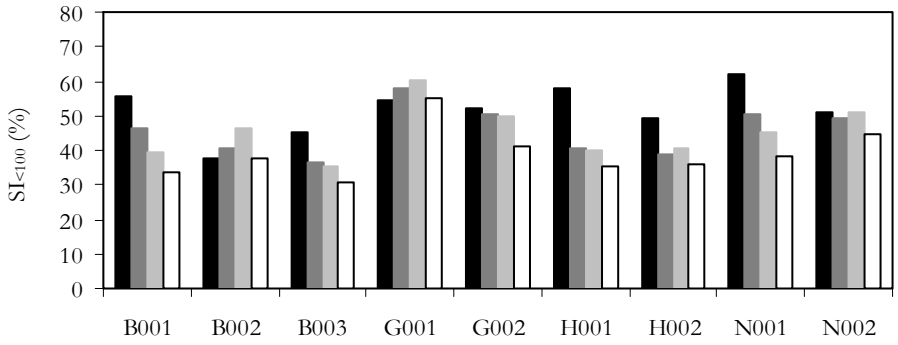

Figure 3.3 $SI_{<100}$ values for all soils treated with four solutions of increasing salt concentration [T102 (■), T301 (■), T401 (■) and T501 (□)] using EOE–disruption.

Like the <100 μm fraction, treating each of the topsoils with the four solutions (T102, T301, T401 or T501) shows that increasing EC_w leads to significantly smaller quantities of dispersed clay (Table 3.6). However, these results show a large effect of sampling region that appears to determine the influence of salt content on the amount of dispersed clay. For example, the B00*i* soils all show a significant stepwise reduction in dispersed clay as solutions of increased EC_w are applied. However, the G002, H002 and N00*i* soils do not disperse in the same way. For these soils, treatment with T102 or T301 solutions leads to similar <2 μm (dag kg^{-1}) values, while using the T401 solution results in significantly less dispersion for the H00*i* and N001 soils. Three soils act very differently to the others; G001 has no significant difference between the T102 and T401 values of <2 μm, while G002 and N002 shows no significant difference in dispersed clay for any of the T102, T301 and T401 treatment solutions. The solution with the largest increment of EC_w (T501) contains sufficient electrolyte to cause the flocculation of all clay reaching suspension during end–over–end shaking, and no dispersed clay is apparent for any of these nine topsoils.

Table 3.6
The <2 μm (dag kg^{-1}) fraction of all soils treated with four solutions of increasing salt concentration using EOE–disruption

	Solution T102 *EC_w 0.0 (dS m^{-1})*			**Solution T301** *EC_w 0.2 (dS m^{-1})*			**Solution T401** *EC_w 0.5 (dS m^{-1})*			**Solution T501** *EC_w 2.7 (dS m^{-1})*
B001	12.77*a*	±	0.18	7.48*b*	±	0.65	3.51*c*	±	0.65	0.00*d*
B002	9.61*a*	±	0.78	6.28*b*	±	0.87	3.36*c*	±	0.36	0.00*d*
B003	10.29*a*	±	0.32	6.01*b*	±	0.21	3.07*c*	±	0.52	0.00*d*
G001	11.01*b*	±	0.37	13.11*a*	±	0.58	10.20*b*	±	0.34	0.00*c*
G002	15.40*a*	±	1.93	14.37*a*	±	4.18	15.00*a*	±	0.4	0.00*b*
H001	7.71*a*	±	0.36	6.19*a*	±	0.6	2.81*b*	±	0.4	0.00*c*
H002	7.72*a*	±	0.33	7.75*a*	±	0.17	2.85*b*	±	0.28	0.00*c*
N001	18.12*a*	±	0.97	18.41*a*	±	0.62	13.43*b*	±	0.09	0.00*c*
N002	7.30*a*	±	0.73	10.19*a*	±	0.37	8.79*a*	±	1.11	0.00*b*

Within rows the letters represent significant difference between treatments using the multiple comparison Tukey–Kramer test where P=0.05.

Comparison of the $SI_{<2}$ values shows the N001 topsoil to consistently have the largest quantities of total clay becoming dispersed after mechanical disruption (Figure 3.4). This is most evident for treatment of this soil with solutions T102 and T301. However, treating the different topsoils using the T401 solution yields similar $SI_{<2}$ values for both the G00*i* and N001 topsoils. In contrast, the most stable topsoils tend to be those sampled from the Bourke and Hillston cotton–producing regions.

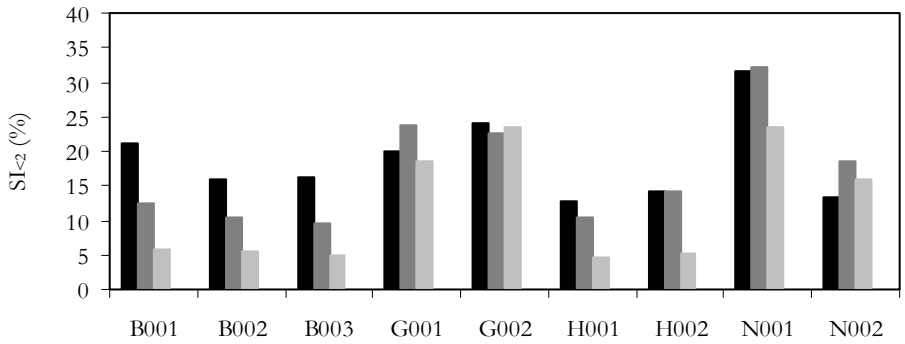

Figure 3.4 $SI_{<2}$ values for all soils treated with four solutions of increasing salt concentration [T102 (■), T301 (■), T401 (■) and T501 (□)] using EOE–disruption.

3.3.5 Structural stability of nine surface soils after EOE–disruption using different increments of water quality (3 increments of EC_w each with 4 levels of SAR_w)

The $SI_{<100}$ and $SI_{<2}$ values of all nine topsoils are compared by sampling region at the three intervals of EC_w and four increments of SAR_w in Figures 3.5 to 3.8. Treating these soils with solutions of different EC_w and SAR_w affects the stability of each soil differently. Each of the Vertosols is most stable where the T50*i* solutions are applied and least stable after treatment with the T30*i* solutions. Meanwhile, increasing the level of SAR_w at each interval of EC_w generally results in decreased stability for each of the topsoils.

For all of these topsoils, the observed trends in values of $SI_{<100}$ and $SI_{<2}$ are dissimilar for the three EC_w intervals, but for solutions T40*i* and T50*i* there are consistent patterns of disruption. Similarly, the topsoils treated with T301, T302 or T303 tend to show larger $SI_{<100}$ and $SI_{<2}$ values as the SAR_w of solution is increased (T301→3). However, after shaking in solution T304 most of these soils have smaller $SI_{<100}$ and $SI_{<2}$ values (B00*i*, G002, H001 and N001) where they are compared with $SI_{<100}$ and $SI_{<2}$ values obtained for the T302 or T303 treatments. This was despite the similar values of actual SAR_w in the T302–4 solutions (SAR_w values of 3.81, 4.39 or 4.40 respectively).

The treatment of the topsoils with T401, T402, T403 and T404 (T401–4) or with T501, T502, T503 and T504 (T501–4) solutions shows trends that are more consistent for the $SI_{<2}$ values. For example, treating each soil using the T401–4 series of solutions results in greater clay dispersion as

the treatment SAR_w is increased (T401→3). However, at the largest increment of SAR_w (T404), $SI_{<2}$ values tend to be similar to the $SI_{<2}$ values obtained after treatment using T403 for all of the topsoils. Concurrently, the $SI_{<100}$ values show a less distinct, but similar trend for topsoils treated using solutions T401–3. The T404 treatment generally results in $SI_{<100}$ values similar to those from the T402 treatment.

The T50*i* solutions show a consistent increase in the $SI_{<100}$ as the level of SAR_w is increased. For the T501–T503 solutions, the $SI_{<2}$ values are consistently less than 5 % for all nine soils. At the largest SAR_w level (T504), $SI_{<2}$ values are generally between 5 and 10 % for these topsoils.

3.3.5.1 Water quality and the stability of the Bourke soils

The B00*i* soils all tend to show similar patterns of aggregate breakdown. The values of $SI_{<100}$ and $SI_{<2}$ (Figure 3.5) are generally largest in low EC_w solutions and smallest in solutions of greatest EC_w (except for B002 $SI_{<100}$ values), while increasing SAR_w tends to result in a decrease in stability for all three soils.

The B00*i* soils all have larger $SI_{<100}$ values after treatment with T302 and T303 than after the T301 treatment, but after treatment with T304 $SI_{<100}$ values were most similar to those to those $SI_{<100}$ values obtained from the T301 treatment. The $SI_{<2}$ values show similar trends for each of the three soils; increasing SAR_w (T301→3) results in larger $SI_{<2}$ values, but after shaking in T304, the $SI_{<2}$ values are less than $SI_{<2}$ value obtained after shaking in either the T302 or T303 treatments.

The topsoil response to the T401, T402 and T403 solutions, for each of the B00*i* soils, shows that larger $SI_{<100}$ and $SI_{<2}$ values occur after treatment with solutions of larger SAR_w. The largest increment of SAR_w (T404) shows these soils to have similar $SI_{<2}$ values to those obtained where the T403 treatment is applied, while the $SI_{<100}$ values obtained for the T404 treatment are similar to those obtained using the T402 solution.

Treating the B00*i* soils with the solutions of largest EC_w (T50*i*) did not tend to result in large differences in either the $SI_{<100}$ or $SI_{<2}$ values. Increasing the SAR_w of treatment solution (T501→4) results in small increases in $SI_{<100}$ for each B00*i* soil; similarly, increased SAR_w leads to larger $SI_{<2}$ values. However, where the treatment solutions T501→3 are applied, no clay dispersion is apparent, but treatment using T504 shows $SI_{<2}$ values of 8 % and 5 % for B001 and B003 soils respectively. The B002 surface soil does not have any dispersed clay in solution after this treatment.

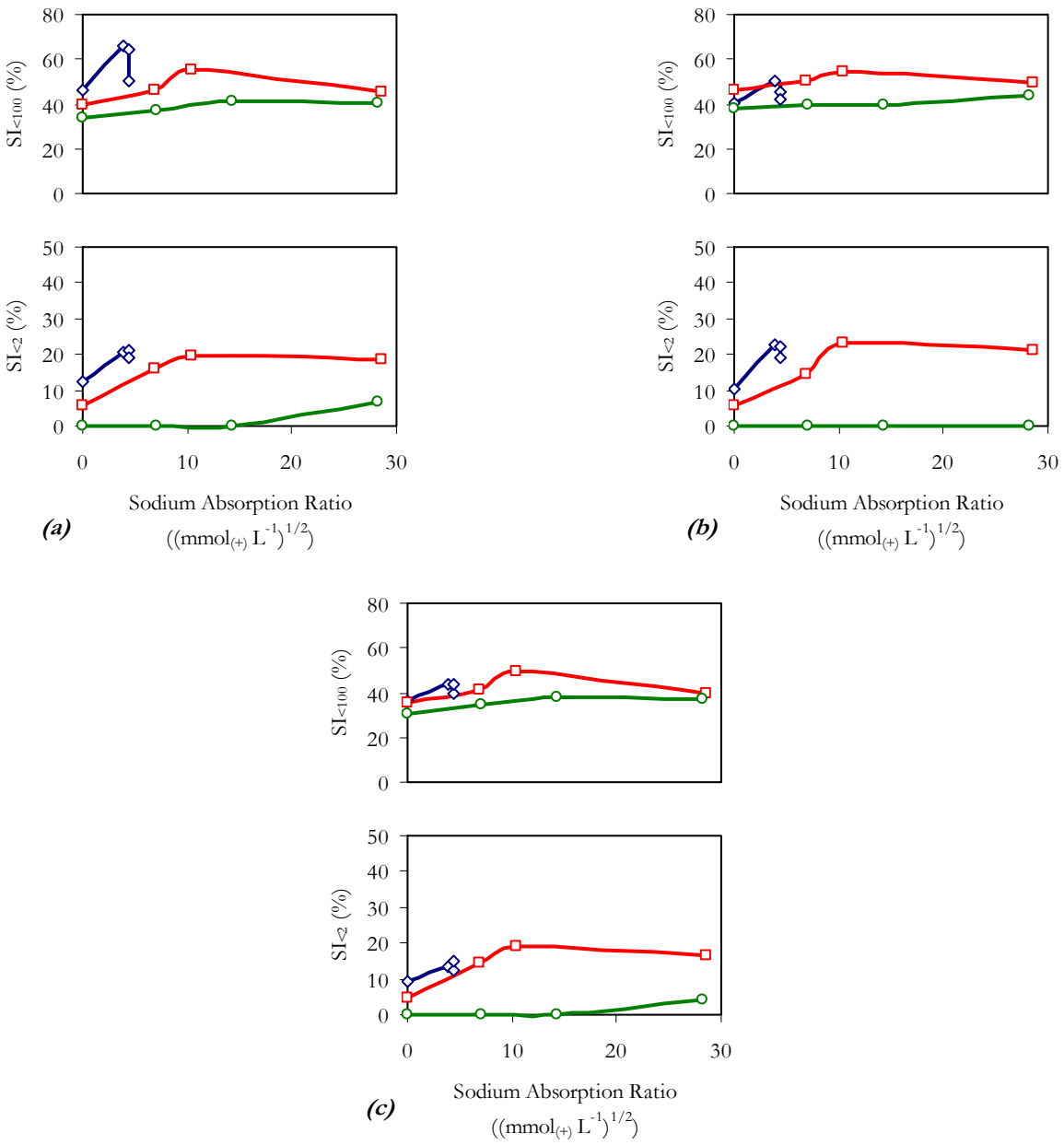

Figure 3.5 The $SI_{<100}$ (%) and the $SI_{<2}$ (%) values of soil B001 (*a*), B002 (*b*) and B003 (*c*) using the treatment solutions T301–4 (◇), T401–4 (□) or T501–4 (○) and EOE–disruption.

3.3.5.2 Water quality and the stability of the lower Gwydir soils

The $SI_{<100}$ and $SI_{<2}$ values determined for the G00*i* soils after end–over–end shaking in each of the treatment solutions are presented in Figure 3.6. Shaking of these soils in solutions T301, T401 or T501 generally led to smaller $SI_{<100}$ values for the larger EC_w solutions, while increasing the SAR_w led to small increases in $SI_{<100}$ values. However, increasing the SAR_w for each of the three treatment series (T30*i*, T40*i* and T50*i*) does not substantially influence the quantity of <100 μm material liberated for either of these soils, particularly when solutions of low SAR_w ($SAR_w \leq 7.5$) are used.

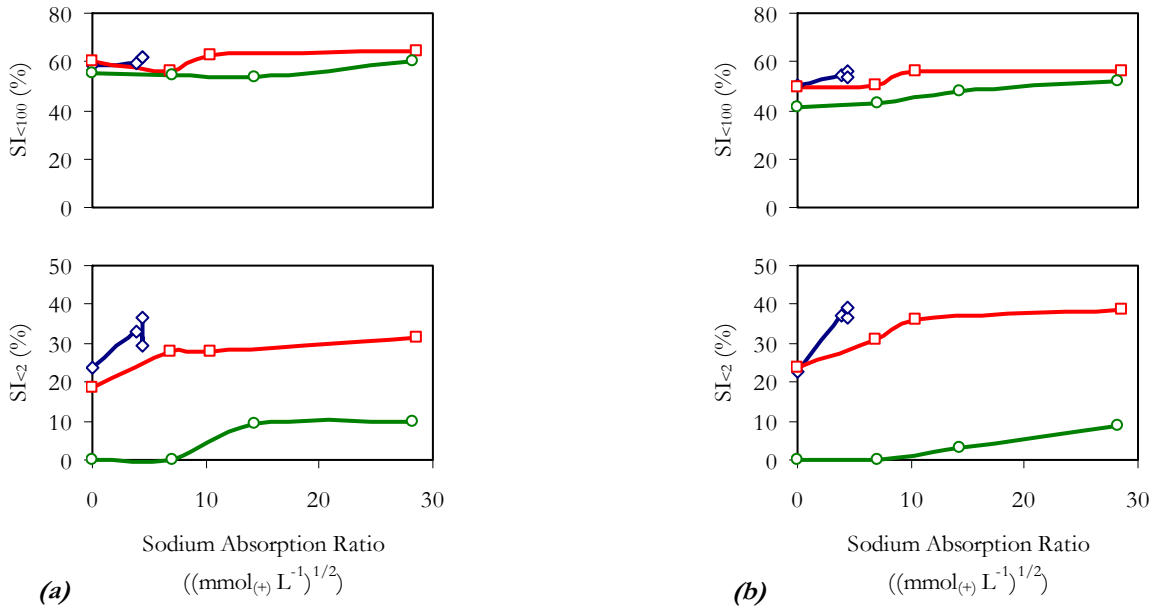

Figure 3.6 The $SI_{<100}$ (%) and the $SI_{<2}$ (%) values of soil G001 (*a*) and G002 (*b*) using treatment solutions T301–4 (◇), T401–4 (□) or T501–4 (○) and EOE–disruption.

In comparison, the combinations of solution EC_w and SAR_w have a much greater effect on the quantities of dispersed clay ($SI_{<2}$ values) for these topsoils. Treating G001 and G002 with solutions T301 and T401 gave similar values of $SI_{<2}$, but increasing the SAR_w shows different responses for the T30*i* and T40*i* treatments. Increasing the SAR_w of the T30*i* series shows a rapid increase in dispersed material, even at low SAR_w values (SAR 3.8–4.4).

Treatment with the T40*i* solutions results in larger $SI_{<2}$ values as SAR_w is increased, however as the T40*i* SAR_w is increased both soils begin to show a plateau in $SI_{<2}$. Comparing the effects of T40*i* (T401 and T402 for G001 and T401–3 for G002) solutions showed a large increase in clay liberation with increasing SAR_w, but following solution T404, the values of $SI_{<2}$ were similar to those obtained using the T403 solution. This gave an inflection point for the T40*i* curves of these topsoils that broadly corresponds to the maximum $SI_{<2}$ obtained using the T30*i* solutions.

The T50*i* treatment series, unlike the T30*i* and T40*i* treatments, shows $SI_{<2}$ values ≤10 % at all SAR_w increments. Here, the small SAR_w solutions (T501 and T502) contain no dispersed clay after shaking, but increasing the SAR_w of solution (T503 and T504) results in some clay dispersion for both soils. Soil G001 is influenced by solution T503 ($SI_{<2}$ =10 %) more than G002 ($SI_{<2}$ =4 %), but where treatment T504 is applied, both surface soils have similar $SI_{<2}$ values.

3.3.5.3 Water quality and the stability of the Hillston soils

The $SI_{<100}$ and $SI_{<2}$ values obtained after shaking the H00*i* surface soils end–over–end in each of the treatment solutions are presented in Figure 3.7. The stabilities of these two topsoils are very similar where the EC_w treatments are compared. Like the other soils, H001 and H002 are most stable after shaking in the saline T50*i* solutions and are generally least stable in the T30*i* solutions.

The T30*i* solutions affected each of these two soils somewhat differently. Soil H001 shows that in the T30*i* solutions, the $SI_{<100}$ and $SI_{<2}$ values increase as SAR_w is raised (solutions T301→3), but using the solution T304, particle liberation is similar to that after the T301 treatment. In contrast, treating H002 with T301–3 gave $SI_{<100}$ and $SI_{<2}$ values that are similar, while using solution T304 results in an increase in $SI_{<100}$ and $SI_{<2}$ values of approximately 5 %.

Treatment using the T40*i* series shows similar patterns of liberation for both soils; both have similar $SI_{<100}$ and $SI_{<2}$ values for each increment of SAR_w. The application of solutions T401–3 shows a continual increase in the stability index of each size fraction for treatments T401–3, while shaking these soils in T404 shows small decreases in the SI indices (particularly $SI_{<100}$) where they are compared with dispersion using the T403 treatment.

In both soils, solutions T501–4 show small increases in $SI_{<100}$, as solution SAR_w is raised. As a result, the application of T504 results in $SI_{<100}$ values approximately 10 % larger than those obtained using T501 for each of the topsoils. In these solutions, clay dispersion ($SI_{<2}$) is very small (<5 %). For the solutions T501–3, no clay dispersion is apparent for either soil, while the application of the T504 solution (SAR_w=28.2) yields similarly small $SI_{<2}$ values ($SI_{<2}$≈3 %) for each soil.

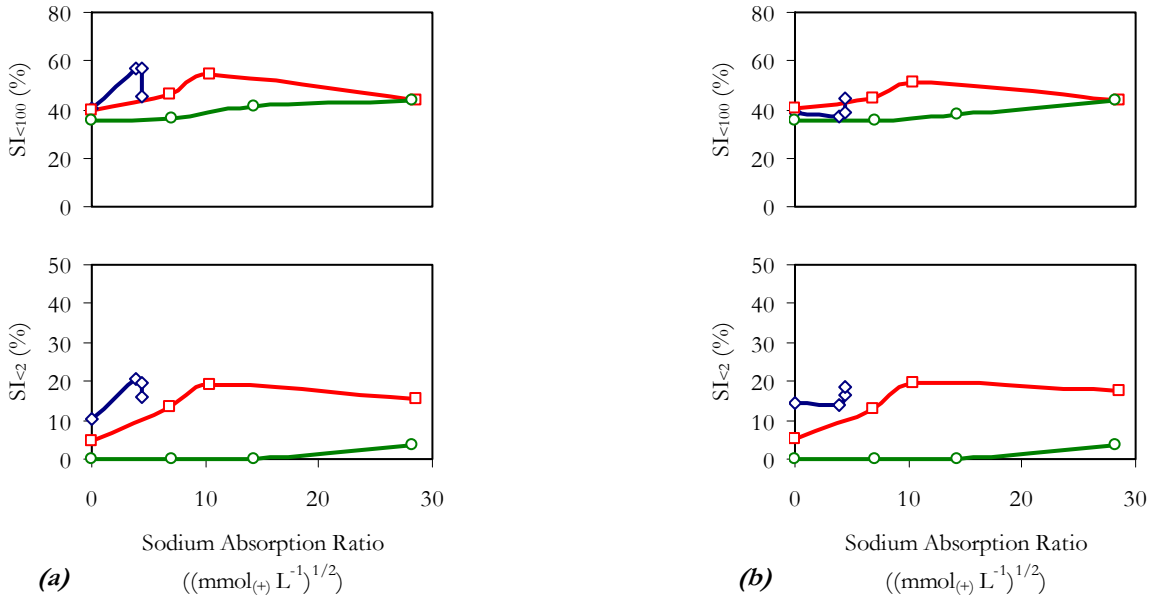

Figure 3.7 The $SI_{<100}$ (%) and the $SI_{<2}$ (%) values of soil H001 (*a*) and H002 (*b*) using treatment solutions T301–4 (◇), T401–4 (□) or T501–4 (○) and EOE–disruption.

3.3.5.4 *Water quality and the stability of the lower Namoi soils*

The $SI_{<100}$ and $SI_{<2}$ values, determined for the N00*i* surface soils, are presented in Figure 3.8. Treating these soils with the T30*i* and T40*i* solutions gives similar trends in $SI_{<100}$. In the T50*i* solutions, the N001 soil has smaller values of $SI_{<100}$ than the N002 soil. Like the other soils, $SI_{<100}$ values are larger after treatment with solutions of larger SAR_w (T301→3, T401→3 or T501→4). However, the T30*i* treatment series gives dissimilar responses for each of the two N00*i* soils: N001 is slightly more stable (smaller $SI_{<100}$) in solution T304 than in T302 or T303, but the N002 soil has similar values of $SI_{<100}$ for the T301–4 treatments.

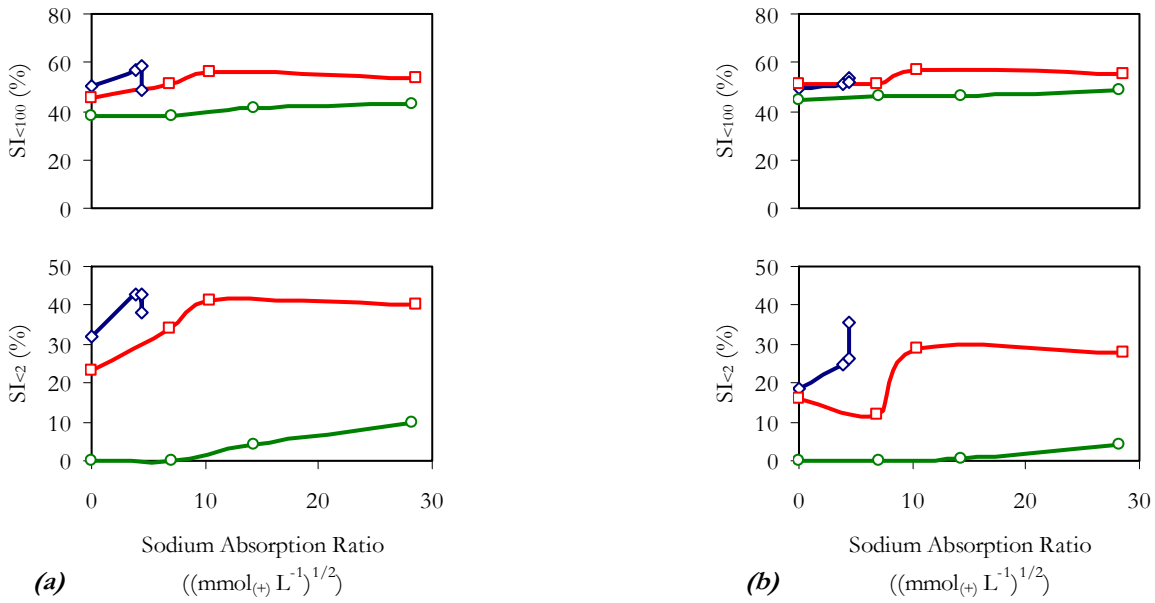

Figure 3.8 The $SI_{<100}$ (%) and the $SI_{<2}$ (%) values of soil N001 (*a*) and N002 (*b*) using treatment solutions T301–4 (◇), T401–4 (□) or T501–4 (○) and EOE–disruption.

For these two N00*i* topsoils, the similar trends of $SI_{<100}$ are not reflected by clay dispersion. In all solutions the clay fraction of N001 is much less stable than the N002 soil. The treatment of N001 with the T30*i* solutions shows a large increase in the quantity of dispersed clay as SAR_w is increased (T301→2). Treating this soil using T302 or T303 results in similar quantities of dispersed clay, but where T304 is applied, the $SI_{<2}$ value is 5 % less than that obtained using the T302 or T303 solutions. In contrast, treating N002 with the T301→4 solutions results in a large increase in $SI_{<2}$.

The T40*i* series highlights the different stabilities of the clay fractions for these two topsoils. Increasing the SAR_w of treatment solutions (T401→3), results in larger quantities of dispersed clay in the N001 surface soil, while treating this soil using the solutions T403 and T404 results in similar values of $SI_{<2}$, where 40 % of clay sized particles are dispersed. The N002 surface soil followed a different trend. Treating this soil using either the T401 or T402 solution results in similar $SI_{<2}$ values. Likewise, treating N002 surface soil with T403 or T404 results in similar $SI_{<2}$ values. However, there

is a sharp increase in $SI_{<2}$ values between treatments of T402 and T403 ($SI_{<2}$ 11 % and $SI_{<2}$ 29 %, respectively).

Treating the N00*i* soils with the T50*i* solutions gives no apparent clay dispersion at low SAR_w; the N001 topsoil does not have dispersed clay in solutions T501 and T502, while N002 has no dispersion after using solutions T501–3. At larger increments of SAR_w the N001 soil has 5 % of clay dispersed after shaking in T503 and 10 % of clay dispersed after shaking in T504. In contrast, the soil N002 has less than 5 % clay dispersion, and this is only after EOE–disruption in T504.

3.3.6 Correlation of the soil physico–chemical attributes with $SI_{<100}$ and $SI_{<2}$ values for each applied treatment

Correlations between selected soil properties and the $SI_{<100}$ and $SI_{<2}$ values of all nine Vertosols, treated with the three different disruptive forces, are given in Table 3.7. These correlation coefficients suggest that only the CEC_{eff} and Ca^{2+}:Mg^{2+}ratio tend to have strong associations with the observed SI indices ($SI_{<100}$ and $SI_{<2}$), particularly $SI_{<2}$, for each treatment of disruptive force and water quality applied. However, some of the other soil properties indicate modest, but important correlation values.

The $SI_{<100}$ values obtained for the spontaneous dispersion treatment are significantly correlated with the soil Na^+ descriptors (SAR, Na^+_{exch}, ESP and ESI) and with the Ca^{2+}:Mg^{2+}. The $SI_{<100}$ values obtained for ultrasonic agitation show the same significant correlations for these same soil properties, with the exception of ESI. However, the $SI_{<100}$ values for the EOE–disruption treatment are not significantly correlated with any of the soil properties presented in Table 3.7.

Overall, the organic carbon content, exchangeable Na^+, the CEC_{eff} and the Ca^{2+}:Mg^{2+} are positively correlated (correlations ≥0.30) with the $SI_{<2}$ values following the three treatments of disruptive force. This suggests that increasing the content of organic carbon, exchangeable Na^+ or the proportion of the Ca^{2+}:Mg^{2+} ratio is associated with increased clay dispersion, while soil systems with larger exchange capacities are also more dispersive. The correlation of ESP with the $SI_{<2}$ values of these treatments is less pronounced and values of ESI and EC/Na^+_{exch} are not correlated with the $SI_{<2}$.

Table 3.7
Correlation of $SI_{<100}$ and $SI_{<2}$ with selected physico–chemical properties of the nine Vertosols, determined for the three disruptive forces[a]

	OC	EC	SAR	Na^+_{exch}	CEC_{eff}	Ca^{2+}:Mg^{2+}	ESP	ESI	$EC_{1:5}/Na^+_{exch}$
Spontaneous dispersion									
$SI_{<100}$	-0.36	0.08	**0.50**	**0.48**	-0.34	**-0.48**	**0.64**	**-0.38**	-0.34
$SI_{<2}$	**0.52**	0.34	-0.11	**0.42**	**0.62**	-0.33	-0.27	-0.00	-0.14
EOE–disruption									
$SI_{<100}$	-0.09	-0.14	-0.02	0.27	-0.04	-0.03	0.25	-0.01	-0.02
$SI_{<2}$	-0.33	-0.37	-0.08	**0.59**	**0.59**	-0.34	**0.43**	-0.09	-0.24
Ultrasonic agitation									
$SI_{<100}$	-0.20	-0.22	**0.61**	**0.62**	**-0.44**	**-0.59**	**0.77**	-0.33	-0.28
$SI_{<2}$	**0.39**	-0.16	-0.23	-0.31	**0.59**	**0.54**	-0.12	-0.02	-0.16

[a] correlations that are significant at the 95 % confidence interval are shown in bold.

The same trends are evidenced in the correlations between the selected soil properties and the $SI_{<100}$ and $SI_{<2}$ values determined using each of the treatment solutions (Table 3.8). In this case, correlation coefficients tend to be largest between $SI_{<100}$ or $SI_{<2}$ and organic carbon content, the CEC_{eff} or the Ca^{2+}:Mg^{2+}. This is particularly evident for the $SI_{<2}$ values, which show a strong positive correlation (>0.50) with the organic carbon content for most of the treatments. There generally appears to be no correlation between SI values and either the electrical conductivity or Na^+ descriptors, with the exception of SAR. The SAR and SI values are negatively correlated for these soils, irrespective of the applied treatment solution. However, this correlation of SAR, and the absence of correlations between SI values and electrical conductivity or the other Na^+ descriptors, is due to the G00*i* and N00*i* soils generally being more dispersive than either the B00*i* or H00*i* soils. The B00*i* and H00*i* soils generally have larger conductivities and Na^+ descriptors, but these soils contain smaller contributions of 2:1 expanding lattice phyllosilicates. Consequently, the B00*i* and H00*i* soils typically have smaller exchange capacities than either the G00*i* or N00*i* topsoils. In addition, the B00*i* and H00*i* soils have smaller organic carbon contents and smaller Ca^{2+}:Mg^{2+} ratios than the G00*i* and N00*i* soils, and hence larger Ca^{2+}:Mg^{2+} ratios and increased organic carbon contents were associated with increased SI indices.

Table 3.8
Correlation of $SI_{<100}$ and $SI_{<2}$ and selected physico–chemical properties of the nine Vertosols, determined for each treatment solution[a]

		OC	EC	SAR	Na^+_{exch}	CEC_{eff}	Ca^{2+}:Mg^{2+}	ESP	ESI	EC/Na^+_{exch}
FW00*i*	$SI_{<100}$	-0.02	-0.24	-0.25	-0.01	-0.37	-0.21	-0.00	-0.28	-0.34
	$SI_{<2}$	**-0.52**	-0.11	**-0.62**	-0.21	**-0.79**	**-0.82**	**-0.40**	-0.31	-0.17
T102	$SI_{<100}$	-0.09	-0.14	-0.02	-0.27	-0.04	-0.03	-0.25	-0.01	-0.02
	$SI_{<2}$	-0.33	-0.37	-0.08	**-0.59**	**-0.59**	-0.34	**-0.43**	-0.09	-0.24
T301	$SI_{<100}$	**-0.42**	-0.30	**-0.54**	-0.14	**-0.74**	**-0.65**	-0.24	-0.09	-0.22
	$SI_{<2}$	-0.36	-0.09	-0.36	-0.11	**-0.75**	**-0.64**	-0.08	-0.12	-0.03
T302	$SI_{<100}$	-0.11	-0.15	-0.07	-0.34	-0.09	-0.03	-0.39	**-0.44**	**-0.47**
	$SI_{<2}$	**-0.54**	-0.02	**-0.42**	-0.13	**-0.75**	**-0.66**	-0.05	-0.09	-0.24
T303	$SI_{<100}$	-0.20	-0.23	-0.23	-0.19	-0.20	-0.13	-0.21	-0.35	**-0.40**
	$SI_{<2}$	**-0.62**	-0.09	**-0.47**	-0.05	**-0.72**	**-0.61**	-0.11	-0.04	-0.18
T304	$SI_{<100}$	**-0.42**	-0.34	**-0.42**	-0.28	**-0.63**	**-0.48**	-0.32	-0.09	-0.18
	$SI_{<2}$	**-0.55**	-0.09	**-0.56**	-0.07	**-0.86**	**-0.83**	-0.27	-0.16	-0.00
T401	$SI_{<100}$	**-0.40**	**-0.53**	**-0.77**	**-0.48**	**-0.74**	**-0.76**	**-0.59**	-0.12	-0.23
	$SI_{<2}$	**-0.65**	-0.02	**-0.45**	-0.05	**-0.86**	**-0.75**	-0.24	-0.17	-0.01
T402	$SI_{<100}$	-0.35	**-0.48**	**-0.68**	-0.24	**-0.53**	**-0.59**	-0.31	-0.33	**-0.43**
	$SI_{<2}$	**-0.55**	-0.07	-0.22	-0.18	**-0.73**	**-0.58**	-0.01	-0.07	-0.22
T403	$SI_{<100}$	-0.28	**-0.46**	**-0.60**	-0.23	**-0.57**	**-0.55**	-0.29	-0.28	-0.37
	$SI_{<2}$	**-0.56**	-0.11	**-0.39**	-0.12	**-0.79**	**-0.73**	-0.10	-0.17	-0.01
T404	$SI_{<100}$	**-0.45**	**-0.39**	**-0.68**	-0.31	**-0.81**	**-0.78**	**-0.44**	-0.08	-0.21
	$SI_{<2}$	**-0.63**	-0.00	**-0.43**	-0.03	**-0.86**	**-0.74**	-0.17	-0.10	-0.06
T501	$SI_{<100}$	-0.29	**-0.51**	**-0.71**	**-0.52**	**-0.67**	**-0.68**	**-0.60**	-0.08	-0.17
	$SI_{<2}$	–	–	–	–	–	–	–	–	–
T502	$SI_{<100}$	-0.32	**-0.50**	**-0.65**	**-0.49**	**-0.67**	**-0.68**	**-0.56**	-0.05	-0.14
	$SI_{<2}$	–	–	–	–	–	–	–	–	–
T503	$SI_{<100}$	**-0.49**	**-0.45**	**-0.55**	**-0.42**	**-0.63**	**-0.55**	**-0.47**	-0.10	-0.19
	$SI_{<2}$	-0.30	-0.10	-0.32	-0.09	**-0.78**	**-0.58**	-0.23	-0.16	-0.29
T504	$SI_{<100}$	**-0.47**	**-0.60**	**-0.70**	**-0.58**	**-0.62**	**-0.55**	**-0.65**	-0.20	-0.28
	$SI_{<2}$	**-0.42**	-0.14	-0.07	-0.20	**-0.65**	-0.36	0.08	-0.01	-0.11

[a] correlations that are significant at the 95 % confidence interval are shown in bold.

3.4 Discussion

3.4.1 Comparing the nine different furrow surface soils with the properties of each profile

The physico–chemical properties showed the nine irrigation furrow topsoils to be mostly similar to the 0.2–0.4 m layer of each respective soil profile described in chapter 2. However, on occasion the

physico–chemical attributes of these furrow topsoils varied between those properties of the 0.0–0.2 m and 0.2–0.4 m layers from the adjacent soil profiles, and for most of the soils investigated, this reflects the formation of ridges and furrows used for cotton production (Figure 1.2).

Of the nine soils, the B00*i* furrow soils tended to have physico–chemical properties that most closely reflected the properties of the surface layers of each soil profile, but generally all nine furrow topsoils were less sodic and more stable than the adjacent profiles. For example, the G00*i*, H00*i* and N00*i* furrow topsoils all had smaller SARs and consequently smaller contributions of exchangeable Na^+ than the upper 0.4 m of the respective profiles. In addition, the G00*i* and H00*i* furrow soils had SARs that tended to be similar to the SAR_w values of the corresponding FW00*i* solutions (Table 3.1). The B00*i* and N00*i* soils did not fit this comparison. Immediately prior to sampling, both N001 and N002 were subjected to a rainfall event. It is expected that this has contributed to the SAR values in these furrow topsoils, which were smaller than the SARs of the adjacent profiles (0.0–0.4 m). Furthermore, the N002 soil formed part of a continuous no–till cotton trial and it is anticipated that the ESP and SAR values of this furrow topsoil were smaller than those of the adjacent soil profile due to leaching of salts by irrigation and rainfall over time. In contrast, the FW001 solution could not be compared with the solution characteristics of the B00*i* soils. This reflects the source of the FW001 solution, which was the Darling River. At the time of sampling, the Darling River had ceased flowing and the electrolyte content had become more concentrated than is expected when water flow occurs.

These nine furrow soils represent an array of different Vertosols used in irrigated cotton production, as indicated by the variation in their physico–chemical properties. Four soils had ASWAT scores of 0 (G00*i*, H002 and N002) and are considered structurally stable. In contrast, the B00*i*, H001 and N001 soils all had ASWAT scores indicative of instability problems, when immersed in de–ionised water. The B001, B002 and N001 furrow topsoils were all sodic (McKenzie 1998), while the B003 and H001 soils had ESP values greater than 2. However, unlike the ASWAT scores for the adjacent soil profiles, ESP alone was not a suitable indicator of structural instability in these furrow soils. The use of ESI or $EC_{1:5}/Na^+_{exch}$ similarly did not assist in predictions of ASWAT instability, as there was no apparent relationship between ASWAT score and either of these indicators. For example, the B001, B003 and N001 furrow soils all had the same ASWAT score, but these soils have three contrasting electrical conductivity values and different ESPs. In contrast, the B002 and N001 soils had similar conductivities (1.19 and 0.96 dS m^{-1}) and ESPs (5.3 and 6.4), but the N001 soil exhibited serious spontaneous dispersion (ASWAT score of 9), while B002 exhibited moderate dispersion only after remoulding (ASWAT score of 3). Nor could ASWAT score be associated with the organic carbon contents, the CEC_{eff} or Ca^{2+}:Mg^{2+} ratios of these soils. In general, it was therefore regarded

that the instability of these soils was at least partly a function of mineral composition. These soils appeared to have ASWAT instability scores that reflected their individual phyllosilicate suites, after which differences in stability were a function of ESP and electrical conductivity.

3.4.2 Critical thresholds of dispersion

Prior to considering the different stabilities of the nine Vertosols, critical thresholds of dispersion must be established. Currently there are no accepted critical dispersion limits set down for Vertosols. Consequently, critical thresholds were devised by adjusting the scheme applied by Hulugalle *et al.* (1999), who used values of $SI_{<20}$ ([<20 μm $_{stability}$ (dag kg^{-1})/<20 μm $_{PSD}$ (dag kg^{-1})]×100) to describe spontaneous dispersion after submersion of air–dry soil aggregates in dilute salt solutions (EC ≤0.05 dS m^{-1}). The adjustment was made in this research, to account for differences between their method of assessment and the EOE–disruption method used to obtain values of $SI_{<2}$ for each of the nine Vertosols. Initially, the $SI_{<2}$ values for all nine furrow topsoils were compared to determine the effect of increased EC_w on stability. It was noted that there was not a large difference in the quantity of dispersed clay where the end–over–end T102 (EC 0.0 dS m^{-1} SAR 0) and T301 (EC 0.2 dS m^{-1} SAR 0) treatments were compared. Hence, the very small salt content of the solutions used in the Hulugalle *et al.* (1999) method were assumed to influence dispersion similarly to the T102 treatment used in this study. Using this hypothesis, values of $SI_{<20}$ obtained in this study after spontaneous dispersion (Table 3.9) (using the method described in chapter 3.2.2) were used to allocate these soils into the classes suggested by Hulugalle *et al.* (1999). The spontaneous dispersion values of $SI_{<20}$ and $SI_{<2}$ were compared (Table 3.9) and showed an average difference of 12 %. Following this comparison, the $SI_{<2}$ values obtained using spontaneous dispersion were compared with the end–over–end $SI_{<2}$ values (T102) and showed an average difference of 12 %. Consequently, the values of each class assigned by Hulugalle *et al.* (1999) tended to fit the observed $SI_{<2}$ values following EOE–disruption in a similar way to the applied classes of spontaneous $SI_{<20}$ values for each soil. However, these classes did not appear of sufficient magnitude to adequately group the nine Vertosols according to observations of spontaneously dispersed clay ($SI_{<2}$). The critical limits of $SI_{<2}$ are given in Table 3.10. These thresholds, applied in this research, were each 5 % larger than those given by Hulugalle *et al.* (1999). This gives a more adequate description of the $SI_{<2}$ values obtained using the EOE–disruption technique.

Table 3.9
Comparing the values of $SI_{<20}$ for the nine furrow soils after spontaneous dispersion with the $SI_{<2}$ values obtained after spontaneous dispersion and after EOE–shaking
The $SI_{<20}$ values presented were obtained from samples used to determine $SI_{<100}$ and $SI_{<2}$ values for each of the soils.

	Spontaneous dispersion		EOE–shaking
	$SI_{<20}$[x]	$SI_{<2}$	$SI_{<2}$
B001	25.7*e*	10.1	21.1
B002	12.0*c*	0.9	16.0
B003	22.3*d*	9.2	16.3
G001	21.9*d*	10.8	20.1
G002	21.4*d*	15.8	24.2
H001	15.2*d*	3.5	12.9
H002	12.2*c*	0.1	14.3
N001	28.1*e*	17.5	31.6
N002	14.7*c*	1.2	13.2

[x] The letters *a*, *b*, *c*, *d* and *e* represent the class criteria for $SI_{<20}$ values applied by Hulugalle *et al.* (1999): *a*, very good (<5 %), *b*, good (5–9 %), *c*, fair (10–14 %), *d*, poor (15–25 %) and, *e*, very poor (>25 %).

Table 3.10
Dispersion classes applied for the description of $SI_{<2}$ (EOE–disruption) for the nine irrigated Vertosols

Dispersion class	Critical $SI_{<2}$ limits	Class description
Class 1	<10 %	very limited dispersion
Class 2	10–15 %	limited dispersion
Class 3	15–20 %	moderate dispersion
Class 4	20–30 %	severe dispersion
Class 5	>30 %	very severe dispersion

The dispersion class ranks applied to each of the nine soils tended to be indicative of the determined ASWAT scores, but each class could not be assigned prescriptive ASWAT scores due to the small number of soil samples included. The only soils not to show an association between ASWAT score and the content of clay dispersed after end–over–end shaking were the G00*i* soils. This reflects the larger CEC_{eff} and greater content of 2:1 expanding phyllosilicates in these soils, but also the low ESP and electrical conductivity values of each of these Vertosols. In contrast, the N001 soil had a similar contribution of CEC_{eff} and phyllosilicate clays to the G00*i* soils, but had a much larger ESP and a greater electrical conductivity. Therefore, except for the G00*i* soils, the remaining seven soils had a correlation coefficient of 0.68, where the end–over–end $SI_{<2}$ values were compared with their ASWAT scores. This comparison was endorsed by Field *et al.* (1997) who compared the ASWAT test with dispersed clay following end–over–end shaking (the method employed involved 20 inversions in 40 seconds), giving a Spearman's rank–order correlation of 0.76.

The applied thresholds (Table 3.10) tend to differentiate the spontaneously dispersed soils from the mechanically dispersed. In this case, the soils that tended to disperse spontaneously are those which had end–over–end $SI_{<2}$ values fitting into *Class* 4 and *Class* 5, while those that did not spontaneously disperse tended to be grouped in *Class* 2. Consequently, for these soils, *Class* 1 represents those soils which have no dispersed clay in solution after mechanical disruption, *Class* 2 represents soils which require mechanical disruption before dispersion occurs, *Class* 3 represents soils that will be readily dispersed with very small disruptive forces, and *Classes* 4 and 5 represent the soils which spontaneously disperse. Consequently, the nine Vertosols were classified using this scheme as:

Class 2	The H00*i* and N002 soils
Class 3	The B002 and B003 soils
Class 4	The B001 and G00*i* soils
Class 5	The N001 soil

3.4.3 Comparing the effect of dispersive energy on the stability of the nine furrow topsoils

The spontaneous dispersion procedure resulted in the smallest values of $SI_{<100}$ and $SI_{<2}$ and the ultrasonic agitation procedure resulted in the largest values of $SI_{<100}$ and $SI_{<2}$ for these nine soils (*e.g.* Watts *et al.* 1996; Raine and So 1997; So *et al.* 1997). Overall, some interesting trends between the $SI_{<100}$ and $SI_{<2}$ values emerged.

The $SI_{<100}$ values of the B00*i* soils were similar irrespective of the disruptive treatment applied, spontaneous dispersion or EOE–disruption. These soils tended to break into particles <100 μm in size much more readily than any of the other soils. The G00*i*, H00*i* and N00*i* soils all had much smaller $SI_{<100}$ values after the spontaneous dispersion treatment rather than after the EOE–disruption treatment, where $SI_{<100}$ values were approximately 20–30 % larger after EOE–disruption rather than after spontaneous dispersion. This difference appears linked to the smaller organic carbon contents of these B00*i* soils (0.22, 0.27 and 0.32 %) compared to all of the other topsoils.

The effect of organic matter was discussed by Warkentin (1982) for clay soils. He quoted Heinonen (1955), who found organic matter to be correlated with aggregate stability in clay soils where the organic matter content is small. In particular Warkentin (1982) suggests that, unlike non–swelling soils, organic contributions tend to influence the stability of Vertosols at the microaggregate (<50 μm) scale. This is the scale investigated in this research using the treatments imposed. However, a similar association differentiating between the mechanical stability and organic carbon contributions was not evident for the other soils (G00*i*, H00*i* and N00*i*). Therefore, the difference in stability for the >100 μm fractions of the G00*i*, H00*i* and N00*i* soils and that of the B00*i* soils may be indicative

of, *(i)*, different types of organic material between the different sampling regions, *(ii)*, different organic matter–clay interactions or, *(iii)*, the presence of a lower threshold minimum of organic carbon in determining the stability of these Vertosols.

There were several distinct differences between the soils when the $SI_{<2}$ values were addressed after spontaneous dispersion and EOE–disruption. However, at this scale it is less likely that organic contributions played a key role in determining the extent of clay dispersion. The $SI_{<2}$ values indicated increasing dispersion where increased force was applied and these increases in $SI_{<2}$, between each of the three disruptive forces, were similar for all the investigated soils. These increases in $SI_{<2}$ were 15–20 % between the spontaneous dispersion and EOE–disruption treatments and 60 % between the EOE–disruption and ultrasonic agitation procedures. The $SI_{<2}$ values generally reflected the physico–chemical properties of these soils more closely than the $SI_{<100}$ values. For example, where spontaneous dispersion was applied, five of these Vertosols (B001, B003, G00*i* and N001) had dispersed clay in suspension (*i.e.* $SI_{<2} >0$). The B001 and N001 soils were sodic (ESP >5), while the B003 soil had an ESP of 3.6 but a very small electrical conductivity. The G00*i* soils had very small ESPs and electrical conductivities. The spontaneous dispersion treatment showed that all of the soils with ESPs greater than 2 dispersed to some extent, except for B002. This sodic Vertosol did not disperse ($SI_{<2} =0$), but had a very large electrical conductivity, which is likely to have caused the flocculation of any dispersed clay resulting from the applied treatment.

The comparison of EOE–disruption and ultrasonic agitation showed different $SI_{<2}$ results for two of the Vertosols (B002 and N001) than for the other soils. Soil B002 was one of the most stable soils when the spontaneous and end–over–end procedures were applied, but was among the least stable under the ultrasonic treatment. This soil was previously described as sodic, but with a large electrical conductivity. In this case, the large disruptive force applied using the ultrasonic treatment appeared sufficient to overcome the suppressive effect of solute composition maintaining clays in a flocculated state and consequently, the $SI_{<2}$ values were more indicative of the large ESP of this irrigated topsoil. The N001 soil was the least stable in all treatments, and using ultrasonic agitation complete dispersion of all clay–sized particles occurred. The conclusion drawn was that the stability of the investigated soils was not adequately described by ESP alone or even by ESP and EC together. Recently, Hulugalle and Finlay (2003) found that the ratio of electrical conductivity to exchangeable Na^+ was a more suitable descriptor of dispersion in Vertosols. This was not supported in this research by the $SI_{<2}$ values after spontaneous dispersion, and neither ESI nor $EC_{1:5}/Na^+_{exch}$ showed any consistent association with $SI_{<2}$. Instead, the $SI_{<2}$ values for these soils tended to reflect differences in the clay phyllosilicate suite of minerals. For example, the G00*i* and N001 soils were the most unstable (largest $SI_{<2}$ values) and had the largest effective cation exchange capacities of any

of the Vertosols investigated. These large CEC_{eff} values were indicative of the larger contributions of 2:1 expanding lattice phyllosilicates in these three soils.

3.4.4 The effect of water quality on the liberation of soil material during end–over–end shaking

In general, increasing the EC_w of the treatment solution resulted in smaller quantities of <100 μm and <2 μm material being liberated, while increasing the SAR_w tended to result in the liberation of larger quantities of the <100 μm and <2 μm fractions. There were two observations; *(i)*, that changes in the <100 μm fraction reflected changes in the <2 μm and, *(ii)*, that the stability of these soils reflected differences in their clay phyllosilicate suites.

The impact of the different water quality treatments on the <100 μm fraction broadly reflected changes in the <2 μm fraction, rather than the accumulation of particles in the 2–100 μm size range (Figures 3.9–11). This observation was particularly evident for soils that had been treated with the T301, T401 and T501 solutions and after these treatments the 2–100 μm fractions were very similar for most of the soils. The 2–100 μm size range tended to show the same trends as the <2 μm size range for the T102 and FW00*i* treatments and for the T30*i*, T40*i* and T50*i* treatments of each soil. However, some exceptions were evident. For example, it is likely that the FW00*i* treatment of the B00*i* soils led to flocculation of clay and consequently values of 2–100 μm were larger after treatment with FW00*i* than after treatment with T102 (Figure 3.9). In contrast, treating the other soils with the FW00*i* solutions led to values of 2–100 μm that were less than those values obtained for the T102 treatment, indicating more material in the <2 μm fraction. For the T30*i*, T40*i* and T50*i* treatments (Figure 3.11), increased SAR_w broadly resulted in a smaller 2–100 μm fraction and a larger <2 μm fraction.

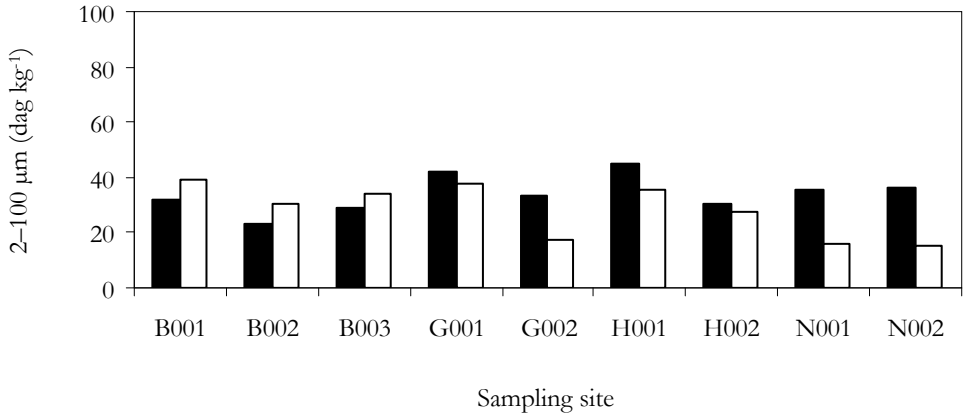

Figure 3.9 Comparing the change in the 2–100 μm fraction after end–over–end treatment of the nine Vertosols using solutions T102 (■) and FW00*i* (□). The 2–100 μm fraction was determined as the difference between the <100 μm and the <2 μm fractions after treatment.

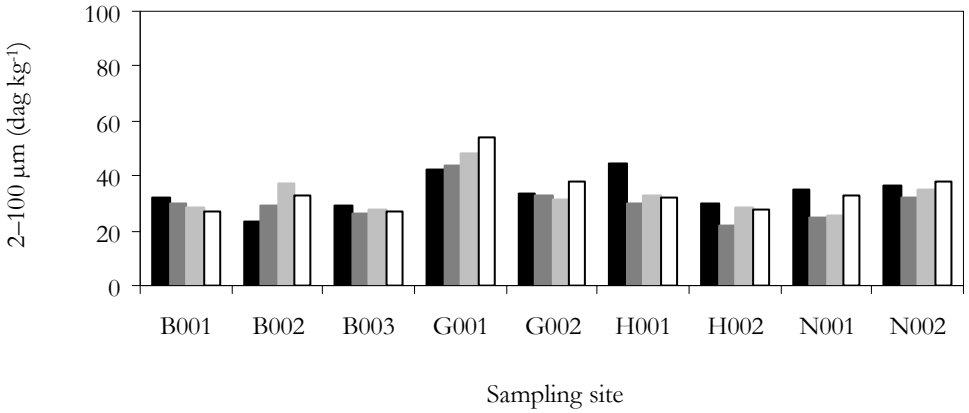

Figure 3.10 Comparing the change in the 2–100 μm fraction after end–over–end treatment of the nine Vertosols using solutions T102 (■), T301 (■), T401 (■) and T501 (□). The 2–100 μm fraction was determined as the difference between the <100 μm and the <2 μm fractions after treatment.

After the T102 and FW00*i* solution treatments there were three distinct groups into which each soil could be placed. These groups reflected different contributions of expanding lattice phyllosilicate clay minerals and consequently, differences in CEC_{eff} values. These three groups are *(i)*, the B00*i* soils, which had significantly smaller $SI_{<2}$ values for the FW00*i* treatment than for the T102 treatment, *(ii)*, the H00*i* soils, which had no significant difference between the treatments and, *(iii)*, the G00*i* and N00*i* soils, which had significantly larger $SI_{<2}$ values for the FW00*i* treatment than for the T102 treatment. Observations of the 2–100 μm fractions (Figure 3.9) showed the opposite trend, *i.e.* B00*i* had larger 2–100 μm fractions after FW00*i*, while the G00*i*, H00*i* and N00*i* soils all had smaller 2–100 μm fractions after shaking in FW00*i* than after shaking in the T102 solution. In comparison, the T30*i*, T40*i* and T50*i* treatments tended to show increased dispersed clay as the SAR_w increased. Concurrently, the 2–100 μm fractions of each soil tended to decrease as the SAR_w increased.

Consequently, the 2–100 μm fraction suggests that the accumulation of particles <100 μm was more dependent on the disruptive energy input applied to each of the soils, rather than a function of the applied treatment solution. The accumulation of particles <100 μm represents the physical breakdown of cementing and binding agents (*e.g.* organic bonds) and the slaking of aggregates during wetting. In contrast, the accumulation of dispersed clay (<2 μm) was a function of the SAR_w and EC_w of the applied solution. Comparing the extent of dispersion for these soils in each of the applied solutions (T102, FW00*i*, T30*i*, T40*i* or T50*i*) was then dependent on other soil physico–chemical properties, *e.g.* the suite of clay phyllosilicates and the proportions of exchangeable Ca^{2+}, Mg^{2+} or Na^{+}. It was expected that the addition of electrolyte solutions would influence the proportions of different exchangeable cations present in the diffuse double layer. However, the altered distribution of cations on clay domains and individual clay particles will not occur uniformly

as exchange surfaces will come into contact with the applied salts in solution at different rates. This will influence the extent of clay liberation taking place, and may account for the different responses of soils with different clay mineral suites.

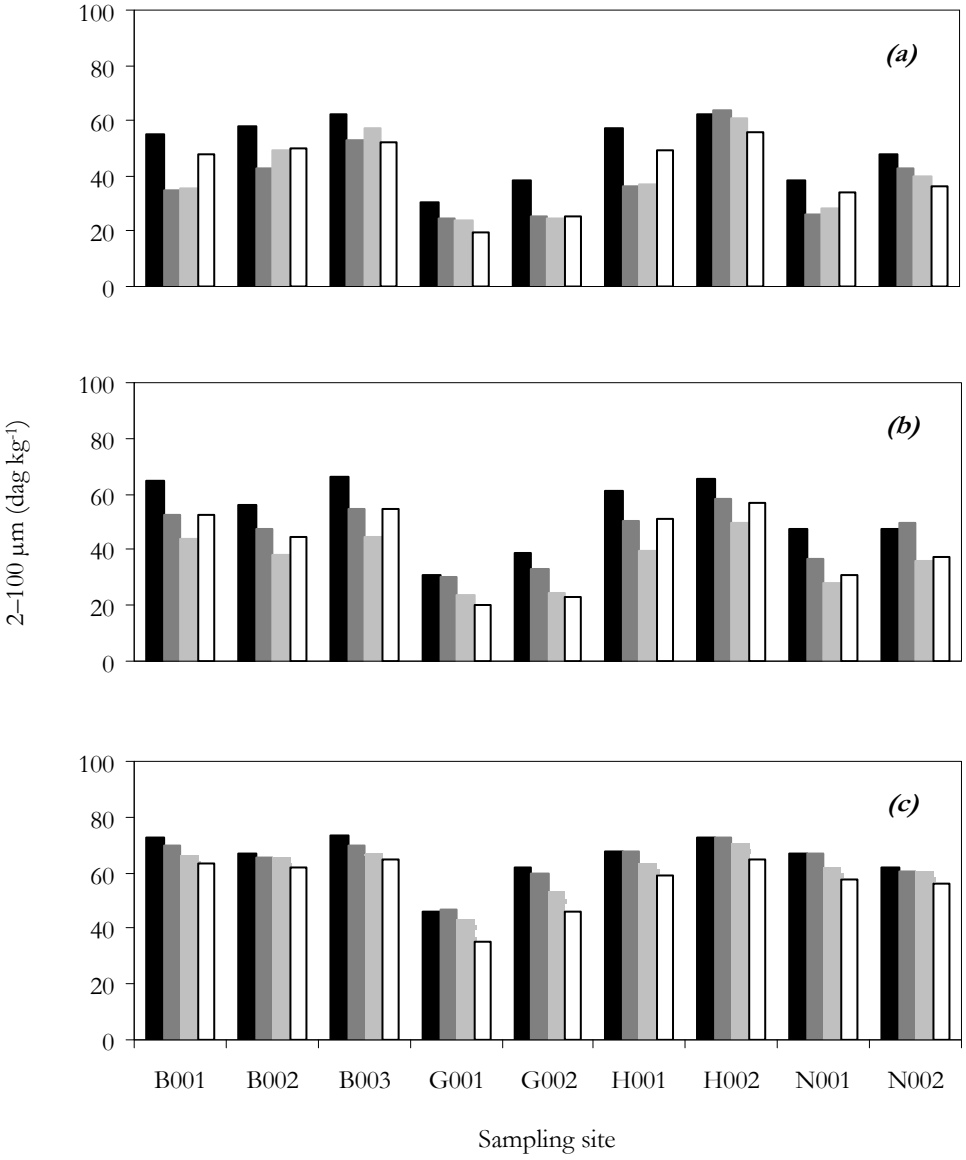

Figure 3.11 Comparing the change in the 2–100 μm fraction determined after end–over–end treatment of the nine Vertosols using the solutions, *(a)*, T30*i*, *(b)*, T40*i*, and *(c)*, T50*i* each at increments of SAR 0 (■), SAR 7.5 (■), SAR 15 (■) and SAR 30 (□). The 2–100 μm fraction was determined as the difference between the <100 μm and the <2 μm fractions after treatment.

3.4.5 Comparisons of soil physico–chemical attributes with the $SI_{<100}$ and $SI_{<2}$ values

The correlation values provided several links between individual physico–chemical properties and values of $SI_{<100}$ and $SI_{<2}$. The $SI_{<2}$ values of all these soils were strongly correlated with CEC_{eff}, but traditional predictors of potential instability (*e.g.* ESP) did not show consistently significant correlations with either of the SI indices ($SI_{<100}$ or $SI_{<2}$) for the different treatments. For these indices, increased organic carbon content and larger Ca^{2+}:Mg^{2+} ratios tended to be significantly

correlated with increased values of $SI_{<100}$ and $SI_{<2}$, while the SAR, Na^{+}_{exch} and ESP values tended to show a negative correlation with the SI indices, where they were compared with each of the treatments. This was not expected primarily as organic matter content and increased Ca^{2+}:Mg^{2+} ratios have long been associated with greater aggregate stability, while Na^{+} is the dominant contributor to dispersion in all soil types, irrespective of the phyllosilicate suite of clays.

In this study, CEC_{eff} tended to be more strongly associated with the observed SI indices than each of the other physico–chemical properties of these nine Vertosols. The soils with largest CEC_{eff} values were those soils that had largest contributions of 2:1 expanding lattice phyllosilicates in the fine and coarse clay fractions (Tables 2.16 and 2.17). The G00*i* and N001 soils had the largest contributions of 2:1 expanding lattice phyllosilicates and the largest CEC_{eff} values; these soils were consistently more dispersive than any of the other soils, irrespective of the disruptive energy applied or the treatment solution used during EOE–disruption. This reflected the general understanding that smectite clays require larger electrolyte concentrations in solution to overcome the activity of Na^{+} than either illitic or kaolinitic clays (Figure 1.12). Consequently, the correlation of SI values with CEC_{eff} was such that the expected correlations between the SI indices and the other physico–chemical properties were not strongly apparent.

3.4 Conclusions

In this study the physical bonding mechanisms tended to be accounted for by comparisons of $SI_{<100}$, while the effects of phyllosilicate suite and chemical disruption were accounted for by comparisons of $SI_{<2}$. For the nine soils investigated, the B00*i* soils tended to have the least stable <100 μm fraction when minimum disruptive force was applied. These B00*i* topsoils slaked rapidly during rapid immersion in de–ionised water, but there were only very small increases in $SI_{<100}$ when this treatment was compared with the $SI_{<100}$ values obtained using EOE–disruption. This can be linked to the very small organic carbon content of these B00*i* soils. However, treating these nine Vertosols with either EOE–disruption or ultrasonic agitation did not tend to differentiate these soils according to $SI_{<100}$ and the measured soil physico–chemical attributes. This was supported by the absence of any strong correlations between the $SI_{<100}$ values obtained for the three disruptive forces and the selected physico–chemical properties. However, there was a general association between increasing Na^{+} content, and decreasing organic carbon and CEC_{eff} values where larger $SI_{<100}$ were obtained, but it is anticipated that these correlations were indicative of changes in $SI_{<2}$ rather than $SI_{<100}$.

The $SI_{<2}$ values tended to be most strongly associated with specific soil physico–chemical properties, particularly those properties that are indicative of the clay phyllosilicate suite. For example, increasing CEC_{eff} was positively correlated with all $SI_{<2}$ values for each treatment of these nine irrigation topsoils. Associated with CEC_{eff}, increasing Ca^{2+}:Mg^{2+} ratios were correlated with larger values of $SI_{<2}$. This is indicative of the different contributions of exchangeable Ca^{2+} to the effective exchange capacity of each soil, while the exchangeable Mg^{2+} content was similar for all nine Vertosols. The other soil properties associated with $SI_{<2}$ tended to be organic carbon and Na^{+} contributions. However, relationships between these characteristics suggest that these attributes were not contributing to stability as anticipated *i.e.* where soils had been treated using the different solutions, a larger exchangeable Na^{+} content was associated with increasing stability (Table 3.8), while larger organic contributions were associated with decreasing stability (Tables 3.7 and 3.8). These observations reflect the dominance of CEC_{eff} in determining differences between the $SI_{<2}$ values for each of these nine Vertosols. Therefore, the differences in clay dispersion were largely indicative of differences in the clay mineral suite. This was shown by the correlation coefficients between SI indices and CEC_{eff}, where the soils with large CEC_{eff} values were dominated by 2:1 expanding lattice phyllosilicate clays. The difference in stability between the soils of comparable mineral suites was then attributed to differences in ESP, exchangeable Na^{+}, electrical conductivity and organic carbon.

In conclusion, the overall stability of these soils tended to represent the dispersion classes into which each soil was classified. The N001 soil (*Class* 5) was the least stable of all these soils and had a large CEC_{eff} and a large ESP. The G00*i* (*Class* 4) and N002 (*Class* 2) soils were intermediate in their stability. These soils each had large CEC_{eff} values but small ESPs and electrical conductivities. The B001 (*Class* 4), B002 (*Class* 3) and B003 (*Class* 3) soils were generally more stable than the G00*i* and N00*i* soils. These soils had much smaller CEC_{eff} values than the G00*i* and N00*i* soils, but their ESPs were all larger than 2. The soils that exhibited the greatest stability were the H00*i* soils (*Class* 2). These soils had the smallest values of CEC_{eff} and contained much smaller contributions of 2:1 expanding lattice phyllosilicate clays than the other soils. Despite their ESPs, they were consistently more stable than the other soils where spontaneous dispersion, ultrasonic agitation and all immersion solution treatments where EOE–disruption was applied.

Chapter 4

ASSESSING THE IMPACT OF IRRIGATION ON SELECTED PHYSICO–CHEMICAL ATTRIBUTES

ASSESSING THE IMPACT OF IRRIGATION ON SELECTED PHYSICO–CHEMICAL ATTRIBUTES

~

Vertic: *vertere (L): to turn or invert; to turn into, change.*

~

4.1 Introduction

In the Australian environment the availability of water for irrigated cotton production is expected to become increasingly limited, and some current irrigation supplies are showing an increasing trend in EC *e.g.* the Lachlan River (Hillston) (Jolly *et al.*, 2001). Furthermore, continued access to current irrigation water sources is not assured. As a consequence, cotton producers are having to continually develop new irrigation techniques to manage the application of different water supplies (*e.g.* Silvertooth 1990; Dugdale *et al.* 2004). Therefore, it is probable that irrigating with water sources of large Na^+ content will become a more common practice among cotton producers. The application of these poor quality water sources will impact on the Na^+ content of soil, and in conjunction with rainfall (clean water), will affect the structural condition of Vertosols and potentially stimulate pre–existing structural instability in these soils. The resulting structural condition is likely to have reduced porosity, problems with surface sealing and such soils will remain waterlogged after irrigation or rainfall events. This is likely to reduce seedling vigour and promote stunted, slow–growing cotton plants (Silvertooth 1990).

The effect of different intervals of water quality on soil physico–chemical properties has been extensively studied in the laboratory and using field trials. For example, an early study by Quirk and Schofield (1955) investigated the effect of electrolyte concentration on the permeability of soils saturated with various exchangeable cations. Many have followed (*e.g.* Curtin *et al.* 1994; Crescimanno *et al.* 1995), but the majority of these works have employed leaching studies on soil columns packed with ground aggregates (*e.g.* Sahin *et al.* 2002), soil pastes (*e.g.* Hussein and Adey 1998) or in combination with sands. This body of research has focused on different phyllosilicate clay systems and on a diverse range of soil types. Consequently, the relationships between physico–chemical properties in determining the structural stability of Vertosols are generally understood. However, there is a dearth of literature describing the impact of irrigation solution composition on the structural stability of intact Vertosols.

The objective in this chapter is to determine the impact of irrigation water quality on soil chemical properties and on the structural stability of six Vertosols (G00*i*, H00*i* and N00*i*). This is achieved by determining the proportion of cations on the exchange complex, and of cations in solution after the completion of six irrigation cycles. The structural stability of these soils is determined using the EOE–procedure where soils are immersed in clean water (T102) and then comparisons are made between the $SI_{<2}$ values for all soils and selected soil chemical properties.

4.2 Materials and Methods

Seventy two soil columns (160 mm *o.d.* × 200 mm *h.*) were sampled from six cotton–growing fields throughout NSW. These soil columns were each extracted from the 0.0–0.2 m layer of an irrigation furrow of each of the G00*i*, H00*i* and N00*i* sites described in chapter 3.

Figure 4.1 Excavation of soil columns from an irrigation furrow of the N001 sampling site.

Twelve soil columns were excavated in polyvinylchloride (PVC) sections (150 mm *i.d.*) from the irrigation furrow of each of the six cotton fields. At each site, soil columns were sampled along a 2 m transect, beginning at the tail drain end of each field. Each column was excavated by firmly pushing individual PVC sections into the soil profile. At the same time, soil was removed from the outer edge of each PVC section to limit possible distortion of soil columns. Using pressure, the bevelled base edge of each PVC section then trimmed any remaining soil, and the intact soil columns were excavated (Figure 4.1). Columns were placed into sample bags, sealed and transported to the laboratory.

4.2.1 Laboratory irrigation of soil columns

In the laboratory an irrigation experiment was designed to mimic the wetting and drying process observed in Vertosols in the field as closely as possible. To conduct the experiment seventy two soil columns were prepared for irrigation by fitting a PVC cap (160 mm *i.d.*) to the base of each soil filled PVC section (Figure 4.2). In the centre of each cap a drainage hole of 4 mm *d.* was inserted and covered by 0.2 mm synthetic gauze. On the inner face of each cap, a silicon sealant was applied to restrict lateral movement of water at the base of each column. This was done to encourage water movement through the soil matrix and to minimise by–pass flow at the soil–PVC interface. Then, a surface reservoir was attached to the upper PVC edge of each soil column. These prepared soil columns were slowly wetted from the base using field–water (FW00*i*) from each site (Table 3.1). This was done by placing each column in a bath; by slowly increasing the height of water in the bath, columns were wetted until free water was present on the soil surface. Each soil column was left with free surface water for a minimum period of 12 hrs, then allowed to drain for a further 48 hrs and column weights were recorded.

Once prepared each soil column was placed above a pre–weighed drainage cup for irrigation. A 150 mm *d.* filter paper was placed on the upper surface of each soil column (*e.g.* Menneer *et al.* 2001) (Figure 4.2) to limit surface soil disruption. One litre of the appropriate irrigation solution (chapter 4.2.2) was poured carefully onto the soil surface and columns were left to drain. This irrigation volume was equivalent to approximately 0.65 of the total pore volume of these Vertosols and was determined from the original soil bulk density.

After soil columns had been allowed to drain for 72 hrs, any remaining surface solution was removed using an applied vacuum (Bakker and Emerson 1973). Post–irrigation, the weights of surface water, of drainage water and of each soil column were recorded and the soil filled columns were placed in an oven to dry at 40 °C (Bresson and Moran 1995). Intermittently, these columns were removed to allow the soil to cool; this was done to mimic alternate periods of day and night. This process was repeated for eight 16 hr periods after each irrigation event.

The irrigation procedure was repeated so that all soil columns were subjected to six of these wetting and drying cycles. Afterward, the soil columns were stored at constant temperature for 50 days to allow further moisture evaporation. At the end of this time period all columns were prepared for analysis of selected physico–chemical properties.

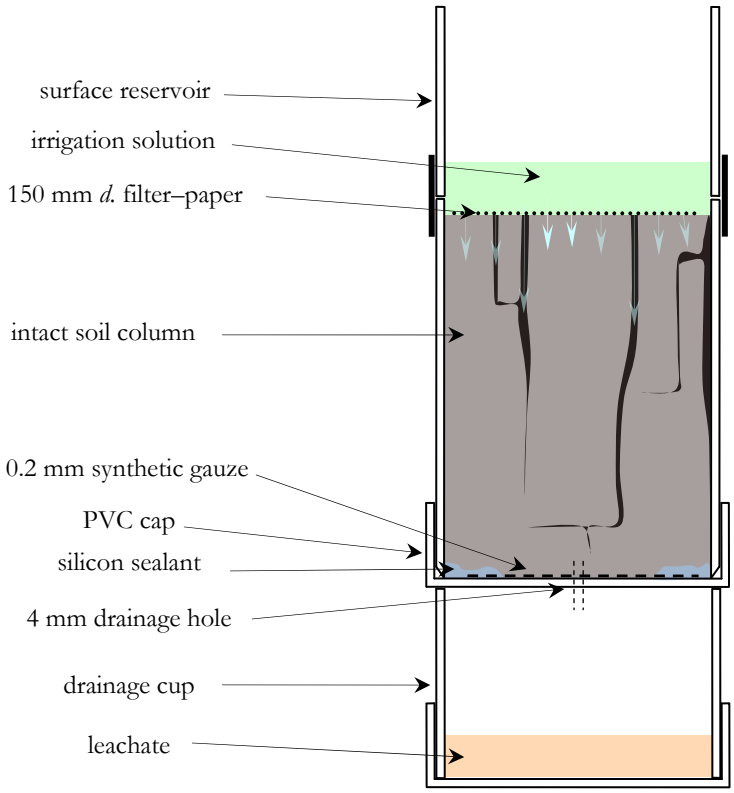

Figure 4.2 The apparatus employed to irrigate soil cores in the laboratory.

4.2.2 The six solutions used to irrigate soil columns

Pairs of soil columns from each site were each irrigated using one of six water solutions (FW00*i*, T102 or T401–4), giving a total of 12 soil cores for each location. A description of the FW00*i* solutions is given in Table 3.1. These solutions were applied to mimic field–like irrigation. The other five solutions, T102 and T401–4, were prepared to give a variety of potential irrigation water qualities for each of the soils investigated. The proposed and actual water qualities of these prepared solutions are given in Table 3.2. Solution T102 has an EC_w <0.01 dS m^{-1} and $SAR_w \rightarrow 0$. This was selected to show the impact of 'clean' water on the physico–chemical condition of Vertosols.

The T401–4 solutions (EC_w=0.5 dS m^{-1}) were prepared so that the solute concentration was not sufficiently large to constitute a salinity risk (Ayers and Westcot, 1985). These solutions had target SAR_w values of 0, 7.5, 15 and 30 respectively, and provided different increments of potential sodicity. The T401–4 solutions were prepared by combining $CaCl_2.2H_2O$, $MgCl_2.6H_2O$ and NaCl. The combinations were determined so that the ratio of Ca^{2+}:Mg^{2+} was 1:1 and the amount of Na^+ satisfied the proposed values of EC_w and SAR_w. This was done using equations 5 and 6.

4.2.3 Monitoring the irrigation of soil columns

Prior to, and after each of the irrigation events, the weights of each soil column and each drainage–cup were recorded. The change in column weight (before irrigation – after irrigation) for each irrigation event is given for each of the irrigated soil columns in appendix 3.1. In addition, the EC_w and SAR_w of drainage water solutions were determined for all leachate fractions. To do this, a conductivity cell was used to determine the electrolyte concentration of drainage water (EC_w dS m^{-1}). Each drainage water sample was then diluted and an ionising suppressant added, containing 2222 µg ml^{-1} CsCl and 1650 µg ml^{-1} $SrCl_2$. The prepared solutions were assessed for contributions of Ca^{2+}, Mg^{2+}, Na^+ and K^+ using Atomic Absorption Spectroscopy ($mmol_{(+)}$ L^{-1}). The concentrations of each cation were used to determine the SAR_w ($(mmol_{(+)}\ L^{-1})^{1/2}$) (equation 2). The EC_w, solution cations and SAR_w values are presented in appendix 3.2 for the leachate fractions of each treatment of the six soils.

4.2.4 Selected chemical properties and the structural stability of laboratory irrigated Vertosols

After six wet–dry irrigation cycles, each of the seventy two soil columns was divided into four depth increments (0–50 mm, 50–100 mm, 100–150 mm and >150 mm) and for each increment, bulk density and wetness were determined. Then, all soil from each layer was air–dried and ground to pass through a 2 mm sieve. This ground soil was placed into a 0.1 mm sieve and later, the <0.1 mm fraction was discarded. The 2.0–0.1 mm fraction was retained for the analysis of selected chemical properties (exchangeable and solution cations) and soil structural stability. The exchangeable cations and soil solution were assessed for all soil samples using the methods described in chapter 2.3.1. The soil exchangeable cations (Ca^{2+}, Mg^{2+}, Na^+ and K^+) were extracted using a 60 % ethanol, 1 M NH_4Cl solution at pH 8.5 (Rayment and Higginson 1992) and analysed using flame Atomic Absorption Spectroscopy. The soil solution was extracted in water using a 1:5 soil–water ratio. Using this solution, the electrical conductivity ($EC_{1:5}$) was determined and the cations of solution were analysed using flame Atomic Absorption Spectroscopy. The soil exchangeable cations were used to determine the CEC_{eff}, ESP, ESI and $EC_{1:5}/Na^+_{exch}$, while the cations of solution were used to determine the SAR.

Once chemical properties were determined, the structural stability of each soil sample was assessed using the EOE–procedure described in chapter 3.2.3. Six gram sub–samples of air–dry soil were immersed in 100 ml of de–ionised water. Each soil was shaken end–over–end for 30 minutes at 30 rpm. The soil solution was transferred to a 500 ml measuring cylinder and each cylinder was filled to volume using de–ionised water. After the appropriate sedimentation period (Gee and Bauder 1986) the <2 µm fraction was sampled using a pipette, and was oven–dried (105 °C). The mass of

dispersed clay (dag kg^{-1}) was determined gravimetrically and $SI_{<2}$ values were calculated using equation 8, where <2 μm $_{PSD}$ (dag kg^{-1}) is the <2 μm fraction given for each of the topsoils described in chapter 3 (Table 3.3).

4.2.5 Data analysis

The effects of irrigating soil columns with each of the different treatment solutions (FW00*i*, T102 and T401–4) was compared for each depth increment of the six Vertosols using selected chemical properties (Ca^{2+}_{exch}, Mg^{2+}_{exch}, Na^{+}_{exch}, K^{+}_{exch}, ESP, EC and SAR) and soil structural stability. To do this, soil properties were compared for each Vertosol using a one–way analysis of variance. The Tukey–Kramer test (P=0.05) was used to determine significant differences between the six treatments at each of the sampled depth increments for each of the six Vertosols. The mean values following each treatment at each depth increment are presented for all measured soil characteristics. The wetness and bulk density values, determined at the time that soil columns were destructively sampled, are given in appendix 4. The exchangeable cations, electrical conductivity, SAR and end–over–end dispersed clay are given in Tables 4.1–12.

After the comparison of selected soil properties, correlation coefficients and linear regression was used to determine any association between $SI_{<2}$ and selected chemical attributes for all the soil samples. To do this, the $SI_{<2}$ values were compared with EC, SAR, Na^{+}_{exch}, Ca^{2+}:Mg^{2+} ratio, ESP, ESI and $EC_{1:5}/Na^{+}_{exch}$. The correlation coefficients were determined using equation 9 and are given in Table 4.13. Then, linear regression was applied between $SI_{<2}$ values and these selected soil attributes. Data transformations were not applied as these did not improve the distribution of any of the measured soil attributes.

4.3 Results

4.3.1 The bulk density and the field wetness of columns at the time of sampling

The mean bulk density and wetness values of each depth increment following the irrigation treatments (FW00*i*, T102 or T401–4), are given in appendix 4 for each of the six Vertosols (G00*i*, H00*i* and N00*i*). Bulk density and wetness both increase with sampling depth, indicative of natural drying processes and overburden pressures. However, the impact of water quality on each of the six Vertosols tends to be represented by either no differences or only small differences in the values of bulk density and wetness for each treatment of the G00*i*, H00*i* and N00*i* soils.

The G00*i* soils do not tend to show any trend in values of bulk density for the treatments of increased SAR_w (T401→4), and the FW00*i* and T102 treatments do not show any significant differences in either attribute where compared to the other treatments. The remaining four soils (H00*i* and N00*i*) all show larger values of bulk density for soils treated with solutions of larger SAR_w (T401→4), but this is only significant for the 50–100 mm depth of the N002 soil. The response of these soils to the T102 and FW00*i* treatments are similar for all six soils (G00*i*, H00*i* and N00*i*). These values of bulk density tend to most closely represent values of bulk density determined for the T401 and T402 treatments. Wetness values do not show any trend for the T401–4 solution treatments of the G00*i*, H002 and N002 soils. However, the H001 and N001 soils both have wetness values that are larger for soil columns treated with solutions of larger SAR_w (T401→4). The FW00*i* and T102 treatments have field wetness values that tend to be similar to the wetness values obtained for soil columns treated with the T401 and T402 solutions, for all six soils.

4.3.2 The impact of irrigating columns on selected soil properties

4.3.2.1 The effect of irrigation treatment on the exchangeable cations

The exchangeable cation contributions (Ca^{2+}, Mg^{2+}, Na^+, K^+ and ESP) are presented in Tables 4.1–6 for the G00*i*, H00*i* and N00*i* soils respectively. There is a general increase in the contributions of particular exchangeable cations (Ca^{2+}, Mg^{2+} and Na^+) as soil depth increases for the T102, FW00*i* and T401–3 treated soils. The T404 treated soil columns have much larger exchangeable Na^+ contributions in the 0–50 mm layer than in the other soil layers.

The irrigation of these Vertosols with the T401–4 range of solutions tends to show smaller contributions of exchangeable Ca^{2+} and Mg^{2+} after treatment with solutions of larger SAR_w (T403 and T404). Contrasting with these smaller contributions, these soil columns all tend to have an increased content of exchangeable Na^+. There is no difference in the exchangeable K^+ content irrespective of the applied irrigation solution. In general, irrigating these six Vertosols with either T102 or FW00*i* tends to result in exchangeable cation contributions that are similar to those determined after treatment with either the T401 or T402 solutions. However, each of the six Vertosols does not show the same response to each of the treatment solutions (FW00*i*, T102 and T401–4).

The H00*i* and N00*i* soils show no significant differences between the exchangeable Ca^{2+}, Mg^{2+} and K^+ contents of the 0–50 mm and 50–100 mm layers where all irrigation treatments are compared. In contrast, the irrigation treatment of soil columns from the G001 and G002 sites show significant differences for different exchangeable cations. Irrigating soil from the G001 site with FW00*i* gave a

soil that contains significantly more exchangeable K^+ in the 0–50 mm layer than where the same soil is irrigated using T404. However, no significant differences are evident for the exchangeable Ca^{2+} or Mg^{2+} contributions for treated columns of this soil.

Soil columns from the G002 site irrigated with the T401–4 solutions contain significantly less exchangeable Mg^{2+} in the 0–50 mm layer after treatment with T404 than after treatment with T401. The treatment of this soil using T102 led to significantly less exchangeable Ca^{2+} for the surface layer, compared to those columns irrigated using FW00*i*. The T401 and FW00*i* treatments of the G002 soil show significantly different exchangeable Ca^{2+} contents to those of G002 soil treated with the T401–4 solutions.

There are much larger variations in exchangeable Na^+ content for all six Vertosols, after treatment using solutions T401–4. Columns treated with the T403 or T404 solutions tend to contain significantly larger exchangeable Na^+ contributions, and consequently, significantly larger ESPs where these are compared with the T401–treated soil columns. This is particularly evident in the surface layers (0–50 mm and 50–100 mm) of the G00*i* and N00*i* soil columns. The H00*i* soils have significantly larger contributions of exchangeable Na^+, but only in the upper–most soil layer. For all these soils, the larger contributions of exchangeable Na^+ correspond to the increased SAR_w of irrigation solution.

In general, the exchangeable Na^+ content of soil columns treated with solutions FW00*i*, T102 or T401 are similar, but there are two exceptions. The treatment of soil columns from G001, using FW00*i*, results in a significantly larger exchangeable Na^+ content in the surface layer than for soil treated using the T102 solution. The treatment of the N001 soil using T102 results in a significantly smaller ESP in the surface layer (0–50 mm) compared to columns irrigated using the FW00*i* treatments. In the T102–treated N001 soil columns, the ESP is significantly larger than the ESP of the T401–treated columns. In this case, the significant difference in ESP is not reflected by differences between the exchangeable Na^+ content for either the FW00*i* or T102 treatments.

Table 4.1
Mean values of exchangeable Ca^{2+}, Mg^{2+}, Na^{+} and K^{+} and of ESP following each irrigation treatment (FW00*i*, T102 and T401–4) of the G001 soil columns

	Depth	FW002	T102	T401	T402	T403	T404
	(mm)	(EC 0.2 SAR 1)	(EC 0.0 SAR 0)	(EC 0.5 SAR 0)	(EC 0.5 SAR 7.5)	(EC 0.5 SAR 15)	(EC 0.5 SAR 30)
Ca^{2+} ($cmol_{(+)}\ kg^{-1}$)	0–50	29.78 ± 0.83	27.72 ± 0.05	28.99 ± 0.16	29.35 ± 1.18	28.83 ± 0.08	28.10 ± 0.51
	50–100	28.94 ± 0.14	28.99 ± 0.84	28.82 ± 0.01	29.06 ± 0.45	28.13 ± 0.63	29.96 ± 1.02
	100–150	29.99 ± 1.22	28.88 ± 1.16	30.40 ± 0.38	30.32 ± 0.43	28.56 ± 1.79	29.98 ± 0.23
	>150	29.77 ± 0.05	29.47 ± 1.57	29.62 ± 0.28	29.94 ± 1.03	29.66 ± 0.86	–
Mg^{2+} ($cmol_{(+)}\ kg^{-1}$)	0–50	10.94 ± 0.14	11.00 ± 0.09	11.10 ± 0.06	11.12 ± 0.11	10.81 ± 0.07	10.76 ± 0.00
	50–100	11.06 ± 0.02	11.08 ± 0.30	10.82 ± 0.02	10.80 ± 0.26	10.80 ± 0.02	11.04 ± 0.00
	100–150	10.85 ± 0.46	11.21 ± 0.34	11.26 ± 0.05	11.23 ± 0.26	10.91 ± 0.17	11.12 ± 0.35
	>150	11.49 ± 0.12	12.18 ± 0.05	11.59 ± 0.02	11.40 ± 0.08	11.54 ± 0.32	–
Na^{+} ($cmol_{(+)}\ kg^{-1}$)	0–50	1.21*c* ± 0.02	1.05*d* ± 0.04	1.01*d* ± 0.03	1.45*b* ± 0.03	1.42*b* ± 0.02	1.72*a* ± 0.02
	50–100	1.28*b* ± 0.03	1.18*b* ± 0.04	1.18*b* ± 0.10	1.34*ab* ± 0.02	1.40*ab* ± 0.00	1.61*a* ± 0.04
	100–150	1.45*ab* ± 0.06	1.37*b* ± 0.02	1.36*b* ± 0.05	1.45*ab* ± 0.02	1.47*ab* ± 0.01	1.59*a* ± 0.00
	>150	1.47 ± 0.05	1.25 ± 0.20	1.42 ± 0.01	1.43 ± 0.08	1.53 ± 0.02	–
K^{+} ($cmol_{(+)}\ kg^{-1}$)	0–50	1.34*a* ± 0.01	1.23*ab* ± 0.08	1.19*ab* ± 0.02	1.21*ab* ± 0.01	1.23*ab* ± 0.07	1.02*b* ± 0.05
	50–100	1.05 ± 0.04	0.98 ± 0.04	0.90 ± 0.01	0.93 ± 0.10	0.88 ± 0.08	0.82 ± 0.02
	100–150	0.71 ± 0.01	0.70 ± 0.01	0.73 ± 0.04	0.71 ± 0.02	0.76 ± 0.01	0.70 ± 0.02
	>150	0.63 ± 0.02	1.19 ± 0.57	0.63 ± 0.04	0.65 ± 0.05	0.63 ± 0.01	–
ESP	0–50	2.79*c* ± 0.01	2.55*cd* ± 0.10	2.40*d* ± 0.07	3.37*b* ± 0.04	3.35*b* ± 0.06	4.12*a* ± 0.01
	50–100	3.02*ab* ± 0.06	2.80*b* ± 0.17	2.83*b* ± 0.23	3.18*ab* ± 0.09	3.39*ab* ± 0.06	3.71*a* ± 0.01
	100–150	3.37 ± 0.01	3.26 ± 0.16	3.11 ± 0.14	3.31 ± 0.01	3.53 ± 0.18	3.67 ± 0.05
	>150	3.39 ± 0.12	2.83 ± 0.38	3.29 ± 0.01	3.28 ± 0.11	3.52 ± 0.06	–

The mean values following each treatment were determined and the standard error of means obtained using a one–way Analysis of Variance and then compared for each of the sampled soil layers (0–50 mm, 50–100 mm, 100–150 mm and >150 mm). Significant differences were determined and are represented within rows by the letters *a*, *b*, *c* and *d*. This was carried out using the Tukey–Kramer test (P=0.05)

Table 4.2

Mean values of exchangeable Ca^{2+}, Mg^{2+}, Na^{+} and K^{+} and of ESP following each irrigation treatment (FW00*i*, T102 and T401–4) of the G002 soil columns

	Depth	FW002		T102		T401		T402		T403		T404	
	(mm)	(EC 0.2 SAR 1)		(EC 0.0 SAR 0)		(EC 0.5 SAR 0)		(EC 0.5 SAR 7.5)		(EC 0.5 SAR 15)		(EC 0.5 SAR 30)	
Ca^{2+} ($cmol_{(+)}\ kg^{-1}$)	0–50	28.77*a*	± 0.52	25.85*b*	± 0.40	26.70*ab*	± 0.53	26.78*ab*	± 0.54	26.27*ab*	± 0.32	27.56*ab*	± 0.38
	50–100	26.50	± 0.94	28.49	± 0.04	29.62	± 0.19	29.84	± 1.03	28.43	± 0.63	27.79	± 1.01
	100–150	28.80	± 0.61	27.08	± 1.13	28.16	± 0.10	25.85	± 0.36	25.66	± 0.29	27.49	± 0.63
	>150	26.94	± 0.73	28.16	± 0.66	28.32	± 0.33	28.21	± 0.42	28.37	± 0.95	–	
Mg^{2+} ($cmol_{(+)}\ kg^{-1}$)	0–50	11.53*ab*	± 0.21	10.89*ab*	± 0.08	11.63*a*	± 0.16	10.93*ab*	± 0.03	10.91*ab*	± 0.13	10.79*b*	± 0.17
	50–100	10.92	± 0.12	11.46	± 0.03	11.96	± 0.17	11.48	± 0.39	11.39	± 0.17	11.23	± 0.35
	100–150	11.73	± 0.07	11.58	± 0.22	11.19	± 0.52	10.91	± 0.16	11.13	± 0.29	11.20	± 0.16
	>150	11.43	± 0.19	11.62	± 0.27	11.72	± 0.31	11.31	± 0.29	12.08	± 0.27	–	
Na^{+} ($cmol_{(+)}\ kg^{-1}$)	0–50	1.03*b*	± 0.02	1.02*b*	± 0.01	0.88*b*	± 0.06	1.38*a*	± 0.08	1.48*a*	± 0.03	1.66*a*	± 0.10
	50–100	1.04*b*	± 0.05	1.18*ab*	± 0.03	0.93*b*	± 0.04	1.34*a*	± 0.04	1.01*a*	± 0.00	1.37*a*	± 0.09
	100–150	1.14	± 0.09	1.32	± 0.02	1.28	± 0.21	1.37	± 0.02	1.29	± 0.06	1.30	± 0.06
	>150	1.25	± 0.03	1.42	± 0.03	1.11	± 0.05	1.39	± 0.02	1.41	± 0.13	–	
K^{+} ($cmol_{(+)}\ kg^{-1}$)	0–50	1.53	± 0.04	1.91	± 0.02	1.81	± 0.32	1.99	± 0.05	1.54	± 0.12	1.86	± 0.03
	50–100	1.66	± 0.18	1.92	± 0.06	1.70	± 0.24	1.92	± 0.02	1.81	± 0.01	1.88	± 0.11
	100–150	1.52	± 0.02	1.56	± 0.02	1.27	± 0.59	1.55	± 0.01	1.39	± 0.05	1.45	± 0.07
	>150	1.42	± 0.15	1.42	± 0.00	1.60	± 0.20	1.31	± 0.06	1.36	± 0.08	–	
ESP	0–50	2.39*b*	± 0.08	2.57*b*	± 0.05	2.14*b*	± 0.12	3.36*a*	± 0.25	3.68*a*	± 0.05	3.97*a*	± 0.16
	50–100	2.60*ab*	± 0.19	2.74*ab*	± 0.08	2.11*b*	± 0.08	3.00*ab*	± 0.01	3.28*a*	± 0.06	3.26*a*	± 0.32
	100–150	2.63	± 0.16	3.19	± 0.06	3.07	± 0.58	3.45	± 0.01	3.26	± 0.19	3.15	± 0.19
	>150	3.04*ab*	± 0.15	3.33*a*	± 0.01	2.60*b*	± 0.13	3.30*ab*	± 0.08	3.26*ab*	± 0.18	–	

The mean values following each treatment were determined and the standard error of means obtained using a one–way Analysis of Variance and then compared for each of the sampled soil layers (0–50 mm, 50–100 mm, 100–150 mm and >150 mm). Significant differences were determined and are represented within rows by the letters *a* and *b*. This was carried out using the Tukey–Kramer test (P=0.05)

Table 4.3
Mean values of exchangeable Ca^{2+}, Mg^{2+}, Na^{+} and K^{+} and of ESP following each irrigation treatment (FW00*i*, T102 and T401–4) of the H001 soil columns

	Depth	FW002	T102	T401	T402	T403	T404
	(mm)	(EC 0.2 SAR 1)	(EC 0.0 SAR 0)	(EC 0.5 SAR 0)	(EC 0.5 SAR 7.5)	(EC 0.5 SAR 15)	(EC 0.5 SAR 30)
Ca^{2+} ($cmol_{(+)}\ kg^{-1}$)	0–50	12.69 ± 0.80	10.61 ± 0.48	10.64 ± 0.06	10.89 ± 0.76	13.39 ± 0.87	13.12 ± 0.94
	50–100	12.97 ± 2.50	12.32 ± 0.52	13.23 ± 0.75	11.90 ± 0.62	15.13 ± 0.36	14.77 ± 1.18
	100–150	13.68 ± 0.09	15.00 ± 0.92	14.27 ± 0.46	13.53 ± 0.57	14.30 ± 0.06	14.73 ± 0.07
	>150	14.98*a* ± 0.10	13.86*ab* ± 0.38	14.59*a* ± 0.41	13.11*b* ± 0.07	14.64*a* ± 0.07	–
Mg^{2+} ($cmol_{(+)}\ kg^{-1}$)	0–50	7.86 ± 0.73	6.32 ± 0.16	6.70 ± 0.13	6.80 ± 0.79	8.54 ± 0.55	8.20 ± 1.24
	50–100	7.87 ± 1.48	7.21 ± 0.34	8.17 ± 0.77	7.51 ± 0.69	9.42 ± 0.26	9.20 ± 0.73
	100–150	8.82 ± 0.47	9.39 ± 0.20	9.26 ± 0.20	8.43 ± 0.21	9.54 ± 0.02	9.36 ± 0.39
	>150	9.95 ± 0.38	8.92 ± 0.16	9.23 ± 0.22	8.76 ± 0.73	9.83 ± 0.02	–
Na^{+} ($cmol_{(+)}\ kg^{-1}$)	0–50	1.37*ab* ± 0.11	1.04*b* ± 0.13	0.78*b* ± 0.16	1.43*ab* ± 0.21	1.98*a* ± 0.06	1.64*ab* ± 0.22
	50–100	1.43 ± 0.17	1.36 ± 0.20	1.24 ± 0.35	1.46 ± 0.12	1.99 ± 0.03	1.72 ± 0.07
	100–150	1.60 ± 0.01	1.70 ± 0.22	1.38 ± 0.31	1.72 ± 0.10	1.89 ± 0.03	1.64 ± 0.04
	>150	1.78 ± 0.01	1.67 ± 0.18	1.51 ± 0.28	1.78 ± 0.03	1.87 ± 0.02	–
K^{+} ($cmol_{(+)}\ kg^{-1}$)	0–50	1.77 ± 0.22	1.90 ± 0.22	1.69 ± 0.34	1.48 ± 0.00	1.54 ± 0.12	1.77 ± 0.12
	50–100	1.56 ± 0.04	1.69 ± 0.05	1.65 ± 0.30	1.49 ± 0.10	1.89 ± 0.16	2.05 ± 0.10
	100–150	1.61 ± 0.04	1.79 ± 0.12	1.29 ± 0.07	1.68 ± 0.26	1.45 ± 0.04	1.71 ± 0.15
	>150	1.63 ± 0.02	1.66 ± 0.13	1.50 ± 0.24	1.55 ± 0.25	1.31 ± 0.10	–
ESP	0–50	5.79*ab* ± 0.13	5.27*ab* ± 0.86	3.95*b* ± 0.84	6.89*ab* ± 0.44	7.80*a* ± 0.16	6.61*ab* ± 0.29
	50–100	6.07 ± 0.36	6.00 ± 0.61	5.05 ± 1.10	6.50 ± 0.16	7.01 ± 0.01	6.23 ± 0.18
	100–150	6.21 ± 0.13	6.14 ± 1.02	5.26 ± 1.17	6.79 ± 0.52	6.95 ± 0.14	5.98 ± 0.09
	>150	6.28 ± 0.06	6.36 ± 0.48	5.62 ± 1.07	7.06 ± 0.06	6.75 ± 0.01	–

The mean values following each treatment were determined and the standard error of means obtained using a one–way Analysis of Variance and then compared for each of the sampled soil layers (0–50 mm, 50–100 mm, 100–150 mm and >150 mm). Significant differences were determined and are represented within rows by the letters *a* and *b*. This was carried out using the Tukey–Kramer test (P=0.05)

Table 4.4

Mean values of exchangeable Ca^{2+}, Mg^{2+}, Na^{+} and K^{+} and of ESP following each irrigation treatment (FW00*i*, T102 and T401–4) of the H002 soil columns

	Depth	FW002		T102		T401		T402		T403		T404	
	(mm)	(EC 0.2 SAR 1)		(EC 0.0 SAR 0)		(EC 0.5 SAR 0)		(EC 0.5 SAR 7.5)		(EC 0.5 SAR 15)		(EC 0.5 SAR 30)	
Ca^{2+} ($cmol_{(+)}\ kg^{-1}$)	0–50	23.29	± 0.93	22.74	± 0.64	22.46	± 1.86	22.68	± 1.01	21.27	± 1.45	20.94	± 0.73
	50–100	19.77	± 0.57	20.68	± 0.32	21.81	± 0.50	21.73	± 0.16	20.82	± 1.03	20.04	± 0.28
	100–150	20.13	± 0.05	19.71	± 0.07	19.42	± 0.30	18.61	± 0.07	18.47	± 1.04	18.52	± 0.27
	>150	18.77	± 0.64	19.48	± 0.26	18.93	± 0.19	18.21	± 0.05	19.87	± 1.14	17.77	± 0.71
Mg^{2+} ($cmol_{(+)}\ kg^{-1}$)	0–50	10.64	± 0.43	10.25	± 0.25	11.11	± 0.96	10.21	± 0.29	10.26	± 1.06	9.90	± 0.32
	50–100	9.60	± 0.27	10.11	± 0.37	9.99	± 0.05	10.03	± 0.15	10.09	± 0.25	9.98	± 0.02
	100–150	10.51	± 0.34	10.01	± 0.10	10.01	± 0.24	9.31	± 0.13	9.68	± 0.23	10.25	± 0.16
	>150	10.79	± 0.21	10.71	± 0.31	10.61	± 0.45	10.59	± 0.40	10.82	± 0.05	10.51	± 0.30
Na^{+} ($cmol_{(+)}\ kg^{-1}$)	0–50	1.38*ab*	± 0.11	1.08*ab*	± 0.02	0.95*b*	± 0.25	1.56*ab*	± 0.02	1.75*a*	± 0.11	1.70*a*	± 0.00
	50–100	1.28	± 0.09	1.16	± 0.03	1.12	± 0.20	1.43	± 0.08	1.49	± 0.11	1.54	± 0.01
	100–150	1.37	± 0.19	1.33	± 0.01	1.34	± 0.34	1.45	± 0.10	1.49	± 0.12	1.59	± 0.03
	>150	1.42	± 0.16	1.35	± 0.03	1.55	± 0.39	1.52	± 0.08	1.55	± 0.20	1.61	± 0.06
K^{+} ($cmol_{(+)}\ kg^{-1}$)	0–50	1.97	± 0.04	1.91	± 0.20	1.68	± 0.15	1.65	± 0.13	1.58	± 0.04	1.58	± 0.07
	50–100	1.52	± 0.06	1.57	± 0.00	1.71	± 0.09	1.80	± 0.04	1.52	± 0.08	1.47	± 0.09
	100–150	1.35	± 0.07	1.37	± 0.06	1.26	± 0.02	1.38	± 0.10	1.24	± 0.04	1.27	± 0.09
	>150	1.12	± 0.05	1.29	± 0.00	1.15	± 0.03	1.21	± 0.07	1.25	± 0.04	1.14	± 0.00
ESP	0–50	3.71*abc*	± 0.42	3.01*bc*	± 0.14	2.60*c*	± 0.48	4.33*ab*	± 0.10	5.02*a*	± 0.06	5.00*a*	± 0.17
	50–100	3.99	± 0.39	3.45	± 0.17	3.21	± 0.51	4.07	± 0.18	4.39	± 0.12	4.64	± 0.04
	100–150	4.09	± 0.51	4.11	± 0.01	4.16	± 1.02	4.72	± 0.30	4.84	± 0.56	5.02	± 0.07
	>150	4.43	± 0.54	4.11	± 0.10	4.79	± 1.10	4.82	± 0.17	4.66	± 0.72	5.19	± 0.02

The mean values following each treatment were determined and the standard error of means obtained using a one–way Analysis of Variance and then compared for each of the sampled soil layers (0–50 mm, 50–100 mm, 100–150 mm and >150 mm). Significant differences were determined and are represented within rows by the letters *a*, *b* and *c*. This was carried out using the Tukey–Kramer test (P=0.05)

Table 4.5
Mean values of exchangeable Ca^{2+}, Mg^{2+}, Na^{+} and K^{+} and of ESP following each irrigation treatment (FW00*i*, T102 and T401–4) of the N001 soil columns

	Depth	FW002	T102	T401	T402	T403	T404
	(mm)	(EC 0.2 SAR 1)	(EC 0.0 SAR 0)	(EC 0.5 SAR 0)	(EC 0.5 SAR 7.5)	(EC 0.5 SAR 15)	(EC 0.5 SAR 30)
Ca^{2+} ($cmol_{(+)}\ kg^{-1}$)	0–50	26.26 ± 1.58	28.07 ± 1.19	27.81 ± 0.62	28.55 ± 1.77	26.34 ± 2.28	24.25 ± 1.55
	50–100	26.98 ± 1.26	29.36 ± 0.17	25.94 ± 1.16	25.88 ± 2.18	27.28 ± 0.44	25.74 ± 0.33
	100–150	27.84 ± 0.71	25.38 ± 2.01	27.41 ± 0.20	27.34 ± 0.25	29.04 ± 1.67	25.69 ± 1.33
	>150	24.90 ± 1.29	28.12 ± 0.70	25.53 ± 0.17	25.35 ± 0.32	26.78 ± 0.37	25.04 ± 1.17
Mg^{2+} ($cmol_{(+)}\ kg^{-1}$)	0–50	10.33 ± 0.45	10.63 ± 0.36	10.97 ± 0.09	10.30 ± 0.48	9.74 ± 0.71	9.24 ± 0.66
	50–100	10.67 ± 0.00	10.94 ± 0.30	10.44 ± 0.18	10.24 ± 0.36	10.59 ± 0.14	9.94 ± 0.66
	100–150	11.30 ± 0.08	10.72 ± 0.53	11.03 ± 0.09	10.73 ± 0.13	11.09 ± 0.35	10.50 ± 0.26
	>150	10.71 ± 0.12	11.44 ± 0.41	10.85 ± 0.03	10.71 ± 0.27	10.78 ± 0.29	10.62 ± 0.00
Na^{+} ($cmol_{(+)}\ kg^{-1}$)	0–50	4.49*a* ± 0.15	3.58*ab* ± 0.25	2.68*b* ± 0.11	3.83*a* ± 0.21	3.85*a* ± 0.23	3.92*a* ± 0.07
	50–100	4.38*a* ± 0.09	4.04*a* ± 0.02	3.36*b* ± 0.05	4.07*a* ± 0.02	4.26*a* ± 0.05	3.99*a* ± 0.19
	100–150	4.62 ± 0.07	4.30 ± 0.33	4.40 ± 0.02	4.51 ± 0.19	4.55 ± 0.19	4.34 ± 0.09
	>150	4.43 ± 0.11	4.65 ± 0.10	4.33 ± 0.15	4.53 ± 0.17	4.41 ± 0.18	4.39 ± 0.01
K^{+} ($cmol_{(+)}\ kg^{-1}$)	0–50	1.88 ± 0.35	1.84 ± 0.37	1.70 ± 0.18	1.71 ± 0.23	1.92 ± 0.27	1.48 ± 0.19
	50–100	2.10 ± 0.14	2.17 ± 0.13	1.96 ± 0.31	1.89 ± 0.12	2.00 ± 0.05	1.93 ± 0.19
	100–150	2.20 ± 0.09	1.99 ± 0.27	1.88 ± 0.13	2.07 ± 0.08	2.14 ± 0.09	1.83 ± 0.04
	>150	1.95 ± 0.12	2.06 ± 0.03	1.79 ± 0.05	1.86 ± 0.09	2.03 ± 0.09	1.92 ± 0.00
ESP	0–50	10.46*a* ± 0.10	8.10*b* ± 0.30	6.20*c* ± 0.12	8.62*b* ± 0.04	9.22*ab* ± 0.22	10.10*a* ± 0.46
	50–100	9.93*a* ± 0.14	8.68*ab* ± 0.02	8.08*b* ± 0.42	9.57*ab* ± 0.56	9.65*ab* ± 0.01	9.59*ab* ± 0.14
	100–150	10.05 ± 0.05	10.14 ± 0.03	9.83 ± 0.01	10.09 ± 0.42	9.71 ± 0.08	10.26 ± 0.20
	>150	10.57 ± 0.50	10.05 ± 0.03	10.19 ± 0.34	10.67 ± 0.48	10.01 ± 0.26	10.46 ± 0.31

The mean values following each treatment were determined and the standard error of means obtained using a one–way Analysis of Variance and then compared for each of the sampled soil layers (0–50 mm, 50–100 mm, 100–150 mm and >150 mm). Significant differences were determined and are represented within rows by the letters *a* and *b*. This was carried out using the Tukey–Kramer test (P=0.05)

Table 4.6

Mean values of exchangeable Ca^{2+}, Mg^{2+}, Na^{+} and K^{+} and of ESP following each irrigation treatment (FW00*i*, T102 and T401–4) of the N002 soil columns

	Depth	FW002	T102	T401	T402	T403	T404
	(mm)	(EC 0.2 SAR 1)	(EC 0.0 SAR 0)	(EC 0.5 SAR 0)	(EC 0.5 SAR 7.5)	(EC 0.5 SAR 15)	(EC 0.5 SAR 30)
Ca^{2+} ($cmol_{(+)}\ kg^{-1}$)	0–50	26.31 ± 0.72	24.09 ± 2.17	26.43 ± 1.48	25.90 ± 0.19	27.39 ± 2.03	26.53 ± 0.50
	50–100	24.52 ± 0.35	25.72 ± 1.47	25.40 ± 0.02	24.99 ± 0.54	26.61 ± 1.20	26.22 ± 0.18
	100–150	26.67 ± 0.74	25.81 ± 1.17	27.06 ± 0.49	28.93 ± 0.88	27.89 ± 0.49	28.06 ± 0.22
	>150	24.26 ± 1.09	25.72 ± 0.52	25.68 ± 0.62	26.89 ± 1.10	26.73 ± 0.80	27.16 ± 0.65
Mg^{2+} ($cmol_{(+)}\ kg^{-1}$)	0–50	9.89 ± 0.28	9.01 ± 0.28	10.16 ± 0.51	9.34 ± 0.23	10.05 ± 0.34	9.65 ± 0.17
	50–100	9.27*ab* ± 0.12	9.08*b* ± 0.13	9.45*ab* ± 0.03	9.20*ab* ± 0.04	9.61*ab* ± 0.17	9.74*a* ± 0.07
	100–150	10.15*ab* ± 0.10	9.39*c* ± 0.06	10.00*abc* ± 0.12	10.53*a* ± 0.04	9.86*bc* ± 0.21	10.48*a* ± 0.04
	>150	10.28 ± 0.34	10.18 ± 0.31	10.33 ± 0.33	10.36 ± 17	10.12 ± 0.31	10.46 ± 0.14
Na^{+} ($cmol_{(+)}\ kg^{-1}$)	0–50	0.97*b* ± 0.01	0.71*c* ± 0.02	0.68*c* ± 0.00	1.06*ab* ± 0.04	1.17*a* ± 0.05	0.94*b* ± 0.04
	50–100	0.91*b* ± 0.03	0.82*b* ± 0.01	0.84*b* ± 0.02	1.01*ab* ± 0.06	1.13*a* ± 0.04	0.95*ab* ± 0.04
	100–150	1.00*ab* ± 0.04	0.90*ab* ± 0.01	0.83*b* ± 0.03	1.04*ab* ± 0.09	1.09*a* ± 0.00	1.08*a* ± 0.01
	>150	1.02*ab* ± 0.05	0.97*ab* ± 0.03	0.89*b* ± 0.03	1.06*ab* ± 0.03	1.09*ab* ± 0.03	1.13*a* ± 0.06
K^{+} ($cmol_{(+)}\ kg^{-1}$)	0–50	1.75 ± 0.01	1.05 ± 0.08	1.81 ± 0.15	1.70 ± 0.08	1.76 ± 0.00	1.86 ± 0.03
	50–100	1.95 ± 0.08	1.45 ± 0.00	1.82 ± 0.25	1.53 ± 0.09	1.79 ± 0.30	1.62 ± 0.21
	100–150	1.33 ± 0.03	1.31 ± 0.04	1.37 ± 0.06	1.31 ± 0.17	1.36 ± 0.08	1.31 ± 0.04
	>150	1.08 ± 0.00	1.12 ± 0.02	1.21 ± 0.15	1.18 ± 0.09	1.11 ± 0.11	1.17 ± 0.03
ESP	0–50	2.51*ab* ± 0.09	2.00*b* ± 0.08	1.74*b* ± 0.09	2.78*a* ± 0.08	2.90*a* ± 0.28	2.42*ab* ± 0.06
	50–100	2.49*ab* ± 0.03	2.22*b* ± 0.08	2.23*ab* ± 0.04	2.76*ab* ± 0.12	2.89*a* ± 0.23	2.47*ab* ± 0.09
	100–150	2.56*ab* ± 0.15	2.42*ab* ± 0.07	2.10*b* ± 0.12	2.49*ab* ± 0.16	2.70*a* ± 0.04	2.64*ab* ± 0.04
	>150	2.78 ± 0.03	2.56 ± 0.09	2.35 ± 0.13	2.69 ± 0.00	2.81 ± 0.15	2.83 ± 0.20

The mean values following each treatment were determined and the standard error of means obtained using a one–way Analysis of Variance and then compared for each of the sampled soil layers (0–50 mm, 50–100 mm, 100–150 mm and >150 mm). Significant differences were determined and are represented within rows by the letters *a*, *b* and *c*. This was carried out using the Tukey–Kramer test (P=0.05)

4.3.2.2 The effect of treatment solution on the soil solution and the quantity of dispersed clay

The mean values of electrical conductivity, SAR and mechanically dispersed clay, for each treated soil layer, are presented in Tables 4.7–12 for the six irrigated Vertosols. The electrical conductivity values are small for all soils following all treatments, and are much less than the EC_w of the applied irrigation solutions (T401–4 and FW00*i*) or the initial electrical conductivity values of the soils (Table 3.3). Generally, the electrical conductivity of the uppermost soil layer is larger than for the lower soil layers of these treated Vertosols. However, the treated soil columns from the G00*i*, H00*i* and N001 sites do not show any significant differences between the values of electrical conductivity after irrigation using any of the T401–4 solutions. Only soil columns from the N002 site that had been irrigated with T404 show a significantly larger soil EC value than those columns irrigated with the T401–3 treatments.

Irrigating with clean water (T102) rather than the other solutions (FW00*i* or T401), did not give significantly smaller electrical conductivities for the G001 or H00*i* soils. However, the G002 and N00*i* soils tend to show significantly smaller electrical conductivities in the surface layers (0–100 mm) where the T102 treated columns are compared with all other treated columns. In these three soils, there is no significant difference between the electrical conductivities of the lower soil layers.

The soil columns irrigated using solutions of large SAR_w (T403–4) generally exhibit largest SARs in the surface layers (0–50 mm and 50–100 mm), but as depth increases, the SAR of the soil solution is less. In contrast, those soil columns irrigated with solutions T102, FW00*i* and T401 tend to have smaller values of SAR at the surface than at depth. Those soils treated with the T401–4 solutions show significantly larger SARs for the soil solution where treatments of larger SAR_w were applied, but all six soils do not show the same level of response. The H00*i* and N001 soils show no significant differences between SAR values for soil columns irrigated using the T401–4 solutions. The G00*i* (0–50 mm and 50–100 mm) and N002 (0–50 mm) soils show significantly smaller SARs for the T401 treated soil than for the T403 treated soil.

The FW00*i* treatments tend to result in SAR values for the six Vertosols that are between those SARs of soil treated with either the T401 or T402 solutions. The soil solution SARs of T102–treated soils tend to be similar to those of the T401–treated soils. There are no significant differences or consistent trends in SAR for these six Vertosols, where T102–treated columns are compared with the FW00*i* or T401 treatments.

The dispersed clay content after end–over–end shaking tends to be larger for soil columns irrigated with larger increments of SAR_w (T401→4). In comparison, columns irrigated with FW00*i* or T102

yield similar levels of dispersed clay, after shaking, to those soil columns irrigated with T401 or T402. The treatment of G001 soil columns using the solutions T401–3 shows an increase in dispersion where solutions of larger SAR_w were applied, and where this soil has been treated with the T403 solution, the quantities of dispersed clay are similar to those resulting from the T102–treated soil. However, when G001 was irrigated with T404 the results show significantly less clay dispersion than for any of the other T40*i* treatments of this Vertosol. Likewise, the G002 soil tends to be most dispersive after being irrigated with the T403. This trend shows a significant difference only between the T401–2 and the T403 treatment, and only in the 50–100 mm soil layer. For this soil, columns treated with either T401 or FW00*i* are most stable, but there are no significant differences between dispersion values for the FW00*i*, T102, T401 and T402 treatments. The H00*i* soils do not have any significant differences in dispersion values after any of the treatments.

The N001 soil appears to be the most dispersive of these six Vertosols, after irrigation with solutions of large SAR_w, but there are no significant differences between the quantities of dispersed clay for any of the irrigation treatments (0–150 mm). At the >150 mm depth only the T403 treatment of the N001 soil is associated with a significantly different value of clay dispersion (significantly less than for the other treatments). The N002 soil does not show any significant differences between the quantities of dispersed clay following any of the applied treatments (FW00*i*, T102 or T404–4).

Table 4.7
Mean values of EC, SAR and Dispersed clay following the completion of each irrigation treatment (FW00*i*, T102 and T401–4) of the G001 soil columns

	Depth	FW002	T102	T401	T402	T403	T404
	(mm)	(EC 0.2 SAR 1)	(EC 0.0 SAR 0)	(EC 0.5 SAR 0)	(EC 0.5 SAR 7.5)	(EC 0.5 SAR 15)	(EC 0.5 SAR 30)
EC (1:5 water) (dS m^{-1})	0–50	0.11 ± 0.02	0.10 ± 0.02	0.13 ± 0.01	0.10 ± 0.00	0.15 ± 0.02	0.11 ± 0.00
	50–100	0.07 ± 0.00	0.06 ± 0.00	0.07 ± 0.00	0.06 ± 0.00	0.07 ± 0.00	0.07 ± 0.00
	100–150	0.06 ± 0.01	0.05 ± 0.00	0.07 ± 0.01	0.06 ± 0.00	0.07 ± 0.00	0.07 ± 0.00
	>150	0.06 ± 0.00	0.06 ± 0.01	0.06 ± 0.00	0.06 ± 0.00	0.07 ± 0.00	–
SAR ($(mmol_{(+)}\ L^{-1})^{1/2}$)	0–50	1.29*b* ± 0.17	1.30*b* ± 0.18	1.13*b* ± 0.12	1.87*ab* ± 0.28	2.43*a* ± 0.12	1.57*ab* ± 0.02
	50–100	1.06*b* ± 0.08	1.05*b* ± 0.07	0.91*b* ± 0.11	1.61*a* ± 0.04	1.60*a* ± 0.09	1.01*b* ± 0.00
	100–150	0.90 ± 0.08	1.02 ± 0.08	0.95 ± 0.13	1.50 ± 0.05	1.42 ± 0.22	1.06 ± 0.03
	>150	0.98 ± 0.09	0.88 ± 0.00	0.94 ± 0.06	1.41 ± 0.15	1.38 ± 0.08	–
Dispersed clay (dag kg^{-1})	0–50	10.39 ± 1.46	10.01 ± 0.87	8.39 ± 1.51	10.42 ± 0.07	10.02 ± 0.94	5.80 ± 0.93
	50–100	9.57*b* ± 0.20	11.44*a* ± 0.23	8.01*c* ± 0.39	10.54*ab* ± 0.44	11.44*a* ± 0.10	5.23*d* ± 0.05
	100–150	10.24*bc* ± 0.41	13.32*a* ± 0.92	8.25*c* ± 0.16	11.38*ab* ± 0.73	11.01*abc* ± 0.26	4.82*d* ± 0.24
	>150	9.82*ab* ± 0.16	14.16*a* ± 0.71	8.68*b* ± 1.31	11.87*ab* ± 0.50	12.26*ab* ± 0.78	–

The mean values following each treatment were determined and the standard error of means obtained using a one–way Analysis of Variance and then compared for each of the sampled soil layers (0–50 mm, 50–100 mm, 100–150 mm and >150 mm). Significant differences were determined and are represented within rows by the letters *a*, *b*, *c* and *d*. This was carried out using the Tukey–Kramer test (P=0.05)

Table 4.8
Mean values of EC, SAR and Dispersed clay following the completion of each irrigation treatment (FW00*i*, T102 and T401–4) of the G002 soil columns

	Depth	FW002	T102	T401	T402	T403	T404
	(mm)	(EC 0.2 SAR 1)	(EC 0.0 SAR 0)	(EC 0.5 SAR 0)	(EC 0.5 SAR 7.5)	(EC 0.5 SAR 15)	(EC 0.5 SAR 30)
EC (1:5 water) (dS m^{-1})	0–50	0.10*ab* ± 0.01	0.05*b* ± 0.00	0.11*a* ± 0.00	0.14*a* ± 0.02	0.11*ab* ± 0.01	0.13*a* ± 0.01
	50–100	0.06*ab* ± 0.00	0.05*b* ± 0.00	0.07*ab* ± 0.01	0.08*a* ± 0.00	0.07*ab* ± 0.01	0.07*ab* ± 0.00
	100–150	0.06 ± 0.00	0.05 ± 0.00	0.06 ± 0.01	0.08 ± 0.00	0.08 ± 0.01	0.07 ± 0.00
	>150	0.06 ± 0.01	0.06 ± 0.01	0.07 ± 0.00	0.07 ± 0.00	0.07 ± 0.01	–
SAR ($(mmol_{(+)}\ L^{-1})^{1/2}$)	0–50	1.61*c* ± 0.12	1.12*d* ± 0.03	1.10*d* ± 0.05	2.50*ab* ± 0.02	2.38*b* ± 0.08	2.85*a* ± 0.09
	50–100	1.46*ab* ± 0.07	1.33*ab* ± 0.17	1.03*b* ± 0.03	1.72*ab* ± 0.23	1.79*a* ± 0.14	1.72*ab* ± 0.01
	100–150	1.37 ± 0.17	1.43 ± 0.02	1.34 ± 0.19	1.80 ± 0.09	1.76 ± 0.16	1.66 ± 0.08
	>150	1.40 ± 0.17	1.43 ± 0.13	1.35 ± 0.10	1.86 ± 0.02	1.59 ± 0.26	–
Dispersed clay (dag kg^{-1})	0–50	8.30 ± 1.33	10.76 ± 1.61	8.84 ± 1.32	9.94 ± 0.64	11.84 ± 1.52	11.49 ± 0.89
	50–100	10.41*b* ± 0.90	9.60*b* ± 0.08	10.14*b* ± 0.89	10.23*b* ± 0.03	14.22*a* ± 0.33	11.91*ab* ± 0.36
	100–150	12.22 ± 0.24	13.03 ± 1.16	10.65 ± 1.17	10.42 ± 0.24	12.61 ± 0.39	11.39 ± 0.31
	>150	12.55 ± 0.43	12.39 ± 0.70	11.59 ± 0.39	13.48 ± 0.45	15.48 ± 2.77	–

The mean values following each treatment were determined and the standard error of means obtained using a one–way Analysis of Variance and then compared for each of the sampled soil layers (0–50 mm, 50–100 mm, 100–150 mm and >150 mm). Significant differences were determined and are represented within rows by the letters *a*, *b*, *c* and *d*. This was carried out using the Tukey–Kramer test (P=0.05)

Table 4.9
Mean values of EC, SAR and Dispersed clay following the completion of each irrigation treatment (FW00*i*, T102 and T401–4) of the H001 soil columns

	Depth	FW002	T102	T401	T402	T403	T404
	(mm)	(EC 0.2 SAR 1)	(EC 0.0 SAR 0)	(EC 0.5 SAR 0)	(EC 0.5 SAR 7.5)	(EC 0.5 SAR 15)	(EC 0.5 SAR 30)
EC (1:5 water) (dS m^{-1})	0–50	0.11 ± 0.01	0.06 ± 0.01	0.16 ± 0.04	0.14 ± 0.01	0.11 ± 0.00	0.11 ± 0.01
	50–100	0.06 ± 0.00	0.05 ± 0.01	0.07 ± 0.01	0.07 ± 0.00	0.08 ± 0.00	0.08 ± 0.01
	100–150	0.07 ± 0.00	0.05 ± 0.01	0.07 ± 0.01	0.07 ± 0.00	0.09 ± 0.00	0.08 ± 0.02
	>150	0.08 ± 0.01	0.06 ± 0.01	0.08 ± 0.00	0.07 ± 0.00	0.08 ± 0.00	–
SAR ($(mmol_{(+)}\ L^{-1})^{1/2}$)	0–50	2.30 ± 0.08	1.49 ± 0.32	1.76 ± 0.69	3.01 ± 0.10	2.59 ± 0.75	2.15 ± 0.13
	50–100	1.61 ± 0.20	1.18 ± 0.22	1.42 ± 0.19	1.58 ± 0.04	1.81 ± 0.41	1.59 ± 0.17
	100–150	1.59 ± 0.07	1.26 ± 0.22	1.56 ± 0.24	1.51 ± 0.01	1.50 ± 0.27	1.80 ± 0.31
	>150	1.78 ± 0.13	1.45 ± 0.23	1.52 ± 0.12	1.61 ± 0.03	1.99 ± 0.15	–
Dispersed clay (dag kg^{-1})	0–50	1.77 ± 1.46	3.50 ± 0.68	5.17 ± 1.79	3.69 ± 0.63	7.04 ± 1.78	7.72 ± 2.93
	50–100	2.72 ± 1.67	3.68 ± 0.66	4.37 ± 0.94	4.90 ± 1.10	6.84 ± 1.78	8.73 ± 0.76
	100–150	5.39 ± 0.66	6.03 ± 0.04	5.87 ± 0.96	6.42 ± 2.64	8.91 ± 1.58	9.83 ± 0.97
	>150	7.43 ± 0.34	6.93 ± 2.54	6.94 ± 2.66	8.67 ± 2.16	9.99 ± 0.13	–

The mean values following each treatment were determined and the standard error of means obtained using a one–way Analysis of Variance and then compared for each of the sampled soil layers (0–50 mm, 50–100 mm, 100–150 mm and >150 mm)

Table 4.10
Mean values of EC, SAR and Dispersed clay following the completion of each irrigation treatment (FW00*i*, T102 and T401–4) of the H002 soil columns

	Depth	FW002	T102	T401	T402	T403	T404
	(mm)	(EC 0.2 SAR 1)	(EC 0.0 SAR 0)	(EC 0.5 SAR 0)	(EC 0.5 SAR 7.5)	(EC 0.5 SAR 15)	(EC 0.5 SAR 30)
EC (1:5 water) (dS m^{-1})	0–50	0.20 ± 0.05	0.13 ± 0.01	0.24 ± 0.05	0.21 ± 0.00	0.21 ± 0.00	0.23 ± 0.01
	50–100	0.13 ± 0.01	0.13 ± 0.00	0.16 ± 0.04	0.15 ± 0.00	0.15 ± 0.01	0.16 ± 0.00
	100–150	0.13 ± 0.01	0.13 ± 0.01	0.15 ± 0.03	0.15 ± 0.00	0.15 ± 0.01	0.17 ± 0.01
	>150	0.14 ± 0.01	0.13 ± 0.01	0.16 ± 0.02	0.15 ± 0.00	0.16 ± 0.01	0.17 ± 0.02
SAR ($(mmol_{(+)}\ L^{-1})^{1/2}$)	0–50	2.61 ± 0.62	1.71 ± 0.20	1.47 ± 0.71	3.10 ± 0.00	3.35 ± 0.19	3.72 ± 0.07
	50–100	2.16 ± 0.46	1.81 ± 0.18	1.87 ± 0.73	2.58 ± 0.06	2.58 ± 0.16	2.88 ± 0.00
	100–150	2.27 ± 0.41	2.06 ± 0.17	2.40 ± 0.86	2.68 ± 0.17	2.59 ± 0.32	3.03 ± 0.11
	>150	2.45 ± 0.44	2.17 ± 0.21	2.72 ± 0.95	2.82 ± 0.10	2.84 ± 0.42	3.11 ± 0.16
Dispersed clay (dag kg^{-1})	0–50	4.89 ± 0.13	5.81 ± 1.15	5.02 ± 0.60	3.24 ± 0.67	6.41 ± 1.27	7.95 ± 1.42
	50–100	5.70 ± 0.25	6.68 ± 1.31	6.27 ± 0.47	7.88 ± 0.73	6.81 ± 1.21	10.54 ± 0.69
	100–150	7.84 ± 0.66	10.17 ± 0.80	9.28 ± 1.63	11.09 ± 1.39	9.52 ± 1.96	11.04 ± 1.85
	>150	7.39 ± 0.84	10.91 ± 2.07	9.93 ± 2.93	13.10 ± 1.56	10.37 ± 0.90	14.80 ± 0.85

The mean values following each treatment were determined and the standard error of means obtained using a one–way Analysis of Variance and then compared for each of the sampled soil layers (0–50 mm, 50–100 mm, 100–150 mm and >150 mm)

Table 4.11
Mean values of EC, SAR and Dispersed clay following the completion of each irrigation treatment (FW00*i*, T102 and T401–4) of the N001 soil columns

	Depth	FW002	T102	T401	T402	T403	T404
	(mm)	(EC 0.2 SAR 1)	(EC 0.0 SAR 0)	(EC 0.5 SAR 0)	(EC 0.5 SAR 7.5)	(EC 0.5 SAR 15)	(EC 0.5 SAR 30)
EC (1:5 water) (dS m^{-1})	0–50	0.20*ab* ± 0.01	0.17*b* ± 0.01	0.20*ab* ± 0.01	0.22*a* ± 0.01	0.23*a* ± 0.01	0.22*a* ± 0.00
	50–100	0.20 ± 0.02	0.18 ± 0.00	0.19 ± 0.01	0.20 ± 0.00	0.20 ± 0.00	0.20 ± 0.00
	100–150	0.19 ± 0.00	0.19 ± 0.00	0.21 ± 0.00	0.21 ± 0.00	0.21 ± 0.00	0.21 ± 0.01
	>150	0.20 ± 0.00	0.20 ± 0.01	0.22 ± 0.00	0.21 ± 0.00	0.21 ± 0.00	0.21 ± 0.00
SAR ($(mmol_{(+)}\ L^{-1})^{1/2}$)	0–50	5.01*ab* ± 0.25	3.70*b* ± 0.48	4.13*ab* ± 0.06	5.12*a* ± 0.06	4.69*ab* ± 0.24	4.95*ab* ± 0.14
	50–100	4.75*a* ± 0.10	3.50*b* ± 0.22	4.28*ab* ± 0.05	4.29*a* ± 0.14	4.18*ab* ± 0.04	4.32*a* ± 0.19
	100–150	4.41 ± 0.30	4.14 ± 0.59	4.73 ± 0.01	4.74 ± 0.02	4.52 ± 0.01	4.28 ± 0.10
	>150	4.76*ab* ± 0.06	4.30*b* ± 0.13	4.88*a* ± 0.16	4.48*ab* ± 0.06	4.63*ab* ± 0.03	4.40*ab* ± 0.08
Dispersed clay (dag kg^{-1})	0–50	14.50 ± 0.59	16.03 ± 1.86	11.60 ± 0.08	11.25 ± 0.15	12.07 ± 1.17	13.43 ± 1.37
	50–100	18.32 ± 0.19	19.29 ± 0.00	16.20 ± 1.51	16.04 ± 0.46	15.66 ± 1.49	15.11 ± 0.72
	100–150	19.86 ± 0.97	19.12 ± 2.40	19.09 ± 1.36	16.79 ± 1.24	15.42 ± 0.76	18.16 ± 0.02
	>150	19.34*a* ± 1.13	20.08*a* ± 0.04	18.53*a* ± 0.89	18.43*a* ± 0.22	14.41*b* ± 0.80	18.92*a* ± 0.43

The mean values following each treatment were determined and the standard error of means obtained using a one–way Analysis of Variance and then compared for each of the sampled soil layers (0–50 mm, 50–100 mm, 100–150 mm and >150 mm). Significant differences were determined and are represented within rows by the letters *a* and *b*. This was carried out using the Tukey–Kramer test (P=0.05)

Table 4.12
Mean values of EC, SAR and Dispersed clay following the completion of each irrigation treatment (FW00*i*, T102 and T401–4) of the N002 soil columns

	Depth	FW002		T102		T401		T402		T403		T404	
	(mm)	(EC 0.2 SAR 1)		(EC 0.0 SAR 0)		(EC 0.5 SAR 0)		(EC 0.5 SAR 7.5)		(EC 0.5 SAR 15)		(EC 0.5 SAR 30)	
EC (1:5 water) (dS m^{-1})	0–50	0.11*bc*	± 0.01	0.08*c*	± 0.00	0.17*b*	± 0.02	0.18*b*	± 0.01	0.16*bc*	± 0.00	0.27*a*	± 0.03
	50–100	0.09	± 0.00	0.07	± 0.01	0.09	± 0.01	0.09	± 0.01	0.10	± 0.00	0.10	± 0.00
	100–150	0.10	± 0.00	0.08	± 0.03	0.09	± 0.02	0.10	± 0.02	0.09	± 0.01	0.09	± 0.01
	>150	0.11	± 0.00	0.08	± 0.02	0.09	± 0.02	0.11	± 0.01	0.09	± 0.01	0.11	± 0.01
SAR ($(mmol_{(+)}\ L^{-1})^{1/2}$)	0–50	1.07*bc*	± 0.04	0.60*c*	± 0.02	0.74*c*	± 0.06	1.68*a*	± 0.00	1.84*a*	± 0.20	1.53*ab*	± 0.02
	50–100	0.98*b*	± 0.06	0.66*c*	± 0.03	0.85*bc*	± 0.02	1.26*a*	± 0.05	1.32*a*	± 0.04	1.21*a*	± 0.00
	100–150	1.04*ab*	± 0.08	0.80*b*	± 0.07	0.88*b*	± 0.01	1.17*a*	± 0.01	1.29*a*	± 0.01	1.26*a*	± 0.05
	>150	1.08*ab*	± 0.01	0.90*b*	± 0.10	0.92*b*	± 0.03	1.24*ab*	± 0.03	1.32*a*	± 0.03	1.36*a*	± 0.12
Dispersed clay (dag kg^{-1})	0–50	4.09	± 0.20	3.50	± 0.93	3.57	± 0.54	3.65	± 1.38	2.89	± 0.07	3.78	± 1.45
	50–100	7.20	± 0.20	4.46	± 0.70	6.40	± 1.25	6.29	± 0.54	6.32	± 0.18	7.04	± 0.19
	100–150	14.64	± 0.57	9.21	± 2.24	9.08	± 2.54	10.07	± 0.09	8.53	± 0.54	9.73	± 0.19
	>150	14.32	± 1.08	11.66	± 4.06	9.08	± 1.70	10.68	± 0.45	9.82	± 1.12	10.35	± 0.34

The mean values following each treatment were determined and the standard error of means obtained using a one–way Analysis of Variance and then compared for each of the sampled soil layers (0–50 mm, 50–100 mm, 100–150 mm and >150 mm). Significant differences were determined and are represented within rows by the letters *a*, *b* and *c*. This was carried out using the Tukey–Kramer test (P=0.05)

4.3.3 The effect of selected soil properties on the $SI_{<2}$ values determined for the six Vertosols

In order to compare the degree of association between the stability index, $SI_{<2}$, and selected soil chemical properties (EC, SAR, Na^+_{exch}, Ca^{2+}:Mg^{2+}, ESP, ESI and $EC_{1:5}/Na^+_{exch}$) following the irrigation treatments, correlation values are given for 'all soils' (G00*i*, H00*i* and N00*i*) and for all soil layers of each individual soil (Table 4.13).

Correlation coefficients between the $SI_{<2}$ values and each of the selected chemical properties are not greater than 0.7, but all correlation values for each of the selected properties and 'all soils' are significant. The strongest correlation coefficients for this comparison are between 0.5–0.7, where $SI_{<2}$ is correlated with SAR, Na^+_{exch} or ESP. The exchangeable Na^+ content is most strongly correlated with $SI_{<2}$ for 'all soils'.

The correlation values between soil properties and $SI_{<2}$ for each individual soil are rarely larger than ±0.5, but all correlation values larger than ±0.28 are significant for each individual soil. Unexpectedly, EC is positively correlated with $SI_{<2}$ for 'all soils', but generally has small negative correlation values with the $SI_{<2}$ values of each individual soil and is significant only for the N00*i* soils. Overall, the evaluation of correlation values for each individual soil shows that the Na^+ descriptors (Na^+_{exch} and ESP) tend to be most strongly correlated with $SI_{<2}$ values. For all of the soils except G001, a larger Na^+_{exch} or ESP is significantly associated with larger $SI_{<2}$ values. The significant negative correlation between the Na^+_{exch} or ESP values and $SI_{<2}$ suggests other soil properties are more influential than Na^+ in determining $SI_{<2}$.

The Ca^{2+}:Mg^{2+}, ESI and $EC_{1:5}/Na^+_{exch}$ values give expected results. These descriptors give significant negative correlations with $SI_{<2}$ for most of the soils. The SARs of H001 and N00*i* are negatively correlated with $SI_{<2}$, and these values are significant for the N00*i* soils.

Table 4.13
Correlation values comparing the $SI_{<2}$ (%) of dispersed clay with the measured soil properties determined from air–dry soil layers for all treatments of all soils and for each soil[a]

	EC	**SAR**	**Na^+_{exch}**	**Ca^{2+}:Mg^{2+}**	**ESP**	**ESI**	**$EC_{1:5}/Na^+_{exch.}$**
$SI_{<2}$ (%) (all soils)	**0.36**	**0.58**	**0.70**	**0.27**	**0.52**	**-0.25**	**-0.38**
G001 $SI_{<2}$ (%)	-0.20	0.15	**-0.32**	**-0.37**	**-0.31**	-0.08	-0.08
G002 $SI_{<2}$ (%)	-0.26	0.14	**0.45**	-0.16	**0.39**	**-0.48**	**-0.49**
H001 $SI_{<2}$ (%)	0.02	-0.02	**0.65**	**-0.67**	**0.42**	-0.15	-0.25
H002 $SI_{<2}$ (%)	-0.18	**0.35**	**0.43**	**-0.78**	**0.60**	**-0.51**	**-0.45**
N001 $SI_{<2}$ (%)	**-0.32**	**-0.33**	**0.57**	**-0.53**	**0.47**	**-0.65**	**-0.68**
N002 $SI_{<2}$ (%)	**-0.35**	-0.09	**0.29**	**-0.53**	**0.29**	**-0.40**	**-0.41**

[a] correlations that are significant at the 95 % confidence interval are shown in bold.

Bivariate comparisons of $SI_{<2}$ against EC, SAR, Na^{+}_{exch}, Ca^{2+}:Mg^{2+}, ESP, ESI and $EC_{1:5}/Na^{+}_{exch}$ are given in Figures 4.3–4.5, and include R^2 estimates of the variability for all soils. In general, the R^2 values for comparisons of $SI_{<2}$ with each soil property are very low, indicating a very poor association between $SI_{<2}$ and each individual soil attribute (Na^{+}_{exch}, Ca^{2+}:Mg^{2+}, ESP, ESI and $EC_{1:5}/Na^{+}_{exch}$). However, these soil attributes tend to show values that are grouped according to the six different Vertosols. For example, the comparisons of Na^{+}_{exch} (Figure 4.4) and ESP (Figure 4.5) against $SI_{<2}$ show all values for the N001 soil to be much larger than those of the other soils. Consequently, other soil properties appear to influence the different stabilities of each of the six Vertosols (*i.e.* the clay phyllosilicate suite or organic matter contributions).

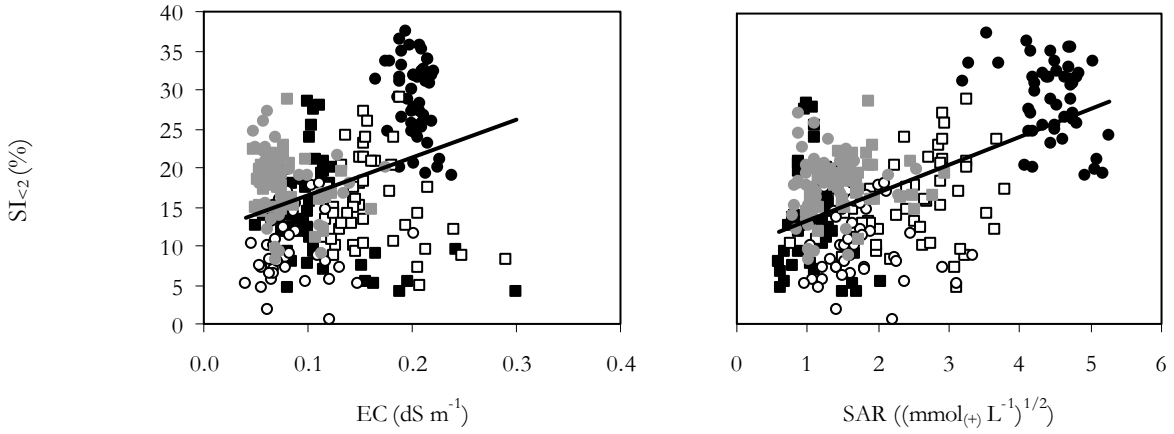

Figure 4.3 Comparison of the $SI_{<2}$ (%) values for all soils with the corresponding values of EC (*y=47.9x+11.8, R^2=0.13*) and SAR (*y=3.6x+9.9, R^2=0.34*) following each of the treatment solutions and for each soil layer analysed. These include values obtained for the G001 (●), G002 (■), H001 (○), H002 (□), N001 (●) and N002 (■) soils.

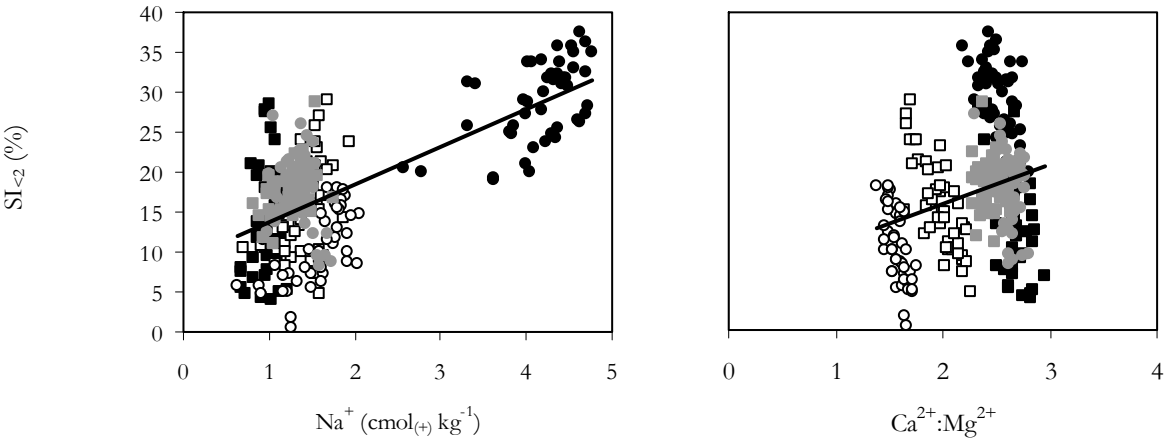

Figure 4.4 Comparison of the $SI_{<2}$ (%) values for all soils with the corresponding values of exchangeable Na^{+} (*y=4.7x+9.0, R^2=0.48*) and Ca^{2+}:Mg^{2+} (*y=5x+5.9, R^2=0.07*) following each of the treatment solutions and for each soil layer analysed. These include values obtained for the G001 (●), G002 (■), H001 (○), H002 (□), N001 (●) and N002 (■) soils.

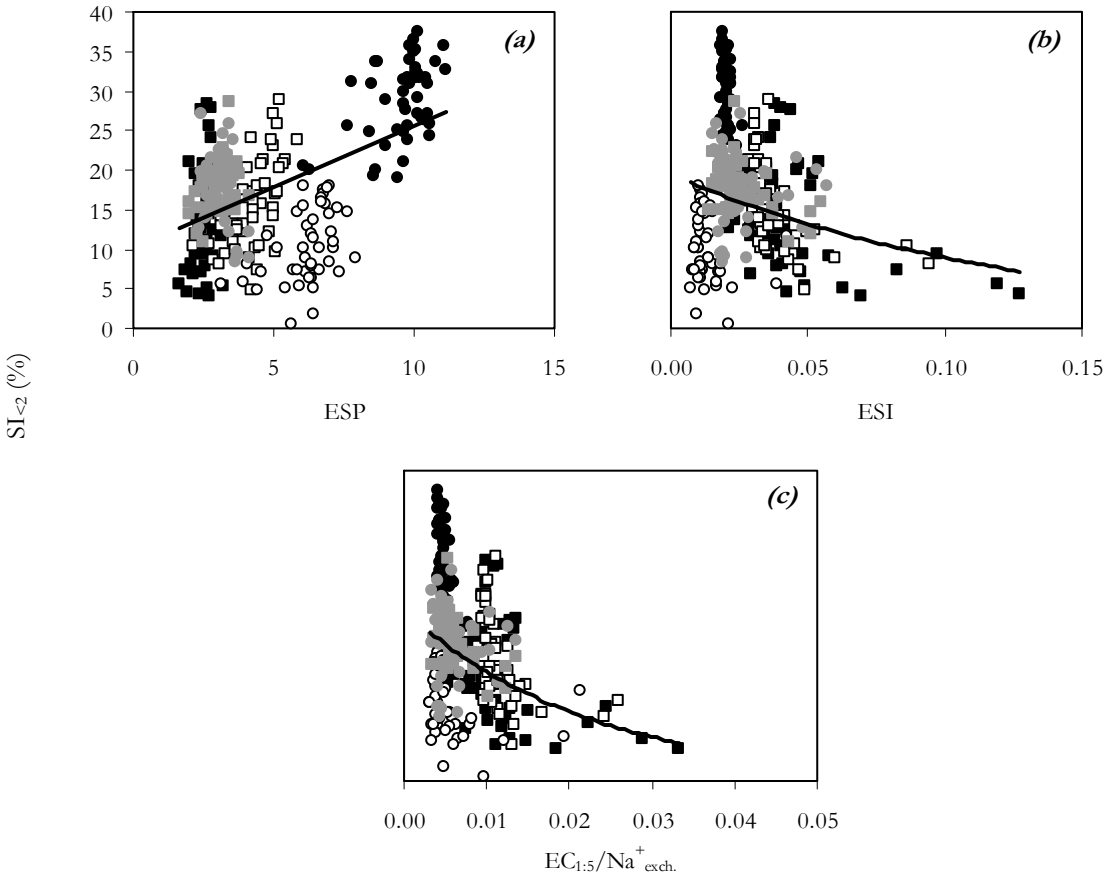

Figure 4.5 Comparison of the $SI_{<2}$ (%) values for all soils with the corresponding, *(a)*, values of ESP ($y=1.5x+10.1$, $R^2=0.27$), *(b)*, ESI ($y=19.5e^{-7.8x}$, $R^2=0.06$) and, *(c)*, $EC_{1:5}/Na^+_{exch.}$ ($y=0.6e^{44.3x}$, $R^2=0.14$) following each of the treatment solutions and for each soil layer analysed. These include values obtained for the G001 (●), G002 (■), H001 (○), H002 (□), N001 (●) and N002 (■) soils.

4.4 Discussion

4.4.1 Irrigating in the laboratory

Soil columns have been used in laboratory studies for many years (*e.g.* Yaron and Thomas 1968), and numerous methods have been used to apply different water quality treatments to soil preparations. In most studies, water treatments have been applied where the volume of solution was comparable to a specified number of pore volumes, or using sufficient solution to elicit specified conditions *i.e.* to increase soil ESP to a certain level. For example, Astaraei and Chauhan (1992) leached soil columns until the parameters of water quality for the percolate (EC_w and SAR_w) were an approximation of the EC_w and SAR_w characteristics of the applied solutions.

In this chapter no attempt was made to obtain percolate EC_w and SAR_w values representative of the applied solution. Rather, this irrigation procedure was adopted to represent the irrigation of cotton–

producing Vertosols. Consequently, the quantity of irrigation water applied in this study was determined from an estimate of total irrigation water (*i.e.* river and/or bore water) applied to cotton crops during the 1996–97 and 1997–98 growing seasons (Dugdale *et al.* 2004). The soil columns were irrigated with this volume of solution because this research aimed to mimic field conditions. In addition, a criterion of the irrigation procedure was to minimise the surface water present at the completion of each irrigation event, as free water would not generally pond on the surface of fields prepared for irrigated cotton production. However, a number of soil columns underwent incomplete percolation of the applied solution (shown in appendix 3.1), particularly where solutions of SAR_w 15 or SAR_w 30 were used. Incomplete percolation is a consequence of two processes; *(i)*, soil swelling and, *(ii)*, the slaking and dispersion of clay particles at the soil surface. These processes are considered to be a result of the rapid wetting of soil aggregates, large solution SAR_w and the movement of water at the soil surface during solution application, which tended to re–distribute small soil aggregates. It is probable that these aggregates then contributed to the infilling of surface cracks in each of these Vertosols and the subsequent restriction of surface infiltration in some of the soil columns, whereby incomplete irrigation resulted.

The problems associated with laboratory–based irrigation have been highlighted throughout the literature. Quirk and Murray (1991) identified reductions in permeability as a response to rapid wetting and the ponding of treatment solutions on the soil surface. Furthermore, the constraints of applying different increments of water quality are well known. Halliwell *et al.* (2001) gave water quality limits that indicate levels of SAR_w that are potentially restrictive, in terms of infiltration, at different intervals of EC_w. They proposed the possibility of slight to moderate infiltration problems when irrigating with solutions of EC_w 0.5, SAR_w <7.5, and severe infiltration difficulties when irrigating with solutions of EC_w 0.5, SAR_w 15–30. Irrigation sources with SAR_w values this large (15–30) are not representative of any current water sources used in irrigated cotton production. However, these SAR_w levels were included in this research so as to determine the extent to which soil properties could be influenced by very large Na^+ contributions from irrigation sources.

4.4.2 Comparing the chemical properties of soil columns with the chemical attributes of the irrigation furrow

After each of the six irrigation treatments, all soils (G00*i*, H00*i* and B00*i*) had different chemical attributes to those determined for each of the initial irrigation furrow soils. The physico–chemical properties of each irrigation furrow soil are given in Table 3.3 (chapter 3.3.1).

The contents of exchangeable Ca^{2+} and Mg^{2+} for the irrigated soil columns were significantly smaller than for the initial soils. Concurrently, the content of exchangeable Na^+ was significantly larger for soil columns irrigated in the laboratory, than for the initial Vertosols sampled from each irrigation

furrow. The laboratory irrigated soils tended to have electrical conductivities that were much more dilute than the initial furrow soil, but only in the N001 soil was this difference significant. Similarly, there tended to be no significant difference between SARs of the irrigated and initial soils.

The altered chemical properties (*e.g.* smaller exchangeable Ca^{2+} and Mg^{2+} contents and larger exchangeable Na^{+} contents) of the irrigated soils did not appear to adversely influence the mechanical stability, where $SI_{<2}$ values were compared with the $SI_{<2}$ of the initial soils (*see* T102 treatment using EOE–disruption, Table 3.4). Overall, the surface soil layers (0–50 mm and 50–100 mm) of the irrigated soil columns tended to be more stable than the initial soils and the 100–150 mm and >150 mm soil layers, irrespective of the applied treatment. This was unexpected, as the surface soil layers tended to have significantly larger ESPs and slightly smaller electrical conductivities than the initial soils. At lower depths (100–150 mm and >150 mm) the quantities of dispersed clay tended to be the same or larger than the dispersed clay contents of the corresponding soil from the irrigation furrow. However, the ESP and electrical conductivity values at these depths did not provide a robust comparison between the irrigated soils and the initial soils. These inconsistencies reflect two potential differences between the soils before and after irrigation. These differences are; *(i)*, the incomplete distribution of cations at exchange surfaces and, *(ii)*, the contributions of organic material.

During the destructive sampling of soil layers, there was no attempt to account for differences in the distribution of exchangeable cations or the organic carbon content of each soil layer. Differences in the distributions of exchangeable cations were expected, in part, because most solution drainage will have taken place through connected pore space between aggregates. Consequently, there would have been only limited solution movement into the soil matrix of individual aggregates. This will have resulted in most changes in the proportions of different exchangeable cations occurring at the outer surfaces of soil aggregates and in some cases at the outer edges of clay domains, rather than at the charged surfaces of individual clay particles. Hence, the altered cation composition of these soils, after irrigation, is likely to reflect ion exchange at the domain/solution interface rather than the particle/solution interface. This results in an uneven distribution of the exchangeable cations in the irrigated soil columns, which will influence the swelling and dispersion of clay particles. Furthermore, this uneven distribution is likely to have encouraged 'de–mixing' (Halliwell *et al.* 2001), a process which results in clay domains remaining intact at ESPs less than 15–25. This occurs in Ca^{2+}–Na^{+} systems as a result of a non–random distribution of exchangeable Ca^{2+} and Na^{+} (Quirk 1994; Nelson *et al.* 1999; Halliwell *et al.* 2001; Quirk 2001). Accordingly, at ESPs less than 25, exchangeable Na^{+} congregates at the outer face of clay domains thereby influencing inter–domain swelling, but not affecting intra–domain expansion.

A second difference between the irrigation furrow soils prior to irrigation and after irrigation is expected to result (in part) from cementing agents (*e.g.* organic matter or $CaCO_3$). In this experiment, the contributions of organic matter or other cementing agents were not determined for each of the irrigated soil columns due to the time and cost constraints involved. Therefore, it is unknown if the irrigation processes to which these soil columns were subjected influenced the production of organic matter (*e.g.* the proliferation of fungi) or by cementation during salt precipitation. However, it is unlikely that salt precipitation contributed to the cementation of aggregates due to the very low EC values that were observed for each of the treated soils post–irrigation. More likely was the impact of organic matter production on the stability of soil aggregates in each of these columns.

In previous research (*e.g.* McNeal *et al.* 1968; Chen and Banin 1975), the potential contributions of organic matter were limited through the addition of controlling agents (*e.g.* NaOCl or $HgCl_2$). Controlling agents were not introduced to the irrigation solutions in this procedure as this would have potentially disrupted the field–like process that had been attempted. However, future work should look to quantify the organic content of soil layers from laboratory irrigated soils. This will go some way to assessing the impact of organic matter on different Na^+–rich Vertosols. For example, the effect of organic contributions on the stability of sodic soils was discussed by Nelson *et al.* (1998). They found that a wet–dry regime appeared to stabilise some clay through particle re–arrangement and cementation. A conclusion they reached suggested that the decomposition of organic matter was able to reduce clay dispersion by impacting on the electrolyte concentration. This work was followed by Nelson *et al.* (1999) who concluded that the dispersibility of clay was a function of the amount and type of organic matter, its CEC and selectivity for specific cations, and the particle size distribution of the soil mineral phase.

4.4.3 Comparison of the assessed soil attributes for these irrigated Vertosols

Prior to irrigation in the laboratory, the six Vertosols were ranked according to various properties (chapter 3). The G00*i* and N00*i* soils had larger Ca^{2+}:Mg^{2+} ratios than the H00*i* soils (N00*i*, G001>G002>H00*i*), while the ESPs showed that the H00*i* and N001 soils are generally more sodic than the G00*i* or N002 soils. However, the G00*i* and N001 soils were the least stable showing *severe* to *very severe dispersion* (*Classes* 4–5) (Table 3.10), while H00*i* and N002 were most stable and show *limited dispersion* (*Class* 2). Consequently, the differences in stability tended to reflect the CEC_{eff}, and therefore, the clay phyllosilicate suites of these soils. In soils with a similar clay phyllosilicate suite, structural stability appeared to be a function of different ESP and electrical conductivity values for each soil.

The selected soil properties of the six Vertosols were ranked in a similar way once the irrigation procedure was complete. Post–irrigation these soils show, very broadly, a similar pattern for the quantities of dispersed clay, regardless of the applied treatment solution *i.e.* the H00*i* and N002 soils appear to be most stable, while the N001 soil appears to be least stable. In the analysis of exchangeable cation contributions, there did not appear to be any preferential exchange for Ca^{2+} or Mg^{2+}, where the T401–4 solutions were applied. The H00*i* soils have the smallest Ca^{2+}:Mg^{2+} ratios following all treatments, while the N00*i* soils have the largest ratios.

The ESPs showed increasing sodicity in the order G00*i*≈N002<H00*i*<N001, but while increasing ESP was associated with increasing values of $SI_{<2}$ for five of the soils, the G001 soil showed decreasing ESP to be associated with $SI_{<2}$. In chapter 1 the impact of Na^+ on individual clay particles was described, *i.e.* increasing Na^+ is associated with less stable systems. Consequently, other soil properties are likely to have had a strong influence on the level of dispersion observed in each of the soil columns.

The electrical conductivities of the irrigated soils were generally the same following all treatments of each soil. Only the irrigated soil columns from the H002 and N001 sites had conductivities that were different to the other soils, but these did not tend to exceed 0.25 dS m^{-1} for any of the treated soil columns. This is indicative of the leaching process brought about by applying irrigation water to the top of soil columns, and consequently the EC of different soil layers was not a good descriptor for characterising the structural stability of these soil samples.

The $SI_{<2}$ values of these soils appeared to reflect differences in the Ca^{2+}:Mg^{2+} ratio and the CEC_{eff} of each soil. The Ca^{2+} and Mg^{2+} cations represent the major proportion of cations on the exchange complex and using this ratio, site specific differences can be identified. The soils showed increasing Ca^{2+}:Mg^{2+} ratios in the order H001<H002<G00*i*≈N00*i*. The CEC_{eff} gave an estimate of negative charge on the surface of clay minerals and consequently, an estimate of the contributions of expanding lattice phyllosilicate clays. This showed the soils to have increasing charge in the order H001<H002<N002<G00*i*≈N001. These distributions (of Ca^{2+}:Mg^{2+} ratio and CEC_{eff}) were very similar to the distribution of soils according to increasing contributions of expanding lattice phyllosilicates (H00*i*≈N002<N001<G00*i*) given in chapter 2.

The apparent influence of clay phyllosilicate suite on the dispersion of the soils investigated in this research is a similar finding to that of Ahmed *et al.* (1969). They found a significant clay type effect on aggregate stability after the preparation of homeoionic clays. Their montmorillonite–based soil had greater stability than a kaolinite based soil, after each had been saturated with Ca^{2+}, Mg^{2+} or K^+.

However, the Na^+–montmorillonite soil was 'very much less' stable than the Na^+–kaolinite soil. They observed the same trends in mixed ionic systems, but noted that the trends were less apparent.

In addition to the influence of swelling clay phyllosilicates on $SI_{<2}$, there appears to be some impact of the size grade of various clay phyllosilicate species (*e.g.* smectite). This observation appears evident as finer clay particles pack more closely, and such systems have a greater ability to swell and flex according to applied pressures (Quirk 1994). In the six Vertosols investigated, the coarse clay fraction (30–40 % of total clay) appeared to influence stability in a different way to the fine clay fraction (60–70 % of total clay). Increased aggregate stability tended to occur were soils contained small amounts of fine 2:1 expanding lattice phyllosilicate clay. Then, soils with similar contributions of fine 2:1 expanding lattice phyllosilicates were differentiated by the contribution of coarse 2:1 expanding lattice phyllosilicates. This may be a result of two factors: *(i)*, thicker 2:1 expanding phyllosilicate clay platelets bend less during swelling than fine clays of the same species and, *(ii)*, the coarse clay fraction has a lower surface area to volume ratio and a smaller charge density. Consequently, coarse clays are likely to swell less, and be less dispersive than fine clays. In chapter 2.6.2 the dominant clay mineral constituents were outlined for each soil; these soils had increasing contributions of expanding 2:1 clay phyllosilicates to the coarse clay fractions, in the order H00*i* < G001 ≈ N00*i* < G002 and had increasing contributions of expanding 2:1 clay phyllosilicates to the fine clay fraction in the order H001 < N002 < H002 < G002 ≈ N001 < G001. Consequently, the lower stability of the G00*i* and N001 soils, which are dominated by smectite clays in both the coarse and fine fractions, appeared to have resulted from increased swelling of clay domains in the de–ionised (T102) solution used for EOE–disruption. The H001 soil tended to have the least dispersed clay after EOE–disruption. This soil was dominated by fine grade illite (<0.2 μm) and consequently, the swelling pressures generated by the very low electrolyte concentration of de–ionised water during end–over–end shaking were not large enough to cause that same level of dispersion as observed in either the G00*i* or N00*i* soils.

4.4.4 Comparing $SI_{<2}$ values with soil properties

In chapter 3, it was shown that the CEC_{eff} of each soil was the property most consistently associated with the observed values of $SI_{<2}$ irrespective of the applied treatment. For the laboratory irrigated soils, the Na^+ descriptors and the Ca^{2+}:Mg^{2+} ratios were the properties most associated with observations of $SI_{<2}$ where all soils were included and for each individual soil. In these six soils (G00*i*, H00*i* and N00*i*), increased Na^+ (exchange or solution) and decreased Ca^{2+}:Mg^{2+} ratios were associated with larger $SI_{<2}$ values. The chapter 3 correlations suggested that an increased Ca^{2+}:Mg^{2+} ratio was associated with larger $SI_{<2}$ values and this was found where the $SI_{<2}$ values for all six

Vertosols were correlated against Ca^{2+}:Mg^{2+} ratios. These correlations reflected the overall influence of the soil mineral suite. This is because the less stable G00*i* and N00*i* soils, that have larger exchange capacities than the H00*i* soils, have larger Ca^{2+}:Mg^{2+} ratios.

The electrical conductivity, ESI and $EC_{1:5}/Na^{+}_{exch}$ attributes were generally not associated with $SI_{<2}$ according to correlation coefficients for individual soils or correlation coefficients for all soils. This reflects the very similar conductivities of all soils irrespective of the sampling site or the treatment solution applied. The ESI and $EC_{1:5}/Na^{+}_{exch}$ predictors presented by Hulugalle and Finlay (2003), were generally less suited for describing $SI_{<2}$ values than ESP when correlation comparisons were assessed, although the ESI and $EC_{1:5}/Na^{+}_{exch}$ were correlated with $SI_{<2}$. The fitted regression model broadly supported the use of an ESI critical level of 0.05 for delineating the less stable Vertosols from the more stable soils. However, both the ESI and $EC_{1:5}/Na^{+}_{exch}$ predictors were strongly influenced by the electrical conductivity values of all included soil samples. This strong EC affect limited the distribution of ESI and $EC_{1:5}/Na^{+}_{exch}$ values and very few soil samples had ESI values greater than 0.05, while most of the $EC_{1:5}/Na^{+}_{exch}$ values were less than 0.015. Consequently, these predictors appeared unsuitable for describing the potential instability of these laboratory irrigated Vertosols.

4.5 Conclusions

Irrigating each of the six Vertosols in the laboratory, using the different water solutions, resulted in larger contributions of exchangeable Na^{+} and smaller values of electrical conductivity compared to the initial furrow soils. However, the irrigated soil columns did not exhibit larger quantities of mechanically dispersed clay than the initial soils. In addition, Na^{+} descriptors (Na^{+}_{exch} and ESP) and Ca^{2+}:Mg^{2+} ratios were the only attributes to show consistent significant individual relationships with the values of $SI_{<2}$ that were determined. This is because of the large influence of clay phyllosilicate suite on the stabilities of these six different Vertosols. However, while the phyllosilicate suite is the main attribute differentiating the stabilities of these six soils, other soil attributes contributed to the different stabilities of irrigated soil columns from each site. The exchangeable Na^{+} content and Ca^{2+}:Mg^{2+} ratios of these soils tended to show consistent relationships with the $SI_{<2}$ values of each soil. However, the distribution of $SI_{<2}$ values suggested that additional soil properties influenced the stability of these irrigated soil columns (*e.g.* organic matter).

Chapter 5

ASSESSING THE IMPACT OF IRRIGATION ON SOIL STRUCTURAL FORM

ASSESSING THE IMPACT OF IRRIGATION ON SOIL STRUCTURAL FORM

~

Form: *forma (L.): the shape and structure of an object*

~

5.1 Introduction

In chapters 3 and 4, soil structural stability was shown to be the result of a myriad of physico–chemical interactions. The structural stability of different soil types is expressed in response to the composition of the clay phyllosilicate suite, total clay content and cation interactions between the diffuse double layer and the soil solution. In addition, irrigation water quality influences the solution and exchangeable cation contents of irrigated soils and consequently, impacts on soil structural stability. As a consequence, it is widely understood that the interactions of different soil physico–chemical properties will influence the expression of structural form (*e.g.* Hubble 1984; McGarry 1996).

Soil structural form describes the arrangement of solid and void space in a heterogeneous or discontinuous manner; it results from the continual development of soil constituents (mineral and organic) into aggregates of increasing size and bound by zones of failure. The development of soil structural form in Vertosols results from swelling and shrinkage, climatic conditions and the physico–chemical attributes of each profile (McGarry 1996). The ability of Vertosols to shrink upon drying causes an arrangement of cracks to develop that are characteristic of particular physico–chemical properties and landuse practices. Thus, the impact of anthropogenic activities on structural form can be quantified by characterising the soil solid and pore phases after different management treatments.

This chapter catalogues the degree of change to soil structural form when undisturbed soil columns are subjected to irrigation water of varying quality. Soil columns, sampled from each of the nine cotton–producing Vertosols, were irrigated in the laboratory with six different solutions. All columns were impregnated with a fluorescent resin and images of structural form collected. These images were analysed using the Solicon© analysis software (Cattle *et al.* 2001) for an array of pore and solid attributes.

5.2 Soil structural form characteristics determined using Solicon©

The Solicon© analysis software (Cattle *et al.* 2001) was developed to apply the stereological techniques described by Moran *et al.* (1989), McBratney and Moran (1990) and McBratney *et al.* (1992) to binary images of soil. This software and its applications are described by Roesner (2003). The key structural form attributes estimated by Solicon© describe the pore and solid phases of soil. These are summarised as (Roesner 2003):

Porosity (P):

P indicates the proportion of pore space that exists within a soil image (length^3 length^{-3}).

Surface area (S_v):

S_v is an estimate of the interfacial area between pore and solid phases in a given volume of soil (length^2 length^{-3}).

Horizontal pore and solid star lengths (l_p^* and l_s^*):

Star length (mm) properties describe the average size of the pore and solid phases. The l_p^* is the expected continuous length of pore in the horizontal plane, encountered in any direction from a point placed at random at a specified image depth. Conversely, l_s^* is the calculation of this attribute for the solid phase.

Horizontal pore and solid genus (g_p and g_s):

Horizontal pore and solid genus descriptors give the number of routes that can be constructed between a pair of points in an image while maintaining passage. It is effectively a measure of the number of loops or the connectedness of an image. Consequently, g_p and g_s represent the minimum connectivity of the pore and solid phases of a binary image.

Pore sieve distribution:

The mean pore sieve size (s_p) is the average radius of pores represented by the largest circles that fit within a pore structure. Consequently, the pore sieve distribution represents the size distribution of all pore units into which different sized shape functions have been fitted.

Distribution of the pore star–shape factor:

The star–area factor (Ra_p^*) is a measure of the 'roundness' estimated form individual pore star areas. Consequently, the histogram of the pore star–shape factor can be used to determine the proportion of certain shape features between the limits of 0 and 1. A factor >0.6 indicates a larger proportion of rounded pore shapes, while a factor <0.4 indicates a larger proportion of fissures or long needle–like pore shapes.

5.3 Methods

5.3.1 Sample preparation and the laboratory irrigation of soil columns

Intact soil columns (160 mm *o.d.* × 200 mm *h.*) were extracted from each of the nine cotton–growing fields (B00*i*, G00*i*, H00*i* and N00*i*) in the same way as those soil columns that were obtained for the chapter 4 irrigation procedure. In the lower Gwydir, Hillston and lower Namoi regions (G00*i*, H00*i* and N00*i*), twelve soil columns were obtained from each sampling site. In the Bourke region, ten soil columns were extracted from each of the B001 and B003 sites, and two soil columns were obtained from the B002 site. This gave a total of ninety four soil columns for the analysis of soil structural form parameters.

Each soil column was prepared and then irrigated in the laboratory according to the procedures outlined in chapter 4.2.1. From each of the G00*i*, H00*i* and N00*i* sampling sites, columns were irrigated using one of the six irrigation solutions (FW00*i*, T102 or T401–4) described in chapter 4.2.2. The B001 and B003 columns were irrigated using one of five irrigation solutions (FW00*i*, T102 or T401–3), and the two soil columns from the B002 site were irrigated using only the corresponding FW00*i* treatment solution. This design resulted in two soil columns from each sampling site being treated using each of the irrigation solutions outlined. The EC_w and SAR_w values for each of these irrigation solutions are presented in Tables 3.1 and 3.2.

During irrigation changes in column weight and drainage solution descriptors were monitored according to the protocol outlined in chapter 4.2.3. The changes in weight for each of the soil columns (before irrigation–after irrigation) are given in appendix 3.1 and the drainage solution descriptors (EC_w, solution cations and SAR_w values) are presented in appendix 3.2 for each treatment of the nine soils.

5.3.2 Image acquisition and analysis

Once six irrigation cycles were completed and after all soil columns had been allowed to dry for 50 days, an image acquisition process was commenced. Following the procedure outlined by Vervoort and Cattle (2003), the soil columns were first impregnated with a slow–curing resin mixture, containing an ultraviolet (UV)–fluorescent yellow dye. This resin mixture filled all surface connected pore–space. The fluid components of the mixture are detailed by McBratney *et al.* (1992). It consisted of resin, diluent, hardener and opacifier at a ratio of 34:34:32:1.

The resin mixture was slowly applied to the surface of each soil column, using sufficient resin to immerse all soil solids. Then each column was left to harden for a minimum of 48 hrs. The subsequent soil–resin blocks were ground using an angle grinder through the horizontal plane (Vervoort and Cattle 2003). Images of the exposed surface were captured using a Canon G3 Powershot digital camera under blacklight blue UV–light. This was done at depth increments of 10 mm, between the soil depths of 0 and 100 mm, and then at depths of 120 mm, 140 mm and 160 mm. The distance between the camera lens and the surface of each soil–resin block was kept constant by raising the exposed face to a given height. Furthermore, all images from individual columns were collected maintaining uniform orientation. This allowed for a comparison between sampling intervals for each of the soil columns to be made post–analysis. The images obtained were composed of yellow pore space and black solids. These were downloaded to a computer and segmented using a threshold histogram. Each was inverted and the subsequent binary image was represented by black (pore space) and white (solid space) pixels, where a single pixel was representative of approximately 0.12 mm^2. Consequently, the porosity detected using this method was the soil macroporosity (Beven and Germann 1982).

A sub–sample of each binary image was collected by taking a circular 1000 pixel *d.* segment from the centre of each sample to remove the edge effects, which resulted from minor soil shrinkage at the PVC–soil interface. The resulting images each had a diameter of approximately 120 mm and this gave each image an area of 1.13×10^{-2} m^2. A schematic representation of an impregnated soil column and the horizontal sampling intervals (10, 30, 50, 70 and 90 mm depths), from which images were collected and prepared, is given in Figure 5.1. Examples of structural form for the six different irrigation treatments of the G001 and H001 soils are given in Figures 5.2 and 5.3 for the 50 mm depth increment of soil columns.

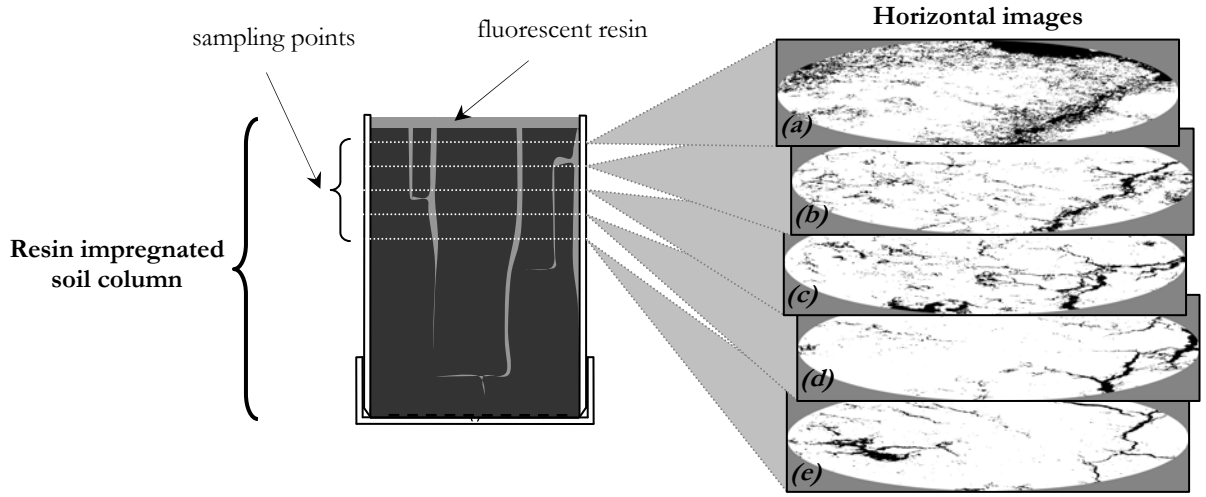

Figure 5.1 Horizontal image samples were collected at 10 mm increments in the 0–100 mm depth of soil columns and then at 20 mm increments in the 100–160 mm zone. In this figure the horizontal images are given for one of the irrigated soil columns at sampling points of, *(a)*, 10 mm depth, *(b)*, 30 mm depth, *(c)*, 50 mm depth, *(d)*, 70 mm depth and, *(e)*, 90 mm depth.

The Solicon© *v2.1* software (Cattle *et al.* 2001) was used to access and assess all soil structural form characteristics of the collected binary images. This program applies various pixel–counting procedures to estimate the proportions, size characteristics and connectivity of the pore and solid phases. The principles behind these calculations are described by Serra (1982), McBratney and Moran (1990) and by Roesner (2003). In this thesis, estimates of six structural parameters were obtained for each image; macroporosity (P), surface area (S_v), pore star length (l_p^*), solid star length (l_s^*), pore genus (g_p) and solid genus (g_s). These were selected to comprehensively describe the pore and solid phases of each soil column. In addition, the pore sieve and pore star–shape distributions were determined for each image to estimate the size and shape of soil macropore space. The pore sieve classes were computed to give a continuous distribution of effective soil pore sizes. To do this, the thresholds for each pore sieve class were assigned according to 0.1 mm increments between 0.1 and 1.0 mm, and then as 0.5 mm increments between 1.0 mm and 2.5 mm. Pore sieve classes with sizes greater than 2.5 mm were not included. Therefore, the twelve pore sieve classes were (mm):

0.1–0.2	0.2–0.3	0.3–0.4	0.4–0.5	0.5–0.6	0.6–0.7
0.7–0.8	0.8–0.9	0.9–1.0	1.0–1.5	1.5–2.0	2.0–2.5

5.3.3 Analysis of soil structural form attributes

All structural form attributes, determined for each of the solution treatments of each Vertosol, were prepared using One–Way Analyses of Variance (ANOVA) to give the mean attributes for each treatment and the corresponding standard error. Using this procedure, the mean treatment effect with increasing soil depth was derived from the replicated treatments of each soil to show changes

in the macroporosity (P), surface area (S_v), pore star length (l_p^*), solid star length (l_s^*), pore connectivity (g_p) and solid connectivity (p_s). These depth functions are presented for the T401–4 treatments of the G001 and H001 soils in Figures 5.4–7. The other depth functions, for each irrigation treatment of the nine Vertosols, are given in appendix 5.1. Once the depth functions were prepared, mean structural attributes were determined for three discrete depth intervals using all images for each irrigation treatment of each soil. These depth intervals were; 0–40 mm, 50–90 mm and 100–160 mm. At each of the three depth intervals, significant differences between means were determined using the Tukey–Kramer test (P=0.05). The mean structural attributes of the 50–90 mm interval are given in Tables 5.1–4, while the mean attributes for the 0–40 mm and 100–160 mm intervals are given in appendix 5.2.

All nine Vertosols were compared to determine differences in structural form between the sites. To do this, the Tukey–Kramer test (P=0.05) was used to compare the nine Vertosols using mean attributes of the 50–90 mm interval. The B001, B003, G00*i*, H00*i* and N00*i* soils were compared using the T102 and T402 treatments. These two solutions were used to compare the soils as 'clean water' (T102) appeared to influence structural form attributes differently to the T40*i* solutions, while the T402 solution included a comparison of soils using a SAR_w treatment. The three B00*i* soils were compared using the FW001 treatment, as this was the only treatment solution used to irrigate the B002 soil. These comparisons are given in Tables 5.5 and 5.6.

The pore sieve and pore star–shape distributions were prepared for the 50–90 mm depth increment. These were used to compare the different treatments of each of the B001, B003, G00*i*, H00*i* and N00*i* soils. The pore sieve and pore star–shape distributions of the B00*i* soils were compared using the FW001 treatment. Figures 5.8 and 5.9 give the pore sieve distributions for the G001 and H001 soils. Figures 5.10 and 5.11 give the pore–star shape distributions for the same soils. The pore sieve and pore star–shape distributions of all the other Vertosols are given in appendix 5.3.

5.4 Results

In Figures 5.2 and 5.3 binary images show the structural arrangement of pore and solid space at the 50 mm depth increment for selected soil columns from the G001 and H001 sites. These images represent soil columns irrigated with the FW00*i*, T102 or T401–4 solutions.

Soil structural attributes are influenced by the SAR_w of the irrigation water applied, but irrespective of the applied treatment solution, these soils all contain very small contributions of macropore space

(frequently <5 % macroporosity) at depths greater than 30 mm. Treating the B001, B003, G00*i,* H00*i* and N00*i* soils with solutions of large SAR_w tends to result in less porosity, less surface area and smaller pore sizes than treating these soils with low SAR_w solutions. Conversely, treating soil treated with low SAR_w solutions gives smaller solid phase attributes than treating soils with large SAR_w solutions.

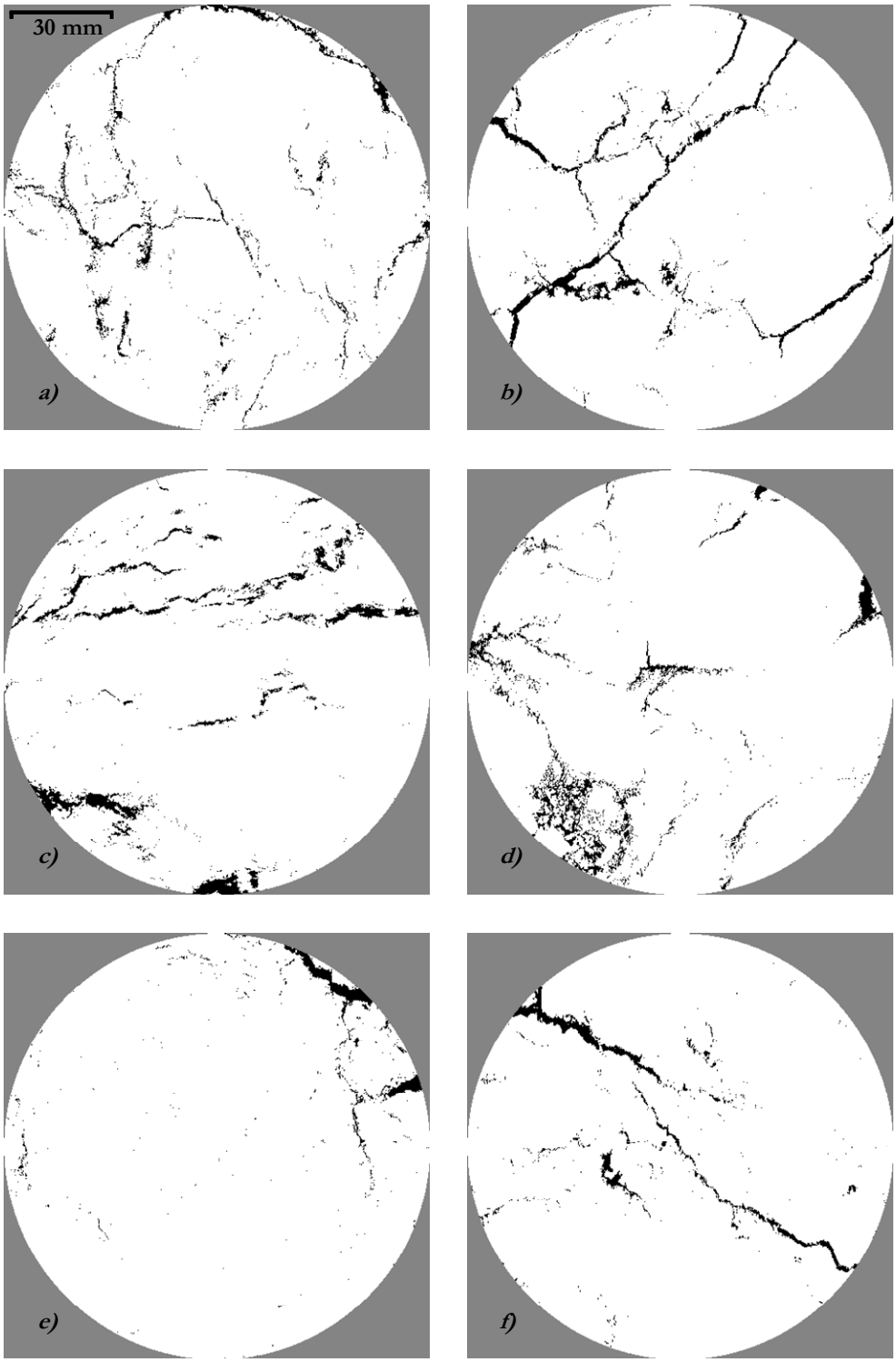

Figure 5.2 The treatment of G001 with each of the irrigation treatment solutions [FW00*i*, *(a)*, T102, *(b)*, T401, *(c)*, T402, *(d)*, T403, *(e)*, and T404, *(f)*]. These selected images were taken from the 50 mm depth increment of soil columns.

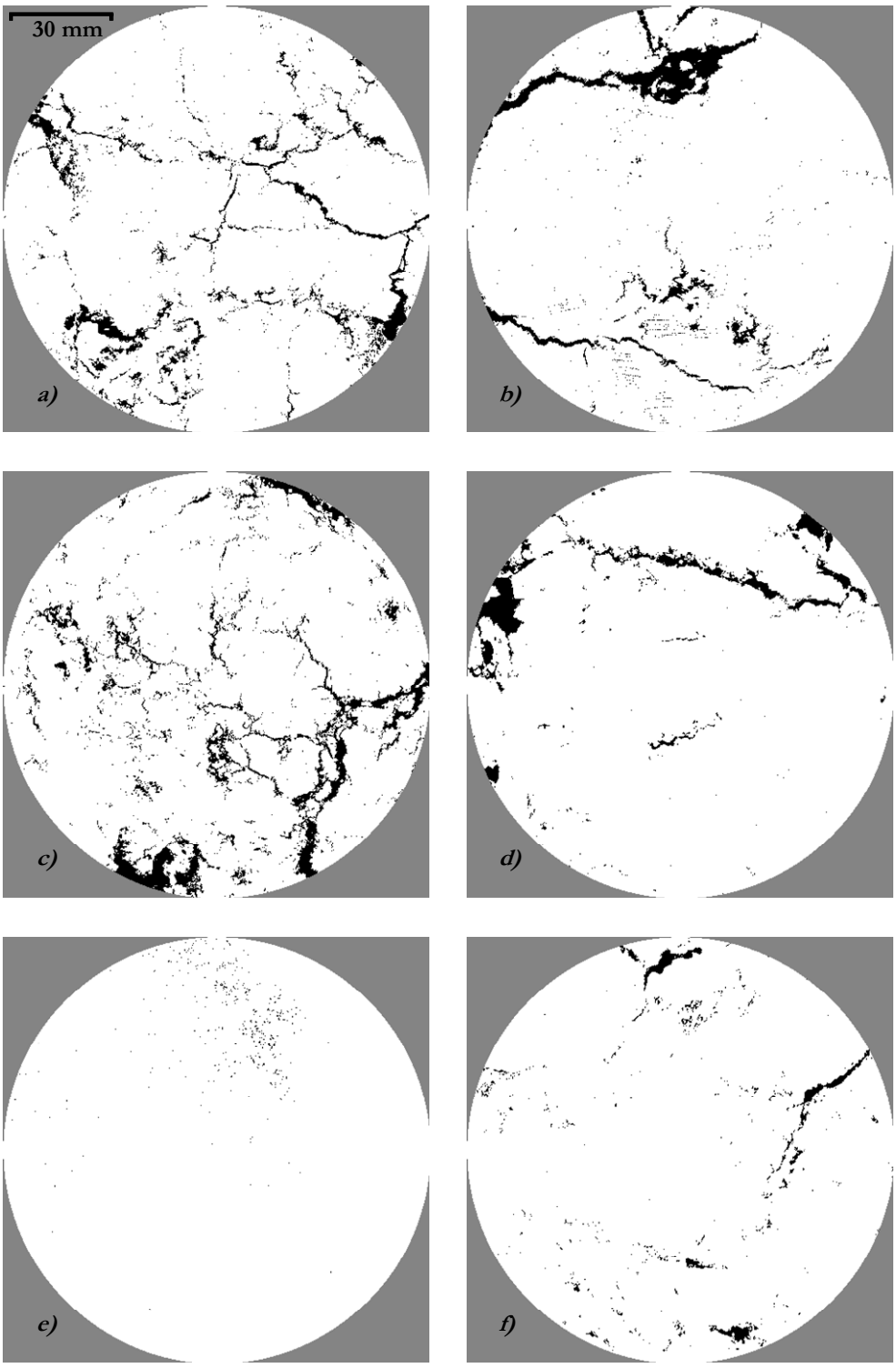

Figure 5.3 The treatment of H001 with each of the irrigation treatment solutions [FW00*i*, *(a)*, T102, *(b)*, T401, *(c)*, T402, *(d)*, T403, *(e)*, and T404, *(f)*]. These selected images were taken from the 50 mm depth increment of soil columns.

5.4.1 The effect of water quality on selected structural parameters for the nine soils investigated

The impact of each of the irrigation solutions on the magnitude of each descriptive parameter is presented by depth for each of the soils studied. Figures 5.4 and 5.5 give the change in structural parameters with depth for the T401–4 treatments of the G001 soil, and Figures 5.6 and 5.7 show the

change in structural parameters with depth for the T401–4 treatments of the H001 soil. The changes in structural parameters with depth, for all the other treatments (FW00*i*, T102 and T401–4) of the nine Vertosols, are given in appendix 5.1

5.4.1.1 Comparative effects of the T40i solutions on structural form attributes

In general, the soils irrigated with the T40*i* solutions tend to show estimates of soil *P*, S_r, g_p and g_s that are smaller for the soil columns treated with solutions of larger SAR_w (T403 or T404) than for soils treated with the T401 solution (SAR_w 0). Concurrently, estimates of l_s^* are typically larger for soil columns irrigated with solutions of greater SAR_w than for soils treated with solution T401. However, the estimates of l_p^* for each of the soils do not tend to be influenced by the SAR_w (T40*i*) treatments applied.

Irrigation using the T40*i* solutions did not result in the same differences between the structural attributes for all soils. In addition, the differences between the structural attributes of soils irrigated, using each of the T40*i* solutions, tend to be less at increased depth. The range of structural attributes of these Vertosols is demonstrated by the G001 and H001 soils.

The G001 soil has *P*, l_p^* and g_p attributes (Figures 5.4 and 5.5) that do not appear to show any differences between the SAR_w treatments (T401–4). At depths of 0–80 mm in this soil, the T403 treated soil tends to have the smallest S_r, while the T404–treated soil tends to have the largest S_r. Similarly, the T404–treated soil has the smallest l_s^*, and the T403–treated columns have the largest l_s^*. The connectivity estimates of solid space (g_s) are similar for the T401–4 treatments, but g_s is generally smallest where the G001 soil has been irrigated with T403. For this soil, the depths below 80 mm have different trends in the structural attributes; the S_r and g_s tend to be least for the T404–treated soil and largest for the T401–treated columns, while the l_s^* values tend to be larger where soil has been treated with larger SAR_w solutions.

The H001 soil (Figures 5.6 and 5.6) appear to have distinct trends in the structural parameters that are apparent at all depths for the T40*i* treatments. This soil has greatest *P* where the T401 treatment had been applied, and least *P* for columns irrigated using T403, while the T402 and T404 treated soils have intermediate values. The S_r and g_s values reflect the trend in *P*, and decreases according to the treatment solution applied during the irrigation of soil columns in the order T401, T402, T404 and T403. The l_s^* values for this soil are consistently larger according to the same order *i.e.* T401 < T402<T404<T403.

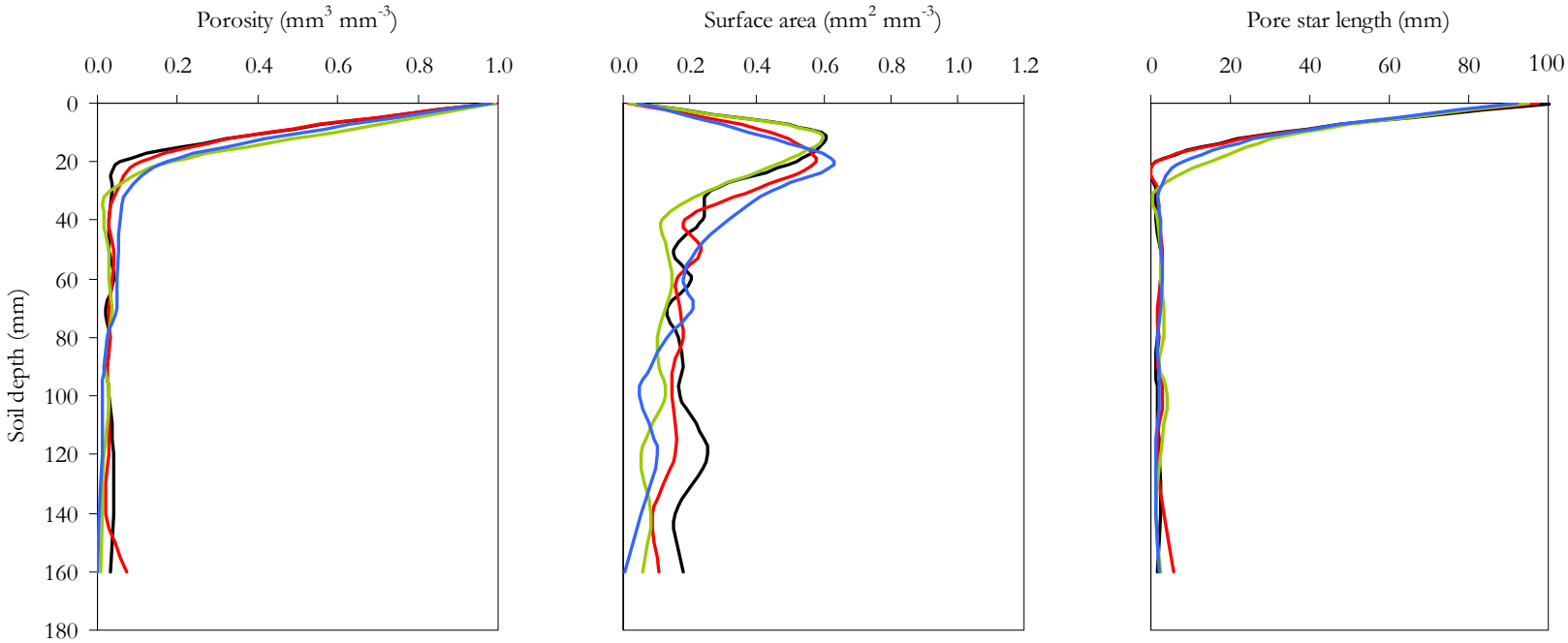

Figure 5.4 Response of selected structural parameters (*P, S_v and l_p^**) of soil G001 to four treatments; T401 (—), T402 (—), T403 (—) and T404 (—).

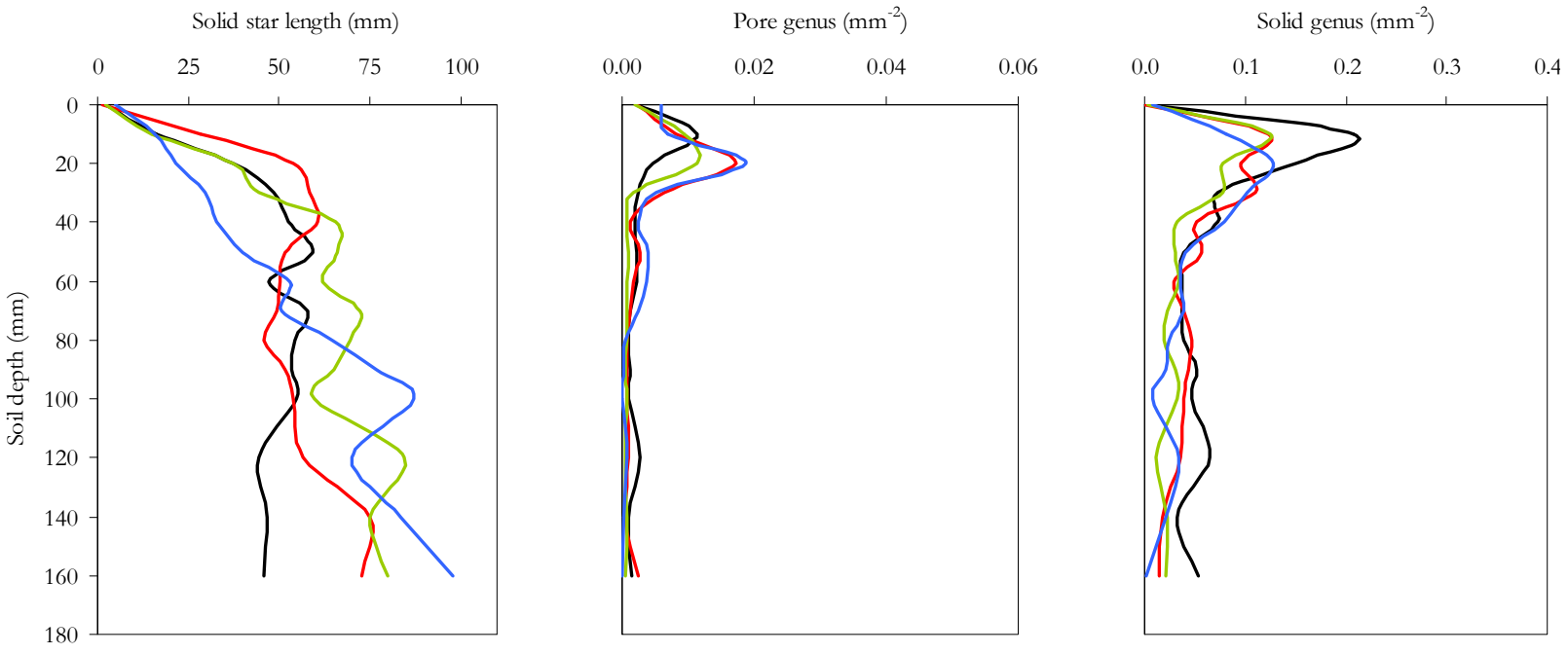

Figure 5.5 Response of selected structural parameters (l_s^*, g_p *and* g_s) of soil G001 to four treatments; T401 (—), T402 (—), T403 (—) and T404 (—).

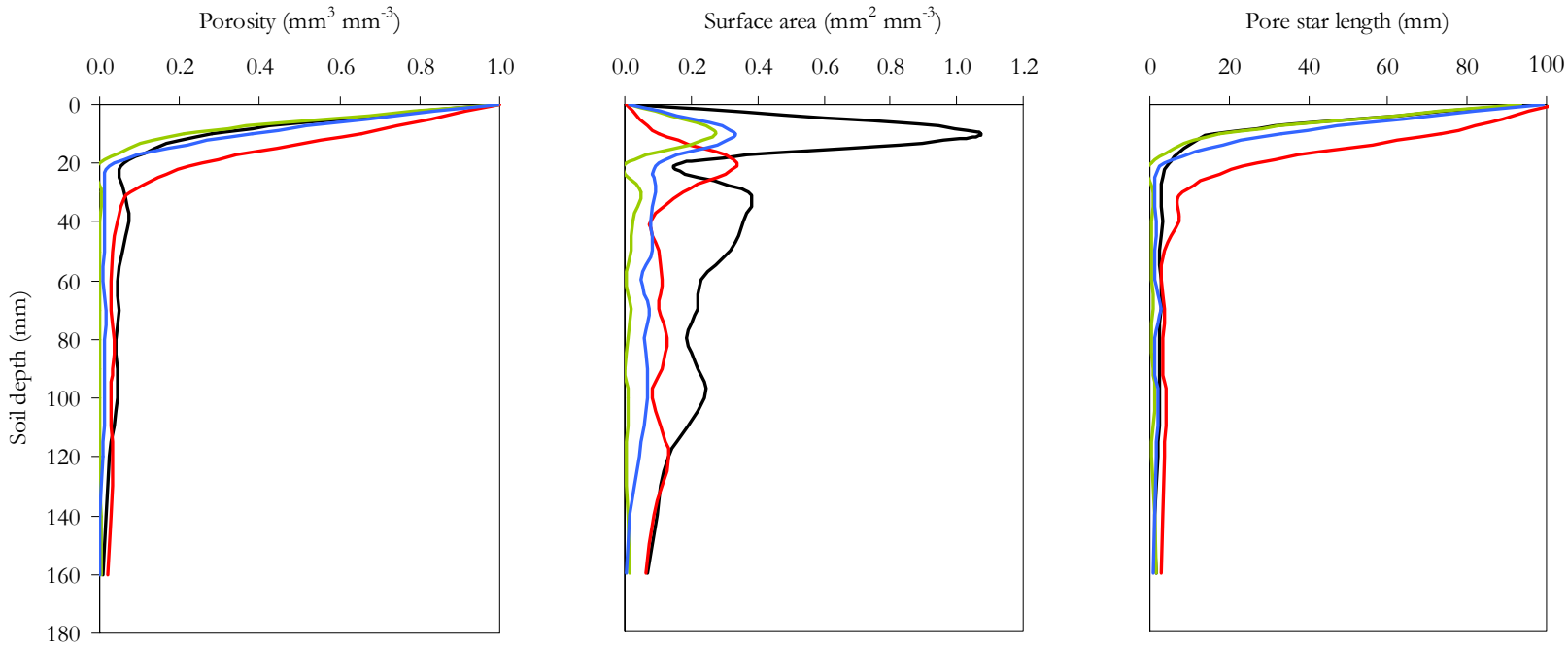

Figure 5.6 Response of selected structural parameters (*P, S_v and l_p^**) of soil H001 to four treatments; T401 (—), T402 (—), T403 (—) and T404 (—).

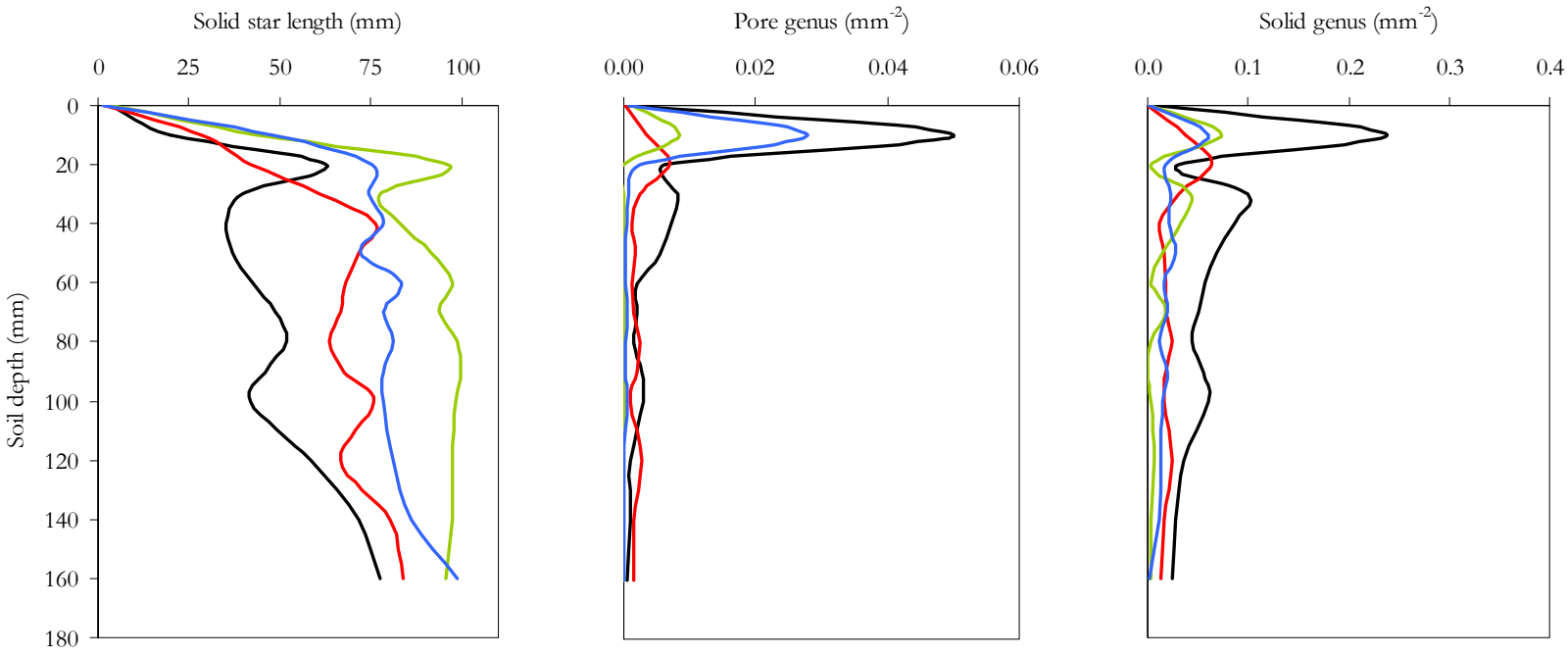

Figure 5.7 Response of selected structural parameters (l_s^*, g_p *and* g_s) of soil H001 to four treatments; T401 (—), T402 (—), T403 (—) and T404 (—).

5.4.1.2 Comparative effects of T401 and T102 solutions on structural form attributes

Differences between the structural parameters, with depth, of the T401 and T102 treatments are shown in appendix 5. The estimates of the S_v attribute for each soil treated using the T401 solution tend to be larger than the surface area estimates for the T102 treatment of soils, especially at depth. The soils irrigated with the T102 solution tend to have larger g_p and g_s, while the P and l_p^* values are generally the same. The l_s^* values for soils irrigated with T401 or T102 do not show any consistent trend.

5.4.1.3 Comparative effects of FW00*i* and T102 solutions on structural form attributes

Differences between the structural parameters, with depth, for the FW00*i* and T102 treatments are shown in appendix 5. Soils treated with the FW00*i* and T102 solutions tend to have similar estimates of P and l_p^*, and while estimates of connectivity (g_p and g_s) are dissimilar, they do not show a consistent trend. The S_v and l_s^* descriptors are consistently different where soils were irrigated using each of these solutions. Estimates of S_v tend to be less for soils irrigated with clean water (T102), while estimates of solid size (l_s^*) are generally smaller for soil columns treated using FW00*i* solutions than for soils that had been irrigated with T102. These trends in S_v and l_s^* values are not consistent for all soils. Two soils, B001 and H002, have larger S_v values and smaller l_s^* values after irrigation with T102.

The comparison of the B00*i* soils using the FW00*i* treatment shows that all these soils have similar P, l_p^* and g_p values. The B002 soil columns tend to have the smallest values of S_v and g_s and the largest values of l_s^*, while the S_v and g_s values of the B001 and B003 soils are similar at all depths.

5.4.2 Comparing the effect of water quality on selected structural parameters of each soil using three depth increments

To overcome the observed effect of depth on the structural form characteristics of these laboratory irrigated Vertosols, the six structural form attributes are compared for each soil at three individual depth increments; 0–40 mm, 50–90 mm and 100–160 mm. The determined mean values of the 50–90 mm depth of soils B001, B003, G00*i*, H00*i* and N00*i* are given in Tables 5.1–4. Tables that include all mean values for the 0–40 mm and 100–160 mm depths are given in appendix 52.

In the soil surface depth (0–40 mm) there tends to be very few significant differences between the structural characteristics, where the treatments are compared, and there is generally a large associated variation for each of the mean values. Similarly, there are few significant differences between the structural attributes of the 100–160 mm depth increment where the different irrigation treatments

have been applied to each Vertosol. This does not reflect a large variation in each mean; rather at this depth the different treatments of each Vertosol have very similar structural form attributes.

For the 50–90 mm depth, soil columns irrigated with the solutions of larger SAR_w (T403–4 solutions) tend to have smaller values of P, S_n, l_p^*, g_p and g_s, and larger values of l_s^*. However, irrigated soil columns from the G00*i* (Table 5.2) and N001 (Table 5.4) sites do not show this trend. These soils generally have larger values of P, S_n, l_p^*, g_p and g_s, and smaller values of l_s^* where columns have been treated using solutions of large SAR_w. However, significant differences between the treatments, for each of the measured attributes, are not evident for some of the soils. The B001 and B003 soils (Table 5.1), and the G001 and N001 soils do not show any significant differences between each of the structural attributes, where the T40*i* irrigation treatments of each soil are compared. The N002 soil only shows a significant increase in l_s^* values between the T402– and T404–treated soil columns.

The G002 soil and the H00*i* (Table 5.3) soils are the only Vertosols in this procedure to show a number of significant differences between the SAR_w treatments (T401→4). The G002 soil has significantly larger P, S_n, g_p and g_s values and significantly smaller l_s^* where solutions of large SAR_w have been used to irrigate columns, but the T401–4 treated columns of this soil contain ≤4 % P. In contrast, the H00*i* soils have significantly smaller P, S_n, g_p and g_s values and significantly larger l_s^* values for soil columns that have been treated using solutions of increasing SAR_w; T401 (SAR_w 0) (*e.g.* P_{H001}=0.05 mm^3 mm^{-3}), T402 (SAR_w 7.5) (*e.g.* P_{H001}=0.03 mm^3 mm^{-3}) or T403 (SAR_w 15) (*e.g.* P_{H001}=0.00 mm^3 mm^{-3}). However, where the H001 soil has been treated using T404, the structural form attributes (P, S_n, g_p, g_s and l_s^*) tend to be of intermediate value (*e.g.* P_{H001}=0.01 mm^3 mm^{-3}); these descriptors have values between those obtained for the T402 and T403 treated soil columns. The T404–treated H002 soil have values for these attributes (P, S_n, g_p, g_s and l_s^*) that are the same as values obtained for soil that has been treated with T401.

Comparisons of the FW00*i*, T102 and T401 treatments of each soil do not result in consistent trends. The G002 (Table 5.2) and N002 (Table 5.4) soils show no significant differences between the structural form attributes where each soil has been irrigated with FW00*i* and T102 or where soil columns have been irrigated using T102 and T401. The irrigation of the B001 and B003 soils (Table 5.1), and the G001 (Table 5.2) and N001 (Table 5.4) soils with the T102, FW00*i* and T401 solutions results in significantly different structural form attributes. Where the B001 soil has been irrigated using the T102 solution it has significantly larger values of P and S_n, and significantly smaller l_s^*, than where this soil has been treated using either FW00*i* or T401. The treatment of the B003 soil with T102 gives significantly smaller values of P, S_n, and g_p and g_s, and a significantly larger l_s^* where these attributes are compared with the structural form descriptors obtained for the FW00*i* treated columns. The G001 soil has a significantly larger estimate of pore size (l_p^*) where soil columns have

been treated with FW00*i* rather than T102, and significantly larger solid connectivity where columns are irrigated using T401 rather than T102. The FW00*i* treatment of the N001 soil results in a significantly larger S_v than the columns irrigated using T401, but for this soil there are no significant differences between the structural form attributes after soil columns are irrigated using either the T102 or T401 solutions. In contrast, the H00*i* soils (Table 5.3) exhibited an array of significant differences where columns of each soil have been irrigated using the T102, FW00*i* and T401 solutions. H001 has significantly larger values of P, S_v, and g_s when the T401 treatment was compared to the T102 solution and significantly smaller l_s^* for the T401 and FW00*i* treated soil columns. The H002 soil has significantly smaller values of P and S_v, and a significantly larger estimate of l_s^*, where the FW00*i*–treated soil is compared to the T102–treated soil. The T401–treated H002 soil has significantly greater g_p than that determined for the FW00*i* and T102–treated soil columns.

Table 5.1
Mean structural parameters derived using image analysis for soils B001 and B003 (50–90 mm) after laboratory irrigation

	FW00*i*			T102			T401			T402			T403		
				EC 0 dS m⁻¹			*EC 0.5 dS m⁻¹*								
				SAR 0 ((mmol(+) L⁻¹)^1/2)			*SAR 0 ((mmol(+) L⁻¹)^1/2)*			*SAR 7.5 ((mmol(+) L⁻¹)^1/2)*			*SAR 15 ((mmol(+) L⁻¹)^1/2)*		
Site B001															
P **(mm³ mm⁻³)**	0.06*b*	±	0.01	0.09*a*	±	0.01	0.04*bc*	±	0.01	0.03*bc*	±	0.00	0.02*c*	±	0.00
Sv **(mm² mm⁻³)**	0.26*b*	±	0.04	0.46*a*	±	0.05	0.25*b*	±	0.05	0.24*b*	±	0.03	0.11*b*	±	0.03
I_p^* **(mm)**	2.53	±	0.38	2.15	±	0.17	2.37	±	0.76	1.26	±	0.10	1.63	±	0.33
I_s^* **(mm)**	52.28*bc*	±	4.69	32.55*c*	±	5.24	58.07*ab*	±	7.11	60.80*ab*	±	4.07	77.93*a*	±	5.46
g_p **(×10⁻² mm²)**	0.33*ab*	±	0.09	0.41*ab*	±	0.08	0.24*ab*	±	0.06	0.42*a*	±	0.10	0.11*b*	±	0.04
gs **(×10⁻² mm²)**	5.16*ab*	±	0.68	8.85*a*	±	0.81	8.80a	±	2.19	7.01*ab*	±	0.97	2.94*b*	±	0.69
Site B003															
P **(mm³ mm⁻³)**	0.05*a*	±	0.00	0.02*b*	±	0.00	0.05*a*	±	0.00	0.04*a*	±	0.00	0.04*a*	±	0.00
Sv **(mm² mm⁻³)**	0.35*a*	±	0.03	0.16*b*	±	0.03	0.32*a*	±	0.03	0.26*ab*	±	0.03	0.30*a*	±	0.02
I_p^* **(mm)**	1.64	±	0.16	1.24	±	0.16	2.32	±	0.36	1.89	±	0.31	1.82	±	0.30
I_s^* **(mm)**	41.32*c*	±	2.69	67.46*a*	±	6.71	44.54*bc*	±	3.15	61.41*ab*	±	3.99	47.13*bc*	±	3.29
g_p **(×10⁻² mm²)**	0.32*a*	±	0.04	0.06*b*	±	0.02	0.45*a*	±	0.06	0.48*a*	±	0.08	0.31*a*	±	0.03
gs **(×10⁻² mm²)**	10.12*a*	±	1.06	3.93*c*	±	0.82	9.06*ab*	±	0.73	6.46*bc*	±	0.93	9.10*ab*	±	0.71

Within rows the letters represent significant difference between mean values for each treatment using the multiple comparison Tukey–Kramer test (P=0.05).

Table 5.2
Mean structural parameters derived using image analysis for soils G001 and G002 (50–90 mm) after laboratory irrigation

	FW00*i*			T102			T401			T402			T403			T404		
				EC 0 dS m⁻¹			*EC 0.5 dS m⁻¹*											
				SAR 0 ((mmol(+) L⁻¹)^1/2)			*SAR 0 ((mmol(+) L⁻¹)^1/2)*			*SAR 7.5 ((mmol(+) L⁻¹)^1/2)*			*SAR 15 ((mmol(+) L⁻¹)^1/2)*			*SAR 30 ((mmol(+) L⁻¹)^1/2)*		
Site G001																		
P **(mm³ mm⁻³)**	0.03*ab*	±	0.00	0.02*b*	±	0.00	0.03*ab*	±	0.00	0.03*ab*	±	0.00	0.03*ab*	±	0.00	0.04*a*	±	0.01
Sv **(mm² mm⁻³)**	0.13*ab*	±	0.02	0.09*b*	±	0.02	0.17*ab*	±	0.02	0.18*a*	±	0.01	0.12*ab*	±	0.01	0.16*ab*	±	0.03
l_p^* **(mm)**	3.69*a*	±	1.03	1.58*b*	±	0.14	2.05*ab*	±	0.24	2.14*ab*	±	0.26	2.69*ab*	±	0.24	2.25*ab*	±	0.21
l_s^* **(mm)**	61.21*ab*	±	4.96	70.15*a*	±	6.61	54.32*ab*	±	3.95	49.87*b*	±	0.80	66.95*ab*	±	3.20	57.01*ab*	±	5.43
g_p **(×10⁻² mm²)**	0.10	±	0.03	0.08	±	0.03	0.16	±	0.04	0.15	±	0.04	0.07	±	0.01	0.21	±	0.09
gs **(×10⁻² mm²)**	2.83*ab*	±	0.66	1.95*b*	±	0.42	4.11*a*	±	0.46	4.27*a*	±	0.45	2.72*ab*	±	0.29	3.20*ab*	±	0.43
Site G002																		
P **(mm³ mm⁻³)**	0.02*bc*	±	0.00	0.02*bc*	±	0.00	0.01*c*	±	0.00	0.01*bc*	±	0.00	0.02*ab*	±	0.01	0.04*a*	±	0.01
Sv **(mm² mm⁻³)**	0.12*bc*	±	0.03	0.12*bc*	±	0.02	0.05*c*	±	0.01	0.11*bc*	±	0.02	0.20*ab*	±	0.04	0.27*a*	±	0.03
l_p^* **(mm)**	1.51	±	0.18	1.10	±	0.20	1.28	±	0.18	1.15	±	0.12	0.99	±	0.07	1.36	±	0.14
l_s^* **(mm)**	78.71*ab*	±	4.72	71.77*ab*	±	4.63	90.43*a*	±	1.48	69.36*b*	±	4.59	60.78*bc*	±	7.32	42.95*c*	±	3.58
g_p **(×10⁻² mm²)**	0.11*ab*	±	0.04	0.06*b*	±	0.01	0.03*b*	±	0.01	0.07*b*	±	0.01	0.18*ab*	±	0.08	0.24*a*	±	0.04
gs **(×10⁻² mm²)**	3.55*bc*	±	1.00	3.90*abc*	±	0.81	1.46*c*	±	0.26	3.88*abc*	±	0.67	5.98*ab*	±	1.08	7.20*a*	±	0.75

Within rows the letters represent significant difference between mean values for each treatment using the multiple comparison Tukey–Kramer test (P=0.05).

Table 5.3
Mean structural parameters derived using image analysis for soils H001 and H002 (50–90 mm) after laboratory irrigation

	FW00*i*	T102	T401	T402	T403	T404
		EC 0 dS m⁻¹	*EC 0.5 dS m⁻¹*			
		SAR 0 ((mmol(+) L⁻¹)^1/2)	*SAR 0 ((mmol(+) L⁻¹)^1/2)*	*SAR 7.5 ((mmol(+) L⁻¹)^1/2)*	*SAR 15 ((mmol(+) L⁻¹)^1/2)*	*SAR 30 ((mmol(+) L⁻¹)^1/2)*
Site H001						
P **(mm³ mm⁻³)**	0.03*ab* ± 0.01	0.02*bc* ± 0.00	0.05*a* ± 0.00	0.03*ab* ± 0.00	0.00*d* ± 0.00	0.01*cd* ± 0.00
Sv **(mm² mm⁻³)**	0.17*ab* ± 0.03	0.09*bcd* ± 0.02	0.23*a* ± 0.04	0.11*bc* ± 0.02	0.01*d* ± 0.00	0.07*cd* ± 0.01
l_p^* **(mm)**	1.72*bc* ± 0.20	1.82*bc* ± 0.26	2.56*ab* ± 0.17	3.41*a* ± 0.17	0.52*d* ± 0.11	1.53*c* ± 0.35
l_s^* **(mm)**	53.17*cd* ± 4.43	73.77*b* ± 6.07	45.20*d* ± 3.38	67.54*bc* ± 5.33	96.19*a* ± 1.89	78.75*ab* ± 4.53
g_P **(×10⁻² mm²)**	0.18*ab* ± 0.04	0.08*ab* ± 0.03	0.27*a* ± 0.09	0.18*ab* ± 0.04	0.00*b* ± 0.00	0.03*b* ± 0.01
gs **(×10⁻² mm²)**	3.55*ab* ± 0.66	2.04*bc* ± 0.54	5.50*a* ± 0.94	1.88*bc* ± 0.34	0.82*c* ± 0.42	1.89*b* ± 0.41
Site H002						
P **(mm³ mm⁻³)**	0.01*c* ± 0.00	0.03*ab* ± 0.00	0.04*a* ± 0.00	0.01*c* ± 0.00	0.02*bc* ± 0.00	0.05*a* ± 0.01
Sv **(mm² mm⁻³)**	0.06*c* ± 0.02	0.17*ab* ± 0.03	0.24*a* ± 0.03	0.04*c* ± 0.01	0.09*bc* ± 0.01	0.24*a* ± 0.02
l_p^* **(mm)**	1.06*b* ± 0.10	1.72*ab* ± 0.34	1.85*ab* ± 0.16	1.89*ab* ± 0.26	1.52*ab* ± 0.16	2.18*a* ± 0.26
l_s^* **(mm)**	83.76*ab* ± 5.52	51.42*c* ± 5.45	52.98*c* ± 6.83	91.26*a* ± 2.41	65.70*bc* ± 5.05	44.65*c* ± 4.45
g_P **(×10⁻² mm²)**	0.05*b* ± 0.02	0.12*b* ± 0.03	0.39*a* ± 0.04	0.04*b* ± 0.01	0.06*b* ± 0.01	0.38*a* ± 0.07
gs **(×10⁻² mm²)**	1.83*bc* ± 0.63	3.72*ab* ± 0.72	5.21*a* ± 0.88	0.87*c* ± 0.17	2.26*bc* ± 0.36	5.42*a* ± 0.50

Within rows the letters represent significant difference between mean values for each treatment using the multiple comparison Tukey–Kramer test (P=0.05).

Table 5.4
Mean structural parameters derived using image analysis for soils N001 and N002 (50–90 mm) after laboratory irrigation

	FW00*i*			T102			T401			T402			T403			T404		
				EC 0 dS m⁻¹			*EC 0.5 dS m⁻¹*											
				SAR 0 ((mmol(+) L⁻¹)^1/2)			*SAR 0 ((mmol(+) L⁻¹)^1/2)*			*SAR 7.5 ((mmol(+) L⁻¹)^1/2)*			*SAR 15 ((mmol(+) L⁻¹)^1/2)*			*SAR 30 ((mmol(+) L⁻¹)^1/2)*		
Site N001																		
P **(mm³ mm⁻³)**	0.08*a*	±	0.02	0.05*ab*	±	0.01	0.04*b*	±	0.01	0.04*ab*	±	0.01	0.05*ab*	±	0.01	0.04*b*	±	0.01
Sv **(mm² mm⁻³)**	0.40*a*	±	0.07	0.23*b*	±	0.02	0.21*b*	±	0.03	0.20*b*	±	0.05	0.28*ab*	±	0.03	0.24*ab*	±	0.04
l_p^* **(mm)**	2.12*ab*	±	0.20	2.61*a*	±	0.31	1.92*ab*	±	0.27	2.20*ab*	±	0.24	1.65*b*	±	0.16	1.43*b*	±	0.15
l_s^* **(mm)**	36.61*b*	±	7.01	48.63*ab*	±	3.81	47.62*ab*	±	4.88	60.01*a*	±	5.50	39.16*ab*	±	4.48	43.67*ab*	±	4.50
g_p **(×10⁻² mm²)**	0.55*a*	±	0.14	0.25*ab*	±	0.04	0.17*b*	±	0.04	0.27*ab*	±	0.09	0.28*ab*	±	0.04	0.19*b*	±	0.04
gs **(×10⁻² mm²)**	8.56*a*	±	1.29	5.47*ab*	±	0.39	5.98*ab*	±	0.75	4.34*b*	±	1.12	7.70*ab*	±	0.84	7.15*ab*	±	1.18
Site N002																		
P **(mm³ mm⁻³)**	0.03	±	0.01	0.02	±	0.00	0.03	±	0.01	0.03	±	0.01	0.02	±	0.00	0.03	±	0.01
Sv **(mm² mm⁻³)**	0.11	±	0.02	0.09	±	0.02	0.13	±	0.02	0.16	±	0.02	0.09	±	0.02	0.10	±	0.02
l_p^* **(mm)**	2.91	±	0.64	1.96	±	0.33	2.12	±	0.22	2.09	±	0.32	2.14	±	0.35	3.14	±	0.50
l_s^* **(mm)**	66.81*ab*	±	5.75	76.27*a*	±	5.56	65.42*ab*	±	4.98	52.46*b*	±	4.01	73.34*ab*	±	4.31	74.44*a*	±	5.36
g_p **(×10⁻² mm²)**	0.19	±	0.06	0.08	±	0.03	0.21	±	0.07	0.20	±	0.04	0.10	±	0.03	0.17	±	0.05
gs **(×10⁻² mm²)**	2.31*ab*	±	0.54	2.06*b*	±	0.42	2.95*ab*	±	0.47	3.95*a*	±	0.44	1.86*b*	±	0.31	1.77*b*	±	0.37

Within rows the letters represent significant difference between mean values for each treatment using the multiple comparison Tukey–Kramer test (P=0.05).

Table 5.5
Mean structural parameters comparing the effects of treatment solution (T102 and T402) on the soils B001, B003, G00*i*, H00*i* and N00*i*

	B001	B003	G001	G002	H001	H002	N001	N002
				Solution T102				
P (mm^3 mm^{-3})	0.09*a*	0.02*bc*	0.02*c*	0.02*c*	0.02*c*	0.03*bc*	0.05*b*	0.02*c*
S_V (mm^2 mm^{-3})	0.46*a*	0.16*bc*	0.09*c*	0.12*bc*	0.09*c*	0.17*bc*	0.23*b*	0.09*c*
l_p^* (mm)	2.15*ab*	1.24*b*	1.58*ab*	1.10*b*	1.82*ab*	1.72*ab*	2.61*a*	1.96*ab*
l_s^* (mm)	32.55*d*	67.46*abc*	70.15*abc*	71.77*abc*	73.77*ab*	51.42*bcd*	48.63*cd*	76.27*a*
g_P (×10^{-2} mm^2)	0.41*a*	0.06*c*	0.08*bc*	0.06*c*	0.08*bc*	0.12*bc*	0.25*ab*	0.08*bc*
g_S (×10^{-2} mm^2)	8.85*a*	3.93*bc*	1.95*c*	3.90*bc*	2.04*c*	3.72*bc*	5.47*b*	2.06*c*
				Solution T402				
P (mm^3 mm^{-3})	0.03*abc*	0.04*a*	0.03*abc*	0.01*bc*	0.03*abc*	0.01*c*	0.04*a*	0.03*ab*
S_V (mm^2 mm^{-3})	0.24*a*	0.26*a*	0.18*ab*	0.11*bc*	0.11*bc*	0.04*c*	0.20*ab*	0.16*ab*
l_p^* (mm)	1.26*bc*	1.89*bc*	2.14*bc*	1.15*c*	3.41*a*	1.89*bc*	2.20*b*	2.09*bc*
l_s^* (mm)	60.80*bc*	61.41*bc*	49.87*c*	69.36*b*	67.54*bc*	91.26*a*	60.01*bc*	52.46*bc*
g_P (×10^{-2} mm^2)	0.42*ab*	0.48*a*	0.15*c*	0.07*c*	0.18*bc*	0.04*c*	0.27*abc*	0.20*bc*
g_S (×10^{-2} mm^2)	7.01*a*	6.46*a*	4.27*ab*	3.88*abc*	1.88*bc*	0.87*c*	4.34*ab*	3.95*abc*

Within rows the letters represent significant difference between mean values for each soil using the multiple comparison Tukey–Kramer test (P=0.05).

5.4.3 Comparing the structural form attributes of the nine Vertosols

The B001, B003, G00*i*, H00*i* and N00*i* soils are compared using the structural form attributes determined for the 50–90 mm depth of the T102 and T402 irrigation treatments (Table 5.5). These eight Vertosols have significantly different structural form attributes and show several significant differences between soils from the same sampling region *i.e.* Bourke, the lower Gwydir, Hillston or the lower Namoi.

The T102 treatment results in significantly different structural form attributes between the B001 and B003 soils and between the N00*i* soils, but not between the G00*i* soils or the H00*i* soils. After being irrigated with T102, the B001 and N001 soils have significantly larger values of P (0.09 and 0.05 $mm^3\ mm^{-3}$), S_v (0.46 and 0.23 $mm^2\ mm^{-3}$), g_p (0.41 and 0.25 $\times 10^{-2}\ mm^2$) and g_s (8.85 and 5.47 $\times 10^{-2}\ mm^2$), and significantly smaller values of l_s^* (32.55 and 48.35 mm) than the B003 and N002 soils, respectively (P=0.02 $mm^3\ mm^{-3}$, S_v=0.16 and 0.09 $mm^2\ mm^{-3}$, g_p=0.06 and 0.08 $\times 10^{-2}\ mm^2$, g_s=3.93 and 2.06 $\times 10^{-2}\ mm^2$ and l_s^* =67.46 and 76.27 mm).

The T402 treatment results in fewer significant differences between the soils than the T102 treatment. The structural attributes of the B001 and B003 soils and the N00*i* soils are not significantly different, while the l_p^* and l_s^* attributes give the only significant differences between the G00*i* soils and between the H00*i* soils respectively, whereas the G001 and H001 soils have larger estimates of pore size (2.14 and 3.41 mm) and smaller estimates of solid size (49.87 and 67.54 mm) than the G002 and H002 soils (l_p^*=1.15 and 1.89 mm, and l_s^*=69.36 and 91.26 mm).

The three B00*i* soils are compared using the FW00*i* irrigation treatment (Table 5.6). For these soils the only significant difference is in values of g_s, where the solid phase of the B001 is significantly less connected than the solid phase of either the B002 or the B003 soils.

Table 5.6
Comparing the different structural parameters for the three B00*i* soils after irrigation using the field water treatment (FW001)

	B001	B002	B003
P ($mm^3\ mm^{-3}$)	0.06	0.07	0.05
S_v ($mm^2\ mm^{-3}$)	0.26	0.38	0.35
l_p^* (mm)	2.53	2.22	1.64
l_s^* (mm)	52.28	39.31	41.32
g_p ($\times 10^{-2}\ mm^2$)	0.33	0.46	0.32
g_s ($\times 10^{-2}\ mm^2$)	5.16*b*	9.01*a*	10.12*a*

Within rows the letters represent significant difference between mean values for each soil using the multiple comparison Tukey–Kramer test (P=0.05).

The comparisons between the T102 and T402 treatments of the B001, B002, G00*i*, H00*i* and N00*i* soils, and the FW001 treatment of the B00*i* soils are used to rank the nine Vertosols according to the structural form characteristics. These soils are ranked based on increasingly large values of P, S_n, l_p^* and g_p, and smaller values of l_s^*. Larger values of P, S_n, l_p^* and g_p, and smaller values of l_s^* represent increasingly desirable soil structural form (*e.g.* Pillai and McGarry 1999). Consequently, these soils have increasingly desirable structural form attributes in the order:

$$H002<G002<H001<N002\approx G001\approx B003\approx B002<N001<B001$$

5.4.4 Determining the effect of water quality on pore sieve distributions

The pore sieve distributions (50–90 mm depth) for irrigation treatments of the G001 and H001 soils are presented in Figures 5.8 and 5.9. The distributions (50–90 mm depth) for irrigation treatments of the B00*i*, G002, H002 and N00*i* soils are given in appendix 5.3.

The nine soils tend to have two pore sieve size ranges that are important where the irrigation treatments are compared. These two size ranges included all effective pore sieve sizes between 0.1–0.5 mm and between 1.0–2.0 mm. In general, soil columns treated with the T401 solution contain a greater volume of macropores of 0.1–0.5 mm and of 1.0–2.0 mm than soils treated with solution T102. Likewise, soils treated with FW00*i* have a greater proportion of macropore space present in the larger pore sieve classes than soil treated with T102. The SAR_w treatments show that soil treated with T402 has a greater proportion of larger pores than soil treated with T401. However, soil treated with solutions of largest SAR_w (T403 or T404) tend to have greater contributions of larger pore sieve sizes and less larger pores than soil irrigated with the small SAR_w solutions (T401 or T402).

The distributions of pore sieve classes for the B00*i*, G00*i*, H002 and N00*i* soils do not show large differences between the different treatments. Unlike these soils, the illitic H001 soil (Figure 5.9) shows large differences between contributing sieve classes for the different SAR_w treatments that have been applied. For this soil, only the T401 and T402 treatments show large contributions of pore sieve sizes 1.0–2.0 mm, but where this soil has been treated using T403 or T404, the pore sieve distribution is dominated by sieve sizes of 0.1–0.5 mm. In addition, the T403–treated soil has a sieve distribution containing no effective porosity in the 1.0–2.0 mm sieve range.

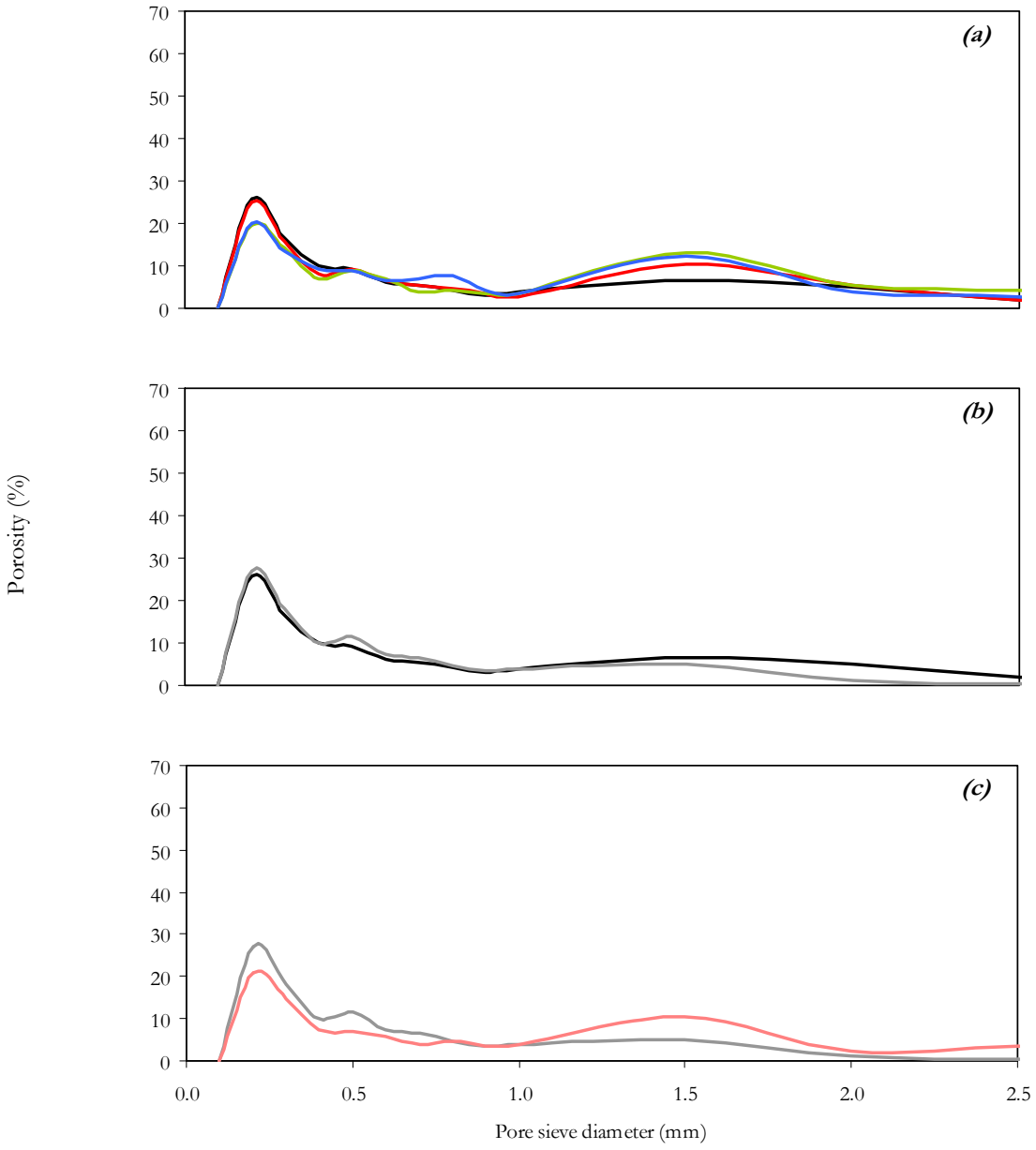

Figure 5.8 The distribution of the pore sieve diameter (s_p) for the 50–90 mm depth of the G001 soil. Comparisons are made between the irrigation treatments; *(a)*, for solutions of increasing SAR_w [T401 (—), T402 (—), T403 (—) and T404 (—)], *(b)*, for salinity treatments [T102 (—) and T401] and, *(c)*, for field water and clean water [FW00*i* (—) and T102 (—)].

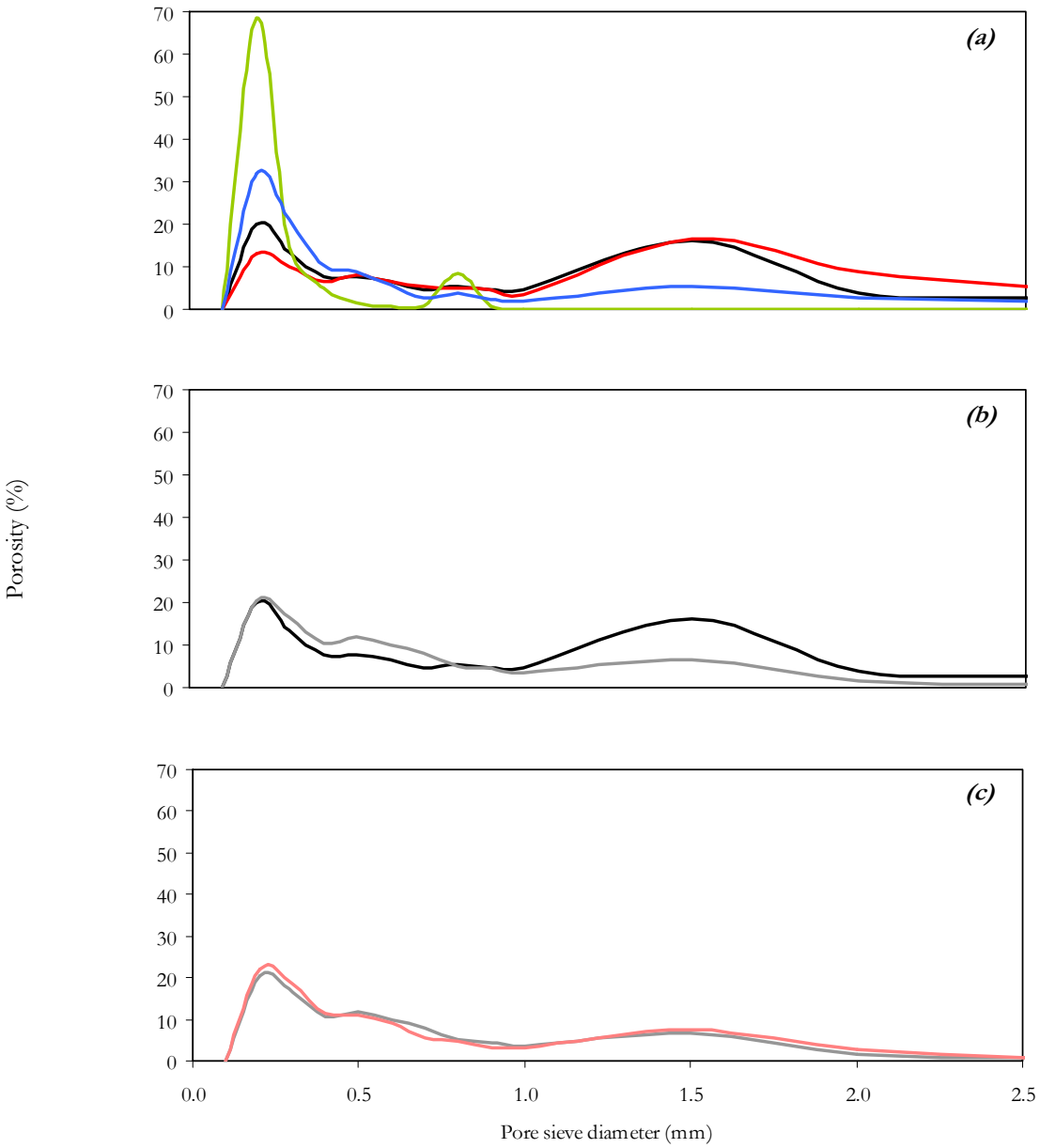

Figure 5.9 The distribution of the pore sieve diameter (s_p) for the 50–90 mm depth of the H001 soil. Comparisons are made between the irrigation treatments; *(a)*, for solutions of increasing SAR_w [T401 (—), T402 (—), T403 (—) and T404 (—)], *(b)*, for salinity treatments [T102 (—) and T401] and, *(c)*, for field water and clean water [FW00*i* (—) and T102 (—)].

5.4.5 Determining the effect of water quality on pore star–shape distributions

The pore star–shape distributions (50–90 mm depth) are presented for the G001 and H001 soils in Figures 5.10 and 5.11. The pore star–shape distributions (50–90 mm depth) for each of the remaining soils are given in appendix 5.4. The distributions of pore star–shape do not tend to show any dominance of pores with either spheroid shapes or long–thin shapes for any of the treatments of the nine Vertosols. However, the centre of each distribution tends to have a mid point at approximately 0.6, indicating that all nine Vertosols tend to contain pore shapes that are more cubic/spheroid than elongated, irrespective of applied irrigation treatments.

One of the nine soils tends to show large differences in the pore star shape distributions of the SAR_w treatments (T401–4). The H001 soil has a large increase in the proportion of rounded pore shapes where solutions of larger SAR_w are applied (T401→3). The B001, B003, H002 and N001 soils also tend to show trends of increasingly rounded pore shapes, where each is irrigated with solutions of increasingly large SAR_w (T401–4), but these trends are much less apparent for these soils than for the H001 soil. The G00*i* and N002 soils generally have star–shape distributions that indicated more long–thin pore star shapes where soils have been irrigated with solutions of larger SAR_w (T401→4), but like the B001, B003, H002 and N001 soils, there are no large differences between the distributions for these treated soils (G00*i* and N002).

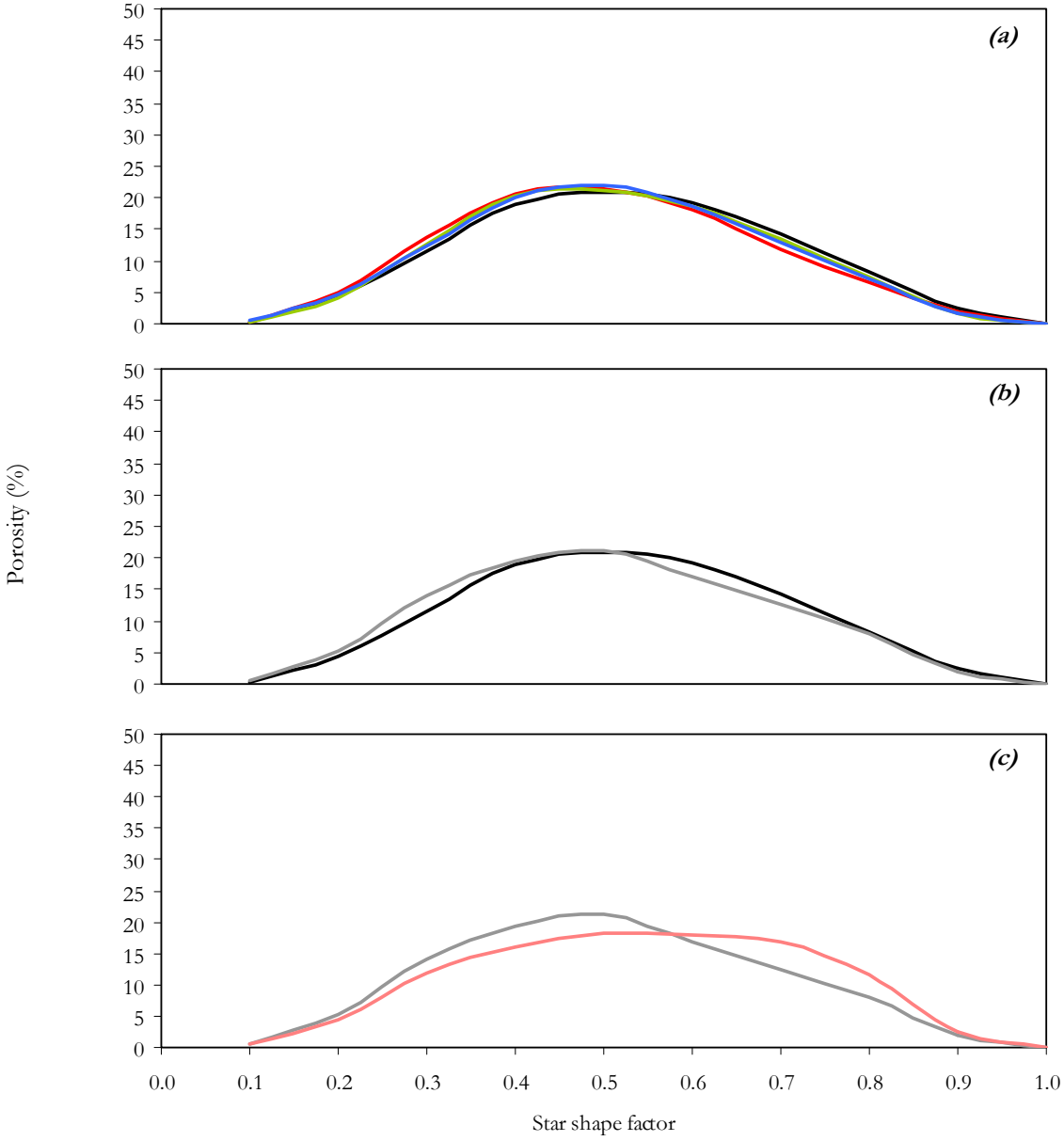

Figure 5.10 The distribution of the pore star shape (Ra_p^*) for the 50–90 mm depth of the G001 soil. Comparisons are made between the irrigation treatments; *(a)*, for solutions of increasing SAR_w [T401 (—), T402 (—), T403 (—) and T404 (—)], *(b)*, for salinity treatments [T102 (—) and T401] and, *(c)*, for field water and clean water [FW00*i* (—) and T102 (—)].

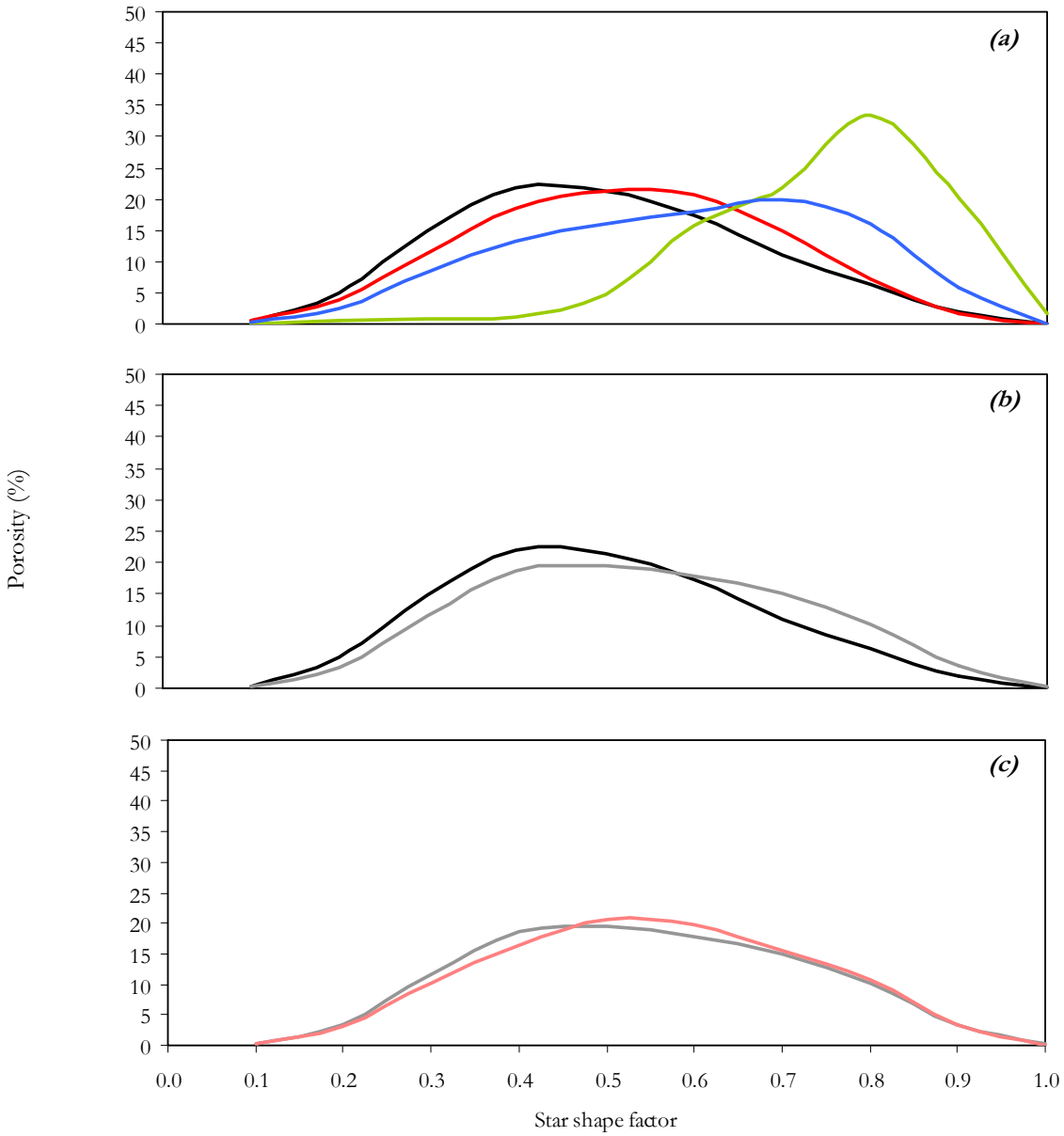

Figure 5.11 The distribution of the pore star shape (Ra_p^*) for the 50–90 mm depth of the H001 soil. Comparisons are made between the irrigation treatments; *(a)*, for solutions of increasing SAR_w [T401 (—), T402 (—), T403 (—) and T404 (—)], *(b)*, for salinity treatments [T102 (—) and T401] and, *(c)*, for field water and clean water [FW00*i* (—) and T102 (—)].

Similarly, where the FW00*i* and T102 treatments and the T102 and T401 treatments are compared, broad trends are observed for each of the soils. The B001, B003, G001 and N00*i* soils all contain more rounded pore star–shapes where they have been treated using the T401 or FW00*i* solutions rather than the T102 solution. The G002 and H001 soils show the same trend between treatments of FW00*i* and T102, but the opposite trend between the T401 and T102 treatments. Treating the H002 soil with the T401 solution, rather than with the T102 solution, results in a larger proportion

of the long, thin pore shapes. Irrigating this H002 soil using the T102 solution, rather than the FW00*i* solution, results in a larger proportion of the long thin, pore star–shapes.

5.5 Discussion

Soils that have large estimates of porosity, surface area and phase connectivity, and which have small size estimates of solid phase components can be regarded as possessing desirable structural attributes. Consequently, desirable soil structural form will consist of a large proportion of small aggregates surrounded by many small, well–connected macropores. This structural arrangement will encourage the flow of water, the diffusion of air and be most suitable for plant root growth (Ringrose–Voase 1996). Any processes that contribute to a decrease in the values of soil macroporosity, surface area and connectivity, and an increase in estimates of aggregate size are detrimental to soil structural form and will be problematic for cotton production.

5.5.1 The impact of irrigation water quality on the different Vertosols

The changes in structural form attributes with increased depth were assessed to compare the treatment solutions used to irrigate each of the nine Vertosols. There were few consistent differences in soil structural form attributes that were attributable to the irrigation solutions, so the mean values of structural form attributes for all images between certain depths were compared. The 0–40 mm and the 100–160 mm layers did not show large irrigation treatment effects for each of the Vertosols. In the uppermost layer (0–40 mm), this reflected the transient features of the surface soil (Moran and McBratney 1992) rather than the impacts of various water quality treatments. In the lowest layer (100–160 mm), the different water treatments resulted in only small differences in structural form attributes and reflected the position of this layer in each of the soil columns. The larger moisture content of this layer (appendix 4) meant more extensive swelling than in the upper layers, and consequently, differences in structural form attributes were less readily identified. Furthermore, it was evident from the soil chemical properties of each irrigation treatment of the soils (chapter 4), that there did not tend to be large differences in the Na^+ content at soil depths greater than 100 mm.

The impact of the different solution treatments on the structural form of these soils was most apparent in the 50–90 mm depth soil layer. The irrigation of each soil with the FW00*i* or clean water (T102) solutions did not consistently yield significant differences in the estimated structural form attributes of this surface layer. This was partly due to the different EC_w and SAR_w attributes of each

FW00*i* solution (Table 3.1). For example, some FW00*i* solutions contained larger solute concentrations and/or larger Na^+ contents (*i.e.* FW001 and FW006) than others (*i.e.* FW002). However, it was clear from the B001 and B003 soils that the different FW00*i* solutions applied were not the only cause of the observed structural form attributes. Where these two Bourke soils were treated with the FW001 solution (EC_w=0.98, SAR_w=4.69), they exhibited similar structural form attributes (Table 5.6), but a comparison of the FW001 and T102 treatments for the B001 and B003 soils resulted in different trends. The B001 soil had more desirable structural form attributes after having been treated using the T102 solution, than where this soil had been treated using FW001. In contrast, the B003 soil had more desirable structural form attributes after treatment using FW001 rather than where it had been treated with T102. Like the FW001 comparison of the three B00*i* soils, the impacts of FW001 or T102 on the structural form attributes of B001 and B003 reflected the different initial soil ESPs and electrical conductivities (ESPs of 8.1 and 3.6 and ECs of 0.37 and 0.14, respectively). In these cases, larger solute concentrations suppressed clay expansion and larger soil Na^+ contents increase the extent of clay swelling.

Comparing the Vertosols that had been irrigated using the T102 solution or the T401 solution did not tend to show significantly different structural form attributes. However, treating each soil using the T401 solution rather than the T102 solution broadly suggested that the former of these solutions led to more desirable structural form attributes. This supported the consideration that the SAR_w and EC_w of each field water solution influenced the extent of expression of the different structural form attributes, rather than other solution properties (*e.g.* anion contributions). In addition, comparison between the FW00*i*–T102 treatments or T102–T401 treatments of the Vertosols showed that irrigation with clean water tended to influence the expression of structural form attributes in these soils differently to the other solutions. The irrigation of the G00*i*, H00*i* and N00*i* soils using each treatment solution reduced the soil solution EC, but using T102 (EC_w 0, SAR_w 0) resulted in ECs that were marginally lower (0.01–0.02 dS m^{-1} less) than those of the FW00*i*– and T401–treated soils (chapter 4.3.2.2). The soil electrical conductivity influences the extent of swelling of 2:1 expanding lattice phyllosilicates; increasing the solute concentration, even by very small amounts, may suppress double layer expansion, and swelling will be determined by the contributions of different cations to solution and soil ESP. Consequently, applying solution T401 (EC_w 0.47, SAR_w 0) tended to result in a 'better' structured soil according to P, S_r, l_s^*, g_p and g_s, while the application of T102 tended to result in structural form descriptors that were comparable to the T402 or T403 treatments of each soil.

The irrigation of the Vertosols with the SAR_w solutions (T401–3) resulted in some clear trends in the structural form descriptors. The G002 soil had more desirable structural attributes for

treatments of larger SAR_w *i.e.* small increases in the values of porosity and surface area, increases in estimates of connectivity and smaller size estimates of the solid phase. However, the T401–3 treated G002 soil columns all had less than 2 % macroporosity. The significant differences in the other structural attributes reflect difference in the distribution of this pore space. Similarly, the T401–3 treated G001 and N00*i* soils all contained 3 % porosity and generally had no differences between estimates of surface area and connectivity, but had an increased estimate of soil ped size for the larger SAR_w treatments. These four soils (G00*i* and N00*i*) were dominated by 2:1 expanding lattice clays in the coarse and fine clay fractions (Tables 2.16 and 2.17). The B00*i* and H002 soils contained less coarse 2:1 expanding lattice clays than the G00*i* and N00*i* soils, while the H001 soil was dominated by illite clay in both size fractions (Tables 2.16 and 2.17). The structural form descriptors of these B00*i* and H00*i* soils showed less porosity, surface area and connectivity, and increased estimates of size for the solid phase where solutions of larger SAR_w had been applied. Of these soils, the H00*i* soils (particularly H001) tended to contain macropore attributes that were most affected by the SAR_w of the applied irrigation solutions.

Irrespective of the soil investigated, the T404 treatment of each Vertosol tended to result in structural form attributes that were similar to the structural form attributes of the T403–treated soil. This was despite the much larger SAR_w of the T404 treatment solution. Soils treated with T404 tended to have greater quantities of ponded surface water post–irrigation. This is because of increased slaking, swelling and dispersion in these soils brought about by the disruptive potential of solution applications and by the impact of large increases in Na^+ at the soil surface. Consequently, very little irrigation solution drained through T404–treated soil columns, and as a result this solution did not impact on soil chemical properties or structural form attributes to the same extent as the other T40*i* treatments.

5.5.2 The pore sieve and star–shape distributions

The pore sieve and pore star–shape distributions provided two pieces of important information. They demonstrated the key pore sizes that were influenced by the quality (EC_w and SAR_w) of applied irrigation water and they highlighted the dominance of more rounded pore shapes relative to the long, thin crack–shaped pores. The pore sieve distributions tended to show two sieve classes that contain most pore volume in the presented range, and which tended to show the largest differences between the treatments. These were pore sieve sizes of 0.1–0.5 mm and 1.0–2.0 mm; very fine macropores are less than 1.0 mm in size and fine macropores are 1.0–2.0 mm in size (Brewer 1964). In general, the soils treated with the FW00*i* and T401 solutions contained more fine macropore space (1.0–2.0 mm sieve sizes), while the T102 treated soils had a larger proportion of very fine

macropore space (0.1–0.5 mm sieve sizes). This was not a consistent trend, and several soils (G001, G002 and H001) that had been treated with FW00*i* or T401 had a larger proportion of very fine macropores (0.1–0.5 mm sieve sizes) than when they had been treated using the T102 solution. The T401–4 treatments of each soil were different. Unlike the structural form attributes previously described (porosity, surface area, size estimates and connectivity), which tended to show a consistent trend of either increasing or decreasing with increasing SAR_w, the pore sieve range tended to show the greatest proportion of fine macropores (1.0–2.0 mm) occurring where each Vertosol had been treated using T402. Then, the T402–4 treatments of each soil generally showed decreases in the contributions of fine macropores as larger SAR_w solutions were applied. This observation was most apparent for the sieve distributions of the G00*i* and N00*i* soils. This implicated the importance of some small quantities of Na^+ in maintaining desirable pore size, particularly in soils with larger contributions of 2:1 expanding lattice clays.

The pore star–shape distributions of each Vertosol were largely unaffected by the application of the different irrigation solutions. This is, in part, a reflection of the number of irrigation treatments and of the moisture content at the time of sampling (appendix 4.3). For example, the number of irrigation events was insufficient to cause a large change in the SAR and exchangeable cation contributions of these soils. Alternatively, the moisture content at the time soil columns were filled with fluorescent resin will influence the extent of structural form expression. The development of surface cracks in an irrigated Vertosol was measured by Ringrose–Voase and Sanidad (1996). However, currently there has been insufficient research in this area to characterise the formation of structural form attributes as different soils dry. At the moisture content of these Vertosols the star–shape factor indicated small trends in the distributions that indicated increasingly long, thin pores or more rounded pores reflecting differences between the shrinkage of soil and the different cracking patterns that are evident for the applied water quality treatments. For example the B00*i*, H00*i* and N001 soils showed a trend toward increasingly rounded pore shapes, while the G00*i* and N002 soils showed a trend toward long, thin pore shapes as the SAR_w of solution was increased. These observations showed a small association with the proportions of 2:1 expanding lattice phyllosilicate clays. Only one of the Vertosols had a large trend in pore star–shape distributions that indicated changing cracking patterns where water of larger SAR_w was applied. Unlike the other soils, the H001 soil was dominated by illite clay. This soil showed a significant increase in the contribution of rounded pores as the SAR_w of treatment increased.

5.5.3 Structural form and the impact of soil physico–chemical properties

For each Vertosol, the impact of irrigation treatment solution on the structural form descriptors tended to correspond to differences in the fundamental soil properties. The extent of differences between structural form attributes for these soils reflected the proportions of fine and coarse clay phyllosilicate minerals in the different soils and the different cation exchange capacities. In the fine clay fraction the B00*i*, G00*i*, H002 and N001 soils contained more than 70 % smectite, while the N002 soil had approximately 60 % smectite. The H001 soil had no detected smectite in this size fraction. The coarse clay fractions of the B00*i* and H00*i* soils contained larger contributions of kaolinite and illite, while the G00*i* and N00*i* soils had coarse fractions with approximately 50–60 % 2:1 expanding lattice clays (smectite and vermiculite). Unlike the stability of these Vertosols (chapter 3), the soils with more 2:1 expanding lattice phyllosilicates and larger CEC_{eff} values tended to have structural form attributes that showed less difference, where the treatments were compared. This potentially reflects the greater ability of these soils to resile structural form after a disruption is introduced (*e.g.* increased soil Na^+ content) through shrink–swell processes. In contrast, the soils with a smaller content of 2:1 expanding lattice phyllosilicates and lower CEC_{eff} values have a smaller capacity to shrink–swell and are less resilient. These soils tend to show different structural form attributes for the different treatment solutions applied.

The G00*i* and N00*i* soils did not show any association between the structural form attributes after each treatment and their chemical properties, either prior to irrigation (Table 3.3) or where irrigated soil columns (chapter 4) had been assessed for changes in soil chemical properties. These four soils (G00*i* and N00*i*) tended to have exchangeable cation contributions that were significantly more affected by irrigation treatments (chapter 4) than the B00*i* or H00*i* soils. In addition, the G00*i* and N00*i* soils had larger moisture contents at the time columns were filled with fluorescent resin. Consequently, the structural form exhibited in these soils may reflect both the increased moisture content of these soils and the distributions of cations, and consequently increased swelling. It is probable that this relates to differences in the adsorption of exchangeable Na^+ at the exchange interface (*e.g.* Quirk 1994). The soils with larger 2:1 expanding lattice phyllosilicates (G00*i* and N00*i*) and with a larger charge (*e.g.* CEC_{eff}) have a greater ability to exchange at the outer face of clay domains with very little Na^+ moving to the charged surfaces of individual clay minerals. In contrast, it is probable that a larger proportion of Na^+ moved to the charged faces of the B00*i* and H00*i* soils, particularly the illite/kaolinite dominated H001 soil, thereby influencing physical properties to a greater extent. The B00*i* and H00*i* soils tended to have structural form descriptors for each of the irrigation treatments that were described by the initial soil chemical properties (Table 3.3) and the soil chemical properties of irrigated soil columns (chapter 4). For these soils, the extent of

degradation to soil structural form depended primarily on the clay phyllosilicate suite, the initial ESPs and ECs and then on the ESPs of soil post–irrigation.

The different Vertosols tended to show associations between certain soil properties and the observed structural form attributes, but these soils did not all show the same treatment effects. Consequently, it was difficult to draw comparisons between those soils with increasingly desirable structural form attributes and their physico–chemical properties (chapter 5.4.3). This is most probably a reflection of the initial differences in the structural form of the intact soil columns prior to irrigation, and may reflect current landuse practices (*e.g.* trafficking or tillage). For example, the B003, G002 and N001 soils had all been tilled prior to sampling, while the other soils had not, but none of the soils showed visible affects of wheel trafficking. Comparing the soils using the T102 solution showed that the B001, B003, H002 and N001 soils had the most desirable soil structural form descriptors, while the G002, H001 and N002 soils tended to have the least desirable structural attributes. Importantly, the G002, H001 and N002 soils were all selected for sampling because of their specific soil attributes; the G002 soil was described by the grower as structurally problematic, the H001 soil was a red illitic Vertosol (unlike the other soils studied), while the N002 soil was part of a continuous no–tillage cotton production trial. Irrigation of soils using the T402 solution showed a similar pattern in the structural form attributes, with the B001, B003 and N00*i* soils tending to have the most desirable characteristics, while the G00*i* and H00*i* soils had the least desirable values for the structural descriptors.

5.6 Conclusions

In general, these laboratory irrigated soils contained very small contributions of macroporosity (frequently <5 %), but despite these small quantities of pore space, irrigation water quality influenced soil structural form attributes. Irrigating with solutions of increased sodicity resulted in increased estimates of the size of soil aggregates, decreased pore surface area and connectivity, and resulted in less desirable soil structural form. However, each of the Vertosols investigated in this study reflected the influence of solution composition differently. These differences were attributed to different suites of clay phyllosilicates in the soils and then to the ESPs and ECs of each soil. Primarily, soils containing larger contributions of fine and coarse 2:1 expanding lattice phyllosilicates had structural form attributes that were least affected by irrigation water quality. Soils with large contributions of fine 2:1 expanding lattice phyllosilicates, but small contributions of coarse 2:1 expanding lattice phyllosilicates had small changes in structural form attributes. The soil containing only sub–dominant contributions of 2:1 expanding lattice phyllosilicates in either size fraction are

least resilient and had structural form descriptors that were most affected by the quality of irrigation water. This may reflect an insufficient number of irrigation events and it is likely that continued irrigation of the more resilient G00*i* and N00*i* soils with the different treatment solutions will elicit changes in desirable structural form descriptors.

Chapter 6

WATER QUALITY AND THE WATER RETENTION CURVES OF TWO VERTOSOLS

THE IMPACT OF WATER QUALITY ON THE WATER RETENTION CURVES OF TWO VERTOSOLS

~

Retention: *cōnservātiō (L): The act of retaining or condition of being retained.*

~

6.1 Introduction

The expression of structural form in Vertosols is related to soil moisture and shrinkage characteristics (Yoshida and Adachi 2004), which are in turn determined by soil physico–chemical properties and the solution composition of any applied irrigation water. Consequently, electrolyte solutions have frequently been used to study the hydraulic properties of soil or soil–sand columns in the laboratory (*e.g.* Martin *et al.* 1964; Shainberg and Gal 1982; Curtin *et al.* 1994). Unfortunately, a large proportion of this research has focused on prepared soil or clay systems and the use of homeoionic preparations of Ca^{2+}, Mg^{2+} or Na^{+} to determine soil–water relations. The use of intact field soil has been less common, but the merits of studying intact soil columns, and improvements in assessment techniques have meant that intact field soils are being used more frequently to determine the impacts of different water quality treatments on soil structure. For example, Barlow and Nash (2002) obtained soil moisture characteristic curves using small intact soil cores obtained from a Ferrosol and a Dermosol. Using pressure plates to determine water retention, they compared the effects of de–ionised water and a NaCl solution, showing that small changes in structure could be observed from differences in the wet–end of soil moisture characteristic curves obtained for each treatment. The wet–end of the soil moisture characteristic gives the water retention curve, and is that part influenced by changes in soil structural porosity. Structural porosity was defined by Quirk (1994) as all pore spaces with a radius greater than 15 μm; textural pores include all spaces with a smaller radius.

The preparation of water retention curves using pressure plates is time–consuming and provides only a small number of data points for the description of soil hydraulic properties. In contrast, the evaporation method is a less time–consuming technique for the determination of soil water retention. For example, Minasny and Field (2004) used the ku/pF–Apparatus (Umwelt–Gerate–Technik GmbH) to measure the hydraulic properties of different soils at potentials of 5 and 600 cm ($|h|$) by applying the evaporation method. Then, they used the van Genuchten (1980) equation to derive models of water retention, hydraulic conductivity and the water capacity functions, where capacity functions can then be used to describe effective pore size distributions.

The aim of chapter 6 is twofold; firstly, to investigate the effect of water quality on the water retention curves of two Vertosols (G001 and H001), and secondly to determine the water capacity functions and effective distribution of structural porosity for each soil. The effect of the water quality treatments on the effective distribution of porosity will also be compared to the total soil porosity and to the pore sieve distributions determined in chapter 5.

6.2 Materials and Methods

6.2.1 Determining the water potential and moisture content using the ku/pF–Apparatus

Soil water retention curves were determined using cores (73 mm *i.d.* × 60 mm *h.*) sampled from the 50–110 mm zone of irrigated soil columns. This was done using the duplicated irrigation treatments (FW00*i*, T102 and T401–4) of two Vertosols; G001 and H001. For this experiment each of the twenty four cores sampled were obtained from the soil columns irrigated in chapter 4.

For each irrigation treatment of the two Vertosols, water retention curves were determined using an evaporation experiment (Minasny and Field 2004). To do this, all of the soil–filled cores were prepared by fitting a perforated plastic bottom, lined with a filter paper (70 mm *d.*), to the base. Two apertures in the side of each metal core, at depths of 15 mm and 45 mm, were sealed and the soil–filled cores were placed into a bath of de–ionised water. The depth of water was gradually increased during a 14 day interval until soil saturation was achieved. The soil–filled cores were then removed from the bath and a bore was inserted horizontally into each of the two apertures. Once soil was removed from each bore channel, the prepared cores were pressed into one of ten baskets of a ku/pF–Apparatus (Figure 6.1) and a tensiometer, calibrated at potentials of 0 and 600 cm (|h|) and with a ceramic tip of 7 mm *o.d.* × 21 mm *l.*, was inserted 53 mm into each bore channel. Each basket was hung from one of the ten extended arms of the machine and the experiment began. The sampling interval used was 30 minutes and the experiment was conducted in a laboratory at 20 °C. The average evaporation rate in this laboratory is 2 mm d^{-1} (Minasny and Field 2004). At each sampling interval the matric potential at each tensiometer and the change in weight were logged by the apparatus. This occurred over a period of 5–14 days and the length of the experiment was determined by the time taken for soil matric potential to reach 700 to 800 cm (|h|), as measured by the upper tensiometer. This generally represented the point at which the upper tensiometer tended to fail. Once soil cores had failed they were taken from the apparatus and the perforated plastic bottom was removed. These soils were oven–dried (105 °C) and the weight of soil solids determined.

Figure 6.1 The ku/pF apparatus. Individual soil cores were hung in each of the ten baskets. This apparatus determines changes in matric potential and soil weight as moisture evaporates from the surface of individual soil cores.

6.2.2 The soil–water retention curves

The change in soil weight and the change in water potential were used to determine the water retention properties of each irrigation treatment of the two Vertosols. First, the Schindler (1980) method was used to calculate the standard water content of each individual soil core. This assumes that each core consists of two compartments (the upper 0–3 cm and the lower 3–6 cm). In the centre of each compartment a tensiometer measures water pressure. Therefore, the change in weight between sampling intervals and the difference in pressure between the two tensiometers gives the average water content, $\overline{\theta}$, and the corresponding average matric potential, $\overline{h}$ (cm):

$$\overline{h} = \frac{h_{1.5} + h_{4.5}}{2} \qquad [10]$$

Using the average water content and the corresponding matric potential, moisture retention curves were prepared for each soil core. These curves were used to derive a simulated model of water retention for each treatment of each Vertosol. This was conducted using the van Genuchten (1980) equation (equation 11), which was fitted to the experimental retention data obtained from duplicate soil cores. This gave six water retention curves for each of the two Vertosols. The van Genuchten equation fits a simulation to the changing soil water content according to the change in potential, and is determined by the unknown parameters of θ_s, θ_r, α and n:

$$\theta = \theta_r + \frac{\theta_s - \theta_r}{\left[1 + (\alpha h)^n\right]^{\left(1-\frac{1}{n}\right)}} \quad [11]$$

where θ_s is the saturated water content and θ_r is the residual water content, and both α and n are fitting parameters of unknown magnitude. The θ_s and θ_r values control the vertical 'legs' of the soil moisture characteristic; θ_s controls the saturated end and θ_r controls the dry end of the function. The parameter α controls the location of the S–shaped function, while the parameter n controls the gradient of the S–shaped function. The inverse of α is accepted as an estimate of the air–entry potential (cm) of a soil. These van Genuchten parameters (θ_s, θ_r, α and n) are shown in Figure 6.2 for the moisture characteristic curves of a compacted soil and an aggregated soil.

For the treated Vertosols examined here, each of the four unknown parameters was determined by minimising the sum of squares error for the fitted van Genuchten equation. The sum of squared error was determined as:

$$SSE = \Sigma(M_1 - X_1)^2 + (M_2 - X_2)^2 ....(M_i - X_i)^2 \quad [12]$$

where X is the measured water content and M is the predicted water content for each increment of matric potential. This was used to calculate the root mean square error:

$$RMSE = \sqrt{\frac{SSE}{N}} \quad [13]$$

where N is the total number of points used in the prediction of θ values using the van Genuchten equation. Once the four unknown parameters were determined (θ_s, θ_r, α and n), the van Genuchten equation was used to plot the water retention curves of the G001 and H001 soils following each of the six treatment solutions (FW00*i*, T102 and T401–4), between the potentials of 0 and 600 cm (|h|). From this point, the simulated water retention curves are indicated by the suffix *. For example, T102 and FW00*i* become $T102^*$ and $FW00i^*$ for each soil, G001 and H001.

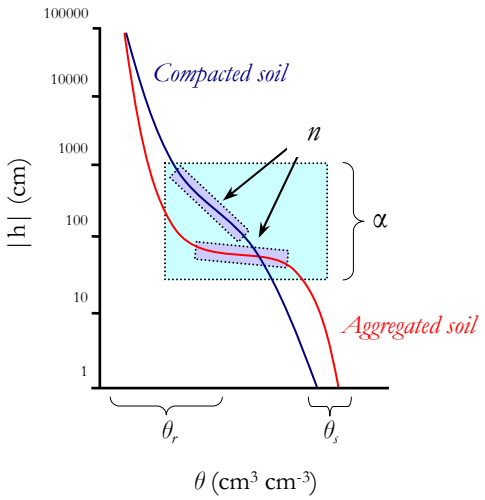

Figure 6.2 The soil moisture characteristics of two differently structured soils (adapted from Hillel 1982).

6.2.3 The water capacity function

Water capacity functions, $C_w(h)$, were determined using the predictions of θ_s, θ_r, α and n for each of the six water retention curves of the G001 and H001 soils. $C_w(h)$ is determined as:

$$C_w(h) = \frac{\alpha(\theta_s - \theta_r)(n-1)h^{n-1}}{\left[1+(\alpha h)^n\right]^{2-1/n}} \quad [14]$$

This function describes the slope of the soil water retention curve and is the change of water content per unit change of matric potential. Hence, large values of C_w are associated with the wet end of the water retention curve, where larger pores are emptying with modest changes in applied pressure. At saturation this function equals zero and again approaches zero as the soil dries, where large increases in pressure are met by small changes in moisture content.

The distribution of pore drainage radii was then determined to give an indication of the volume of moisture contained in pore spaces with a particular drainage aperture. The radius of this aperture (r) is related to the matric potential (h) by:

$$r(cm) = \frac{0.15}{h(cm)} \quad [15]$$

This function may be used to give an estimate of the hierarchical arrangement of pore drainage radii from which water loss occurs during evaporation.

6.2.4 Total porosity of the treated columns

The total porosity of each soil core was determined to identify the effect of treatment on the volume contribution of each soil phase (solid, liquid and gaseous). This was calculated from the bulk density of soil cores used in determining the soil water retention properties and the moisture content of these cores at the time each was sampled from the irrigated soil columns. The bulk density and moisture content were used to determine the volume fraction of soil solid, V_s, of soil solution, V_l, and of soil air, V_g.

$$V_s\,(cm^3\,cm^{-3}) = \frac{\rho}{\rho_s} \qquad [16]$$

$$V_l\,(cm^3\,cm^{-3}) = \rho \times w \qquad [17]$$

$$V_{s,l}\,(\%) = \frac{V_{s,l}}{V} \times 100 \qquad [18]$$

$$V_g\,(\%) = 1 - V_s - V_l \qquad [19]$$

where ρ is the bulk density of soil, ρ_s is the bulk density of soil solids (estimated as 2.65 g cm^{-3}) and w is the soil wetness at the time cores were sampled from each of the soil columns.

6.3 Results

6.3.1 The simulated water retention curves of G001 and H001

The parameters of θ_s, θ_r, α and n are given in Table 6.1 for each of the treatments of G001 and H001. The RMSE values are given in Table 6.1. These values indicate a similar level of accuracy for the van Genuchten model for all the treatments of the two soils, with two exceptions. The *T102** and *T404** curves for the G001 soil and the *T402** curve for the H001 soil show much larger RMSE values. This shows that the two retention curves, to which the van Genuchten model was fitted for each treatment, lost moisture during the evaporation experiment at different rates and that the contained different θ values at each interval of potential.

The predicted saturated water content following the *T404** treatment for the G001 soil and following the *T102** treatment for the H001 soil are larger than those of the θ_s values obtained for the other treatments of these soils, and are least for the *T403** curve of the G001 soil and for the

*T401** and *T403** curves of the H001 soil. The predicted residual water content (θ_r) approaches 0 for treatment curves of each soil. The α and *n* values do not show a consistent trend for the simulated water retention curves for either of these soils. This reflects the absence of the characteristic S–shaped curve of the soil moisture characteristic.

Table 6.1
Parameter values for the van Genuchten Model of the treated soils and the associated RMSE values. The θ_s, θ_r, α and *n* values were used to derive the water capacity function for each treatment of each soil (G001 and H001)

Treatment	θ_s	θ_r	α ($cm^{1/n}$)	*n*	*RMSE*
			Site *G001*		
FW00i*	0.58	0.00	2.31	1.04	0.01
T102*	0.53	0.00	0.83	1.03	0.06
T401*	0.52	0.00	0.96	1.05	0.01
T402*	0.55	0.00	0.96	1.04	0.00
T403*	0.49	0.00	0.00	1.21	0.01
T404*	0.68	0.00	2.92	1.07	0.06
			Site *H001*		
FW00i*	0.56	0.00	0.39	1.07	0.01
T102*	0.72	0.00	1.36	1.11	0.01
T401*	0.55	0.00	0.03	1.19	0.01
T402*	0.61	0.00	2.86	1.11	0.05
T403*	0.55	0.00	0.79	1.07	0.01
T404*	0.62	0.00	2.52	1.08	0.01

* denotes attributes derived for the two soils using the van Genuchten equation

The predicted parameters in Table 6.1 are used to model water retention according to the irrigation treatments of each soil. The curves developed using the van Genuchten equation are given, for both soils, in Figure 6.3 and as a natural log function in Figure 6.4. The *T401**, *T403** and *T404** treated soils tend to have fitted water retention characteristics that are similar for both G001 and H001, where |h| was between 200 and 600 cm. However, where |h| is between 0 and 200 cm, the *T401** and *T402** retention curves are different for each of the two soils.

The treatment of the G001 soil with increasingly sodic solutions (T401→4) does not show any trend in the water retention curves. For this soil, the *T401** treatment gives a θ_s value less than that of the *T402** treatment, and the fitted curves following treatment with these solutions have the same α values and give the same estimate of air–entry point. These two curves have a similar gradient at |h| 100 to 600 cm, showing a similar unit decrease in θ per increase in potential, while at lower potentials (|h| 0 to 100 cm), small changes in |h| give large changes in θ. In contrast, the *T403** and *T404** curves have different water retention properties for both the 0–100 cm and 100–600 cm potentials. The *T403** curve has an estimated air entry potential of zero (Figure 6.3), and appears to have a consistent gradient of decreasing θ as |h| is increased. At |h| 100–600 cm, the *T404** water

retention curve is similar to the *T403** retention curve, but where |h| is less than 100 cm, *T404** has the largest loss of water of all four of the G001 *T401–4** curves.

The H001 soil has similar *T403** and *T404** water retention curves. These systems have similar *n* values, but α is much larger for the *T404** retention curve. These treatments have a similar gradient to the *T402** treatment in the |h| 200–600 cm, but *T402** has smaller θ values at all potentials. The *T401** curve is most similar to the curve of the *T402** treated soil. However, unlike the air–entry values for the other SAR_w curves, which are between 0 and 3 cm, *T401** has an estimate of air–entry point at |h| 33 cm.

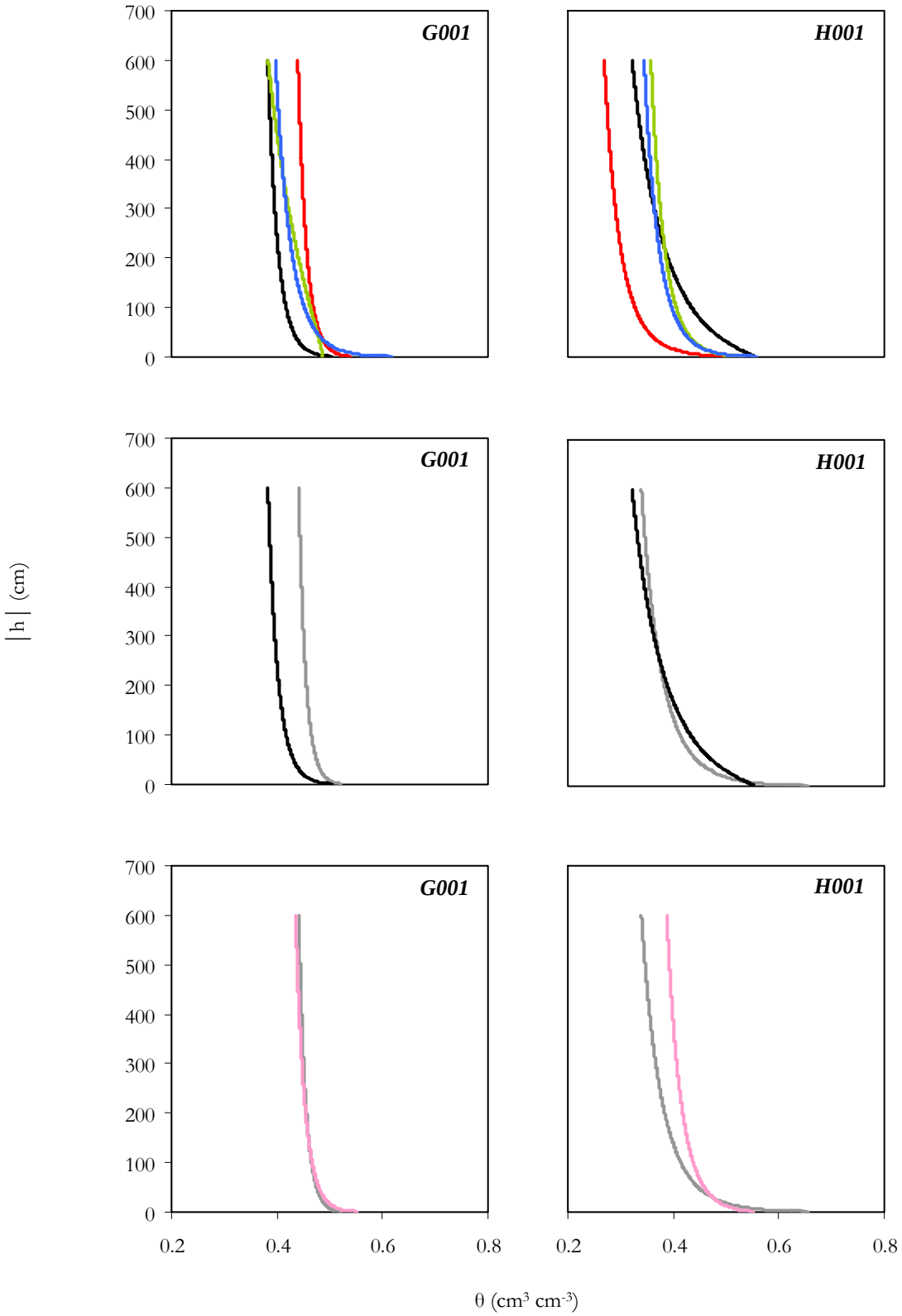

Figure 6.3 Predicted water retention curves for the soils G001 and H001 for each of the laboratory irrigation treatments [*FW00i** (—), *T102** (—), *T401** (—), *T402** (—), *T403** (—) and *T404** (—)].

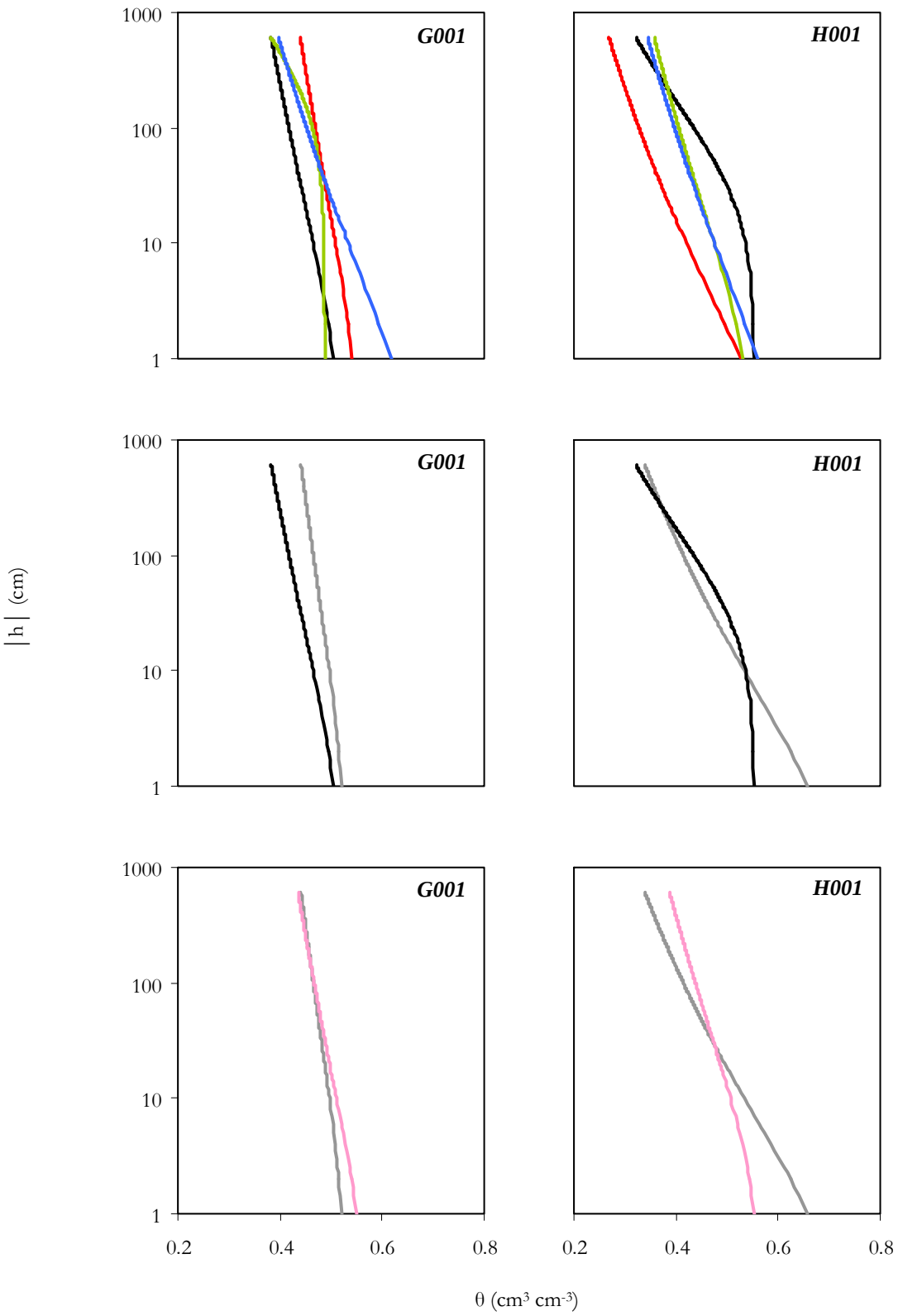

Figure 6.4 Predicted water retention curves, using a natural log scale, for the soils G001 and H001 for each of the laboratory irrigation treatments [*FW00i** (—), *T102** (—), *T401** (—), *T402** (—), *T403** (—) and *T404** (—)].

6.3.2 The water capacity of irrigation treatments for G001 and H001

The water capacity functions of the simulated G001 and H001 water retention curves are given in Figures 6.5 and 6.6. In general, the modelled functions of these two soils tend to have largest values of C_w occurring at a potential of 2–3 cm.

The *FW00i**, *T102**, *T401**, *T402** and *T404** capacity functions of G001 have largest C_w values at potentials of 2–3 cm, but the *T403** treatment does not show any large changes in C_w at any of the measured matric potentials (0–50 cm). The water retention curves following the *T401** and *T402** treatments of G001 tend to have capacity functions that are similar, while the *T404** treatment has a much larger C_w at potentials of 2–3 cm. The C_w of the *T102** and *FW00i** treated soils are similar to those curves of the *T401** and *T402** examples.

Following the *T401** treatment, the H001 soil tends to have similar C_w values for all matric potentials between saturation (0 cm) and 50 cm (|h|). For this soil, the *T402–4** capacity functions have largest C_w values at |h| 2–3 cm, but as matric potential is increased the water capacity decreases rapidly. The *T402** curve has the largest C_w and the *T403** curve has the smallest C_w. The *T404** treatment has a water capacity at 2–3 cm potential that is intermediate between those values for the *T402** and *T403** systems.

The functions presented in Figures 6.5 and 6.6 show changes in C_w for pore spaces with a drainage radius greater than 10 μm (0.01 mm). These figures show that H001 tends to have a greater volume of structural porosity than G001 for all fitted retention curves. Generally, all curves show a similar distribution of connected pore space, but two capacity functions have different distributions of effective porosity. The distribution of pore drainage radii of the G001 *T403** curve shows only small contributions of porosity throughout. The H001 soil, following treatment using solution *T401**, has pore size contributions from a broad range of radius sizes. This is not a characteristic of any of the other retention curves. In this case, the largest C_w values of this curve are indicative of effective drainage porosity with a radius of approximately 0.15 mm. Like the other treatments of the G001 and H001 soils, C_w then approaches 0 cm^{-1} for this water capacity function.

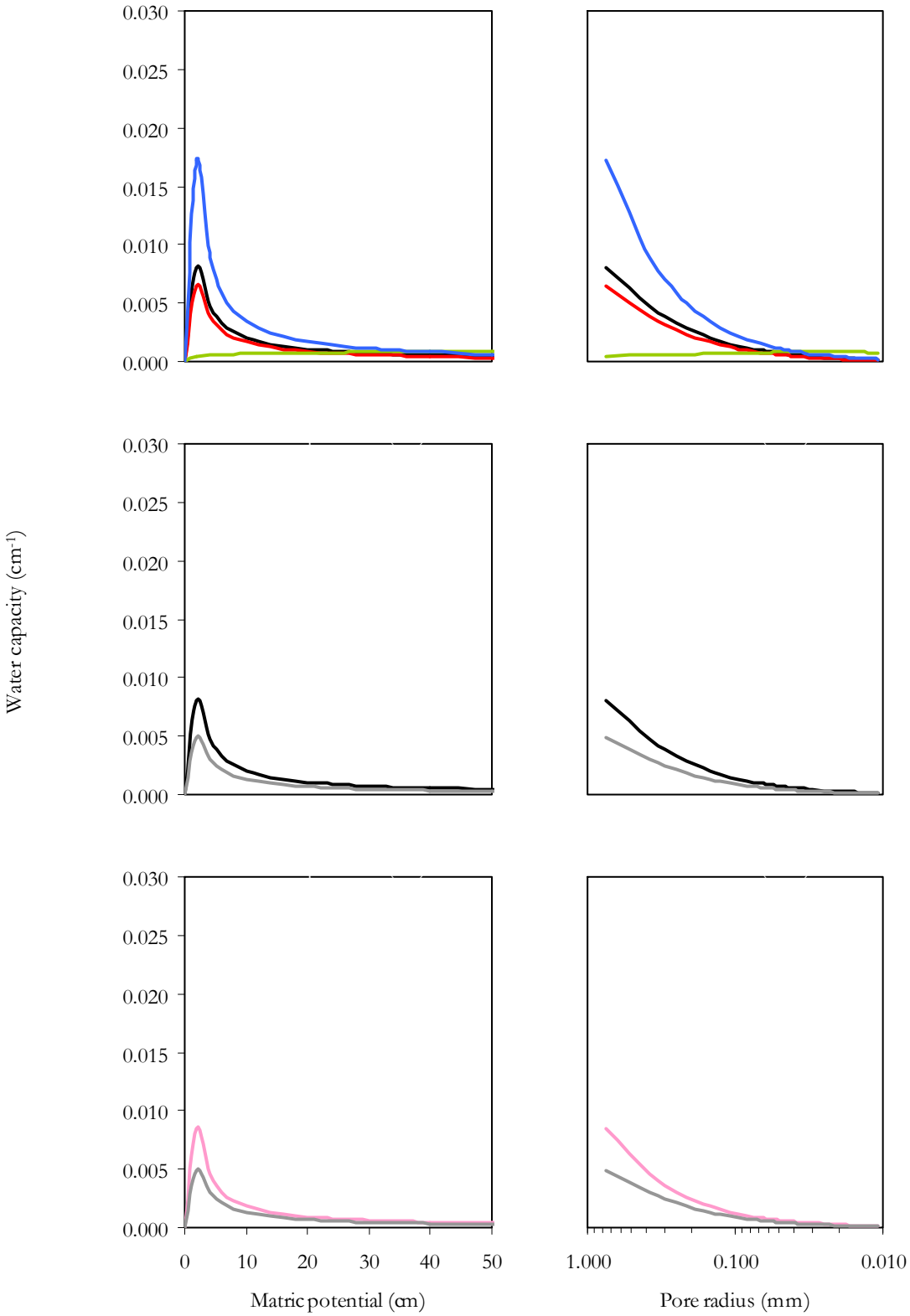

Figure 6.5 Water capacity as a function of matric potential and of effective pore radii for each of the laboratory irrigation treatments of G001 [*FW00i** (—), *T102** (—), *T401** (—), *T402** (—), *T403** (—) and *T404** (—)].

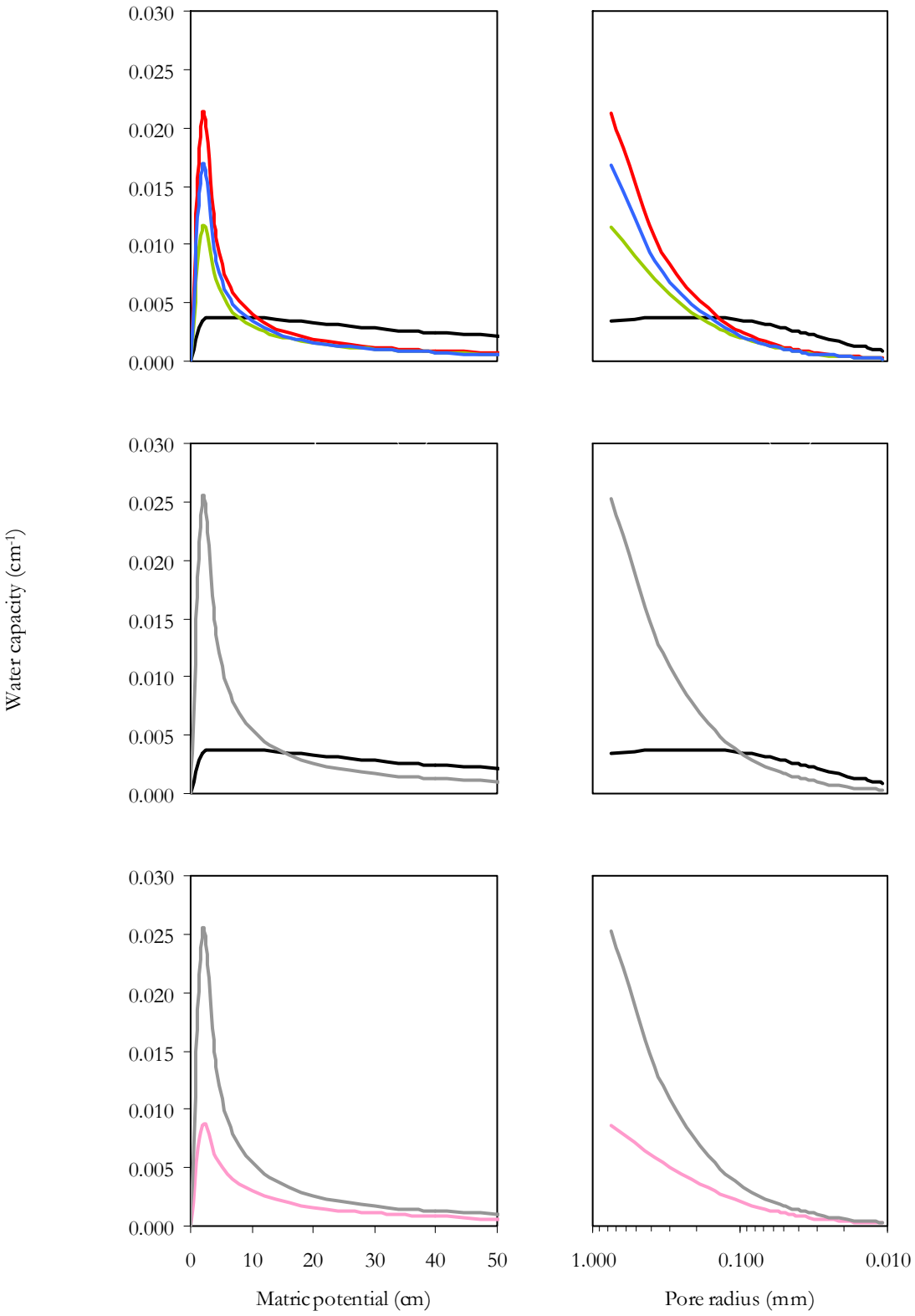

Figure 6.6 Water capacity as a function of matric potential and of effective pore radii for each of the laboratory irrigation treatments of H001 [*FW00i** (—), *T102** (—), *T401** (—), *T402** (—), *T403** (—) and *T404** (—)].

6.3.3 The effect of irrigation water quality on the total soil porosity

For the G001 and H001 soils, the volume fractions of solid and pore (solution and air) space are given in Figure 6.7. This comparison shows two general trends. The T401–4 treatments of each soil tends to result in a small decrease in the volume of solid, where solutions of larger SAR_w (0, 7.5, 15 or 30) have been used to irrigate soil columns. This is indicative of the greater swelling of 2:1 expanding lattice phyllosilicates in the presence of increased Na^+. However, the change in moisture content for these same treatment applications is different for each of the two soils. The G001 soil tends to have greater air–filled porosity for the larger SAR_w treatments. In contrast, the T401 and T402–treated H001 soil cores have greater air–filled porosity than the T403 and T404–treated H001 soils.

The T102 treatment of each soil tends to result in a greater volume fraction of pore space than either the FW00*i* or the T401 treatments. This suggested that an increase in swelling took place in these soils due to increased expansion of the diffuse double layer where the soil solution had a small ionic concentration. In the G001 soil, the T102 treatment tends to result in less solid volume than is observed for all other treatments of this soil. The FW00*i*–treated soil contains a solid volume that is comparable to the T403–treated soil. For H001, the T102 and T403–treated soil cores have a similar volume of solids, while the FW00*i* and T401–treated cores have similar values.

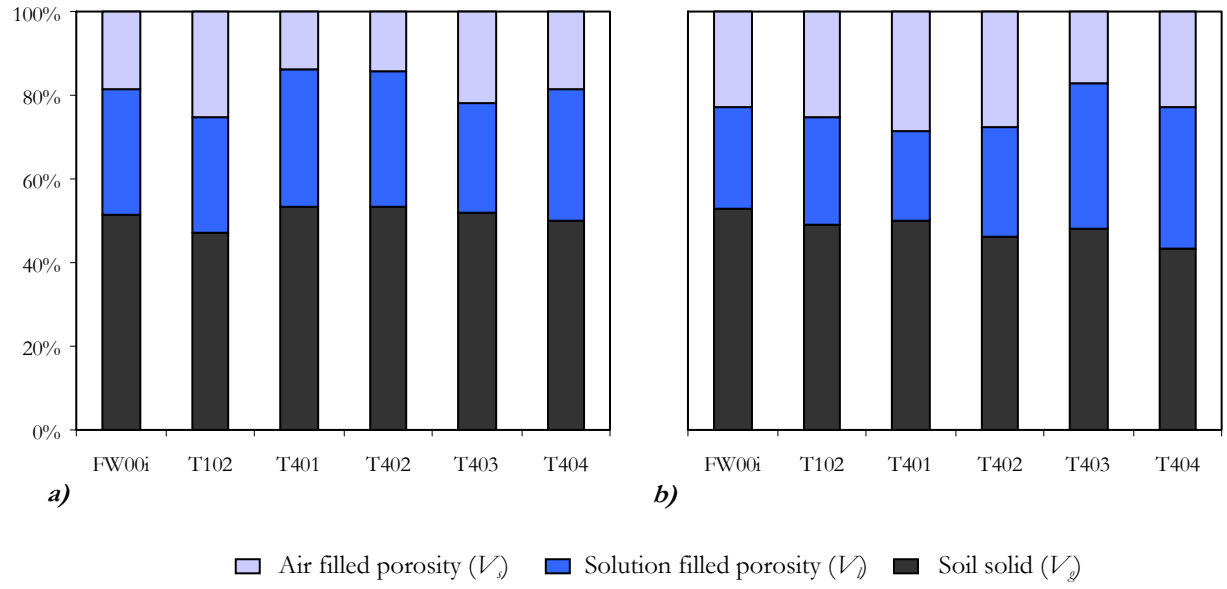

Figure 6.7 The contribution of each phase (solid, liquid and air) to soil volume for soils G001 *(a)* and H001 *(b)*.

6.4 Discussion

6.4.1 Determination of unknown parameters using the van Genuchten equation

Historically, the unknown parameters of θ_s, θ_r, α and n have been estimated using the saturated moisture content of a soil with a specified clay texture (*e.g.* Carsel and Parrish 1988). However, fitting the van Genuchten equation to develop simulated retention curves for the treated G001 and H001 soils tended to result in different estimates to those obtained by Carsel and Parrish (1988) (θ_s =0.38, θ_r =0.068, α =0.008 and n =1.09) *i.e.* the G001 and H001 soils had larger θ_s values and smaller θ_r values.

The values of n obtained for the G001 and H001 curves in this study are similar to the Carsel and Parrish (1988) value, but the estimated α values obtained here did not show a similarity with their estimate for clay textured soils. Richard *et al.* (2001) determined the unknown parameters by fitting the van Genuchten equation to soil moisture characteristic curves. They found a range of α values (0.2–9.5 m^{-1}) that were independent of the applied treatment for non–clay soils.

The values of θ_s, θ_r, α and n obtained in this thesis (chapter 6.3.1) were estimated using only the wet–end of the moisture characteristic, and the predicted water retention curves included only part of, or none, of the characteristic S–shape (Figure 6.2). This will impact on the values derived for θ_r, n and α. The parameters n and α are determined by the contribution of different pore sizes; a soil containing a large proportion of macropores of similar size will drain at potentials close to zero, while a soil containing a distribution of smaller pores will drain at larger potentials. The θ_r parameter controls the dry–end of the soil moisture characteristic, but with no data for potentials larger than |h| 600 cm and in the absence of all, or part of, the S–shaped zone, this estimate is unlikely to give an accurate prediction of the residual water content of these soils. However, given the fit (RMSE <0.06) of the simulated retention properties to the experimental retention curves, these values were acceptable for investigations of the fitted water retention curves applied to different irrigation treatments of the G001 and H001 soils.

6.4.2 The moisture retention of soils G001 and H001

The fitted water retention curves for the two Vertosols are similar to those of other swelling soils (*e.g.* Minasny and Field 2004). The water retention curves for treatments of G001 and H001 all had one zone of significant moisture loss and this occurred at very small suction (|h|=0 to 100 cm), as the soil commenced draining from saturation. Unlike the moisture characteristic curves of non–swelling soils and soils with smaller clay contents, none of the treatments tended to show the

distinct S–shaped function (Figure 6.2), within the measured potential range (|h|=0 to 600 cm). The absence of this S–shaped function between matric potentials of 0 to 600 cm is indicative of fine–textured swelling clay soils. These soils contain porosity that closes during wetting, and consequently, there is often a large proportion of very small pores.

The water retention properties of the two soils were influenced by the quality of water applied in irrigation, but G001 tended to be affected less by water quality than H001. Treating these soils with sodic water tended to result in increased saturated water contents, but where these soils had been treated with the T403 and T404 solutions, they tended to lose more water with smaller changes in potential. In chapter 5, the H001 soil had structural form that was influenced most by the SAR_w of applied solutions, while G001 did not have significantly different structural form attributes after soil had been irrigated with the SAR_w solutions. These observations are reflected by the simulated water retention curves determined for the treatments of these two Vertosols. The H001 soil tended to show a trend in water retention curves that was consistent with its structural form attributes after each SAR_w treatment. The T401–treatment of this H001 soil had a fitted water retention curve that showed a more consistent moisture loss with changes in matric potential, where this was compared to the other solution treatments. This trend suggested a larger distribution of structural porosity in the T401–treated soil cores, than in cores treated with the other solutions. Overall, the H001 *T402** curve tended to show larger water loss than the other sodicity treatments, while *T403** and *T404** indicated similar moisture losses.

There were two key differences in the physical properties of these two soil types that were identified in chapter 2 and 3; these soils had different organic carbon contributions and clay mineral suites. The G001 soil contained more than twice as much organic carbon than the H001 soil (0.96 % and 0.45 % respectively). Organic matter has been reported as contributing to the stability of small aggregates (<500 μm) in Vertosols (Warkentin 1982). However, it is unlikely that these very small organic contributions significantly influenced the different water retention properties of these two soils.

The G001 soil contained a much larger content of 2:1 swelling phyllosilicates (smectite and vermiculite) than the H001 soil, which was dominated by illite. Moderate differences in the content of 2:1 swelling phyllosilicates (smectite and vermiculite) have been consistently associated with different soil stabilities and structural form attributes in this work. It was shown in chapter 3 and in chapter 4 that soils with a larger contribution of smectite tended to have a larger amount of dispersed clay after shaking. This reflected less compression of the diffuse double layer of swelling clays in dilute soil solutions and was discussed by Wilding and Tessier (1988) as a major contributor

to the swelling of Na^+–smectite soils. In this chapter, the increased swelling of these treated G001 soil columns was expected to reduce the content of structural porosity making treatment comparisons difficult. In comparison, the illitic H001 soil should swell less and thus, cores from the irrigated H001 columns appeared to contain larger contributions of structural porosity.

The contributions of Na^+ to the 50–100 mm soil layer (chapter 4) following the irrigation of soil columns in the laboratory tended to be broadly associated with the different water retention curves of each of these Vertosols. The other chemical attributes (*e.g.* Ca^{2+}, Mg^{2+} and EC) did not appear to be linked with different water retention properties. In the G001 soil, the T401–treated soil had a smaller ESP than the other SAR_w treated columns (50–100 mm). The T402–3 treated soil columns had similar ESPs, but the T404–treated soil had a larger ESP and SAR than the other SAR_w treatments. For the G001 soil, the irrigation treatments that led to larger ESPs and SARs resulted in larger moisture contents at saturation. This reflects increased swelling in the G001 soil where the soil Na^+ content is larger. The treatment of the H001 soil with larger SAR_w solutions, similarly, led to increases in ESP and SAR. In this soil, these larger ESPs and SARs were generally associated with the observed water retention properties; soil with larger Na^+ contents had smaller changes in moisture content as matric potential increased. Similar associations were observed between the Na^+ content and the *FW00i** and *T102** water retention curves of each soil.

6.4.3 Water capacity as a function of effective pore drainage radii for the two Vertosols investigated

In the soil matrix there exists an array of complex inter–aggregate and intra–aggregate cavities which vary in amount, size, shape, tortuosity and continuity (Danielson and Sutherland 1986). Soil–water relations provide one method for characterising the hydraulic connectivity of this soil matrix. However, it does not account for any soil moisture retained on the surfaces of microstructures, in non–connected pore spaces (*i.e.* in a collapsed structure) or within pores that have a drainage radius less than 2.5 μm.

During the evaporation experiment in this thesis, most of the moisture loss occurred at potentials less than 10 cm (|h|). This is indicative of drainage from the larger pore spaces, which remained filled with water after saturation of these swelling soils. These larger pores have an effective drainage radius of greater than 150 μm, and these pores correspond to soil macroporosity (Brewer 1964). These macropores were characterised using image analysis in chapter 5. The smallest effective pore drainage radius identified in the water capacity functions (Figures 6.5 and 6.6) was approximately 10 μm; these are micropores (Brewer 1964) and drain at a potential of 150 cm (|h|). Consequently, this distribution of pore radii represents the macropore (>75 μm *d.*), mesopore (30–75 μm *d.*) and micropore (5–30 μm *d.*) spaces (Brewer 1964); or according to Quirk (1994) the total distribution of

soil macropores. Quirk (1994) considered mesopores and macropores as one class with an effective radius greater than 15 μm; these pores he considered to represent soil structural porosity.

The irrigation treatments of the two Vertosols (G001 and H001) tended to result in water capacity functions that reflected the contributions of Na^+ content. For the G001 soil, the irrigation treatments (T401–3) that led to larger ESPs and SARs tended to result in less pore space reflecting increased soil swelling, but the T404–treated cores had largest ESPs and had a larger contribution of pores with a drainage radius greater than 100 μm. This potentially reflects other soil properties *i.e.* the initial soil structural form. The treatment of the H001 soil with larger SAR_w solutions, similarly, led to increased swelling and treating this soil with solutions of larger SAR_w, led to a reduction in the contribution of connected pore spaces. Treating either of these soils with the FW00*i* and T102 solutions led to similar associations between the distributions of pore drainage radii and the soil Na^+ content.

6.4.4 The soil solid, liquid and gaseous phases

Soil water capacity functions can be used to derive the effective pore size distribution, but give no indication of total soil porosity. The determination of soil bulk density and the contribution of discrete phases (solid, liquid and gaseous) is perhaps the most frequently used measure of assessing soil porosity and structural condition. In this research, irrigating soil columns with each of the treatment solutions affected the volume fractions of solid, liquid and gas in both the G001 and H001 soils. These two soils showed similar small changes in bulk density for the applied irrigation treatments, but comparison of the air–filled and solution–filled phases showed differences between G001 and H001. Generally, these soils contained more pore space (*i.e.* all space occupied by liquid and gas) where soil had been treated with solutions of larger SAR_w. This showed that treatment of the G001 and H001 soils with waters of larger sodicity, led to small increases in swelling due to increased expansion of the diffuse double layer (*e.g.* Slade *et al.* 1991). This larger porosity for soils treated using solutions of larger SAR_w did not reflect the distribution of air–filled and solution–filled porosity. The G001 soil samples tended to have increasing contributions of soil air, where soil had been irrigated with solutions of greater SAR_w. In contrast, the H001 had the opposite relationship, containing less soil air and more soil solution after treatments of larger SAR_w. This is presumably indicative of a less connected pore network, brought about by structural collapse. The G001 soil, with a much larger content of 2:1 swelling phyllosilicate clays, does not appear to have collapsed in this way. In so doing, the G001 soil has a structural form consistent with increased mineral swelling where larger SAR_w solutions were applied, but the structural arrangement of soil aggregates has not

been changed. Consequently, changes in the effective drainage radius of pore space or the pore sieve distribution did not reflect the different irrigation treatments of this soil.

Irrigating these soils with FW00*i* and T401 led to less total porosity than treating soil using the T102 solution. This did not reflect observations of the effective distributions of porosity. For example, the FW00*i* and T401–treated G001 soil samples appeared to contain more porosity (radius >10 μm) than the T102–treated G001 soil. Consequently, the larger volume of total porosity in the T102–treated G001 cores is a reflection of increased clay swelling. In contrast, the T102 treatment of the H001 soil tended to have a similar contribution of effective drainage porosity (radius >10 μm) to that of the T401 treatment of this soil, but this tended to be in the larger effective pore sizes (Figure 6.6). The comparison of the FW00*i* and T102 treatments of H001 indicated that the treatment of this soil using clean water similarly led to larger pore spaces than the field water treatment. This reflected increased crack development in the T102–treated H001 soil. For example, the analysis of soil structural form in chapter 5 indicated that the treatment of this soil using T102 led to an estimate of soil solid size that was comparable to the T403–treated soil columns, while the estimated size of pore space was significantly larger for the T102–treated soil.

6.4.5 Comparing the pore distributions obtained from the soil moisture retention curve and from the image analysis procedure

The effective distributions of pore drainage radii provided a cumulative account of soil textural porosity. This measurement is dependent on the connectivity of pore space and on the neck size of the smallest pores in the connected network; the smallest pores in the network determine the potential required for drainage to occur (Dexter 2004). These effective distributions of pore radius were compared with the pore sieve distributions determined using image analysis (chapter 5). Both the distributions of pore radius and pore sieve size tended to give similar relationships between the different irrigation treatments of each soil *i.e.* treatment of the H001 soil with solutions of larger SAR_w resulted in less porosity which was less connected. However, the estimates of the pore distribution derived from water capacity functions tended to be better related to the observed physico–chemical properties of each soil. This could have occurred for several reasons: *(i)*, the resolution of porosity studied using each of the methods, *(ii)*, the water content at the time images were obtained for analysis and, *(iii)*, the impact of re–wetting soil cores for determination of hydraulic properties. The image analysis procedure addressed all pore spaces with a minimum diameter of 120 μm. This image analysis method provided a much coarser resolution than determinations of the effective pore radii, which included connected pore space with an effective radius greater than 10 μm. The different water contents at which these cores were studied will influence the extent of development in structural characteristics. For example, the assessment of soil

columns to determine structural form characteristics contained much smaller volumetric water contents than cores that had been re–wetted to determine water retention properties. Consequently, as the soils used for the assessment of soil structural form were drier, this method of analysis will include a greater contribution of large pores, due to soil shrinkage. The moisture retention curves were wetted to saturation using clean water (T102) and left to equilibrate. This diluted the soil solution, promoting the re–distribution of exchangeable and solution cations within the structural arrangement of clay domains, and potentially resulting in the collapse of soil aggregates. This will account for the observed association between the ESP, SAR and the stability and moisture retention properties. In contrast, the pore sieve distributions did not show the same association with Na^+ contributions. This was attributed to the distribution of Na^+ on exchange sites prior to water retention samples being re–wetted. In the soil columns 'de–mixing' (Halliwell *et al.* 2001) was likely to have resulted in Na^+ occupying the outer faces of clay domains rather than on the surfaces of individual clay particles. During re–wetting with clean water, this distribution is likely to have changed, with Na^+ becoming more evenly distributed at the exchange sites of clay particles.

6.5 Conclusions

In this chapter, the impact of irrigation treatment on the water retention properties of the G001 and H001 soils was investigated. This allowed the comparison of the effective distribution of pore drainage radii with total soil porosity and with pore sieve distributions (chapter 5). These methods provided a descriptive analysis of two different swelling soils (G001 and H001). In addition, they provide an understanding of the activity of intact soil samples after treatment with different water quality solutions. These methods showed that the clay phyllosilicate suite was the most influential property contributing to soil structural form and hydraulic properties where irrigation water quality is changed. In this case, soil dominated by 2:1 expanding lattice clays (G001) was affected by solution quality much less than the illite–dominated H001 soil. This tended to reflect changes in structural condition; the G001 soil appeared to maintain a connected pore distribution, but the illitic H001 soil seemed to show structural collapse where solutions of large SAR_w were applied.

Chapter 7

DEVELOPING A DESCRIPTIVE MODEL OF THE STRUCTURAL STABILITY OF IRRIGATED VERTOSOLS

DEVELOPING A DESCRIPTIVE MODEL OF THE STRUCTURAL STABILITY OF IRRIGATED VERTOSOLS

~

Description: *dēscriptio (L): a representation in words of the nature or characteristics of a thing*

~

7.1 Introduction

One of the most perplexing issues in soil science has proven to be the development of a suitable description of structural stability in agricultural soils. Consequently, a large body of research has focused on this objective, and the principles of aggregate liberation, clay dispersion and soil hydraulic properties are generally understood. This understanding has been used to develop several descriptors that characterise the structural behaviour of particular soil types; these have related physico–chemical properties to soil structural stability (*e.g.* Rengasamy *et al.* 1984; Sumner *et al.* 1998; Hulugalle and Finlay 2003), soil structural form and soil hydraulic characteristics (*e.g.* Quirk and Schofield 1955; Quirk 2001; Dexter 2004). However, to maintain or improve soil structural stability, land managers have tended to focus on reducing sodicity (ESP) or clay dispersion by changing the balance of specific ionic species in a soil system *e.g.* increasing exchangeable Ca^{2+} and reducing Na^{+} contributions, or by raising the cation concentration of irrigation waters (*e.g.* Quirk and Schofield 1955). These methods have tended to consider exchangeable Na^{+}, ESP, SAR and EC singularly, or in combination, as the dominating descriptors of structural behaviour. In this thesis, and other work (*e.g.* Rengasamy *et al.* 1984; Wilding and Tessier 1988), structural responses have been linked to differences in the clay phyllosilicate suite. However, while the clay mineral suite is often discussed, it is rarely quantified in soil stability studies, and techniques predicting soil structural stability have not included the suite of clay minerals.

This chapter aims to compare the stability of the nine soils investigated using current assessment practices. Then, a descriptive model of the structural stability of irrigated Vertosols is presented. This model uses soil physico–chemical properties to describe potential instability where soil is immersed in different water quality solutions. The objective of this model is to demonstrate how irrigation sources of differing quality will impact on the stability of different Vertosols.

7.2 Estimating the structural stability of the nine Vertosols using current methods

7.2.1 The soil samples and data used for comparisons

The soils to be assessed using current methods of predicting stability include those nine surface soils assessed in chapter 3, and each of the individual soil layers (0–50 mm, 50–100 mm, 100–150 mm and >150 mm) sampled from soil columns (G00*i*, H00*i* and N00*i*) irrigated in the laboratory in chapter 4. The important physico–chemical attributes of each soil layer, and the estimated contributions of phyllosilicate minerals to the coarse and fine clay fractions at each of the sites investigated, are presented in appendix 6. $SI_{<2}$ values are used as indicators of stability for each soil sample; these values were determined after the EOE–disruption of soil immersed in solution T102.

The ASWAT score for each of the nine surface Vertosols is first compared with the key stability thresholds provided in the SOILpak manual. Then, the stabilities of all soil samples are compared using the:

1. Exchangeable Sodium Percentage (ESP)
2. Electrochemical Stability Index (ESI)
3. $EC_{1:5}/Na^{+}_{exch}$
4. Classification scheme for dispersive behaviour in red–brown earths (Rengasamy *et al.* 1984) (to be referred to as the *Rengasamy classification scheme*)

7.2.2 Factors affecting the structural stability of cotton–producing Vertosols in water

The SOILpak manual (McKenzie 1998) was developed by the cotton industry to assist growers and extension staff in the management of Vertosols for cotton production. In this resource, the ASWAT test (Field *et al.* 1997) is used as a method of assessing the extent of clay dispersion from aggregates and from re–moulded soil (Figure 7.1). The SOILpak resource also provides key stability thresholds for some soil properties of cotton–growing Vertosols. These key stability thresholds are given in Table 7.1, and are compared with the estimates of stability given by the ASWAT test for the nine furrow soils (Table 7.2).

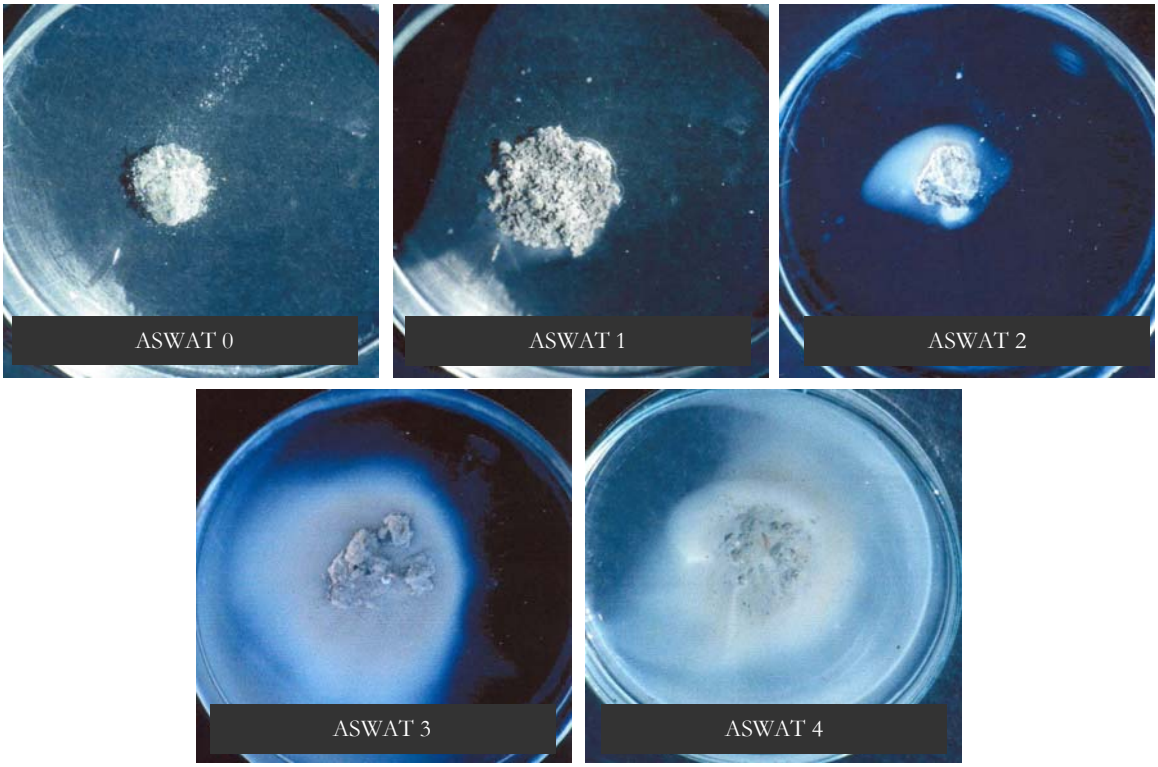

Figure 7.1 The ASWAT dispersion classes (Field 2000). ASWAT scores (0–4) are determined at intervals of 10 minutes and 2 hrs by immersing air–dry soil aggregates, and then re–moulded soil, in de–ionised water. The result is an ASWAT score out of 16, where 0–1 represents negligible dispersion, 2–6 represents moderate dispersion and 7–16 represents serious dispersion.

Table 7.1
Thresholds associated with the structural stability or structural instability of cotton–growing Vertosols (McKenzie 1998)

	Values associated with stability	**Values associated with instability**
	(small ASWAT scores *i.e.* <2)	(large ASWAT scores *i.e.* >7)
ESP	<2	>2 (small EC) >15 (large EC)
Electrochemical Stability Index (ESI) ($EC_{1:5}$/ESP)	>0.05	<0.05
Ca^{2+}:Mg^{2+} ratio	>2.0	<2.0
$CaCO_3$ content (%)	>0.3	<0.3
Organic matter (%)	*	*

* Critical limits for organic matter contributions have not been established for the different Vertosols used in cotton production. However, in terms of soil structural condition, larger values of organic matter are considered more beneficial, if accompanied by an adequate supply of calcium ions (McKenzie 1998).

The ASWAT scores assigned to each of the nine Vertosols are not consistently correlated with the measured values of ESI or Ca^{2+}:Mg^{2+} ratio. The stable G00*i*, H002 and N002 soils (ASWAT <2) all have ESI values greater than 0.05, but the unstable soils (ASWAT >2) have a mixture of ESI values.

The unstable B001 and B003 soils have ESI values <0.05, whereas the unstable B002, H001 and N001 soils all have ESI values that indicated stability. The Ca^{2+}:Mg^{2+} ratios are all close to the minimum suggested as a threshold for stable soils. These values tend to be similar for all the Vertosols, and show no relationship with ASWAT scores. The content of organic carbon is very small for all soils and does not appear to be linked with the observed ASWAT scores, except for the B00*i* soils. These soils have the smallest organic carbon contents and all have ASWAT scores greater than 3. The ASWAT dispersion scores are much more closely linked with soil ESP. The soils with ESPs larger than 2 all have ASWAT scores of 3 or greater. For these soils, the magnitude of each ASWAT score tends to reflect different ESP and electrical conductivity values, but this relationship is not described by the values of ESI.

Table 7.2
Selected physico–chemical chemical attributes of the nine furrow soils described in chapter 3

	Sampled field								
	B001	**B002**	**B003**	**G001**	**G002**	**H001**	**H002**	**N001**	**N002**
ASWAT score	9	3	9	0	0	4	0	9	0
ESP	8.1	5.3	3.6	1.3	1.6	3.1	1.8	6.4	0.7
EC (dS m^{-1})	0.37	1.19	0.14	0.09	0.15	0.21	0.20	0.96	0.17
ESI	0.05	0.22	0.04	0.07	0.10	0.07	0.11	0.15	0.26
Ca^{2+}:Mg^{2+}	1.9	2.3	2.6	2.9	2.6	1.9	2.1	2.9	3.0
Organic carbon (%)	0.22	0.27	0.32	0.96	0.39	0.45	0.40	0.62	0.88

The ASWAT procedure provides a method of allocating potential dispersion classes to the nine soils investigated. However, while descriptive, this method is qualitative, and in the absence of laboratory analysis it gives no measure of the soil properties that may cause potential instability. Furthermore, the absence of a clear relationship between electrical conductivity and ESP (or ESI), for the ASWAT scores, highlights the difficulty of using these descriptive comparisons as stability predictors; this is because other soil physico–chemical properties affect structural stability. This is demonstrated by two examples; *(i)*, the B002 soil has an ESI of 0.22 and the N001 soil has an ESI of 0.15 (indicating stability for both soils), yet neither soil is stable according to their ASWAT scores and, *(ii)*, both the B003 and H001 soils have similar ESP and electrical conductivity values, yet the assigned ASWAT scores indicated dissimilar structural stability. This may be, in part, explained by the suite of clay phyllosilicates in each Vertosol. The H001 soil has a much smaller content of 2:1 swelling phyllosilicates than the B003 soil, while the B002 soil has a smaller content of 2:1 swelling phyllosilicates than the N001 soil. This link is observed in chapter 3 and chapter 4 between the content of 2:1 swelling phyllosilicate clays and the $SI_{<2}$ values of each soil. Similarly, it is apparent that an important factor controlling the ASWAT scores of the nine Vertosols is the contributions of

specific phyllosilicate minerals (*i.e.* smectite and vermiculite) in the clay fraction. Soils with similar clay mineral suites tend to have ASWAT scores that are differentiated by ESP and electrical conductivity values.

7.2.3 Comparing ESP, ESI *and* $EC_{1:5}/Na^{+}_{exch}$ *with the stability index of clay dispersion*

7.2.3.1 Comparing all chapter 3 *soils and all chapter* 4 *soils*

To test the suitability of ESP, ESI and $EC_{1:5}/Na^{+}_{exch}$ as predictors of the stability of different Vertosols, each attribute is compared (in chapter 3) with the $SI_{<2}$ values of the nine furrow soils, and with each of the soil layers collected from the irrigated columns (chapter 4 soils). The nine furrow soils do not show any relationship where $SI_{<2}$ values are compared with either ESP, ESI or $EC_{1:5}/Na^{+}_{exch}$ (Figure 7.2*a,b,c*), while comparing the ESP, ESI and $EC_{1:5}/Na^{+}_{exch}$ values with $SI_{<2}$ values for the laboratory–irrigated soils does not show any conclusive relationship (Figure 7.2*d,e,f*). For example, the chapter 4 soil samples that have large values of $SI_{<2}$ have small ESI and $EC_{1:5}/Na^{+}_{exch}$ values, but the soil samples that have small $SI_{<2}$ values are not associated with either large or small ESI and $EC_{1:5}/Na^{+}_{exch}$ values.

Despite there being no overall relationships, the $SI_{<2}$ values are larger for soil samples with bigger ESPs for each Vertosol. For each of the six Vertosols irrigated in the laboratory, increased ESPs are reflected by larger values of dispersion ($SI_{<2}$) (*e.g.* G00*i*, H002 and N002). However, ESP is not the only determinant of stability in these soils and other physico–chemical attributes are influential in determining a linear description of $SI_{<2}$. The laboratory–irrigated soils have much smaller values of ESI and $EC_{1:5}/Na^{+}_{exch}$ than the furrow soils, yet the $SI_{<2}$ values suggest that the chapter 4 soil samples have similar stability to the chapter 3 topsoil samples. This suggested that either soil electrical conductivity is not as influential in determining the stability of these soils as considered in previous research, or that other soil properties are more influential in determining soil stability *i.e.* the clay mineral suite, the exchangeable Mg^{2+} content and/or organic matter contributions. In this work, the irrigation of the soil columns in the laboratory tends to dilute the soil solution, and the subsequent electrical conductivity values tend to be similar for all treatments and all soil layers. This was likely to be the reason for the limited association between electrical conductivity and the stability of these irrigated soil samples. Consequently, the small $EC_{1:5}$ values tend to result in small values of ESI and $EC_{1:5}/Na^{+}_{exch}$, and hence, the critical ESI of 0.05 for Vertosols (McKenzie 1998) is not a useful stability descriptor for these soil samples.

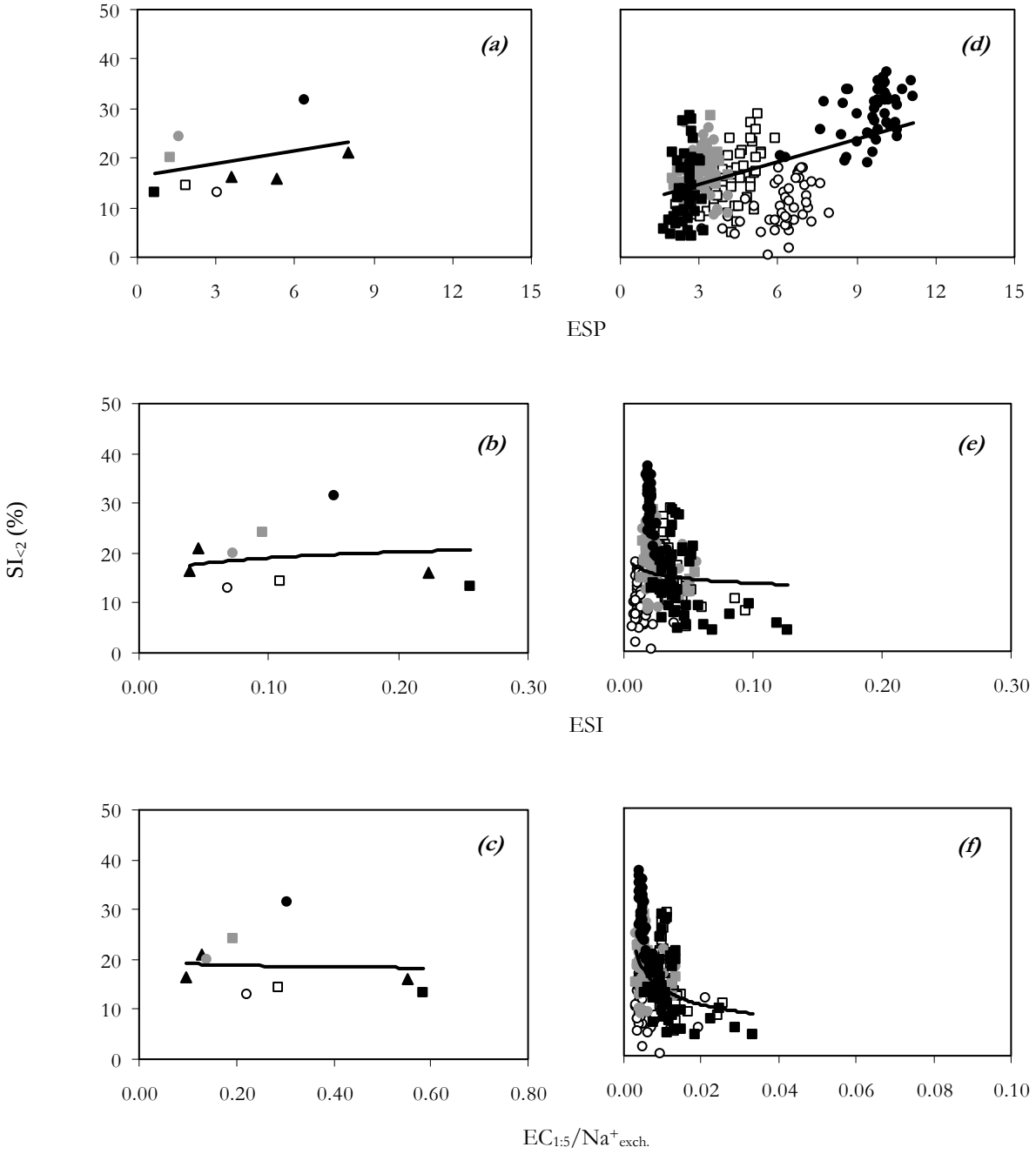

Figure 7.2 The $SI_{<2}$ values for the furrow soils related to, *(a)*, ESP (*$y=0.9x+16.3$ $R^2=0.12$*), *(b)*, ESI ($y=23.3x^{0.1}$ $R^2=0.03$) and, *(c)*, $EC_{1:5}/Na^+_{exch}$ (*$y=18.1x^{-0.1}$ $R^2=0.00$*) and the $SI_{<2}$ values for the laboratory–irrigated soils according to, *(d)*, ESP (*$y=1.5x+10.1$ $R^2=0.27$*), *(e)*, ESI (*$y=11.1x^{-0.1}$ $R^2=0.01$*) and, *(f)*, $EC_{1:5}/Na^+_{exch}$ (*$y=2.3x^{-0.4}$ $R^2=0.11$*). The soils B00*i* (▲), G001 (●), G002 (■), H001 (○), H002 (□), N001 (●) and N001 (■) are given individually.

7.2.3.2 Differentiating the irrigated Vertosols (chapter 4 *soils) according to the suite of clay phyllosilicates*

The contribution of organic matter to the irrigated soil columns is not considered in this research, due primarily to time and financial constraints. While organic contributions are not considered, the clay phyllosilicate suite is consistently associated with the different stabilities of the nine Vertosols investigated. Consequently, by grouping the soils according to those with a very small contribution of expanding lattice clays (H001) and the 'other soils' (the G00*i*, H002 and N00*i* soils), which

contain larger contributions of expanding lattice clays, the relationships between $SI_{<2}$ and ESI or $EC_{1:5}/Na^{+}_{exch}$ are improved. Figure 7.3 presents the $SI_{<2}$ values as a function of ESI and $EC_{1:5}/Na^{+}_{exch}$ for the H001 soil and for the five 'other soils'. The fitted curves for the 'other soils' have R^2 values of 0.36 for $SI_{<2}$ against ESI or $EC_{1:5}/Na^{+}_{exch}$, while the R^2 for the different H001 comparisons are 0.03 and 0.11 respectively. The R^2 values for the 'other soils' (G00*i*, H002 and N00*i*) are consistent with those obtained by Hulugalle and Finlay (2003) for the comparison of the ESI and $EC_{1:5}/Na^{+}_{exch}$ indices with the stability of several Grey Vertosols from northern NSW. However, the exclusion of laboratory–irrigated soil layers of the illitic Red Vertosol (the H001 soil) highlighted the poor suitability of these indices as predictors of stability for different irrigated Vertosols used in cotton production.

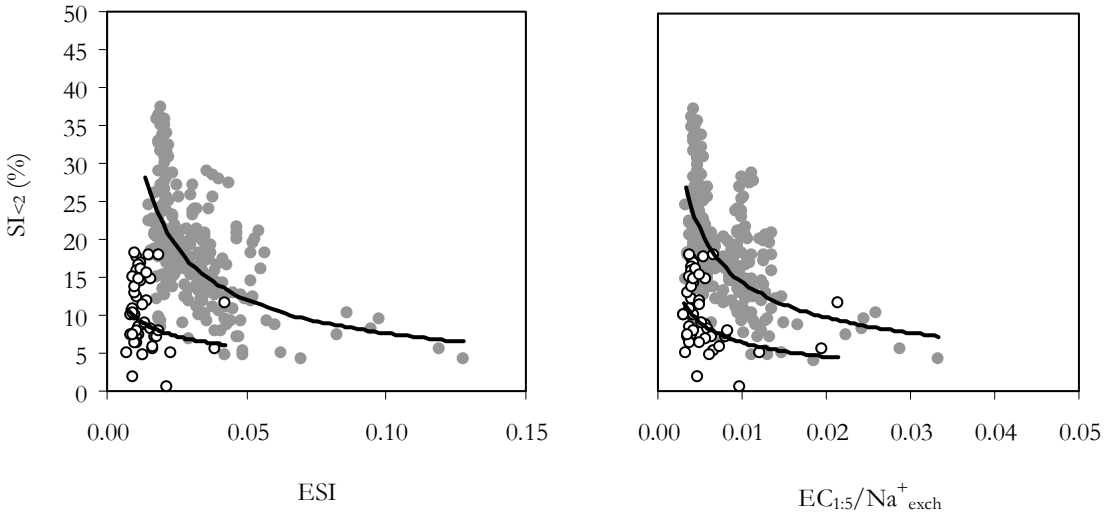

Figure 7.3 The $SI_{<2}$ values determined for the laboratory–irrigated soils as a function of ESI and of $EC_{1:5}/Na^{+}_{exch}$. The B00*i*, G00*i*, H002 and N00*i* soils (●) form one group (ESI $y=1.7x^{-0.66}$ $R^2=0.36$ and $EC_{1:5}/Na^{+}_{exch}$ $y=1.0x^{-0.57}$ $R^2=0.36$), the second group are the H001 (○) samples (ESI $y=2.2x^{-0.33}$ $R^2=0.03$ and $EC_{1:5}/[Na^{+}]_{exch}$ $y=0.64x^{-0.59}$ $R^2=0.11$).

7.2.4 The Rengasamy classification scheme

The ESI descriptor (Blackwell *et al.* 1991; McKenzie 1998; Hulugalle and Finlay 2003) was preceded by the Rengasamy classification scheme (Rengasamy *et al.* 1984). This classification scheme uses soil electrical conductivity and the Na^{+} concentration, in the forms of Total Cation Concentration (equation 1) (where TCC≈10×EC (dS m^{-1})) and SAR, to class soils according to observations of spontaneous and mechanical dispersion. In their description, Rengasamy *et al.* (1984) noted the different dispersive activity of Vertosols compared to red–brown earths (*i.e.* Chromosols and Sodosols). So to overcome this observation, they only included red–brown earths in their scheme, as these soils have similar suites of clay minerals. This exclusion highlighted the difficulties associated with considering soils dominated by different phyllosilicate clay suites.

7.2.4.1 The furrow topsoils (chapter 3 soils)

In this research, the nine initial furrow soils and the laboratory–irrigated soil samples are compared using the Rengasamy *et al.* (1984) format to demonstrate the poor suitability of this classification scheme for describing the stability of Vertosols. The TCC and SAR attributes of the furrow soils are presented in Figure 7.4. In this figure, all but three of the soils are described as potentially dispersive (*class* 2a) and have small SARs, while two other soils are potentially dispersive but contain larger SARs (*class* 2b). This classification does not appear to be consistent with the behaviour of these soils according to the ASWAT test or the values of $SI_{<2}$ obtained after spontaneous dispersion (Figure 3.1). This was shown where the different Vertosols are identified according to their dispersion classes (described in chapter 3.4.2) (Figure 7.5*a*) and according to the region from which each soil was sampled (B00*i*, G00*i*, H00*i* or N00*i*) (Figure 7.5*b*). In Figure 7.5*a*, the Rengasamy classification scheme gives a poor description of the behaviour of the nine Vertosols. For example, the N001 soil is positioned in *class* 3a (flocculated), yet it has an ASWAT score indicative of serious dispersion, and it exhibits the largest $SI_{<2}$ values of all nine soils, where spontaneous dispersion and EOE–disruption were applied. In Figure 7.5*b* each of the nine soils is grouped according to sampling region. The B00*i*, G00*i* and H00*i* soils all tend to show the same linear relationship between SAR and TCC, irrespective of stability, but the N00*i* soils both tend to have a larger ratio of TCC to SAR. This suggested that the N00*i* soils should have greater stability than the other soils, but this is not supported by the dispersion classes indicated in Figure 7.5*a*.

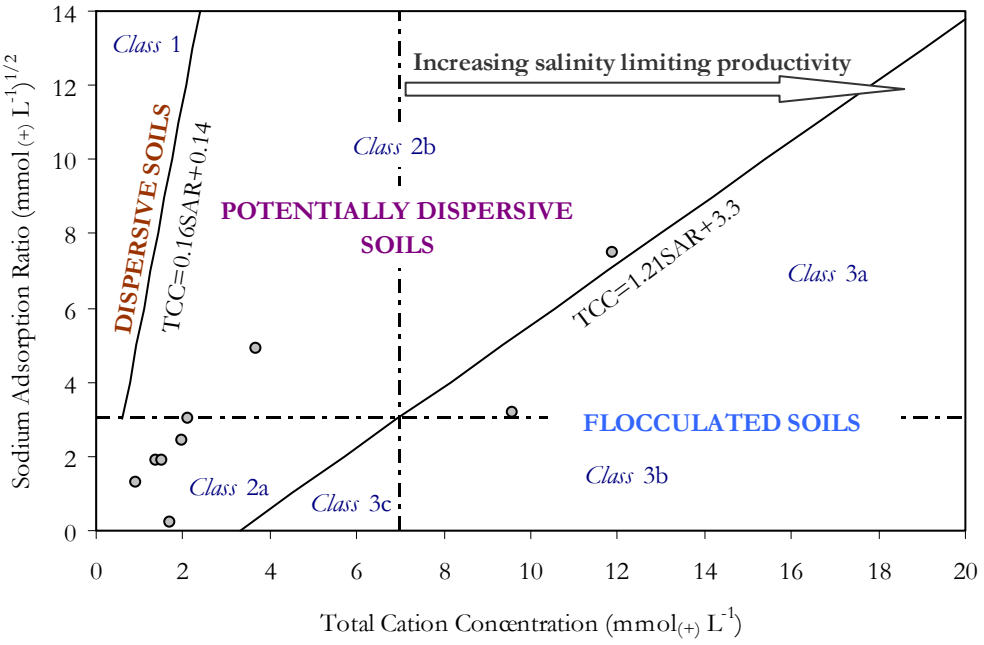

Figure 7.4 The Rengasamy classification scheme (Rengasamy *et al.* 1984); the nine Vertosols from chapter 3 have been added to estimate stability according to this classification scheme. The descriptions of each *Class* are given in Table 1.4.

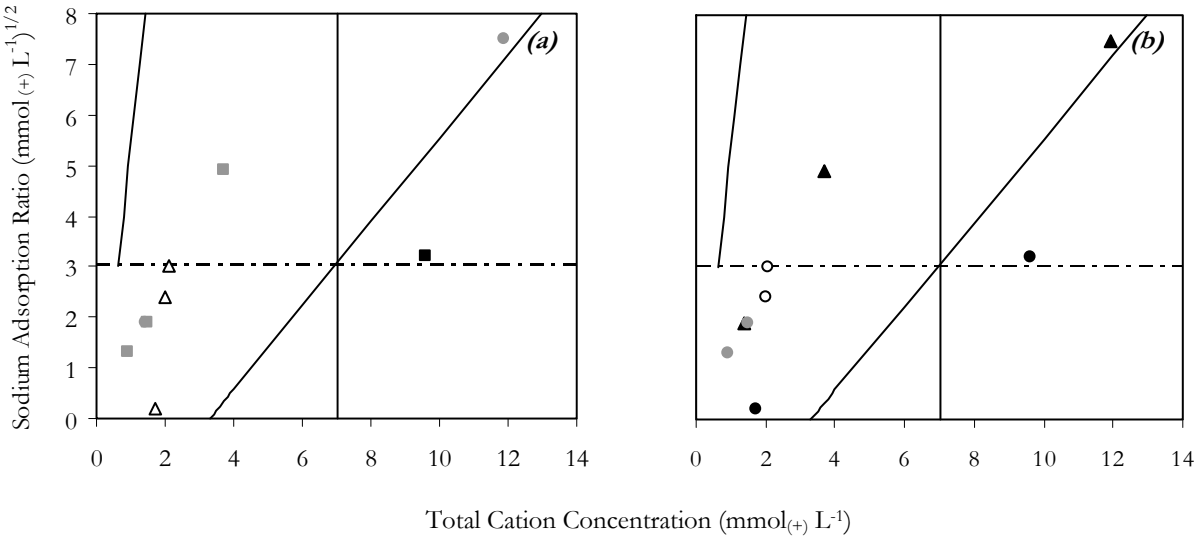

Figure 7.5 The Rengasamy classification scheme (Rengasamy *et al.* 1984) is presented for the furrow soils according to, *(a)*, $SI_{<2}$ values [0–5 (○), 5–10 (□), 10–15 (△), 15–20 (●), 20–25 (■), 25–30 (●) and >30 (■) %] and, *(b)*, as a function of sampling region [B00*i* (▲),G00*i* (●), H00*i* (○), and N00*i* (●)].

7.2.4.2 The laboratory irrigated soils (chapter 4 *soils)*

The soil samples collected from the laboratory irrigated columns (chapter 4 soils) (Figure 7.6) are all described as potentially dispersive according to their SARs and TCCs. These soil samples have very similar conductivities, and hence similar TCC values, irrespective of the applied irrigation treatment or the sampling site from which soil columns were obtained. This is indicative of leaching during irrigation, which reduced the electrical conductivity values of the G00*i*, H00*i* and N002 soil columns by approximately 0.1 dS m^{-1}, and the electrical conductivities of the N001 soil columns by approximately 0.8 dS m^{-1}. Like the ESI and $EC_{1:5}/Na^{+}_{exch}$ descriptors, this influenced the classification of these soils using the Rengasamy classification scheme (Rengasamy *et al.* 1984).

The irrigated soil samples all tend to have TCCs less than 4 and SARs less than 6, which gives a small distribution of data, and this distribution does not reflect the range of observed $SI_{<2}$ values of these soils. Figure 7.7*a* shows that the soils with $SI_{<2}$ values of greater than thirty, have largest SARs and TCCs, while the soils that have smaller TCCs and SARs have consistently smaller $SI_{<2}$ values. However, this trend is more a reflection of the individual soils, rather than the SAR and TCC values of each soil sample. Figure 7.7*b* shows the distribution of the six different Vertosols (G00*i*, H00*i* and N00*i*) marked by sampling region, and shows three distinct groups. The G00*i* and N002 soils tend to have SARs less than 3, while the N001 samples tend to have SAR values of 3–6. The H00*i* soils generally have a broad distribution of SARs (1–4 $(mmol_{(+)}\ L^{-1})^{1/2}$).

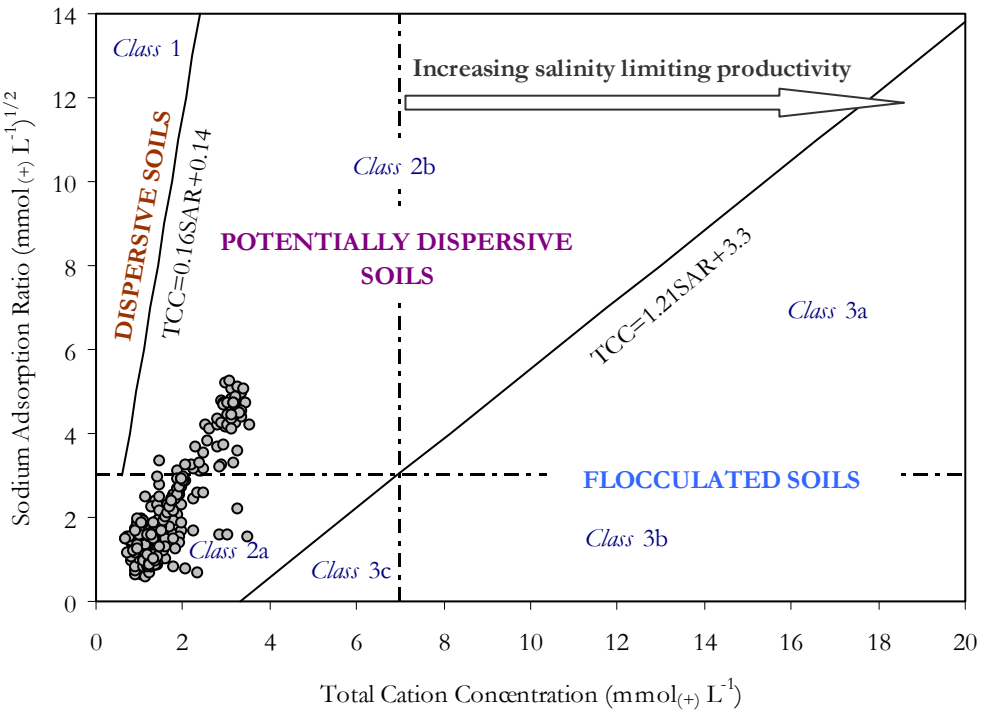

Figure 7.6 The Rengasamy classification scheme (Rengasamy *et al.* 1984) showing all soil layers from the laboratory–irrigated Vertosols (chapter 4). The descriptions of each *Class* are given in Table 1.4.

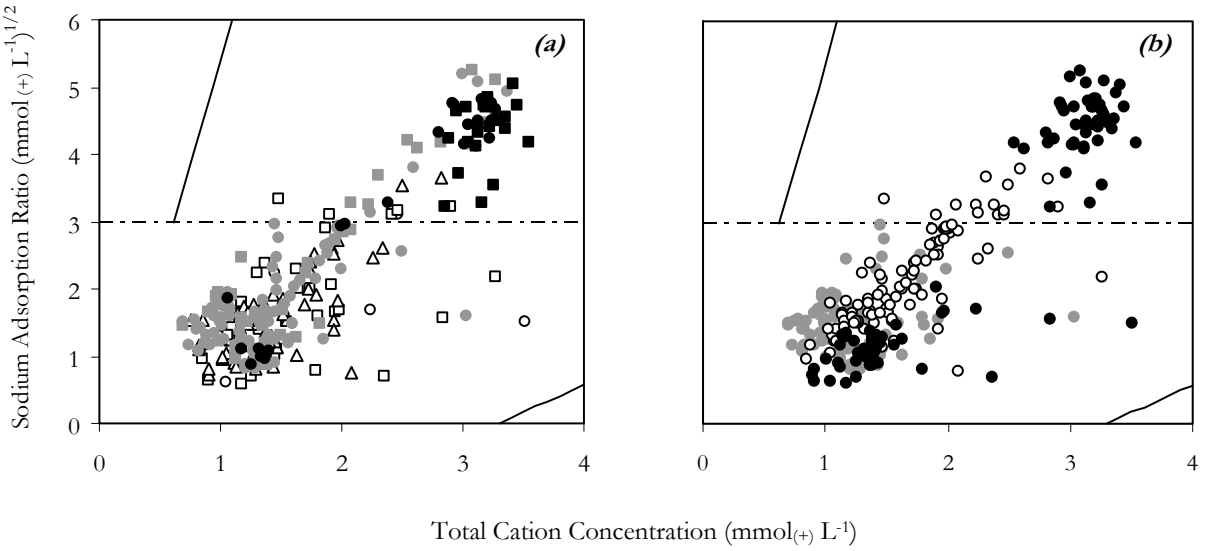

Figure 7.7 The Rengasamy classification scheme (Rengasamy *et al.* 1984) is presented for the soils irrigated in the laboratory according to, *(a)*, $SI_{<2}$ values for each soil [0–5 (○), 5–10 (□), 10–15 (△), 15–20 (●), 20–25 (■), 25–30 (●) and >30 (■) %] and, *(b)*, as a function of sampling region [B00*i* (▲),G00*i* (●), H00*i* (○), and N00*i* (●)].

7.2.5 The problems with these current predictive models

The current techniques used for predicting the dispersive potential of soils generally classify different soils according to the concentration of the soil solution (EC) and soil Na^+ contributions (Na^+_{exch}, ESP or SAR). They do not include any other soil physico–chemical attributes (Ca^{2+}_{exch}, Mg^{2+}_{exch}, organic carbon content or clay phyllosilicate suite), and discount the effect of irrigation

water quality on the stability of immersed soils. For example, Rengasamy *et al.* (1984) only included soils dominated by similar clay mineral species (*i.e.* illite and kaolinite), while the critical ESI level (ESI <0.1 considered detrimental) for red–brown earths (Blackwell *et al.* 1991) is double the critical level applied to Vertosols (ESI <0.05 considered detrimental) (Table 7.1).

This research has shown that the quantity of 2:1 expanding phyllosilicates in the fine clay fraction, and subsequently the CEC_{eff} (determined by the clay phyllosilicate suite and organic contributions), is positively correlated with increased mechanically dispersed clay ($SI_{<2}$) for the Vertosols investigated. Furthermore, soils with larger contributions of 2:1 expanding clay minerals (G00*i* and N001) tend to have chemical properties that are influenced to a greater extent, than soils with a smaller content of these phyllosilicates, where different irrigation water treatments are compared (chapter 4).

The use of irrigation water will also influence the electrical conductivity and the SAR of the soil solution directly. For example, shaking each of the nine soils end–over–end using solutions of differing EC_w and SAR_w has a significant impact on values of $SI_{<2}$ (chapter 3). These solution effects have been well understood for more than 50 years (Quirk and Schofield 1955), yet predictions of dispersive potential do not consider these characteristics. Furthermore, there have been only limited attempts to differentiate the impacts of treatment solutions of different EC_w and SAR_w values from the impact of clean water (EC_w 0, SAR_w 0) on stability. This may be appropriate for non–irrigated rain–fed soils, but Vertosols used in cotton production are reliant on alternate water resources to supplement annual rainfall. Consequently, it is important to predict the impact of differing water quality on soil structural stability.

7.3 Developing predictions of structural stability according to soil physico–chemical properties and water quality

This research provides the opportunity to develop a prediction of the impact of different water quality parameters (EC_w and SAR_w) on the stability of Vertosols with different physico–chemical properties (*e.g.* phyllosilicate suite, exchangeable Na^+ and soil EC). Generally, the different soil samples (appendix 6) tend to have a broad range of soil chemical properties (*e.g.* ESPs range from 0–11). The soil physical properties (*e.g.* clay content) are typically less wide ranging, but the differences in clay phyllosilicate suites are substantial, and have a major impact on the different structural stabilities of these soils.

To develop a prediction of stability according to soil physico–chemical attributes and water quality parameters, three processes are undertaken: *(i)*, to identify those physico–chemical properties associated with the observed values of $SI_{<2}$, *(ii)*, to identify the impact of differing water quality on $SI_{<2}$ values and, *(iii)*, to consider the different dispersion thresholds described in chapter 3, in light of the proposed prediction technique.

7.3.1 The association between soil physico–chemical properties and $SI_{<2}$

The soil physico–chemical properties reported in the literature as those that are most influential in determining the structural condition of Vertosols are the exchangeable cations (Ca^{2+}, Mg^{2+} and Na^{+}), electrical conductivity, clay content, the proportion of fine clay and the clay phyllosilicate suite (McGarry 1996). However, previous prediction models describing potential instability do not include clay content, the proportions of different phyllosilicates (or cation exchange capacity) or the contents of exchangeable Ca^{2+} and Mg^{2+}. These properties must be considered, particularly as different Australian Vertosols show large variations in these attributes (*e.g.* Isbell 1989; McKenzie *et al.* 2004). Therefore, in this study, other soil properties, in addition to the ESP, SAR and EC, are considered. The soil attributes that were used to derive a prediction of $SI_{<2}$ were:

Soil physical properties	*Soil chemical properties*
Total clay content*	Ca^{2+}_{exch} ($cmol_{(+)}$ kg^{-1})
Coarse clay content*	Mg^{2+}_{exch} ($cmol_{(+)}$ kg^{-1})
Fine clay content*	Na^{+}_{exch} ($cmol_{(+)}$ kg^{-1})
$C_{2:1}$ clay* (contribution of coarse 2:1 phyllosilicates)	CEC_{eff} ($cmol_{(+)}$ kg^{-1})
$F_{2:1}$ clay* (contribution of fine 2:1 phyllosilicates)	Ca^{2+}:Mg^{2+} ratio
Illite clay*	ESP
Kaolinite clay*	EC ($dS\ m^{-1}$)
* *denotes estimated contributions of soil properties as a percentage of all soil material*	SAR ($mmol_{(+)}$ $L^{-1})^{1/2}$

The quantity of mechanically dispersed clay ($SI_{<2}$) is predicted for all soil samples (including all chapter 3 and chapter 4 soils) (appendix 6), using stepwise linear regression. This was done using the $SI_{<2}$ values obtained after EOE–disruption of each soil sample for 30 minutes in de–ionised water (solution T102). The stepwise model is used to recognise those soil attributes that are most strongly associated with the observed $SI_{<2}$ values. In addition, all soil properties strongly associated with $SI_{<2}$ values are examined, and dependent soil attributes are not included *i.e.* only Na^{+}_{exch} or ESP was included, not both.

Once soil attributes were selected, standard least squares regression is used to derive a linear prediction of mechanically dispersed clay using the $SI_{<2}$ values. The selected predictor of dispersion (*Dispersion in water*) is given by equation 20.

$$\begin{aligned} \textit{Dispersion in water } (D_w) = {} & 8.65 + 3.32Na^{+}_{exch} + 0.92CEC_{eff} - 4.55EC \\ & + 0.12SAR - 0.18Clay - 9.08Ca^{2+} : Mg^{2+} \end{aligned} \qquad [20]$$

The predicted *Dispersion in water* (D_w) of all soil samples is presented in Figure 7.8 against the measured $SI_{<2}$ values. This model gives a robust description of $SI_{<2}$ (R^2 of 0.65), but the linear trend tends to reflect the influence of two soils in particular. In this research, the N001 soil samples are consistently more dispersive than the other soils, and dominate the larger prediction values of D_w. The least dispersive illitic H001 soil dominates the smaller estimates of mechanically dispersed clay. The other soils tend to occupy the central positions of this function.

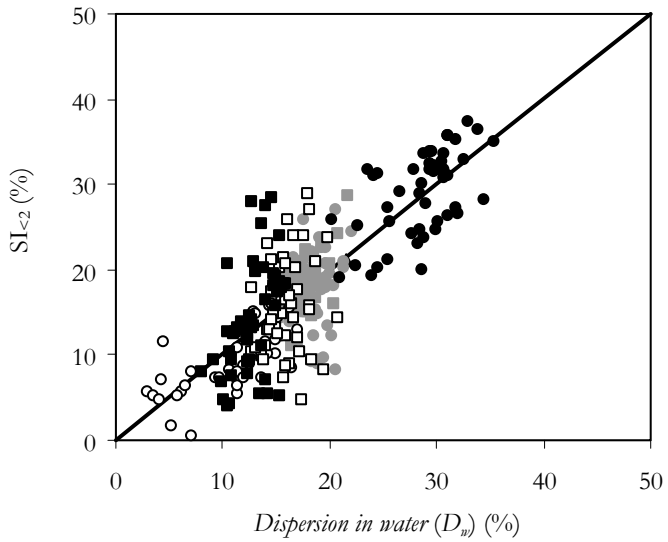

Figure 7.8 The measured $SI_{<2}$ values for all soil samples as a function of the *Dispersion in water* (D_w) prediction ($y=x+0.03$, $R^2=0.65$). The soils have been labelled according to soil site [B00*i* (▲), G001 (●), G002 (■), H001 (○), H002 (□), N001 (●) and N001 (■)].

Using the D_w prediction, increased contributions of Na^+ (Na^+_{exch} and SAR) and a larger CEC_{eff} are associated with increased dispersion (larger values of $SI_{<2}$), while larger values of electrical conductivity, clay content and a reduced Ca^{2+}:Mg^{2+} ratio are associated with increased stability (smaller values of $SI_{<2}$). Throughout this research, the suite of clay phyllosilicates has been consistently linked with the structural condition of the different Vertosols. However, in this prediction, no contribution of clay phyllosilicate type is directly included by the stepwise regression approach. Instead, this model includes the CEC_{eff} and clay content as descriptors of the clay mineral environment. In chapter 3, the CEC_{eff} was the soil property which gave the strongest correlation

with the observed values of $SI_{<2}$; those soils with larger exchange capacities are those soils with larger contributions of 2:1 expanding lattice phyllosilicates (the G00*i* and N001 soils).

7.3.2 The impact of water quality on $SI_{<2}$

7.3.2.1 Development of a prediction of $SI_{<2}$ according to water quality characteristics

The stability of the nine Vertosols, after EOE–disruption using 'clean' water (solution T102), is predicted according to physico–chemical attributes using equation 20. However, this prediction does not account for the effects of increasing the EC_w and SAR_w of immersion solution on the mechanical dispersion of clay–sized particles. Consequently, the $SI_{<2}$ values obtained using EOE–disruption, where soils are shaken in the FW00*i*, T102, T30*i*, T40*i* and T50*i* solutions, were used to estimate the effect of water quality treatments on mechanical dispersion.

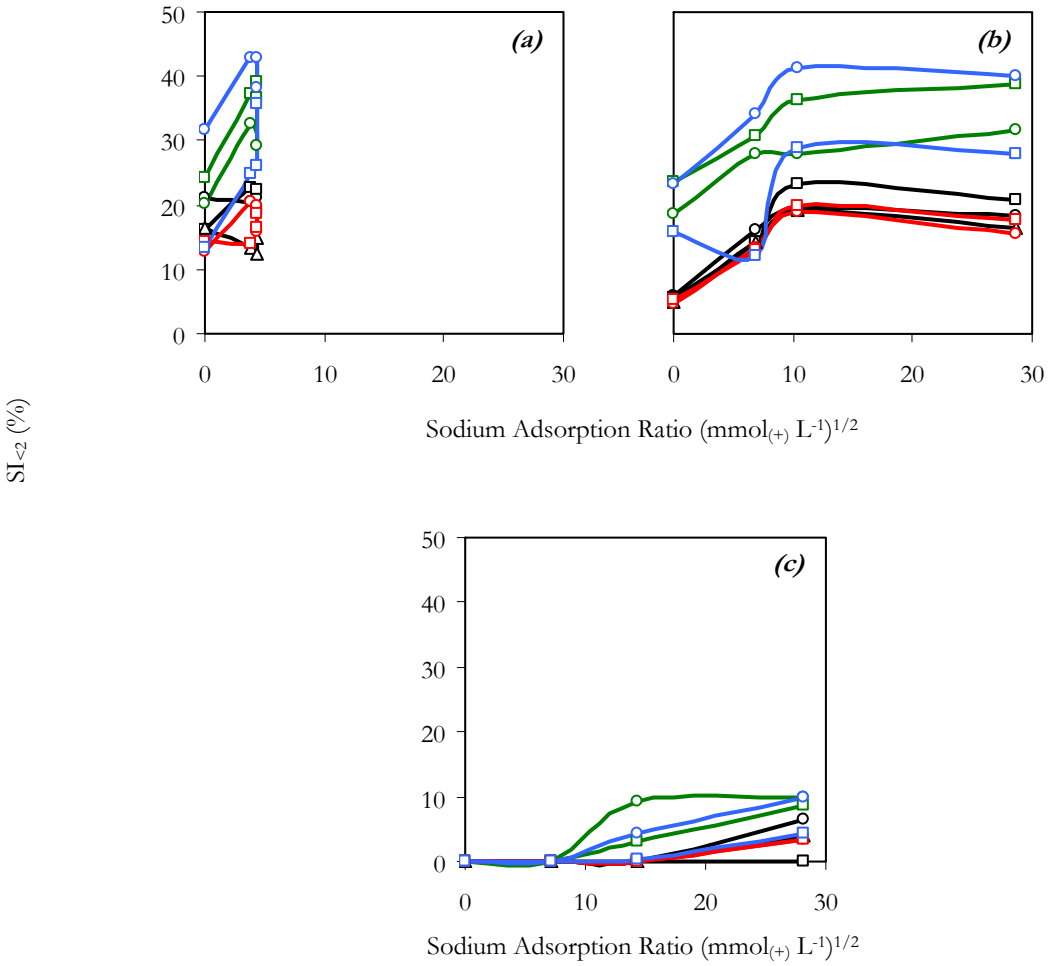

Figure 7.9 Values of $SI_{<2}$, at each of three different EC_w intervals of 0.2 *(a)*, 0.5 *(b)* and 2.7 *(c)* (dS m^{-1}), with increasing SAR_w [B001 (○), B002 (□), B003 (△), G001 (○), G002 (□), H001 (○), H002 (□), N001 (○) and N002 (□)].

In chapter 3, it was shown that the T30*i*, T40*i* and T50*i* solution treatments generally resulted in similar dispersion trends for each of the nine Vertosols, but the magnitude of $SI_{<2}$ values differed

for each of the different furrow topsoils (Figure 7.9). The B00*i* and H00*i* soils tend to have similar $SI_{<2}$ values for each of the T30*i*, T40*i* and T50*i* treatments applied, while the N002, G001, G002 and N001 soils all tend to show larger values of $SI_{<2}$ for each treatment SAR_w applied.

As the nine Vertosols all have similar trends in $SI_{<2}$ values for the SAR_w treatments, the impact of the different irrigation solution parameters (EC_w and SAR_w) is used to develop a prediction of average $SI_{<2}$. Unlike the soil physico–chemical properties that described $SI_{<2}$ by *Dispersion in water* (D_w), there is no linear relationship that describe the interaction of EC_w and SAR_w for descriptions of the observed $SI_{<2}$ values. Therefore, a non–linear function is applied for this description. Initially, a stepwise statistical model is applied to derive associations between the input attributes (EC_w and SAR_w) and the $SI_{<2}$ values using a surface response function. Then, multi–linear regression is applied to develop a prediction of the $SI_{<2}$ values (the *Dispersion under irrigation* function) obtained using EOE–disruption and the FW00*i*, T102, T30*i*, T40*i* and T50*i* solutions. The *Dispersion under irrigation* function is given by equation 21, where EC_w (dS m^{-1}) and SAR_w are the characteristics of each treatment solution applied (Tables 3.1–2).

$$\begin{aligned} \textit{Dispersion under irrigation } (D_i) = \; & 23.66 - 13.07EC_w + (EC_w - 0.90)(2.02\,(EC_w - 0.90)) \\ & + 0.61SAR_w + (SAR_w - 7.98)(-0.02\,(SAR_w - 7.98)) \end{aligned} \qquad [21]$$

The model given in Figure 7.10 shows the fitted D_i function by using all EC_w values of 0–3 dSm^{-1} and all SAR_w values of 0–30. Thus, the predicted average $SI_{<2}$ value for these Vertosols, where EOE–disruption is applied using 'clean water' (T102), is indicated by the point ○ in Figure 7.10; where EC_w and SAR_w are both equal to 0. Any point along the *x*–axis (the EC_w axis) represents the effect of increasing the electrolyte concentration of immersion solution on stability, while maintaining SAR_w at zero. Similarly, the effect of increased SAR_w, on stability, can be described at any interval of EC_w.

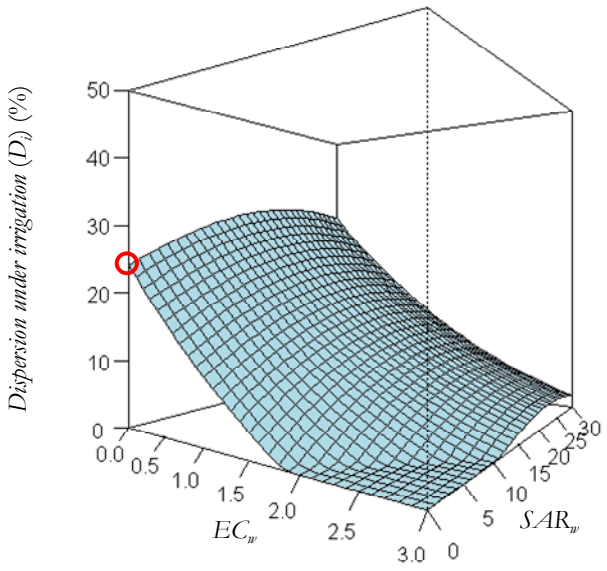

Figure 7.10 The predicted *Dispersion under irrigation* (D_i) response surface fitted to all EC_w values between 0.0 and 3.0 (dS m^{-1}) and all SAR_w values between 0 and 30 ($mmol_{(+)}\ L^{-1})^{1/2}$. The predicted average $SI_{<2}$ value for these Vertosols where EC_w and SAR_w are both equal to 0 is indicated by ○.

This D_i prediction averages the extent of dispersion for all nine Vertosols for each combination of EC_w and SAR_w. However, to develop a predictive tool describing the structural stability of these Vertosols in different EC_w and SAR_w solutions, and to link this to the physico–chemical attributes of each soil, it is necessary to consider the effect of water quality in the same way for all the investigated soils.

7.3.2.2 Predicting $SI_{<2}$ for individual Vertosols according to water quality characteristics

Due to the similar trends in $SI_{<2}$, where soils are treated using the T30*i*, T40*i* and T50*i* solutions, it was expected that the D_i function could be used to describe the stability of each different Vertosol. To do this, the D_i prediction needed to be adjusted for each soil. This can be done by considering equation 21 at the point where EC_w and SAR_w are equal to zero (the *y*–intercept). This point of the D_i function represents the predicted $SI_{<2}$ after EOE–disruption in the T102 solution; this is termed $SI_{<2\ (T102)}$, and the given value of the $SI_{<2\ (T102)}$ in equation 21 is 23.66. Consequently, by substituting the actual $SI_{<2\ (T102)}$ values for each of the different Vertosols into equation 21, the D_i function can be adjusted to describe the response of each of the different Vertosols to changes in water quality. This is described by the *Dispersion of irrigated Vertosols* (D_iV) function, shown in equation 22.

$$\begin{aligned} \textit{Dispersion of irrigated Vertosols}\,(D_iV) = {} & SI_{<2\,(T102)} - 13.07EC_w + (EC_w - 0.90)(2.02\,(EC_w - 0.90)) \\ & + 0.61SAR_w + (SAR_w - 7.98)(-0.02\,(SAR_w - 7.98)) \end{aligned} \quad [22]$$

Figure 7.11 gives the *Dispersion of irrigated Vertosols* function for two of the soils investigated (G001 [$SI_{<2\ (T102)}$=20.1] and H001 [$SI_{<2\ (T102)}$=12.9]). The actual $SI_{<2}$ values obtained after EOE–disruption using the T30*i*, T40*i* and T50*i* solutions and the D_i prediction (equation 21) are included for each of the soils. Generally, the D_iV function tends to underestimate the $SI_{<2}$ values for the G001 soil, but gives an accurate prediction of the $SI_{<2}$ values of the H001 soil.

Similarly, when the *Dispersion of irrigated Vertosols* function is fitted using the $SI_{<2\ (T102)}$ values for the B00*i*, G002, H002 and N00*i* soils there are two trends. The B00*i* and H002 soils tend to have $SI_{<2}$ values that are accurately predicted by the D_iV function. In contrast, D_iV tends to under–estimate the $SI_{<2}$ values for the G002 and N00*i* soils. This reflects the differences between the $SI_{<2}$ values for the nine Vertosols, where the four G00*i* and N00*i* soils are less stable than the five B00*i* and H00*i* soils. In this case, the similar stabilities of the B00*i* and H00*i* soils are expected to have a greater influence on the derived model of stability (equation 21).

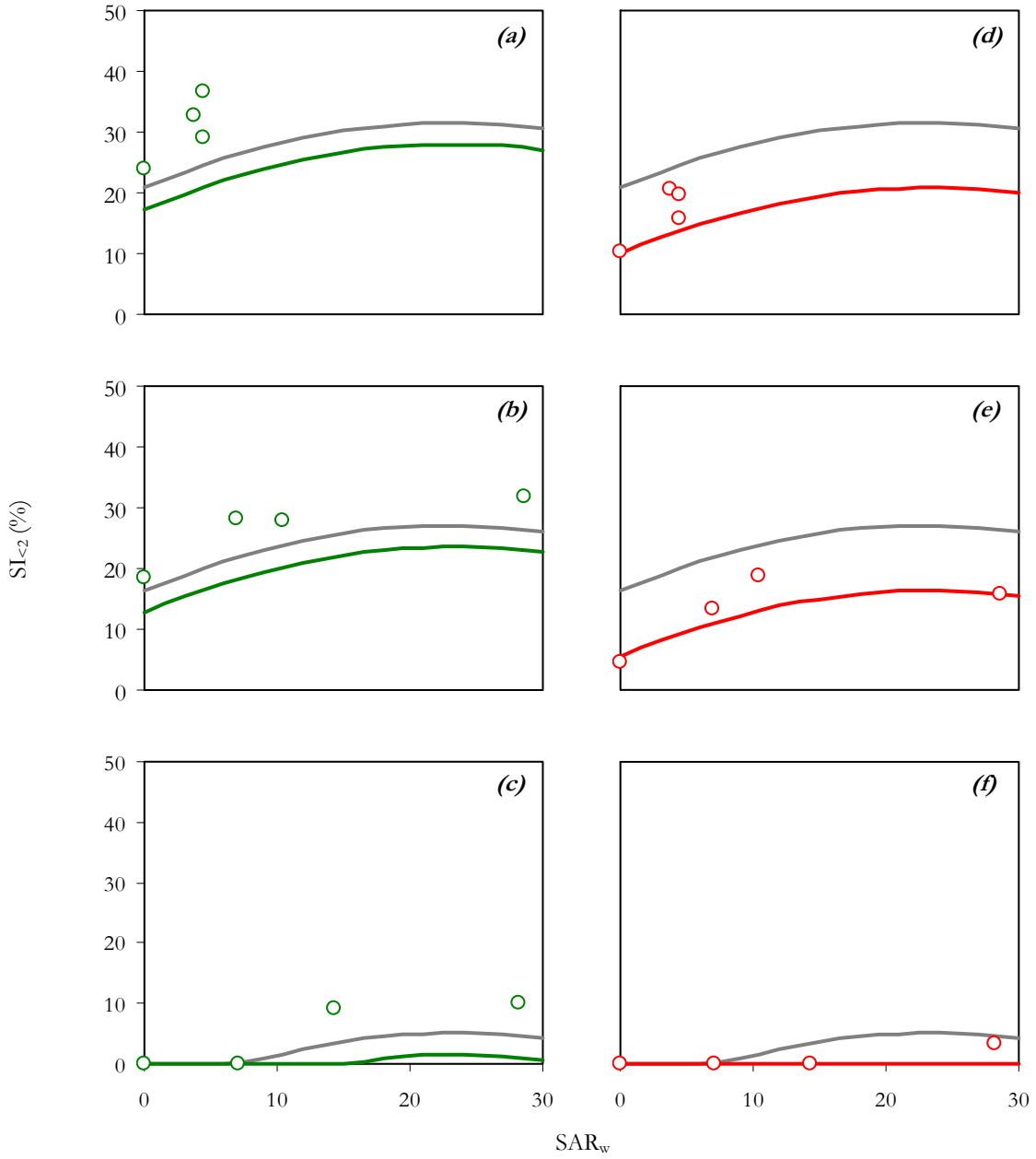

Figure 7.11 The actual values of $SI_{<2}$ obtained after the EOE–disruption of the G001 (○) soil in solutions of, *(a)*, EC 0.19, *(b)*, EC 0.47 and, *(c)*, EC 2.35 (dS m^{-1}) and of the H001 (○) soil in solutions of, *(d)*, EC 0.19, *(e)*, EC 0.47 and, *(f)*, EC 2.35 (dS m^{-1}). For each of the soils the D_iV [G001 (—) and H001 (—)] and D_i (—) are given.

7.3.3 Summary of the dispersion classes

In chapter 3 classes were derived to characterise the magnitude of $SI_{<2}$ after soils were treated with EOE–disruption for 30 minutes. These dispersion classes are:

Class 1	$SI_{<2}$ 0–10 %	very limited dispersion
Class 2	$SI_{<2}$ 10–15 %	limited dispersion
Class 3	$SI_{<2}$ 15–20 %	moderate dispersion
Class 4	$SI_{<2}$ 20–30 %	severe dispersion
Class 5	$SI_{<2}$ >30 %	very severe dispersion

The *dispersion classes* are included here so that they may be incorporated into the descriptive model of structural stability. These classes provide the threshold increments that classify soils according to their behaviour in solutions of different EC_w and SAR_w increments.

7.4 A model of the structural stability of the nine Vertosols

7.4.1 The structural stability of irrigated Vertosols

A predictive model of structural stability is derived using the *Dispersion of irrigated Vertosols* (D_iV) function, where $SI_{<2\ (T102)}$ values are predicted using D_w. The *dispersion classes* are used to classify the predicted stability of the different Vertosols according to changes in EC_w and SAR_w. This model (Figure 7.12) is prepared to predict the extent of clay dispersion at all intervals of EC_w between 0 and 3 (dS m^{-1}), which represent the usual range of EC_w values of irrigation waters (Ayers and Westcot 1985), and all SAR_w intervals between 0 and 30 $(mmol_{(+)}\ L^{-1})^{1/2}$. The x– and z–axes of the predictive model are described by the irrigation solution parameters EC_w and SAR_w, respectively. The y–axis is described by the D_iV function, which includes a prediction of $SI_{<2\ (T102)}$ given by D_w for different Vertosols according to different physico–chemical properties (equation 20). Therefore, the D_iV function gives a predicted response describing the expected dispersion of a soil with a specific D_w, where EC_w and SAR_w are not equal to zero.

For the prediction model given in Figure 7.12, the FAO criterion describing saline irrigation solutions is included (Ayers and Westcot 1985). According to the FAO, irrigation solutions that have an EC_w greater than 0.7 (dS m^{-1}) should restrict the growth of certain sensitive crop species. Cotton (*Gossypium hirsutum*) is a crop which is tolerant of salinity and can be irrigated with waters with much larger EC_w values than 0.7 (dS m^{-1}), but some crops grown in rotation with cotton (*e.g.*

soybean [*Glycine max*] and maize [*Zea mays*]) are less tolerant of saline conditions. In addition, where the climate is not suitable for cotton production, other irrigated Vertosols are used for the production of much more sensitive crops *e.g.* paddy rice (*Oriza sativa*) and sugarcane (*Saccharum officinarum*). Ayers and Westcot (1985) indicated that cotton suffers potential losses in yield only after the EC_w of irrigation water exceeds 5 (dS m^{-1}); maize, sugarcane, rice and soybean crops are likely to suffer yield losses where the EC_w of irrigation water exceeds between approximately 1.0 and 3.3 (dS m^{-1}). However, the overall impact of salinity on the yield of these crops will depend on soil texture. For example, McKenzie (1998) indicated that cotton grown on 'very highly saline' Vertosols would potentially suffer yield losses. He suggested that a 'very highly saline medium' clay soil would have a root zone $EC_{1:5}$ of 1.33 (dS m^{-1}), while a 'very highly saline' heavy clay soil would have a root zone $EC_{1:5}$ of 1.72 (dS m^{-1}).

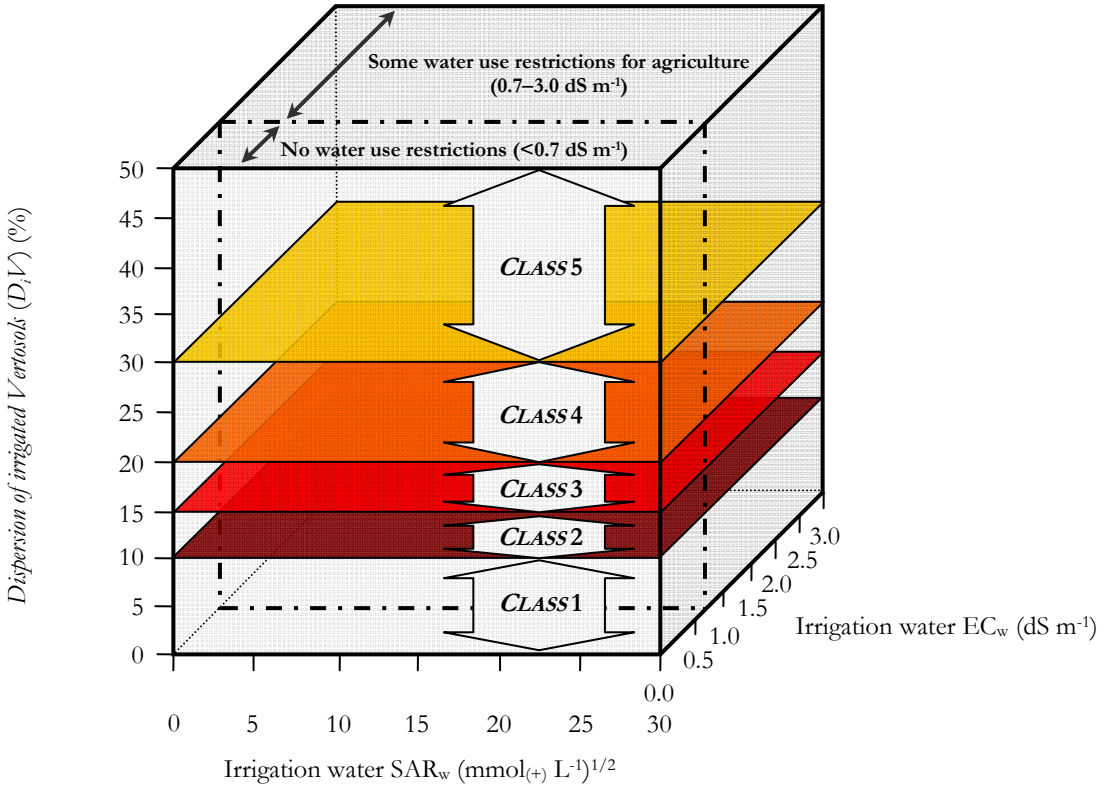

Figure 7.12 The predictive model, describing the structural stability of the nine different Vertosols in solutions of different EC_w and SAR_w. In this model the dispersion class limits occur at D_iV values of 10 (■), 15 (■), 20 (■) and 30 (■) %. The impact of water quality on the stability of different Vertosols is described by D_iV, where the D_w function gives the predicted value of $SI_{<2\ (T102)}$. The regions of 'No water use restrictions' and 'Some water use restriction for agriculture' represent the degree of restrictions applied by the FAO on irrigation supplies according to crop water availability (Ayers and Westcot 1985).

7.4.2 Modelling the stability of each of the nine Vertosols

For each of the nine Vertosols, the $SI_{<2}$ values obtained using the T30*i*, T40*i* and T50*i* solutions are compared to the prediction model described in Figure 7.12. The actual $SI_{<2}$ values are compared

with the D_iV stability predictions for each soil at three intervals; *(i)*, for changes in SAR_w at EC_w 0.19, *(ii)*, for changes in SAR_w at EC_w 0.47 and, *(iii)*, for changes in SAR_w at EC_w 2.35. At each of these three EC_w intervals a slice is taken through the z–axis (Figure 7.13), and the D_iV function prepared using the specified EC_w and all values of SAR_w (0–30). These predictions are presented for each Vertosol individually in Figures 7.14–17 (the B00*i*, G00*i*, H00*i* and N00*i* soils, respectively). Each figure gives all three fitted D_iV predictions (*(i)*, *(ii)* and *(iii)*) and the actual $SI_{<2}$ values of each individual soil for each treatment series (T30*i*, T40*i* and T50*i*).

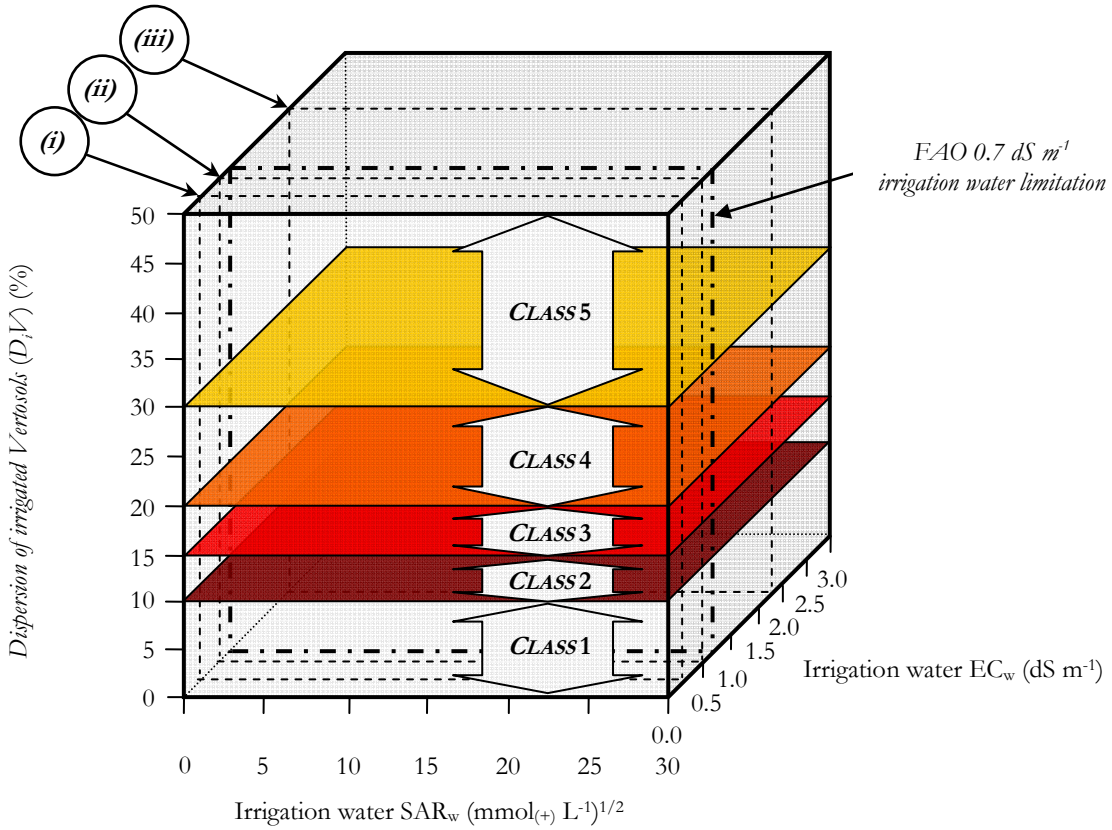

Figure 7.13 A predictive model for describing the structural stability of the nine different Vertosols in solutions of different EC_w and SAR_w. In this model the dispersion class limits occur at D_iV values of 10 (■), 15 (■), 20 (■) and 30 (■) %. The impact of water quality on the stability of different Vertosols is described by D_iV, where the D_w function gives the predicted value of $SI_{<2\ (T102)}$. The cross section slices (*(i)*, *(ii)* and *(iii)*) represent the irrigation water EC_w intervals used during the treatment of each of the nine Vertosols using the different T30*i*, T40*i* and T50*i* solutions.

Figures 7.14–17 show the suitability of the developed model for describing the stability of the nine topsoils. The best predictions tend to occur where soils have been treated in solutions of largest EC_w (at any SAR_w) or with solutions that contained SAR_w values approaching zero. Overall, the D_iV function gave a robust description of the actual $SI_{<2}$ values of the B00*i* and H00*i* soils for all the treatments. However, the D_iV function tends to underestimate the extent of dispersion occurring for the G00*i* and the N00*i* soils. For these soils, D_iV tends to be consistently less than the actual $SI_{<2}$ values, where the T30*i* (EC_w 0.19 dS m^{-1}) and T40*i* (0.47 dS m^{-1}) series treatments are compared. These inconsistencies reflect the dataset used to prepare the response functions; the G00*i* and N00*i*

soils exhibit more variable $SI_{<2}$ values for each EC_w–SAR_w treatment solution, while the five B00*i* and H00*i* soils all have very similar stabilities, irrespective of the applied treatment solution.

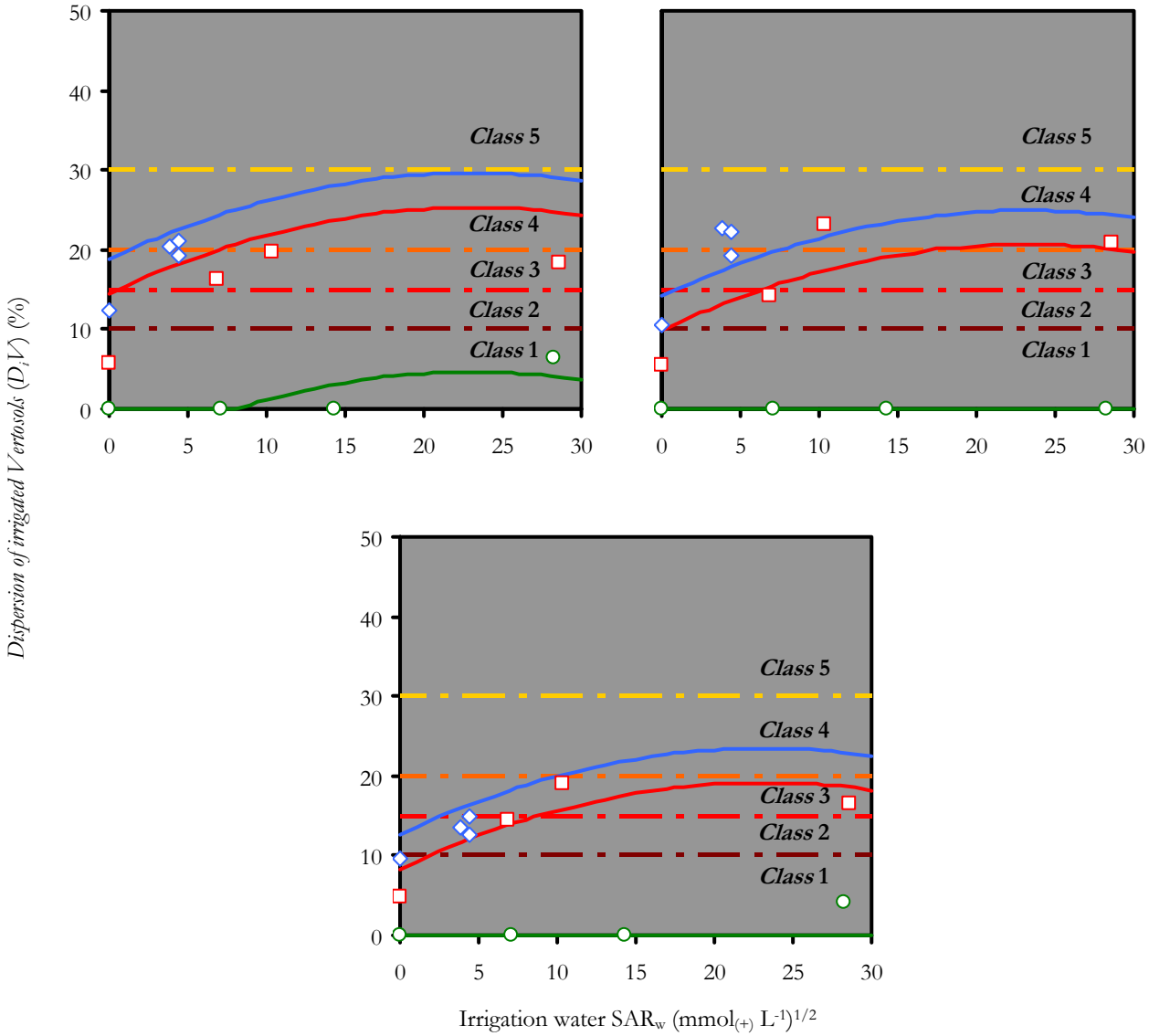

Figure 7.14 Predicted D_iV for the soils, *(a)*, B001, *(b)*, B002, and *(c)*, B003. For each soil, the three slices *(i)*, *(ii)* and *(iii)* represent predicted mechanically dispersed clay after EOE–disruption using solutions of EC_w 0.19 (—), 0.47 (—) and 2.35 (—) dSm^{-1}, between the SAR_w values of 0 and 30. The dispersion class thresholds are given where D_iV equals 10 (—), 15 (—), 20 (—) and 30 (—) %. The actual values of $SI_{<2}$ are given according to the EC_w of the treatment solutions applied; EC 0.19 (◇), 0.47 (□) and 2.35 (○) dS m^{-1}.

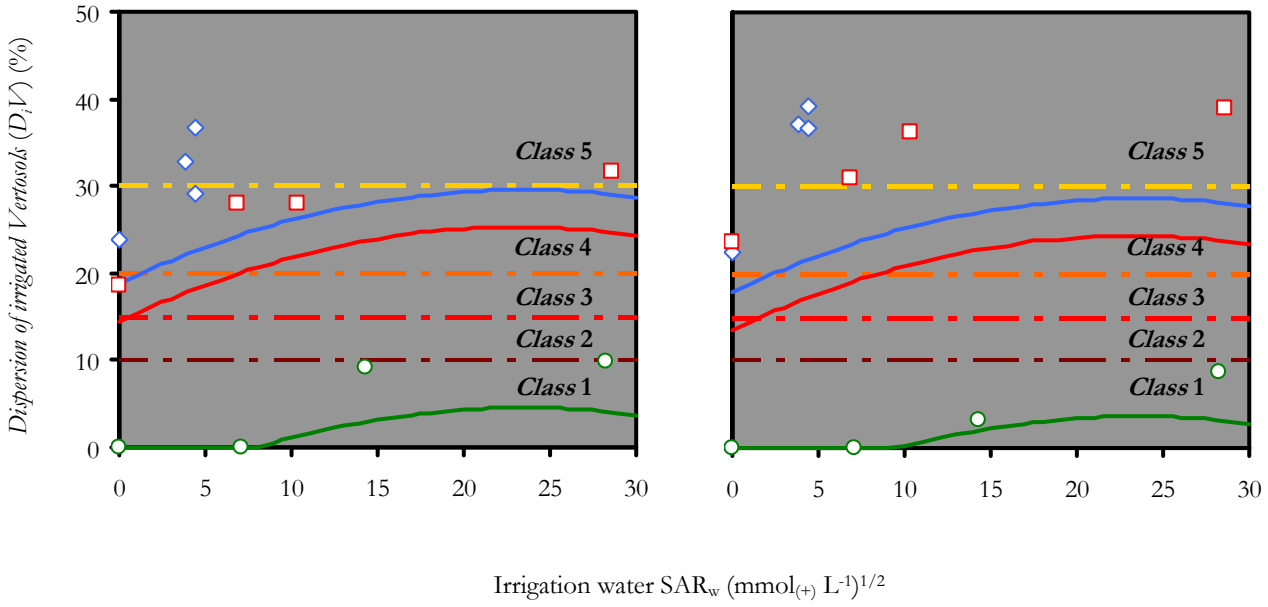

Figure 7.15 Predicted D_iV for the soils, *(a)*, G001, and *(b)*, G002. For each soil, the three slices *(i)*, *(ii)* and *(iii)* represent predicted mechanically dispersed clay after EOE–disruption using solutions of EC_w 0.19 (—), 0.47 (—) and 2.35 (—) dSm^{-1}, between the SAR_w values of 0 and 30. The dispersion class thresholds are given where D_iV equals 10 (—), 15 (—), 20 (—) and 30 (—) %. The actual values of $SI_{<2}$ are given according to the EC_w of the treatment solutions applied; EC 0.19 (◇), 0.47 (□) and 2.35 (○) dS m^{-1}.

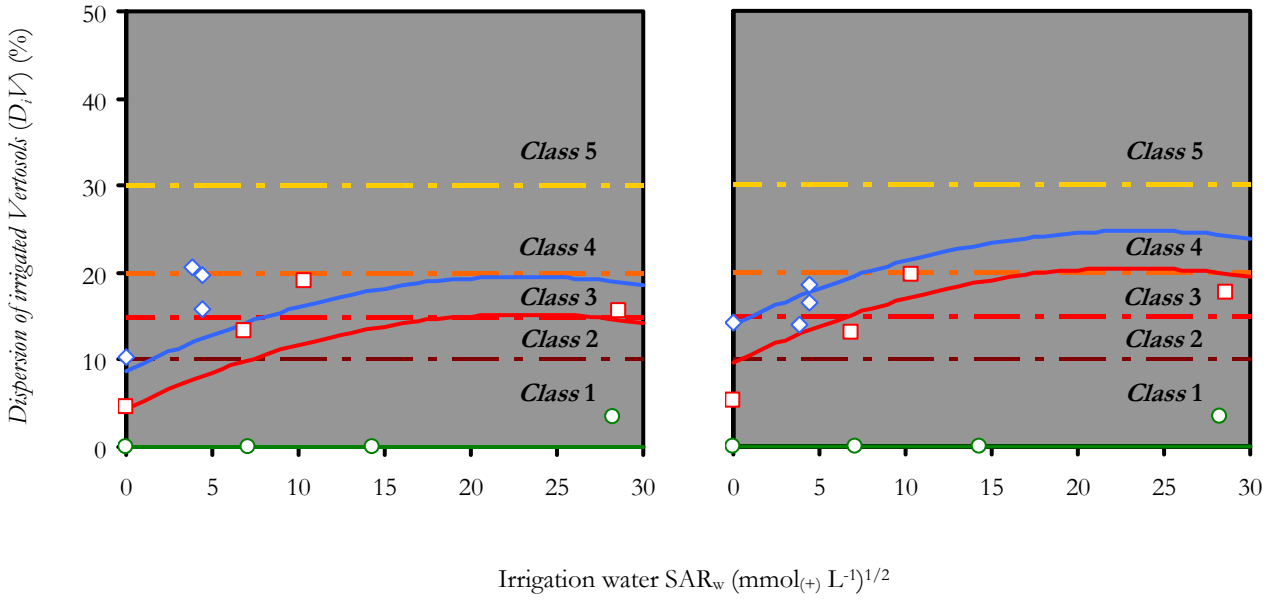

Figure 7.16 Predicted D_iV for the soils, *(a)*, H001, and *(b)*, H002. For each soil, the three slices *(i)*, *(ii)* and *(iii)* represent predicted mechanically dispersed clay after EOE–disruption using solutions of EC_w 0.19 (—), 0.47 (—) and 2.35 (—) dSm^{-1}, between the SAR_w values of 0 and 30. The dispersion class thresholds are given where D_iV equals 10 (—), 15 (—), 20 (—) and 30 (—) %. The actual values of $SI_{<2}$ are given according to the EC_w of the treatment solutions applied; EC 0.19 (◇), 0.47 (□) and 2.35 (○) dS m^{-1}.

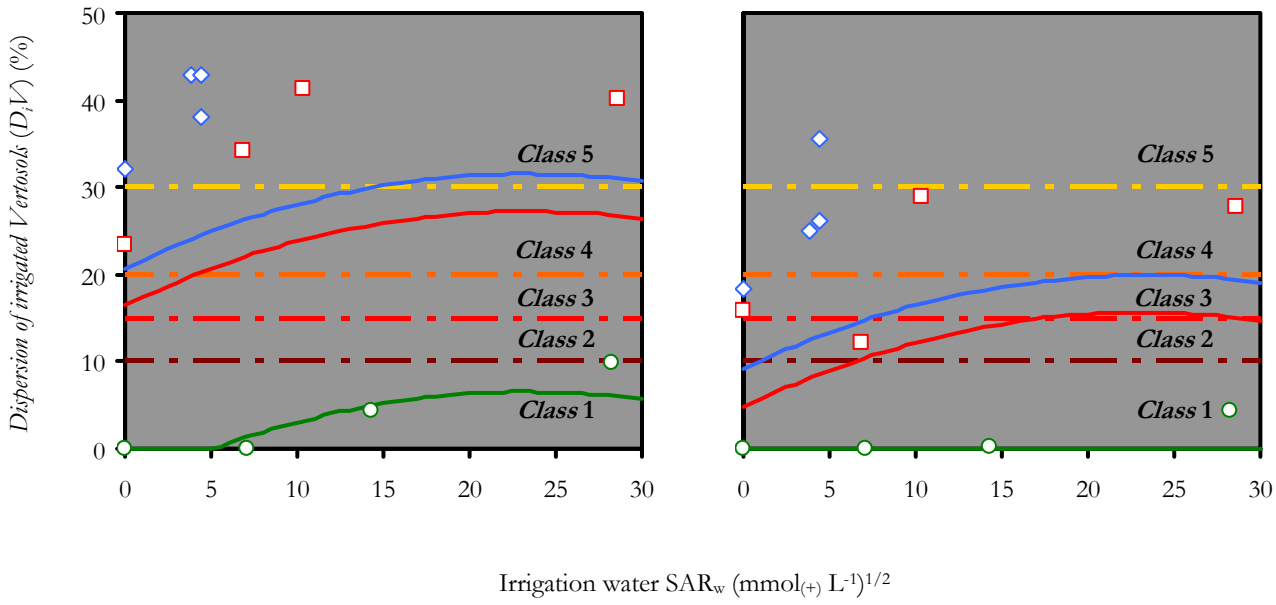

Figure 7.17 Predicted D_iV for the soils, *(a)*, N001, and *(b)*, N002. For each soil, the three slices *(i)*, *(ii)* and *(iii)* represent the predicted increments of mechanically dispersed clay after EOE–disruption using solutions of EC_w 0.19 (—), 0.47 (—) and 2.35 (—) dSm^{-1}, between the SAR_w values of 0 and 30. The dispersion class thresholds are given where D_iV equals 10 (—), 15 (—), 20 (—) and 30 (—) %. The actual values of $SI_{<2}$ are given according to the EC_w of the treatment solutions applied; EC 0.19 (◇), 0.47 (□) and 2.35 (○) dS m^{-1}.

In each of these prediction models (Figures 7.14–17), increasing the SAR_w of the T30*i* and T40*i* series led to increased estimates of clay dispersion, particularly where SAR_w is less than 15. For stability predictions at SAR_w values greater than 15, the D_iV function tends to show much smaller increases in the predicted dispersion of the Vertosols. In this region of the prediction, it is assumed that other soil attributes determine differences in the extent of clay dispersion for different Vertosols *i.e.* organic bonds or other cementing agents. These models show that only the N001 soil have predicted values of $SI_{<2}$ that occurred in *Class* 5, and this occurs only at very large values of SAR_w (15–30). This N001 soil is the least stable according to the developed prediction. The N001 soil and the B00*i*, G00*i* and H002 soils all have dispersion classes indicating spontaneous dispersion (*Classes* 4 and 5) at some increment of SAR_w for the T30*i* and T40*i* predictions. In general, the least dispersive soils (H001 and N002) do not have predicted dispersion values in any *Class* greater than 3, meaning that these soils are only moderately dispersive when shaken in solutions of SAR_w =7.5–30 (T30*i* solutions) and SAR_w =17.5–30 (T40*i* solutions). In solutions with smaller SAR_w values these soils are much more stable. Consequently, these predictions ranked the nine Vertosols in the same way as had been done using the *dispersion classes* in chapter 3.4.2. These soils have decreasing stability in the order: H001≈N002<H002<B003≈B002<B001≈G00*i*<N001.

7.5 Conclusions

In this chapter, a critical ESP of 2 appears to delineate the stable soils from those that are non–stable, where the ASWAT test is used to describe potential instability. However, when the $SI_{<2}$ values are compared using the ESP, ESI and $EC_{1:5}/Na^{+}_{exch}$ values, there does not appear to be any critical threshold intervals that delineate the stable soils from those that are not stable. Similarly, the prediction of stability using the SAR and TCC thresholds, provided by the Rengasamy classification scheme (Rengasamy *et al.* 1984), does not provide a suitable description of clay dispersion for the Vertosols investigated. This is because the stability of these Vertosols is partly determined by the suite of clay phyllosilicates and consequently, by the exchange capacity of each soil. Once these properties are considered, stability is a function of other soil attributes *i.e.* the Na^{+} content and the electrical conductivity. Consequently, a predictive model is developed to determine the extent of clay dispersion for a soil of specific physico–chemical attributes. This model incorporates the soil physico–chemical properties of each Vertosol to predict the extent of clay dispersion (*Dispersion in water*). A surface response function (*Dispersion of irrigated Vertosols*) is then used to predict the extent of dispersion in different water solutions at various increments of EC_w and SAR_w. This allows the nine Vertosols to be presented in terms of the impact of water quality on dispersion.

Initially, it was proposed that a predictive scheme similar to that developed by Rengasamy *et al.* (1984) could be developed to consider dispersion as a function of the soil electrical conductivity, the Na^{+} content (either SAR, Na^{+}_{exch} or ESP) and the clay mineral suite or the soil exchange capacity. This was not possible with the soil data set developed. This task must be undertaken as a future research opportunity.

Chapter 8

GENERAL DISCUSSION, CONCLUSIONS AND FUTURE RESEARCH OPPORTUNITIES

GENERAL DISCUSSION, CONCLUSIONS AND FUTURE RESEARCH OPPORTUNITIES

~

Future: *futūrus (L): the indefinite time yet to come*

~

8.1 The structural integrity of cotton–producing Vertosols

In eastern Australia, the Vertosols on which most irrigated cotton production occurs frequently contain sodic subsoils (ESP >5), and in some cases exhibit sodicity at the soil surface. The elevated Na^+ contributions of these soils and their other physico–chemical properties (*i.e.* clay content, clay phyllosilicate suite and solution concentrations) result in significant swelling and potential instability. In addition, the cotton industry is expected to become increasingly reliant on finite supplies of good quality irrigation water *i.e.* waters of low EC_w and small SAR_w. This is leading to the use of alternate water sources, which are potentially of poor quality and have elevated levels of EC_w and/or SAR_w. Irrigation using these solutions is likely to impact on the structural condition of both sodic and non–sodic Vertosols.

8.1.1 The irrigated Vertosols: their physico–chemical properties

In non–swelling soils, stability is generally determined by the contribution of Na^+, the electrolyte concentration of solution (EC) and by other transient soil properties (*i.e.* organic matter content). However, the primary attribute controlling the structural behaviour of Vertosols is the contribution of expanding phyllosilicate clays (*e.g.* smectite and less frequently, vermiculite). In this soil type, 2:1 expanding clays do not always dominate the phyllosilicate suite (*e.g.* Vervoort *et al.* 2003), and consequently different Vertosols may exhibit dissimilar behaviour when wetted. For example, illite and kaolinite clays have shrink swell activity that is $^1/_2$–$^1/_5$ that of the 2:1 expanding lattice phyllosilicates (Wilding and Tessier 1988). Consequently, when illite and kaolinite clays co–dominate or dominate the suite of phyllosilicates, soil structural behaviour will reflect these differences. In addition, the proportions of exchangeable Ca^{2+}, Mg^{2+}, and Na^+ influence the extent of mineral expansion during hydration. Thus, the concentration of the soil solution that is required to maintain stability will depend on the clay species and on the proportions of different exchangeable cations.

Nine Vertosols (B00*i*, G00*i*, H00*i* and N00*i*) were sampled to represent variations in phyllosilicate suites and in physico–chemical properties of cotton–producing soils from eastern Australia (Table 8.1). The distribution of the measured soil properties for these soils is generally consistent with the

documented physico–chemical attributes of other Vertosols from eastern Australia (*e.g.* Isbell 1989; Hulugalle *et al.* 1999; Hulugalle and Finlay 2003; Vervoort *et al.* 2003). The G00*i* and N00*i* soils are Black Vertosols (Isbell 1989) dominated by 2:1 expanding phyllosilicates, the B00*i* and H002 soils are Grey Vertosols, and the H001 soil is an illitic Red Vertosol. Each of these nine soils contains a topsoil clay content of between 55 and 65 %, of which 60–70 % is fine clay. The nine soils have ESPs that range between 1 and 10, ECs of 0.1 to 1.2 dS m^{-1} and CEC_{eff} values that are largest for those soils that contain more 2:1 expanding phyllosilicates.

Table 8.1
A summary of selected physico–chemical properties for the nine Vertosols
The number of (+) represent increasing contributions of 2:1 expanding lattice phyllosilicates

	Sampled furrow topsoil								
	B001	**B002**	**B003**	**G001**	**G002**	**H001**	**H002**	**N001**	**N002**
Clay content (%)	60.5	60.0	63.0	54.9	63.7	59.9	54.1	57.3	55.3
Fine 2:1 expanding clays	++++	++++½	++++	+++++	++++½	+½	+++½	++++½	+++
Coarse 2:1 expanding clays	–	+	½	++½	+++	–	+	++½	++½
Organic Carbon (%)	0.22	0.27	0.32	0.96	0.39	0.45	0.40	0.62	0.88
EC (dS m^{-1})	0.37	1.19	0.14	0.09	0.15	0.21	0.20	0.96	0.17
CEC_{eff} ($cmol_{(+)}$ kg^{-1})	35.5	40.5	40.5	51.3	48.8	30.8	38.2	49.0	43.7
Ca^{2+}:Mg^{2+} ratio	1.9	2.3	2.6	2.9	2.6	1.9	2.1	2.9	3.0
ESP (%)[a]	8.1	5.3	3.6	1.3	1.6	3.1	1.8	6.4	0.7
ASWAT score	9	3	9	0	0	4	0	9	0

[a] Vertosols with ESPs >5 % are sodic, while Vertosols with ESPs 2–5 % have been identified as potentially unstable (McKenzie 1998).

8.1.2 The irrigated Vertosols: structural stability

In the laboratory, each of the nine furrow topsoils was subjected to different stability assessment techniques involving the immersion of soil aggregates in different solutions and the application of different disruptive forces. The ASWAT test (Field *et al.* 1997) generally differentiated the dispersive potential of the nine Vertosols according to their individual physico–chemical attributes (Table 8.1). The soils with ESPs greater than 2 are moderately to seriously dispersive, while the soils with ESPs less than 2 each have ASWAT scores of 0. The magnitude of the assigned ASWAT scores for the dispersive soils is a function of the ESP and solution EC, but soils with similar ESPs and ECs do not have the same ASWAT scores. For example, the B003 and H001 soils have similar ESPs and

ECs, but have different stabilities according to the ASWAT test. Thus, the different ASWAT scores appear to reflect different contributions of 2:1 expanding lattice clays in these soils. This relationship, between phyllosilicate suite (or cation exchange capacity) and stability, is more apparent for the different Vertosols where sub–samples are treated using different disruptive forces and then using different water quality treatments. The extent of dispersion for each of the soils, after each applied disruptive force and after disruption using each treatment solution, is given in Table 8.2. In all treatments, the G00*i* and N00*i* soils are less stable than the B00*i* and H00*i* soils.

Table 8.2
A summary of the dispersion of the nine Vertosols
The (+) signs provide a rank to each of the soils according to the observed dispersion of clay after each applied treatment. Soil that was not dispersive in an applied treatment is given the sign (–)

	Sampled furrow topsoil								
	B001	**B002**	**B003**	**G001**	**G002**	**H001**	**H002**	**N001**	**N002**
Disruptive force treatments after immersion in clean water									
Spontaneous dispersion	+	–	+	+	++	–	–	++	–
EOE–disruption	++	+	+	++	++	+	+	+++	+
Ultrasonic agitation	+	++	+	+	++	+	+	+++	+
Water quality treatments applied during EOE–disruption									
T102	+	+	+	++	++	+	+	+++	+
FW00*i*	+	+	+	+++	+++	+	+	++++	+++
T30*i*	+	++	+	+++	+++	+	+	++++	+++
T40*i*	+	+	+	++	++	+	+	+++	++
T50*i*	+	–	+	++	++	+	+	++	+

In general, the application of increased disruptive force (spontaneous dispersion → EOE–disruption → ultrasonic agitation) gives greater liberation of particles of <100 μm and <2 μm. The G00*i*, H00*i* and N00*i* soils tend to show the same trends of increased $SI_{<100}$ for larger disruptive forces, but the B00*i* soils have $SI_{<100}$ values that showed a different trend. Comparing all of the Vertosols shows that the B00*i* soils have the largest $SI_{<100}$ values after the small disruptive force is applied, but these $SI_{<100}$ values are the same after EOE–disruption. This reflected the smaller organic carbon content of the Bourke soils (Table 8.1). These B00*i* soils appear to slake more extensively than the other soils when they are immersed in de–ionised water and this reflects less organic binding of soil aggregates.

The organic carbon content of each soil does not appear to be related to the dispersed clay content ($SI_{<2}$) of soils treated with different disruptive forces. For all nine Vertosols, the extent of clay dispersion is determined by the disruptive energy applied, the content of 2:1 expanding lattice clays (or CEC_{eff}), Na^+ contributions and soil solution EC (Table 8.1). The G00*i* and N001 soils have the largest CEC_{eff} values and are the most dispersive, while those soils with smaller CEC_{eff} values (the H00*i* and N002 soils) are much more stable (Table 8.2). In addition to this trend, the B002 soil shows an additional response to the disruptive treatments that is not observed for the other soils. The sodic B002 soil has similar stability to the B001 and B003 soils, where the small and medium forces are applied, but is less stable than the other Bourke soils where the largest disruptive force is applied. In this case, the force applied using ultrasonic agitation was sufficient to overcome the influence of this soils large solution EC (1.19 dS m^{-1}) on the expansion of clay particles, but the EC of the subsequent soil suspension is insufficient to cause the flocculation of dispersed clay in solution.

The different water quality solutions differentiated the nine Vertosols based on the extent of dispersion occurring as a response to treatment solution characteristics (*i.e.* EC_w and SAR_w). The treatment solutions have only a small influence on the liberation of <100 μm particles, and the observed trends in $SI_{<100}$ are typically the result of increased clay liberation in solutions of larger SAR_w.

The different Vertosols dispersed in the different water quality treatments (FW00*i*, T102, T30*i*, T40*i* and T50*i*) according to their content of 2:1 expanding lattice phyllosilicates (and the CEC_{eff}). Consequently, the G00*i* and N00*i* soils are more dispersive than the B00*i* and H00*i* soils (Table 8.2). The soils with similar clay phyllosilicate suites then tend to disperse in the different solutions according to the soil Na^+ contributions (*i.e.* Na^+_{exch} and soil solution SAR) and the electrical conductivity of each treatment solution. Treating each of these soils with solutions of larger SAR_w (*e.g.* T301–4, T401–4 or T501–4) gives more clay dispersion, while shaking the soils in solutions of larger EC_w (*e.g.* T30*i*, T40*i* or T50*i*) gives less clay dispersion.

8.1.3 The impact of irrigation water quality on selected soil properties, structural form and water retention

The treatment of each of the Vertosols using the three disruptive forces and the different water quality solutions identified the mechanisms controlling their differing stabilities after immersion. This did not necessarily describe potential changes in 'field' characteristics of Vertosols irrigated with different water quality treatments *i.e.* changes in soil chemical properties or structural condition. To investigate the impact of water quality on structurally–intact soils, columns of field soil were irrigated using different water quality solutions (FW00*i*, T102 and T401–4). The impacts of these

solutions on selected chemical properties and on soil structural condition (structural stability after immersion, structural form and water retention properties) were determined.

Irrigating these structurally–intact soils meant that, unlike the immersion techniques used to determine stability (chapter 3), the solution treatments flowed differentially through the soil matrix, according to the distribution of connected porosity. This affects changes in soil chemical and structural attributes. Each of the irrigated soils subsequently has larger ESPs where larger SAR_w solutions had been applied, and soils with larger ESPs tend to be more dispersive. However, the response of each Vertosol to the applied irrigation treatments reflected the 2:1 suite of phyllosilicate clays. The soils that have larger contributions of 2:1 phyllosilicates, and consequently larger CEC_{eff} values, are more dispersive when immersed in clean water and shaken. In addition, the soils with large CEC_{eff} values generally have greater differences in the chemical attributes (*e.g.* ESP) for soil columns irrigated with the different solutions.

The structural form attributes of the intact soils show a different response to the applied solutions than was observed during the immersion assessments of stability. Intact field soils with larger contributions of 2:1 expanding lattice clays (the G00*i* and N00*i* soils) contained a macropore distribution that does not alter greatly under the irrigation treatments. The B001, B002 and H002 soils have less 2:1 expansive clays and these soils show some small decreases in desirable structural form attributes as the SAR_w of treatment solution is increased (T401→4). The soil with a very small content of expansive clays, the illitic H001 soil, is the most stable soil where immersion and shaking techniques are applied, but is the soil most affected by the different irrigation solutions. Treating this soil using increasingly Na^+–rich waters (T401→4) results in much less porosity, smaller estimates of surface area and reduced connectivity than for the other soils. Consequently, the application of increasingly Na^+–rich waters give a rapid reduction in the desirable structural form attributes that is not observed for the other soils. A similar response is observed for the water retention properties of the G001 and H001 soils. The illitic H001 Vertosol has water retention properties that show a strong influence of the solution SAR_w treatments applied; while the 2:1 expansive clay dominated G001 soil appears much less affected by solution Na^+ content.

The structural form and the water retention studies of the structurally–intact field soils do not account for the impact of solution SAR_w on phyllosilicate swelling. The determination of the different volume contributions (solid, pore and solution) (chapter 6) shows that both the G001 and H001 soils have smaller volume fractions of solid space and more porosity where they have been treated using the increasingly Na^+–rich T40*i* solutions or using clean water (the T102 solution). Consequently, the irrigation of these soils with solutions of increasing SAR_w or with clean water results in increased phyllosilicate swelling, indicated by a smaller volume fraction of solid space. This

is despite the small observed effects of treatment solution on the chemical attributes of both soils and on the structural form attributes of the G001 soil. However, these two soils have different additional responses to the SAR_w treatments that explain the different observations of structural form and water retention. The G001 soil is more swollen after being treated with large SAR_w solutions, but appeared to maintain structural form. This is indicated by similar volume contributions of solution to each of the treated soil cores (Figure 6.7*a*). In contrast, the large SAR_w treatments of the H001 soil have a larger volume of pore space, but contain larger volumes of soil solution. In this soil, the increasingly large SAR_w treatments result in the collapse of structure and a less connected pore network. Consequently, the structural form attributes and hydraulic properties of this soil tend to describe this collapsed condition as reductions in desirable structural form attributes and degraded hydraulic properties.

8.1.4 A model describing the stability of Vertosols in solutions of different EC_w and SAR_w characteristics

The structural stability of all Vertosol samples (chapter 3 and chapter 4 soils) is comprehensively characterised by treating immersed soil using different increments of disruptive energy and different treatment solutions. The dispersed clay contributions of these soils are compared with current indicators of potential instability *i.e.* ESP, ESI or EC/Na^+_{exch}, but these do not describe the observed dispersion that occurs where these soils are subjected to wetting and disruption in the laboratory. In addition, there does not appear to be any suitable critical stability thresholds that delineate stable soils from the unstable soils using ESP, ESI or EC/Na^+_{exch}. This results from fundamental differences between these Vertosols, particularly differences between the clay phyllosilicate suites, but the ESI and EC/Na^+_{exch} ratios are also strongly influenced by the diluted electrical conductivity of the irrigated soil columns.

The predictive model developed (Figure 7.12) integrates a multitude of soil physico–chemical attributes (Na^+_{exch}, EC, SAR, Ca^{2+}:Mg^{2+}, CEC_{eff} and clay content) to describe the laboratory measured structural stability of Vertosols in a clean water solution. In this predictive model, CEC_{eff} and clay content are used to account for the different phyllosilicate suites of the soils studied. This prediction is then extended to consider the stability of Vertosols according to water quality attributes (EC_w and SAR_w). Consequently, the predictive model describes the attenuation of dispersion for different Vertosols as the EC_w of irrigation solutions is increased, or conversely as the SAR_w of treatment solutions is reduced. This model provides considerable benefit for predicting the mechanical liberation of Vertosols immersed in different solutions, and it has potential for use beyond the cotton industry for describing the stability of other soil types. However, to extend the model in this way, the *Dispersion in water* term and the *Dispersion of irrigated Vertosols* function may

require calibration to account for differences in the clay phyllosilicate suites (or clay content and CEC_{eff} values) of other soil types.

8.1.5 Cotton soils that are most likely to exhibit structural degradation where poor quality solutions are applied as irrigation supplies

The research conducted can be used to derive an estimate of those soils that will be most dispersive and those soils that will be influenced most by the application of poor quality irrigation waters *i.e.* solutions with large SAR_w. The nine Vertosols investigated all tend to show the effects of irrigation SAR_w and EC_w attributes on soil structural condition. However, the soils exhibit two different trends; *(i)*, the soils with largest CEC_{eff} values are potentially the most dispersive when immersed in different solutions, but *(ii)*, these soils have structural form attributes that are influenced less by the applied solutions during the irrigation procedure. Those soils that have smaller CEC_{eff} values are less dispersive when immersed and shaken in solution, but these soils tend to undergo changes in structural form that reflect the collapse of the structured soil matrix in solutions of large SAR_w (*e.g.* the H001 soil).

In solution, the hydration of these soils with larger contributions of 2:1 expanding lattice phyllosilicates results in sufficient expansion of clays that attractive forces are overcome and dispersion occurs. However, the swelling of these minerals in structurally–intact soils is confined by the volume of each soil column and aggregates, while swollen, remain intact. In contrast, the soils that contain increasing contributions of non–expansive clays (*i.e.* illite and kaolinite) appear to swell less, and consequently, the increased Na^+ content of large SAR_w solutions results in aggregate breakdown and structural collapse.

This research shows that the structurally–intact field soils most likely to exhibit structural degradation, where poor quality water supplies are used to irrigate cotton–producing Vertosols, are those soils with small contributions of 2:1 expanding lattice clays and which have smaller exchange capacities. Thus, in NSW the cotton–producing Vertosols that are likely to suffer structural degradation due to the application of sodic irrigation waters (elevated SAR_w), or clean water (EC_w 0, SAR_w 0) are those from the Hillston, Bourke and Macquarie cotton–producing valleys. In this thesis, soils from the Macquarie valley are not included. McKenzie (1992) and Vervoort *et al.* (2003) determined the clay mineral suite and exchange capacities of different soils from this region. These reports show many soils from this region to contain smaller contributions of smectite and have exchange capacities that are much smaller than those determined for soils from the lower Gwydir and lower Namoi investigated by Vervoort *et al.* (2003). However, all nine of the intact Vertosols irrigated in the laboratory contain increased Na^+ contributions after being treated with the larger

Na^+–rich solutions. Consequently, the continued application of sodic waters is likely to impact on the structural condition of all Vertosols.

The soils dominated by 2:1 expansive clays are likely to be influenced less by poor quality irrigation waters over time than those soils with larger contributions of illite and kaolinite clays. For example, the irrigation of a Namoi Vertosol dominated by 2:1 expansive clays (Soil 1) using a water source with an SAR_w of 15 through 10 wetting events will lead to an increased soil ESP and more swelling, but this soil is likely to maintain a desirable structural form. The irrigation of an illitic Macquarie Vertosol (Soil 2) with this same water source and 10 wetting events will lead to an increased ESP, but the structural form of this soil will deteriorate and be much less desirable for cotton production. However, applying the SAR_w 15 solution and a solution of SAR_w 1 (*i.e.* FW002) alternately to Soil 1 and Soil 2 will lead to a less rapid increase in soil ESP. Consequently, Na^+ will contribute less to swelling in these soils and the structural condition maintained for cotton production over a longer period.

However, all Vertosols are likely to be degraded by the application of irrigation solutions with large SAR_w values to some extent. Consequently, to maintain a porous soil structure, which contains many small well–connected macropores and small aggregates, the contribution of exchangeable Na^+ in irrigation waters should be minimised. If possible the topsoil ESP should be maintained at less than 2. This is a difficult proposal for many sodic Vertosols (*e.g.* the B001 and H001 soils), but an ESP of 2 has previously been suggested as a lower limit of exchangeable Na^+, above which Vertosols may disperse (Cook *et al.* 1992; McKenzie 1998). This was supported by the ASWAT test conducted on each of the soils in this research. To achieve this reduction in ESP, both Soil 1 and Soil 2 could be treated with waters of large EC_w, but small SAR_w or with soil ameliorants (*e.g.* Gypsum). Applying these water sources or ameliorants would reduce the content of Na^+ at exchange sites and raise the soil solution EC, thereby reducing soil swelling and the potential for structural collapse. In so doing the limitation guidelines of irrigation EC_w for different crops (Ayers and Westcot 1985) should be consulted so as to minimise the risk of crop yield reductions.

8.2 Conclusions

Regarding the structural stability of the nine different Vertosols after immersion and shaking in different solutions:

The dispersion of clay for the different Vertosols is determined by the contributions of 2:1 expanding lattice phyllosilicates irrespective of the applied disruption force or treatment solution. The soils with larger contributions of 2:1 expanding lattice clays are more dispersive than soils with smaller contributions of these clays. In these soils, this relationship is reflected by the strong correlations between the $SI_{<2}$ values and CEC_{eff}. Soils that have similar contributions of 2:1 expanding lattice phyllosilicates then disperse according to exchangeable Na^+ contents (and ESP) and soil solution EC.

Vertosols immersed in increasingly sodic solutions (increased SAR_w), at constant EC_w, are more dispersive, until a threshold limit is reached. This threshold limit reflected the maximum level of dispersion for each of the soils after they have been immersed and shaken in the T30*i* and T40*i* solutions.

Vertosols immersed in increasingly saline solutions (increased EC_w), at constant SAR_w, are less dispersive. In solutions of very large EC_w (*i.e.* T50*i*) at low SAR_w (*i.e.* <7.5 $(mmol_{(+)}\ L^{-1})^{1/2}$) these Vertosols are not dispersive. This potentially reflects the flocculation of suspended clays from solution after the shaking procedure is complete.

Regarding the impact of irrigation water quality on the condition of the nine different structurally intact Vertosols:

The soils with larger contributions of 2:1 expanding lattice phyllosilicates tend to have bigger changes in the contributions of specific exchangeable cations after irrigation and are more dispersive after immersion than soils with smaller contributions of these clays. Consequently, irrigating different Vertosols with large SAR_w solutions leads to smaller contributions of exchangeable Ca^{2+} and Mg^{2+} and larger contributions of exchangeable Na^+.

The 2:1 expansive clay dominated G00*i* and N00*i* soils have structural form attributes that do not show treatment effects where the different irrigation treatments are compared. The soils that have only the fine clay fraction dominated by 2:1 expanding lattice phyllosilicates (the B00*i* and H002 soils) show small reductions in desirable structural form attributes after being treated with solutions of increased SAR_w, while the illitic Red Vertosol (the H001 soil) has structural form attributes that are much less desirable after the large SAR_w treatments than after the small SAR_w treatments.

The water retention curves and effective distributions of connected porosity show the effect of clay mineral suite for the two different Vertosols that are compared in this way (the G001 and H001 soils). The G001 soil does not appear to show any effect of treatment SAR_w on the soil water retention properties. The H001 soil shows a large treatment effect and treating this soil with solutions of larger SAR_w results in smaller contributions of connected porosity.

For the G001 and H001 soils, it is evident from the volume fractions of solid, solution and soil air that increased swelling occurred in response to large SAR_w treatments or in response to clean water. However, the different response of the illitic H001 soil reflects the collapse of the structural arrangement in this soil; increasing the SAR_w of the treatment solution leads to more swelling, but more of the pore space is occupied by soil solution in an unconnected network of soil porosity. The G001 soil does not show any sign of structural collapse.

Regarding the prediction of structural stability in Vertosols:

A model of structural stability is developed to describe the interaction of selected soil physico–chemical properties and irrigation solution attributes. The proposed model provides an estimate of the attenuation of dispersion for different Vertosols, where soils are immersed in solutions of varying SAR_w and EC_w.

Regarding those cotton–producing regions of eastern Australia that are most likely to suffer changes in soil structural conditions where alternative water supplies are used to irrigate cotton fields:

Those cotton producing regions that are most likely to suffer structural degradation, where waters of increased SAR_w are used to irrigate fields, are the soils with smaller contributions of 2:1 expanding lattice phyllosilicates, and hence those soils with smaller exchange capacities. The regions that incorporate these soil types are the Bourke, Macquarie valley and Hillston cotton producing regions.

The soils dominated by the 2:1 expanding lattice phyllosilicates (*e.g.* the G00*i* and N001 soils) are likely to suffer structural degradation if prolonged application of sodic solutions takes place, but overall these soils tend to have structural form attributes that are less affected by application of sodic irrigation solutions than the B00*i* and H00*i* soils.

8.3 Future research opportunities

The research undertaken during the completion of this thesis highlighted several future research opportunities.

8.3.1 Current methods of determining structural stability and the clay mineral suite

The current methods of quantifying structural stability involve the immersion of soil aggregates in either de–ionised water or solutions of variable quality. These methods have several inherent problems; it is difficult to compare the stability of soils treated in different laboratories or using different methods of analysis to quantify aggregate liberation and the dispersed clay content. In addition, this research identified the large clay mineral effect on the dispersion of clay from immersed soil samples. Soils with larger contributions of 2:1 expanding lattice minerals were consistently more dispersive than those soils with smaller contributions of these particular clay mineral species, irrespective of the soil ESP or soil solution EC. However, irrigating structurally–intact soils with different solutions showed that soils with larger contributions of 2:1 expanding lattice clays had structural form attributes that showed less solution SAR_w effects than the soils with smaller contributions of 2:1 expanding lattice clays, which appeared to slump. Rengasamy *et al.* (1984) made a similar observation. They noted that the heavy clay soils (Vertosols) dispersed differently to the red–brown earth soils after immersion. Hence, they excluded Vertosols from their classification scheme and concentrated solely on the red–brown earths.

Vertosols are used widely for irrigated agriculture and they show a wide variation in the contributions of different phyllosilicate clays. For these soils the different swelling capacities of different clay mineral species contribute significantly to differences in stabilities where immersion techniques are applied. Future work must quantify the different stabilities of Vertosols containing different phyllosilicate clays and will assist in developing a more robust understanding of the liberation of clay during immersion methods of testing stability. This will make comparisons between immersion tests and the field behaviour of Vertosol more relevant for management decisions.

8.3.2 The impact of organic carbon contributions

There is currently no specific threshold organic matter content for Vertosols that has been categorically linked to the stability of soil aggregates (McKenzie 1998), but increased organic matter

in these soils is generally associated with increased stability. This general understanding was observed for these soils in chapter 3 where the liberation of material of the <100 μm fraction during spontaneous dispersion appeared to be associated with the organic carbon content. The three B00*i* soils contained less organic carbon than the other soils and they slaked much more extensively when immersed in water. In addition, the irrigation procedure applied to structurally–intact soil columns tended to result in soil samples that had similar stabilities to the initial furrow topsoils. This was despite the irrigated soils having larger ESPs and smaller ECs than the corresponding furrow topsoils. The organic carbon content of the different irrigated soil columns was not quantified due to cost and labour restrictions. In addition, the different organic carbon contents of each soil are likely to have been composed of different organic matter types. For example, organic matter contributing to the stabilisation of soil structure of the irrigated soil columns was likely to result from fungal proliferation, while the organic content of the furrow soils was likely to have consisted of mineralised organic carbon types. These different types of organic material and their impact on the structural stability of Vertosols must be characterised.

8.3.3 The structural form of Vertosols: the impact of moisture content

The Vertosols that were irrigated in the laboratory for the analysis of soil structural form attributes were allowed to dry for 50 days prior to being filled with fluorescent resin. However, at this time the intact soil columns contained significant moisture (0.10–0.35 g g^{-1}). This moisture content may have influenced the expression of structural form attributes, and could have masked differences between the structural form of soil columns treated using the different irrigation solutions. In chapter 5 it was observed that the soils containing large contributions of both coarse and fine 2:1 expanding lattice phyllosilicates (the G00*i* and N001 soils) did not show any significant differences between the desirable soil structural form descriptors where the six treatments were applied. This may reflect the moisture content of these soil columns.

Currently, only limited research has addressed the formation of cracks in Vertosols as they dry. For example, Ringrose–Voase and Sanidad (1996) looked at the development of cracks in two Philippines Vertosols by measuring the width and depth of cracks along a 7 m transect as each soil dried. However, this method is unsuitable for describing the development of smaller cracking patterns in Vertosols *i.e.* cracks that are <10 mm in width. Recent developments in the area of X–ray computed tomography (CT–scanning) are likely to provide a method by which soil–filled columns (*e.g.* 150 mm *d.*) can be used to identify the formation of cracks for Vertosols as they dry. CT–scanning is frequently used for the determination of root development in soil columns (*e.g.* Mooney 2002; McNeill and Kolesik 2004), but until recently the resolution of scanners appears to have been

a limitation restricting the analysis of soils at fine resolutions. However, Gregory *et al.* (2003) recently reported on a CT–scanner with the potential to analyses soil samples of approximately 120 mm *d.* at a resolution of 50 μm. Using an apparatus such as this, the development of cracks during drying could be characterised, and an understanding of the formation of cracks in Vertosols developed. This is likely to provide a more descriptive indication of what soil moisture content is best suited for the analysis of soil structural form attributes.

8.3.4 Developing a model of soil structural stability

The predictive tool that was developed in this research project was not that which was initially proposed. Initially, this project aimed to develop a predictive model of potential instability that considered soil chemical properties (*i.e.* ESP, SAR and electrical conductivity) in relation to other soil attributes (*i.e.* the suite of clay phyllosilicates, CEC_{eff} or organic contributions). This was expected to be completed using a three dimensional approach to discriminate between the spontaneous and mechanical dispersion of the different Vertosols. However, the number of different Vertosols assessed in this research was insufficient. Initially, it was anticipated that the laboratory irrigated soil samples would provide an array of different chemical conditions (large variations in EC and SAR) that could be used to differentiate these soils, but this procedure led to the dilution of the soil solution. This resulted in only small distributions of electrical conductivity and SAR values (0.05–0.40 dS m^{-1} and 0.5–5.5 $(mmol_{(+)}\ L^{-1})^{1/2}$) for all soil samples.

To develop the proposed predictive model, future research must undertake three tasks. A large number of soil samples must be collected, which are representative of the different clay phyllosilicate suites (or cation exchange capacities) of Vertosols used for cotton production throughout eastern Australia. For example, Rengasamy *et al.* (1984) used 138 different red–brown earth soil samples in their classification scheme. The sampled Vertosols need to be assessed for an array of soil physico–chemical attributes (*e.g.* clay content, exchangeable cations and the cation exchange capacity, electrical conductivity and organic matter contributions). Then, the structural stability of these Vertosols should be assessed using different immersion techniques *i.e.* spontaneously dispersion and EOE–disruption. This information will help to categorise the dispersion of different soils and should consider the impact of swelling on the liberation of clay during stability assessments.

8.3.5 Remediation of sodic conditions in Vertosols

During this research no attempt was made to address the remediation of structural behaviour resulting from inherent sodicity or from increased contributions of Na^+ due to irrigation water

quality. However, the research conducted for this project provides a basis for this future research opportunity.

Research into remediation methods should specifically focus on the application of lime or gypsum as an amendment, where either of these salts is applied directly to the field in the absence of irrigated crops or as an additive to poor quality water supplies prior to field irrigation. This is an issue that should be considered as a high priority for the cotton industry given the current condition of some irrigation water resources and recent predictions of increasing salt content in some river systems (Jolly *et al.* 2001) used for the irrigation of cotton.

Bibliography

Abu–Sharar TM, Bingham FT, Rhoades JD (1987) Stability of soil aggregates as affected by electrolyte concentration and composition. *Soil Science Society of America Journal* **51**, 309–314.

Agassi M, Shainberg I, Morin J (1981) Effect of electrolyte concentration and soil sodicity on infiltration rate and crust formation. *Soil Science Society of America Journal* **45**, 848–851.

Ahmad N (1983) Vertisols. In 'Pedogenesis and Soil Taxonomy, Vol. 2. The Soil Orders'. (Ed.s NES L.P. Wilding, G.F. Hall) pp. 91–123. (Elsevier: Amsterdam)

Ahmad N (1996) Occurrence and Distribution of Vertisols. In 'Vertisols and technologies for their management. Developments in soil science 24'. (Eds N Ahmad and A Mermut) pp. 1–41 (Elservier Sciences: Netherlands)

Ahmad N, Mermut A (1996) 'Vertisols and technologies for their management.' (Elservier Sciences: Netherlands)

Ahmed S, Swindale LD, El–Swaify SA (1969) Effects of adsorbed cations on physical properties of tropical red earths and tropical black earths. *Journal of Soil Science* **20**, 255–268.

Allen BL, Hajek BF (1989) Mineral occurrence in soil environments. In 'Minerals in Soil Environments'. (Eds JB Dixon and SB Weed) pp. 199–278 (Soil Science Society of America: Madison, Wisconsin, USA)

Alperovitch N, Shainberg I, Keren R, Singer MJ (1985) Effect of clay mineralogy and aluminum and iron oxides on the hydraulic conductivity of clay–sand mixtures. C*lays and Clay Minerals* **33**, 443–450.

Amézketa E (1999) Soil aggregate stability: A review. *Journal of Sustainable Agriculture* **14**, 83–151.

Anderson JV, Fadul KE, O'Connor GA (1973) Factors effecting the coefficient of linear extensibility in Vertosols. *Soil Science Society of America Proceedings* **37**, 296–299.

Ashton D, Hanna N (2002) Fibers: outlook to 2006–07. *Australian Commodities* **9**, 41–49.

Astaraei AR, Chauhan RPS (1992) Effect of Ca:Mg ratio on soil sodicity at different levels of Sodium Adsorption ratio and Electrolyte Concentration. *Australian Journal of Soil Research* **30**, 751–756.

Australian Department of Trade and Resources (1982) 'Australian Farming Systems.' (Australian Government Printing Services: Canberra)

Ayers RS, Westcot DW (1985) 'Water quality for agriculture'. (FAO Irrigation and drainage paper 29 Rev. 1) (Food and Agriculture Organisation of the United Nations: Rome)

Bakker AC, Emerson WW (1973) The comparative effect of exchangeable calcium, magnesium, and sodium on some physical properties of red–brown subsoils. III. The permeability of Shepparton soil and comparison of methods. *Australian Journal of Soil Research* **11**, 159–165.

Barlow K, Nash D (2002) Investigating structural stability using the soil water characteristic curve. *Australian Journal of Experimental Agriculture* **42**, 291–296.

Barzegar AR, Nelson PN, Oades JM, Rengasamy P (1997) Organic matter, sodicity, and clay type: Influence on soil aggregation. *Soil Science Society of America Journal* **61**, 1131–1137.

Batey TJ (2001) Soil profile description and evaluation. In 'Soil and environmental analysis'. (Eds KA Smith and CE Mullins) pp. 595–628. (Marcel Dekker, Inc.: New York)

Ben-Hur M, Stern R, van der Merwe AJ, Shainberg I (1992) Slope and gypsum effects on infiltration and erodibility of dispersive and non–dispersive soils. *Soil Science Society of America Journal* **56**, 1571–1576.

Beven K, Germann P (1982) Macropores and Water flow in soils. *Water Resources Research* **18**, 1311–1325.

Black CA (1986) 'Soil–Plant Relationships.' (John Wiley and Sons: New York)

Blackwell PS, Jayawardane NS, Green TW, Wood JT, Blackwell J, Beatty HJ (1991) Subsoil macropore space of a transitional red–brown earth after either deep tillage, gypsum or both. II. Chemical effects and long term changes. *Australian Journal of Soil Research* **29**, 141–154.

Blokhuis WA (1982) Morphology and genesis of Vertisols. In 'Vertisols and rice soils of the tropics. Symposia papers II. Transactions of the 12th International Congress of Soil Science'. New Delhi, India pp. 23–47. (Indian Society of Soil Science)

Blum WH (1998) Basic Concepts: Degradation, Resilience and rehabilitation. In 'Methods for Assessment of Soil Degradation'. (Ed.s R Lal, Blum, W.H., Valentine, C., Stewart, B.A.) pp. 1–16. (CRC Press LLC: Florida)

Bresson LM, Moran CJ (1995) Structural change induced by wetting and drying in seedbeds of a hardsetting soil with contrasting aggregate size distribution. *European Journal of Soil Science* **46**, 205–214.

Brewer R (1964) 'Fabric and Mineral Analysis of Soils.' (John Wiley: New York)

Brewer R, Sleeman JR (1988) 'Soil Structure and Fabric.' (S.R. Frankland Pty. Ltd.: Melbourne)

Brindley GW, Brown G (1984) 'Crystal structures of clay minerals and their x–ray identification.' (Spottiswoode Ballantyne Ltd.: Great Britain)

Bullock P, Loveland PJ (1974) Mineralogical analysis. In 'Soil survey laboratory methods'. (Eds BW Avery and CL Bascombe) pp. 57–69. (Soil survey technical monograph. No. 6.: Rothamsted Experimental Station)

Carsel R, Parrish R (1988) Developing joint probability distributions of soil water retention characteristics. *Water Resources Research* **24**, 755–769.

Cass A, Sumner ME (1982a) Soil pore structural stability and irrigation water quality: I. Empirical sodium stability model. *Soil Science Society of America Journal* **46**, 503–506.

Cass A, Sumner ME (1982b) Soil pore structural stability and irrigation water quality: III. Evaluation of soil stability and crop yield in relation to salinity and sodicity. *Soil Science Society of America Journal* **46**, 513–517.

Cattle SR, Farrell RA, McBratney AB, Moran CJ, Roesner EA, Koppi AJ (2001) © Solicon–PC Version 2.1. (The University of Sydney and the Cotton Research and Development Corporation)

Chan KY, Mullins CE (1994) Slaking characteristics of some Australian and British soils. *European Journal of Soil Science* **45**, 273–283.

Chang CW, Dregne HE (1955) Effect of exchangeable sodium on soil properties and on growth and cation content of alfalfa and cotton. *Soil Science Society of America Proceedings*, 29–35.

Chen Y, Banin A (1975) Scanning electron microscope (SEM) observations of soil structure changes induced by sodium–calcium exchange in relation to hydraulic conductivity. *Soil Science* **120**, 428–436.

Chen Y, Banin A, Borochovitch A (1983) Effect of potassium on soil structure in relation to hydraulic conductivity. *Geoderma* **30**, 135–147.

Chenu C (1989) Influence of a fungal polysaccharide, scleroglucan, on clay microstructures. *Soil Biology and Biochemistry* **21**, 299–305.

Chiang SC, Radcliffe DE, Miller RW, Newman KD (1987) Hydraulic conductivity of three southeastern soils as affected by sodium, electrolyte concentration and pH. *Soil Science Society of America Journal* **51**, 1293–1299.

Churchman GJ, Skjemstad JO, Oades JM (1993) Influence of clay minerals and organic matter on effects of sodicity on soils. *Australian Journal of Soil Research* **31**, 779–800.

Cook GD, So HB, Dalal RC (1992) Structural degradation of two Vertisols under continuous cultivation. *Soil and Tillage Research* **24**, 47–64.

Coughlan KJ (1979) 'Influence of micro-structure on the physical properties of cracking clay soils.' Report to the Reserve Bank, Adelaide.

Coughlan KJ (1984) The structure of Vertisols. In 'The properties and Utilisation of Cracking Clay Soils'. (Ed.s EHH J.W. McGarity, H.B. So) pp. 87–96. (University of New England: Armidale)

Coulombe CE, Dixon JB, Wilding LP (1996a) Mineralogy and chemistry of Vertisols. In 'Vertisols and technologies for their management'. (Ed.s N Ahmad, Mermut, A.R.) pp. 115–200. (Elsevier Science B.V.: Amsterdam)

Coulombe CE, Wilding LP, Dixon JB (1996b) Overview of Vertisols: Characteristics and impacts on society. *Advances in Agronomy* **57**, 289–375.

Crescimanno G, Provenzano G, Iovino M (1995) Influence of salinity and sodicity on soil structural and hydraulic characteristics. *Soil Science Society of America Journal* **59**, 1701–1708.

Curtin D, Steppuhn H, Selles F (1994a) Clay dispersion in relation to sodicity, electrolyte concentration and mechanical effects. *Soil Science Society of America Journal* **58**, 955–962.

Curtin D, Steppuhn H, Selles F (1994b) Effects of magnesium on cation selectivity and structural stability of sodic soils. *Soil Science Society of America Journal* **58**, 730–737.

Curtin D, Steppuhn H, Selles F (1994c) Structural stability of chernozemic soils as affected by exchangeable sodium and electrolyte concentration. *Canadian Journal of Soil Science* **74**, 157–164.

Dalal RC (1989) Long–term effects of no-tillage, crop residue, and nitrogen application on properties of a Vertisol. *Soil Science Society of America Journal* **53**, 1511–1515.

Dalal RC, Mayer RJ (1986a) Long–term trends in fertility of soils under continuous cultivation and cereal cropping in southern QLD. I. Overall changes in soil properties and trends in winter cereal yields. *Australian Journal of Soil Research* **24**, 265–279.

Dalal RC, Mayer RJ (1986b) Long–term trends in fertility of soils under continuous cultivation and cereal cropping in southern QLD. II. Total organic carbon and its rate of loss from the soil profile. *Australian Journal of Soil Research* **24**, 281–292.

Daniells IG (1989) degradation and restoration of soil structure in a cracking grey clay used for cotton production. *Australian Journal of Soil Research* **27**, 455–469.

Danielson RE, Sutherland PL (1986) Porosity. In 'Methods of soil analysis. Part I. Physical and Mineralogical Methods'. (Ed.s A Klute) pp. 443–461. (American Society of Agronomy Inc., Soil Science Society of America Inc.: Madison, Wisconsin, USA)

De Vos JH, Virgo KJ (1969) Soil structure in Vertisols of the Blue Nile clay plains. *Sudan Journal of Soil Science* **20**, 189–206.

Del Villar EH (1944) The tirs of Morocco, Rabat, Morocco. *Soil Science* **57**, 313–339.

Dexter AR (2004) Soil physical quality. Part I. Theory, effects of soil texture, density, and organic matter, and effects on root growth. *Geoderma* **120**, 201–214.

Dontsova KM, Norton LD (2002) Clay dispersion, infiltration, and erosion as influenced by exchangeable calcium and magnesium. *Soil Science* **167**, 184–193.

Dudal R (1963) Dark clay soils of tropical and subtropical regions. *Soil Science Society of America Journal* **95**, 264–270.

Dudal R (1965) 'Dark Clay Soils of tropical and Subtropical Regions.' (FAO: Rome)

Dudal R, Eswaran H (1988) Distribution, properties and classification of Vertisols. In 'Vertisols: Their distribution, properties, classification and management'. (Ed.s LP Wilding, Puentes, R.) pp. 1–22. (Texas A&M University Printing Center: College Station)

Dugdale H, Harris G, Neilson J, Richards D, Roth G, Williams D (Eds) (2004) 'WATERpak: a guide for irrigation management in cotton.' (Cotton Research and Development Corporation)

Edwards AP, Bremner JM (1967) Dispersion of soil particles by sonic vibration. *Journal of Soil Science* **18**, 47–63.

Elliott ET (1986) Aggregate structure and carbon, nitrogen, and phosphorous in native and cultivated soils. *Soil Science Society of America Journal* **50**, 627–633.

Ellison WD (1947) Some effects of soil erosion on infiltration and surface runoff. *Agricultural Engineering*, 245–248.

Emerson WW (1954) The determination of the stability of soil crumbs. *Journal of Soil Science* **5**, 233–250.

Emerson WW (1967) A classification of soil aggregates based on their coherence in water. *Australian Journal of Soil Research* **5**, 47–57.

Emerson WW (1983) Inter-particle bonding. In 'Soils: An Australian Viewpoint' pp. 477–498. (Division of Soils, CSIRO, Academic Press: London)

Emerson WW, Bakker AC (1973) The comparative effects of exchangeable calcium, magnesium, and sodium on some physical properties of red–brown earth subsoils. II. The spontaneous dispersion of aggregates in water. *Australian Journal of Soil Research* **11**, 151–157.

Emerson WW, Chi CL (1977) Exchangeable calcium, magnesium and sodium and the dispersion of illites in water. II. Dispersion of illites in water. *Australian Journal of Soil Research* **15**, 255–262.

Emerson WW, Greenland DJ (1990) Soil aggregates–formation and stability. In 'Soil colloids and their associations in aggregates'. (Eds MF De Boodt, MHB Hayes and A Herbillon) pp. 485–511. (NATO ASI Series)

Emerson WW, Smith BH (1970) Magnesium, organic matter and soil structure. *Nature* **31**, 453–454.

FAO (1998) 'World Reference Base for Soils.' (Food and Agriculture Organisation of the United Nations: Rome)

Favre F, Boivin P, Wopereis MCS (1997) Water movement and soil swelling in a dry, cracked Vertisol. *Geoderma* **78**, 113–123.

Felhendler R, Shainberg I, Frenkel H (1974) Dispersion and the hydraulic conductivity of soils in mixed solutions. In '10th International Congress of Soil Science'. Moscow, USSR pp. 103–111.

Field DJ (2000) The bricks and mortar of Vertosols: The characteristics of aggregation and assessing aggregate stability of Vertosols used for cotton production. Unpublished thesis, The University of Sydney.

Field DJ, McKenzie DC, Koppi AJ (1997) Development of an improved Vertisol stability test for SOILpak. *Australian Journal of Soil Research* **35**, 843–852.

Field DJ, Minasny B (1999) A description of aggregate liberation and dispersion in A horizons of Australian Vertosols by ultrasonic agitation. *Geoderma* **91**, 11–26.

Fireman M, Bodman GB (1939) The effect of saline irrigation water upon the permeability and base status of soils. *Soil Science Society of America Proceedings* **4**, 71–77.

Fox D, Bryan R, Fox C (2004) Changes in pore characteristics with depth for structural crusts. *Geoderma* **120**, 109–120.

Frenkel H, Goertzen JO, Rhoades JD (1978) Effects of clay type and content, exchangeable sodium percentage and electrolyte concentration on clay dispersion and soil hydraulic conductivity. *Soil Science Society of America Journal* **42**, 32–39.

Gee GW, Bauder JW (1986) Particle–size Analysis. In 'Methods of Soil Analysis'. (Ed.s A Klute) pp. 383–410. (Madison: Wisconsin, USA)

Grant CD, Blackmore AV (1991) Self-mulching behaviour in clay soils: its definition and measurement. *Australian Journal of Soil Research* **29**, 155–173.

Gregory P, Hutchison DJ, Read DB, Jenneson P, Gilboy W, Morton E (2003) Non–invasive imaging of roots with high resolution X–ray micro–tomography. *Plant and Soil* **255**, 351–359.

Halliwell DJ, Barlow K, Nash D (2001) A review of the effects of waste water sodium on soil physical properties and their implications for irrigation systems. *Australian Journal of Soil Research* **39**, 1259–1267.

Hamza MA, Anderson SH, Alymore LAG (2001) Studies of soil water draw–downs by single radish roots at decreasing soil water content using computer–assisted tomography. *Australian Journal of Soil Research* **39**, 1387–1396.

Heeraman D, Hopmans J, Clausnitzer V (1997) Three dimensional imaging of plant roots in situ with X–ray computed tomography. *Plant and Soil* **189**, 167–179.

Heinonen R (1955) Soil aggregation in relation to texture and organic matter. *Agrogeol. Julk.* **No. 64**.

Herrick JE, Wander MM (1998) Relationships between soil organic carbon and soil quality in cropped and rangeland soils: The importance of distribution, composition, and soil biological activity. In 'Soil Processes and the Carbon Cycle.' (Ed.s JMK R. Lal, R.F. Follett, and B.A. Stewart) pp. 461–425. (CRC Press LLC)

Hewitt AE, Shepherd TG (1997) Structural vulnerability of New Zealand soils. *Australian Journal of Soil Research* **35**, 461–474.

Hillel D (1982) 'Introduction to Soil Physics.' (Academic Press, Inc.: New York)

Holmgren GGS, Juve RL, Geschwender RC (1977) A mechanically controlled variable rate leaching device. *Soil Science Society of America Journal* **41**, 1207–1208.

Horn R, Taubner H, Wuttke M, Baumgartl T (1994) Soil physical properties related to soil structure. *Soil and Tillage Research* **30**, 187–216.

Hubble GD (1984) The cracking clay soils: definition, nature, genesis and use. In 'The properties and Utilisation of Cracking Clay Soils'. (Ed.s EHH J.W. McGarity, H.B. So) pp. 3–13. (University of New England: Armidale)

Hulugalle NR, Entwistle P (1997) Soil properties, nutrient uptake and crop growth in an irrigated Vertisol after nine years of minimum tillage. *Soil and Tillage Research* **42**, 15–32.

Hulugalle NR, Entwistle PC, Mensah RK (1999) Can Lucerne (*Medicago sativa L.*) strips improve soil utility in irrigated cotton (*Gossypium hirsutum L.*) fields? *Applied Soil Ecology* **12**, 81–92.

Hulugalle NR, Entwistle PC, Scott F, Kahl J (2001) Rotation crops for irrigated cotton in a medium–fine, self–mulching, grey Vertosol. *Australian Journal of Soil Research* **39**, 317–328.

Hulugalle NR, Finlay LA (2003) $EC_{1:5}$/exchangeable Na, a sodicity index for cotton farming systems in irrigated and rain–fed Vertosols. *Australian Journal of Soil Research* **41**, 761–769.

Hussein J, Adey MA (1995) Changes of structure and tilth mellowing in a Vertisol due to wet/dry cycles in the liquid and vapor phases. *European Journal of Soil Science* **46**, 357–368.

Hussein J, Adey MA (1998) Changes in microstructure, voids and b–fabric of surface samples of a Vertisol caused by wet / dry cycles. *Geoderma* **85**, 63–82.

Isbell RF (1989) Australian Vertisols. In 'Characterisation, classification and utilization of cold Aridisols and Vertisols. Sixth International Soil Correlation Meeting (VI ISCOM)'. (Ed.s JM Kimble) p. 73–80. (Soil Management Support Services, Washington DC)

Isbell RF (1996) 'The Australian Soil Classification.' (CSIRO Publishing: Collingwood, Victoria)

Isbell RF, McDonald WS, Ashton LJ (1997) 'Concepts and Rationale of the Australian Soil Classification.' (CSIRO Land and Water: Australia)

Jackson ML (1956) 'Soil Chemical Analysis–Advanced course.' (Published by the Author, Department of Soils, University of Wisconsin: Madison 6, Wisconsin)

Jewitt TN, Law RD, Virgo KJ (1979) Vertisol soils of the tropics and subtropics: their management and use. *Outlook on Agriculture* **10**, 30–40.

Jolly ID, Williamson DR, Gilfedder M, Walker GR, Morton R, Robinson G, Jones H, Zhang L, Dowling TI, Dyce P, Nathan RJ, Nandakumar N, Clarke R, McNeill V (2001) Historical stream salinity trends and catchment salt balances in the Murray–Darling Basin, Australia. *Marine and Freshwater Research* **52**, 53–63.

Kanwar JS, Kanwar BS (1968) Quality of irrigation water. In '9th International congress of soil science'. Adelaide, Australia pp. 391–403. (International Society of Soil Science and Angus and Robertson)

Kay BD (1990) Rates of change of soil structure under different cropping systems. *Advances in Soil Science* **12**, 1–52.

Kay BD (1998) Soil structure and organic carbon: A review. In 'Soil Processes and the Carbon Cycle'. (Ed.s JMK R. Lal, R.F. Follett, and B.A. Stewart) pp. 169–197. (CRC Press LLC)

Kay BD, Rasiah V, Perfect E (1994) Structural aspects of soil resilience. In 'Soil Resilience and Sustainable Land Use.' (Ed.s DJ Greenland, Szabolcs, I.) pp. 449–468. (CAB international.: Wallingford, Oxon, UK.)

Kemper WD, Rosenau RC (1984) Soil cohesion as affected by time and water content. *Soil Science Society of America Journal* **48**, 1001–1006.

Kemper WD, Rosenau RC (1986) Aggregate stability and size distribution. In 'Methods of Soil Analysis. Part 1–Physical and Mineralogical Methods'. (Ed.s A Klute) pp. 425–441. (Soil Science Society of America: Madison, Wisconsin)

Keren R, Ben–Hur M (2003) Interaction effects of clay swelling and dispersion and $CaCO_3$ content on saturated hydraulic conductivity. *Australian Journal of Soil Research* **41**, 979–989.

Kossovitch P (1912) Die Schwarzerde. In 'Tschernosion'. (Ed.s V f.Fachliteratur) pp. 137–139. (GMBH: Berlin)

Lal R (1993) Tillage effects on soil degradation, soil resilience, soil quality, and sustainability. *Soil and Tillage Research* **27**, 1–8.

Lal R (1998) Soil Quality and Sustainability. In 'Methods for Assessment of Soil Degradation'. (Ed.s R Lal, Blum, W.H., Valentine, C., Stewart, B.A.) pp. 17–30 (CRC Press LLC: Florida)

Le Bissonnais Y (1996) Aggregate stability and assessment of soil crustability and erodibility: I. Theory and methodology. *European Journal of Soil Science* **47**, 425–437.

Lebron I, Suarez DI, Schaap MG (2002) Soil pore size and geometry as a result of aggregate-size distribution and chemical composition. *Soil Science* **167**, 165–172.

Levy GJ, Eisenberg H, Shainberg I (1993) Clay dispersion as related to soil properties and water permeability. *Soil Science* **155**, 15–22.

Levy GJ, Torrento JR (1995) Clay dispersion and macroaggregate stability is affected by exchangeable potassium and sodium. *Soil Science* **160**, 352–358.

Levy GJ, van der Watt HVH (1988) Effects of clay mineralogy and soil sodicity on soil infiltration rate. *South African Journal of Plant and Soil* **5**, 92–96.

Levy GJ, van der Watt HVH (1990) Effect of exchangeable potassium on the hydraulic conductivity and infiltration rate of some South African soils. *Soil Science* **149**, 69–77.

Lieffering RE, McLay (1996) Effects of pH solutions with large monovalent cation concentrations on cation exchange properties. *Australian Journal of Soil Research* **34**, 229–242.

Loch RJ (1982) Rainfall simulator methodology: concepts for realistic research. In 'Resources, Efficient Use and Conservation: Agricultural engineering conference'. Armidale, NSW pp. 99–103.

Loveday J (1984) Management of Vertisols under irrigated agriculture (invited paper). In 'The properties and Utilisation of Cracking Clay Soils'. (Ed.s EHH J.W. McGarity, H.B. So) pp. 269–277. (University of New England: Armidale)

Lu G, Sakagami K, Tanaka H, Hamada R (1998) Role of organic matter in stabilisation of water stable aggregates under different types of land use. *Soil Science and Plant Nutrition* **44**, 147–155.

Martin JP, Richards SJ, Pratt PF (1964) Relationship of exchangeable Na percentage at different soil pH levels to hydraulic conductivity. *Soil Science Society of America Proceedings* **28**, 620–622.

Matkin EA, Smart P (1987) A comparison of tests of soil structural stability. *Journal of Soil Science* **38**, 123–135.

McBratney AB, Moran CJ (1990) A rapid method of analysis for soil macropore structure: II. Stereological model, statistical analysis, and interpretation. *Soil Science Society of America Journal* **54**, 509–515.

McBratney AB, Moran CJ, Stewart JB, Cattle SR, Koppi AJ (1992) Modifications to a method of rapid assessment of soil macropore structure by image analysis. *Geoderma* **53**, 255–274.

McDonald RC, Isbell RF (1998) Soil profile. In 'Australian soil and land survey: Field handbook'. (Eds RC McDonald, RF Isbell, JG Speight, J Walker and MS Hopkins) pp. 103–152. (CSIRO Land and Water: Canberra)

McGarry D (1993) Degradation of soil structure. In 'Land degradation processes in Australia'. (Eds G McTainsh and WC Boughton) pp. 271–305. (Longman Cheshire: Melbourne)

McGarry D (1996) The structure and grain size distribution of Vertisols. In 'Vertisols and technologies for their management'. (Eds N Ahmad, A Mermut) pp. 231–259. (Elsevier: Amsterdam)

McIntyre DS (1956) The effect of free ferric oxide on the structure of some Terra Rossa and Rendzina soils. *Journal of Soil Science* **7**, 302–306.

McIntyre DS (1974) Soil sampling techniques for physical measurement. In 'Methods for Analysis of Irrigated Soils (Ed J Loveday) pp. 12–20. (Commonwealth Agricultural Bureaux: Farnham Royal)

McIntyre DS (1979) Exchangeable sodium, sub plasticity and hydraulic conductivity of some Australian soils. *Australian Journal of Soil Research* **17**, 115–120.

McKenzie DC (Ed) (1998) 'SOILpak for cotton growers (3rd edn).' (N.S.W. Agriculture: Orange, N.S.W.)

McKenzie DC, Abbott TS, Higginson FR (1991) The effect of irrigated crop production on the properties of a sodic Vertisol. *Australian Journal of Soil Research* **29**, 443–453.

McKenzie NJ (1992) Soils of the lower Macquarie Valley, new South Wales. Divisional Report No. 117. (CSIRO Division of Soils: Canberra)

McKenzie NJ, Jacquier D, Isbell RF, Brown K (2004) 'Australian soils and landscapes.' (CSIRO publishing: Collingwood, Vic, Australia)

McKenzie DC, Abbott TS, Chan KY, Slavich PG, Hall DJM (1995) The nature, distribution and management of sodic soils in New South Wales. In 'Australian Sodic Soils: Distribution, Properties and Management'. (Eds R Naidu, ME Sumner, P Rengasamy) pp. 247–264. (CSIRO: Australia)

McLeod S (1975) Studies on wet oxidation procedures for the determination of organic carbon in soil. In 'Notes on Soil Techniques' pp. 73–79. (CSIRO Division of Soils: Canberra)

McNeal BL, Layfield DA, Norvell WA, Rhoades JD (1968) Factors influencing hydraulic conductivity of soils in the presence of mixed salt solutions. *Soil Science Society of America Journal* **32**, 187–190.

McNeill A, Kolesik P (2004) X–ray CT investigations of intact soil cores with and without living cop roots. In 'SuperSoil 2004, 3rd Australian New Zealand Soils Conference'. University of Sydney, Australia. (Ed.s B Singh)

Menneer JC, McLay CDA, Lee R (2001) Effects of sodium-contaminated wastewater on soil permeability of two New Zealand soils. *Australian Journal of Soil Research* **39**, 877–891.

Mermut AR, Padmanabham E, Eswaran H, Dasog GS (1996) Pedogenesis. In 'Vertisols and Technologies for their management'. (Eds N Ahmad and A Mermut) pp. 43–61. (Elsevier Science)

Middleton HE (1930) Properties of soils which influence soil erosion. *Technical Bulletin, US Department of Agriculture* **No 178**.

Miller RW, Donahue RL (1995) 'Soils in our environment.' (Prentice–Hall Inc.: United States of America)

Minasny B, Field DJ (2004) Estimating soil hydraulic properties and their uncertainty: the use of stochastic simulation in the inverse modeling of the evaporation method. *Geoderma* **126**, 277–290.

Mooney SJ (2002) Three–dimensional visualization and quantification of soil macroporosity and water flow patterns using computed tomography. *Soil Use and Management* **18**, 142–151.

Moran CJ, McBratney AB (1992) Acquisition and analysis of three–component digital images of soil pore structure. I. Method. *Journal of Soil Science* **43**, 541–549.

Moran CJ, McBratney AB, Koppi AJ (1989) A rapid method for analysis of macropore structure: I. Specimen preparation and digital binary image production. *Soil Science Society of America Journal* **53**, 921–928.

Muhammed S (1996) Soil salinity, sodicity, and water logging. In 'Soil Science'. (Eds A Rashid and KS Memon). (National Book Foundation: Islamabad)

Mukhtar OMA, Swowoba AR, Godfrey CL (1974) The effect of sodium and calcium chlorides on structure stability of two Vertisols: Gezira clay form Sudan, Africa and Houston Black clay from Texas, USA. *Soil Science* **118**, 109–119.

Mullins CE, MacLeod DA, Northcote KH, Tisdall JM, Young IM (1990) Hardsetting soils: behaviour, occurrence and management. *Advances in Soil Science* **11**, 37–108.

Murthy RS, Bhattacharjee JC, Landey RJ, Pofali RM (1984) Distribution, characteristics and classification of Vertisols. In 'Vertisols and rice soils of the tropics. Symposia papers II. Transactions of the 12th International Congress of Soil Science'. New Delhi, India pp. 3–22. (Indian Society of Soil Science)

Naidu R, Sumner ME, Rengasamy P (1995) 'Australian Sodic Soils: Distribution, Properties and Management.' (CSIRO Australia)

Narawimha R, Mathew PK (1995) Effects of exchangeable cations on hydraulic conductivity of a marine clay. *Clays and Clay Minerals* **43**, 433–437.

Nelson PN, Baldock JA, Clarke P, Oades JM, Churchman GJ (1999) Dispersed clay and organic matter in soil: their nature and associations. *Australian Journal of Soil Research* **37**, 289–315.

Nelson PN, Baldock JA, Oades JM (1998) Changes in dispersible clay content, organic carbon content, and electrolyte composition following incubation of sodic soil. *Australian Journal of Soil Research* **36**, 883–897.

Nikiforoff CC (1941) Morphological classification of soil structure. *Soil Science* **52**, 193–212.

Nimmo JR, Perkins KS (2002) Aggregate stability and size distribution. In 'Methods of Soil Analysis. Part 4–Physical Methods'. (Eds JH Dane and GC Topp) pp. 317–328. (Soil Science Society of America, Inc.: Madison, Wisconsin)

Nordt L, Wilding L, Lynn W, Crawford C (2004) Vertisol genesis in a humid climate of the coastal plain of Texas, U.S.A. *Geoderma* **122**, 83–102.

Norrish K, Pickering JG (1977) Clay mineralogical properties. In 'Soil Factors in crop production in a semi–arid environment'. (Ed.s ELG J.S. Russell) pp. 33–53. (University of Queensland Press, St. Lucia: Brisbane)

North PF (1976) Towards an absolute measurement of soil structural stability using ultrasound. *Journal of Soil Science* **27**, 451–459.

Northcote KH, Skene JKM (1972) 'Australian Soils with Saline and Sodic properties.' (CSIRO, Australia)

NSW Agriculture (1995) 'Soil management for irrigated cotton, Agfact P5.3.6, 2nd edition.' Division of Plant Industries, NSW Agriculture.

Oades JM, Waters AG (1991) Aggregate hierarchy in soils. *Australian Journal of Soil Research* **29**, 815–828.

Oakes H, Thorp J (1950) Dark–clay soils of warm regions variously called Rendzina, Black Cotton Soils, Regur, and Tris. *Soil Science Society of America Proceedings* **15**, 347–354.

Odeh IOA, Cattle SR, Triantafilis J, McBratney AB, Taylor J (2004) A simple soil database management assistant for the Australian Cotton Industry. In 'SuperSoil 2004, 3rd Australian New Zealand Soils Conference'. University of Sydney, Australia. (Ed.s B Singh).

Oster JD, Shainberg I (2001) Soil responses to sodicity and salinity: challenges and opportunities. *Australian Journal of Soil Research* **39**, 1219–1224.

Oster JD, Shainberg I, Wood JD (1980) Flocculation value and gel structure of sodium/calcium montmorillonite and illite suspensions. *Soil Science Society of America Journal* **44**, 955–959.

Piccolo A, Mbagwu JSC (1989) Effects of humic substances and surfactants on the stability of soil aggregates. *Soil Science* **147**, 47–54.

Pierret A, Capowiez Y, Belzunces L, Moran CJ (2002) 3D reconstruction and quantification of macropores using X–ray computed tomography and image analysis. *Geoderma* **106**, 247–271.

Pierret A, Kirby M, Moran CJ (2003) Simultaneous X–ray imaging of plant root growth and water uptake in thin–slab systems. *Plant and Soil* **255**, 361–373.

Pillai UP, McGarry D (1999) Structure repair of a compacted Vertisol with wet–dry cycles and crops. *Soil Science Society of America Journal* **63**, 201–210.

Pillai–McGarry UPP, Collis–George N (1990) Laboratory simulation of the surface morphology of self–mulching and non–self mulching Vertisols. I. Materials, methods and preliminary results. *Australian Journal of Soil Research* **28**, 129–139.

Probert ME, Fergus IF, Bridge BJ, McGarry D, Thomson CH, Russell JS (1987) 'The Properties and Management of Vertisols.' (CAB International: Wallingford, U.K)

Quirk JP (1950) The measurement of stability of soil micro–aggregates in water. *Australian Journal of Agricultural Research* **1**, 276–284.

Quirk JP (1994) Interparticle forces: A basis for the interpretation of soil physical behavior. *Advances in Agronomy* **53**, 121–183.

Quirk JP (2001) The significance of the threshold and turbidity concentrations in relation to sodicity and microstructure. *Australian Journal of Soil Research* **39**, 1185–1217.

Quirk JP, Murray RS (1991) Towards a model for soil structural behaviour. *Australian Journal of Soil Research* **29**, 829–867.

Quirk JP, Schofield RK (1955) The effect of electrolyte concentration on soil permeability. *Journal of Soil Science* **6**, 163–178.

Raine SR, So HB (1993) An energy based parameter for the assessment of aggregate bond energy. *Journal of Soil Science* **44**, 249–259.

Raine SR, So HB (1994) Ultrasonic dispersion of soil in water: the effect of suspension properties on energy dissipation and soil dispersion. *Australian Journal of Soil Research* **32**, 1157–1174.

Raine SR, So HB (1997) An investigation of the relationships between dispersion, power and mechanical energy using the end–over–end shaking and ultrasonic methods of aggregate stability assessment. *Australian Journal of Soil Research* **35**, 41–53.

Rayment GE, Higginson FR (1992) 'Australian Laboratory Handbook of Soil and Water Chemical Methods.' (Inkata Press: Sydney)

Reichert JM, Norton LD (1994) Aggregate stability and rain–impacted sheet erosion of air–dried and pre–wetted clayey surface soils under intense rain. *Soil Science* **158**, 159–169.

Rengasamy P (1982) Dispersion of calcium clay. *Australian Journal of Soil Research* **20**, 153–157.

Rengasamy P, Naidu R (1993) Dispersive potential of sodic soils as influenced by charge on their clay fractions. In 'Proceedings of the 10th International Clay Conference'. Adelaide, Australia, July 18–23. (Eds GJ Churchman, RW Fitzpatrick and RA Egglton) pp. 469–472. (CSIRO Publishing, Melbourne, Australia)

Rengasamy P, Ford GW, Greene RSB (1987) Classification of aggregate stability. In 'Effects of Management Practice on Soil Physical Properties'. Queensland Department of Primary Industries Conference and Workshop Series QC87006, Brisbane. (Eds KJ Coughlan and PN Troung) pp. 97–101.

Rengasamy P, Greene RSB, Ford GW (1986) Influence of magnesium on aggregate stability in sodic red–brown earths. *Australian Journal of Soil Research* **24**, 229–237.

Rengasamy P, Greene RSB, Ford GW, Mehanni AH (1984) Identification of dispersive behaviour and the management of red–brown earths. *Australian Journal of Soil Research* **22**, 413–431.

Rhoades JD (1982) Soluble salts. In 'Methods of soil analysis, II, Chemical and microbial properties'. (Eds AL Page, RH Miller and DR Keeney) pp. 167–179. (ASA–SSSA, Madison: Wisconsin, USA)

Richard G, Sillion JF, Marloie O (2001) Comparison of inverse and direct evaporation methods for estimating soil hydraulic properties under different tillage practices. *Soil Science Society of America Journal* **65**, 215–224.

Ringrose–Voase AJ (1996) Measurement of soil macropore geometry by image analysis of sections through impregnated soil. *Plant and Soil* **183**, 27–47.

Ringrose-Voase AJ, Sanidad WB (1996) A method for measuring the development of surface cracks in soils: application to crack development after lowland rice. *Geoderma* **71**, 245–261.

Roesner EA (2003) Development of an Image Analysis Technique for the Practical Assessment of Soil Pore Structure. Unpublished thesis, The University of Sydney.

Rowell DL, Payne D, Ahmad N (1969) The effect of the concentration and movement of solutions on the swelling, dispersion and movement of clay in saline and alkaline soils. *Journal of Soil Science* **20**, 176–188.

Sahin U, Anapali O, Hanay A (2002) The effect of consecutive applications of leaching water applied in equal, increasing or decreasing quantities on soil hydraulic conductivity of a saline sodic soil in the laboratory. *Soil Use and Management* **18**, 152–154.

Sarmah AK, Pillai-McGarry U, McGarry D (1996) Repair of the structure of a compacted Vertisol via wet / dry cycles. *Soil and Tillage Research* **38**, 17–34.

Schindler U (1980) Ein Schnellverfahren zur Messung der Wasserleitfähigkeit im teilgesättigten Boden. *Archiv fur Acker- und Pflanzenbau und Bodenkunde* **24ä**, 1–7.

Serra J (1982) 'Image analysis and mathematical morphology.' (Academic Pree: London)

Seybold CA, Herrick JE, Brejda JJ (1999) Soil resilience: a fundamental component of soil quality. *Soil Science* **164**, 224–234.

Shainberg I, Gal M (1982) The effect of lime on the response of soils to sodic conditions. *Journal of Soil Science* **33**, 489–498.

Shainberg I, Letey J (1984) Response of soils to sodic and saline conditions. *Hilgardia* **52**, 1–57.

Shainberg I, Levy GJ, Goldstein D, Levin J (1997) Aggregate size and seal properties. *Soil Science* **162**, 470–478.

Shainberg I, Rhoades JD, Prather RJ (1981) Effect of low electrolyte concentration on clay dispersion and hydraulic conductivity of a sodic soil. *Soil Science Society of America Journal* **45**, 273–277.

Shainberg I, Sumner ME, Miller WP, Farina MPW, Pavan MA, Fey MV (1989) Use of gypsum on soils: a review. *Advances in Soil Science* **9**, 1–111.

Shiel RS, Adey MA, Lodder M (1988) The effect of successive wet/dry cycles on aggregate size distribution. *European Journal of Soil Science* **39**, 71–79.

Silvertooth JC (1990) Water management for upland and pima cotton. In 'Belt wide Cotton Conference, 6–12 January 1990'. San Antonio, Texas pp. 64–67.

Singh B, Heffernan S (2002) Layer charge characteristics of smectites from Vertosols (Vertisols) of New South Wales. *Australian Journal of Soil Research* **40**, 1159–1170.

Slade PG, Quirk JP, Norrish K (1991) Crystalline swelling of smectite samples in concentrated NaCl solutions in relation to layer charge. *Clays and Clay Minerals* **39**, 234–238.

So HB, Cook GD (1987) Measuring dispersion of clay soils. In 'Effects of Management Practice on Soil Physical Properties'. Queensland Department of Primary Industries Conference and Workshop Series QC87006, Brisbane. (Eds KJ Coughlan and PN Troung) p. 102–105.

So HB, Cook GD (1993) The effect of slaking and dispersion on the hydraulic conductivity of clay soils. *Catena* **24**, 55–64.

So HB, Cook GD, Raine SR (1997) An examination of the end–over–end shaking technique for measuring soil dispersion. *Australian Journal of Soil Research* **35**, 31–39.

Soil Science Society of America (1997) 'Glossary of Soil Science Terms, 1996.' (Soil Science Society of America, Inc.: Wisconsin 53711 USA)

Soil Survey Staff (1998) 'Keys to Soil Taxonomy.' (United States Department of Agriculture, Natural Resources Conservation Service: Washington DC)

Soil Survey Staff (2003) 'Keys to Soil Taxonomy.' (United States Department of Agriculture, Natural Resources Conservation Service: Washington DC)

Stace HCT, Hubble GD, Brewer R, Northcote KH, Sleeman JR, Mulcahy MJH, E.G. (1968) 'A Handbook of Australian Soils.' (Rellim: Adelaide)

Stannard ME, Kelly ID (1977) 'Irrigation Potential of the Lower Namoi Valley.' (NSW Water Resources Department: Sydney)

Suarez DL, Rhoades JD, Lavado R, Grieve CM (1984) Effect of pH on saturated hydraulic conductivity and soil dispersion. *Soil Science Society of America Journal* **48**, 50–55.

Sumner ME (1993) Sodic soils: new perspectives. *Australian Journal of Soil Research* **31**, 683–750.

Sumner ME, Rengasamy P, Naidu R (1998) Sodic Soils: A Reappraisal. In 'Sodic Soils: Distribution, Properties, Management, and Environmental Consequences'. (Ed.s ME Sumner, Naidu, R.) pp. 3–17. (Oxford University Press: New York Oxford)

Surapaneni A, Olsson KA, Burrow DP, Beecher HG, Hanm GJ, Stevens RM, Hulugalle NR, McKenzie DC, Rengasamy P (2002) Tatura sodicity conference: knowledge gaps in sodicity research for major agricultural industries. *Australian Journal of Experimental Agriculture* **42**, 379–387.

Tessier D (1990) Behaviour and microstructure of clay minerals. In 'Soil colloids and their associations in aggregates'. (Eds MF De Boodt, MHB Hayes and A Herbillon) pp. 387–416. (NATO ASI Series)

Tessier D, Beaumont A, Pedro G (1990) Influence of clay mineralogy and rewetting rate on clay microstructure. In 'Soil micromorphology: A basic and applied science'. (Ed.s LA Douglas) pp. 115–121)

Thomasson AJ (1978) Towards an objective classification of soil structure. *Journal of Soil Science* **29**, 38–46.

Tisdall JM, Oades JM (1982) Organic matter and water stable aggregates in soils. *Journal of Soil Science* **33**, 141–163.

United States Salinity Laboratory Staff (1954) 'Diagnosis and improvement of saline and alkali soils.' (United States Department of Agriculture: Washington DC)

van Genuchten MT (1980) A closed–form equation for predicting the hydraulic conductivity of unsaturated soils. *Soil Science Society of America Journal* **44**, 892–898.

van Olphen H (1963) 'An Introduction to Clay Colloid Chemistry.' (Interscience Publishers: New York)

van Olphen H (1987) Dispersion and flocculation. In 'Chemistry of clays and clay minerals'. (Ed.s ACD Newman) pp. 203–224. (Longman Scientific and Technical: London)

Vervoort RW, Cattle SR, Minasny B (2003) The hydrology of Vertosols used for cotton production: I. Hydraulic, structural and fundamental soil properties. *Australian Journal of Soil Research* **41**, 1255–1272.

Vervoort RW, Cattle SR (2003) Linking hydraulic conductivity and tortuosity parameters to pore space geometry and pore–size distribution. *Journal of Hydrology* **272**, 36–49.

Warkentin BP (1982) Clay soil structure related to soil management. *Tropical Agriculture (Trinidad)* **59**, 82–91.

Watts CW, Dexter AR, Longstaff DJ (1996) An assessment of the vulnerability of soil structure to de–stabilisation during tillage. Part II. Field trials. *Soil and Tillage Research* **37**, 175–190.

Whittig LD, Allardice WR (1986) X-Ray diffraction techniques. In 'Methods of soil analysis: physical and mineralogical methods.' (Ed.s A Flute) pp. 331–361. (Soil Science Society of America: Madison, Wisconsin, USA)

Wilding LP, Puentes R (1988) 'Vertisols: Their distribution, properties, classification and management.' (Texas A&M University Printing Center: College Station)

Wilding LP, Tessier D (1988) Genesis of Vertisols: shrink-swell phenomena. In 'Vertisols: Their distribution, properties, classification and management'. (Ed.s LP Wilding, Puentes, R.) pp. 55–81. (Texas A&M University Printing Center: College Station)

Yaron B, Thomas GW (1968) Soil hydraulic conductivity as affected by sodic water. *Water Resources Research* **4**, 545–552.

Yerima BPK, Calhoun FG, Senkayi AL, Dixon JB (1985) Occurrence of interstratified kaolinite-smectite in El Salvador Vertisols. *Soil Science Society of America Journal* **49**, 462–466.

Yerima BPK, Wilding LP, Calhoun FG, Hallmark CT (1987) Volcanic ash-influenced Vertisols and associated Mollisols of El Salvador: physical, chemical and morphological properties. *Soil Science Society of America Journal* **51**, 699–708.

Yoshida S, Adachi K (2004) Numerical analysis of crack generation in saturated deformable soil under row–planted vegetation. *Geoderma* **120**, 63–74.

Yule DF, Willcocks TF (1996) Tillage and cultural practices. In 'Vertisols and technologies for their management'. (Ed.s N Ahmad, Mermut, A.) pp. 231–259. (Elsevier: Amsterdam)

Appendices

Appendix 1: Position of the nine different Vertosols according to the topographic and geological landscapes

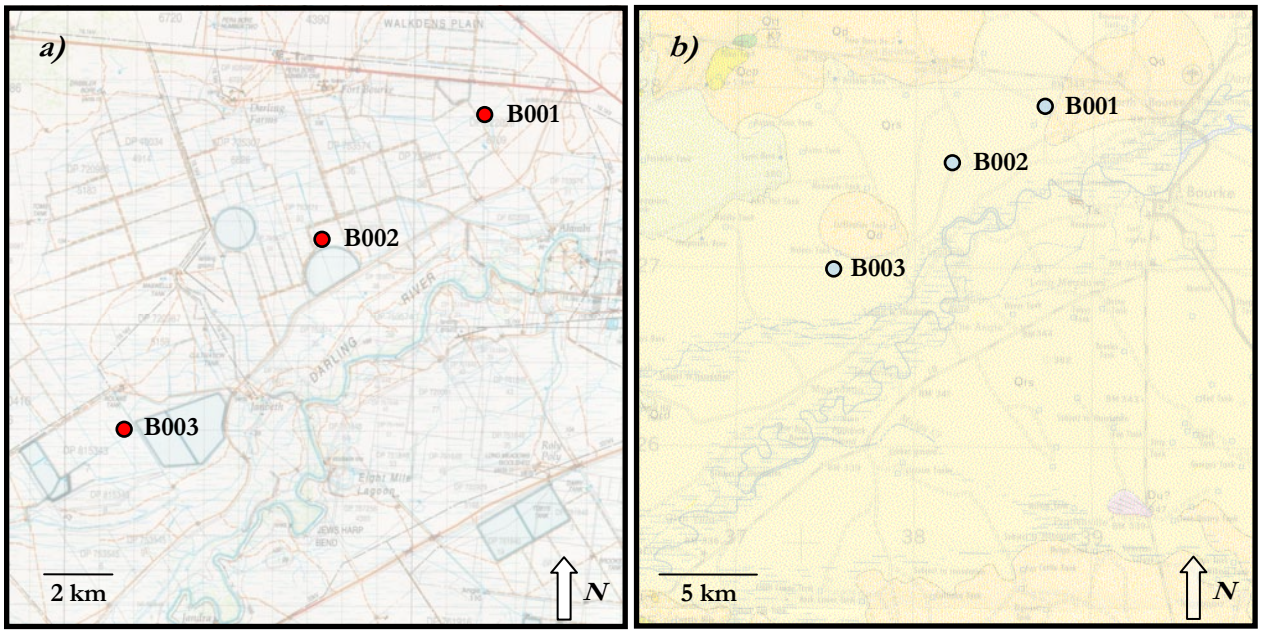

Figure A1.1 Position of each of the B00*i* soils according to, *a)*, the topographic landscape (*topographic map 8037, NSW Department of Lands*) and, *b)*, the geological landscape (*Bourke geological map, NSW Department of Primary Industries*). Geological reference unit *Qd* represents red sand forming undulating plains, and reference unit *Qrs* represents alluvial floodplains of clayey silt, sand and gravel.

Figure A1.2 Position of each of the G00*i* soils according to, *a)* and *b)*, the topographic landscape (*topographic map 8839–II and III, NSW Department of Lands*) and, *c)*, the geological landscape (*Moree geological map, NSW Department of Primary Industries*). Geological landscape consists of alluvial riverine deposits of black and red clayey silt, sand and coarse gravel.

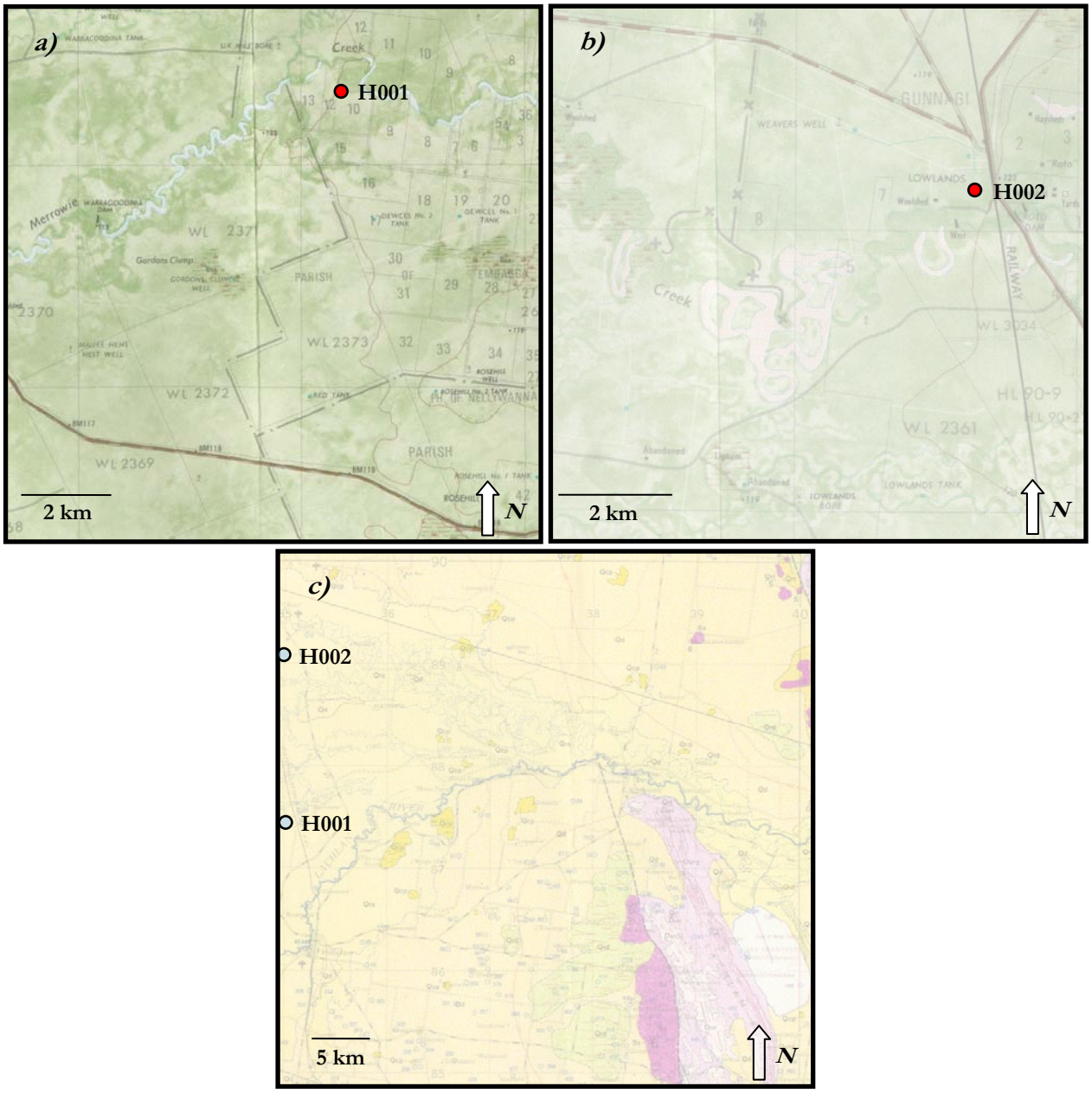

Figure A1.3 Position of each of the H00*i* soils according to, *a)* and *b)*, the topographic landscape (*topographic map 7931, NSW Department of Lands*) and, *c)*, the geological landscape (*Cargelliogo geological map, NSW Department of Primary Industries*). The H00*i* soils are both positioned on alluvial deposits of black and red clayey silt, sand and gravel in the geological landscape.

Figure A1.4 Position of each of the N00*i* soils according to, *a)* and *b)*, the topographic landscape (*N001 is positioned on the 8738–II and III topographic map and N002 is positioned on the 8837–I and IV topographic map, NSW Department of Lands*) and, *c)* and *d)*, the geological landscape (*N001 is positioned on the Moree geological map and N002 is positioned on the Narrabri geological map, NSW Department of Primary Industries*). The N001 and N002 geological landscapes consists of alluvial riverine plain deposits of black and red clayey silt, sand and coarse gravel.

Appendix 2.1: **X–ray diffraction patterns of randomly arranged soil minerals for the B00*i*, G002, H002 and N00*i* Vertosols**

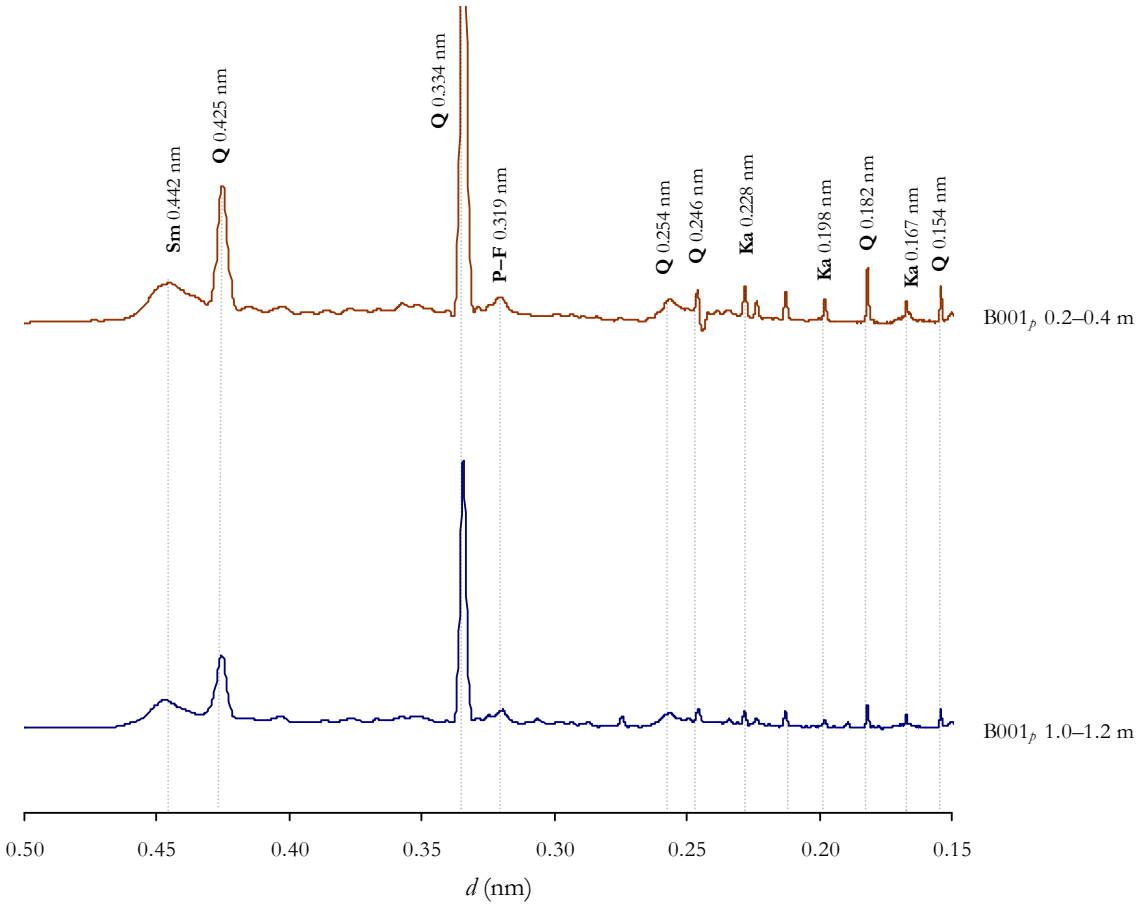

Figure A2.1 The primary suite of soil minerals from site B001 at depths of 0.2–0.4 and 1.0–1.2m. The labels identify the basal spacings (nm) corresponding to the dominant mineral species: quartz (Q), plagioclase feldspars (P–F), smectite clay (Sm) and kaolinite clay (Ka).

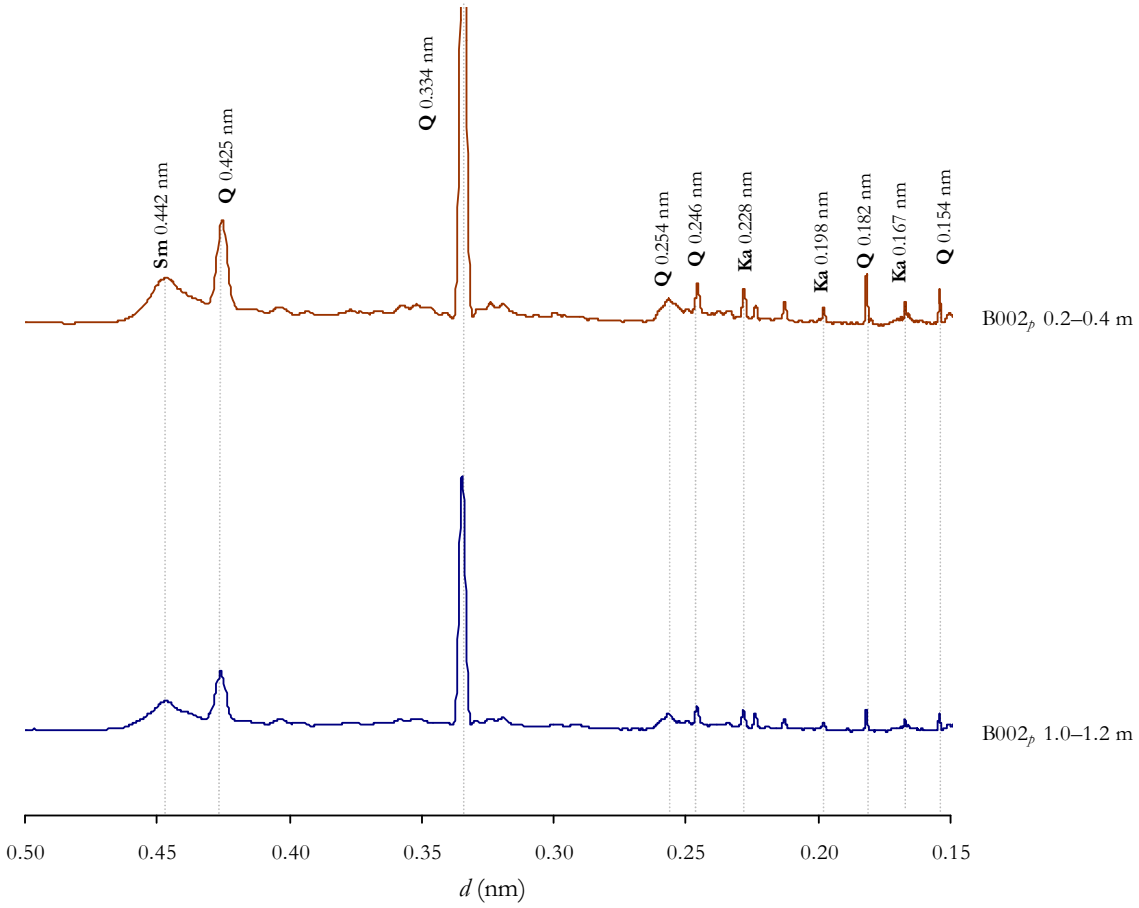

Figure A2.2 The primary suite of soil minerals from site B002 at depths of 0.2–0.4 and 1.0–1.2m. The labels identify the basal spacings (nm) corresponding to the dominant mineral species: quartz (Q), smectite clay (Sm) and kaolinite clay (Ka).

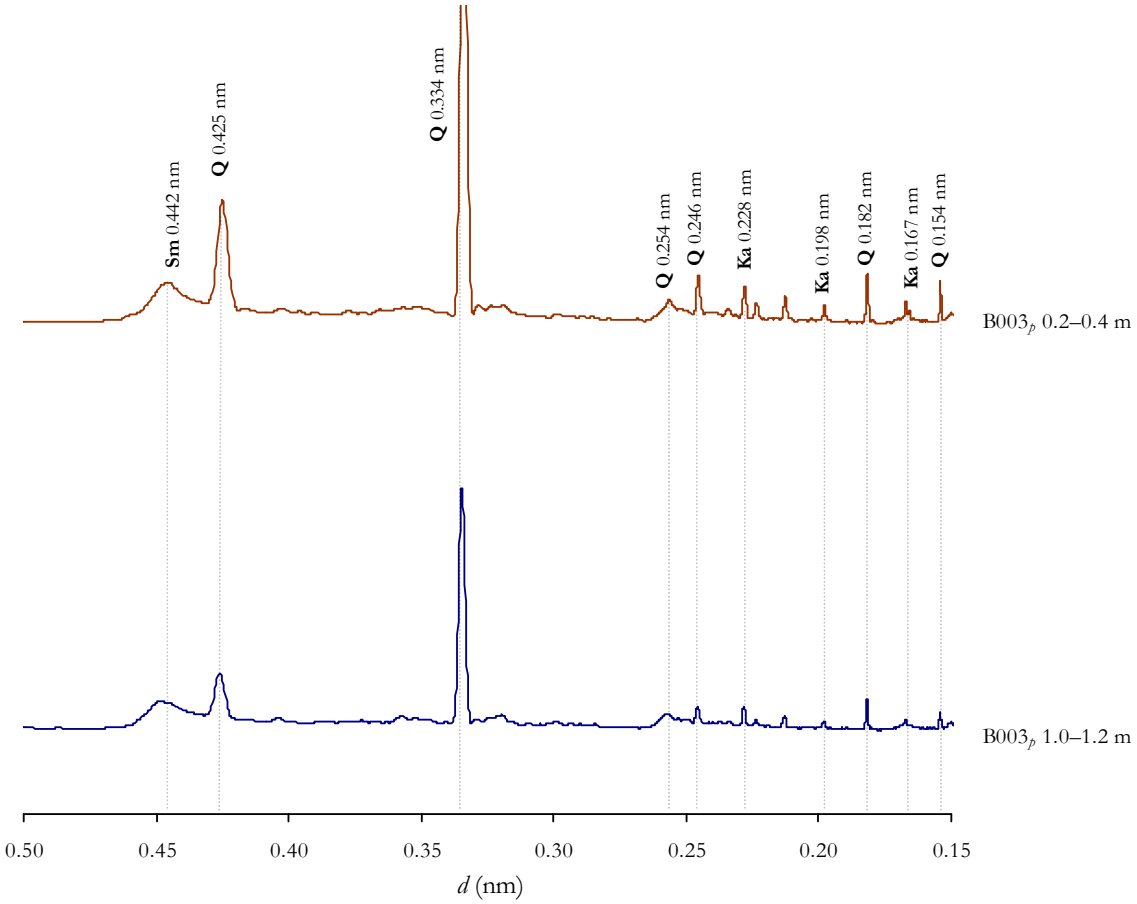

Figure A2.3 The primary suite of soil minerals from site B003 at depths of 0.2–0.4 and 1.0–1.2m. The labels identify the basal spacings (nm) corresponding to the dominant mineral species: quartz (Q), smectite clay (Sm) and kaolinite clay (Ka).

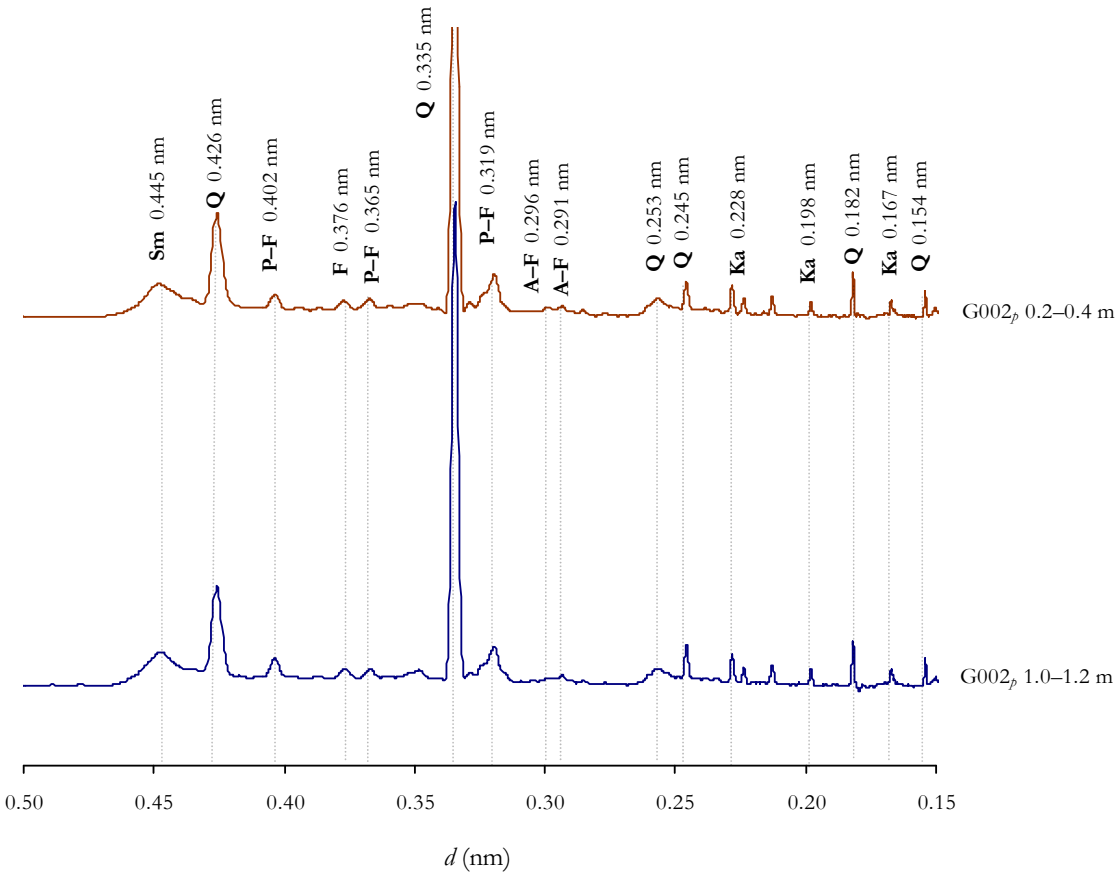

Figure A2.4 The primary suite of soil minerals from site G002 at depths of 0.2–0.4 and 1.0–1.2m. The labels identify the basal spacings (nm) corresponding to the dominant mineral species: quartz (Q), feldspars (F), plagioclase feldspars (P–F), alkali–feldspars (A–F), smectite clay (Sm) and kaolinite clay (Ka).

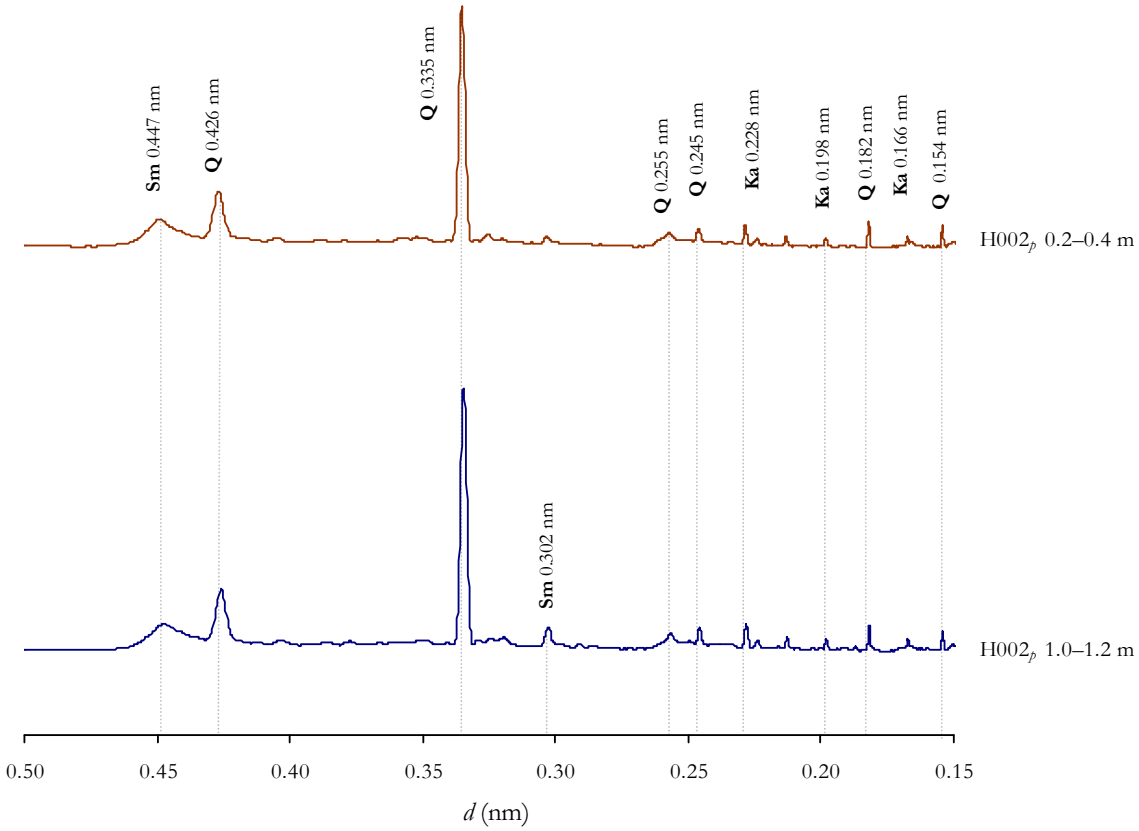

Figure A2.5 The primary suite of soil minerals from site H002 at depths of 0.2–0.4 and 1.0–1.2m. The labels identify the basal spacings (nm) corresponding to the dominant mineral species: quartz (Q), smectite clay (Sm) and kaolinite clay (Ka).

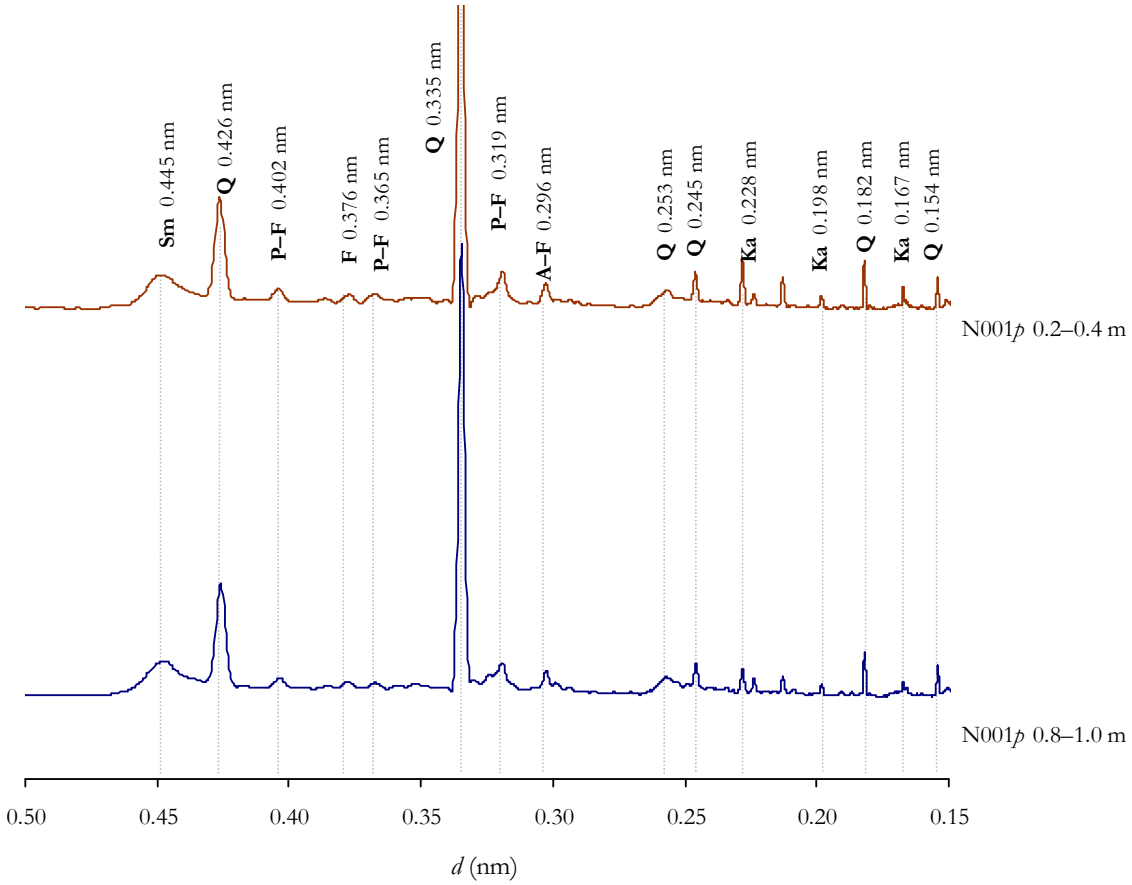

Figure A2.6 The primary suite of soil minerals from site N001 at depths of 0.2–0.4 and 1.0–1.2m. The labels identify the basal spacings (nm) corresponding to the dominant mineral species: quartz (Q), feldspars (F), plagioclase feldspars (P–F), alkali–feldspars (A–F), smectite clay (Sm) and kaolinite clay (Ka).

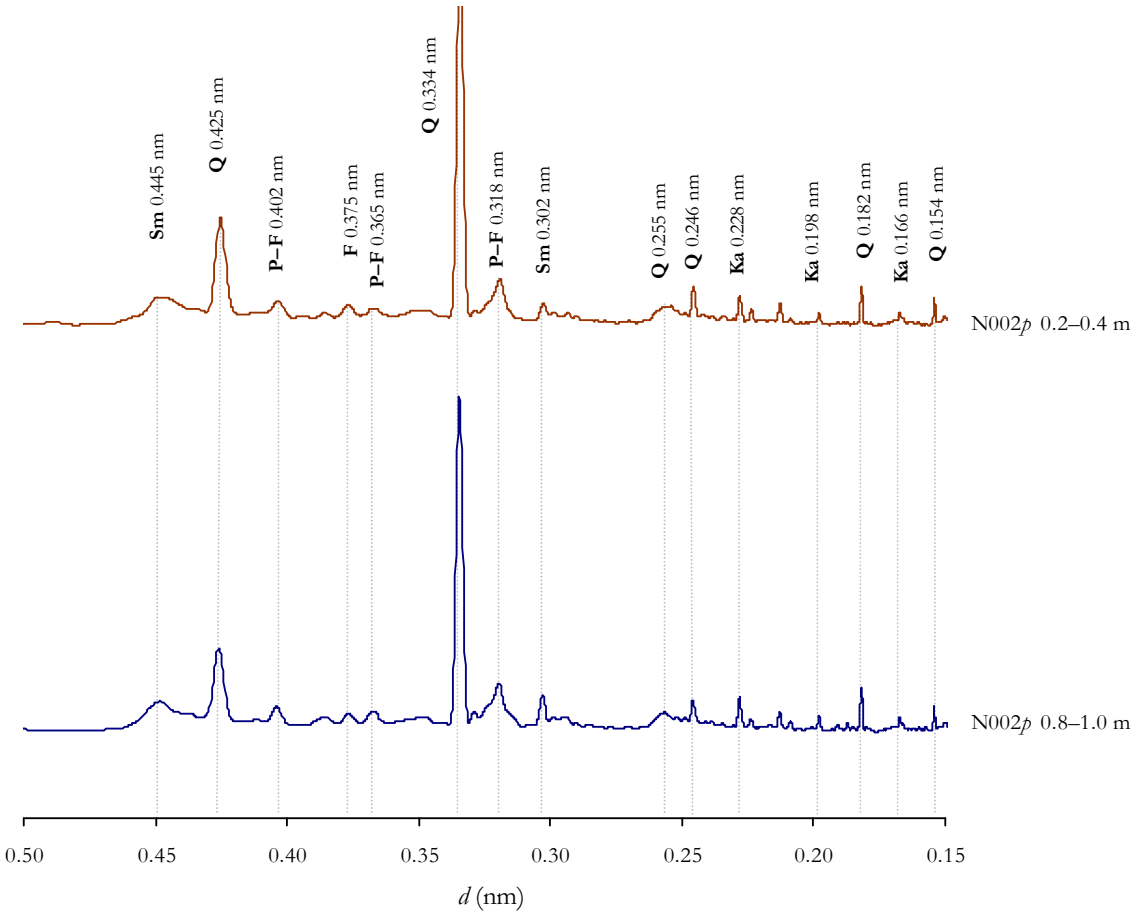

Figure A2.7 The primary suite of soil minerals from site N002 at depths of 0.2–0.4 and 1.0–1.2m. The labels identify the basal spacings (nm) corresponding to the dominant mineral species: quartz (Q), feldspars (F), plagioclase feldspars (P–F), smectite clay (Sm) and kaolinite clay (Ka).

Appendix 2.2: **X–ray diffraction patterns of the fine (<0.2 μm) and coarse (0.2–2 μm) mineral suites of each of the B00*i*, G002, H002 and N00*i* Vertosols**

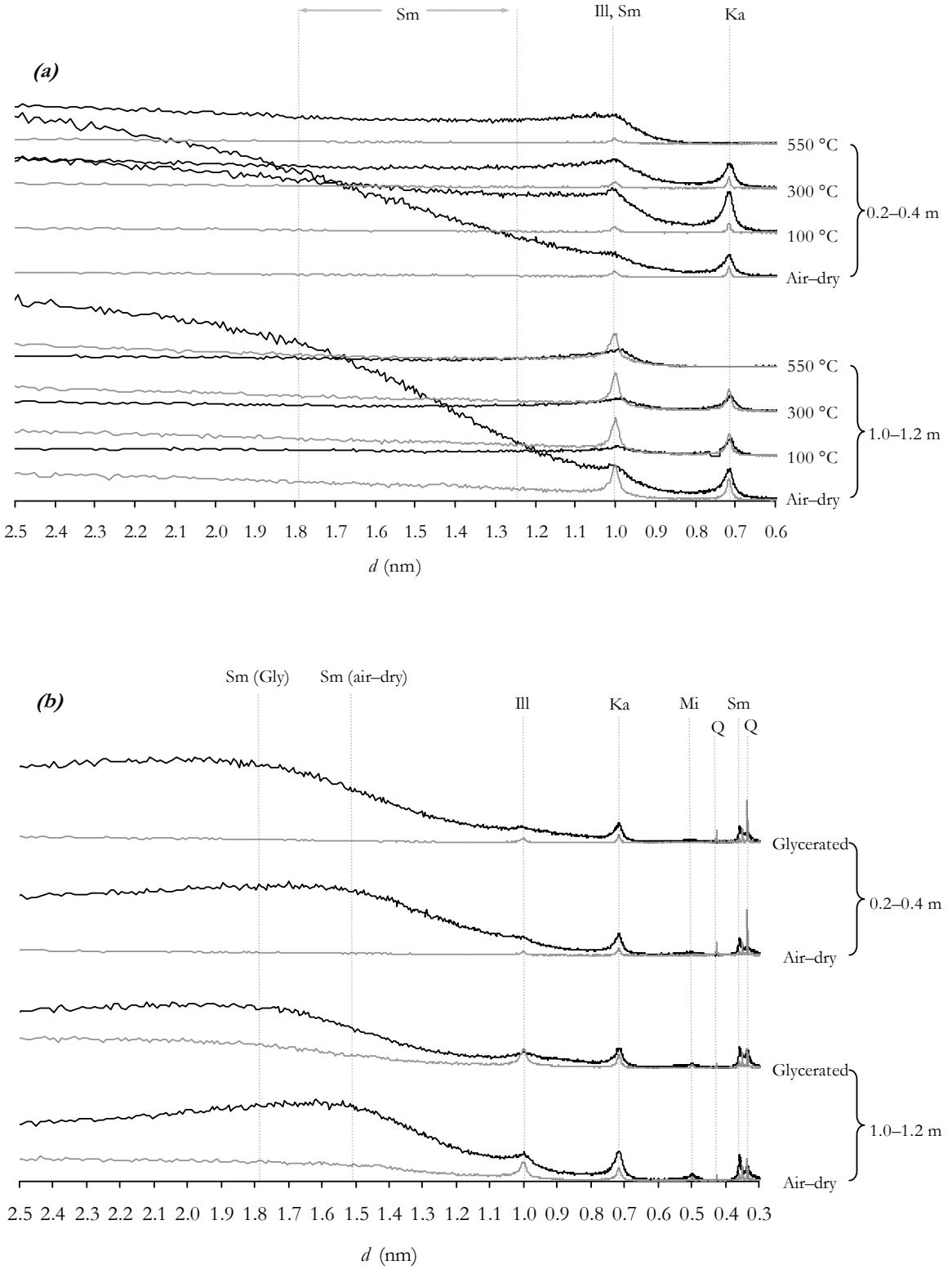

Figure A2.8 Fine (▬) and coarse clay minerals (▬) sampled at depths of 0.2–0.4 and 1.0–1.2 m from site B001, after treatment with,*(a)*, KCl (air–dry, 100 °C, 300 °C and 550 °C) and, *(b)*, $MgCl_2$ (air–dry and glycerated). The labels identify the different clay minerals; smectite clay (Sm), illite clay (Ill), kaolinite clay (Ka), quartz (Q) and mica (Mi).

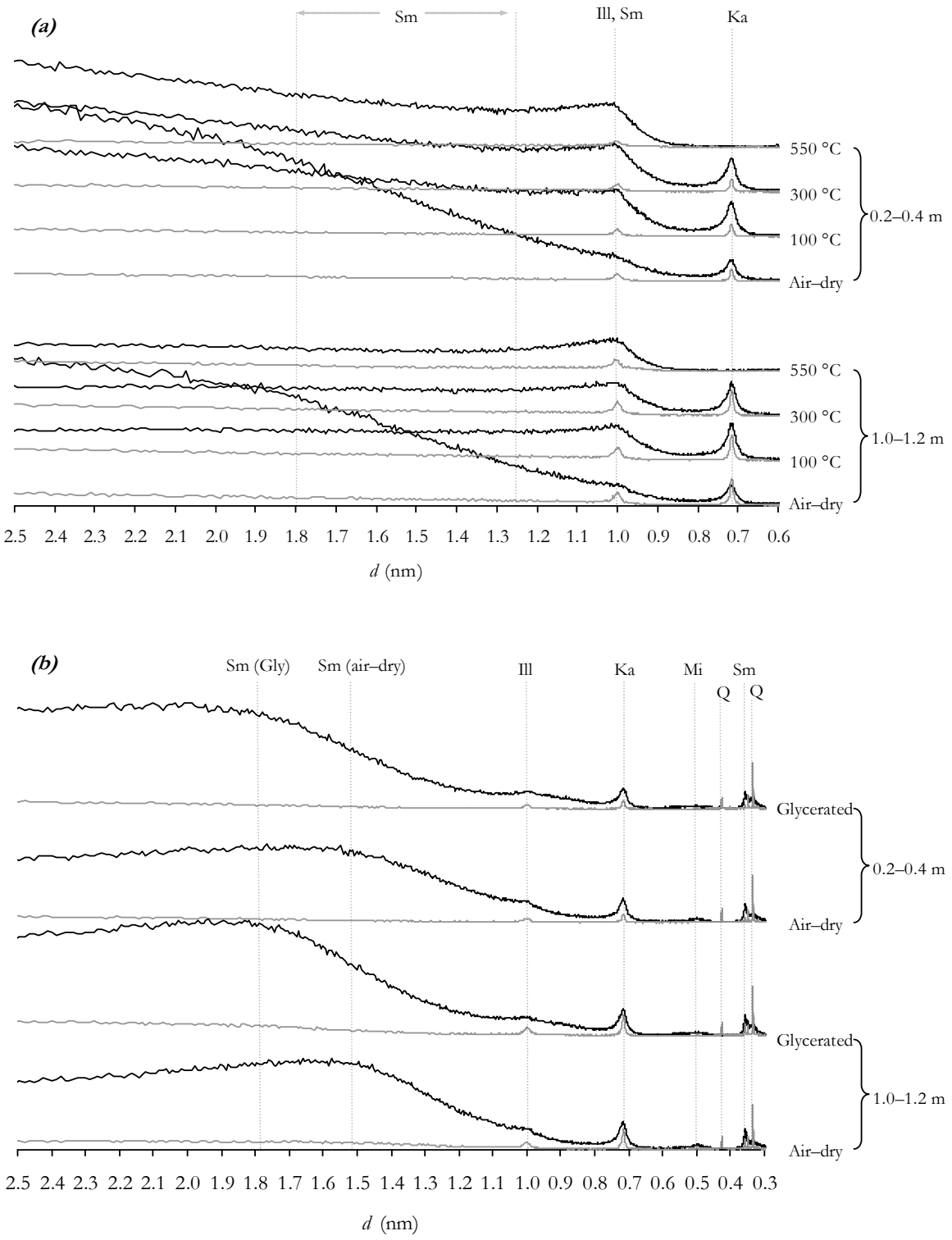

Figure A2.9 Fine (▬) and coarse clay minerals (▬) sampled at depths of 0.2–0.4 and 1.0–1.2 m from site B002, after treatment with,*(a)*, KCl (air–dry, 100 °C, 300 °C and 550 °C) and, *(b)*, $MgCl_2$ (air–dry and glycerated). The labels identify the different clay minerals; smectite clay (Sm), illite clay (Ill), kaolinite clay (Ka), quartz (Q) and mica (Mi).

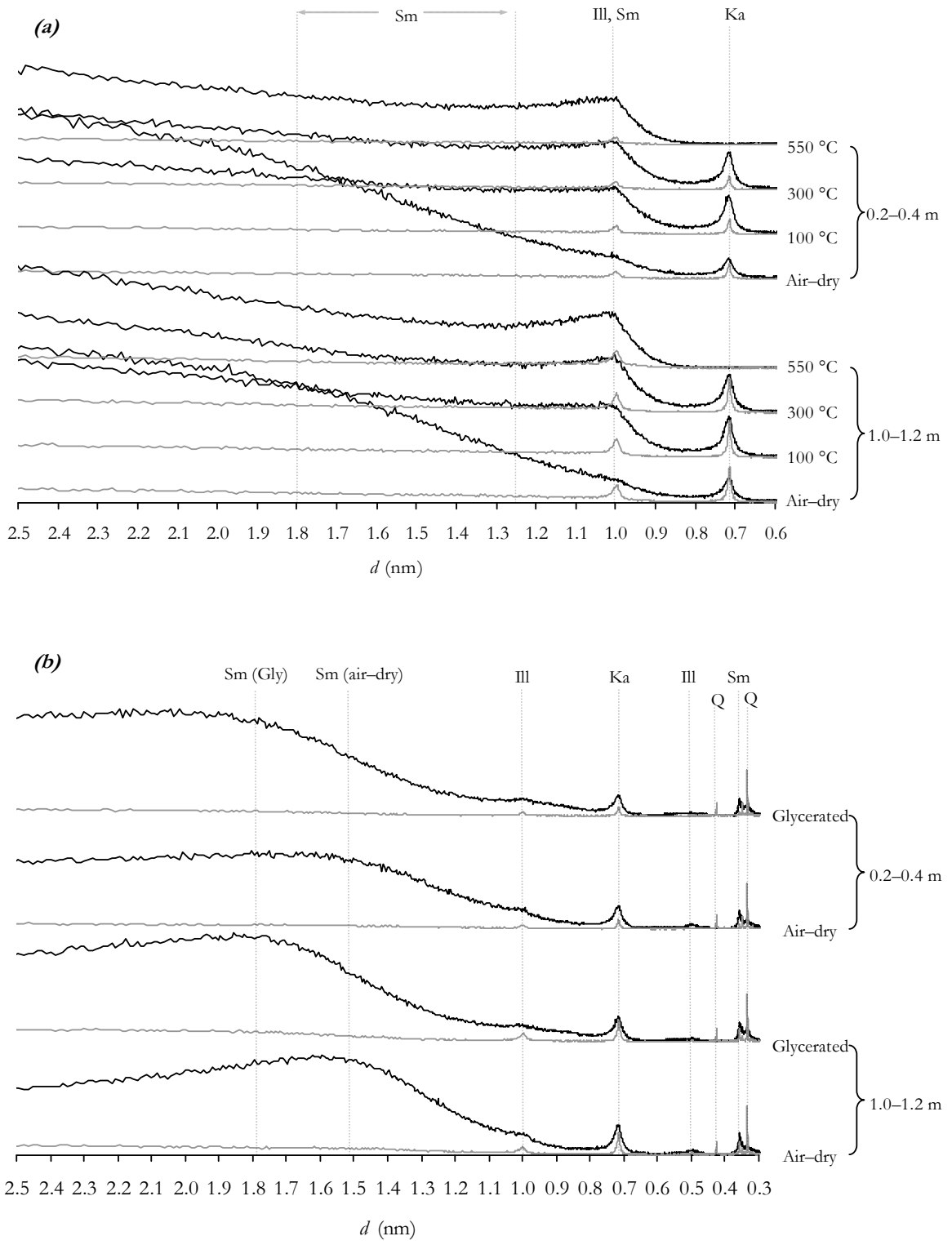

Figure A2.10 Fine (▬) and coarse clay minerals (▬) sampled at depths of 0.2–0.4 and 1.0–1.2 m from site B003, after treatment with,*(a)*, KCl (air–dry, 100 °C, 300 °C and 550 °C) and, *(b)*, $MgCl_2$ (air–dry and glycerated). The labels identify the different clay minerals; smectite clay (Sm), illite clay (Ill), kaolinite clay (Ka), quartz (Q) and mica (Mi).

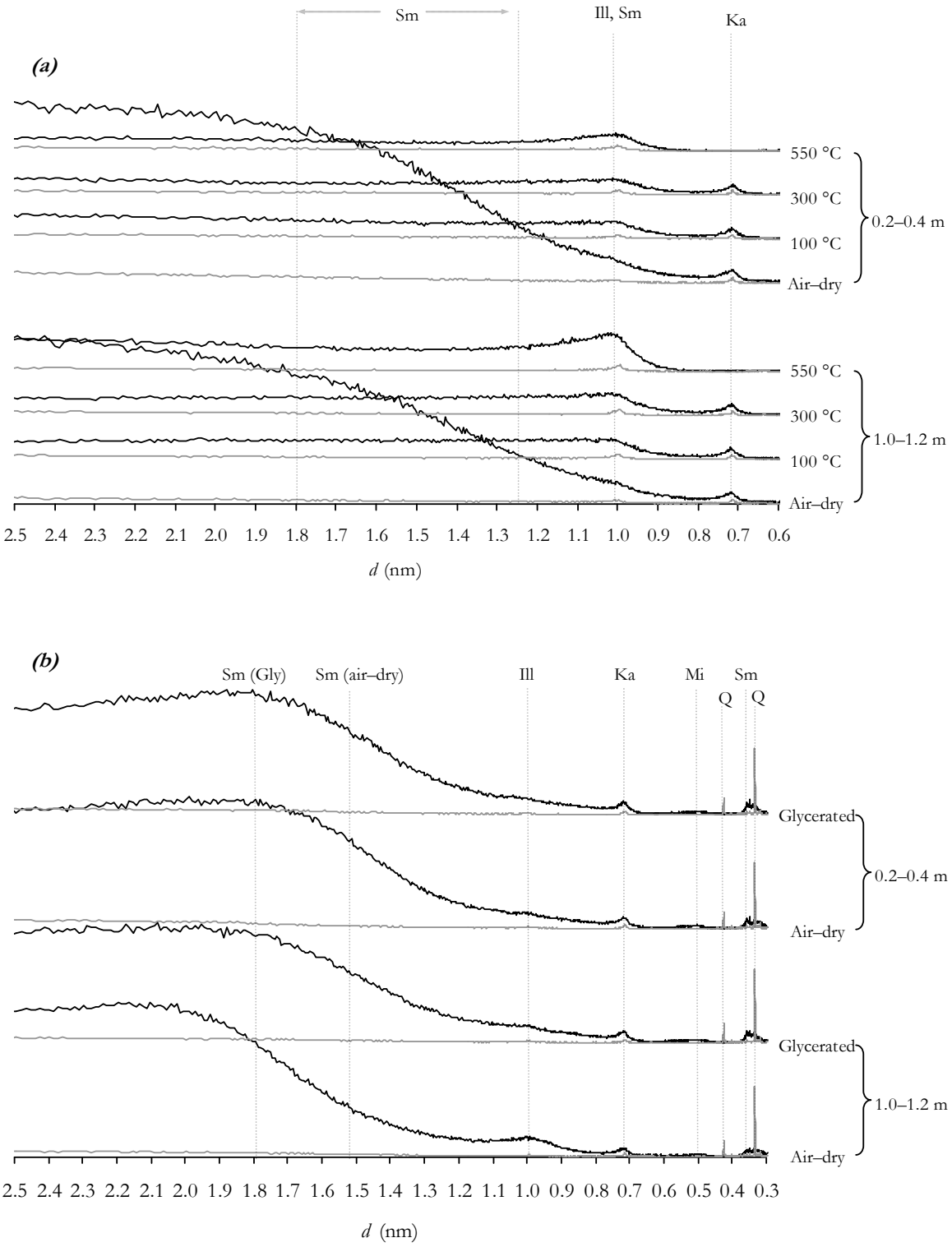

Figure A2.11 Fine (▬) and coarse clay minerals (▬) sampled at depths of 0.2–0.4 and 1.0–1.2 m from site G002, after treatment with,*(a)*, KCl (air–dry, 100 °C, 300 °C and 550 °C) and, *(b)*, $MgCl_2$ (air–dry and glycerated). The labels identify the different clay minerals; smectite clay (Sm), illite clay (Ill), kaolinite clay (Ka), quartz (Q) and mica (Mi).

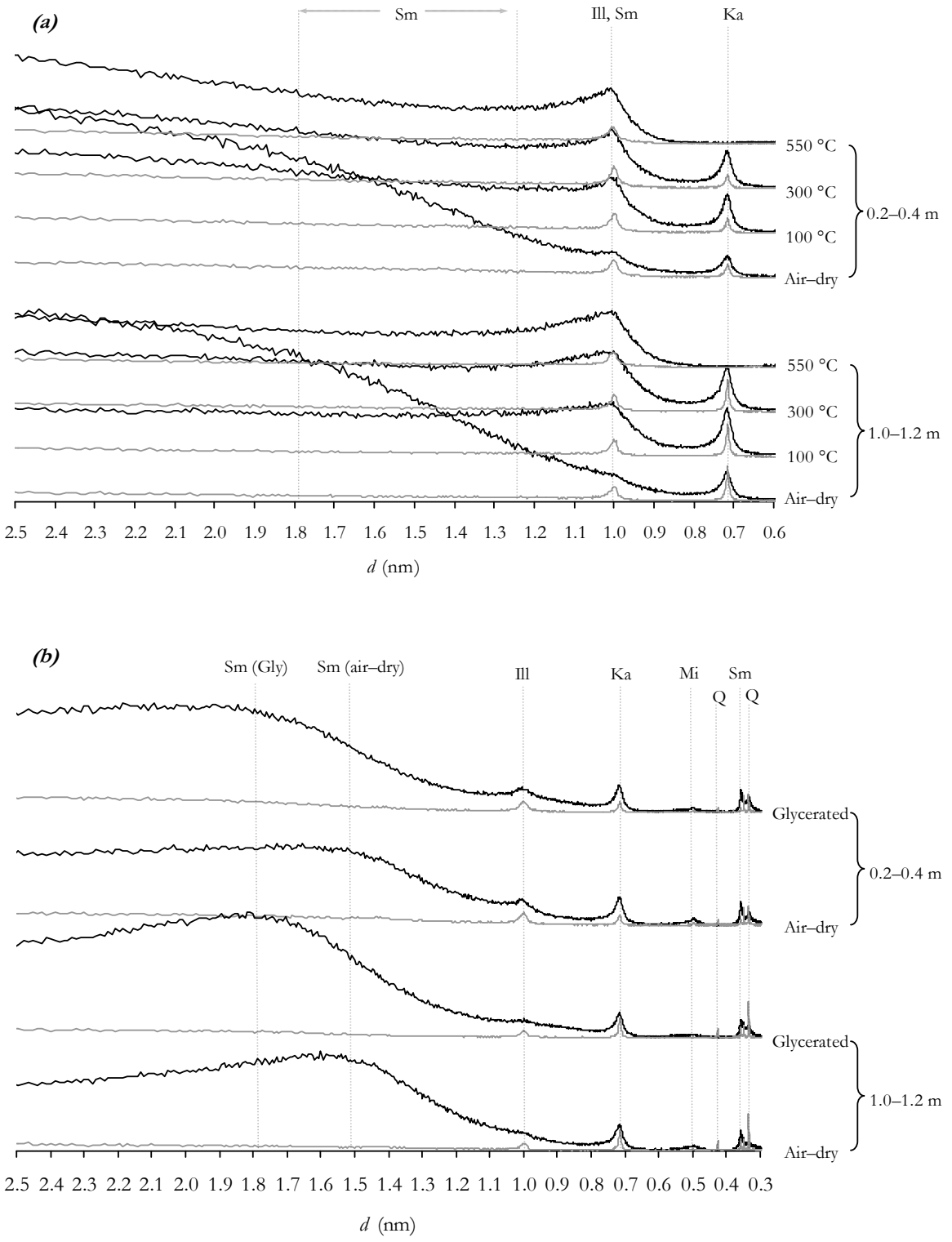

Figure A2.12 Fine (▬) and coarse clay minerals (▬) sampled at depths of 0.2–0.4 and 1.0–1.2 m from site H002, after treatment with,*(a)*, KCl (air–dry, 100 °C, 300 °C and 550 °C) and, *(b)*, $MgCl_2$ (air–dry and glycerated). The labels identify the different clay minerals; smectite clay (Sm), illite clay (Ill), kaolinite clay (Ka), quartz (Q) and mica (Mi).

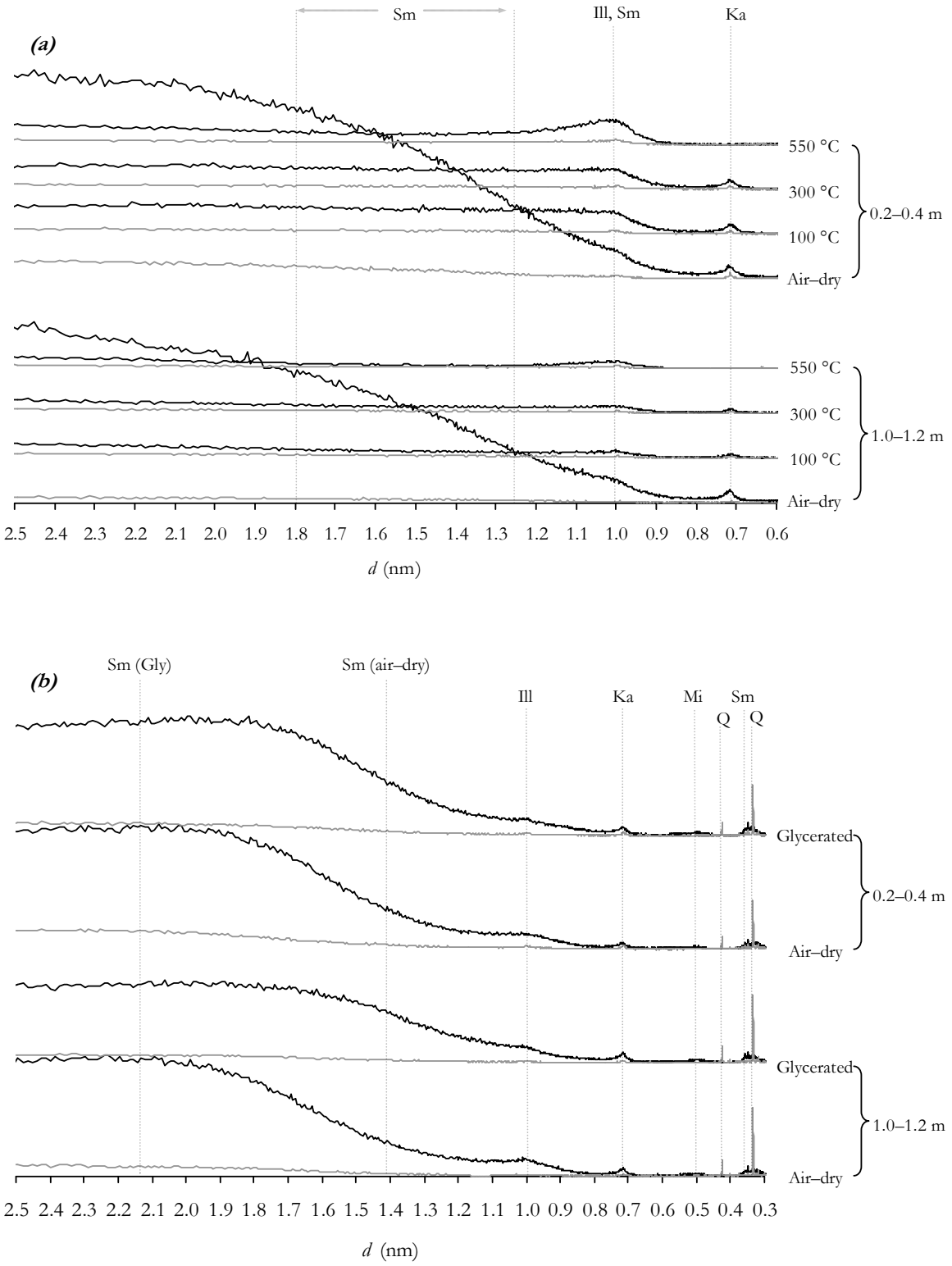

Figure A2.13 Fine (▬) and coarse clay minerals (▬) sampled at depths of 0.2–0.4 and 1.0–1.2 m from site N001, after treatment with,*(a)*, KCl (air–dry, 100 °C, 300 °C and 550 °C) and, *(b)*, $MgCl_2$ (air–dry and glycerated). The labels identify the different clay minerals; smectite clay (Sm), illite clay (Ill), kaolinite clay (Ka), quartz (Q) and mica (Mi).

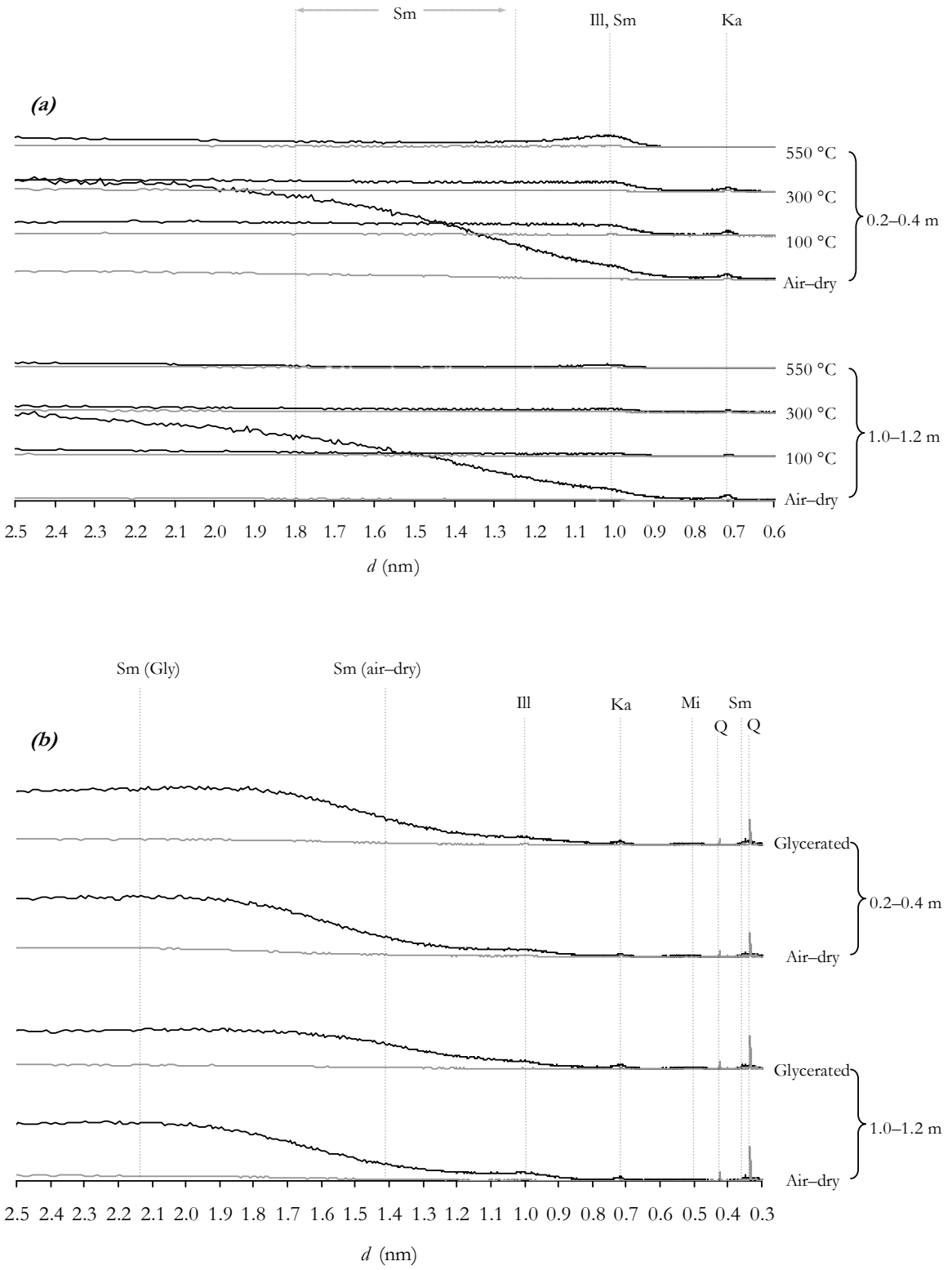

Figure A2.14 Fine (▬) and coarse clay minerals (▬) sampled at depths of 0.2–0.4 and 1.0–1.2 m from site N002, after treatment with,*(a)*, KCl (air–dry, 100 °C, 300 °C and 550 °C) and, *(b)*, $MgCl_2$ (air–dry and glycerated). The labels identify the different clay minerals; smectite clay (Sm), illite clay (Ill), kaolinite clay (Ka), quartz (Q) and mica (Mi).

Appendix 3.1: The change in weight for all individual intact soil columns (B00*i*, G00*i*, H00*i* and N00*i*) irrigated in the laboratory

Table A3.1
The change in weight for soil columns sampled from B001 and B003 after irrigation in the laboratory
The weights recorded represent the difference between before and after each irrigation event

Treatment Solution	Irrigation event	Replicate 1	Replicate 2	Replicate 1	Replicate 2
		(kg)			
		Site B001		Site B003	
FW00*i*	1	–	–	–	–
	2	–	–	–	–
	3	–	0.38	–	0.31
	4	0.30	0.60	0.30	0.43
	5	0.42	0.42	0.42	0.31
	6	0.32	0.36	0.33	0.24
T102	1	–	–	–	–
	2	0.30	0.38	0.30	0.30
	3	0.44	0.56	0.42	0.40
	4	0.33	0.43	0.31	0.32
	5	0.27	0.37	0.25	0.24
	6	–	–	–	–
T401	1	0.32	0.33	0.31	0.32
	2	0.24	0.29	0.08	0.24
	3	0.38	0.39	0.35	0.40
	4	0.21	0.19	0.19	0.20
	5	0.30	0.31	0.35	0.31
	6	0.21	0.21	0.20	0.19
T402	1	0.23	0.28	0.26	0.28
	2	0.37	0.43	0.38	0.41
	3	–	–	–	–
	4	–	–	–	–
	5	0.29	0.36	0.30	0.30
	6	0.30	0.38	0.26	0.33
T403	1	0.26	0.29	0.28	0.20
	2	0.39	0.41	0.42	0.34
	3	–	–	–	–
	4	–	–	–	–
	5	0.31	0.35	0.32	0.27
	6	0.34	0.40	0.30	0.26

Table A3.2
The change in weight for soil columns sampled from B002 after irrigation in the laboratory
The weights recorded represent the difference between before and after each irrigation event

Treatment Solution	Irrigation event	Replicate 1	Replicate 2	
		(kg)		
FW00*i*	1	–	–	*
	2	–	–	*
	3	–	–	*
	4	0.27	0.45	*
	5	0.37	0.35	*
	6	6.86	0.26	*

* Represents soil columns with surface water after the completion of irrigation.

Table A3.3
The change in weight for soil columns sampled from G001 after irrigation in the laboratory
The weights recorded represent the difference between before and after each irrigation event

Treatment Solution	Irrigation event	Replicate 1	Replicate 2	Replicate 3	Replicate 4
		(kg)			
FW00*i*	1	0.20	0.25	0.20	0.15 *
	2	0.20	0.19	0.14	0.22 *
	3	0.31	0.29	0.26	0.41 **
	4	0.14	0.16	0.15	0.26
	5	0.24	0.27	0.24	0.39 *
	6	0.19	0.20	0.16	0.20
T102	1	0.21	0.21	0.19	0.26 *
	2	0.21	0.20	0.18	0.24 *
	3	0.29	0.29	0.26	0.38 *
	4	0.21	0.17	0.23	0.23 **
	5	0.25	0.26	0.24	0.34 *
	6	0.18	0.18	0.19	0.21 **
T401	1	0.34 **	0.34 *	0.30	0.30
	2	0.23 **	0.22 *	0.23	0.22
	3	0.35 **	0.43 *	0.30	0.31
	4	0.20 **	0.25 *	0.17	0.19
	5	0.37 **	0.38 *	0.35	0.29
	6	0.20 **	0.30	0.22	0.22
T402	1	0.22	0.25 *	0.24	0.17
	2	0.20	0.26 *	0.28 *	0.23
	3	0.28	0.40 *	0.40 *	0.29
	4	0.02	0.22 **	0.16	0.24
	5	0.26	0.34 *	0.33	0.26
	6	0.20	0.19 **	0.21	0.21 *
T403	1	0.30 *	0.26	0.23	0.22
	2	0.26 **	0.21	0.19	0.20
	3	0.38 **	0.30	0.32	0.31
	4	0.19 **	0.13	0.17	0.22
	5	0.34 *	0.24	0.28	0.26
	6	0.27 **	0.18	0.20	0.19
T404	1	0.21	0.27 **	0.23	0.19
	2	0.24	0.31 **	0.32 *	0.23
	3	0.31	0.39 *	0.39 *	0.29
	4	0.30	0.41 *	0.41 *	0.31
	5	0.35	0.43 *	0.43 *	0.36
	6	0.29	0.38 *	0.39 *	0.29

* Represents soil columns with surface water after the completion of irrigation.
** Represents soil columns with no drainage water after the completion of the irrigation event.

Table A3.4
The change in weight for soil columns sampled from G002 after irrigation in the laboratory
The weights recorded represent the difference between before and after each irrigation event

Treatment Solution	Irrigation event	Replicate 1	Replicate 2	Replicate 3	Replicate 4
		(kg)			
FW00*i*	1	0.27	0.30	0.29	0.31
	2	0.19	0.23	0.21	0.23
	3	0.29	0.33	0.30	0.34
	4	0.19	0.20	0.22	0.27 *
	5	0.33	0.33	0.32	0.33
	6	0.21	0.20	0.19	0.29 *
T102	1	0.30	0.28	0.43 *	0.26
	2	0.24	0.21	0.33 *	0.24
	3	0.30	0.32	0.36 *	0.32
	4	0.28 *	0.21	0.22 *	0.21
	5	0.40 *	0.29	0.38 *	0.43 *
	6	0.27 *	0.23	0.23 *	0.28
T401	1	0.28	0.28	0.28	0.34 *
	2	0.20	0.22	0.22	0.23 *
	3	0.28	0.27	0.26	0.38 *
	4	0.23	0.19	0.23	0.24 *
	5	0.32	0.28	0.34	0.35
	6	0.21	0.21	0.22	0.31
T402	1	0.29	0.31 *	0.39	0.27
	2	0.21	0.23 *	0.32 *	0.35 *
	3	0.31	0.30 *	0.40 *	0.37 *
	4	0.24	0.21 *	0.23 *	0.27 *
	5	0.42	0.40 *	0.41 *	0.41 *
	6	0.27 *	0.29 *	0.27 *	0.41
T403	1	0.32	0.29	0.29 *	0.24
	2	0.21	0.31 *	0.21 *	0.23
	3	0.32	0.38 *	0.34 *	0.41
	4	0.22	0.26 *	0.16	0.32 *
	5	0.31	0.42 *	0.35 *	0.43 *
	6	0.23	0.26 *	0.21 *	0.30 *
T404	1	0.25	0.19	0.35 *	0.19
	2	0.37 *	0.23	0.35 *	0.24
	3	0.39 *	0.29 *	0.39 *	0.33
	4	0.42 *	0.31	0.40 *	0.41
	5	0.51 *	0.45	0.47 *	0.51 *
	6	0.37 *	0.31	0.33 *	0.39

* Represents soil columns with surface water after the completion of irrigation.

Table A3.5
The change in weight for soil columns sampled from H001 after irrigation in the laboratory
The weights recorded represent the difference between before and after each irrigation event

Treatment Solution	Irrigation event	Replicate 1	Replicate 2	Replicate 3	Replicate 4
		(kg)			
FW00*i*	1	0.22	0.27	0.26 *	0.22 *
	2	0.28	0.33	0.34 *	0.32 *
	3	0.20	0.19	0.23 *	0.25 *
	4	0.16	0.18	0.21 *	0.23 *
	5	0.27	0.29	0.34 *	0.33 *
	6	0.28	0.27	0.32 *	0.35 *
T102	1	0.21	0.21	0.21	0.20
	2	0.28	0.31 *	0.34 *	0.31
	3	0.19	0.22 *	0.24 *	0.26 *
	4	0.20 *	0.18 *	0.19 *	0.21 *
	5	0.32 *	0.35 *	0.28 *	0.34 *
	6	0.32 *	0.28 **	0.32 *	0.34 *
T401	1	0.38	0.29	0.43 *	0.38 *
	2	0.35 *	0.28	0.37	0.33 *
	3	0.48 *	0.35	0.50 *	0.43 *
	4	0.24	0.16	0.26	0.21 *
	5	0.39 *	0.28	0.40	0.39 *
	6	0.29	0.26	0.26 *	0.21 *
T402	1	0.21	0.18	0.22	0.31 *
	2	0.35	0.24	0.37 *	0.39 *
	3	–	–	– *	– *
	4	–	–	–	–
	5	0.33	0.19	0.27 *	0.30 *
	6	0.29	0.24	0.26 *	0.37 *
T403	1	0.27 *	0.25 *	0.30 *	0.21
	2	0.26 *	0.38 *	0.41 *	0.34
	3	– *	– *	– *	–
	4	–	–	–	–
	5	0.27 *	0.27 *	0.32 *	0.21
	6	0.28 *	0.29 *	0.33 *	0.28
T404	1	0.28	0.27	0.35 *	0.33
	2	0.29	0.24	0.27 *	0.28 *
	3	0.22 *	0.24 *	0.25 *	0.24 *
	4	0.28 *	0.30	0.25 *	0.27 *
	5	0.23	0.21 *	0.20 *	0.27 *
	6	0.18 *	0.20 *	0.18 *	0.18 *

* Represents soil columns with surface water after the completion of irrigation.
** Represents soil columns with no drainage water after the completion of the irrigation event.

Table A3.6
The change in weight for soil columns sampled from H002 after irrigation in the laboratory
The weights recorded represent the difference between before and after each irrigation event

Treatment Solution	Irrigation event	Replicate 1	Replicate 2	Replicate 3	Replicate 4
		(kg)			
FW00*i*	1	0.18	0.20	0.21	0.19
	2	0.28	0.28	0.28	0.28
	3	0.19	0.15	0.23	0.20
	4	0.16	0.18	0.17	0.19
	5	0.29	0.31	0.27	0.29
	6	0.29	0.31	0.30	0.30
T102	1	0.21	0.21	0.20	0.21
	2	0.25	0.29	0.34	0.29
	3	0.19	0.20	0.26 *	0.18
	4	0.16	0.18	0.25 *	0.20
	5	0.29	0.34	0.31 *	0.26
	6	0.26	0.30	0.33 *	0.30
T401	1	0.08	0.36	0.34 *	0.28 *
	2	0.36 *	0.25	0.24	0.28 *
	3	0.59 *	0.60	0.48	0.48 *
	4	0.25 *	0.21	0.29	0.26 *
	5	0.44 *	0.29	0.31	0.36 *
	6	0.26 *	0.21	0.25 *	0.21 *
T402	1	0.25 *	0.18	0.19	0.21
	2	0.38 *	0.30	0.35	0.34
	3	– *	–	–	–
	4	–	–	–	–
	5	0.27 *	0.22	0.20	0.30
	6	0.34 *	0.28	0.28	0.31
T403	1	0.28 *	0.19	0.24 *	0.18
	2	0.45 *	0.29	0.33 *	0.29
	3	–	– *	–	–
	4	–	–	–	–
	5	0.32 *	0.34 *	0.27 *	0.23
	6	0.30 *	0.36 *	0.26	0.28
T404	1	0.19	0.31	0.25	0.27
	2	0.25	0.33	0.28	0.30
	3	0.31 *	0.41 *	0.37 *	0.40 *
	4	0.32 *	0.40 *	0.35 *	0.40 *
	5	0.41 *	0.44 *	0.47 *	0.49 *
	6	0.34 *	0.41 *	0.33 *	0.36 *

* Represents soil columns with surface water after the completion of irrigation.

Table A3.7
The change in weight for soil columns sampled from N001 after irrigation in the laboratory
The weights recorded represent the difference between before and after each irrigation event

Treatment Solution	Irrigation event	Replicate 1	Replicate 2	Replicate 3	Replicate 4
		(kg)			
FW00*i*	1	0.26	0.27	0.25	0.36 *
	2	0.27	0.23	0.25	0.23 *
	3	0.18	0.14	0.14	0.24 *
	4	0.21	0.19	0.31	0.26 *
	5	0.14	0.16	0.13	0.20 *
	6	0.16	0.16	0.19	0.20 *
T102	1	0.28	0.25	0.39 *	0.27
	2	0.24	0.27	0.24 *	0.28
	3	0.17	0.17	0.24 *	0.16
	4	0.23	0.22	0.29 *	0.19
	5	0.18	0.18	0.20 *	0.15
	6	0.19	0.17	0.22 *	0.17
T401	1	0.29	0.23	0.28	0.27
	2	0.16	0.17	0.17	0.15
	3	0.17	0.23	0.21	0.14
	4	0.23	0.20	0.23	0.24
	5	0.25 *	0.16	0.13	0.16
	6	0.23	0.19	0.13	0.21
T402	1	0.28	0.25	0.38	0.27
	2	0.05	0.18	0.15	0.13
	3	0.13	0.14	0.26	0.17
	4	0.23	0.24	0.26	0.22
	5	0.17	0.15	0.25 *	0.19
	6	0.18	0.21	0.24 *	0.14
T403	1	0.25	0.26	0.28	0.33
	2	0.21	0.16	0.16	0.17
	3	0.17	0.23	0.20	0.18
	4	0.20	0.10	0.22	0.19
	5	0.18	0.14	0.08	0.21
	6	0.15	0.13	0.17	0.20
T404	1	0.31 *	0.37	0.39 *	0.24
	2	0.25 *	0.26	0.18	0.21
	3	0.23 *	0.26	0.20	0.21
	4	0.27 *	0.26	0.18	0.19
	5	0.28 *	0.19	0.18	0.13
	6	0.27 *	0.25	0.22	0.09

* Represents soil columns with surface water after the completion of irrigation.

Table A3.8
The change in weight for soil columns sampled from N002 after irrigation in the laboratory
The weights recorded represent the difference between before and after each irrigation event

Treatment Solution	Irrigation event	Replicate 1	Replicate 2	Replicate 3	Replicate 4
		(kg)			
FW00*i*	1	0.17	0.18	0.27	0.26 *
	2	0.19	0.17	0.23	0.20
	3	0.16	0.13	0.20	0.23
	4	0.16	0.19	0.22	0.25 *
	5	0.11	0.12	0.16	0.14
	6	0.20	0.27	0.24	0.29
T102	1	0.16	0.21 *	0.33	0.17
	2	0.18	0.20 *	0.19	0.18
	3	0.17	0.21 *	0.26 *	0.18
	4	0.18	0.21 *	0.28 *	0.30
	5	0.11	0.18 *	0.26 *	0.28 *
	6	0.22	0.16 *	0.25 *	0.31
T401	1	0.23	0.20	0.20	0.18
	2	0.22	0.23	0.03	0.13
	3	0.22	0.20	0.15	0.19
	4	0.25	0.22	0.23	0.23
	5	0.13	0.10	0.25	0.16
	6	0.24	0.13	0.22 *	0.18
T402	1	0.25 *	0.16	0.24 *	0.18
	2	0.25 *	0.18	0.24 *	0.19
	3	0.20 *	0.17	0.14 *	0.18
	4	0.24 *	0.24	0.21 *	0.25
	5	0.19 *	0.17	0.22 *	0.12
	6	0.17 *	0.19	0.18 *	0.19
T403	1	0.19	0.20	0.21 *	0.15
	2	0.18	0.18	0.21 *	0.15
	3	0.20	0.17	0.18 *	0.18
	4	0.20	0.25	0.24 *	0.25
	5	0.12	0.12	0.18 *	0.12
	6	0.16	0.17	0.19 *	0.15
T404	1	0.32 *	0.18	0.16	0.25
	2	0.31 *	0.23	0.17	0.17
	3	0.29 *	0.11	0.17	0.22
	4	0.27 *	0.17	0.16	0.17
	5	0.25	0.17	0.11	0.18
	6	0.26 *	0.21	0.19	0.20

* Represents soil columns with surface water after the completion of irrigation.

Appendix 3.2: ***The electrical conductivity, solution cations and SAR_w values determined after the analysis of all percolate solutions for each of the irrigation treatments of B00i, G00i, H00i and N00i.***

Table A3.9
Chemical attributes of drainage water for each irrigation event of B001 using the FW00*i* and T102 treatment solutions

Treatment Solution	Irrigation Event	Ca^{2+} ($mmol_{(+)}$ L^{-1})	Mg^{2+} ($mmol_{(+)}$ L^{-1})	Na^{+} ($mmol_{(+)}$ L^{-1})	K^{+} ($mmol_{(+)}$ L^{-1})	EC_w ($dS\ m^{-1}$)	SAR_w ($(mmol_{(+)}\ L^{-1})^{1/2}$)
FW00*i*	1	5.07 ± 0.18	4.35 ± 0.01	17.87 ± 3.54	0.19 ± 0.02	2.25 ± 0.30	8.25 ± 1.71
	2	5.43 ± 0.48	4.83 ± 0.22	23.39 ± 1.63	0.41 ± 0.04	2.79 ± 0.08	10.37 ± 1.07
	3	3.27 ± 1.00	2.80 ± 0.79	18.82 ± 1.47	0.17 ± 0.06	2.16 ± 0.31	11.05 ± 0.81
	4	2.49 ± 0.77	2.21 ± 0.60	17.51 ± 0.98	0.15 ± 0.05	1.90 ± 0.18	11.71 ± 1.10
	5	1.88 ± 0.47	1.75 ± 0.41	15.76 ± 3.35	0.11 ± 0.03	1.69 ± 0.19	11.67 ± 1.09
	6	1.75 ± 0.49	1.54 ± 0.37	16.66 ± 0.65	0.10 ± 0.04	1.57 ± 0.16	13.27 ± 1.25
T102	1	4.24 ± 0.57	3.80 ± 0.72	18.42 ± 3.49	0.15 ± 0.02	2.16 ± 0.45	9.14 ± 1.01
	2	3.89 ± 1.17	3.12 ± 1.11	20.50 ± 6.09	0.34 ± 0.02	2.30 ± 0.69	10.85 ± 1.48
	3	2.78 ± 0.84	2.53 ± 0.82	18.61 ± 5.57	0.11 ± 0.02	2.07 ± 0.60	11.30 ± 1.65
	4	1.90 ± 0.54	1.73 ± 0.61	15.83 ± 3.56	0.18 ± 0.09	1.55 ± 0.37	11.78 ± 0.76
	5	1.20 ± 0.40	1.22 ± 0.35	10.27 ± 7.64	0.07 ± 0.02	1.01 ± 0.61	8.56 ± 5.69
	6	1.03 ± 0.30	0.90 ± 0.27	11.32 ± 3.13	0.06 ± 0.01	0.94 ± 0.25	11.45 ± 1.52

Table A3.10
Chemical attributes of drainage water for each irrigation event of B001 using the T401–3 treatment solutions

Treatment Solution	Irrigation Event	Ca^{2+} ($mmol_{(+)}\ L^{-1}$)	Mg^{2+} ($mmol_{(+)}\ L^{-1}$)	Na^{+} ($mmol_{(+)}\ L^{-1}$)	K^{+} ($mmol_{(+)}\ L^{-1}$)	EC_w ($dS\ m^{-1}$)	SAR_w ($((mmol_{(+)}\ L^{-1})^{1/2}$)
T401	1	9.02 ± 2.70	8.33 ± 2.24	31.46 ± 3.64	0.36 ± 0.01	3.76 ± 0.63	10.84 ± 0.33
	2	5.35 ± 0.54	4.81 ± 0.46	25.96 ± 1.56	0.25 ± 0.12	2.90 ± 0.03	11.59 ± 1.26
	3	3.23 ± 0.01	2.80 ± 0.03	18.87 ± 0.29	0.12 ± 0.01	2.71 ± 0.07	10.87 ± 0.20
	4	2.18 ± 0.07	1.98 ± 0.02	14.76 ± 0.39	0.09 ± 0.01	2.12 ± 0.06	10.24 ± 0.38
	5	1.95 ± 0.06	1.63 ± 0.01	14.45 ± 0.38	0.09 ± 0.01	1.90 ± 0.05	10.82 ± 0.36
	6	1.32 ± 0.03	1.09 ± 0.02	11.40 ± 0.43	0.08 ± 0.01	1.55 ± 0.03	10.40 ± 0.40
T402	1	4.40 ± 1.83	3.59 ± 1.51	26.73 ± 6.81	0.08 ± 0.01	2.70 ± 0.81	13.58 ± 0.51
	2	4.86 ± 0.88	3.37 ± 0.83	27.57 ± 0.88	0.08 ± 0.01	2.45 ± 0.50	13.78 ± 1.01
	3	3.00 ± 0.76	2.64 ± 0.69	23.62 ± 5.04	0.07 ± 0.01	2.13 ± 0.46	14.03 ± 1.20
	4	2.18 ± 0.48	1.97 ± 0.51	19.36 ± 4.01	0.07 ± 0.01	1.74 ± 0.31	13.40 ± 1.19
	5	1.80 ± 0.37	1.47 ± 0.26	16.14 ± 3.23	0.07 ± 0.01	1.53 ± 0.17	12.56 ± 1.33
	6	1.36 ± 0.27	1.10 ± 0.17	13.23 ± 1.73	0.06 ± 0.01	1.64 ± 0.19	11.93 ± 0.49
T403	1	5.76 ± 1.20	4.91 ± 1.15	27.84 ± 0.40	0.12 ± 0.00	3.13 ± 0.35	12.26 ± 1.19
	2	4.57 ± 0.08	3.19 ± 0.34	19.47 ± 6.32	0.09 ± 0.00	2.39 ± 0.09	9.98 ± 3.48
	3	2.30 ± 0.34	2.15 ± 0.36	20.43 ± 1.80	0.08 ± 0.00	1.84 ± 0.14	13.74 ± 0.13
	4	1.77 ± 0.22	1.64 ± 0.25	17.19 ± 1.17	0.07 ± 0.00	1.59 ± 0.12	13.20 ± 0.02
	5	1.43 ± 0.10	1.27 ± 0.16	14.80 ± 0.52	0.07 ± 0.00	1.41 ± 0.08	12.77 ± 0.16
	6	1.27 ± 0.20	1.06 ± 0.10	13.50 ± 0.48	0.07 ± 0.01	1.61 ± 0.04	12.56 ± 0.36

Table A3.11
Chemical attributes of drainage water for each irrigation event of B002 using the FW00*i* treatment solution

Treatment Solution	Irrigation Event	Ca^{2+} ($mmol_{(+)}$ L^{-1})	Mg^{2+} ($mmol_{(+)}$ L^{-1})	Na^{+} ($mmol_{(+)}$ L^{-1})	K^{+} ($mmol_{(+)}$ L^{-1})	EC_w ($dS\ m^{-1}$)	SAR_w ($(mmol_{(+)}\ L^{-1})^{1/2}$)
FW00*i*	1	22.83 ± 0.60	16.87 ± 0.10	47.07 ± 5.44	0.34 ± 0.00	6.71 ± 0.43	10.57 ± 1.29
	2	9.05 ± 1.60	6.28 ± 0.78	23.86 ± 8.21	0.17 ± 0.13	3.18 ± 0.79	8.46 ± 2.31
	3	15.65 ± 8.36	12.59 ± 6.76	44.57 ± 15.23	0.28 ± 0.02	5.77 ± 2.29	12.15 ± 0.70
	4	14.03 ± 8.23	11.73 ± 7.39	44.24 ± 18.62	0.29 ± 0.02	5.59 ± 2.59	12.60 ± 1.22
	5	13.69 ± 8.53	9.37 ± 5.71	38.32 ± 14.52	0.16 ± 0.11	4.68 ± 1.84	11.79 ± 0.45
	6	2.80 ± 0.64	2.02 ± 0.63	14.36 ± 9.33	0.03 ± 0.00	1.49 ± 0.83	8.67 ± 4.90

Table A3.12
Chemical attributes of drainage water for each irrigation event of B003 using the FW00*i* and T102 treatment solutions

Treatment Solution	Irrigation Event	Ca^{2+} ($mmol_{(+)}$ L^{-1})	Mg^{2+} ($mmol_{(+)}$ L^{-1})	Na^{+} ($mmol_{(+)}$ L^{-1})	K^{+} ($mmol_{(+)}$ L^{-1})	EC_w ($dS\ m^{-1}$)	SAR_w ($(mmol_{(+)}\ L^{-1})^{1/2}$)
FW00*i*	1	4.65 ± 0.41	2.85 ± 0.05	8.81 ± 0.37	0.18 ± 0.02	1.41 ± 0.01	4.55 ± 0.05
	2	4.11 ± 0.57	2.53 ± 0.38	8.66 ± 0.14	0.28 ± 0.11	1.22 ± 0.07	4.78 ± 0.27
	3	2.73	1.98	7.73	0.11	1.10	5.04
	4	3.38 ± 0.26	2.08 ± 0.12	7.89 ± 0.22	0.13 ± 0.01	1.15 ± 0.02	4.78 ± 0.03
	5	3.59 ± 0.59	2.23 ± 0.24	8.23 ± 0.76	0.22 ± 0.13	1.18 ± 0.07	4.83 ± 0.10
	6	3.49 ± 0.67	2.07 ± 0.19	6.14 ± 3.97	0.10 ± 0.00	1.18 ± 0.06	3.53 ± 2.12
T102	1	4.56 ± 0.31	3.43 ± 0.54	10.44 ± 1.14	0.14 ± 0.01	1.50 ± 0.07	5.21 ± 0.29
	2	3.16 ± 0.40	1.97 ± 0.35	8.98 ± 0.21	0.11 ± 0.01	1.17 ± 0.12	5.64 ± 0.29
	3	2.63 ± 0.73	1.53 ± 0.38	7.61 ± 1.09	0.21 ± 0.12	0.93 ± 0.12	5.32 ± 0.04
	4	1.43 ± 0.31	0.93 ± 0.22	4.83 ± 1.87	0.06 ± 0.00	0.67 ± 0.09	4.33 ± 1.24
	5	1.39 ± 0.51	0.80 ± 0.25	5.70 ± 0.16	0.16 ± 0.11	0.53 ± 0.08	5.69 ± 0.86
	6	1.03 ± 0.31	0.77 ± 0.41	5.98 ± 1.96	0.05 ± 0.00	0.51 ± 0.22	6.28 ± 0.81

Table A3.13
Chemical attributes of drainage water for each irrigation event of B003 using the T401–3 treatment solutions

Treatment Solution	Irrigation Event	Ca^{2+} ($mmol_{(+)}$ L^{-1})	Mg^{2+} ($mmol_{(+)}$ L^{-1})	Na^{+} ($mmol_{(+)}$ L^{-1})	K^{+} ($mmol_{(+)}$ L^{-1})	EC_w ($dS\ m^{-1}$)	SAR_w ($(mmol_{(+)}\ L^{-1})^{1/2}$)
T401	1	6.46 ± 0.39	3.75 ± 0.39	13.01 ± 0.13	0.10 ± 0.02	1.63 ± 0.10	5.77 ± 0.27
	2	3.89 ± 0.34	2.57 ± 0.29	10.00 ± 0.16	0.10 ± 0.02	1.35 ± 0.06	5.59 ± 0.36
	3	3.32 ± 0.48	2.16 ± 0.18	8.98 ± 0.22	0.10 ± 0.02	1.54 ± 0.05	5.45 ± 0.19
	4	2.87 ± 0.29	1.96 ± 0.20	6.31 ± 1.70	0.09 ± 0.02	1.43 ± 0.06	4.02 ± 0.89
	5	2.78 ± 0.13	1.66 ± 0.12	7.48 ± 0.01	0.09 ± 0.02	1.28 ± 0.05	5.03 ± 0.13
	6	2.54 ± 0.32	1.56 ± 0.16	7.40 ± 1.20	0.08 ± 0.02	1.20 ± 0.06	5.15 ± 0.54
T402	1	2.66 ± 1.91	1.73 ± 1.14	7.73 ± 2.08	0.08 ± 0.02	1.27 ± 0.12	5.99 ± 0.91
	2	5.06 ± 0.13	2.49 ± 0.23	9.53 ± 0.16	0.09 ± 0.01	1.24 ± 0.10	4.91 ± 0.03
	3	3.12 ± 0.27	2.18 ± 0.21	6.01 ± 3.42	0.09 ± 0.01	1.14 ± 0.09	3.61 ± 1.94
	4	2.89 ± 0.06	1.97 ± 0.09	8.18 ± 0.20	0.09 ± 0.01	1.08 ± 0.04	5.25 ± 0.05
	5	3.22 ± 0.19	1.91 ± 0.03	8.71 ± 0.12	0.10 ± 0.01	1.07 ± 0.01	5.45 ± 0.18
	6	3.29 ± 0.40	1.95 ± 0.11	8.10 ± 0.02	0.12 ± 0.02	1.42 ± 0.05	5.02 ± 0.23
T403	1	3.56 ± 0.57	2.25 ± 0.41	10.55 ± 0.64	0.07 ± 0.02	1.35 ± 0.15	6.23 ± 0.15
	2	4.78 ± 0.40	2.30 ± 0.25	6.80 ± 2.85	0.07 ± 0.01	1.33 ± 0.09	3.69 ± 1.68
	3	3.41 ± 0.09	2.11 ± 0.17	9.65 ± 0.00	0.08 ± 0.01	1.19 ± 0.03	5.82 ± 0.13
	4	3.19 ± 0.09	2.00 ± 0.02	8.91 ± 0.26	0.09 ± 0.01	1.20 ± 0.04	5.54 ± 0.22
	5	2.62 ± 0.03	1.69 ± 0.06	8.28 ± 0.04	0.08 ± 0.01	1.09 ± 0.01	5.64 ± 0.01
	6	2.76 ± 0.36	1.69 ± 0.13	8.59 ± 0.77	0.08 ± 0.01	1.37 ± 0.12	5.76 ± 0.21

Table A3.14
Chemical attributes of drainage water for each irrigation event of G001 using the FW00*i* and T102 treatment solutions

Treatment Solution	Irrigation Event	Ca^{2+} ($mmol_{(+)}$ L^{-1})	Mg^{2+} ($mmol_{(+)}$ L^{-1})	Na^{+} ($mmol_{(+)}$ L^{-1})	K^{+} ($mmol_{(+)}$ L^{-1})	EC_w ($dS\ m^{-1}$)	SAR_w ($(mmol_{(+)}\ L^{-1})^{1/2}$)
FW00*i*	1	1.74 ± 0.07	1.11 ± 0.03	3.80 ± 0.31	0.04 ± 0.01	0.40 ± 0.02	3.20 ± 0.30
	2	1.26 ± 0.35	0.77 ± 0.24	2.34 ± 0.70	0.05 ± 0.01	0.43 ± 0.04	2.23 ± 0.47
	3	1.42 ± 0.56	0.94 ± 0.29	2.54 ± 0.72	0.05 ± 0.01	0.48 ± 0.12	2.75 ± 0.54
	4	1.70 ± 0.11	0.96 ± 0.04	3.15 ± 0.38	0.05 ± 0.01	0.46 ± 0.04	2.74 ± 0.32
	5	1.23 ± 0.06	0.81 ± 0.04	3.31 ± 0.30	0.04 ± 0.00	0.47 ± 0.02	3.30 ± 0.34
	6	1.33 ± 0.06	0.86 ± 0.04	2.91 ± 0.32	0.04 ± 0.01	0.44 ± 0.03	2.79 ± 0.31
T102	1	2.07 ± 0.31	1.33 ± 0.24	4.43 ± 0.38	0.04 ± 0.00	0.49 ± 0.06	3.43 ± 0.11
	2	1.44 ± 0.87	1.02 ± 0.64	3.15 ± 1.20	0.03 ± 0.00	0.44 ± 0.23	3.08 ± 0.19
	3	0.79 ± 0.52	0.99 ± 0.68	2.64 ± 1.29	0.04 ± 0.00	0.45 ± 0.20	3.03 ± 0.34
	4	0.12 ± 0.09	0.07 ± 0.05	0.63 ± 0.33	0.02 ± 0.01	0.13 ± 0.02	2.70 ± 0.10
	5	0.87 ± 0.54	0.83 ± 0.61	2.73 ± 1.36	0.03 ± 0.00	0.37 ± 0.20	3.07 ± 0.41
	6	0.15 ± 0.05	0.10 ± 0.03	0.66 ± 0.18	0.03 ± 0.00	0.10 ± 0.01	1.89 ± 0.23

Table A3.15
Chemical attributes of drainage water for each irrigation event of G001 using the T401–4 treatment solutions

Treatment Solution	Irrigation Event	Ca^{2+} ($mmol_{(+)}$ L^{-1})	Mg^{2+} ($mmol_{(+)}$ L^{-1})	Na^{+} ($mmol_{(+)}$ L^{-1})	K^{+} ($mmol_{(+)}$ L^{-1})	EC_w ($dS\ m^{-1}$)	SAR_w ($(mmol_{(+)}\ L^{-1})^{1/2}$)
T401	1	2.12 ± 0.87	1.32 ± 0.47	2.98 ± 1.14	0.05 ± 0.01	0.82 ± 0.10	2.63 ± 0.20
	2	2.74 ± 0.86	1.51 ± 0.51	4.35 ± 1.35	0.04 ± 0.01	0.98 ± 0.03	2.85 ± 0.56
	3	2.70 ± 0.89	1.65 ± 0.55	4.57 ± 1.47	0.04 ± 0.01	1.08 ± 0.05	3.00 ± 0.56
	4	2.29 ± 0.74	1.44 ± 0.47	3.42 ± 1.04	0.04 ± 0.01	0.91 ± 0.02	2.52 ± 0.33
	5	2.15 ± 0.71	1.52 ± 0.51	2.90 ± 0.95	0.03 ± 0.00	0.95 ± 0.07	2.06 ± 0.39
	6	3.12 ± 0.49	2.09 ± 0.14	3.71 ± 0.55	0.11 ± 0.08	0.81 ± 0.08	2.29 ± 0.26
T402	1	2.77 ± 0.45	1.79 ± 0.26	6.05 ± 0.21	0.05 ± 0.01	0.67 ± 0.03	4.12 ± 0.31
	2	2.52 ± 0.45	1.84 ± 0.36	5.78 ± 0.48	0.04 ± 0.00	0.75 ± 0.07	4.08 ± 0.45
	3	2.23 ± 0.43	1.63 ± 0.34	6.07 ± 0.66	0.04 ± 0.00	0.90 ± 0.13	4.53 ± 0.46
	4	1.36 ± 0.55	0.92 ± 0.34	3.38 ± 1.12	0.03 ± 0.00	0.68 ± 0.01	3.86 ± 0.85
	5	2.25 ± 0.57	1.46 ± 0.39	5.51 ± 0.68	0.03 ± 0.00	0.82 ± 0.15	4.23 ± 0.27
	6	1.41 ± 0.56	0.90 ± 0.35	3.63 ± 1.14	0.03 ± 0.00	0.76 ± 0.06	3.54 ± 0.65
T403	1	1.82 ± 0.67	1.10 ± 0.42	4.37 ± 1.18	0.04 ± 0.01	0.61 ± 0.05	3.60 ± 0.70
	2	1.23 ± 0.49	0.87 ± 0.34	4.21 ± 1.20	0.04 ± 0.01	0.63 ± 0.07	4.06 ± 0.91
	3	0.62 ± 0.44	0.49 ± 0.28	2.46 ± 1.33	0.03 ± 0.01	0.75 ± 0.02	4.25 ± 0.33
	4	0.96 ± 0.33	0.65 ± 0.23	3.28 ± 1.05	0.04 ± 0.01	0.59 ± 0.03	3.42 ± 0.85
	5	1.58 ± 0.67	1.05 ± 0.42	4.64 ± 1.02	0.09 ± 0.06	0.64 ± 0.19	4.24 ± 0.15
	6	1.12 ± 0.38	0.72 ± 0.25	3.76 ± 1.15	0.04 ± 0.01	0.73 ± 0.04	3.73 ± 0.81
T404	1	2.15 ± 0.18	1.65 ± 0.06	3.97 ± 0.16	0.05 ± 0.00	0.63 ± 0.03	2.89 ± 0.11
	2	3.33 ± 0.46	2.20 ± 0.31	5.54 ± 0.45	0.01 ± 0.01	0.90 ± 0.07	3.35 ± 0.04
	3	2.61 ± 0.44	1.82 ± 0.28	5.06 ± 0.34	0.02 ± 0.01	0.81 ± 0.07	3.45 ± 0.06
	4	2.55 ± 0.37	1.78 ± 0.27	5.16 ± 0.32	0.03 ± 0.01	0.82 ± 0.06	3.54 ± 0.05
	5	2.66 ± 0.29	1.79 ± 0.21	5.13 ± 0.22	0.02 ± 0.00	0.83 ± 0.04	3.46 ± 0.07
	6	2.95 ± 0.42	1.82 ± 0.23	5.22 ± 0.22	0.03 ± 0.00	0.85 ± 0.05	3.43 ± 0.10

Table A3.16
Chemical attributes of drainage water for each irrigation event of G002 using the FW00*i* and T102 treatment solutions

Treatment Solution	Irrigation Event	Ca^{2+} ($mmol_{(+)}$ L^{-1})	Mg^{2+} ($mmol_{(+)}$ L^{-1})	Na^{+} ($mmol_{(+)}$ L^{-1})	K^{+} ($mmol_{(+)}$ L^{-1})	EC_w ($dS\ m^{-1}$)	SAR_w ($(mmol_{(+)}\ L^{-1})^{1/2}$)
FW00*i*	1	3.54 ± 0.29	2.38 ± 0.17	6.19 ± 0.45	0.10 ± 0.01	1.14 ± 0.07	3.59 ± 0.14
	2	2.63 ± 0.13	1.53 ± 0.05	6.00 ± 0.36	0.08 ± 0.00	0.84 ± 0.03	4.17 ± 0.24
	3	1.87 ± 0.07	1.14 ± 0.05	4.44 ± 0.24	0.07 ± 0.00	0.68 ± 0.02	3.63 ± 0.22
	4	1.54 ± 0.09	0.96 ± 0.05	3.65 ± 0.12	0.07 ± 0.01	0.59 ± 0.01	3.27 ± 0.10
	5	1.48 ± 0.11	0.91 ± 0.05	3.27 ± 0.11	0.08 ± 0.01	0.55 ± 0.02	3.00 ± 0.14
	6	1.64 ± 0.21	1.01 ± 0.06	3.04 ± 0.07	0.28 ± 0.03	0.51 ± 0.01	2.67 ± 0.16
T102	1	3.33 ± 0.62	2.12 ± 0.42	5.91 ± 0.74	0.10 ± 0.00	1.04 ± 0.15	3.60 ± 0.21
	2	2.28 ± 0.57	1.36 ± 0.37	5.79 ± 0.86	0.07 ± 0.01	0.77 ± 0.15	4.36 ± 0.11
	3	1.66 ± 0.45	1.00 ± 0.28	4.59 ± 0.71	0.06 ± 0.00	0.62 ± 0.13	4.05 ± 0.12
	4	1.12 ± 0.32	0.73 ± 0.21	3.34 ± 0.66	0.07 ± 0.00	0.47 ± 0.10	3.49 ± 0.21
	5	1.08 ± 0.25	0.71 ± 0.15	2.93 ± 0.45	0.08 ± 0.01	0.44 ± 0.08	3.10 ± 0.15
	6	0.76 ± 0.15	0.58 ± 0.13	2.47 ± 0.38	0.08 ± 0.02	0.33 ± 0.07	3.02 ± 0.16

Table A3.17
Chemical attributes of drainage water for each irrigation event of G002 using the T401–4 treatment solutions

Treatment Solution	Irrigation Event	Ca^{2+} ($mmol_{(+)}$ L^{-1})	Mg^{2+} ($mmol_{(+)}$ L^{-1})	Na^{+} ($mmol_{(+)}$ L^{-1})	K^{+} ($mmol_{(+)}$ L^{-1})	EC_w ($dS\ m^{-1}$)	SAR_w ($(mmol_{(+)}\ L^{-1})^{1/2}$)
T401	1	3.38 ± 0.24	2.09 ± 0.17	5.52 ± 0.11	0.11 ± 0.01	0.94 ± 0.05	3.36 ± 0.17
	2	2.88 ± 0.88	1.48 ± 0.50	5.49 ± 1.66	0.08 ± 0.02	1.08 ± 0.04	3.51 ± 0.73
	3	3.06 ± 0.18	2.15 ± 0.32	6.69 ± 0.73	0.09 ± 0.01	1.06 ± 0.04	4.14 ± 0.38
	4	3.46 ± 0.43	2.06 ± 0.24	5.80 ± 0.67	0.11 ± 0.01	1.05 ± 0.09	3.48 ± 0.20
	5	2.90 ± 0.27	1.94 ± 0.16	4.45 ± 0.49	0.10 ± 0.01	1.00 ± 0.07	2.85 ± 0.20
	6	3.29 ± 0.21	2.11 ± 0.06	4.20 ± 0.32	0.15 ± 0.05	0.88 ± 0.03	2.57 ± 0.21
T402	1	3.47 ± 0.40	2.22 ± 0.09	6.47 ± 0.16	0.10 ± 0.00	1.07 ± 0.04	3.87 ± 0.22
	2	3.11 ± 0.63	2.28 ± 0.37	7.91 ± 0.61	0.08 ± 0.00	1.07 ± 0.06	4.81 ± 0.18
	3	2.67 ± 0.33	2.02 ± 0.41	6.76 ± 0.50	0.08 ± 0.00	1.00 ± 0.10	4.42 ± 0.11
	4	2.62 ± 0.22	1.87 ± 0.37	6.24 ± 0.53	0.08 ± 0.00	0.95 ± 0.09	4.17 ± 0.12
	5	2.40 ± 0.10	2.07 ± 0.45	5.53 ± 0.86	0.09 ± 0.01	0.92 ± 0.04	3.66 ± 0.35
	6	3.30 ± 0.52	2.01 ± 0.27	5.39 ± 0.59	0.11 ± 0.02	0.91 ± 0.08	3.31 ± 0.13
T403	1	3.94 ± 0.19	2.43 ± 0.09	6.24 ± 0.30	0.11 ± 0.00	1.11 ± 0.07	3.49 ± 0.12
	2	3.19 ± 0.31	1.99 ± 0.24	7.43 ± 0.52	0.08 ± 0.00	1.04 ± 0.06	4.62 ± 0.11
	3	2.25 ± 0.37	1.48 ± 0.31	5.88 ± 0.69	0.07 ± 0.00	0.85 ± 0.10	4.32 ± 0.13
	4	2.11 ± 0.31	1.30 ± 0.21	4.99 ± 0.57	0.08 ± 0.00	0.78 ± 0.08	3.83 ± 0.18
	5	2.42 ± 0.17	1.56 ± 0.16	4.51 ± 0.33	0.08 ± 0.00	0.90 ± 0.06	3.19 ± 0.12
	6	3.04 ± 0.31	1.86 ± 0.13	4.81 ± 0.45	0.13 ± 0.03	0.86 ± 0.04	3.06 ± 0.16
T404	1	3.41 ± 0.56	2.22 ± 0.27	4.71 ± 0.44	0.11 ± 0.01	0.84 ± 0.11	2.82 ± 0.09
	2	3.57 ± 0.25	2.41 ± 0.04	5.61 ± 0.12	0.08 ± 0.00	0.93 ± 0.03	3.26 ± 0.13
	3	3.19 ± 0.18	2.15 ± 0.09	5.11 ± 0.20	0.09 ± 0.01	0.87 ± 0.02	3.13 ± 0.10
	4	3.14 ± 0.14	2.10 ± 0.10	4.95 ± 0.26	0.09 ± 0.00	0.86 ± 0.03	3.05 ± 0.13
	5	3.47 ± 0.17	2.29 ± 0.09	5.19 ± 0.23	0.10 ± 0.01	0.93 ± 0.03	3.06 ± 0.12
	6	3.73 ± 0.33	2.27 ± 0.15	5.05 ± 0.31	0.09 ± 0.01	0.94 ± 0.04	2.92 ± 0.11

Table A3.18
Chemical attributes of drainage water for each irrigation event of H001 using the FW00*i* and T102 treatment solutions

Treatment Solution	Irrigation Event	Ca^{2+} ($mmol_{(+)}$ L^{-1})	Mg^{2+} ($mmol_{(+)}$ L^{-1})	Na^{+} ($mmol_{(+)}$ L^{-1})	K^{+} ($mmol_{(+)}$ L^{-1})	EC_w ($dS\ m^{-1}$)	SAR_w ($(mmol_{(+)}\ L^{-1})^{1/2}$)
FW00*i*	1	1.82 ± 0.29	1.73 ± 0.32	6.77 ± 0.39	0.10 ± 0.02	0.82 ± 0.08	5.17 ± 0.40
	2	1.15 ± 0.31	2.40 ± 0.79	8.25 ± 1.88	0.11 ± 0.01	0.94 ± 0.17	6.04 ± 0.83
	3	1.70 ± 0.47	1.61 ± 0.41	7.76 ± 1.27	0.07 ± 0.01	0.86 ± 0.21	6.14 ± 0.44
	4	2.37 ± 0.45	2.12 ± 0.74	8.40 ± 2.21	0.09 ± 0.01	1.01 ± 0.26	5.47 ± 0.83
	5	1.52 ± 0.19	1.27 ± 0.18	5.69 ± 0.84	0.06 ± 0.02	0.49 ± 0.07	4.77 ± 0.44
	6	1.87 ± 0.63	1.81 ± 0.58	6.28 ± 1.77	0.08 ± 0.01	0.88 ± 0.23	4.95 ± 0.97
T102	1	3.90 ± 0.54	3.69 ± 0.35	8.57 ± 1.75	0.20 ± 0.06	1.55 ± 0.05	4.34 ± 0.82
	2	2.35 ± 0.32	2.16 ± 0.28	8.99 ± 0.98	0.12 ± 0.01	1.11 ± 0.10	6.00 ± 0.45
	3	1.29 ± 0.18	1.14 ± 0.15	7.60 ± 0.65	0.07 ± 0.01	1.00 ± 0.26	6.90 ± 0.16
	4	2.19 ± 0.46	1.57 ± 0.27	8.45 ± 0.34	0.08 ± 0.01	0.85 ± 0.10	6.38 ± 0.56
	5	1.92 ± 0.74	1.95 ± 0.77	8.22 ± 1.88	0.08 ± 0.01	0.88 ± 0.25	6.16 ± 0.54
	6	0.53 ± 0.17	0.39 ± 0.13	2.41 ± 0.81	0.05 ± 0.01	0.26 ± 0.03	3.14 ± 1.00

Table A3.19
Chemical attributes of drainage water for each irrigation event of H001 using the T401–4 treatment solutions

Treatment Solution	Irrigation Event	Ca^{2+} ($mmol_{(+)}$ L^{-1})	Mg^{2+} ($mmol_{(+)}$ L^{-1})	Na^{+} ($mmol_{(+)}$ L^{-1})	K^{+} ($mmol_{(+)}$ L^{-1})	EC_w ($dS\ m^{-1}$)	SAR_w ($(mmol_{(+)}\ L^{-1})^{1/2}$)
T401	1	3.12 ± 0.66	2.41 ± 0.49	8.99 ± 0.26	0.09 ± 0.01	0.96 ± 0.13	5.61 ± 0.41
	2	2.76 ± 0.56	2.88 ± 0.64	7.96 ± 1.54	0.11 ± 0.02	1.23 ± 0.20	5.16 ± 1.16
	3	2.71 ± 0.37	2.70 ± 0.25	7.02 ± 1.29	0.12 ± 0.01	1.58 ± 0.07	4.44 ± 1.01
	4	1.78 ± 0.64	1.68 ± 0.57	6.34 ± 2.00	0.08 ± 0.02	1.40 ± 0.02	5.53 ± 0.27
	5	2.55 ± 0.23	2.27 ± 0.24	8.37 ± 0.80	0.11 ± 0.01	1.40 ± 0.10	5.41 ± 0.43
	6	1.66 ± 0.55	1.42 ± 0.48	6.15 ± 1.93	0.13 ± 0.06	1.15 ± 0.13	4.91 ± 0.76
T402	1	2.48 ± 0.39	2.46 ± 0.40	8.48 ± 0.53	0.10 ± 0.01	1.11 ± 0.11	5.48 ± 0.12
	2	2.87 ± 0.62	2.12 ± 0.46	8.63 ± 1.13	0.08 ± 0.02	1.01 ± 0.13	5.58 ± 0.42
	3	1.98 ± 0.31	1.72 ± 0.26	9.22 ± 0.31	0.08 ± 0.01	0.91 ± 0.09	6.94 ± 0.44
	4	1.74 ± 0.24	1.61 ± 0.19	7.74 ± 0.59	0.09 ± 0.01	0.92 ± 0.07	6.00 ± 0.11
	5	1.72 ± 0.28	1.57 ± 0.20	8.03 ± 0.51	0.09 ± 0.01	0.91 ± 0.08	6.37 ± 0.37
	6	1.76 ± 0.26	1.60 ± 0.20	6.76 ± 1.03	0.09 ± 0.01	1.17 ± 0.10	5.39 ± 0.93
T403	1	2.02 ± 0.43	2.05 ± 0.30	7.05 ± 1.22	0.09 ± 0.02	0.97 ± 0.09	4.96 ± 0.73
	2	3.53 ± 0.36	3.23 ± 0.20	11.88 ± 0.46	0.11 ± 0.02	1.33 ± 0.05	6.50 ± 0.31
	3	2.95 ± 0.37	2.66 ± 0.31	11.07 ± 1.10	0.11 ± 0.02	1.26 ± 0.11	6.63 ± 0.42
	4	2.88 ± 0.46	2.53 ± 0.29	9.79 ± 0.80	0.12 ± 0.02	1.22 ± 0.09	5.99 ± 0.28
	5	2.35 ± 0.33	2.09 ± 0.24	9.48 ± 0.74	0.11 ± 0.02	1.10 ± 0.10	6.41 ± 0.29
	6	2.07 ± 0.24	1.97 ± 0.20	8.83 ± 1.04	0.11 ± 0.02	1.29 ± 0.17	6.20 ± 0.54
T404	1	3.74 ± 0.38	3.55 ± 0.35	9.51 ± 0.39	0.16 ± 0.01	1.72 ± 0.11	5.00 ± 0.05
	2	4.00 ± 0.35	3.12 ± 0.31	10.91 ± 0.73	0.13 ± 0.02	1.48 ± 0.11	5.79 ± 0.21
	3	3.34 ± 0.43	2.84 ± 0.39	8.94 ± 1.59	0.20 ± 0.07	1.40 ± 0.15	5.10 ± 0.74
	4	2.71 ± 0.49	2.50 ± 0.45	7.47 ± 0.73	0.26 ± 0.05	1.29 ± 0.18	4.82 ± 0.65
	5	2.60 ± 0.38	2.25 ± 0.43	8.53 ± 1.11	0.30 ± 0.06	1.20 ± 0.17	5.47 ± 0.29
	6	1.93 ± 0.43	2.15 ± 0.43	8.30 ± 1.08	0.10 ± 0.01	1.15 ± 0.16	5.86 ± 0.14

Table A3.20
Chemical attributes of drainage water for each irrigation event of H002 using the FW00*i* and T102 treatment solutions

Treatment Solution	Irrigation Event	Ca^{2+}	Mg^{2+}	Na^{+}	K^{+}	EC_w	SAR_w
		($mmol_{(+)}$ L^{-1})	($mmol_{(+)}$ L^{-1})	($mmol_{(+)}$ L^{-1})	($mmol_{(+)}$ L^{-1})	(dS m^{-1})	(($mmol_{(+)}$ L^{-1})$^{1/2}$)
FW00*i*	1	1.62 ± 0.18	1.44 ± 0.13	4.75 ± 0.37	0.06 ± 0.00	0.65 ± 0.06	3.84 ± 0.18
	2	1.92 ± 0.32	1.62 ± 0.24	5.05 ± 0.64	0.11 ± 0.05	0.63 ± 0.08	3.80 ± 0.20
	3	1.94 ± 0.22	1.41 ± 0.15	5.71 ± 0.64	0.05 ± 0.00	0.57 ± 0.06	4.40 ± 0.28
	4	2.79 ± 0.18	1.38 ± 0.13	6.02 ± 0.55	0.04 ± 0.00	0.58 ± 0.06	4.23 ± 0.52
	5	0.35 ± 0.35	0.29 ± 0.29	1.27 ± 1.27	0.01 ± 0.01	0.47 ± 0.00	4.47 ± 0.00
	6	1.50 ± 0.08	1.20 ± 0.05	4.85 ± 0.15	0.04 ± 0.00	0.47 ± 0.01	4.18 ± 0.12
T102	1	1.44 ± 0.17	1.22 ± 0.09	5.08 ± 0.47	0.06 ± 0.00	0.62 ± 0.03	4.42 ± 0.32
	2	1.24 ± 0.21	1.04 ± 0.17	3.99 ± 0.28	0.05 ± 0.01	0.49 ± 0.05	3.80 ± 0.16
	3	1.62 ± 0.24	1.23 ± 0.28	5.33 ± 0.54	0.05 ± 0.00	0.55 ± 0.11	4.53 ± 0.24
	4	2.29 ± 0.19	1.25 ± 0.27	6.70 ± 0.66	0.04 ± 0.00	0.52 ± 0.09	5.07 ± 0.44
	5	1.76 ± 0.23	1.40 ± 0.19	5.35 ± 0.55	0.05 ± 0.00	0.52 ± 0.03	4.27 ± 0.17
	6	0.97 ± 0.12	0.81 ± 0.13	4.17 ± 0.53	0.04 ± 0.00	0.36 ± 0.05	4.40 ± 0.29

Table A3.21
Chemical attributes of drainage water for each irrigation event of H002 using the T401–4 treatment solutions

Treatment Solution	Irrigation Event	Ca^{2+} ($mmol_{(+)}$ L^{-1})	Mg^{2+} ($mmol_{(+)}$ L^{-1})	Na^{+} ($mmol_{(+)}$ L^{-1})	K^{+} ($mmol_{(+)}$ L^{-1})	EC_w ($dS\ m^{-1}$)	SAR_w ($(mmol_{(+)}\ L^{-1})^{1/2}$)
T401	1	4.22 ± 0.69	2.51 ± 0.47	8.19 ± 0.48	0.06 ± 0.00	0.84 ± 0.12	4.66 ± 0.55
	2	2.79 ± 0.58	2.93 ± 0.10	8.38 ± 1.01	0.07 ± 0.00	1.00 ± 0.02	5.12 ± 0.94
	3	3.19 ± 0.76	3.31 ± 0.23	7.07 ± 0.51	0.09 ± 0.01	1.23 ± 0.14	3.93 ± 0.11
	4	2.80 ± 0.48	3.14 ± 0.43	8.48 ± 1.48	0.07 ± 0.01	1.41 ± 0.13	4.94 ± 0.89
	5	3.40 ± 0.86	3.50 ± 0.42	8.93 ± 1.66	0.08 ± 0.00	1.46 ± 0.14	4.95 ± 1.13
	6	3.51 ± 0.83	3.43 ± 0.41	8.79 ± 1.80	0.08 ± 0.00	1.46 ± 0.16	4.84 ± 1.17
T402	1	2.20 ± 0.20	1.94 ± 0.20	7.89 ± 0.63	0.05 ± 0.00	0.92 ± 0.10	5.48 ± 0.19
	2	2.27 ± 0.79	2.15 ± 0.68	7.19 ± 2.19	0.05 ± 0.01	1.06 ± 0.03	4.64 ± 1.06
	3	3.04 ± 0.50	2.95 ± 0.31	8.77 ± 1.81	0.06 ± 0.00	1.15 ± 0.05	5.04 ± 1.02
	4	3.07 ± 0.40	2.73 ± 0.40	9.84 ± 1.17	0.05 ± 0.00	1.05 ± 0.08	5.81 ± 0.67
	5	2.36 ± 0.34	2.43 ± 0.49	8.55 ± 1.22	0.06 ± 0.00	1.03 ± 0.13	5.62 ± 0.70
	6	2.21 ± 0.47	2.43 ± 0.38	8.77 ± 0.97	0.07 ± 0.00	1.24 ± 0.12	5.84 ± 0.73
T403	1	2.67 ± 0.26	2.43 ± 0.26	7.88 ± 0.32	0.07 ± 0.00	0.99 ± 0.07	4.97 ± 0.22
	2	2.53 ± 0.41	2.97 ± 0.31	6.50 ± 2.85	0.06 ± 0.00	1.06 ± 0.07	3.76 ± 1.62
	3	2.83 ± 0.09	2.82 ± 0.33	9.72 ± 1.01	0.06 ± 0.00	1.08 ± 0.10	5.76 ± 0.43
	4	3.18 ± 0.42	2.80 ± 0.46	9.87 ± 1.41	0.06 ± 0.00	1.07 ± 0.11	5.66 ± 0.59
	5	2.64 ± 0.20	2.39 ± 0.31	8.60 ± 0.87	0.07 ± 0.00	1.06 ± 0.11	5.41 ± 0.30
	6	2.59 ± 0.14	2.28 ± 0.25	7.92 ± 0.81	0.07 ± 0.00	1.22 ± 0.14	5.06 ± 0.36
T404	1	1.80 ± 0.34	1.59 ± 0.22	5.28 ± 0.46	0.06 ± 0.01	0.71 ± 0.07	4.12 ± 0.29
	2	2.49 ± 0.42	4.04 ± 0.28	10.96 ± 1.09	0.05 ± 0.00	1.31 ± 0.08	6.11 ± 0.67
	3	2.07 ± 0.48	4.62 ± 0.49	11.68 ± 1.50	0.05 ± 0.01	1.33 ± 0.10	6.39 ± 0.82
	4	2.07 ± 0.61	4.39 ± 0.55	10.98 ± 1.58	0.05 ± 0.00	1.32 ± 0.09	6.13 ± 0.90
	5	2.10 ± 0.60	4.23 ± 0.49	10.87 ± 1.49	0.05 ± 0.01	1.33 ± 0.10	6.14 ± 0.88
	6	3.03 ± 0.57	3.95 ± 0.44	8.58 ± 1.34	0.06 ± 0.00	1.34 ± 0.09	4.63 ± 0.80

Table A3.22
Chemical attributes of drainage water for each irrigation event of N001 using the FW00*i* and T102 treatment solutions

Treatment Solution	Irrigation Event	Ca^{2+} ($mmol_{(+)}$ L^{-1})	Mg^{2+} ($mmol_{(+)}$ L^{-1})	Na^{+} ($mmol_{(+)}$ L^{-1})	K^{+} ($mmol_{(+)}$ L^{-1})	EC_w ($dS\ m^{-1}$)	SAR_w ($(mmol_{(+)}\ L^{-1})^{1/2}$)
FW00*i*	1	0.75 ± 0.12	0.45 ± 0.06	8.99 ± 0.56	0.05 ± 0.00	0.98 ± 0.07	11.73 ± 0.17
	2	0.90 ± 0.09	0.58 ± 0.17	11.41 ± 1.52	0.04 ± 0.00	0.92 ± 0.13	13.21 ± 0.84
	3	0.55 ± 0.17	0.55 ± 0.21	10.73 ± 1.80	0.09 ± 0.04	0.87 ± 0.12	15.10 ± 1.57
	4	0.24 ± 0.07	0.44 ± 0.22	9.76 ± 1.49	0.10 ± 0.05	0.83 ± 0.12	18.17 ± 1.16
	5	0.58 ± 0.09	0.53 ± 0.17	9.28 ± 1.34	0.10 ± 0.07	0.80 ± 0.12	12.54 ± 0.56
	6	0.15 ± 0.18	0.49 ± 0.19	9.01 ± 1.38	0.02 ± 0.01	0.78 ± 0.12	19.49 ± 3.75
T102	1	0.73 ± 0.26	0.42 ± 0.15	7.61 ± 2.53	0.05 ± 0.01	1.15 ± 0.09	9.08 ± 2.50
	2	0.98 ± 0.10	0.61 ± 0.22	11.06 ± 2.04	0.05 ± 0.00	0.93 ± 0.17	12.22 ± 1.48
	3	0.57 ± 0.10	0.49 ± 0.21	9.38 ± 1.90	0.05 ± 0.01	0.75 ± 0.15	12.69 ± 1.60
	4	0.53 ± 0.20	0.53 ± 0.19	9.28 ± 1.68	0.12 ± 0.04	0.78 ± 0.13	12.81 ± 1.94
	5	0.24 ± 0.07	0.51 ± 0.22	8.56 ± 1.99	0.18 ± 0.01	0.74 ± 0.16	14.16 ± 1.05
	6	0.07 ± 0.07	0.44 ± 0.16	6.82 ± 0.68	0.02 ± 0.01	0.70 ± 0.11	16.38 ± 3.21

Table A3.23
Chemical attributes of drainage water for each irrigation event of N001 using the T401–4 treatment solutions

Treatment Solution	Irrigation Event	Ca^{2+} ($mmol_{(+)}$ L^{-1})	Mg^{2+} ($mmol_{(+)}$ L^{-1})	Na^{+} ($mmol_{(+)}$ L^{-1})	K^{+} ($mmol_{(+)}$ L^{-1})	EC_w ($dS\ m^{-1}$)	SAR_w ($(mmol_{(+)}\ L^{-1})^{1/2}$)
T401	1	0.80 ± 0.07	0.49 ± 0.03	8.08 ± 1.13	0.05 ± 0.00	1.09 ± 0.05	10.04 ± 1.23
	2	1.20 ± 0.10	0.54 ± 0.05	10.04 ± 0.77	0.04 ± 0.00	1.19 ± 0.25	10.72 ± 0.44
	3	1.07 ± 0.23	0.61 ± 0.09	9.27 ± 1.42	0.07 ± 0.02	1.03 ± 0.06	10.32 ± 1.33
	4	0.75 ± 0.21	0.54 ± 0.06	9.56 ± 0.57	0.05 ± 0.01	0.95 ± 0.04	12.19 ± 1.15
	5	1.17 ± 0.18	0.57 ± 0.06	9.24 ± 0.46	0.11 ± 0.05	0.96 ± 0.03	10.02 ± 0.42
	6	0.58 ± 0.13	0.54 ± 0.05	8.73 ± 0.38	0.04 ± 0.00	0.91 ± 0.03	11.86 ± 0.46
T402	1	0.75 ± 0.11	0.47 ± 0.05	8.30 ± 1.26	0.05 ± 0.01	1.10 ± 0.06	10.70 ± 1.43
	2	1.26 ± 0.15	0.55 ± 0.08	10.83 ± 0.75	0.04 ± 0.00	1.02 ± 0.07	11.44 ± 0.13
	3	0.89 ± 0.13	0.60 ± 0.07	7.36 ± 2.29	0.07 ± 0.03	1.02 ± 0.06	8.34 ± 2.36
	4	0.78 ± 0.09	0.52 ± 0.05	9.08 ± 1.39	0.05 ± 0.01	0.97 ± 0.05	11.27 ± 1.75
	5	0.82 ± 0.06	0.55 ± 0.06	9.74 ± 0.45	0.07 ± 0.03	0.96 ± 0.05	11.79 ± 0.45
	6	0.35 ± 0.08	0.50 ± 0.06	8.95 ± 0.33	0.02 ± 0.00	0.92 ± 0.04	14.00 ± 0.53
T403	1	0.88 ± 0.14	0.51 ± 0.09	9.40 ± 1.01	0.05 ± 0.00	1.12 ± 0.12	11.38 ± 0.22
	2	1.34 ± 0.15	0.58 ± 0.10	11.14 ± 1.25	0.05 ± 0.00	1.06 ± 0.11	11.33 ± 0.57
	3	1.16 ± 0.22	0.61 ± 0.11	11.22 ± 1.34	0.06 ± 0.01	1.06 ± 0.10	12.06 ± 0.63
	4	1.09 ± 0.22	0.60 ± 0.09	10.64 ± 1.05	0.05 ± 0.01	1.04 ± 0.09	11.81 ± 0.54
	5	0.91 ± 0.10	0.59 ± 0.07	9.96 ± 0.65	0.13 ± 0.05	1.02 ± 0.06	11.52 ± 0.20
	6	0.73 ± 0.22	0.60 ± 0.08	10.02 ± 0.75	0.03 ± 0.01	1.00 ± 0.06	12.94 ± 0.93
T404	1	0.75 ± 0.12	0.45 ± 0.08	8.66 ± 0.72	0.05 ± 0.00	0.97 ± 0.10	11.30 ± 0.14
	2	1.22 ± 0.28	0.95 ± 0.20	13.55 ± 1.55	0.05 ± 0.01	1.19 ± 0.10	13.14 ± 1.36
	3	0.98 ± 0.33	0.95 ± 0.20	12.97 ± 1.47	0.06 ± 0.01	1.18 ± 0.08	13.60 ± 1.61
	4	0.83 ± 0.29	1.00 ± 0.24	10.23 ± 2.93	0.14 ± 0.06	1.23 ± 0.11	10.38 ± 2.71
	5	1.13 ± 0.15	0.94 ± 0.22	12.21 ± 1.67	0.18 ± 0.07	1.18 ± 0.11	12.04 ± 1.43
	6	0.66 ± 0.19	0.84 ± 0.18	11.25 ± 1.43	0.05 ± 0.00	1.10 ± 0.09	13.25 ± 1.54

Table A3.24
Chemical attributes of drainage water for each irrigation event of N002 using the FW00*i* and T102 treatment solutions

Treatment Solution	Irrigation Event	Ca^{2+} ($mmol_{(+)}$ L^{-1})	Mg^{2+} ($mmol_{(+)}$ L^{-1})	Na^{+} ($mmol_{(+)}$ L^{-1})	K^{+} ($mmol_{(+)}$ L^{-1})	EC_w ($dS\ m^{-1}$)	SAR_w ($(mmol_{(+)}\ L^{-1})^{1/2}$)
FW00*i*	1	5.04 ± 0.39	3.08 ± 0.06	3.80 ± 0.07	0.12 ± 0.04	0.89 ± 0.02	1.89 ± 0.07
	2	4.27 ± 0.17	3.09 ± 0.51	3.80 ± 0.45	0.07 ± 0.01	0.81 ± 0.05	1.97 ± 0.17
	3	3.45 ± 0.22	2.84 ± 0.62	3.54 ± 0.66	0.05 ± 0.01	0.76 ± 0.07	1.97 ± 0.23
	4	3.07 ± 0.14	2.51 ± 0.50	3.12 ± 0.41	0.03 ± 0.01	0.67 ± 0.06	1.85 ± 0.15
	5	3.28 ± 0.12	2.35 ± 0.37	3.10 ± 0.22	0.04 ± 0.01	0.63 ± 0.03	1.84 ± 0.07
	6	2.68 ± 0.24	2.45 ± 0.45	3.02 ± 0.27	0.04 ± 0.01	0.60 ± 0.03	1.88 ± 0.13
T102	1	3.50 ± 0.56	2.59 ± 0.20	3.53 ± 0.35	0.11 ± 0.04	0.73 ± 0.04	2.04 ± 0.20
	2	3.43 ± 0.74	2.95 ± 0.57	3.87 ± 0.64	0.04 ± 0.01	0.75 ± 0.10	2.16 ± 0.28
	3	2.83 ± 0.32	2.97 ± 0.67	3.70 ± 0.64	0.05 ± 0.01	0.71 ± 0.08	2.14 ± 0.27
	4	1.80 ± 0.43	2.77 ± 0.77	3.17 ± 0.71	0.00 ± 0.00	0.63 ± 0.08	2.05 ± 0.35
	5	2.15 ± 0.26	2.83 ± 0.89	3.36 ± 0.80	0.03 ± 0.01	0.62 ± 0.10	2.07 ± 0.35
	6	1.90 ± 0.23	2.71 ± 0.95	3.25 ± 0.89	0.02 ± 0.01	0.57 ± 0.11	2.06 ± 0.39

Table A3.25
Chemical attributes of drainage water for each irrigation event of N002 using the T401–4 treatment solutions

Treatment Solution	Irrigation Event	Ca^{2+} ($mmol_{(+)}$ L^{-1})	Mg^{2+} ($mmol_{(+)}$ L^{-1})	Na^{+} ($mmol_{(+)}$ L^{-1})	K^{+} ($mmol_{(+)}$ L^{-1})	EC_w ($dS\ m^{-1}$)	SAR_w ($(mmol_{(+)}\ L^{-1})^{1/2}$)
T401	1	4.58 ± 0.21	2.87 ± 0.10	3.23 ± 0.23	0.14 ± 0.04	0.88 ± 0.03	1.67 ± 0.11
	2	5.07 ± 0.33	3.06 ± 0.18	3.00 ± 0.32	0.10 ± 0.05	0.92 ± 0.05	1.48 ± 0.11
	3	5.04 ± 0.60	3.43 ± 0.42	3.07 ± 0.54	0.05 ± 0.01	0.97 ± 0.07	1.47 ± 0.17
	4	4.87 ± 0.41	3.07 ± 0.28	2.73 ± 0.34	0.03 ± 0.02	0.91 ± 0.05	1.36 ± 0.11
	5	5.40 ± 0.35	3.32 ± 0.29	2.75 ± 0.41	0.04 ± 0.01	0.93 ± 0.06	1.31 ± 0.14
	6	5.00 ± 0.31	3.23 ± 0.30	2.58 ± 0.35	0.03 ± 0.01	0.90 ± 0.06	1.26 ± 0.12
T402	1	3.80 ± 0.81	2.70 ± 0.39	3.68 ± 0.27	0.16 ± 0.06	0.83 ± 0.09	2.08 ± 0.11
	2	3.67 ± 0.89	3.67 ± 0.64	4.74 ± 0.26	0.05 ± 0.01	0.97 ± 0.10	2.54 ± 0.17
	3	4.08 ± 0.96	3.82 ± 0.59	4.91 ± 0.39	0.04 ± 0.00	1.02 ± 0.07	2.51 ± 0.19
	4	3.44 ± 0.76	3.84 ± 0.64	5.59 ± 1.08	0.02 ± 0.01	1.01 ± 0.08	2.95 ± 0.54
	5	3.86 ± 0.53	3.99 ± 0.96	4.80 ± 0.41	0.03 ± 0.01	0.99 ± 0.08	2.45 ± 0.13
	6	3.76 ± 0.57	4.10 ± 0.93	4.88 ± 0.45	0.03 ± 0.01	1.00 ± 0.07	2.47 ± 0.15
T403	1	3.04 ± 0.40	2.37 ± 0.50	3.88 ± 0.45	0.14 ± 0.06	0.77 ± 0.06	2.39 ± 0.21
	2	3.83 ± 0.75	2.52 ± 0.56	4.76 ± 0.43	0.06 ± 0.01	0.90 ± 0.09	2.75 ± 0.23
	3	3.68 ± 0.66	2.82 ± 0.67	4.67 ± 0.34	0.10 ± 0.04	0.92 ± 0.08	2.66 ± 0.19
	4	3.13 ± 0.74	2.86 ± 0.75	4.66 ± 0.42	0.01 ± 0.01	0.91 ± 0.08	2.80 ± 0.29
	5	3.42 ± 0.48	2.91 ± 0.79	4.94 ± 0.39	0.03 ± 0.01	0.92 ± 0.07	2.84 ± 0.23
	6	3.21 ± 0.52	2.96 ± 0.89	4.80 ± 0.44	0.03 ± 0.00	0.90 ± 0.08	2.80 ± 0.26
T404	1	4.37 ± 0.76	2.59 ± 0.46	3.82 ± 0.20	0.07 ± 0.01	0.83 ± 0.08	2.13 ± 0.24
	2	4.14 ± 0.91	2.86 ± 0.86	4.37 ± 0.12	0.12 ± 0.06	0.94 ± 0.11	2.56 ± 0.41
	3	4.00 ± 0.85	2.68 ± 0.63	4.15 ± 0.17	0.05 ± 0.01	0.92 ± 0.09	2.48 ± 0.44
	4	3.95 ± 0.90	2.51 ± 0.51	4.56 ± 0.16	0.02 ± 0.01	0.93 ± 0.08	2.78 ± 0.51
	5	4.77 ± 0.64	2.87 ± 0.41	4.66 ± 0.09	0.05 ± 0.01	0.99 ± 0.05	2.45 ± 0.24
	6	4.33 ± 0.76	2.76 ± 0.48	4.43 ± 0.05	0.04 ± 0.00	0.94 ± 0.08	2.48 ± 0.29

Appendix 4: Bulk density and wetness values of irrigated soil columns.

Table A4.1
Mean values of bulk density and wetness for each treatment (FW00*i*, T102 and T401–4) of the G001 soil columns at the completion laboratory irrigation

	Depth	FW002	T102	T401	T402	T403	T404
	(mm)	(EC 0.2 SAR 1)	(EC 0.0 SAR 0)	(EC 0.5 SAR 0)	(EC 0.5 SAR 7.5)	(EC 0.5 SAR 15)	(EC 0.5 SAR 30)
Bulk density ($g\ cm^{-1}$)	0–50	1.09 ± 0.12	1.18 ± 0.05	1.32 ± 0.15	1.20 ± 0.01	1.24 ± 0.06	1.31 ± 0.00
	50–100	1.34	1.35 ± 0.08	1.35 ± 0.08	1.37 ± 0.02	1.34 ± 0.04	1.26 ± 0.10
	100–150	1.19	1.33	1.06 ± 0.06	1.20 ± 0.15	1.32 ± 0.02	1.16
Wetness ($\times 10^{-2}$) ($g\ g^{-1}$)	0–50	0.15 ± 0.01	0.16 ± 0.04	0.15 ± 0.02	0.16 ± 0.03	0.13 ± 0.01	0.18 ± 0.01
	50–100	0.22 ± 0.03	0.22 ± 0.04	0.21 ± 0.02	0.23 ± 0.02	0.19 ± 0.01	0.23 ± 0.05
	100–150	0.27 ± 0.02	0.26 ± 0.04	0.24	0.27 ± 0.01	0.25 ± 0.01	0.29 ± 0.00
	>150	0.28 ± 0.02	0.28 ± 0.03	0.25 ± 0.03	0.28 ± 0.00	0.26 ± 0.00	0.29

The mean values of each treatment were determined and the standard error of means obtained using a one–way Analysis of Variance and then compared for each of the sampled soil layers (0–50 mm, 50–100 mm, 100–150 mm and >150 mm).

Table A4.2
Mean values of bulk density and wetness for each treatment (FW00*i*, T102 and T401–4) of the G002 soil columns at the completion laboratory irrigation

	Depth	FW002	T102	T401	T402	T403	T404
	(mm)	(EC 0.2 SAR 1)	(EC 0.0 SAR 0)	(EC 0.5 SAR 0)	(EC 0.5 SAR 7.5)	(EC 0.5 SAR 15)	(EC 0.5 SAR 30)
Bulk density ($g\ cm^{-1}$)	0–50	0.92 ± 0.00	0.95 ± 0.04	0.98 ± 0.06	0.99 ± 0.01	1.05 ± 0.08	0.84 ± 0.19
	50–100	0.94 ± 0.08	0.97 ± 0.13	1.09 ± 0.09	0.95 ± 0.02	1.02 ± 0.06	1.05 ± 0.06
	100–150	1.12 ± 0.08	1.09 ± 0.03	1.07 ± 0.00	1.20 ± 0.05	1.20 ± 0.05	
Wetness ($\times 10^{-2}$) ($g\ g^{-1}$)	0–50	0.20 ± 0.04	0.22 ± 0.07	0.12	0.22 ± 0.03	0.23 ± 0.02	0.22 ± 0.05
	50–100	0.26 ± 0.01	0.25 ± 0.04	0.25 ± 0.04	0.27 ± 0.01	0.28 ± 0.01	0.28 ± 0.02
	100–150	0.26 ± 0.01	0.28 ± 0.01	0.27 ± 0.02	0.28 ± 0.01	0.29 ± 0.01	0.28 ± 0.01
	>150	0.27 ± 0.01	0.29 ± 0.01	0.27 ± 0.02	0.29 ± 0.00	0.29 ± 0.00	

The mean values of each treatment were determined and the standard error of means obtained using a one–way Analysis of Variance and then compared for each of the sampled soil layers (0–50 mm, 50–100 mm, 100–150 mm and >150 mm).

Table A4.3
Mean values of bulk density and wetness for each treatment (FW00*i*, T102 and T401–4) of the H001 soil columns at the completion laboratory irrigation

	Depth	FW002	T102	T401	T402	T403	T404
	(mm)	(EC 0.2 SAR 1)	(EC 0.0 SAR 0)	(EC 0.5 SAR 0)	(EC 0.5 SAR 7.5)	(EC 0.5 SAR 15)	(EC 0.5 SAR 30)
Bulk density ($g\ cm^{-1}$)	0–50	1.27	1.34 ± 0.06	1.07 ± 0.06	1.12 ± 0.10	1.12 ± 0.05	1.27 ± 0.06
	50–100	1.16	1.13 ± 0.07	1.23 ± 0.21	1.12 ± 0.05	1.07 ± 0.02	0.93 ± 0.21
	100–150	1.25	1.04 ± 0.15	1.19 ± 0.06	0.96 ± 0.06	1.15 ± 0.06	1.06
Wetness ($\times 10^{-2}$) ($g\ g^{-1}$)	0–50	0.10 ± 0.00	0.09 ± 0.01	0.13 ± 0.04	0.14 ± 0.02	0.18 ± 0.01	0.22 ± 0.07
	50–100	0.17*ab* ± 0.01	0.20*ab* ± 0.03	0.16*b* ± 0.02	0.21*ab* ± 0.03	0.28*ab* ± 0.01	0.29*a* ± 0.02
	100–150	0.23*ab* ± 0.01	0.25*ab* ± 0.00	0.22*b* ± 0.03	0.26*ab* ± 0.02	0.27*ab* ± 0.01	0.32*a* ± 0.02
	>150	0.24 ± 0.02	0.26 ± 0.00	0.23 ± 0.02	0.28 ± 0.01	0.28 ± 0.00	

The mean values of each treatment were determined and the standard error of means obtained using a one–way Analysis of Variance and then compared for each of the sampled soil layers (0–50 mm, 50–100 mm, 100–150 mm and >150 mm). Significant differences were determined and are represented within rows by the letters *a* and *b*. This was carried out using the Tukey–Kramer test (P=0.05).

Table A4.4
Mean values of bulk density and wetness for each treatment (FW00*i*, T102 and T401–4) of the H002 soil columns at the completion laboratory irrigation

	Depth	FW002	T102	T401	T402	T403	T404
	(mm)	(EC 0.2 SAR 1)	(EC 0.0 SAR 0)	(EC 0.5 SAR 0)	(EC 0.5 SAR 7.5)	(EC 0.5 SAR 15)	(EC 0.5 SAR 30)
Bulk density ($g\ cm^{-1}$)	0–50	1.01 ± 0.02	1.02 ± 0.03	1.00 ± 0.17	0.95 ± 0.08	0.92 ± 0.09	1.02 ± 0.10
	50–100	1.09 ± 0.07	1.04 ± 0.09	1.06 ± 0.05	1.05 ± 0.01	1.08 ± 0.08	1.13 ± 0.08
	100–150	1.05 ± 0.16	1.05 ± 0.07	1.30 ± 0.07	1.18 ± 0.11	1.11 ± 0.03	1.18 ± 0.07
Wetness ($\times 10^{-2}$) ($g\ g^{-1}$)	0–50	0.13 ± 0.01	0.21 ± 0.02	0.21 ± 0.09	0.24 ± 0.02	0.25 ± 0.00	0.21 ± 0.02
	50–100	0.21 ± 0.00	0.24 ± 0.01	0.23 ± 0.05	0.28 ± 0.00	0.27 ± 0.01	0.25 ± 0.02
	100–150	0.23 ± 0.01	0.25 ± 0.00	0.23 ± 0.02	0.26 ± 0.00	0.27 ± 0.01	0.25 ± 0.00
	>150	0.24 ± 0.00	0.25 ± 0.00	0.23 ± 0.02	0.27 ± 0.00	0.27 ± 0.00	0.26 ± 0.01

The mean values of each treatment were determined and the standard error of means obtained using a one–way Analysis of Variance and then compared for each of the sampled soil layers (0–50 mm, 50–100 mm, 100–150 mm and >150 mm).

Table A4.5
Mean values of bulk density and wetness for each treatment (FW00*i*, T102 and T401–4) of the N001 soil columns at the completion laboratory irrigation

	Depth	FW002	T102	T401	T402	T403	T404
	(mm)	(EC 0.2 SAR 1)	(EC 0.0 SAR 0)	(EC 0.5 SAR 0)	(EC 0.5 SAR 7.5)	(EC 0.5 SAR 15)	(EC 0.5 SAR 30)
Bulk density ($g\ cm^{-1}$)	0–50	0.95 ± 0.02	1.03 ± 0.14	0.87 ± 0.02	0.90 ± 0.08	1.01 ± 0.04	0.96 ± 0.01
	50–100	0.98 ± 0.04	0.97 ± 0.13	0.84 ±	0.95 ± 0.02	0.87 ± 0.04	1.04 ± 0.01
	100–150	0.94 ± 0.04	1.04 ± 0.10	0.99 ± 0.08	0.99 ± 0.09	0.89 ± 0.05	0.96 ± 0.03
Wetness ($\times 10^{-2}$) ($g\ g^{-1}$)	0–50	0.29 ± 0.04	0.26 ± 0.11	0.28 ± 0.01	0.31 ± 0.02	0.26 ± 0.02	0.33 ± 0.00
	50–100	0.32 ± 0.03	0.33 ± 0.05	0.34 ± 0.00	0.32 ± 0.04	0.34 ± 0.00	0.37 ± 0.01
	100–150	0.33 ± 0.00	0.35 ± 0.02	0.36 ± 0.01	0.37 ± 0.01	0.37 ± 0.00	0.36 ± 0.02
	>150	0.36 ± 0.04	0.34 ± 0.01	0.36 ± 0.01	0.37 ± 0.03	0.36 ± 0.00	0.35 ± 0.01

The mean values of each treatment were determined and the standard error of means obtained using a one–way Analysis of Variance and then compared for each of the sampled soil layers (0–50 mm, 50–100 mm, 100–150 mm and >150 mm).

Table A4.6
Mean values of bulk density and wetness for each treatment (FW00*i*, T102 and T401–4) of the N002 soil columns at the completion laboratory irrigation

	Depth	FW002	T102	T401	T402	T403	T404
	(mm)	(EC 0.2 SAR 1)	(EC 0.0 SAR 0)	(EC 0.5 SAR 0)	(EC 0.5 SAR 7.5)	(EC 0.5 SAR 15)	(EC 0.5 SAR 30)
Bulk density ($g\ cm^{-1}$)	0–50	1.20 ± 0.01	1.06 ± 0.02	1.10 ± 0.08	1.21 ± 0.14	1.13 ± 0.02	1.03 ± 0.02
	50–100	0.98*c* ± 0.05	1.07*bc* ± 0.04	1.10*bc* ± 0.04	0.97*c* ± 0.02	1.24*ab* ± 0.00	1.31*a* ± 0.04
	100–150	1.08 ± 0.03	1.00 ± 0.04	1.05 ± 0.02	1.01 ± 0.05	0.96 ± 0.06	0.96 ± 0.05
Wetness ($\times 10^{-2}$) ($g\ g^{-1}$)	0–50	0.19 ± 0.02	0.18 ± 0.03	0.18 ± 0.02	0.20 ± 0.00	0.16 ± 0.04	0.14 ± 0.02
	50–100	0.25 ± 0.01	0.25 ± 0.00	0.24 ± 0.01	0.24 ± 0.00	0.22 ± 0.01	0.22 ± 0.00
	100–150	0.26 ± 0.01	0.28 ± 0.02	0.26 ± 0.00	0.25 ± 0.01	0.25 ± 0.00	0.24 ± 0.01
	>150	0.27 ± 0.02	0.28 ± 0.01	0.26 ± 0.01	0.26 ± 0.00	0.26 ± 0.00	0.24 ± 0.00

The mean values of each treatment were determined and the standard error of means obtained using a one–way Analysis of Variance and then compared for each of the sampled soil layers (0–50 mm, 50–100 mm, 100–150 mm and >150 mm). Significant differences were determined and are represented within rows by the letters *a*, *b* and *c*. This was carried out using the Tukey–Kramer test (P=0.05).

Appendix 5.1: ***The effect of water quality on*** **P, S_v, l_p^*, l_s^*, g_p** ***and*** **g_s** ***for each of the Vertosols (B00i, G00i, H00i, N00i) as a function of depth.***

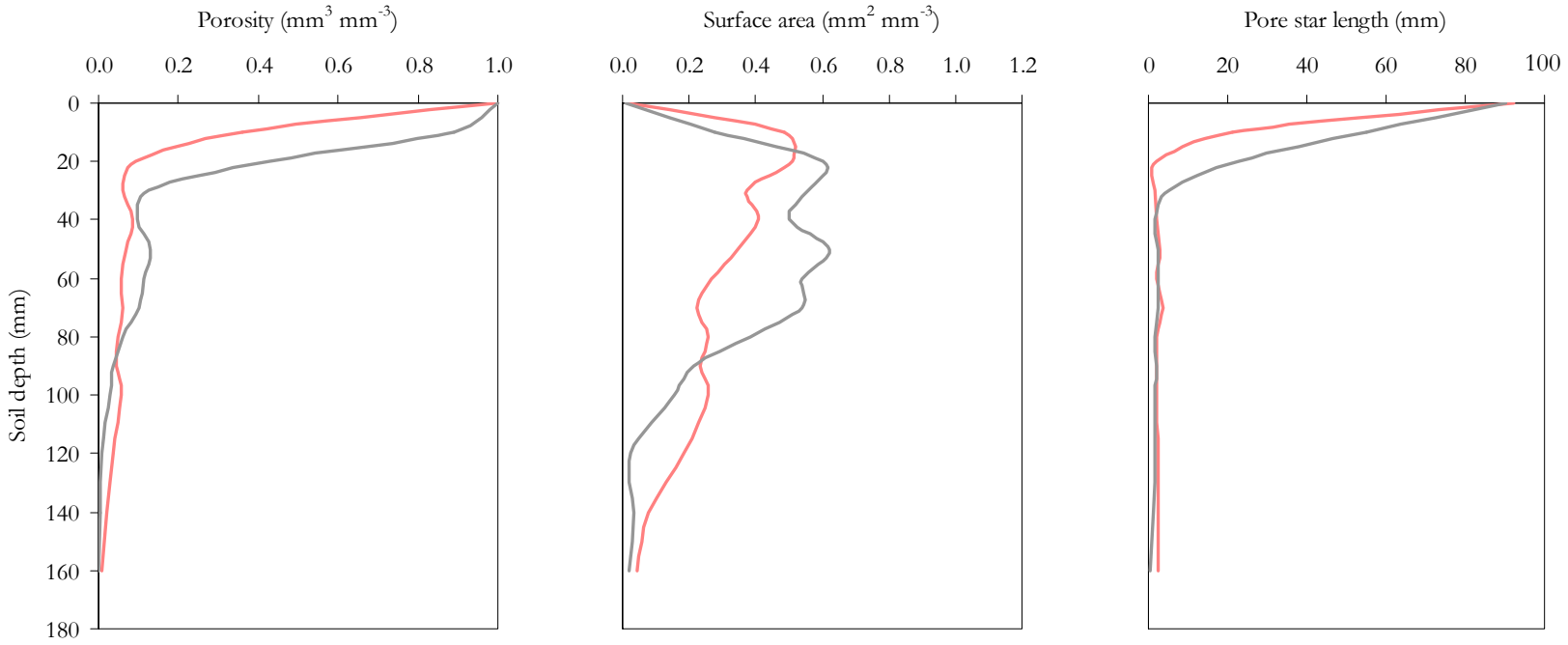

Figure A5.1 Response of selected soil structural parameters (*P, S_v and l_p^**) of soil B001 to two treatments, FW00*i* (—) and T102 (—).

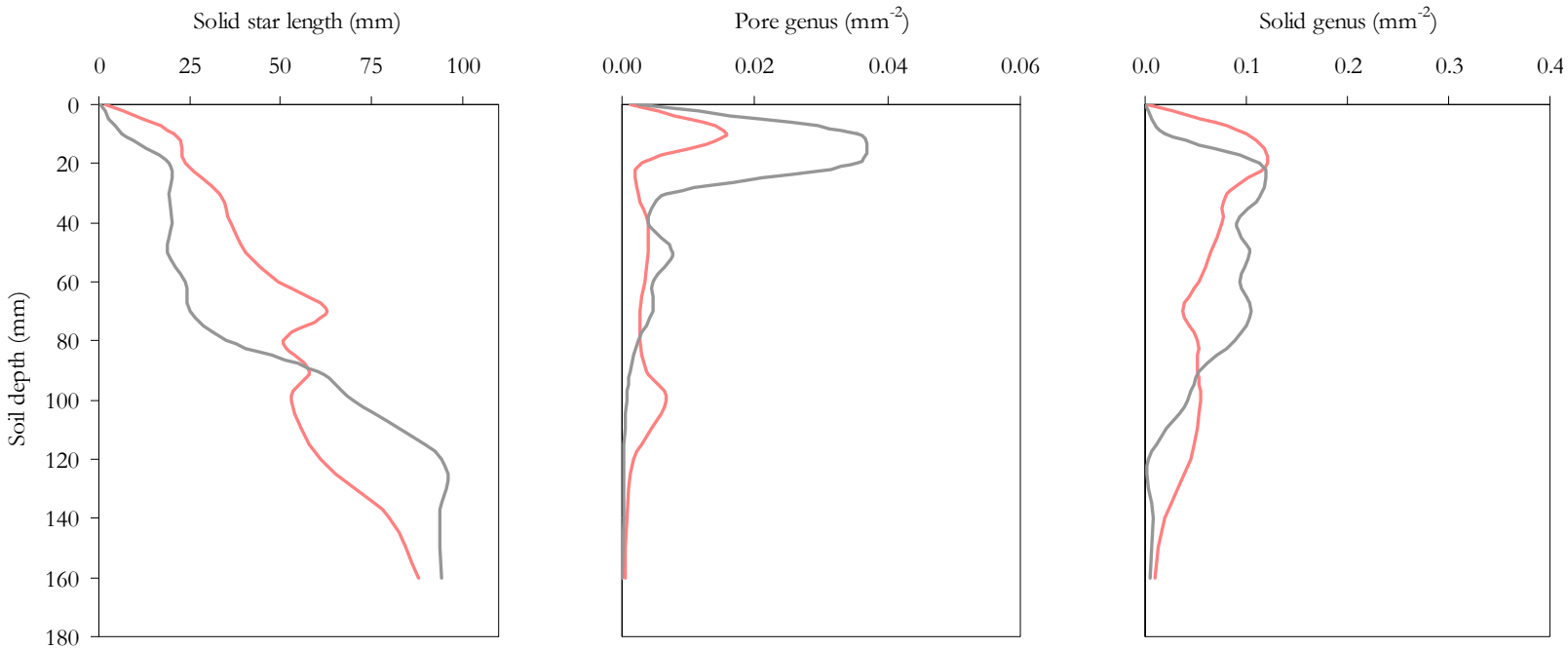

Figure A5.2 Response of selected soil structural parameters (l_s^*, g_p *and* g_s) of soil B001 to two treatments, FW00*i* (—) and T102 (—).

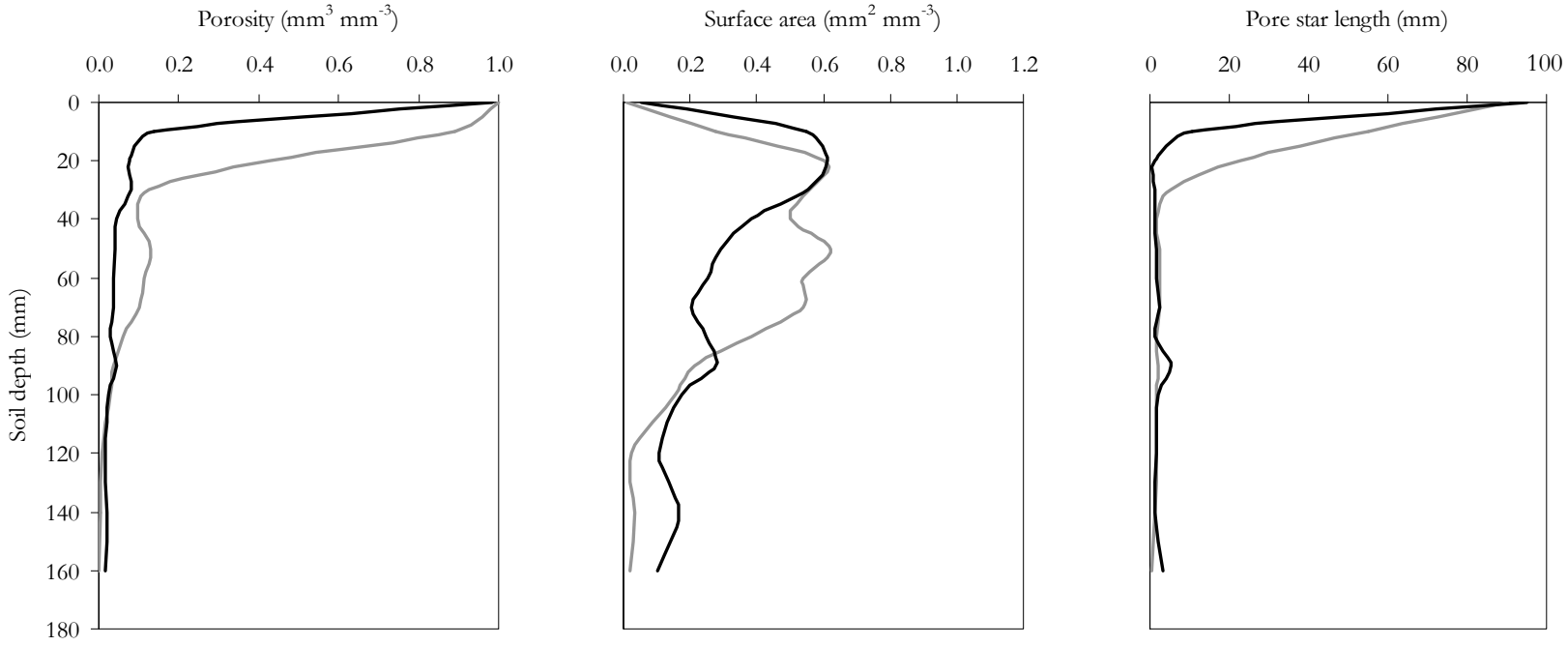

Figure A5.3 Response of selected soil structural parameters (*P, S_v and l_p^**) of soil B001 to two treatments, T102 (—) and T401 (—).

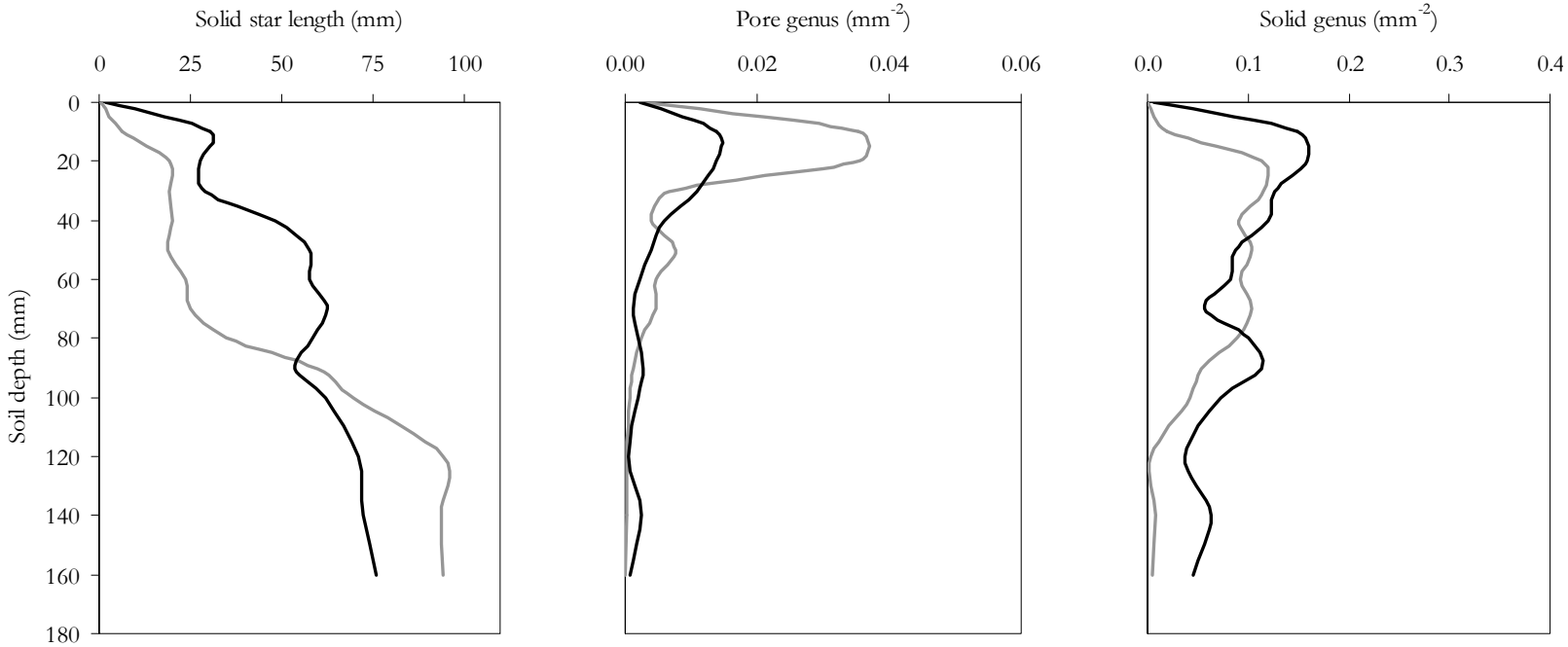

Figure A5.4 Response of selected soil structural parameters (l_s^*, g_p *and* g_s) of soil B001 to two treatments, T102 (▬) and T401 (▬).

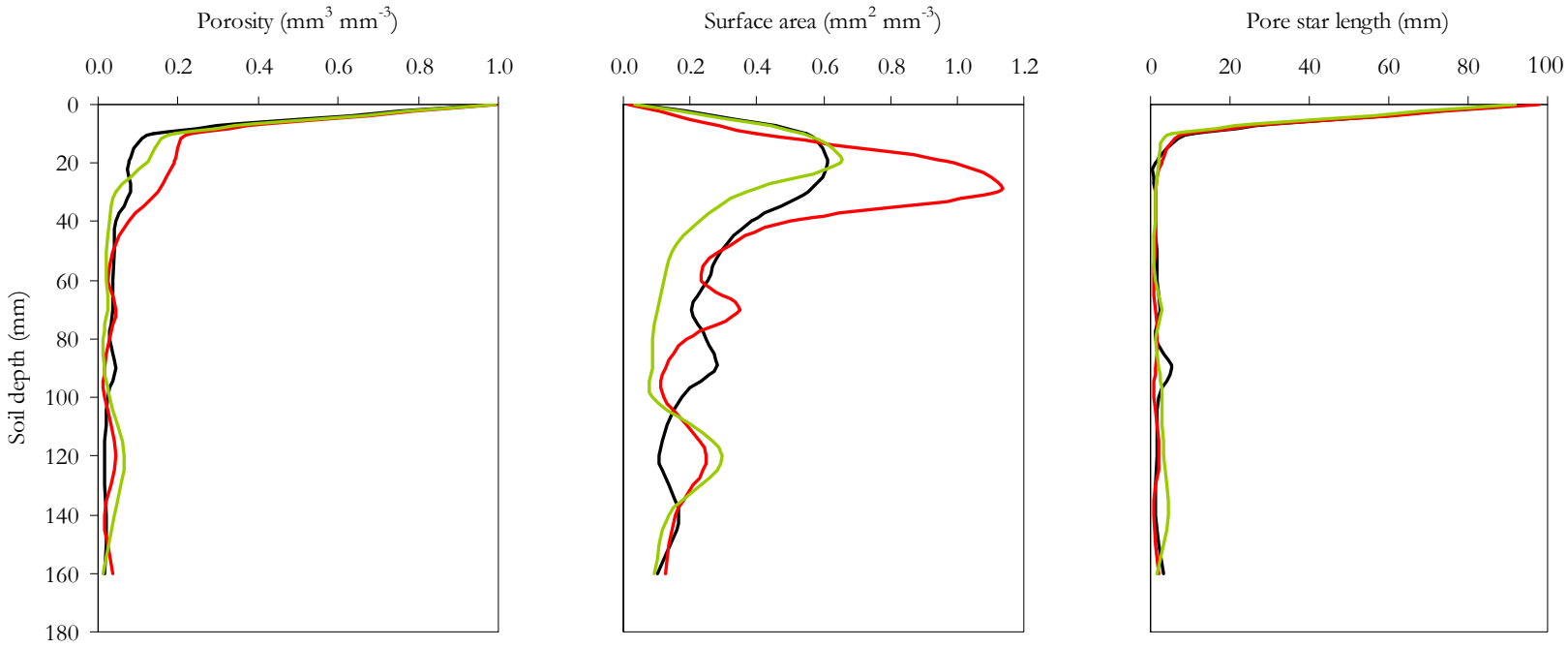

Figure A5.5 Response of selected soil structural parameters (*P, S_v and l_p^**) of soil B001 to three treatments; T401 (—), T402 (—) and T403 (—).

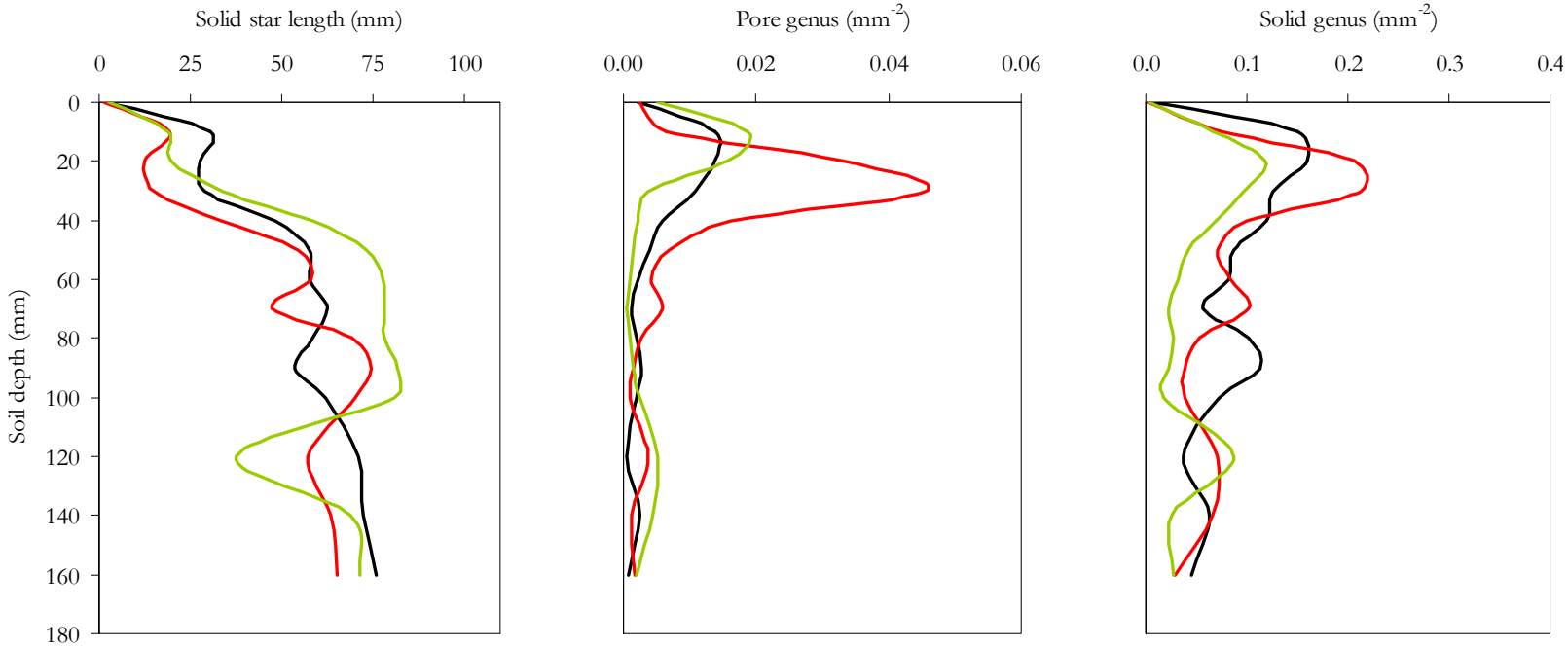

Figure A5.6 Response of selected soil structural parameters (l_s^*, g_p *and* g_s) of soil B001 to three treatments; T401 (—), T402 (—) and T403 (—).

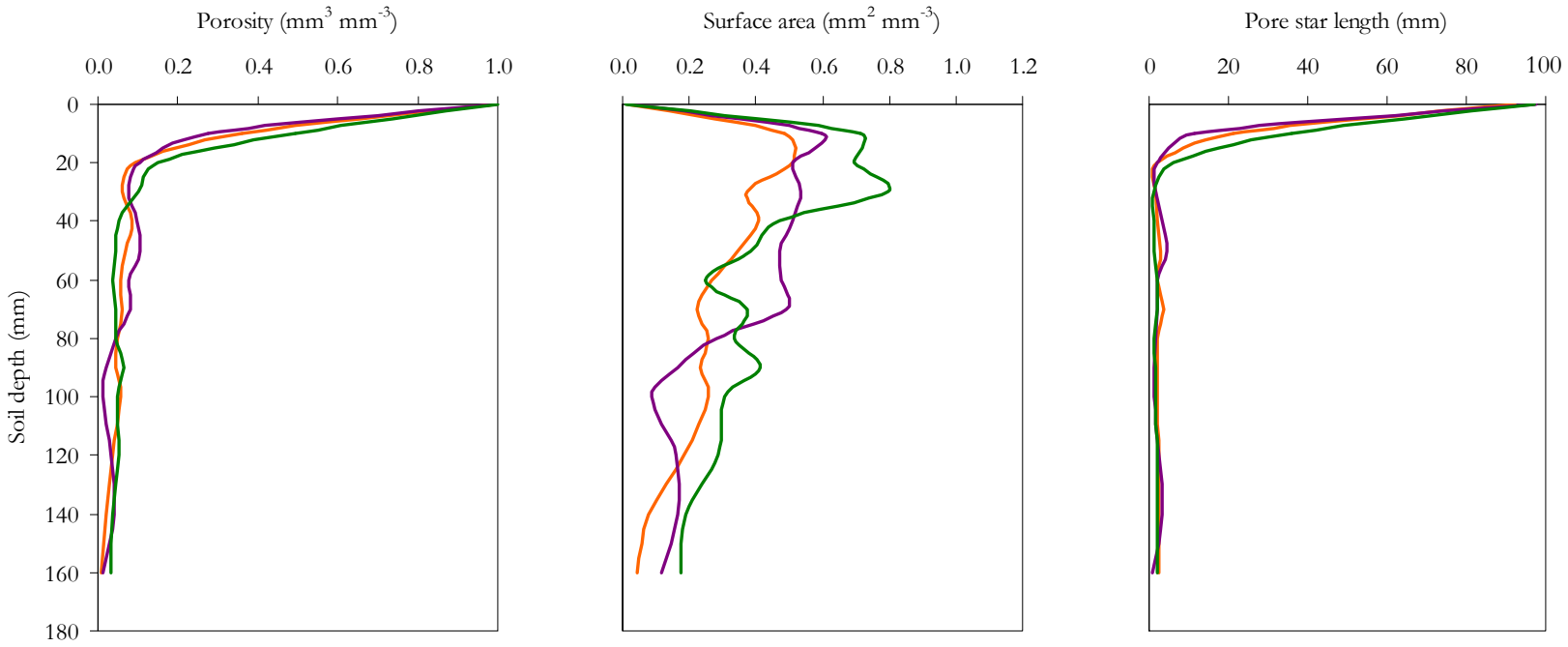

Figure A5.7 Response of selected soil structural parameters (*P, S_v and l_p^**) of soils B001 (—), B002 (—) and B003 (—) treated with FW001.

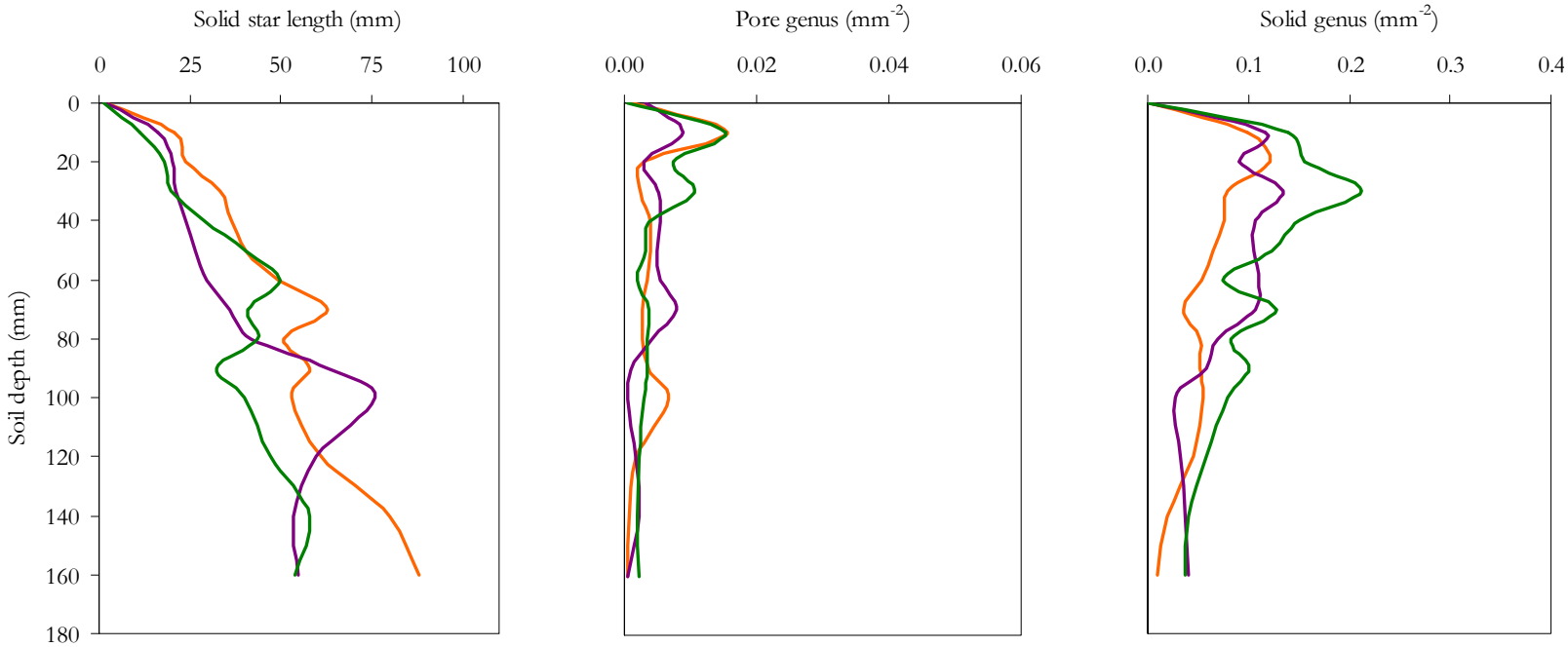

Figure A5.8 Response of selected soil structural parameters (l_s^*, g_p *and* g_s) of soils B001 (—), B002 (—) and B003 (—) treated with FW001.

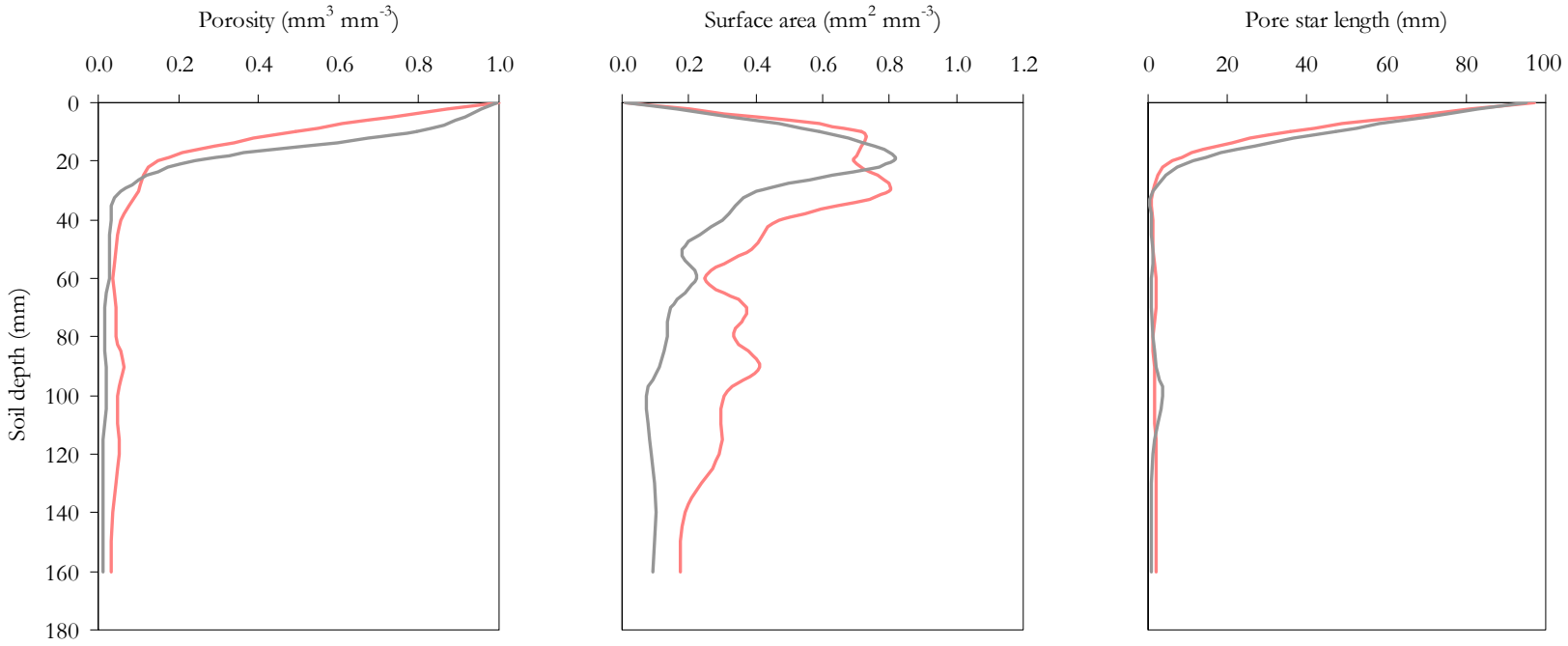

Figure A5.9 Response of selected soil structural parameters (P, S_v *and* l_p^*) of soil B003 to two treatments, FW00*i* (—) and T102 (—).

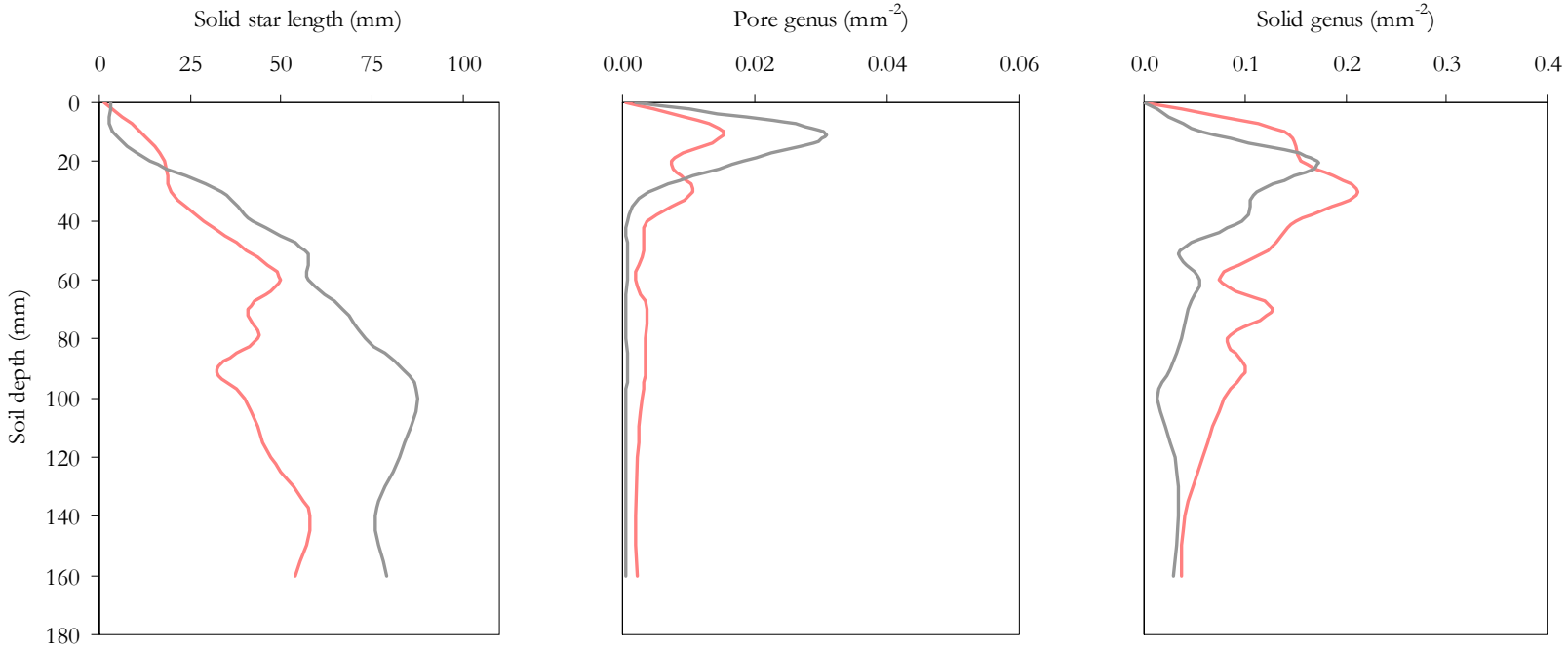

Figure A5.10 Response of selected soil structural parameters (l_s^*, g_p *and* g_s) of soil B003 to two treatments, FW00*i* (—) and T102 (—).

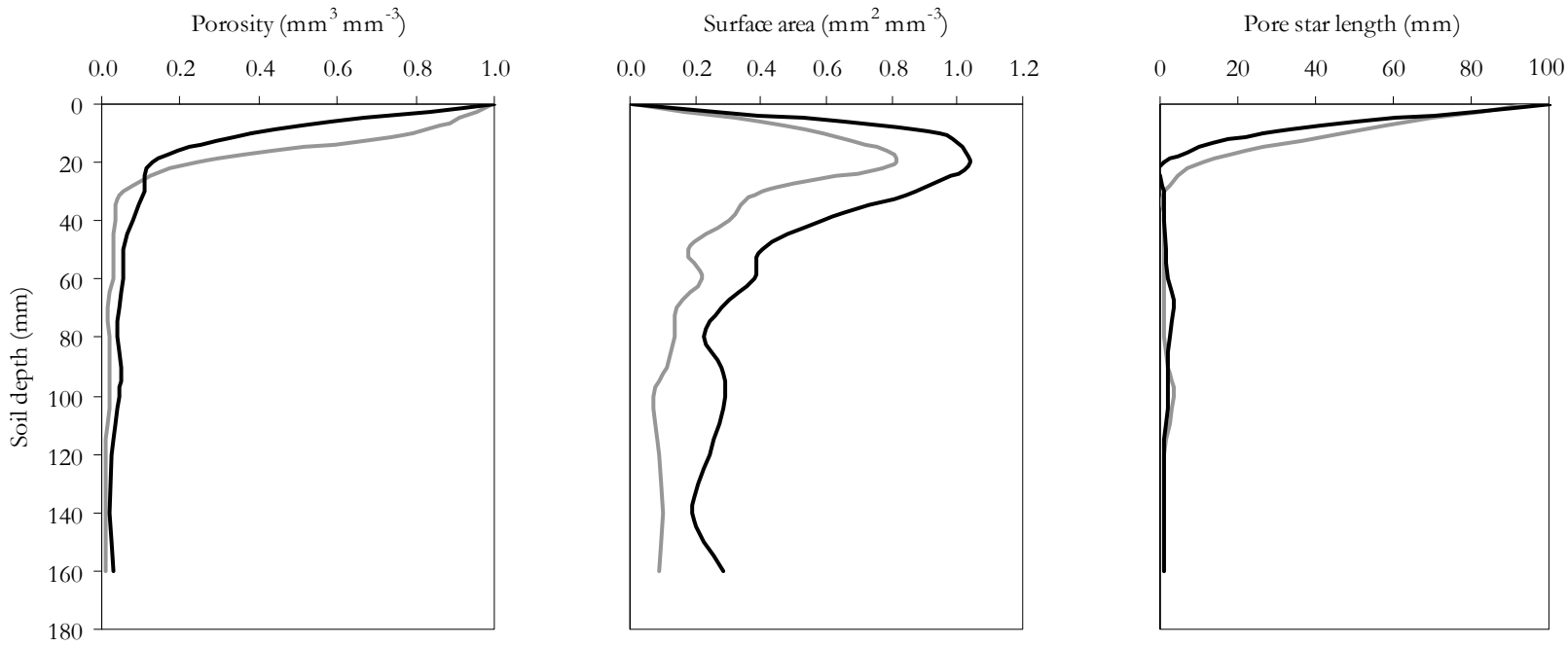

Figure A5.11 Response of selected soil structural parameters (*P, S_v and l_p^**) of soil B003 to two treatments, T102 (—) and T401 (—).

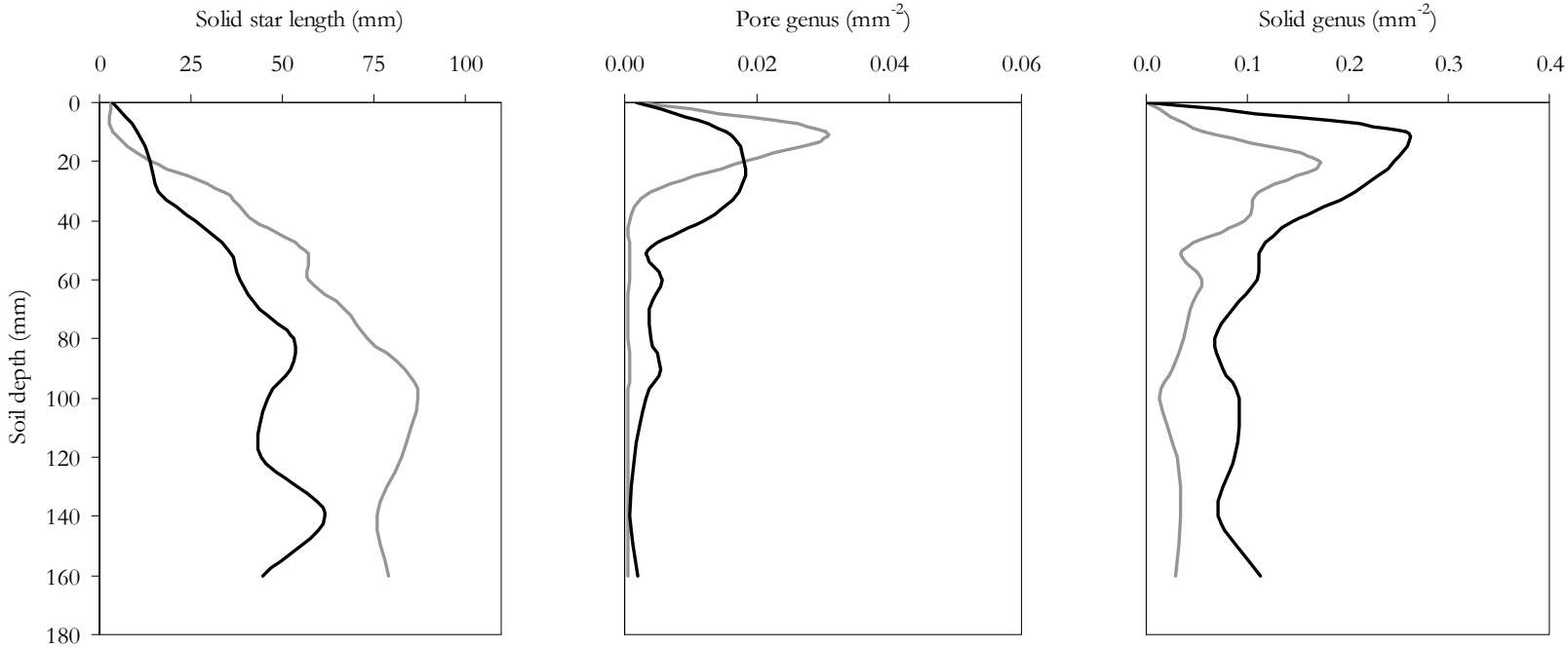

Figure A5.12 Response of selected soil structural parameters (l_s^*, g_p *and* g_s) of soil B003 to two treatments, T102 (▬) and T401 (▬).

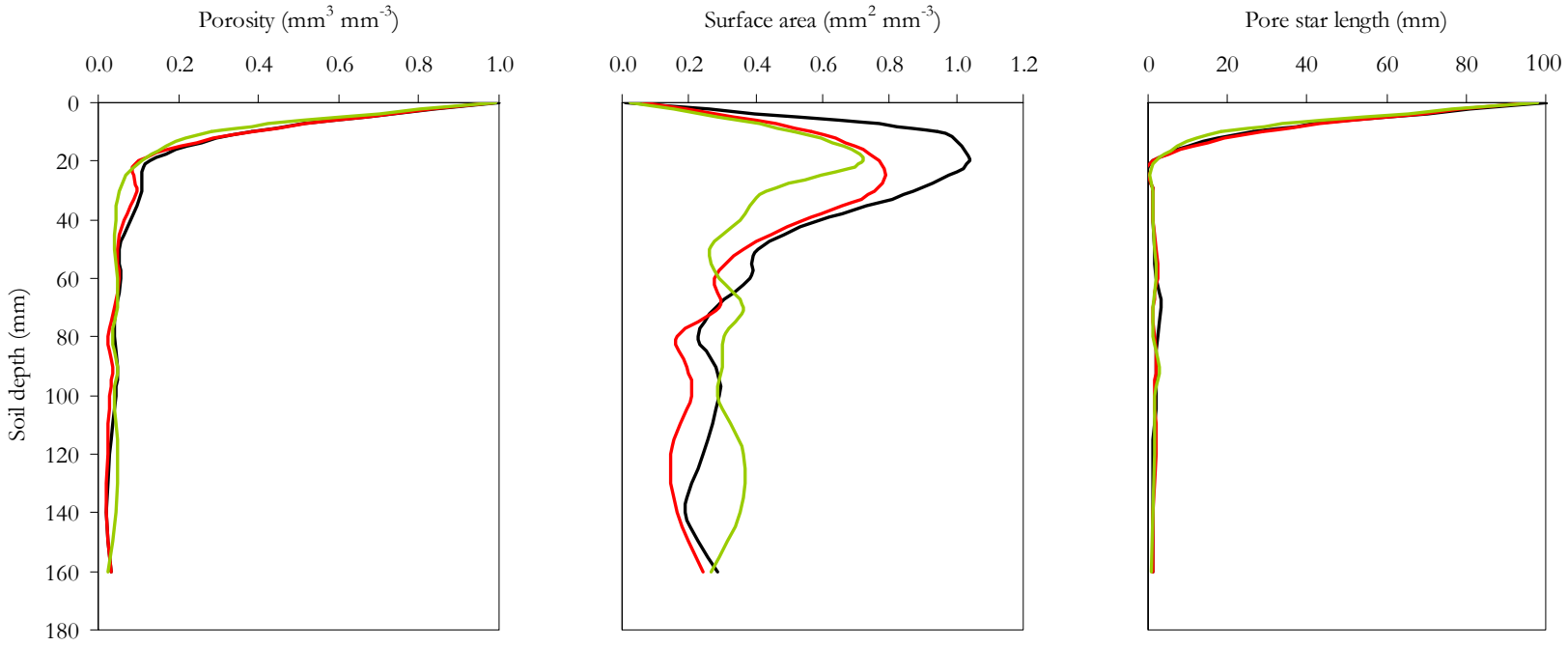

Figure A5.13 Response of selected soil structural parameters (*P, S_v and l_p^**) of soil B003 to three treatments; T401 (—), T402 (—) and T403 (—).

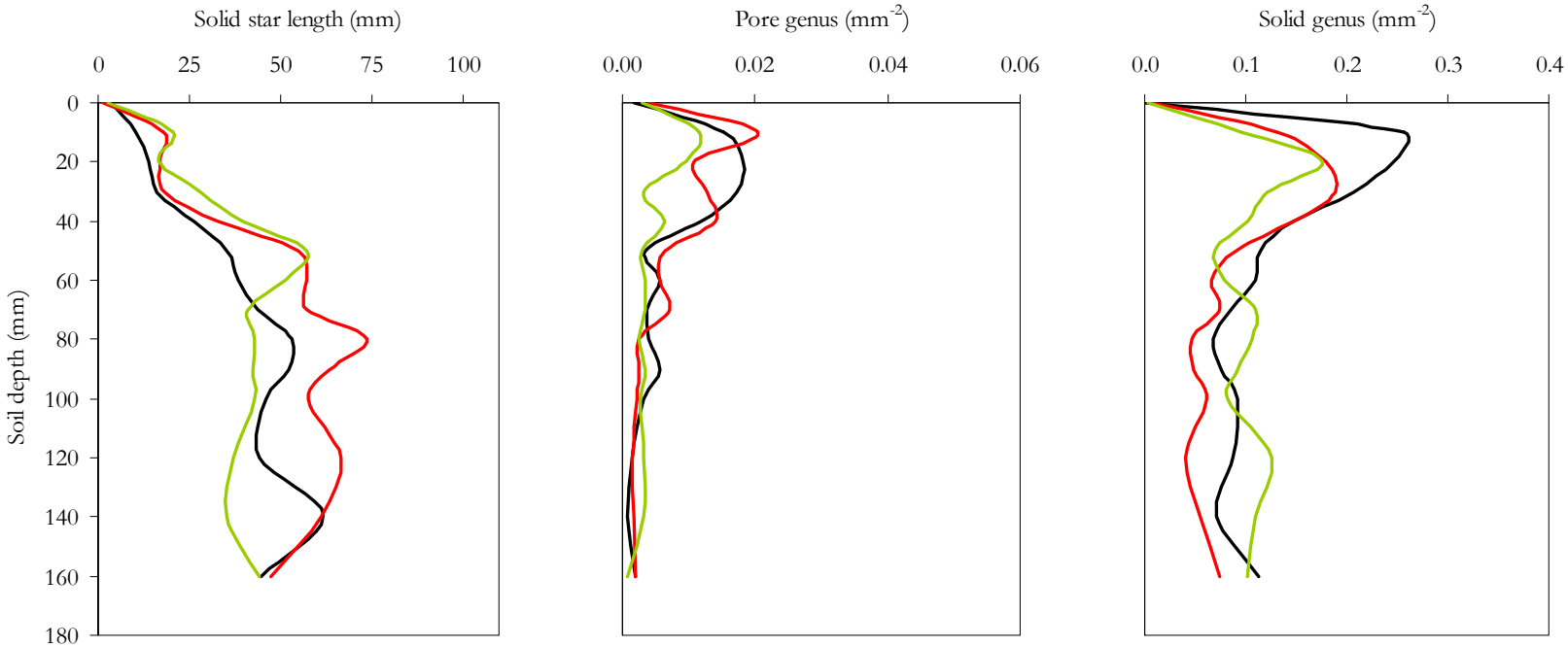

Figure A5.14 Response of selected soil structural parameters (l_s^*, g_p *and* g_s) of soil B003 to three treatments; T401 (—), T402 (—) and T403 (—).

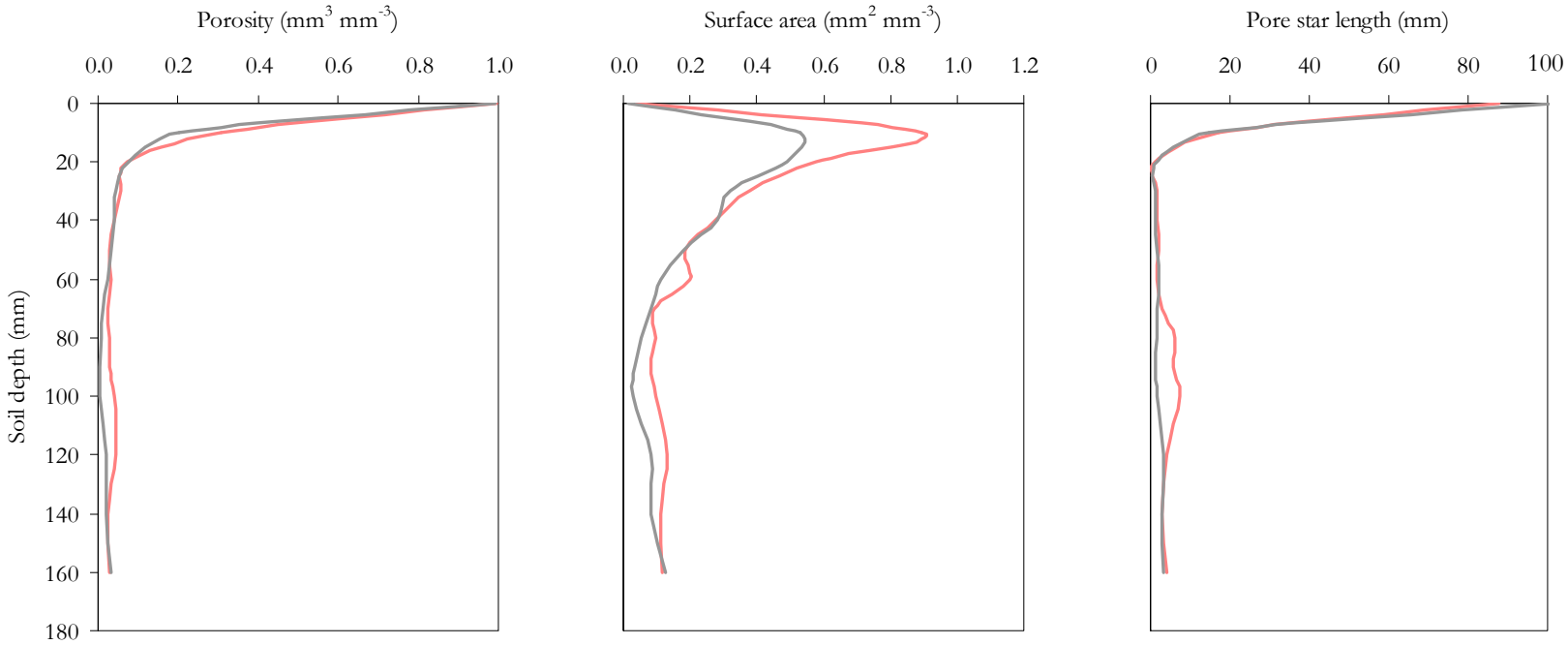

Figure A5.15 Response of selected soil structural parameters (*P, S_v and l_p^**) of soil G001 to two treatments, FW00*i* (—) and T102 (—).

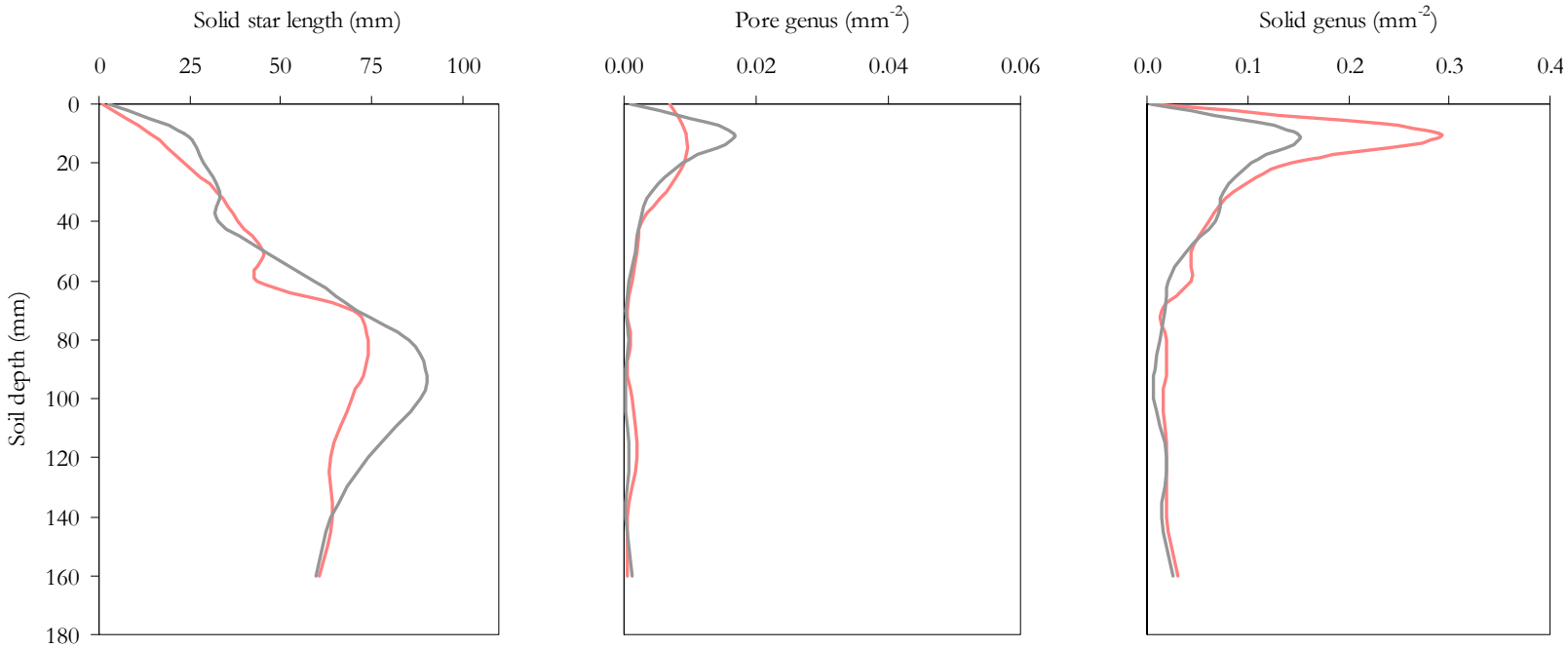

Figure A5.16 Response of selected soil structural parameters (l_s^*, g_p *and* g_s) of soil G001 to two treatments, FW00*i* (—) and T102 (—).

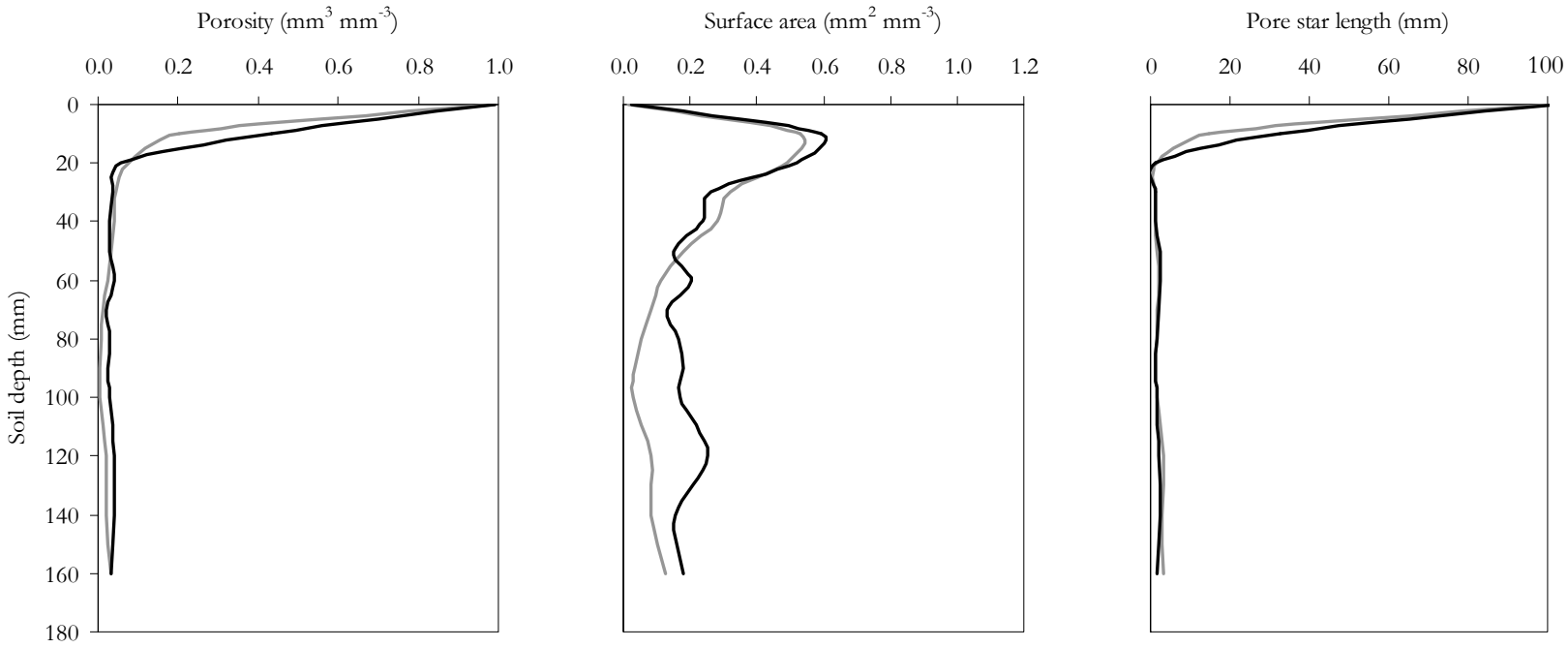

Figure A5.17 Response of selected soil structural parameters (*P, S_v and l_p^**) of soil G001 to two treatments, T102 (—) and T401 (—).

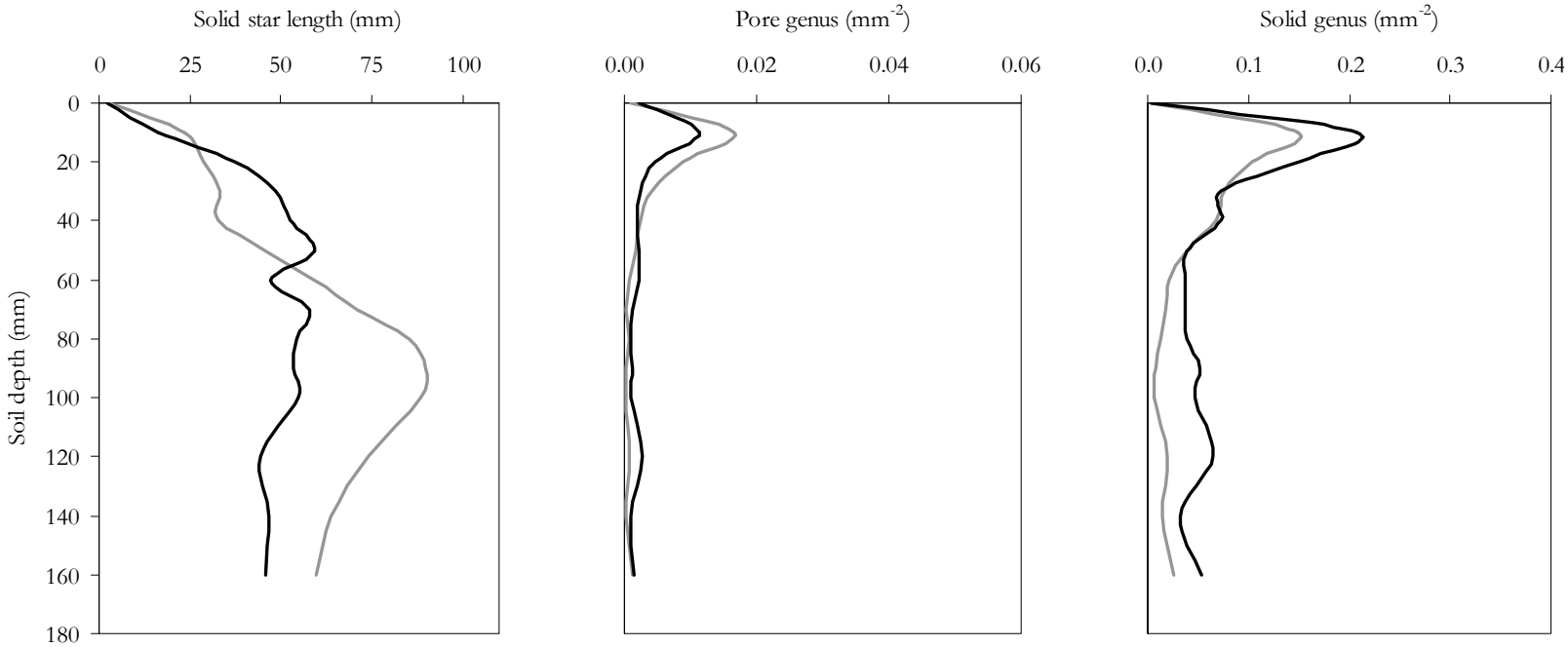

Figure A5.18 Response of selected soil structural parameters (l_s^*, g_p *and* g_s) of soil G001 to two treatments, T102 (—) and T401 (—).

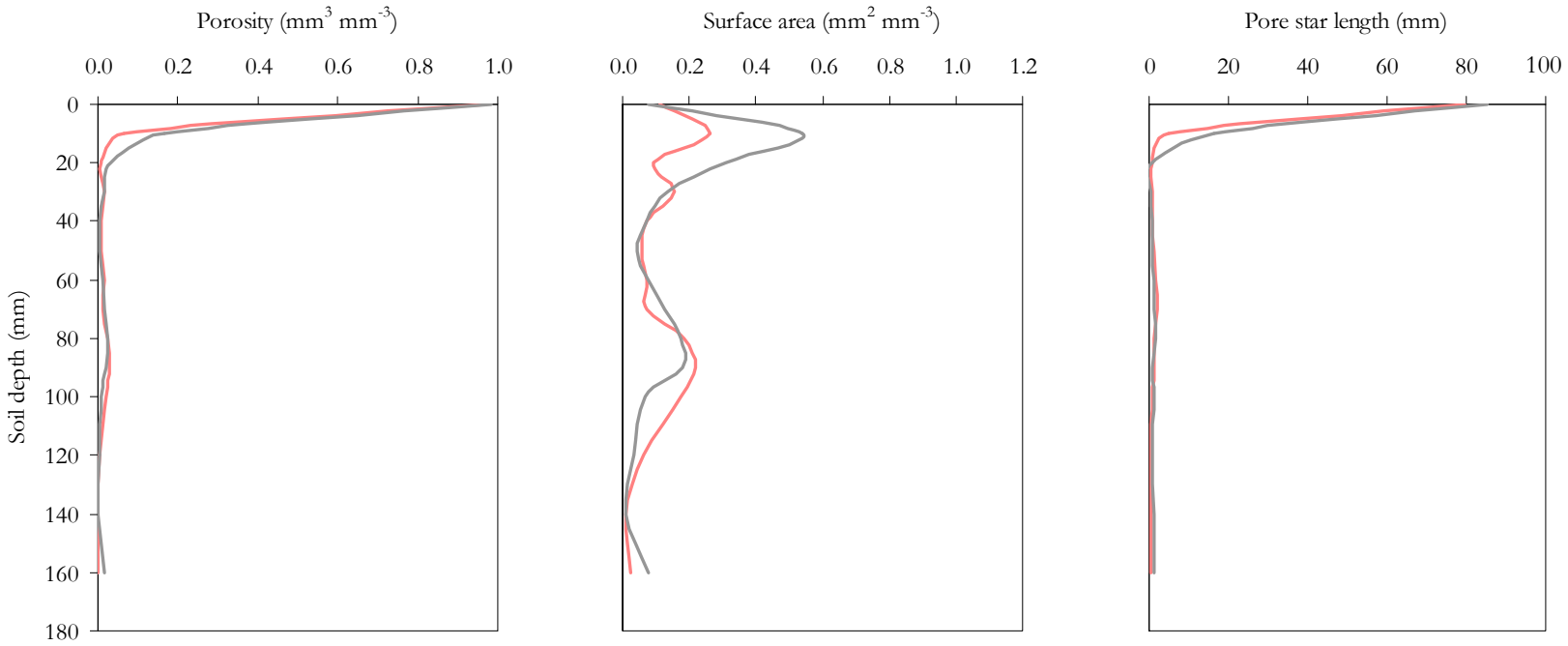

Figure A5.19 Response of selected soil structural parameters (*P, S_v and l_p^**) of soil G002 to two treatments, FW00*i* (—) and T102 (—).

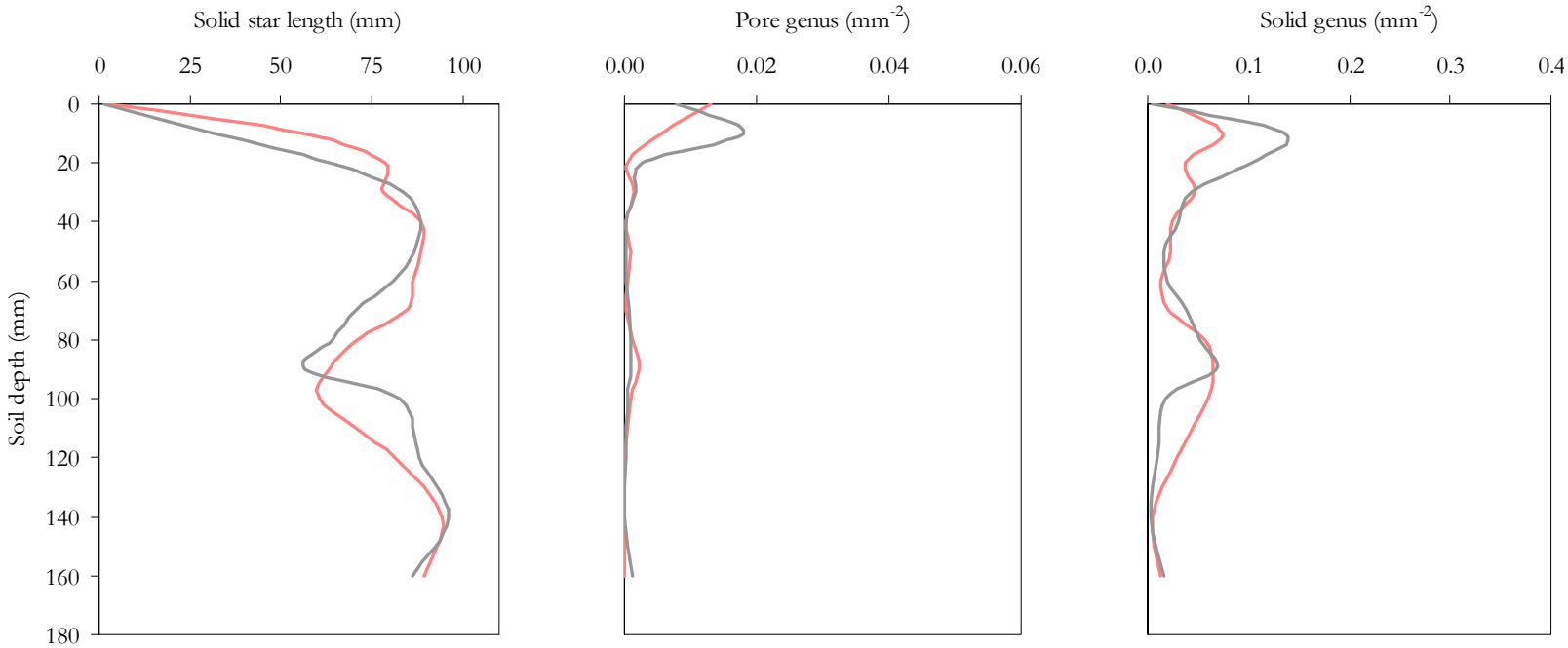

Figure A5.20 Response of selected soil structural parameters (l_s^*, g_p *and* g_s) of soil G002 to two treatments, FW00*i* (—) and T102 (—).

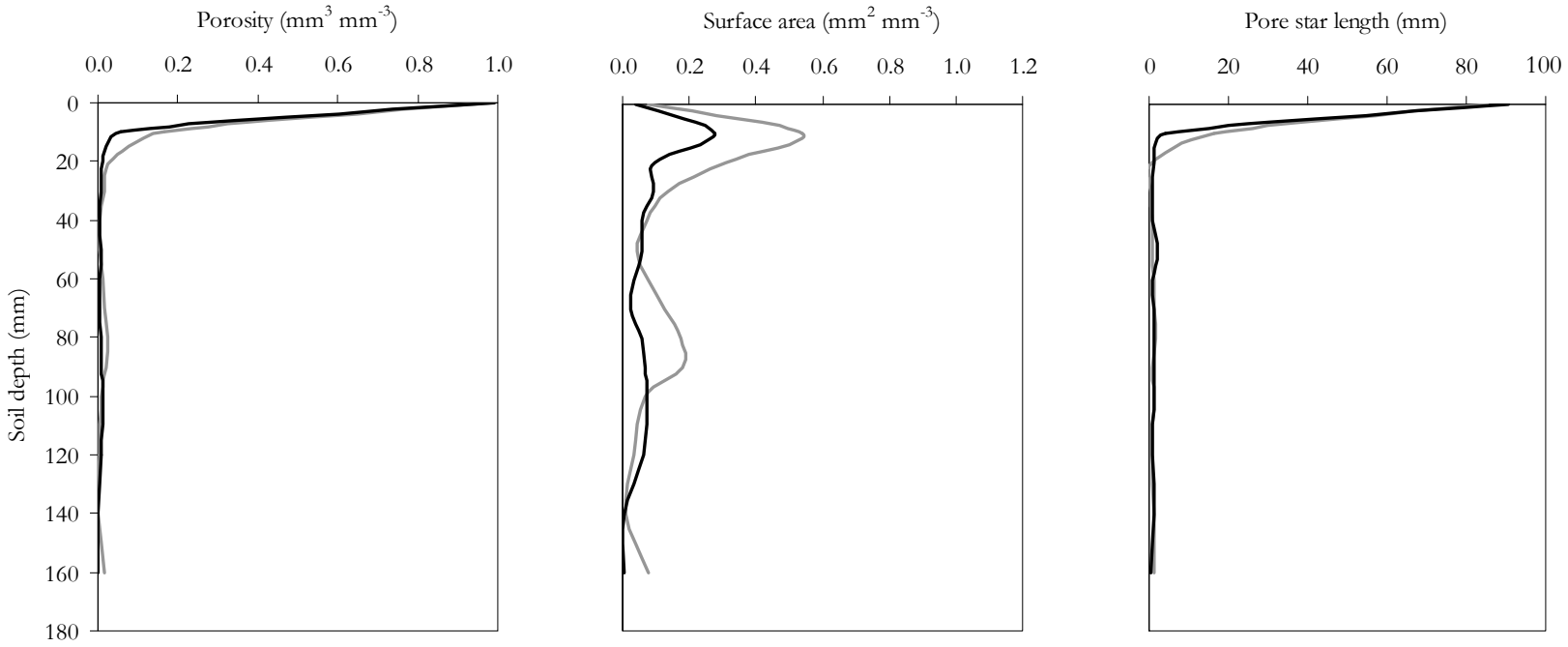

Figure A5.21 Response of selected soil structural parameters (*P, S_v and l_p^**) of soil G002 to two treatments, T102 (—) and T401 (—).

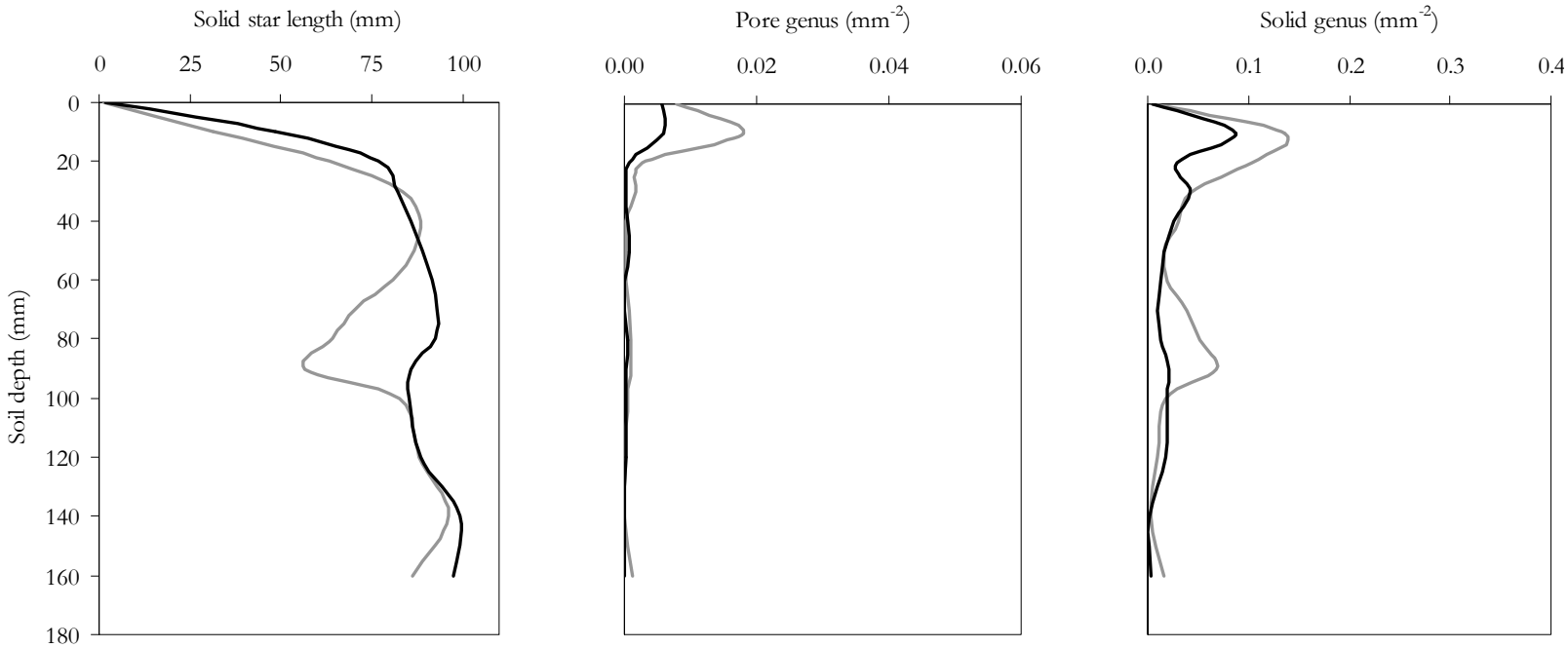

Figure A5.22 Response of selected soil structural parameters (l_s^*, g_p *and* g_s) of soil G002 to two treatments, T102 (—) and T401 (—).

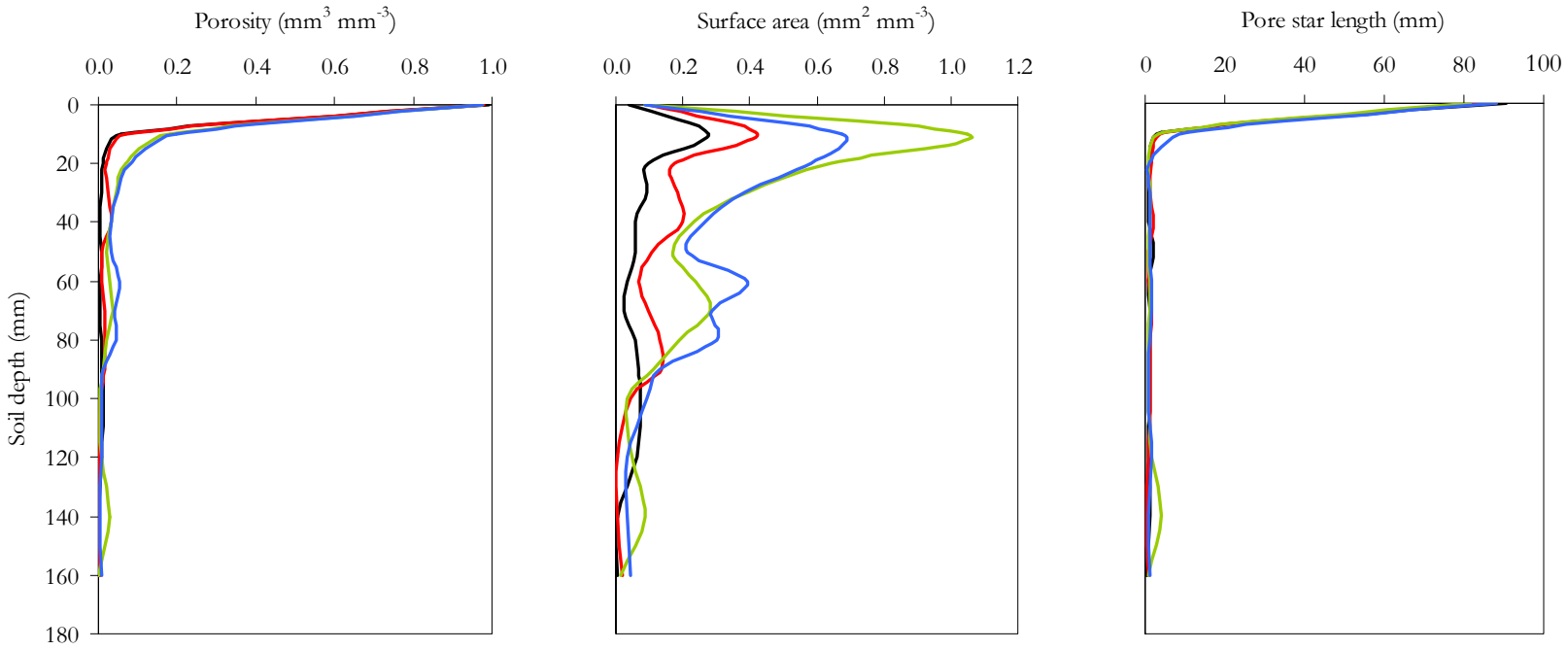

Figure A5.23 Response of selected soil structural parameters (*P, S_v and l_p^**) of soil G002 to four treatments; T401 (—), T402 (—), T403 (—) and T404 (—).

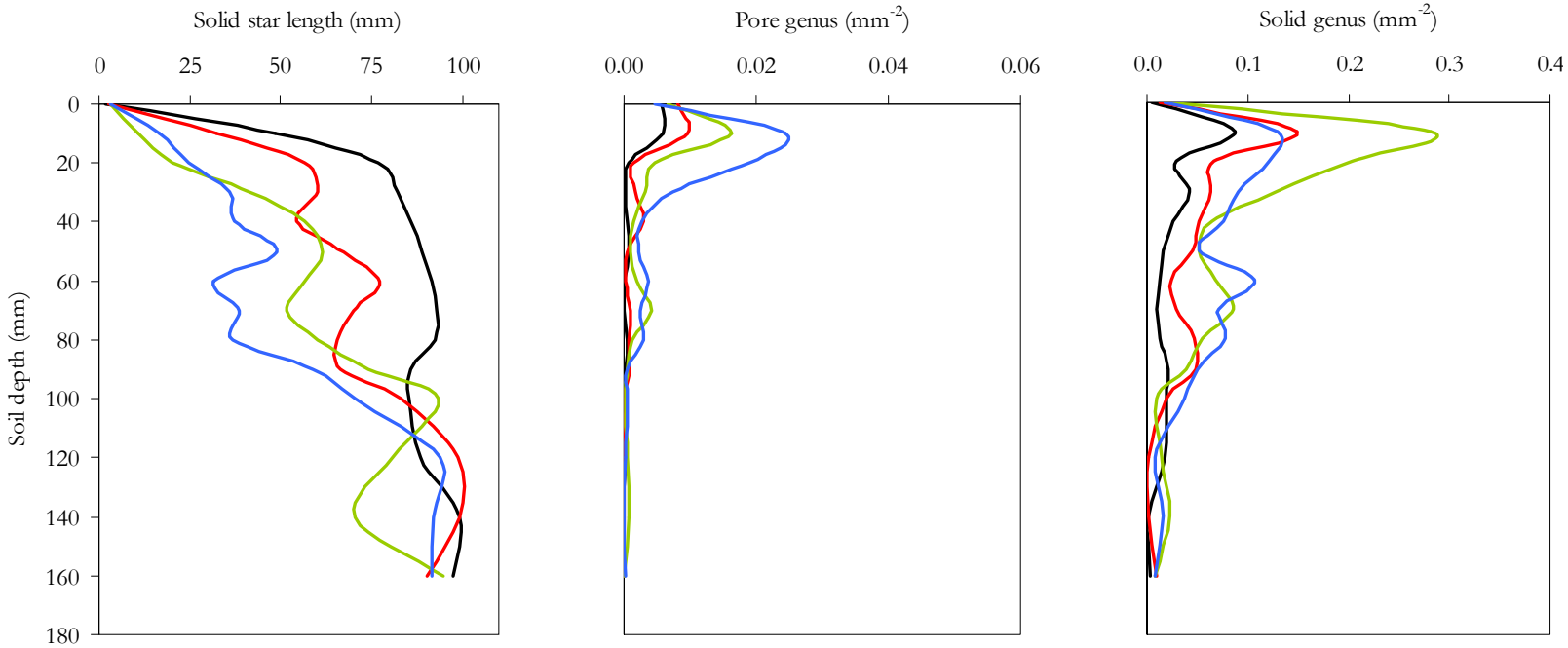

Figure A5.24 Response of selected soil structural parameters (l_s^*, g_p *and* g_s) of soil G002 to four treatments; T401 (—), T402 (—), T403 (—) and T404 (—).

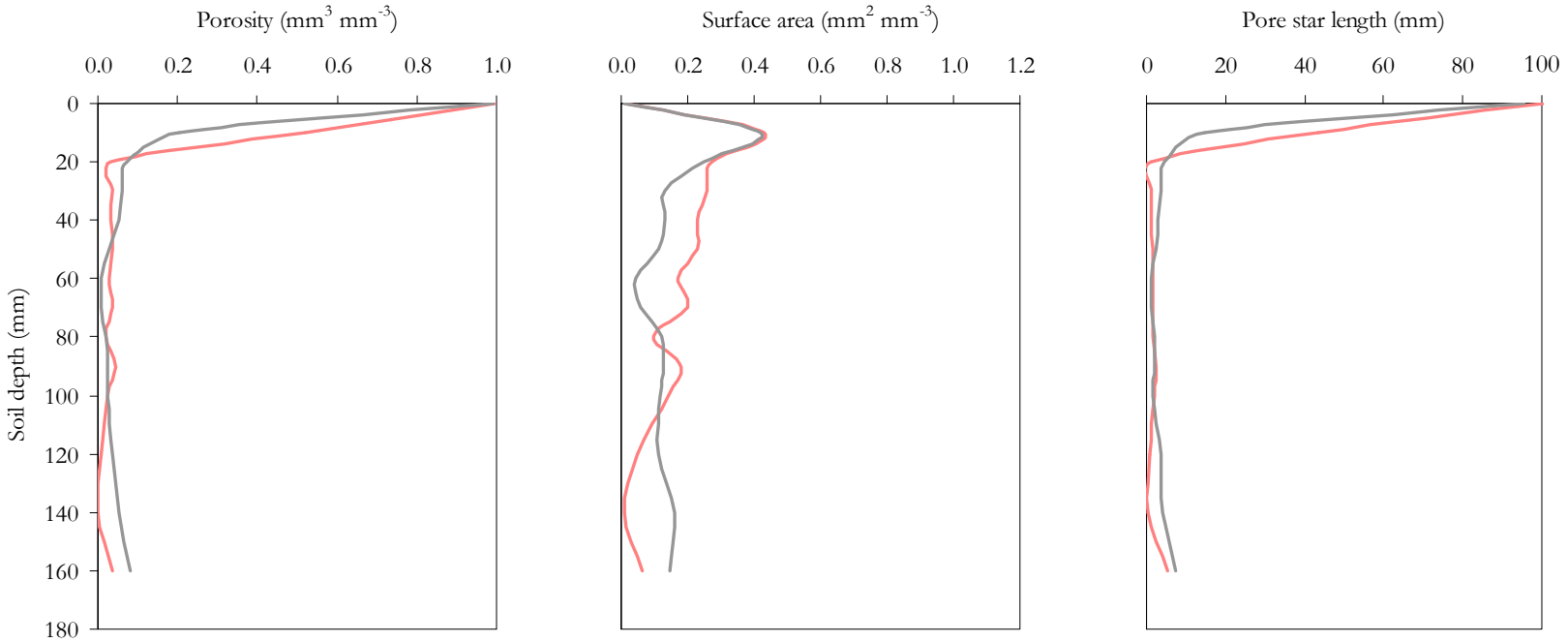

Figure A5.25 Response of selected soil structural parameters (*P, S_v and l_p^**) of soil H001 to two treatments, FW00*i* (—) and T102 (—).

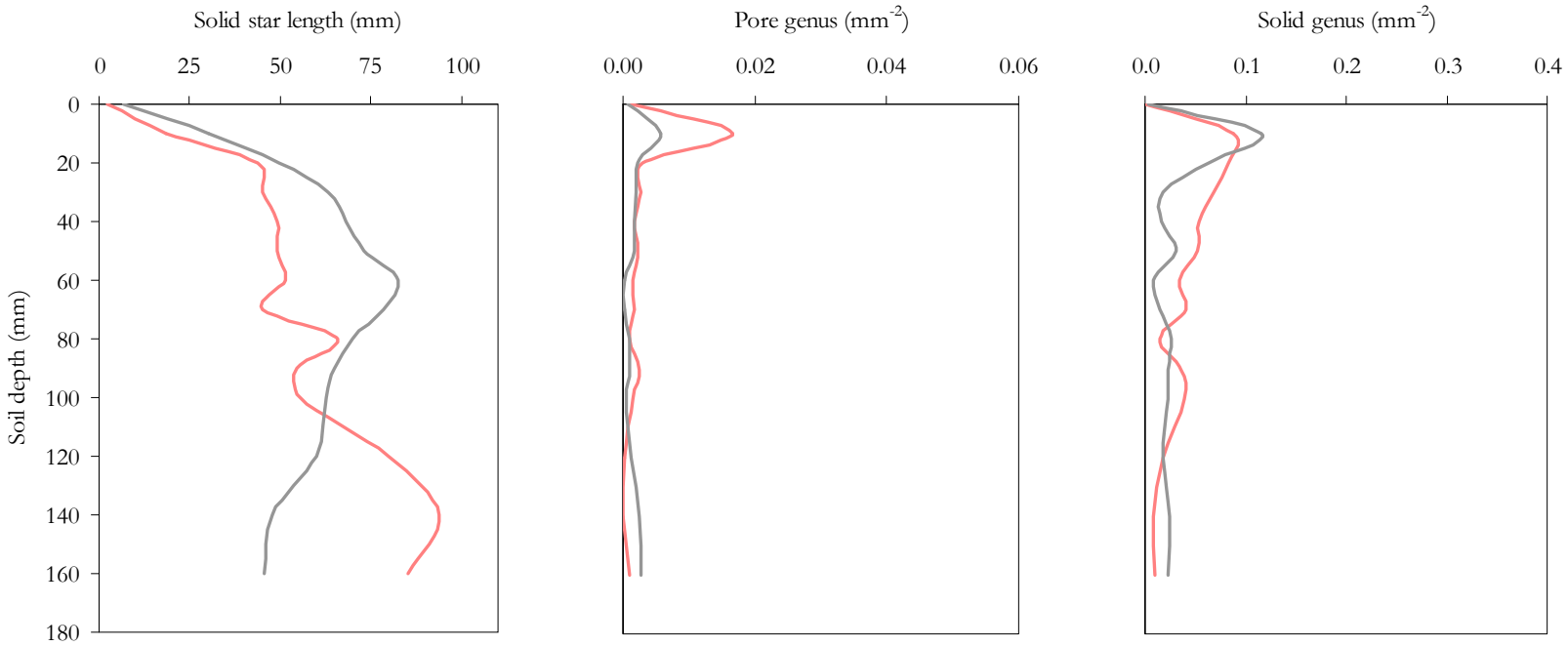

Figure A5.26 Response of selected soil structural parameters (l_s^*, g_p *and* g_s) of soil H001 to two treatments, FW00*i* (—) and T102 (—).

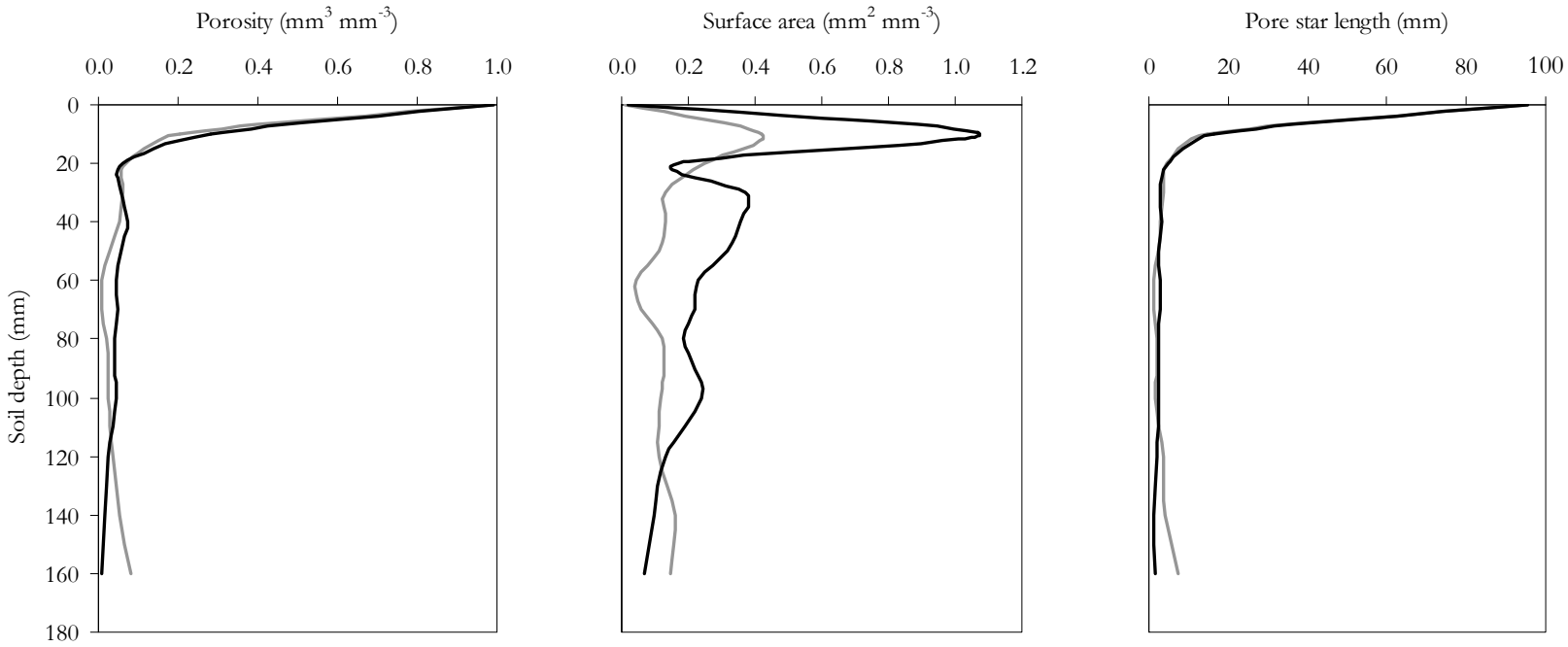

Figure A5.27 Response of selected soil structural parameters (*P, S_v and l_p^**) of soil H001 to two treatments, T102 (—) and T401 (—).

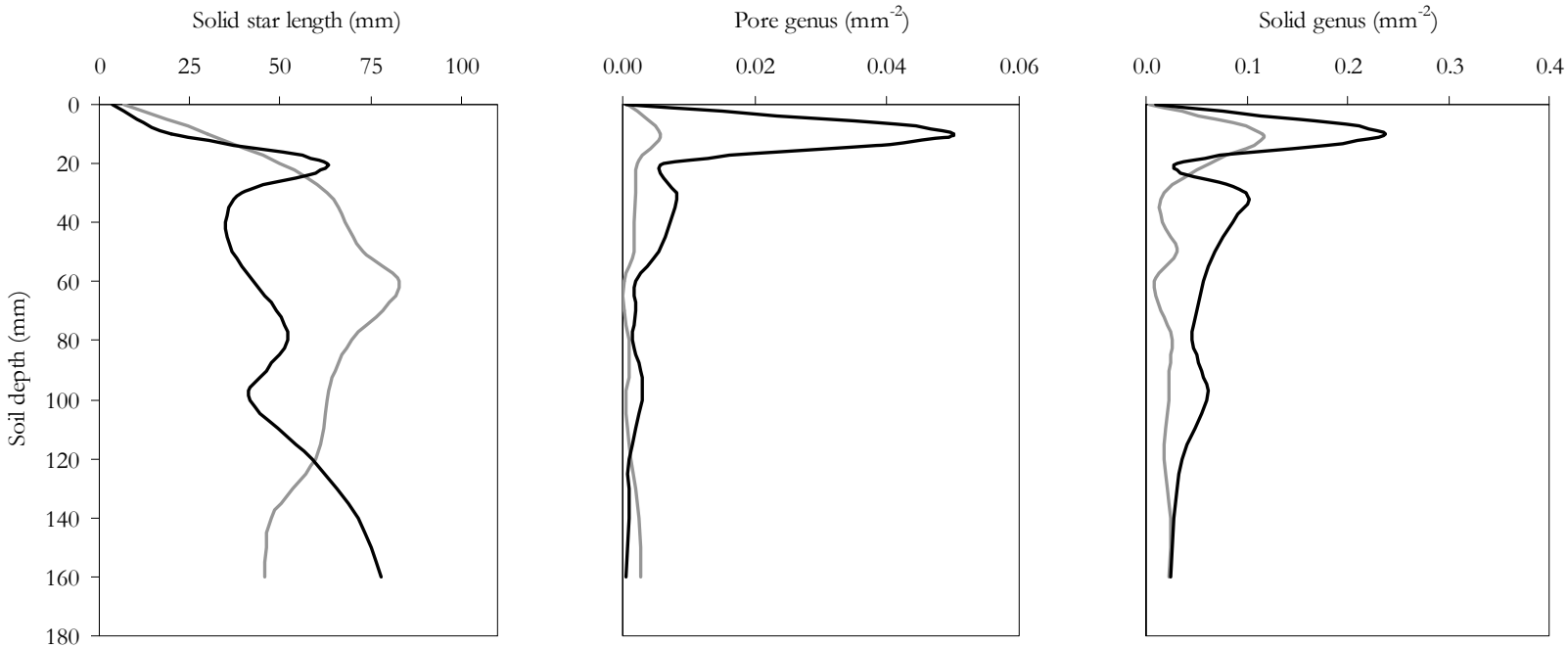

Figure A5.28 Response of selected soil structural parameters (l_s^*, g_p *and* g_s) of soil H001 to two treatments, T102 (—) and T401 (—).

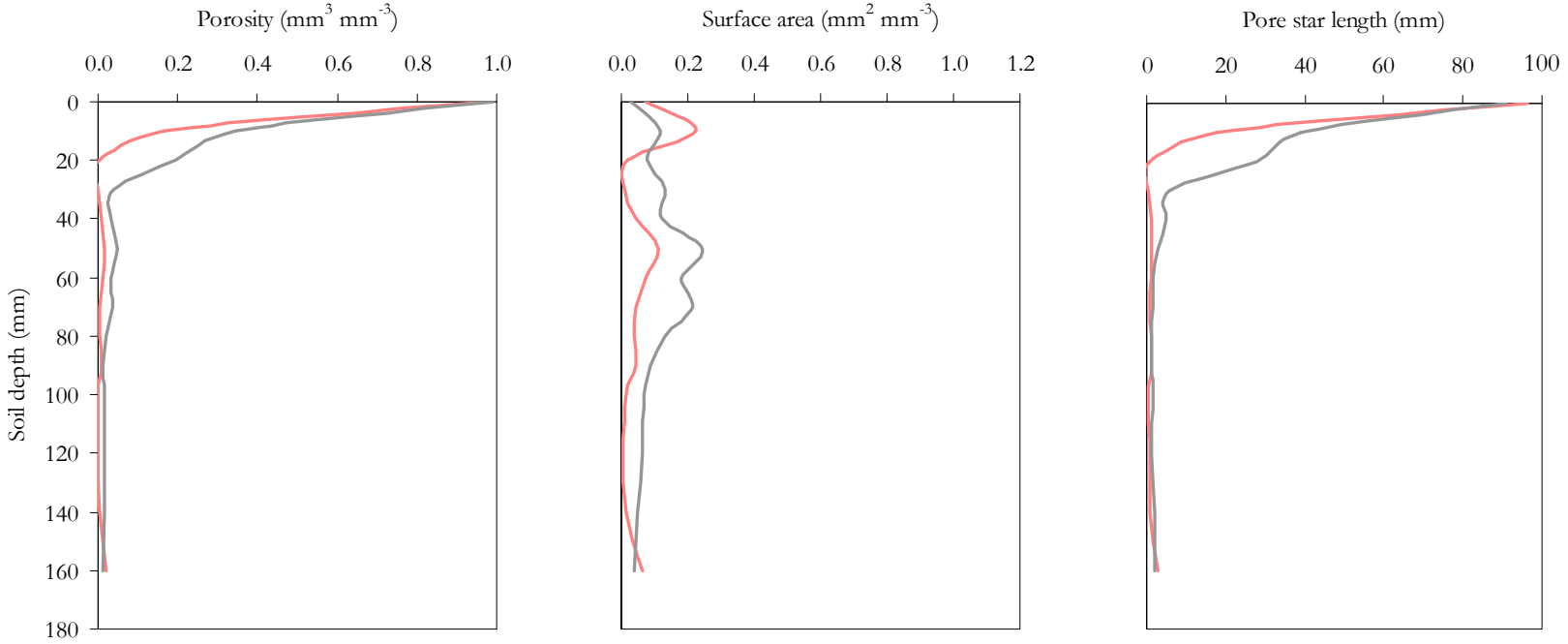

Figure A5.29 Response of selected soil structural parameters (*P, S_v and l_p^**) of soil H002 to two treatments, FW00*i* (—) and T102 (—).

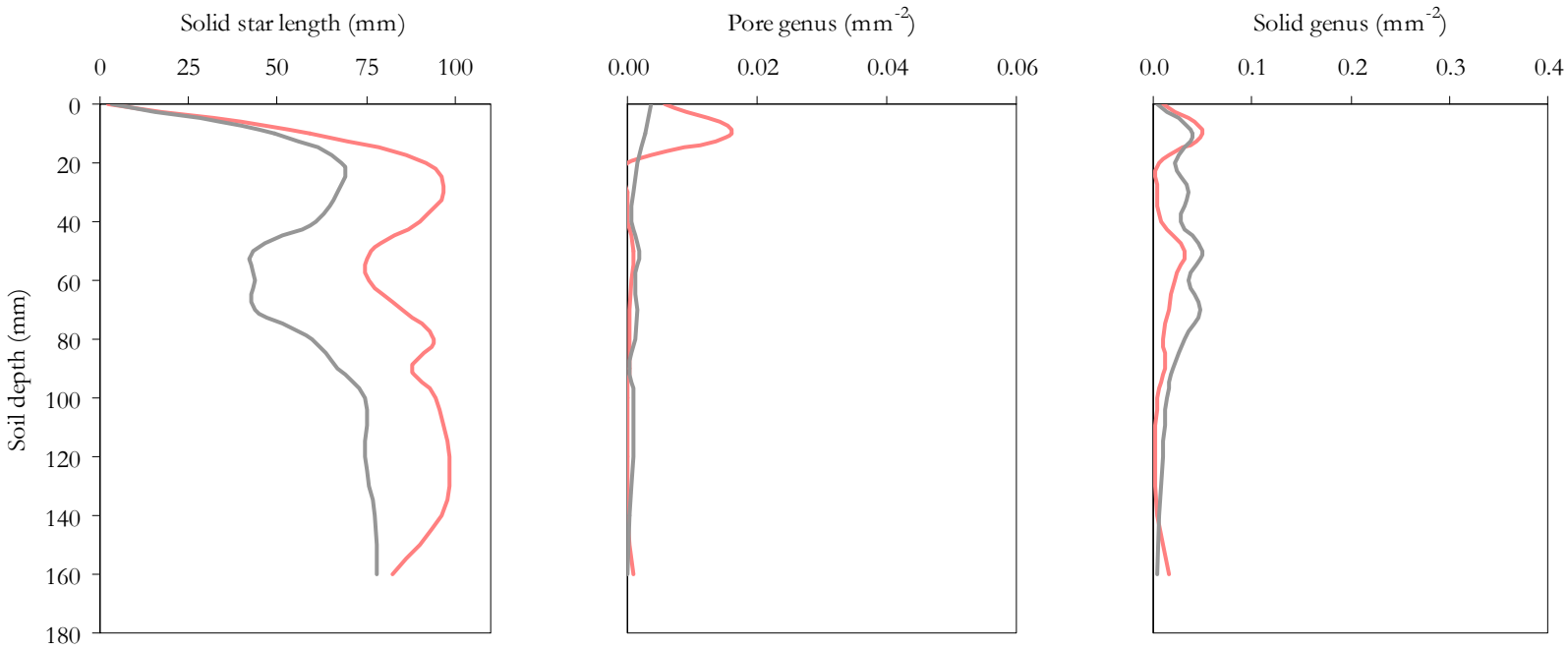

Figure A5.30 Response of selected soil structural parameters (l_s^*, g_p *and* g_s) of soil H002 to two treatments, FW00*i* (—) and T102 (—).

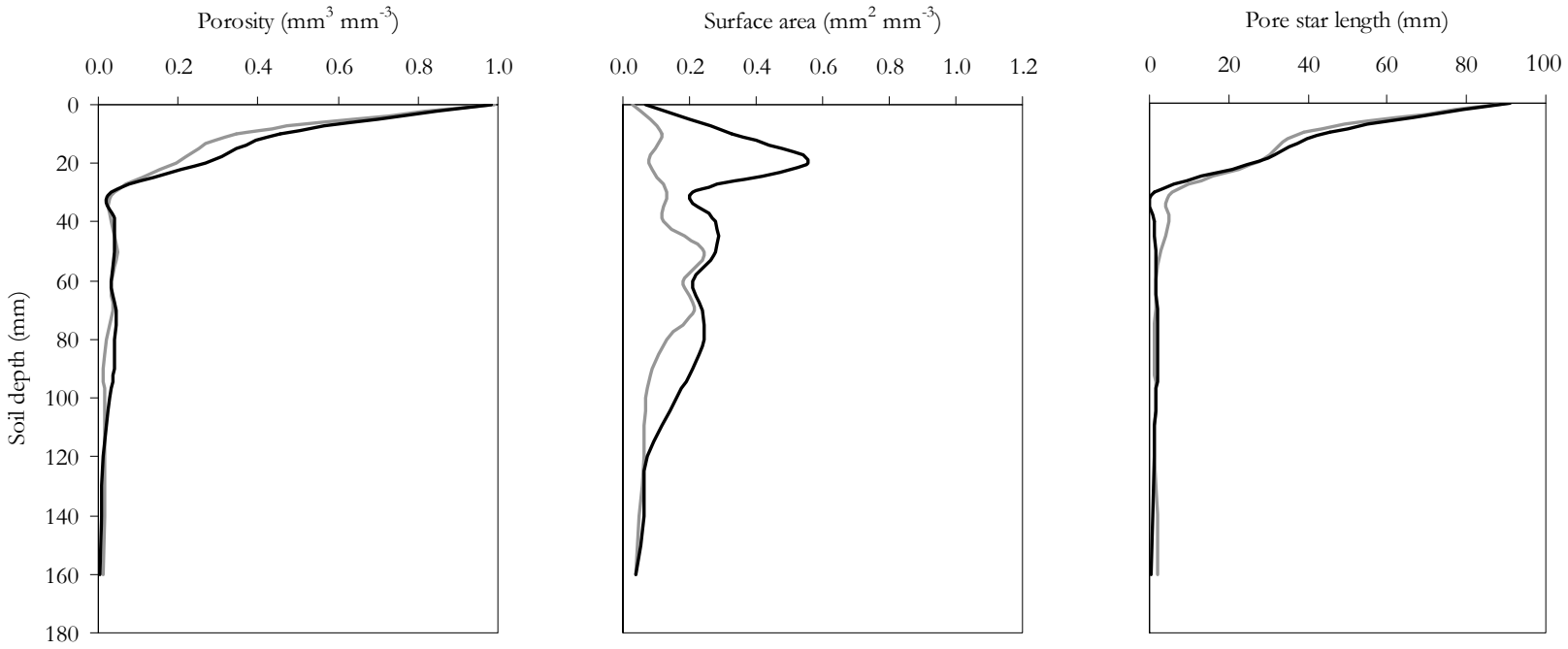

Figure A5.31 Response of selected soil structural parameters (*P, S_v and l_p^**) of soil H002 to two treatments, T102 (—) and T401 (—).

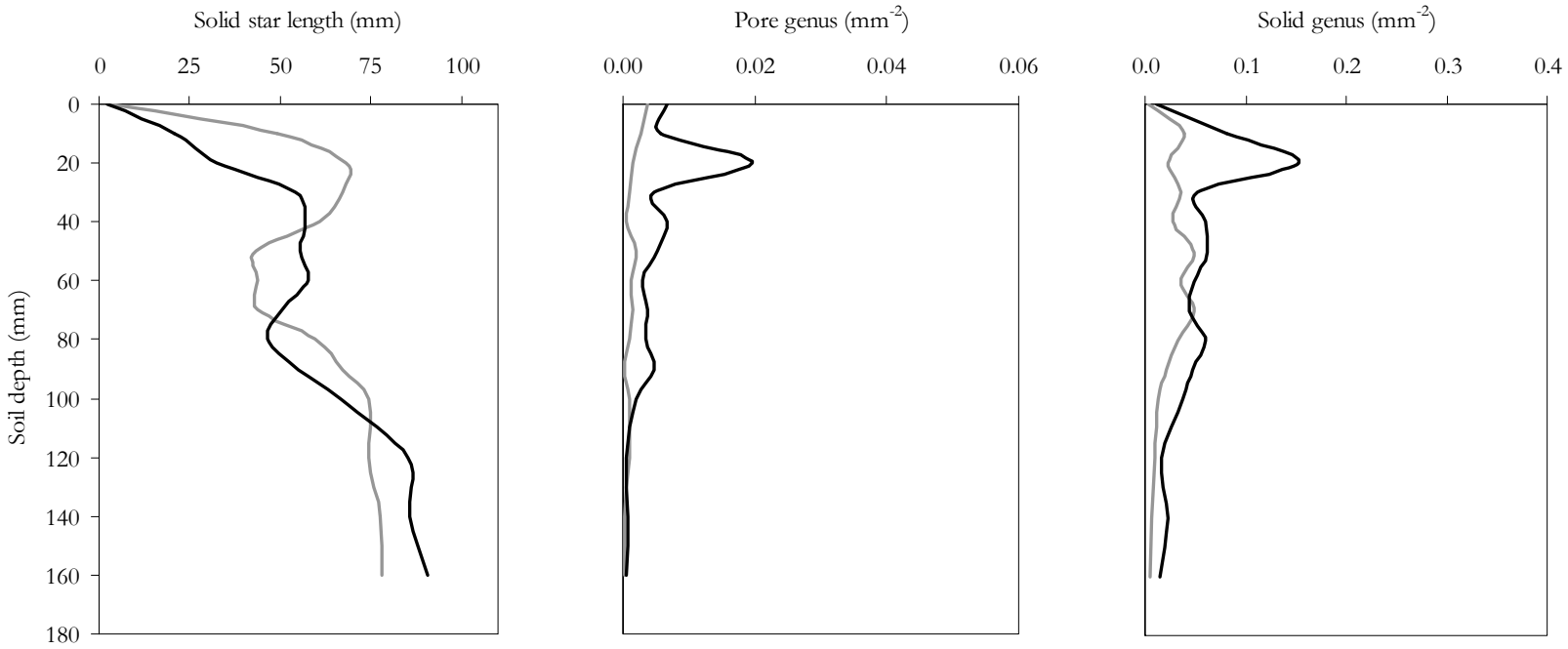

Figure A5.32 Response of selected soil structural parameters (l_s^*, g_p *and* g_s) of soil H002 to two treatments, T102 (—) and T401 (—).

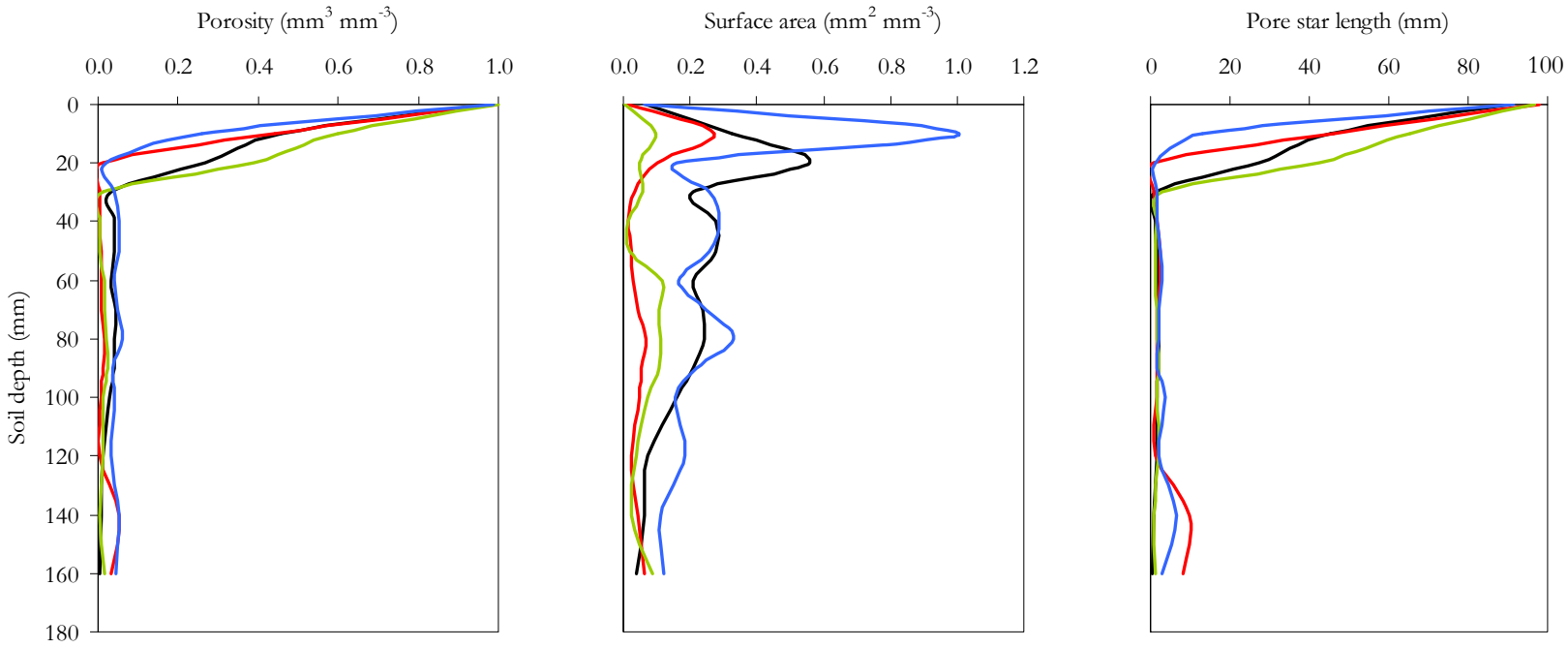

Figure A5.33 Response of selected soil structural parameters (*P, S_v and l_p^**) of soil H002 to four treatments; T401 (—), T402 (—), T403 (—) and T404 (—).

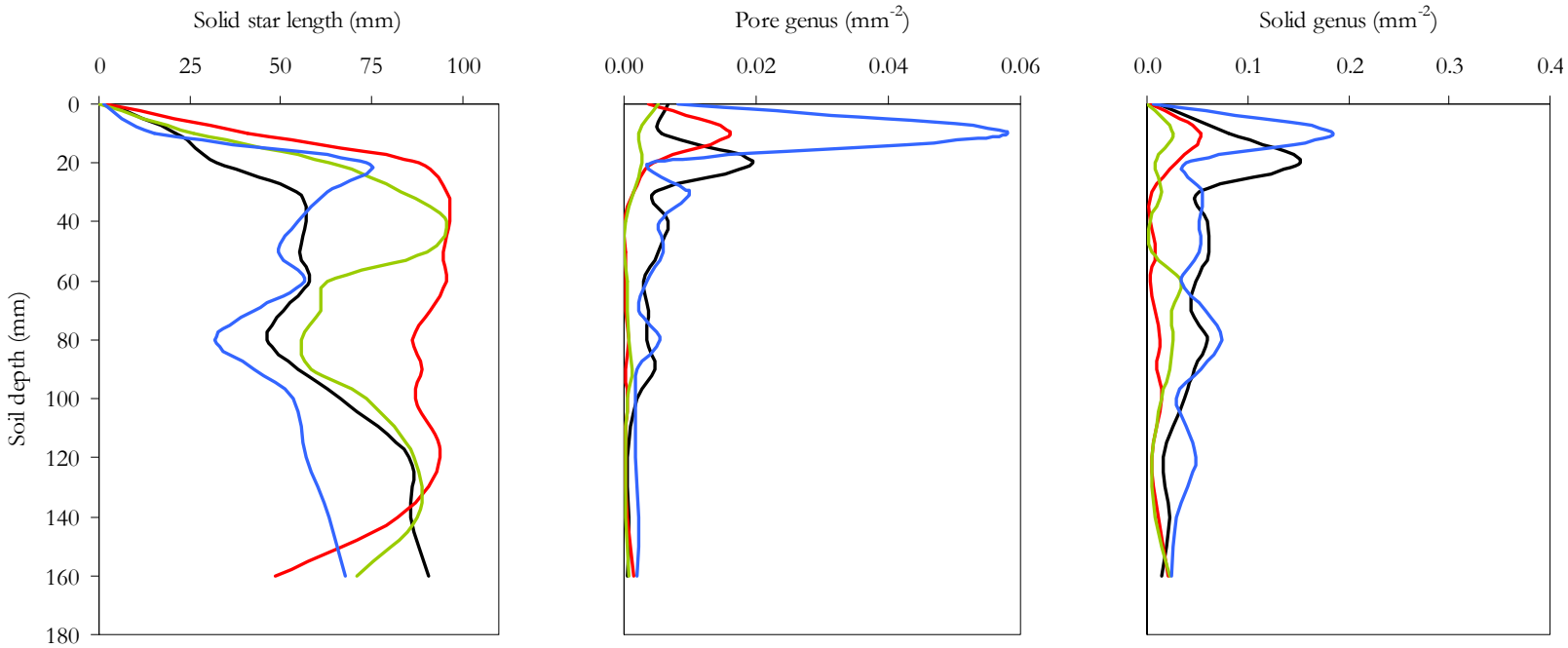

Figure A5.34 Response of selected soil structural parameters (l_s^*, g_p *and* g_s) of soil H002 to four treatments; T401 (—), T402 (—), T403 (—) and T404 (—).

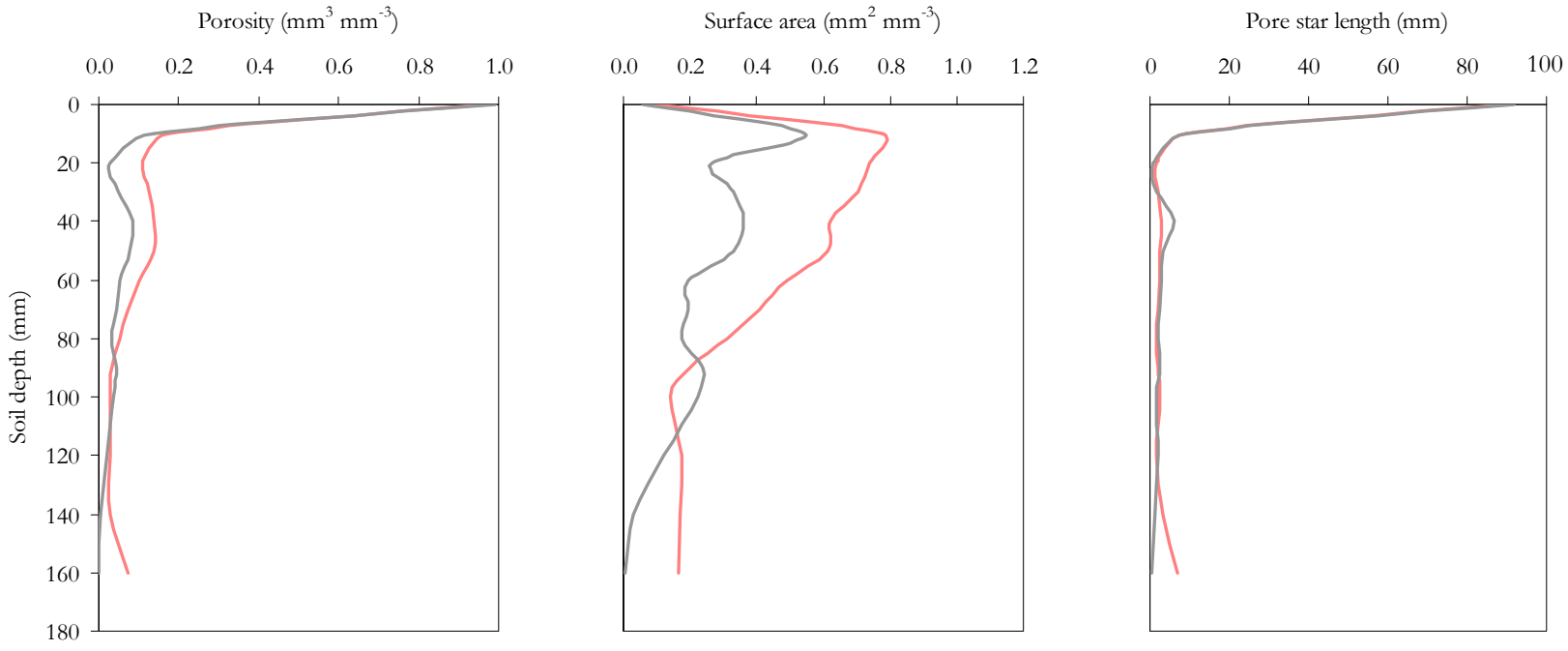

Figure A5.35 Response of selected soil structural parameters (*P, S_v and l_p^**) of soil N001 to two treatments, FW00*i* (—) and T102 (—).

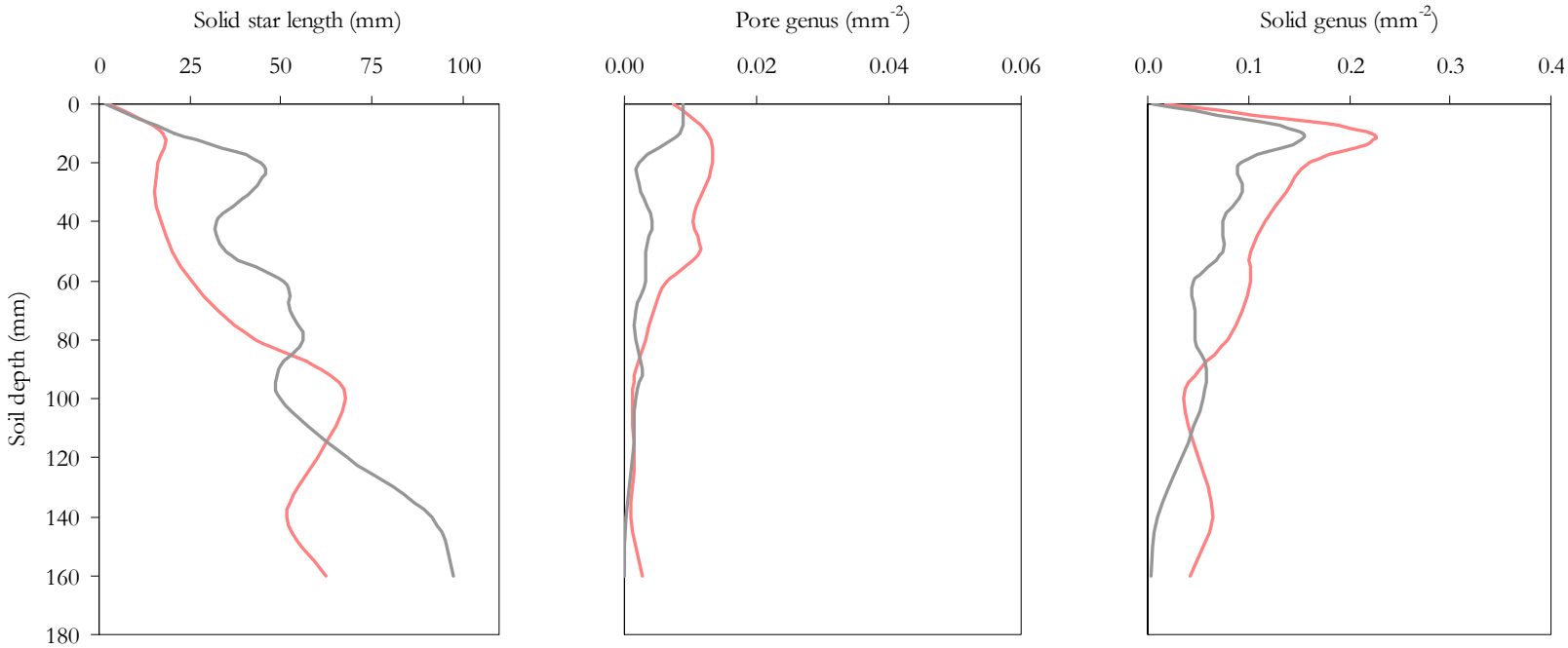

Figure A5.36 Response of selected soil structural parameters (l_s^*, g_p *and* g_s) of soil N001 to two treatments, FW00*i* (—) and T102 (—).

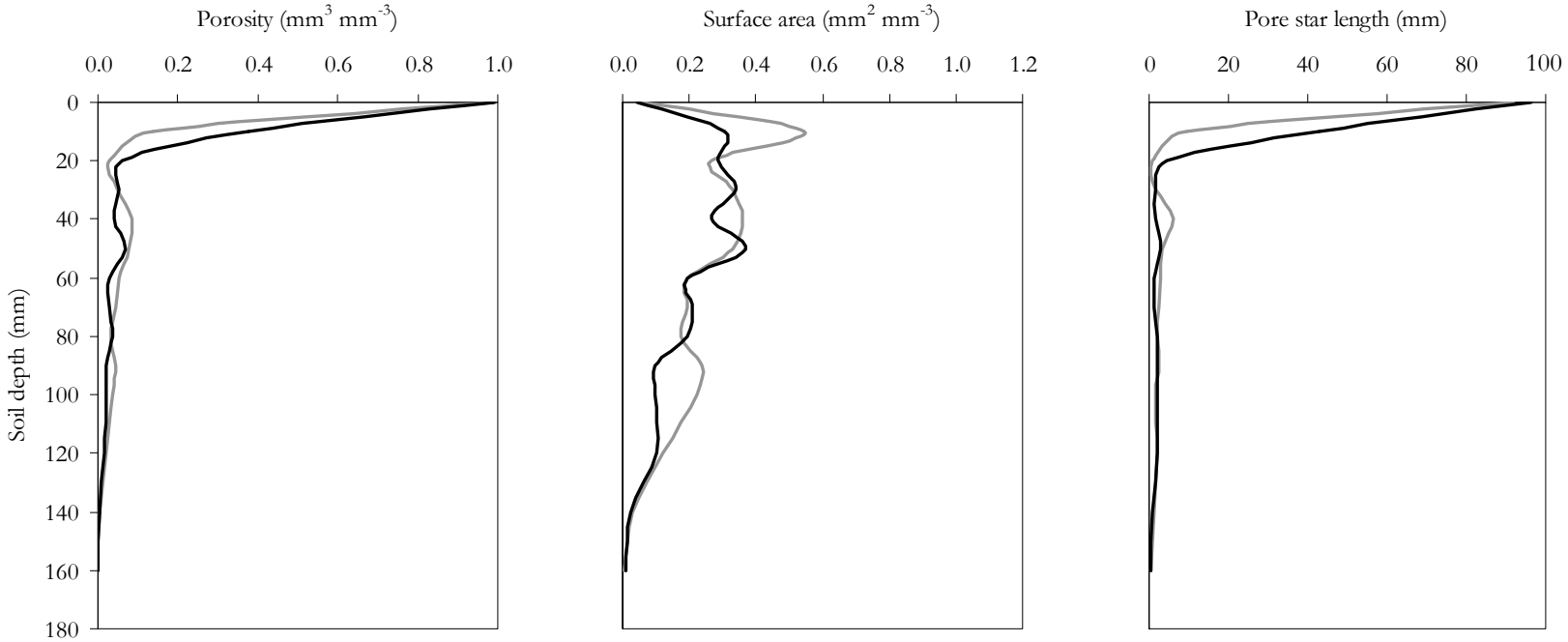

Figure A5.37 Response of selected soil structural parameters (*P, S_v and l_p^**) of soil N001 to two treatments, T102 (—) and T401 (—).

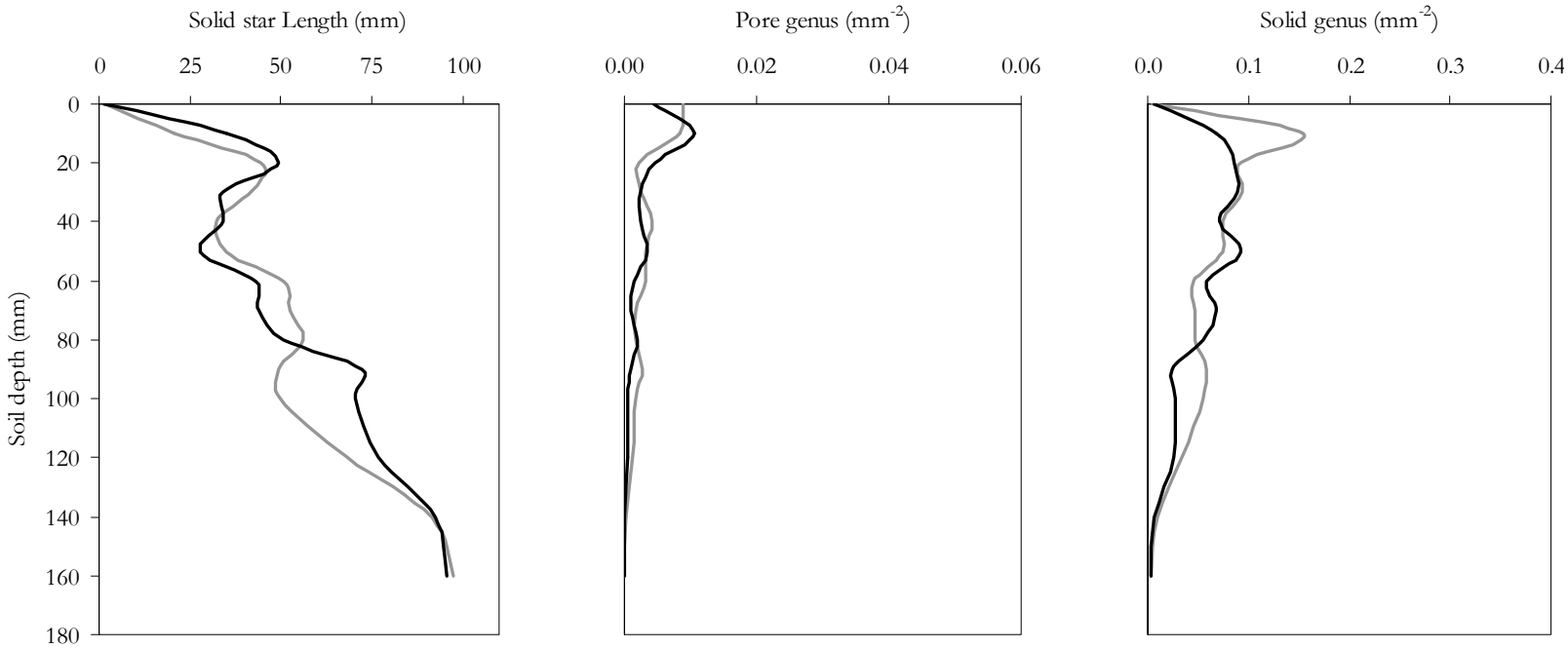

Figure A5.38 Response of selected soil structural parameters (l_s^*, g_p *and* g_s) of soil N001 to two treatments, T102 (—) and T401 (—).

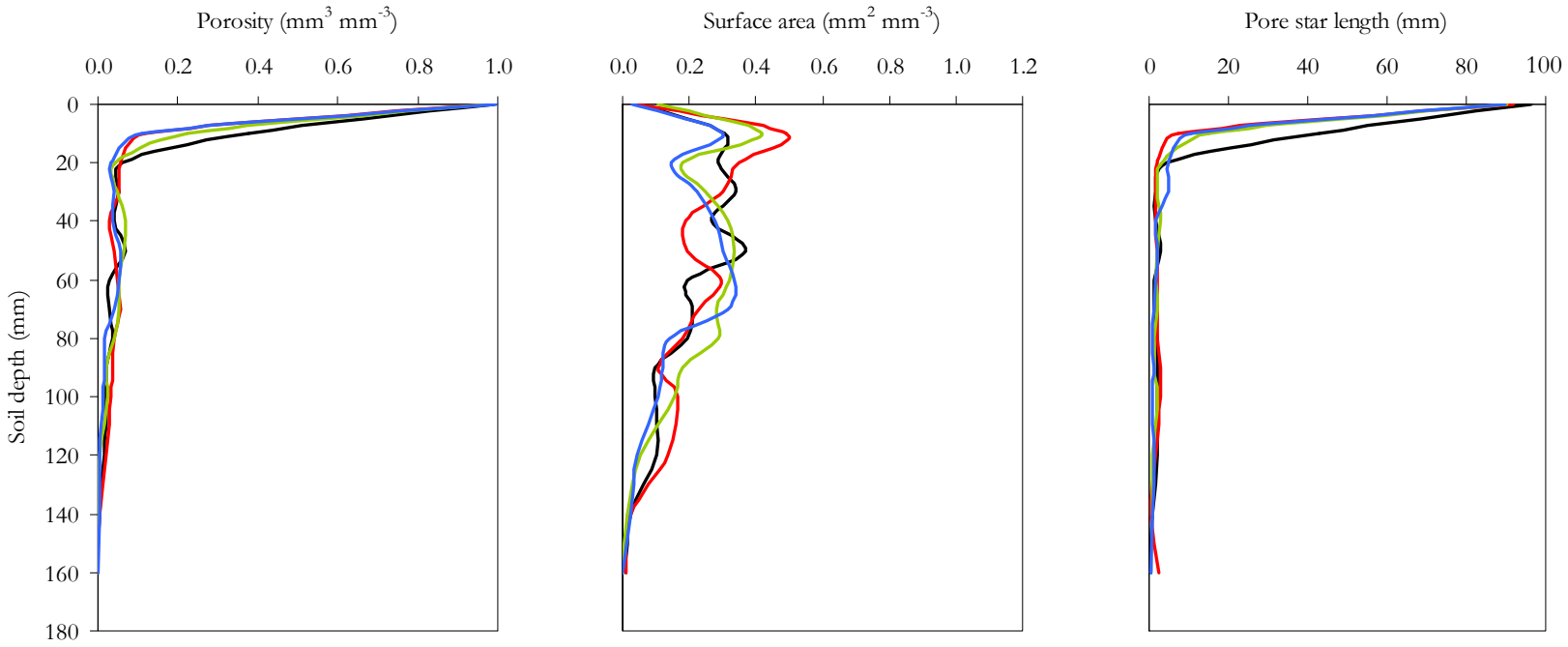

Figure A5.39 Response of selected soil structural parameters (*P, S_v and l_p^**) of soil N001 to four treatments; T401 (—), T402 (—), T403 (—) and T404 (—).

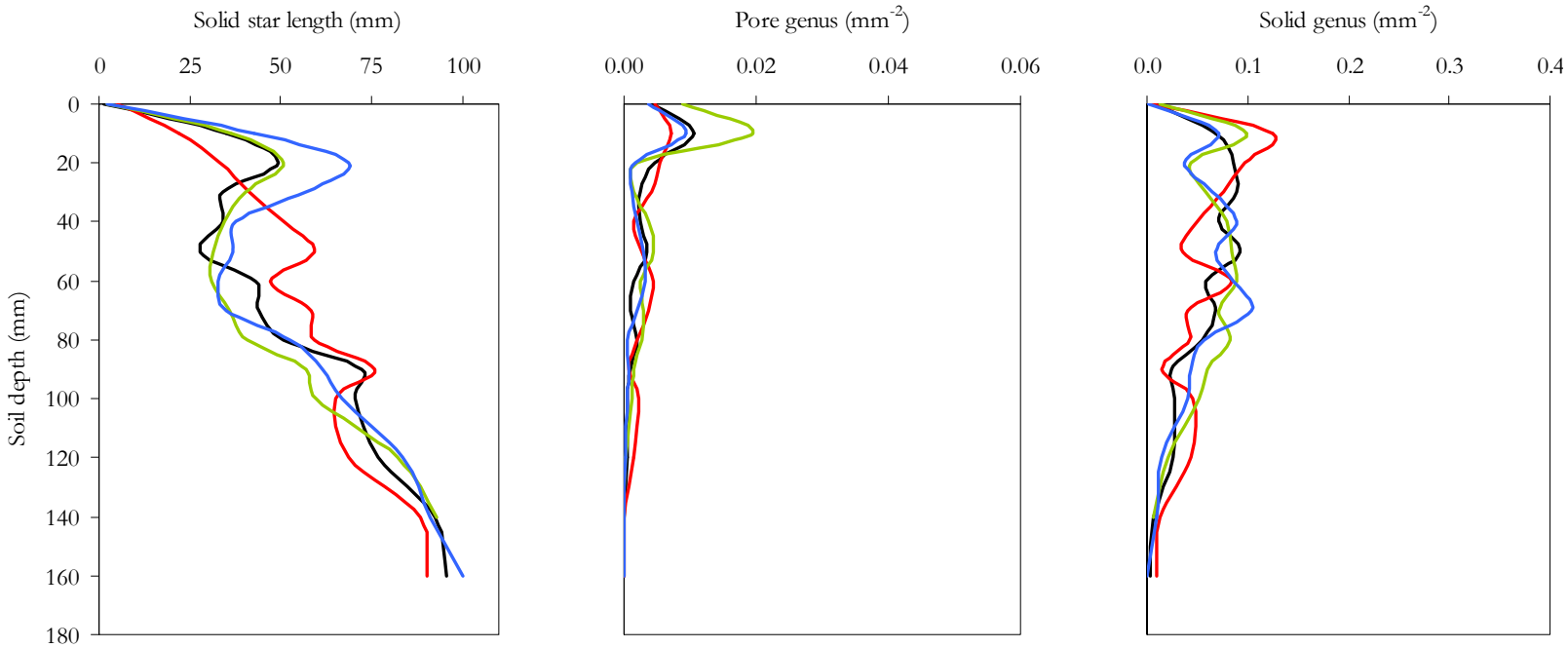

Figure A5.40 Response of selected soil structural parameters (l_s^*, g_p *and* g_s) of soil N001 to four treatments; T401 (—), T402 (—), T403 (—) and T404 (—).

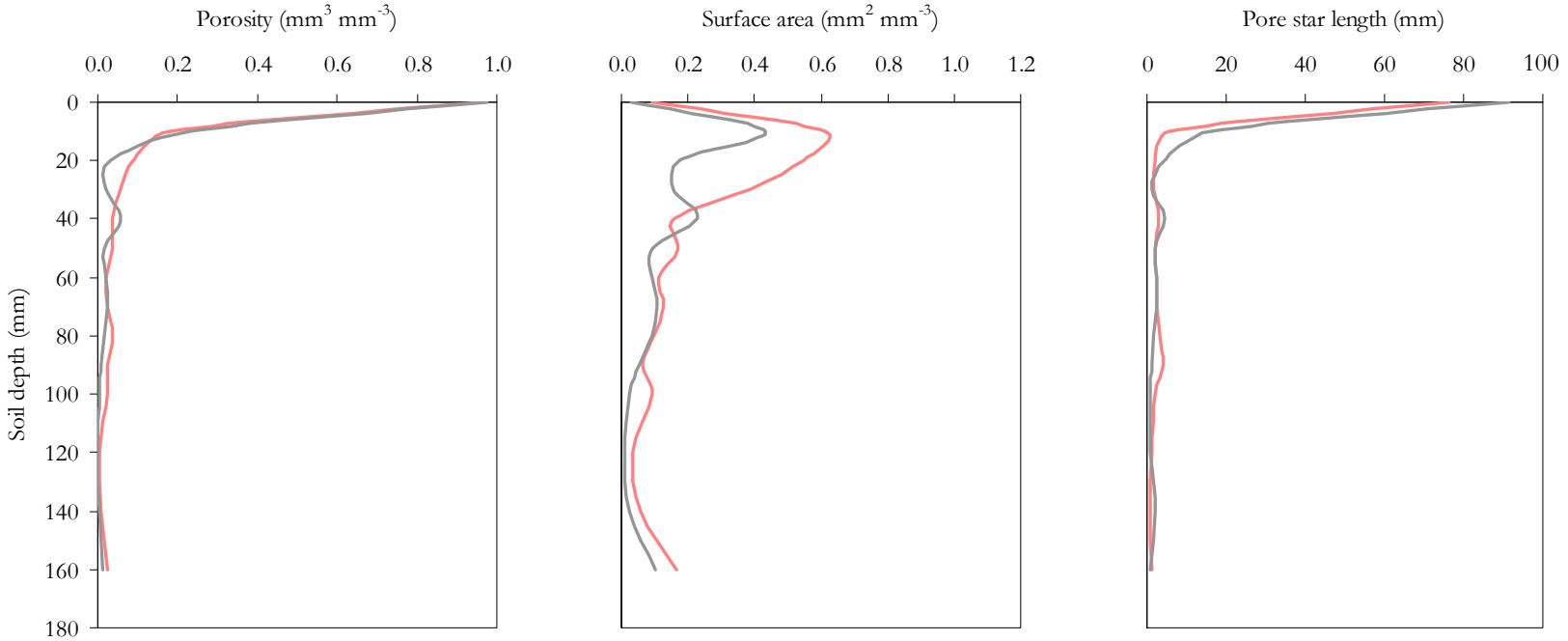

Figure A5.41 Response of selected soil structural parameters (*P, S_v and l_p^**) of soil N002 to two treatments, FW00*i* (—) and T102 (—).

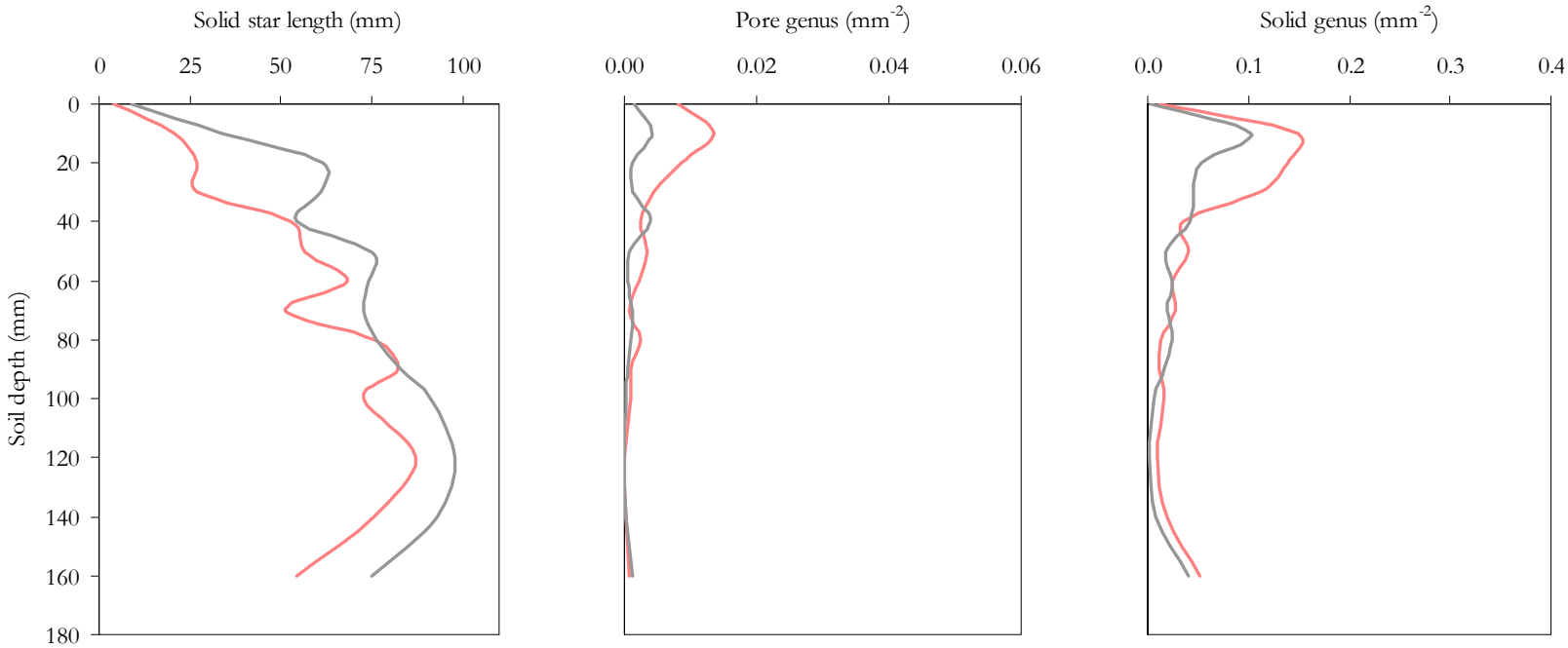

Figure A5.42 Response of selected soil structural parameters (l_s^*, g_p *and* g_s) of soil N002 to two treatments, FW00*i* (—) and T102 (—).

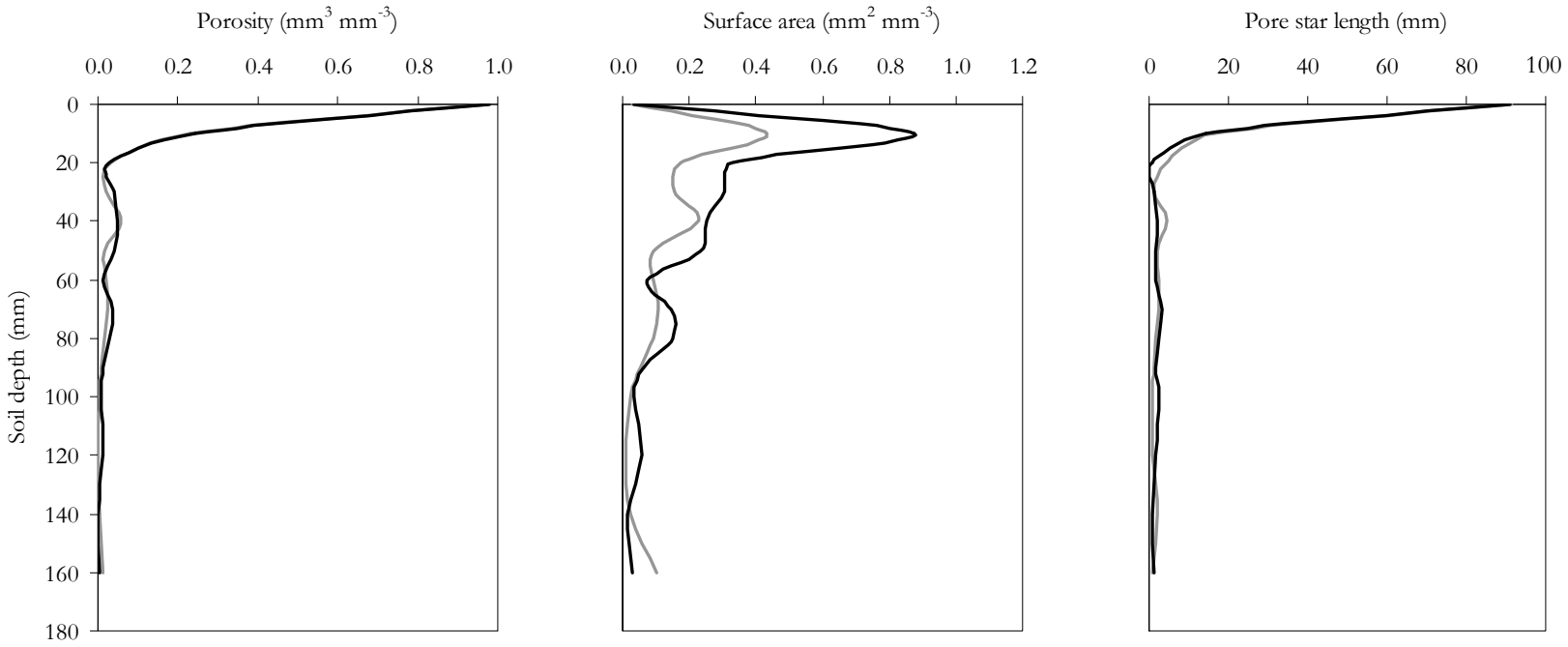

Figure A5.43 Response of selected soil structural parameters (*P, S_v and l_p^**) of soil N002 to two treatments, T102 (▬) and T401 (▬).

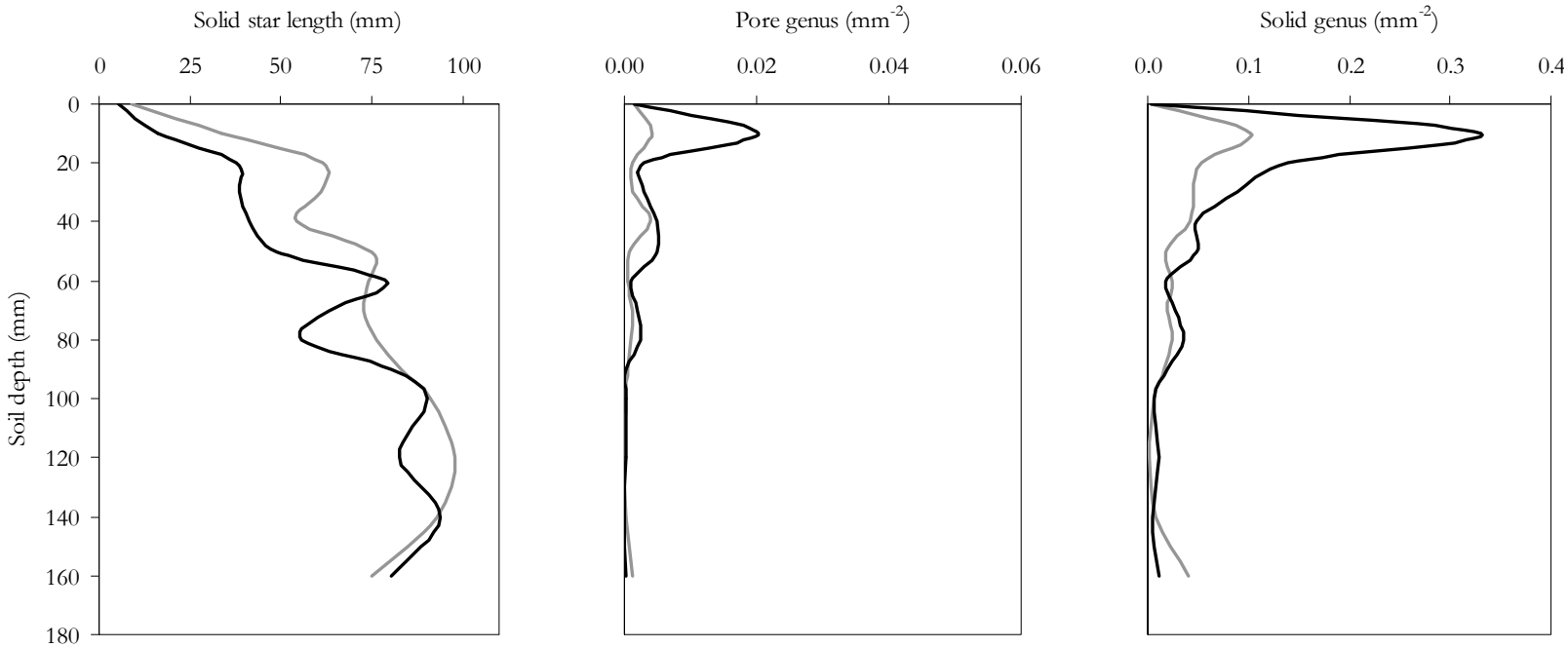

Figure A5.44 Response of selected soil structural parameters (l_s^*, g_p *and* g_s) of soil N002 to two treatments, T102 (—) and T401 (—).

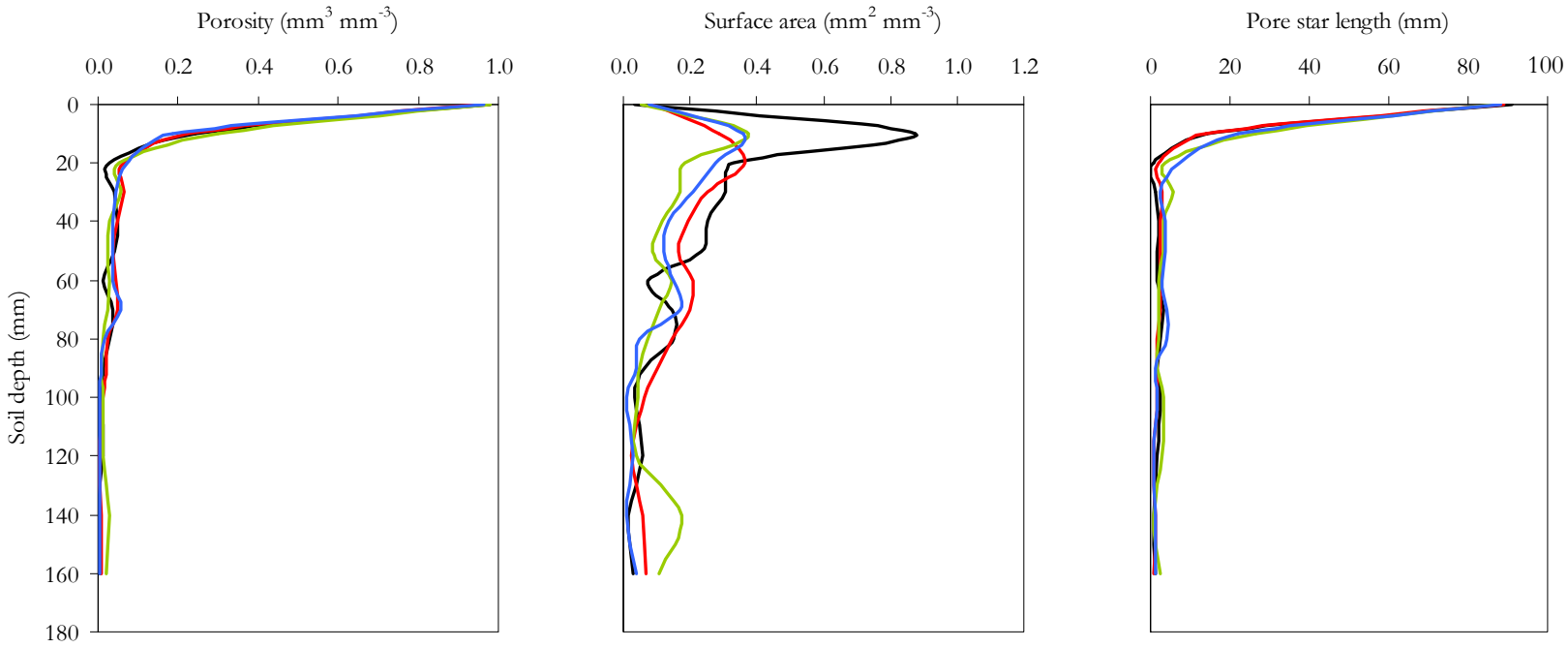

Figure A5.45 Response of selected soil structural parameters (*P, S_v and l_p^**) of soil N002 to four treatments; T401 (—), T402 (—), T403 (—) and T404 (—).

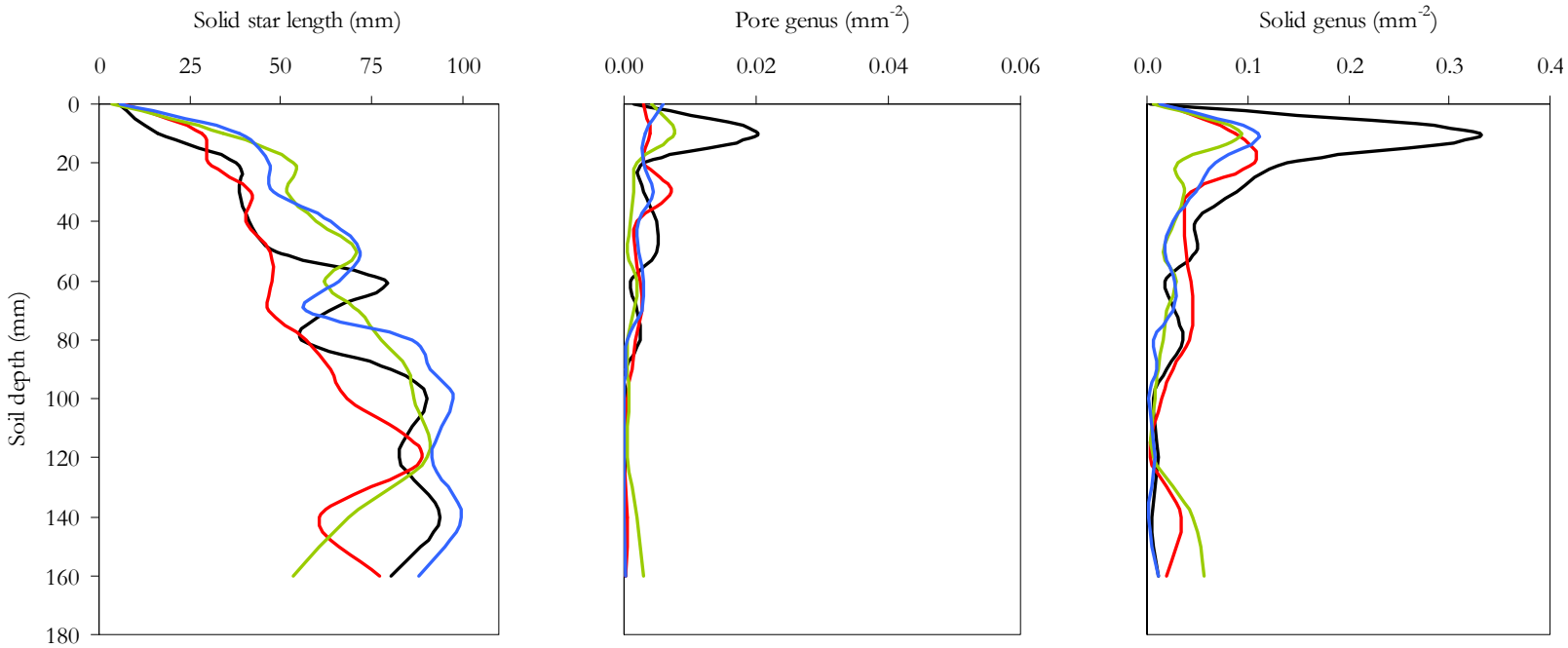

Figure A5.46 Response of selected soil structural parameters (l_s^*, g_p *and* g_s) of soil N002 to four treatments; T401 (—), T402 (—), T403 (—) and T404 (—).

Appendix 5.2: ***The effect of water quality on* P, S_v, l_p^*, l_s^*, g_p *and* g_s *for each of the Vertosols (B00i, G00i, H00i, N00i) at depth intervals of 0–40 mm and 100–160 mm.***

Table A5.1
Mean structural parameters derived using image analysis for sites B001 and B003 (0–40 mm) after laboratory irrigation

	FW00*i*			T102			T401			T402			T403		
				EC 0 dS m⁻¹			*EC 0.5 dS m⁻¹*								
				SAR 0 ((mmol(+) L⁻¹)^1/2)			*SAR 0 ((mmol(+) L⁻¹)^1/2)*			*SAR 7.5 ((mmol(+) L⁻¹)^1/2)*			*SAR 15 ((mmol(+) L⁻¹)^1/2)*		
Site B001															
P **(mm³ mm⁻³)**	0.32	±	0.12	0.51	±	0.13	0.27	±	0.12	0.33	±	0.11	0.28	±	0.12
Sv **(mm² mm⁻³)**	0.36	±	0.07	0.39	±	0.07	0.43	±	0.08	0.61	±	0.14	0.36	±	0.08
l_p^* **(mm)**	23.81	±	11.95	35.17	±	11.52	21.92	±	12.39	22.47	±	12.66	20.33	±	11.99
l_s^* **(mm)**	23.20	±	5.31	13.11	±	2.84	27.47	±	5.43	16.33	±	3.67	26.70	±	7.01
g_P **(×10⁻² mm²)**	0.52	±	0.21	1.68	±	0.79	0.93	±	0.20	2.07	±	0.65	0.91	±	0.24
gs **(×10⁻² mm²)**	7.55	±	1.65	6.77	±	1.81	11.22	±	2.02	11.85	±	2.88	7.10	±	1.44
Site B003															
P **(mm³ mm⁻³)**	0.36	±	0.12	0.42	±	0.14	0.27	±	0.11	0.33	±	0.12	0.36	±	0.13
Sv **(mm² mm⁻³)**	0.54	±	0.10	0.42	±	0.11	0.77	±	0.12	0.54	±	0.09	0.37	±	0.08
l_p^* **(mm)**	28.30	±	12.29	31.04	±	12.87	17.77	±	11.64	25.72	±	12.34	30.81	±	13.16
l_s^* **(mm)**	15.76	±	3.16	19.39	±	6.31	15.14	±	3.18	17.48	±	3.48	19.85	±	4.16
g_P **(×10⁻² mm²)**	0.75	±	0.20	1.11	±	0.43	1.41	±	0.26	1.23	±	0.19	0.64	±	0.13
gs **(×10⁻² mm²)**	13.15*ab*	±	2.37	8.79*b*	±	2.18	19.05*a*	±	3.32	13.03*ab*	±	2.28	9.05*b*	±	2.01

Within rows the letters represent significant difference between mean values for each treatment using the multiple comparison Tukey–Kramer test (P=0.05).

Table A5.2
Mean structural parameters derived using image analysis for sites B001 and B003 (100–160 mm) after laboratory irrigation

	FW00*i*			T102			T401			T402			T403		
				EC 0 dS m⁻¹			*EC 0.5 dS m⁻¹*								
				SAR 0 ((mmol(+) L⁻¹)^1/2)			*SAR 0 ((mmol(+) L⁻¹)^1/2)*			*SAR 7.5 ((mmol(+) L⁻¹)^1/2)*			*SAR 15 ((mmol(+) L⁻¹)^1/2)*		
Site B001															
P **(mm³ mm⁻³)**	0.03	±	0.01	0.01	±	0.00	0.02	±	0.00	0.03	±	0.01	0.04	±	0.01
Sv **(mm² mm⁻³)**	0.14	±	0.05	0.06	±	0.02	0.14	±	0.04	0.16	±	0.05	0.15	±	0.04
l_p^* **(mm)**	2.37	±	0.54	1.35	±	0.25	2.05	±	0.47	1.49	±	0.39	3.01	±	0.73
l_s^* **(mm)**	70.47	±	7.02	88.08	±	4.40	70.37	±	7.45	64.02	±	9.36	64.74	±	9.23
g_p **(×10⁻² mm²)**	0.24	±	0.15	0.03	±	0.01	0.14	±	0.06	0.19	±	0.09	0.35	±	0.11
gs **(×10⁻² mm²)**	3.26	±	0.99	1.45	±	0.64	5.49	±	1.57	5.12	±	1.45	3.98	±	1.42
Site B003															
P **(mm³ mm⁻³)**	0.04*a*	±	0.01	0.01*b*	±	0.00	0.03*ab*	±	0.01	0.03*ab*	±	0.00	0.04*a*	±	0.00
Sv **(mm² mm⁻³)**	0.24*a*	±	0.05	0.09*b*	±	0.02	0.25*a*	±	0.04	0.19*ab*	±	0.04	0.32*a*	±	0.02
l_p^* **(mm)**	1.95	±	0.06	1.58	±	0.45	1.30	±	0.15	1.61	±	0.24	1.21	±	0.12
l_s^* **(mm)**	49.75*b*	±	6.37	81.25*a*	±	3.84	49.19*b*	±	6.24	58.29*b*	±	7.79	39.89*b*	±	2.11
g_p **(×10⁻² mm²)**	0.23*a*	±	0.05	0.05*b*	±	0.02	0.19*ab*	±	0.05	0.18*ab*	±	0.05	0.25*a*	±	0.04
gs **(×10⁻² mm²)**	5.38*bc*	±	1.13	2.65*c*	±	0.82	9.09*ab*	±	1.63	5.80*abc*	±	1.35	10.47*a*	±	0.69

Within rows the letters represent significant difference between mean values for each treatment using the multiple comparison Tukey–Kramer test (P=0.05).

Table A5.3
Mean structural parameters derived using image analysis for sites G001 and G002 (0–40 mm) after laboratory irrigation

	FW00*i*	T102	T401	T402	T403	T404
		EC 0 dS m⁻¹	*EC 0.5 dS m⁻¹*			
		SAR 0 ((mmol(+) L⁻¹)^1/2)	*SAR 0 ((mmol(+) L⁻¹)^1/2)*	*SAR 7.5 ((mmol(+) L⁻¹)^1/2)*	*SAR 15 ((mmol(+) L⁻¹)^1/2)*	*SAR 30 ((mmol(+) L⁻¹)^1/2)*
Site G001						
P **(mm³ mm⁻³)**	0.30 ± 0.12	0.27 ± 0.12	0.31 ± 0.13	0.32 ± 0.12	0.36 ± 0.13	0.36 ± 0.12
Sv **(mm² mm⁻³)**	0.43 ± 0.10	0.33 ± 0.06	0.33 ± 0.09	0.32 ± 0.13	0.29 ± 0.10	0.36 ± 0.08
I_p^* **(mm)**	14.48 ± 9.60	24.18 ± 13.07	27.70 ± 13.44	27.28 ± 12.44	30.13 ± 12.26	27.95 ± 11.51
I_s^* **(mm)**	24.15 ± 4.65	24.30 ± 3.80	31.33 ± 7.01	40.53 ± 11.84	32.99 ± 8.89	20.95 ± 3.84
g_p **(×10⁻² mm²)**	0.69 ± 0.11	0.66 ± 0.24	0.45 ± 0.14	0.71 ± 0.34	0.50 ± 0.16	0.79 ± 0.22
gs **(×10⁻² mm²)**	13.00 ± 3.53	7.95 ± 1.60	10.18 ± 3.03	7.63 ± 2.77	6.31 ± 2.20	7.94 ± 1.85
Site G002						
P **(mm³ mm⁻³)**	0.21 ± 0.13	0.24 ± 0.13	0.22 ± 0.13	0.23 ± 0.13	0.26 ± 0.12	0.27 ± 0.12
Sv **(mm² mm⁻³)**	0.14*b* ± 0.03	0.23*ab* ± 0.09	0.11*b* ± 0.04	0.22*ab* ± 0.04	0.48*a* ± 0.12	0.40*ab* ± 0.08
I_p^* **(mm)**	17.37 ± 10.40	20.72 ± 11.17	19.46 ± 11.85	18.87 ± 11.05	17.93 ± 10.72	20.53 ± 11.46
I_s^* **(mm)**	60.79 ± 11.00	53.53 ± 12.68	58.94 ± 11.16	41.18 ± 7.38	26.43 ± 7.28	23.54 ± 4.76
g_p **(×10⁻² mm²)**	0.42 ± 0.19	0.61 ± 0.28	0.26 ± 0.09	0.48 ± 0.14	0.64 ± 0.22	1.17 ± 0.31
gs **(×10⁻² mm²)**	4.06*b* ± 1.00	6.39*ab* ± 2.42	3.79*b* ± 1.19	6.87*ab* ± 1.50	13.98*a* ± 3.34	8.74*ab* ± 1.50

Within rows the letters represent significant difference between mean values for each treatment using the multiple comparison Tukey–Kramer test (P=0.05).

Table A5.4
Mean structural parameters derived using image analysis for sites G001 and G002 (100–160 mm) after laboratory irrigation

	FW00*i*	T102	T401	T402	T403	T404
		EC 0 dS m⁻¹	*EC 0.5 dS m⁻¹*			
		SAR 0 ((mmol(+) L⁻¹)^1/2)	*SAR 0 ((mmol(+) L⁻¹)^1/2)*	*SAR 7.5 ((mmol(+) L⁻¹)^1/2)*	*SAR 15 ((mmol(+) L⁻¹)^1/2)*	*SAR 30 ((mmol(+) L⁻¹)^1/2)*
Site G001						
P **(mm³ mm⁻³)**	0.03 ± 0.01	0.02 ± 0.00	0.04 ± 0.01	0.04 ± 0.02	0.02 ± 0.01	0.01 ± 0.00
Sv **(mm² mm⁻³)**	0.11*ab* ± 0.01	0.08*b* ± 0.02	0.19*a* ± 0.03	0.12*ab* ± 0.03	0.08*b* ± 0.02	0.05*b* ± 0.02
l_p^* **(mm)**	4.60*a* ± 0.75	2.79*ab* ± 0.39	1.89*ab* ± 0.28	3.39*ab* ± 1.22	2.55*ab* ± 0.75	1.53*b* ± 0.19
l_s^* **(mm)**	64.44*ab* ± 2.77	71.45*a* ± 5.80	48.02*b* ± 4.28	64.62*ab* ± 7.39	74.78*a* ± 5.36	84.66*a* ± 5.84
g_p **(×10⁻² mm²)**	0.11 ± 0.03	0.06 ± 0.02	0.15 ± 0.04	0.13 ± 0.06	0.06 ± 0.02	0.03 ± 0.02
gs **(×10⁻² mm²)**	2.18*b* ± 0.31	1.66*b* ± 0.28	4.91*a* ± 0.67	2.71*ab* ± 0.70	2.19*b* ± 0.38	1.58*b* ± 0.78
Site G002						
P **(mm³ mm⁻³)**	0.01 ± 0.00	0.01 ± 0.00	0.00 ± 0.00	0.00 ± 0.00	0.01 ± 0.01	0.01 ± 0.00
Sv **(mm² mm⁻³)**	0.07 ± 0.03	0.05 ± 0.02	0.04 ± 0.02	0.02 ± 0.01	0.05 ± 0.02	0.05 ± 0.01
l_p^* **(mm)**	0.54 ± 0.09	1.09 ± 0.21	0.87 ± 0.10	0.75 ± 0.17	1.91 ± 0.94	1.06 ± 0.19
l_s^* **(mm)**	81.29 ± 7.11	88.23 ± 4.26	91.66 ± 3.09	92.74 ± 3.29	83.37 ± 7.01	86.93 ± 4.00
g_p **(×10⁻² mm²)**	0.03 ± 0.02	0.05 ± 0.03	0.02 ± 0.01	0.01 ± 0.01	0.04 ± 0.02	0.03 ± 0.01
gs **(×10⁻² mm²)**	2.64 ± 1.05	1.19 ± 0.46	1.17 ± 0.43	0.79 ± 0.40	1.44 ± 0.41	1.72 ± 0.49

Within rows the letters represent significant difference between mean values for each treatment using the multiple comparison Tukey–Kramer test (P=0.05).

Table A5.5
Mean structural parameters derived using image analysis for sites H001 and H002 (0–40 mm) after laboratory irrigation

	FW00*i*			T102			T401			T402			T403			T404		
				EC 0 dS m⁻¹			*EC 0.5 dS m⁻¹*											
				SAR 0 ((mmol(+) L⁻¹)^1/2)			*SAR 0 ((mmol(+) L⁻¹)^1/2)*			*SAR 7.5 ((mmol(+) L⁻¹)^1/2)*			*SAR 15 ((mmol(+) L⁻¹)^1/2)*			*SAR 30 ((mmol(+) L⁻¹)^1/2)*		
Site H001																		
P **(mm³ mm⁻³)**	0.32	±	0.13	0.28	±	0.12	0.29	±	0.12	0.41	±	0.13	0.24	±	0.13	0.29	±	0.13
Sv **(mm² mm⁻³)**	0.24*ab*	±	0.06	0.19*ab*	±	0.07	0.40*a*	±	0.13	0.14*ab*	±	0.06	0.07*b*	±	0.04	0.12*ab*	±	0.04
l_p^* **(mm)**	29.57	±	13.50	16.43	±	10.09	16.66	±	10.21	43.65	±	12.83	22.46	±	12.24	27.80	±	12.55
l_s^* **(mm)**	31.78	±	7.76	47.56	±	10.39	35.32	±	7.78	41.82	±	10.19	60.75	±	12.12	55.41	±	10.92
g_p **(×10⁻² mm²)**	0.51	±	0.20	0.27	±	0.09	1.60	±	0.66	0.29	±	0.10	0.19	±	0.15	0.65	±	0.44
gs **(×10⁻² mm²)**	5.90*ab*	±	1.39	4.78*ab*	±	2.29	10.19*a*	±	3.33	2.85*ab*	±	1.10	3.08*ab*	±	1.18	2.47*b*	±	0.80
Site H002																		
P **(mm³ mm⁻³)**	0.23	±	0.13	0.32	±	0.13	0.36	±	0.13	0.29	±	0.13	0.40	±	0.15	0.27	±	0.12
Sv **(mm² mm⁻³)**	0.07*b*	±	0.03	0.10*b*	±	0.02	0.29*ab*	±	0.07	0.09*b*	±	0.04	0.04*b*	±	0.02	0.36*a*	±	0.12
l_p^* **(mm)**	23.34	±	12.39	33.83	±	12.64	33.20	±	13.57	21.91	±	12.34	41.69	±	14.53	21.80	±	11.87
l_s^* **(mm)**	68.10	±	11.84	49.65	±	8.73	33.37	±	8.03	71.47	±	11.96	53.65	±	13.42	41.53	±	9.93
g_p **(×10⁻² mm²)**	0.44*ab*	±	0.23	0.19*b*	±	0.04	0.86*ab*	±	0.29	0.53*ab*	±	0.26	0.24*b*	±	0.11	1.72*a*	±	0.71
gs **(×10⁻² mm²)**	1.58*bc*	±	0.63	2.58*abc*	±	0.66	7.17*a*	±	1.94	2.03*abc*	±	1.04	1.04*c*	±	0.53	6.74*ab*	±	2.13

Within rows the letters represent significant difference between mean values for each treatment using the multiple comparison Tukey–Kramer test (P=0.05).

Table A5.6
Mean structural parameters derived using image analysis for sites H001 and H002 (100–160 mm) after laboratory irrigation

	FW00*i*	T102	T401	T402	T403	T404
		EC 0 dS m⁻¹	*EC 0.5 dS m⁻¹*			
		SAR 0 ((mmol(+) L⁻¹)^1/2)	*SAR 0 ((mmol(+) L⁻¹)^1/2)*	*SAR 7.5 ((mmol(+) L⁻¹)^1/2)*	*SAR 15 ((mmol(+) L⁻¹)^1/2)*	*SAR 30 ((mmol(+) L⁻¹)^1/2)*
Site H001						
P **(mm³ mm⁻³)**	0.02*b* ± 0.01	0.05*a* ± 0.01	0.02*ab* ± 0.01	0.03*ab* ± 0.01	0.00*b* ± 0.00	0.01*b* ± 0.00
Sv **(mm² mm⁻³)**	0.07*ab* ± 0.02	0.13*a* ± 0.01	0.14*a* ± 0.03	0.09*ab* ± 0.02	0.01*b* ± 0.00	0.03*b* ± 0.02
l_p^* **(mm)**	2.27*ab* ± 1.22	4.21*a* ± 0.80	1.79*ab* ± 0.18	3.49*ab* ± 0.52	1.22*b* ± 0.27	1.58*ab* ± 0.39
l_s^* **(mm)**	78.54*ab* ± 6.53	54.02*c* ± 5.21	62.47*bc* ± 5.95	76.71*abc* ± 6.82	97.10*a* ± 0.88	84.05*ab* ± 6.95
g_p **(×10⁻² mm²)**	0.08 ± 0.04	0.17 ± 0.04	0.14 ± 0.05	0.17 ± 0.06	0.00 ± 0.00	0.02 ± 0.02
gs **(×10⁻² mm²)**	1.87*ab* ± 0.58	2.18*ab* ± 0.13	3.71*a* ± 0.74	1.77*ab* ± 0.41	0.34*b* ± 0.07	1.14*b* ± 0.43
Site H002						
P **(mm³ mm⁻³)**	0.01*b* ± 0.00	0.02*ab* ± 0.01	0.01*ab* ± 0.00	0.02*ab* ± 0.01	0.01*ab* ± 0.00	0.04*a* ± 0.01
Sv **(mm² mm⁻³)**	0.02*b* ± 0.01	0.06*b* ± 0.02	0.08*ab* ± 0.02	0.05*b* ± 0.02	0.05*b* ± 0.02	0.14*a* ± 0.03
l_p^* **(mm)**	1.26 ± 0.56	1.84 ± 0.50	1.18 ± 0.25	4.67 ± 2.64	1.43 ± 0.23	3.83 ± 1.33
l_s^* **(mm)**	92.94*a* ± 4.16	76.17*ab* ± 8.35	81.96*ab* ± 4.53	82.06*ab* ± 7.04	79.71*ab* ± 5.91	60.43*b* ± 5.29
g_p **(×10⁻² mm²)**	0.03*b* ± 0.02	0.06*b* ± 0.03	0.10*ab* ± 0.03	0.06*ab* ± 0.02	0.04*b* ± 0.02	0.19*a* ± 0.05
gs **(×10⁻² mm²)**	0.65*b* ± 0.34	0.84*b* ± 0.30	2.29*ab* ± 0.64	1.14*b* ± 0.32	1.25*b* ± 0.39	3.31*a* ± 0.60

Within rows the letters represent significant difference between mean values for each treatment using the multiple comparison Tukey–Kramer test (P=0.05).

Table A5.7
Mean structural parameters derived using image analysis for sites N001 and N002 (0–40 mm) after laboratory irrigation

	FW00*i*	T102	T401	T402	T403	T404
		EC 0 dS m⁻¹	*EC 0.5 dS m⁻¹*			
		SAR 0 ((mmol(+) L⁻¹)^1/2)	*SAR 0 ((mmol(+) L⁻¹)^1/2)*	*SAR 7.5 ((mmol(+) L⁻¹)^1/2)*	*SAR 15 ((mmol(+) L⁻¹)^1/2)*	*SAR 30 ((mmol(+) L⁻¹)^1/2)*
Site N001						
P **(mm³ mm⁻³)**	0.30 ± 0.11	0.26 ± 0.12	0.30 ± 0.12	0.25 ± 0.12	0.27 ± 0.12	0.24 ± 0.13
Sv **(mm² mm⁻³)**	0.59*a* ± 0.09	0.31*b* ± 0.06	0.25*b* ± 0.04	0.27*b* ± 0.07	0.25*b* ± 0.05	0.20*b* ± 0.05
I_p^* **(mm)**	21.07 ± 11.56	21.92 ± 11.73	29.35 ± 12.33	20.90 ± 11.91	22.78 ± 11.42	22.34 ± 11.35
I_s^* **(mm)**	13.67*b* ± 1.91	28.22*ab* ± 6.45	30.81*ab* ± 5.76	30.43*ab* ± 6.26	32.77*ab* ± 6.99	41.59*a* ± 9.95
g_p **(×10⁻² mm²)**	1.11*a* ± 0.15	0.52*ab* ± 0.15	0.49*ab* ± 0.15	0.46*ab* ± 0.12	0.71*ab* ± 0.31	0.36*b* ± 0.11
gs **(×10⁻² mm²)**	13.05*a* ± 2.24	8.42*ab* ± 1.86	6.38*ab* ± 1.15	7.06*ab* ± 1.54	5.89*b* ± 1.37	5.26*b* ± 1.49
Site N002						
P **(mm³ mm⁻³)**	0.27 ± 0.12	0.26 ± 0.12	0.27 ± 0.12	0.27 ± 0.12	0.28 ± 0.12	0.26 ± 0.12
Sv **(mm² mm⁻³)**	0.36 ± 0.07	0.20 ± 0.07	0.36 ± 0.11	0.24 ± 0.04	0.18 ± 0.06	0.21 ± 0.05
I_p^* **(mm)**	17.65 ± 9.91	23.64 ± 11.66	21.87 ± 11.83	22.08 ± 11.48	25.23 ± 10.98	24.72 ± 11.19
I_s^* **(mm)**	26.31 ± 5.33	43.97 ± 9.93	27.85 ± 5.35	29.47 ± 4.73	40.40 ± 8.14	40.45 ± 6.70
g_p **(×10⁻² mm²)**	0.75 ± 0.18	0.24 ± 0.06	0.64 ± 0.24	0.39 ± 0.11	0.33 ± 0.11	0.37 ± 0.06
gs **(×10⁻² mm²)**	8.93 ± 2.04	4.97 ± 1.63	12.22 ± 4.30	5.79 ± 1.52	3.94 ± 1.54	5.28 ± 1.84

Within rows the letters represent significant difference between mean values for each treatment using the multiple comparison Tukey–Kramer test (P=0.05).

Table A5.8
Mean structural parameters derived using image analysis for sites N001 and N002 (100–160 mm) after laboratory irrigation

	FW00*i*			T102			T401			T402			T403			T404		
				EC 0 dS m⁻¹			*EC 0.5 dS m⁻¹*											
				SAR 0 ((mmol(+) L⁻¹)^1/2)			*SAR 0 ((mmol(+) L⁻¹)^1/2)*			*SAR 7.5 ((mmol(+) L⁻¹)^1/2)*			*SAR 15 ((mmol(+) L⁻¹)^1/2)*			*SAR 30 ((mmol(+) L⁻¹)^1/2)*		
Site N001																		
P **(mm³ mm⁻³)**	0.04*a*	±	0.02	0.02*ab*	±	0.01	0.01*ab*	±	0.00	0.01*ab*	±	0.01	0.01*ab*	±	0.00	0.01*b*	±	0.00
Sv **(mm² mm⁻³)**	0.16	±	0.04	0.09	±	0.03	0.06	±	0.02	0.08	±	0.03	0.06	±	0.02	0.04	±	0.02
l_p^* **(mm)**	3.52	±	1.47	1.31	±	0.26	1.37	±	0.28	1.73	±	0.39	1.28	±	0.29	0.89	±	0.12
l_s^* **(mm)**	60.53	±	6.85	76.74	±	7.57	83.81	±	4.28	76.43	±	7.97	78.40	±	7.34	83.26	±	5.61
g_p **(×10⁻² mm²)**	0.16	±	0.06	0.08	±	0.03	0.03	±	0.01	0.11	±	0.05	0.05	±	0.03	0.02	±	0.01
gs **(×10⁻² mm²)**	4.80	±	0.91	2.54	±	0.83	1.57	±	0.44	3.03	±	1.15	2.66	±	0.87	1.85	±	0.77
Site N002																		
P **(mm³ mm⁻³)**	0.01	±	0.01	0.01	±	0.00	0.01	±	0.00	0.01	±	0.00	0.02	±	0.01	0.00	±	0.00
Sv **(mm² mm⁻³)**	0.09	±	0.03	0.04	±	0.02	0.03	±	0.01	0.05	±	0.02	0.09	±	0.04	0.02	±	0.01
l_p^* **(mm)**	1.35	±	0.25	1.06	±	0.28	1.57	±	0.44	1.08	±	0.34	2.41	±	0.51	1.15	±	0.34
l_s^* **(mm)**	72.28	±	8.54	88.75	±	6.27	86.73	±	4.14	75.50	±	7.16	77.75	±	8.62	94.17	±	2.81
g_p **(×10⁻² mm²)**	0.05	±	0.03	0.05	±	0.04	0.02	±	0.01	0.04	±	0.02	0.13	±	0.06	0.01	±	0.01
gs **(×10⁻² mm²)**	2.47	±	0.89	1.51	±	1.11	0.84	±	0.24	1.59	±	0.59	2.57	±	1.25	0.57	±	0.23

Within rows the letters represent significant difference between mean values for each treatment using the multiple comparison Tukey–Kramer test (P=0.05).

Appendix 5.3: **The effect of water quality on the pore sieve distributions for each of the Vertosols (B00*i*, G00*i*, H00*i*, N00*i*) at the 50–90 mm depth.**

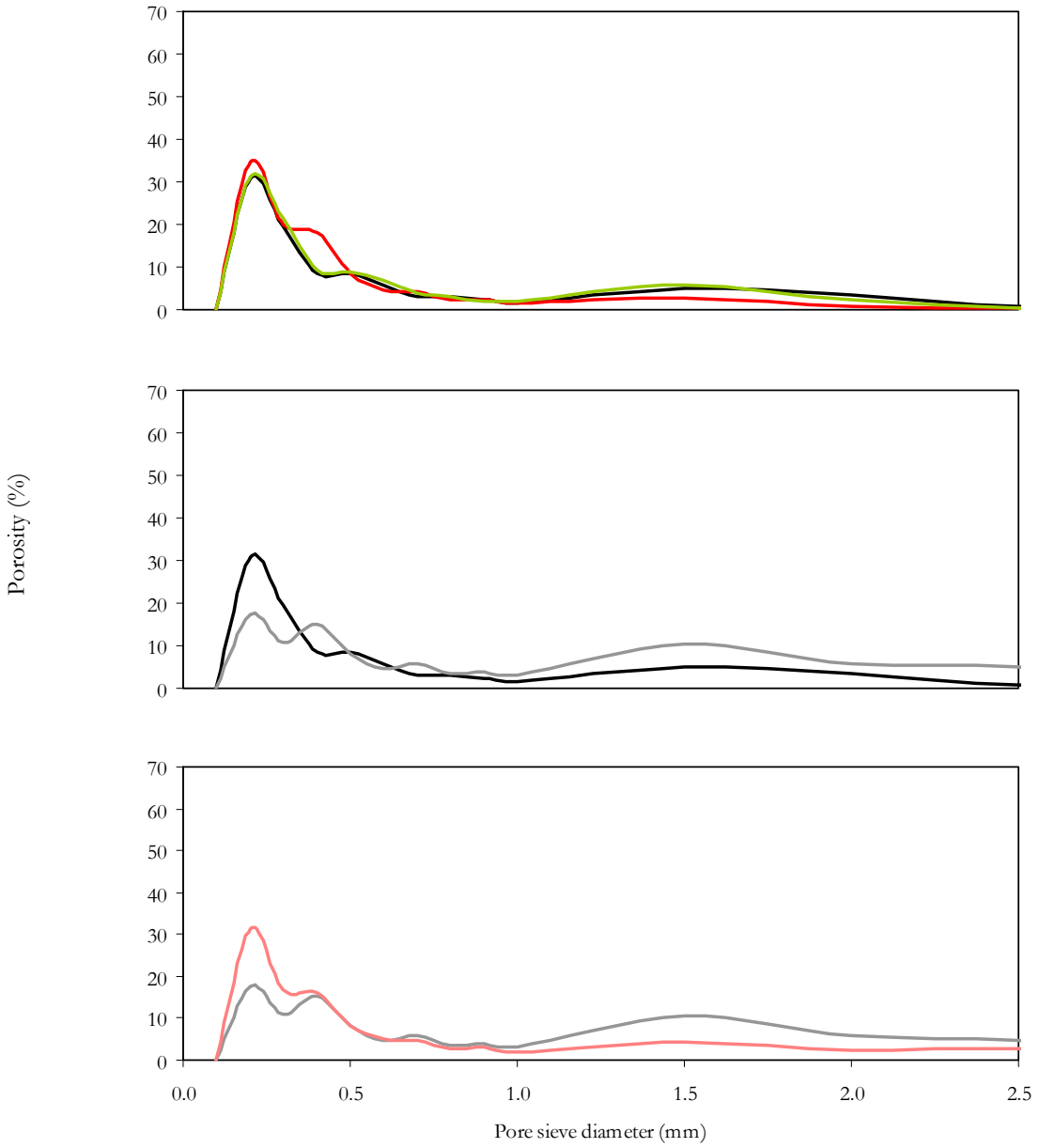

Figure A5.47 The distribution of pore sieve diameter (s_p) for the 50–90 mm depth of the B001 soil. Comparisons are made between the irrigation treatments; field water and 'clean' water [FW00*i* (—) and T102 (—)], salinity treatments [T102 (—) and T401] and for solutions of increasing SAR [T401 (—), T402 (—), T403 (—) and T404 (—)].

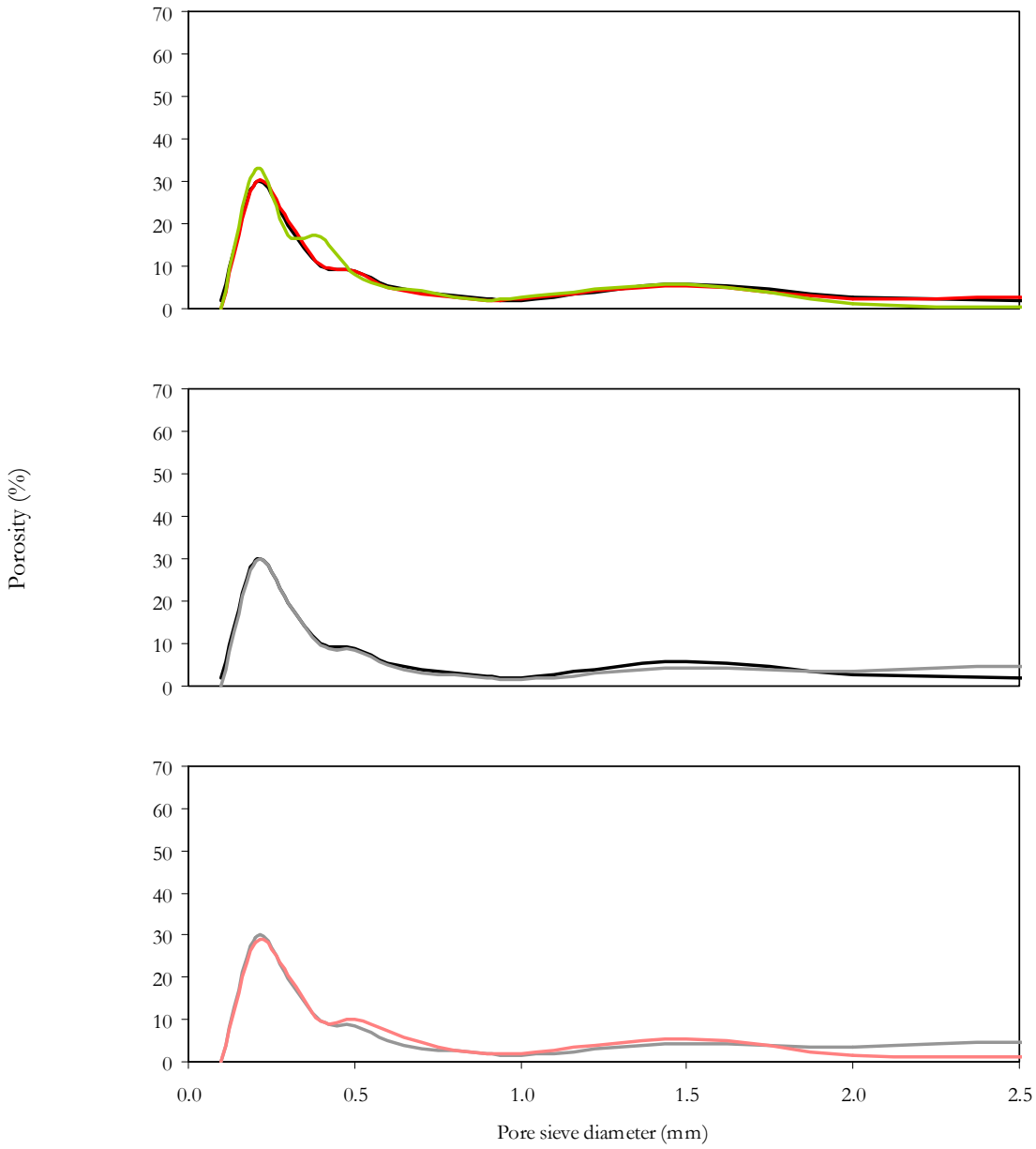

Figure A5.48 The distribution of pore sieve diameter (s_p) for the 50–90 mm depth of the B003 soil. Comparisons are made between the irrigation treatments; field water and 'clean' water [FW00*i* (—) and T102 (—)], salinity treatments [T102 (—) and T401] and for solutions of increasing SAR [T401 (—), T402 (—), T403 (—) and T404 (—)].

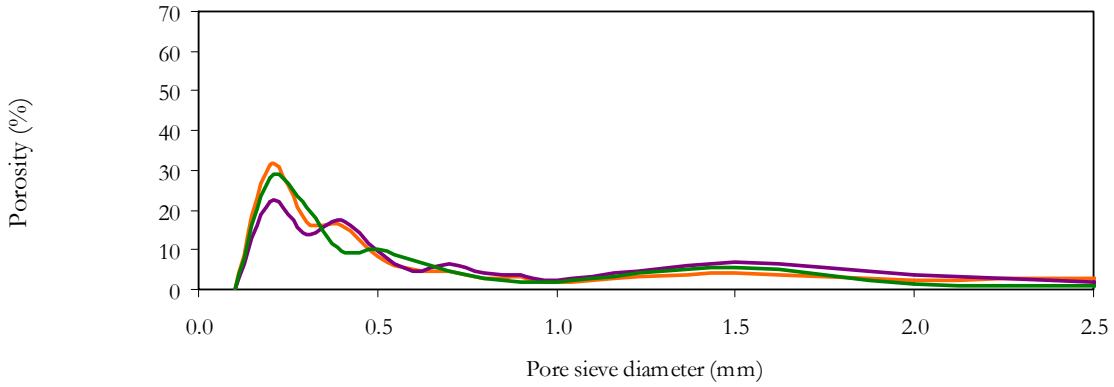

Figure A5.49 The distribution of pore sieve diameter (s_p) for the 50–90 mm depth of the B00*i* soils after irrigation with FW001 [B001 (—), B002 (—) and B003 (—)].

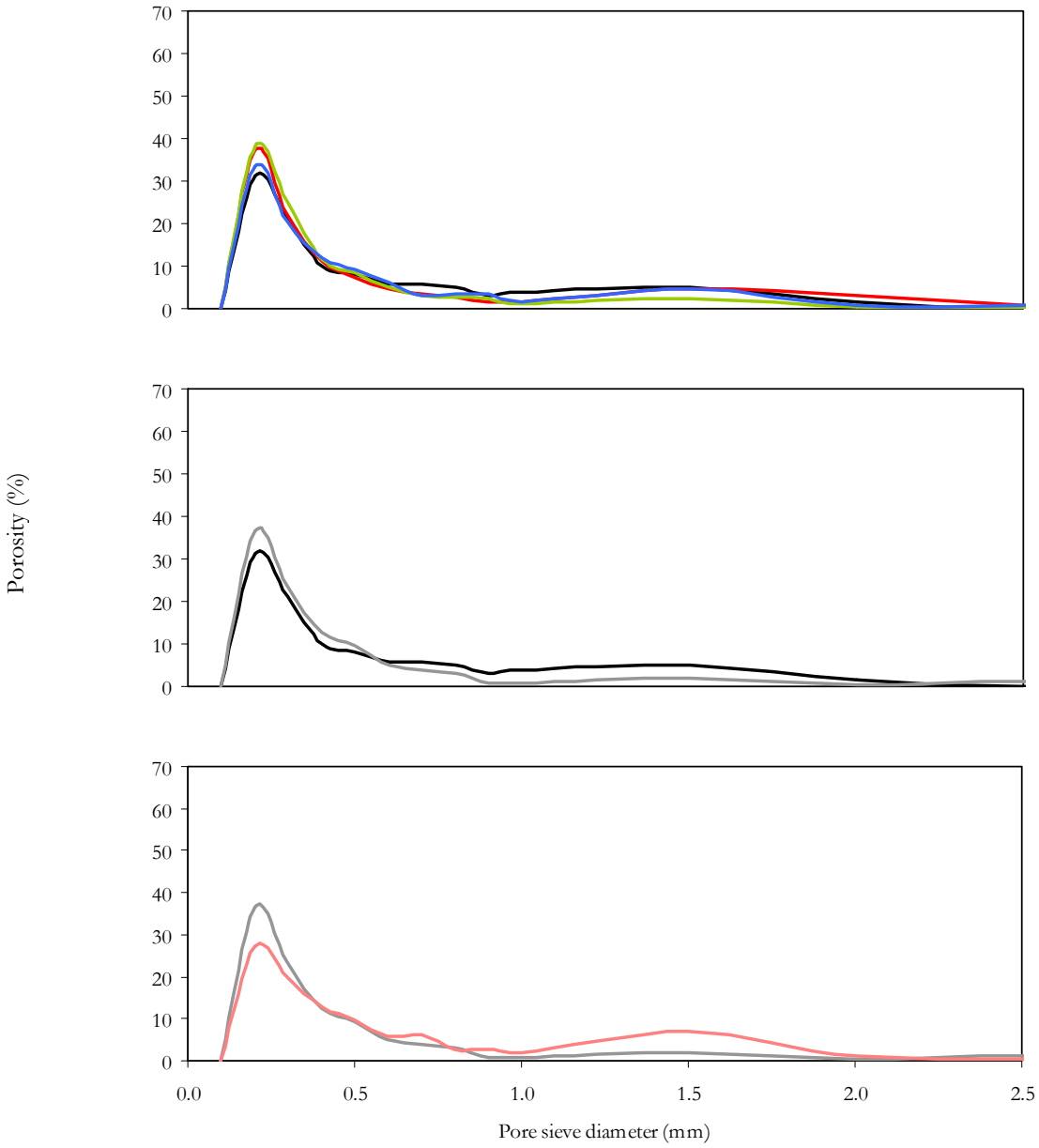

Figure A5.50 The distribution of pore sieve diameter (s_p) for the 50–90 mm depth of the G002 soil. Comparisons are made between the irrigation treatments; field water and 'clean' water [FW00*i* (—) and T102 (—)], salinity treatments [T102 (—) and T401] and for solutions of increasing SAR [T401 (—), T402 (—), T403 (—) and T404 (—)].

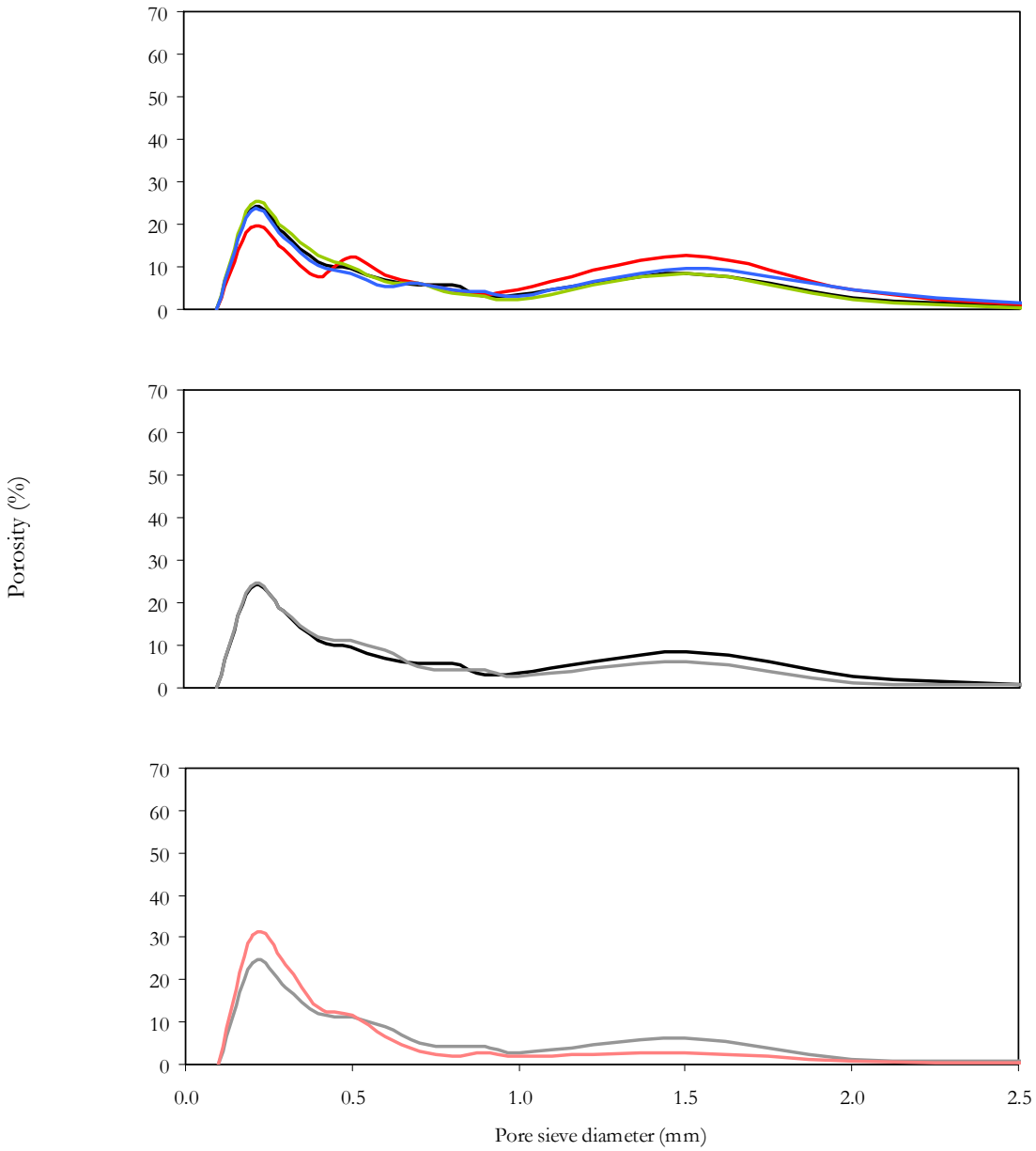

Figure A5.51 The distribution of pore sieve diameter (s_p) for the 50–90 mm depth of the H002 soil. Comparisons are made between the irrigation treatments; field water and 'clean' water [FW00*i* (—) and T102 (—)], salinity treatments [T102 (—) and T401] and for solutions of increasing SAR [T401 (—), T402 (—), T403 (—) and T404 (—)].

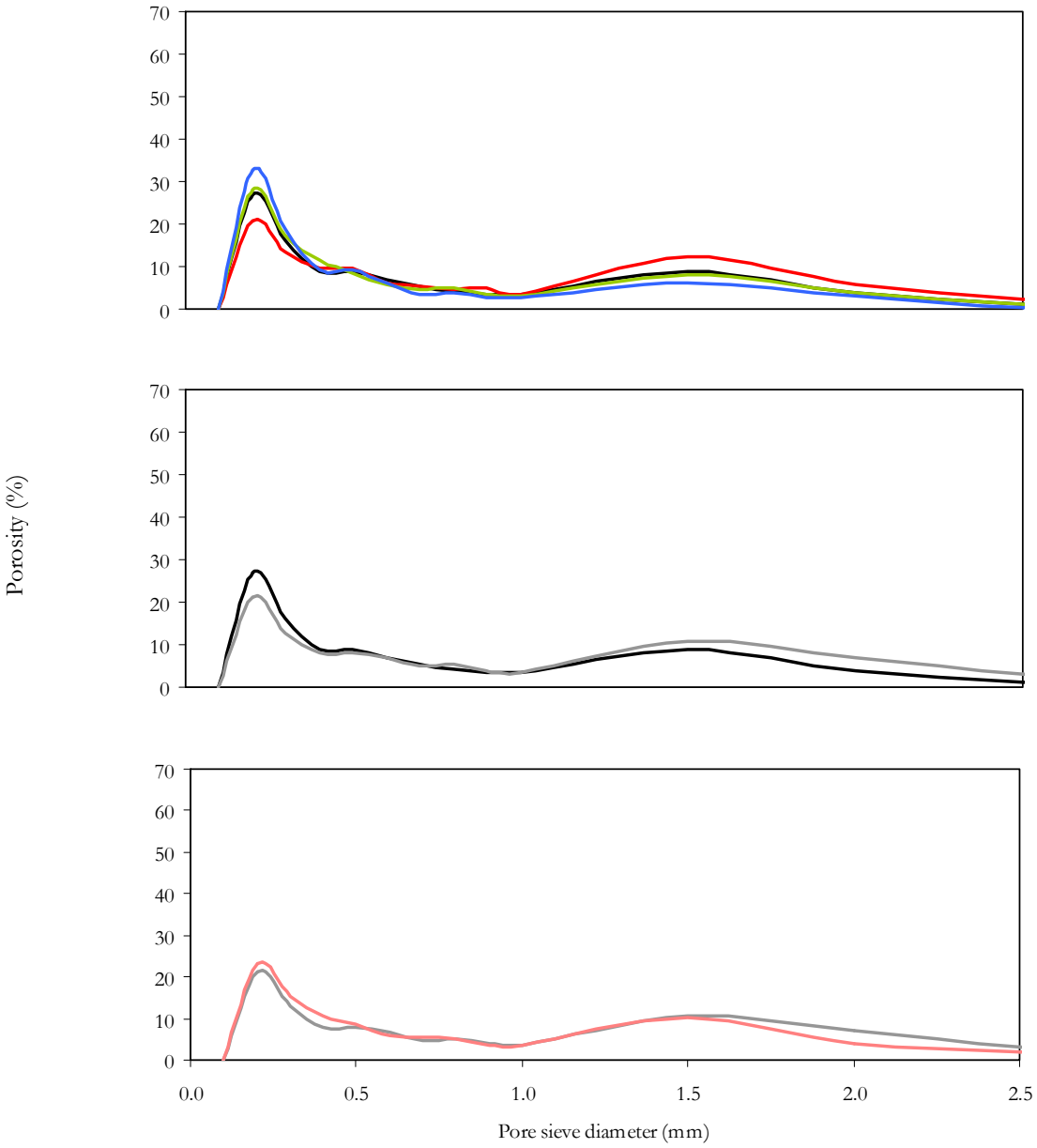

Figure A5.52 The distribution of pore sieve diameter (s_p) for the 50–90 mm depth of the N001 soil. Comparisons are made between the irrigation treatments; field water and 'clean' water [FW00*i* (—) and T102 (—)], salinity treatments [T102 (—) and T401] and for solutions of increasing SAR [T401 (—), T402 (—), T403 (—) and T404 (—)].

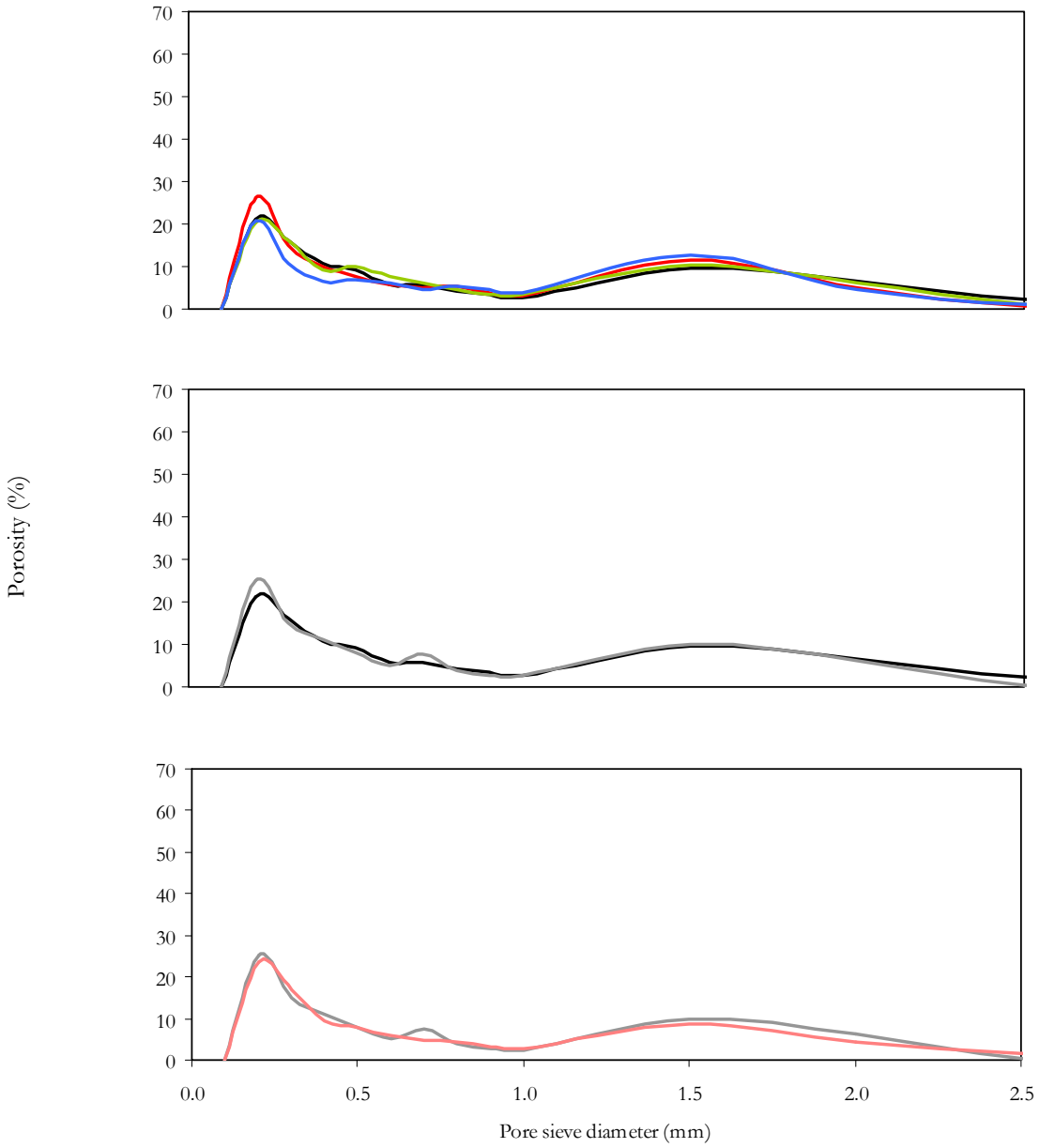

Figure A5.53 The distribution of pore sieve diameter (s_p) for the 50–90 mm depth of the N002 soil. Comparisons are made between the irrigation treatments; field water and 'clean' water [FW00*i* (—) and T102 (—)], salinity treatments [T102 (—) and T401] and for solutions of increasing SAR [T401 (—), T402 (—), T403 (—) and T404 (—)].

Appendix 5.4: **The effect of water quality on pore star–shape distributions for each of the Vertosols (B00*i*, G00*i*, H00*i*, N00*i*) at the 50–90 mm depth.**

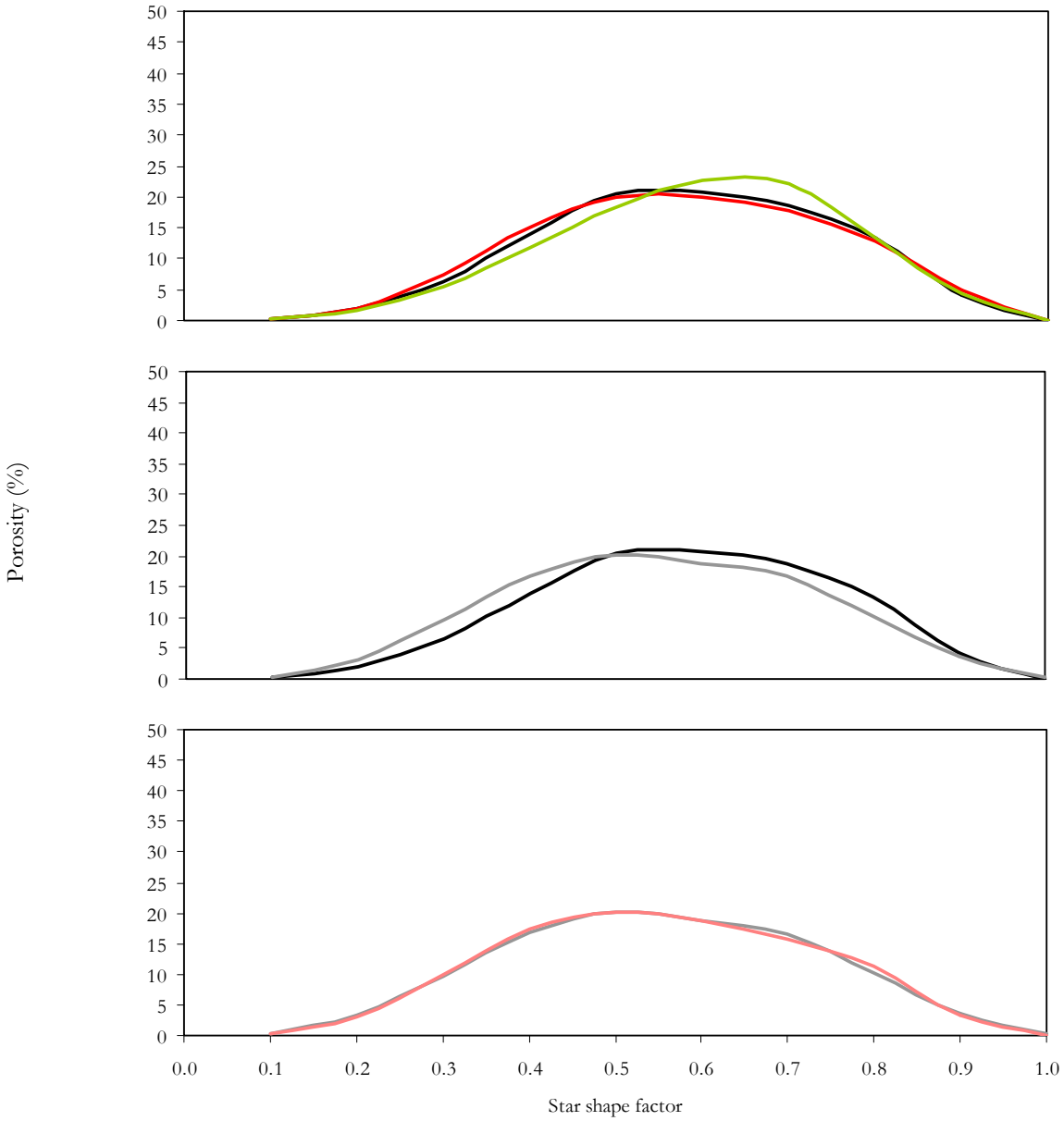

Figure A5.54 The distribution of the pore star shape (Ra_p^*) for the 50–90 mm depth of the B001 soil. Comparisons are made between the irrigation treatments; field water and 'clean' water [FW00*i* (—) and T102 (—)], salinity treatments [T102 (—) and T401] and for solutions of increasing SAR [T401 (—), T402 (—), T403 (—) and T404 (—)].

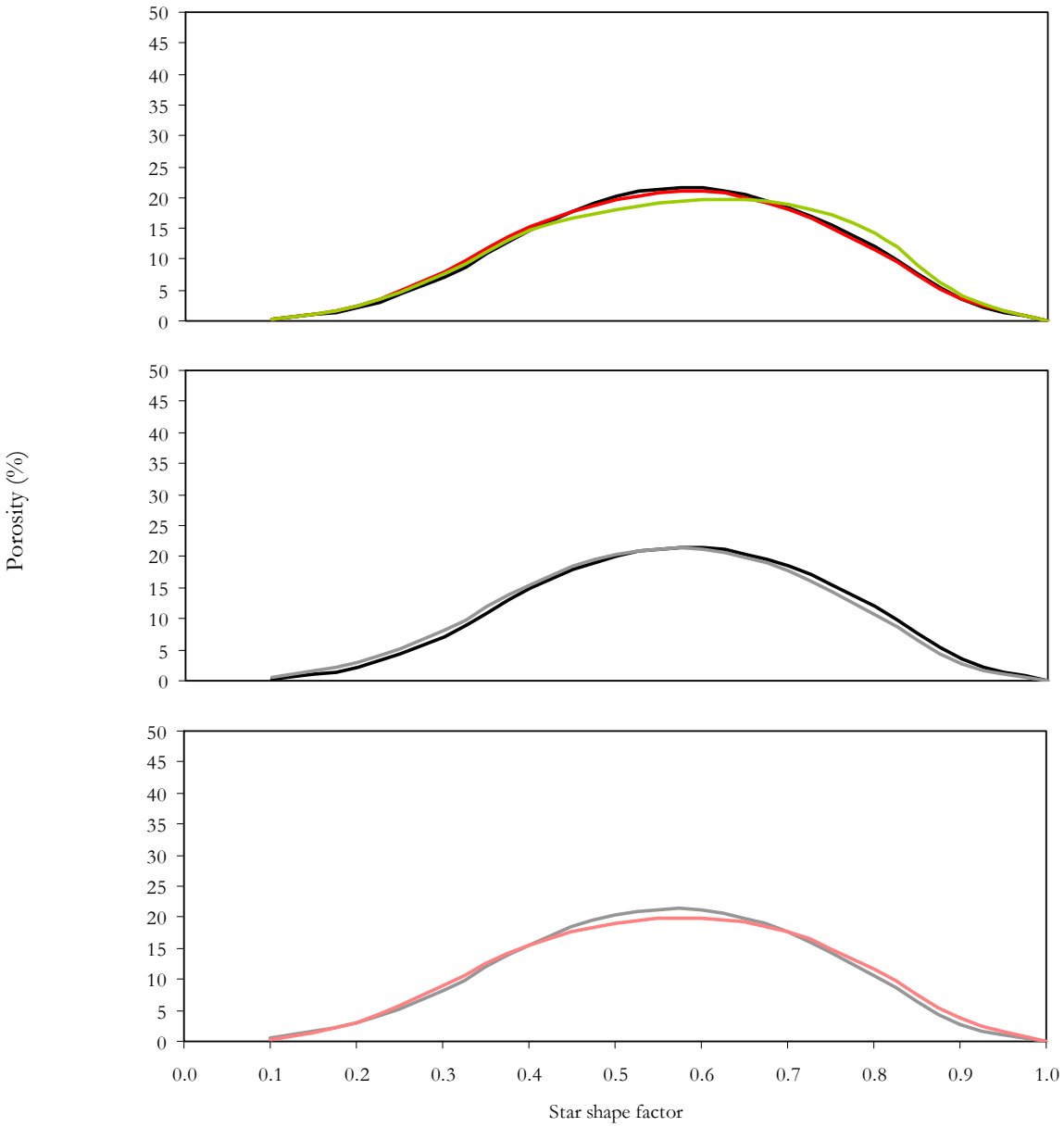

Figure A5.55 The distribution of the pore star shape (Ra_p^*) for the 50–90 mm depth of the B003 soil. Comparisons are made between the irrigation treatments; field water and 'clean' water [FW00*i* (—) and T102 (—)], salinity treatments [T102 (—) and T401] and for solutions of increasing SAR [T401 (—), T402 (—), T403 (—) and T404 (—)].

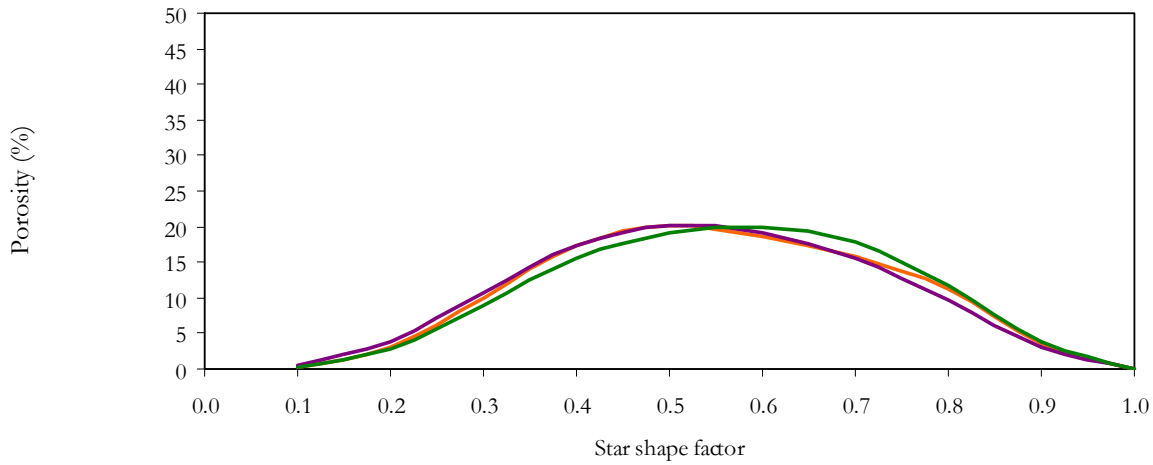

Figure A5.56 The distribution of the pore star shape (Ra_p^*) for the 50–90 mm depth of the B00*i* soils after irrigation with FW001 [B001 (—), B002 (—) and B003 (—)].

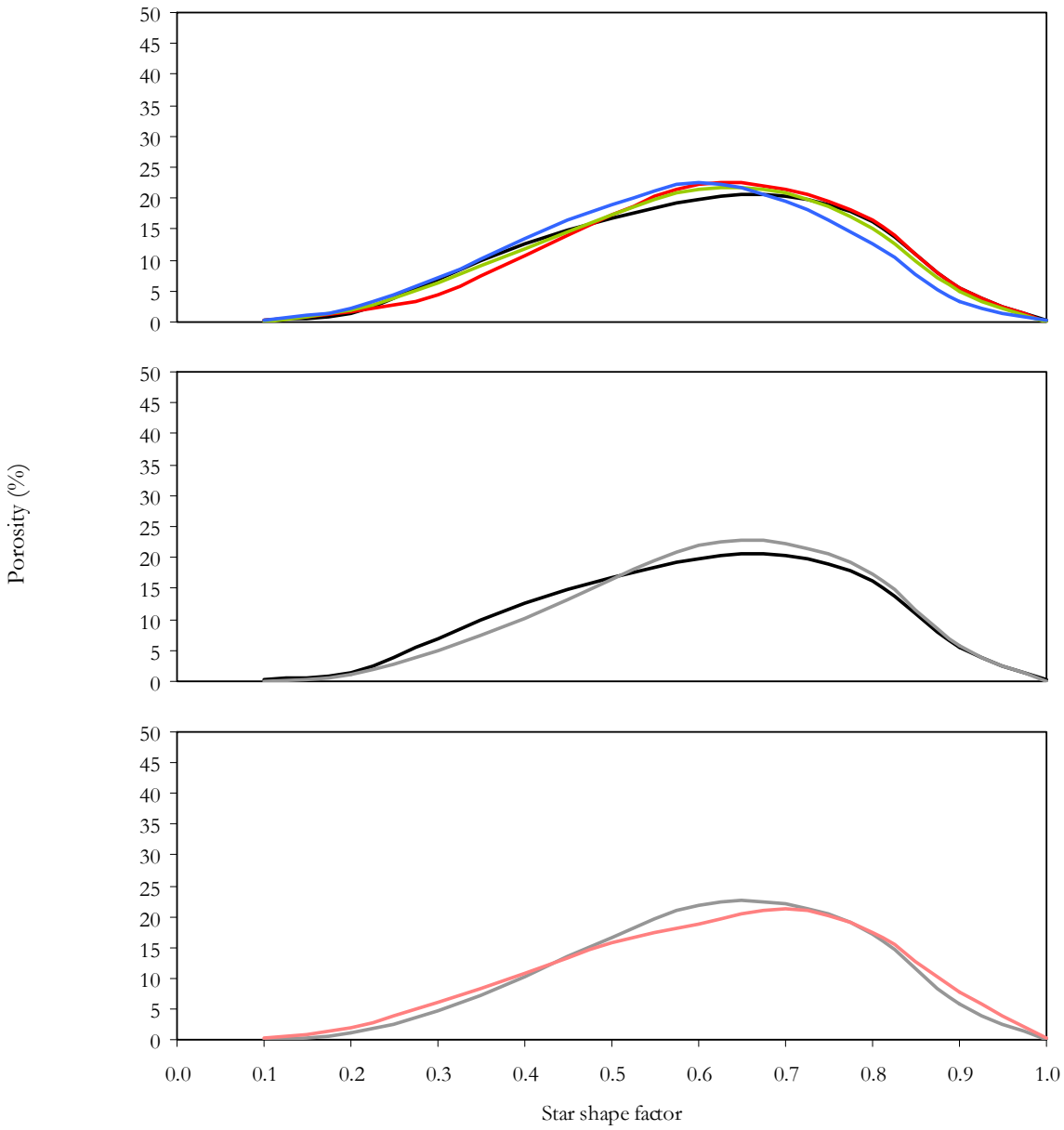

Figure A5.57 The distribution of the pore star shape (Ra_p^*) for the 50–90 mm depth of the G002 soil. Comparisons are made between the irrigation treatments; field water and 'clean' water [FW00*i* (—) and T102 (—)], salinity treatments [T102 (—) and T401] and for solutions of increasing SAR [T401 (—), T402 (—), T403 (—) and T404 (—)].

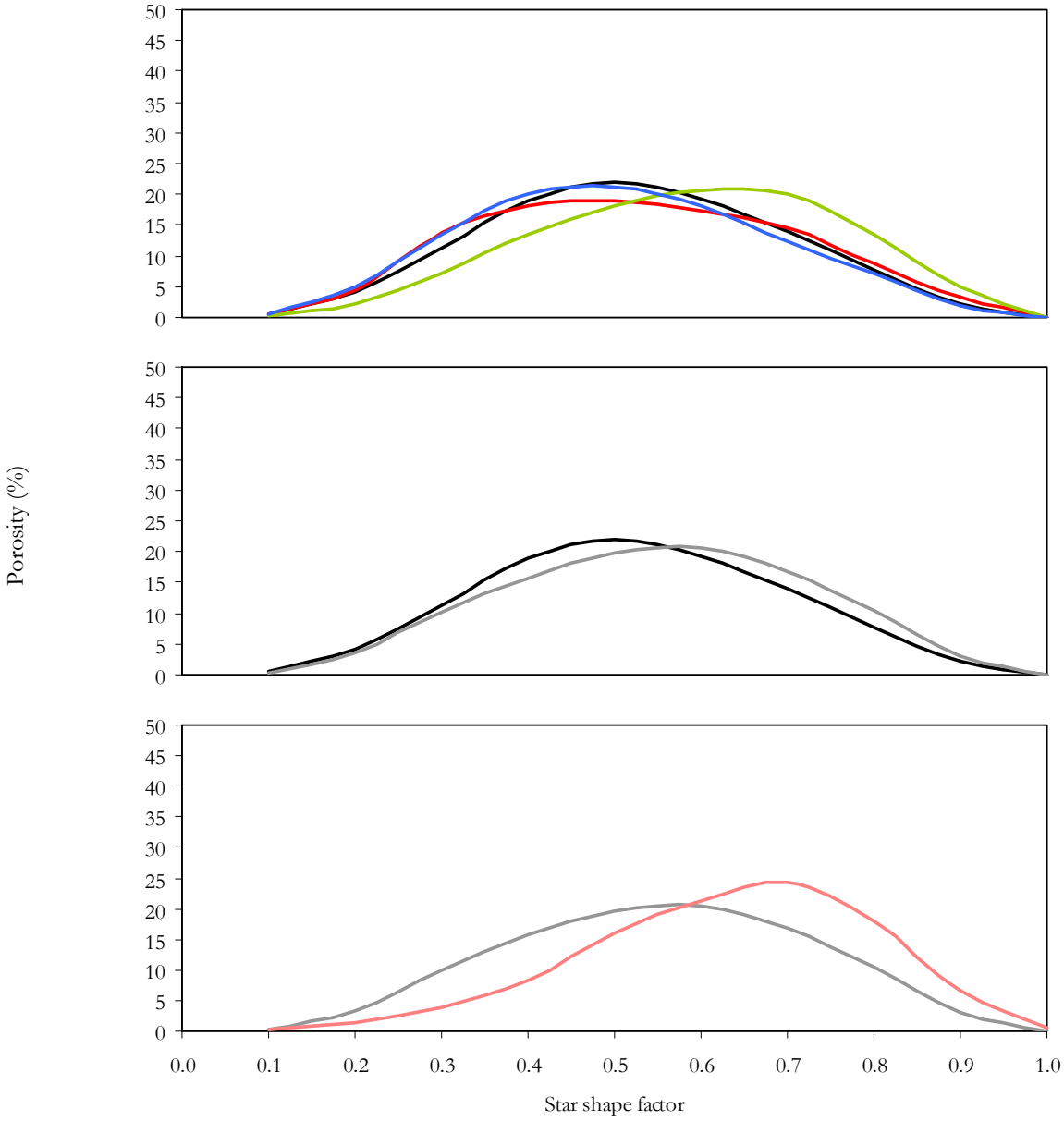

Figure A5.58 The distribution of the pore star shape (Ra_p^*) for the 50–90 mm depth of the H002 soil. Comparisons are made between the irrigation treatments; field water and 'clean' water [FW00*i* (—) and T102 (—)], salinity treatments [T102 (—) and T401] and for solutions of increasing SAR [T401 (—), T402 (—), T403 (—) and T404 (—)].

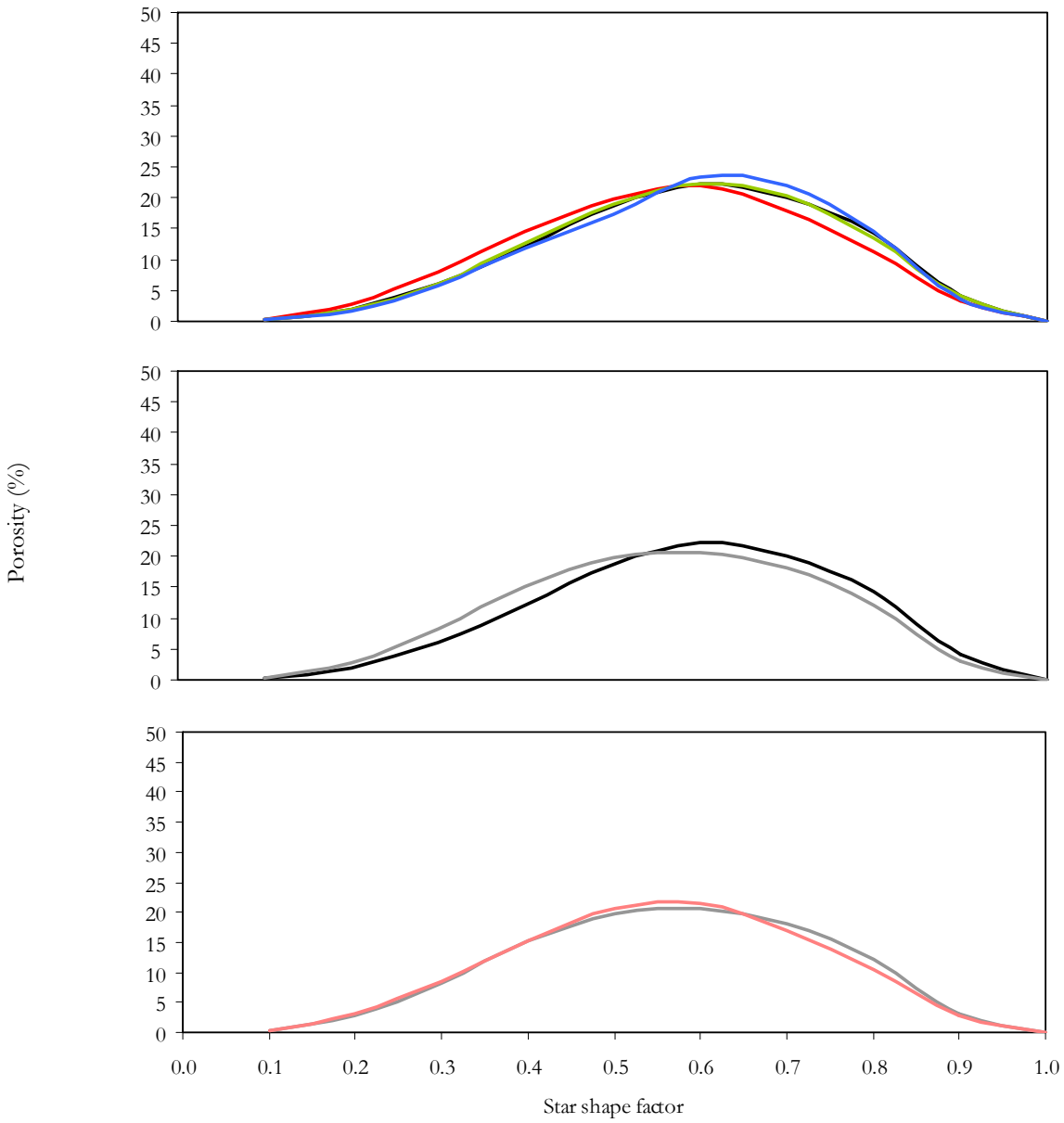

Figure A5.59 The distribution of the pore star shape (Ra_p^*) for the 50–90 mm depth of the N001 soil. Comparisons are made between the irrigation treatments; field water and 'clean' water [FW00*i* (—) and T102 (—)], salinity treatments [T102 (—) and T401] and for solutions of increasing SAR [T401 (—), T402 (—), T403 (—) and T404 (—)].

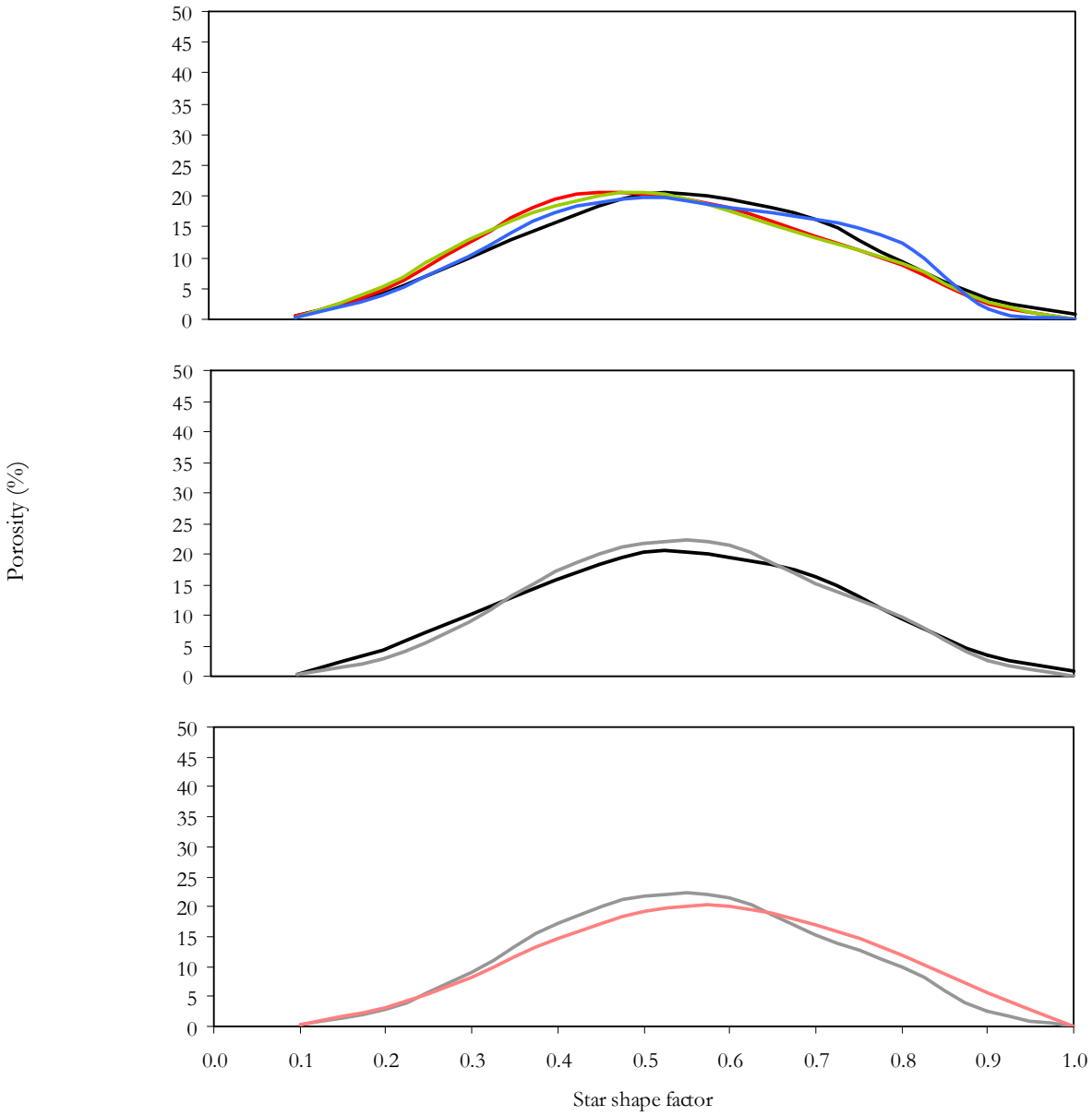

Figure A5.60 The distribution of the pore star shape (Ra_p^*) for the 50–90 mm depth of the N002 soil. Comparisons are made between the irrigation treatments; field water and 'clean' water [FW00*i* (—) and T102 (—)], salinity treatments [T102 (—) and T401] and for solutions of increasing SAR [T401 (—), T402 (—), T403 (—) and T404 (—)].

Appendix 6.1: The contributions of the fine and coarse clay fractions to total clay and the estimated proportions of different phyllosilicate clay minerals in each Vertosol.

Table A6.1
The contributions of each clay fraction (total clay (<2 μm), coarse clay (<2–0.2 μm) and fine clay (<0.2 μm)) and estimated contributions of clay phyllosilicate minerals to all soil material for each of the nine Vertosols

$C_{2:1}$ clay and *$F_{2:1}$ clay* each represent the proportions of coarse and fine 2:1 expanding lattice phyllosilicates, *Illite clay* and *Kaolinite clay* represent the proportions of these phyllosilicate minerals in the soil as a function of the total clay fraction.

	Clay content	Coarse clay	Fine clay	Phyllosilicate clay mineral suite (%)			
	(%)			$C_{2:1}$ clay	$F_{2:1}$ clay	Illite clay	Kaolinite clay
B001	61	17	43	1	35	15	9
B002	60	21	39	4	35	12	8
B003	63	18	45	2	34	20	8
G001	55	18	37	9	35	5	5
G002	64	21	43	12	39	6	6
H001	60	17	43	–	13	37	10
H002	54	16	38	3	26	9	15
N001	57	18	39	9	33	9	6
N002	55	19	36	10	22	19	6

Appendix 6.2: Selected physico–chemical attributes of the nine irrigation furrow Vertosols assessed in chapter 3.

Table A6.2
Selected physico–chemical attributes of the nine irrigation furrow Vertosols used for comparison of soils with current predictors of stability and for the development of a model of structural stability

Soil Site	$SI_{<2}$	Ca^{2+}	Mg^{2+}	Na^{+}	CEC_{eff}	Ca^{2+}:Mg^{2+}	ESP	EC	SAR
	(%)	$cmol_{(+)}\ kg^{-1}$						$dS\ m^{-1}$	$(mmol_{(+)}\ L^{-1})^{1/2}$
B001	21.1	20.4	10.7	2.9	35.5	1.9	8.1	0.37	4.9
B002	16.0	25.7	11.1	2.2	40.5	2.3	5.3	1.19	7.5
B003	16.3	26.9	10.4	1.5	40.5	2.6	3.6	0.14	1.9
G001	20.1	37.1	12.7	0.6	51.3	2.9	1.2	0.09	1.3
G002	24.2	33.6	13.0	0.8	48.8	2.6	1.6	0.15	1.9
H001	12.9	18.6	9.9	0.9	30.8	1.9	3.1	0.21	3.0
H002	14.3	24.7	11.7	0.7	38.2	2.1	1.8	0.20	2.4
N001	31.6	32.9	11.4	3.1	49.0	2.9	6.4	0.96	3.2
N002	13.2	31.4	10.3	0.3	43.7	3.0	0.7	0.17	0.2

Appendix 6.3: Selected physico–chemical attributes of all soil layers sampled from the laboratory irrigated soil columns assessed in chapter 4.

Table A6.3
Selected physico–chemical attributes of the laboratory irrigated G001 soil used for comparison of soils with current predictors of stability and for the development of a model of structural stability

$SI_{<2}$	Ca^{2+}	Mg^{2+}	Na^{+}	CEC_{eff}	$Ca^{2+}:Mg^{2+}$	ESP	EC	SAR
(%)		$cmol_{(+)}\ kg^{-1}$					$dS\ m^{-1}$	$(mmol_{(+)}\ L^{-1})^{1/2}$
18.9	28.2	11.0	1.4	41.8	2.6	3.4	0.09	1.6
20.0	28.6	10.5	1.4	41.5	2.7	3.3	0.06	1.6
22.1	29.9	11.0	1.4	43.0	2.7	3.3	0.06	1.6
22.5	28.9	11.5	1.3	42.4	2.5	3.2	0.06	1.6
19.1	30.5	11.2	1.5	44.4	2.7	3.3	0.10	2.2
18.4	29.5	11.1	1.3	42.7	2.7	3.1	0.07	1.6
19.4	30.8	11.5	1.5	44.4	2.7	3.3	0.06	1.5
20.7	31.0	11.3	1.5	44.4	2.7	3.4	0.06	1.3
16.5	28.7	10.7	1.4	42.1	2.7	3.4	0.13	2.3
20.7	27.5	10.8	1.4	40.5	2.5	3.5	0.07	1.5
19.6	30.4	11.1	1.5	43.7	2.7	3.3	0.07	1.6
20.9	30.5	11.9	1.5	44.5	2.6	3.5	0.06	1.5
20.0	28.9	10.9	1.4	42.5	2.7	3.3	0.17	2.6
21.0	28.8	10.8	1.4	41.9	2.7	3.3	0.08	1.7
20.5	26.8	10.7	1.5	39.7	2.5	3.7	0.06	1.2
23.7	28.8	11.2	1.5	42.2	2.6	3.6	0.07	1.3
16.7	27.7	10.9	1.1	41.0	2.5	2.7	0.11	1.5
21.3	28.1	10.8	1.2	41.1	2.6	3.0	0.06	1.1
25.9	27.7	10.9	1.4	40.7	2.5	3.4	0.06	1.1
27.1	27.9	12.1	1.1	42.9	2.3	2.5	0.06	0.9
19.8	27.8	11.1	1.0	41.0	2.5	2.4	0.08	1.1
20.4	29.8	11.4	1.1	43.4	2.6	2.6	0.06	1.0
22.6	30.0	11.5	1.3	43.6	2.6	3.1	0.05	0.9
24.5	31.0	12.2	1.5	45.3	2.5	3.2	0.05	0.9
21.6	30.6	11.1	1.2	44.2	2.8	2.8	0.13	1.5
17.1	28.8	11.0	1.2	42.1	2.6	3.0	0.07	1.1
19.4	28.8	10.4	1.4	41.3	2.8	3.4	0.07	1.0
17.6	29.8	11.4	1.4	43.3	2.6	3.3	0.06	1.1
16.3	29.0	10.8	1.2	42.3	2.7	2.8	0.08	1.1
17.8	29.1	11.1	1.3	42.6	2.6	3.1	0.07	1.0
17.9	31.2	11.3	1.5	44.7	2.8	3.4	0.05	0.8
18.2	29.7	11.6	1.5	43.5	2.6	3.5	0.05	0.9
18.0	28.8	11.0	1.0	42.1	2.6	2.5	0.14	1.2
15.3	28.8	10.8	1.3	41.8	2.7	3.1	0.08	1.0
14.7	30.0	11.2	1.4	43.4	2.7	3.3	0.08	1.1
13.4	29.9	11.6	1.4	43.6	2.6	3.3	0.07	1.0
12.5	29.1	11.2	1.0	42.5	2.6	2.3	0.11	1.0
13.9	28.8	10.8	1.1	41.6	2.7	2.6	0.07	0.8
15.3	30.8	11.3	1.3	44.1	2.7	3.0	0.06	0.8
18.2	29.3	11.6	1.4	43.0	2.5	3.3	0.06	0.9

Table A6.3 continued

$SI_{<2}$	Ca^{2+}	Mg^{2+}	Na^{+}	CEC_{eff}	Ca^{2+}:Mg^{2+}	ESP	EC	SAR
(%)	$cmol_{(+)}\ kg^{-1}$						$dS\ m^{-1}$	$(mmol_{(+)}\ L^{-1})^{1/2}$
8.9	28.6	10.8	1.7	42.2	2.7	4.1	0.11	1.6
9.4	28.9	11.0	1.6	42.3	2.6	3.7	0.07	1.0
9.2	29.7	10.9	1.6	42.9	2.7	3.7	0.07	1.1
12.2	30.5	11.5	1.5	44.1	2.6	3.4	0.06	0.9
12.3	27.6	10.8	1.7	41.0	2.6	4.1	0.12	1.5
9.6	31.0	11.0	1.7	44.5	2.8	3.7	0.07	1.0
8.3	30.2	11.5	1.6	44.1	2.6	3.6	0.07	1.0

Table A6.4
Selected physico–chemical attributes of the laboratory irrigated G002 soil used for comparison of soils with current predictors of stability and for the development of a model of structural stability

$SI_{<2}$	Ca^{2+}	Mg^{2+}	Na^{+}	CEC_{eff}	Ca^{2+}:Mg^{2+}	ESP	EC	SAR
(%)	$cmol_{(+)}\ kg^{-1}$						$dS\ m^{-1}$	$(mmol_{(+)}\ L^{-1})^{1/2}$
16.0	26.2	11.5	0.8	40.6	2.3	2.0	0.11	1.0
14.5	29.4	12.1	0.9	43.9	2.4	2.0	0.08	1.0
18.6	28.3	11.7	1.1	42.9	2.4	2.5	0.07	1.2
18.8	28.0	12.0	1.2	42.6	2.3	2.7	0.07	1.3
11.8	27.2	11.8	0.9	41.4	2.3	2.3	0.12	1.1
17.3	29.8	11.8	1.0	44.5	2.5	2.2	0.06	1.1
14.9	28.1	10.7	1.5	40.9	2.6	3.7	0.05	1.5
17.6	28.7	11.4	1.1	42.9	2.5	2.5	0.08	1.4
16.6	26.2	10.9	1.5	40.6	2.4	3.6	0.12	2.5
16.0	30.9	11.9	1.4	46.1	2.6	3.0	0.08	1.5
16.7	25.5	10.7	1.4	39.1	2.4	3.5	0.07	1.7
20.5	27.8	11.0	1.4	41.6	2.5	3.4	0.07	1.9
14.6	27.3	11.0	1.3	41.6	2.5	3.1	0.16	2.5
16.1	28.8	11.1	1.3	43.1	2.6	3.0	0.08	2.0
16.0	26.2	11.1	1.4	40.2	2.4	3.4	0.08	1.9
21.9	28.6	11.6	1.4	42.8	2.5	3.2	0.08	1.8
21.0	26.6	11.0	1.5	40.6	2.4	3.7	0.10	2.5
21.8	27.8	11.2	1.4	42.3	2.5	3.3	0.06	1.6
19.2	26.0	11.4	1.2	40.0	2.3	3.1	0.07	1.6
19.9	27.4	11.8	1.3	41.8	2.3	3.1	0.06	1.3
16.2	25.9	10.8	1.4	39.8	2.4	3.6	0.12	2.3
22.8	29.1	11.6	1.4	43.8	2.5	3.2	0.08	1.9
20.4	25.4	10.8	1.3	38.9	2.3	3.5	0.08	1.9
28.7	29.3	12.4	1.5	44.6	2.4	3.4	0.08	1.9
14.4	25.5	10.8	1.0	39.2	2.4	2.6	0.06	1.1
15.2	28.5	11.5	1.1	43.1	2.5	2.7	0.05	1.5
22.3	25.9	11.4	1.3	40.2	2.3	3.2	0.05	1.5
20.5	28.8	11.9	1.4	43.6	2.4	3.3	0.07	1.6
19.4	26.2	11.0	1.0	40.2	2.4	2.5	0.05	1.2
14.9	28.4	11.4	1.2	42.9	2.5	2.8	0.05	1.2
18.6	28.2	11.8	1.3	42.9	2.4	3.1	0.05	1.4

Table A6.4 continued

$SI_{<2}$	Ca^{2+}	Mg^{2+}	Na^{+}	CEC_{eff}	$Ca^{2+}:Mg^{2+}$	ESP	EC	SAR
(%)	$cmol_{(+)}\ kg^{-1}$						$dS\ m^{-1}$	$(mmol_{(+)}\ L^{-1})^{1/2}$
18.3	27.5	11.3	1.4	41.7	2.4	3.3	0.05	1.3
15.1	29.3	11.7	1.0	43.6	2.5	2.3	0.09	1.5
17.7	27.4	11.0	1.0	40.9	2.5	2.4	0.06	1.4
18.7	28.2	11.8	1.1	42.5	2.4	2.5	0.06	1.5
19.0	27.7	11.6	1.2	42.1	2.4	2.9	0.07	1.6
10.9	28.2	11.3	1.0	42.1	2.5	2.5	0.11	1.7
14.9	25.6	10.8	1.1	39.3	2.4	2.8	0.07	1.5
19.6	29.4	11.7	1.2	43.8	2.5	2.8	0.05	1.2
20.4	26.2	11.2	1.3	40.0	2.3	3.2	0.06	1.2
19.4	27.2	10.6	1.6	41.2	2.6	3.8	0.13	2.9
19.3	26.8	10.9	1.5	40.9	2.5	3.6	0.07	1.7
18.4	26.9	11.0	1.4	40.6	2.4	3.3	0.07	1.6
16.6	27.9	11.0	1.8	42.5	2.6	4.1	0.12	2.8
18.1	28.8	11.6	1.3	43.6	2.5	2.9	0.07	1.7
17.4	28.1	11.4	1.2	42.3	2.5	3.0	0.07	1.7

Table A6.5
Selected physico–chemical attributes of the laboratory irrigated H001 soil used for comparison of soils with current predictors of stability and for the development of a model of structural stability

$SI_{<2}$	Ca^{2+}	Mg^{2+}	Na^{+}	CEC_{eff}	$Ca^{2+}:Mg^{2+}$	ESP	EC	SAR
(%)	$cmol_{(+)}\ kg^{-1}$						$dS\ m^{-1}$	$(mmol_{(+)}\ L^{-1})^{1/2}$
14.7	14.3	9.1	2.0	26.8	1.6	7.6	0.12	1.8
14.4	14.8	9.2	2.0	27.9	1.6	7.0	0.09	1.4
17.5	14.4	9.5	1.9	27.2	1.5	6.8	0.08	1.2
16.9	14.7	9.8	1.9	27.8	1.5	6.8	0.08	2.1
8.8	12.5	8.0	1.9	24.1	1.6	8.0	0.11	3.3
8.4	15.5	9.7	2.0	28.9	1.6	7.0	0.08	2.2
12.2	14.2	9.6	1.9	27.1	1.5	7.1	0.08	1.8
16.5	14.6	9.8	1.8	27.4	1.5	6.7	0.08	1.8
5.4	13.5	8.6	1.5	25.1	1.6	5.9	0.10	2.4
7.3	15.5	9.3	1.6	27.9	1.7	5.7	0.07	1.8
10.1	13.6	9.3	1.6	26.1	1.5	6.1	0.06	1.7
13.0	15.1	10.3	1.8	28.8	1.5	6.2	0.06	1.7
5.6	10.7	6.6	0.6	19.9	1.6	3.1	0.12	1.1
5.7	12.5	7.4	0.9	22.7	1.7	3.9	0.07	1.2
8.2	14.7	9.1	1.1	26.2	1.6	4.1	0.06	1.3
7.1	15.0	9.0	1.2	27.0	1.7	4.5	0.08	1.4
7.0	10.1	6.2	1.2	19.1	1.6	6.1	0.07	1.8
7.2	12.8	7.6	1.6	23.7	1.7	6.6	0.05	1.4
10.0	14.1	9.2	1.9	26.9	1.5	7.2	0.06	1.5
15.8	14.2	9.1	1.8	27.0	1.6	6.8	0.07	1.7
7.2	11.6	7.6	1.6	22.3	1.5	7.3	0.13	2.9
10.0	12.5	8.2	1.6	23.7	1.5	6.7	0.07	1.5
15.1	13.0	8.6	1.8	24.8	1.5	7.3	0.07	1.5
18.1	13.2	9.5	1.8	25.8	1.4	7.0	0.07	1.6
5.1	10.1	6.0	1.2	18.8	1.7	6.5	0.15	3.1

Table A6.5 continued

$SI_{<2}$	Ca^{2+}	Mg^{2+}	Na^{+}	CEC_{eff}	Ca^{2+}:Mg^{2+}	ESP	EC	SAR
(%)		$cmol_{(+)}\ kg^{-1}$					$dS\ m^{-1}$	$(mmol_{(+)}\ L^{-1})^{1/2}$
6.3	11.3	6.8	1.3	21.0	1.7	6.3	0.07	1.6
6.3	14.1	8.2	1.6	25.9	1.7	6.3	0.06	1.5
10.9	13.0	8.0	1.8	24.6	1.6	7.1	0.07	1.6
0.5	11.9	7.1	1.3	22.3	1.7	5.7	0.12	2.2
1.7	10.5	6.4	1.3	19.7	1.6	6.4	0.06	1.4
7.9	13.8	8.3	1.6	25.3	1.6	6.3	0.07	1.5
11.8	14.9	9.6	1.8	27.9	1.6	6.3	0.09	1.9
11.6	10.6	6.8	0.9	19.7	1.6	4.8	0.20	2.5
8.9	14.0	8.9	1.6	25.8	1.6	6.1	0.08	1.6
11.4	13.8	9.5	1.7	26.2	1.5	6.4	0.08	1.8
16.0	14.2	9.5	1.8	26.7	1.5	6.7	0.08	1.6
4.7	11.1	6.5	0.9	20.6	1.7	4.4	0.06	1.2
5.0	11.8	6.9	1.2	21.5	1.7	5.4	0.04	1.0
10.1	15.9	9.6	1.5	28.9	1.7	5.1	0.05	1.0
7.3	13.5	8.8	1.5	25.3	1.5	5.9	0.05	1.2
8.0	12.2	7.0	1.4	22.5	1.7	6.3	0.12	2.3
13.7	13.6	8.5	1.7	25.9	1.6	6.4	0.07	1.4
14.8	14.8	9.0	1.6	27.2	1.6	5.9	0.07	1.5
17.8	14.1	9.4	1.9	27.0	1.5	6.9	0.10	2.0
15.5	15.9	9.9	1.8	29.6	1.6	6.0	0.09	1.8
18.0	14.7	9.8	1.7	27.6	1.5	6.1	0.11	2.1

Table A6.6
Selected physico–chemical attributes of the laboratory irrigated H002 soil used for comparison of soils with current predictors of stability and for the development of a model of structural stability

$SI_{<2}$	Ca^{2+}	Mg^{2+}	Na^{+}	CEC_{eff}	Ca^{2+}:Mg^{2+}	ESP	EC	SAR
(%)		$cmol_{(+)}\ kg^{-1}$					$dS\ m^{-1}$	$(mmol_{(+)}\ L^{-1})^{1/2}$
8.8	22.4	10.2	1.5	36.0	2.2	4.1	0.25	3.2
10.1	19.2	9.3	1.4	31.4	2.1	4.4	0.14	2.6
15.7	20.1	10.8	1.6	33.9	1.9	4.6	0.14	2.7
15.2	18.1	11.0	1.6	31.8	1.6	5.0	0.15	2.9
9.3	24.2	11.1	1.3	38.6	2.2	3.3	0.15	2.0
11.0	20.3	9.9	1.2	33.0	2.1	3.6	0.12	1.7
13.3	20.2	10.2	1.2	32.8	2.0	3.6	0.12	1.9
12.1	19.4	10.6	1.3	32.4	1.8	3.9	0.13	2.0
12.9	22.1	10.0	1.1	34.9	2.2	3.2	0.14	1.9
9.9	20.4	9.7	1.2	32.9	2.1	3.6	0.13	2.0
20.3	19.8	10.1	1.3	32.7	2.0	4.1	0.13	2.2
24.0	19.2	11.0	1.4	32.9	1.7	4.2	0.14	2.4
8.6	23.4	10.5	1.1	37.0	2.2	2.9	0.12	1.5
14.8	21.0	10.5	1.1	34.2	2.0	3.3	0.12	1.6
17.3	19.6	9.9	1.3	32.2	2.0	4.1	0.12	1.9
16.3	19.7	10.4	1.3	32.8	1.9	4.0	0.12	2.0
7.2	21.7	9.9	1.5	34.9	2.2	4.4	0.21	3.1
15.9	21.9	10.2	1.5	35.3	2.2	4.3	0.15	2.6

Table A6.6 continued

$SI_{<2}$	Ca^{2+}	Mg^{2+}	Na^{+}	CEC_{eff}	$Ca^{2+}:Mg^{2+}$	ESP	EC	SAR
(%)	$cmol_{(+)}\ kg^{-1}$						$dS\ m^{-1}$	$(mmol_{(+)}\ L^{-1})^{1/2}$
23.1	18.7	9.4	1.6	30.9	2.0	5.0	0.15	2.8
27.1	18.3	11.0	1.6	32.0	1.7	5.0	0.15	2.9
4.8	23.7	10.5	1.6	37.3	2.3	4.2	0.21	3.1
13.2	21.6	9.9	1.3	34.6	2.2	3.9	0.15	2.5
17.9	18.5	9.2	1.3	30.5	2.0	4.4	0.15	2.5
21.3	18.2	10.2	1.4	31.1	1.8	4.6	0.15	2.7
14.2	22.7	11.3	1.9	37.4	2.0	5.0	0.21	3.5
10.4	21.9	10.3	1.6	35.4	2.1	4.5	0.15	2.7
21.2	17.4	9.4	1.6	29.8	1.8	5.4	0.15	2.9
20.8	18.7	10.9	1.8	32.6	1.7	5.4	0.17	3.3
9.5	19.8	9.2	1.6	32.3	2.2	5.1	0.21	3.2
14.8	19.8	9.8	1.4	32.5	2.0	4.3	0.14	2.4
14.0	19.5	9.9	1.4	32.0	2.0	4.3	0.14	2.3
17.5	21.0	10.8	1.4	34.4	2.0	3.9	0.15	2.4
10.4	20.6	10.2	0.7	33.3	2.0	2.1	0.18	0.8
10.7	21.3	9.9	0.9	33.8	2.1	2.7	0.12	1.1
14.2	19.7	9.8	1.0	31.8	2.0	3.1	0.13	1.5
12.9	19.1	10.2	1.2	31.6	1.9	3.7	0.13	1.8
8.2	24.3	12.1	1.2	39.1	2.0	3.1	0.29	2.2
12.5	22.3	10.0	1.3	35.5	2.2	3.7	0.19	2.6
20.2	19.1	10.2	1.7	32.3	1.9	5.2	0.18	3.3
23.8	18.7	11.1	1.9	32.9	1.7	5.9	0.18	3.7
12.1	21.7	10.2	1.7	35.2	2.1	4.8	0.24	3.6
20.7	20.3	10.0	1.5	33.4	2.0	4.6	0.16	2.9
17.0	18.8	10.1	1.6	31.8	1.9	5.1	0.18	3.1
28.9	18.5	10.8	1.7	32.1	1.7	5.2	0.19	3.3
17.3	20.2	9.6	1.7	33.0	2.1	5.2	0.22	3.8
18.2	19.8	10.0	1.5	32.6	2.0	4.7	0.15	2.9
23.8	18.2	10.4	1.6	31.4	1.8	4.9	0.16	2.9
25.8	17.1	10.2	1.5	30.0	1.7	5.2	0.16	3.0

Table A6.7
Selected physico–chemical attributes of the laboratory irrigated N001 soil used for comparison of soils with current predictors of stability and for the development of a model of structural stability

$SI_{<2}$	Ca^{2+}	Mg^{2+}	Na^{+}	CEC_{eff}	$Ca^{2+}:Mg^{2+}$	ESP	EC	SAR
(%)	$cmol_{(+)}\ kg^{-1}$						$dS\ m^{-1}$	$(mmol_{(+)}\ L^{-1})^{1/2}$
31.2	26.9	10.3	3.3	42.7	2.6	7.8	0.17	3.2
33.7	29.2	10.6	4.0	46.1	2.7	8.7	0.18	3.3
37.4	27.4	11.2	4.6	45.5	2.4	10.2	0.19	3.5
35.1	27.4	11.0	4.5	45.1	2.5	10.1	0.21	4.2
24.7	29.3	11.0	3.8	45.5	2.7	8.4	0.18	4.2
33.7	29.5	11.2	4.1	46.9	2.6	8.7	0.18	3.7
29.0	23.4	10.2	4.0	39.3	2.3	10.1	0.19	4.7
35.0	28.8	11.8	4.8	47.5	2.4	10.0	0.19	4.4
24.3	24.7	9.9	4.3	41.1	2.5	10.6	0.20	5.3
32.3	25.7	10.7	4.3	42.6	2.4	10.1	0.22	4.9

Table A6.7 continued

$SI_{<2}$	Ca^{2+}	Mg^{2+}	Na^{+}	CEC_{eff}	$Ca^{2+}:Mg^{2+}$	ESP	EC	SAR
(%)	$cmol_{(+)}\ kg^{-1}$						$dS\ m^{-1}$	$(mmol_{(+)}\ L^{-1})^{1/2}$
33.0	27.1	11.2	4.5	45.0	2.4	10.1	0.19	4.7
31.8	26.2	10.6	4.3	42.9	2.5	10.1	0.21	4.8
26.3	27.8	10.8	4.6	44.8	2.6	10.4	0.19	4.8
31.6	28.2	10.7	4.5	45.6	2.6	9.8	0.19	4.6
36.4	28.5	11.4	4.7	46.9	2.5	10.0	0.19	4.1
35.7	23.6	10.8	4.5	41.1	2.2	11.1	0.20	4.7
20.4	27.2	10.9	2.6	42.2	2.5	6.1	0.20	4.1
25.6	27.1	10.6	3.3	43.3	2.5	7.7	0.20	4.3
30.9	27.6	10.9	4.4	45.0	2.5	9.8	0.21	4.7
33.9	25.7	10.8	4.2	42.4	2.4	9.8	0.21	5.0
20.1	28.4	11.1	2.8	44.2	2.6	6.3	0.19	4.2
30.9	24.8	10.3	3.4	40.1	2.4	8.5	0.19	4.2
35.7	27.2	11.1	4.4	44.5	2.4	9.8	0.21	4.7
30.8	25.4	10.9	4.5	42.6	2.3	10.5	0.22	4.7
19.4	26.8	9.8	3.6	42.2	2.7	8.6	0.21	5.2
28.8	28.1	10.6	4.0	44.7	2.6	9.0	0.20	4.4
31.5	27.6	10.6	4.3	44.7	2.6	9.7	0.21	4.7
31.8	25.7	11.0	4.4	42.8	2.3	10.2	0.20	4.4
19.9	30.3	10.8	4.0	46.6	2.8	8.7	0.22	5.1
27.2	23.7	9.9	4.0	39.3	2.4	10.1	0.20	4.1
27.1	27.1	10.9	4.7	44.6	2.5	10.5	0.21	4.8
32.6	25.0	10.4	4.7	42.1	2.4	11.1	0.21	4.5
23.1	28.6	10.5	4.1	45.4	2.7	9.0	0.22	4.5
29.9	26.8	10.5	4.2	43.6	2.6	9.7	0.20	4.2
25.6	27.4	10.7	4.4	44.5	2.6	9.8	0.21	4.5
23.7	26.4	10.5	4.2	43.3	2.5	9.8	0.21	4.6
19.0	24.1	9.0	3.6	38.4	2.7	9.4	0.24	4.9
24.7	27.7	10.7	4.3	44.7	2.6	9.6	0.20	4.1
28.2	30.7	11.4	4.7	49.1	2.7	9.6	0.21	4.5
26.5	27.2	11.1	4.6	44.8	2.5	10.3	0.21	4.7
21.0	25.8	9.9	4.0	41.4	2.6	9.6	0.23	5.1
27.6	26.1	10.6	4.2	43.0	2.5	9.7	0.20	4.1
31.7	27.0	10.8	4.4	44.1	2.5	10.1	0.22	4.4
33.8	23.9	10.6	4.4	40.8	2.2	10.8	0.21	4.5
25.8	22.7	8.6	3.8	36.4	2.6	10.6	0.22	4.8
25.1	25.4	9.3	3.8	40.2	2.7	9.5	0.21	4.5
31.7	24.4	10.2	4.3	40.6	2.4	10.5	0.20	4.2
32.3	26.2	10.6	4.4	43.1	2.5	10.2	0.21	4.3

Table A6.8
Selected physico–chemical attributes of the laboratory irrigated N002 soil used for comparison of soils with current predictors of stability and for the development of a model of structural stability

$SI_{<2}$	Ca^{2+}	Mg^{2+}	Na^{+}	CEC_{eff}	$Ca^{2+}:Mg^{2+}$	ESP	EC	SAR
(%)	$cmol_{(+)}\ kg^{-1}$						$dS\ m^{-1}$	$(mmol_{(+)}\ L^{-1})^{1/2}$
8.0	21.9	8.7	0.7	32.9	2.5	2.1	0.08	0.6
9.3	24.2	9.0	0.8	35.5	2.7	2.3	0.08	0.7
20.7	24.6	9.3	0.9	36.2	2.6	2.5	0.12	0.9

Table A6.8 continued

$SI_{<2}$	Ca^{2+}	Mg^{2+}	Na^{+}	CEC_{eff}	Ca^{2+}:Mg^{2+}	ESP	EC	SAR
(%)	$cmol_{(+)}\ kg^{-1}$						$dS\ m^{-1}$	$(mmol_{(+)}\ L^{-1})^{1/2}$
28.4	25.2	10.5	1.0	37.8	2.4	2.7	0.10	1.0
4.7	26.3	9.3	0.7	38.0	2.8	1.9	0.08	0.6
6.8	27.2	9.2	0.8	38.7	3.0	2.1	0.06	0.6
12.6	27.0	9.4	0.9	38.7	2.9	2.3	0.05	0.7
13.8	26.2	9.9	0.9	38.2	2.7	2.5	0.06	0.8
7.8	25.6	9.6	1.0	37.9	2.7	2.6	0.10	1.0
13.4	24.9	9.4	0.9	37.2	2.6	2.5	0.09	1.0
25.4	25.9	10.1	1.0	38.3	2.6	2.7	0.10	1.1
24.0	25.3	10.6	1.1	38.1	2.4	2.8	0.10	1.1
7.0	27.0	10.2	1.0	39.9	2.7	2.4	0.11	1.1
12.6	24.2	9.2	0.9	36.1	2.6	2.5	0.10	0.9
27.5	27.4	10.3	1.0	40.0	2.7	2.4	0.11	1.0
27.8	23.2	9.9	1.0	35.2	2.3	2.8	0.11	1.1
7.4	24.9	9.7	0.7	36.9	2.6	1.8	0.15	0.8
13.8	25.4	9.5	0.9	37.8	2.7	2.3	0.08	0.8
11.8	26.6	9.9	0.9	38.6	2.7	2.2	0.08	0.9
13.3	25.1	10.0	0.9	37.0	2.5	2.5	0.07	0.9
5.5	27.9	10.7	0.7	41.2	2.6	1.6	0.20	0.7
9.3	25.4	9.4	0.8	37.2	2.7	2.2	0.11	0.9
21.0	27.5	10.1	0.8	39.9	2.7	2.0	0.11	0.9
19.5	26.3	10.7	0.9	39.2	2.5	2.2	0.12	0.9
9.1	26.1	9.6	1.1	38.4	2.7	2.9	0.17	1.7
10.4	24.4	9.2	1.0	36.1	2.6	2.6	0.11	1.2
18.0	28.0	10.5	1.0	41.0	2.7	2.3	0.12	1.2
20.1	25.8	10.2	1.0	38.3	2.5	2.7	0.12	1.3
4.1	25.7	9.1	1.0	37.6	2.8	2.7	0.19	1.7
12.3	25.5	9.2	1.1	37.4	2.8	2.9	0.08	1.3
18.4	29.8	10.6	1.1	42.7	2.8	2.6	0.07	1.2
18.5	28.0	10.5	1.1	40.7	2.7	2.7	0.10	1.2
5.1	29.4	10.4	1.1	42.7	2.8	2.6	0.16	1.6
11.1	27.8	9.8	1.1	40.8	2.8	2.7	0.10	1.3
16.4	28.4	10.1	1.1	40.8	2.8	2.7	0.08	1.3
19.8	25.9	9.8	1.1	37.9	2.6	3.0	0.08	1.3
5.4	25.4	9.7	1.2	38.0	2.6	3.2	0.16	2.0
11.8	25.4	9.4	1.2	37.5	2.7	3.1	0.09	1.4
14.5	27.4	9.7	1.1	39.6	2.8	2.7	0.10	1.3
15.7	27.5	10.4	1.1	40.3	2.6	2.7	0.10	1.3
9.5	27.0	9.8	1.0	39.7	2.8	2.5	0.24	1.6
13.1	26.0	9.7	1.0	38.5	2.7	2.6	0.10	1.2
17.3	27.8	10.4	1.1	40.6	2.7	2.7	0.10	1.3
19.3	26.5	10.3	1.2	39.2	2.6	3.0	0.11	1.5
4.2	26.0	9.5	0.9	38.3	2.7	2.4	0.30	1.5
12.4	26.4	9.8	0.9	38.5	2.7	2.4	0.10	1.2
17.8	28.3	10.5	1.1	41.2	2.7	2.6	0.09	1.2
18.1	27.8	10.6	1.1	40.7	2.6	2.6	0.10	1.2